



Aalborg Universitet

AALBORG UNIVERSITY
DENMARK

Automatic generation of elevation data over Danish landscape

Wind, Lissi Marianne

Publication date:
2008

Document Version
Publisher's PDF, also known as Version of record

[Link to publication from Aalborg University](#)

Citation for published version (APA):
Wind, L. M. (2008). *Automatic generation of elevation data over Danish landscape*. Institut for Samfundsudvikling og Planlægning, Aalborg Universitet.

General rights

Copyright and moral rights for the publications made accessible in the public portal are retained by the authors and/or other copyright owners and it is a condition of accessing publications that users recognise and abide by the legal requirements associated with these rights.

- Users may download and print one copy of any publication from the public portal for the purpose of private study or research.
- You may not further distribute the material or use it for any profit-making activity or commercial gain
- You may freely distribute the URL identifying the publication in the public portal -

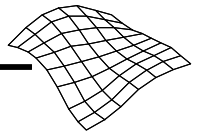
Take down policy

If you believe that this document breaches copyright please contact us at vbn@aub.aau.dk providing details, and we will remove access to the work immediately and investigate your claim.



Automatic generation of elevation data over Danish landscape

**Ph D-Thesis
Marianne Wind
Aalborg University
2008**



Abstract

This thesis consists of two parts; a main part and an appendix. To get the full benefit and understanding of the thesis both parts should be read.

This thesis is a review and analysis of an investigation into the automatic collection of elevation data. Elevation data can be collected “automatically” with IFSAR (InterFerometric Synthetic Aperture Radar), LI-DAR (Light Detection And Ranging, or “laser scanning”) or by automatic correlation of digital images. The focus of this thesis is on the automatic generation of elevation data from digital images based on automatic correlation. The programme Match-T is the basis for this investigation. A method for the proposal of combining/integrating new z-measurements will also be mentioned. This method is to handle historic, present and future elevation data obtained from different sources.

The thesis uses as its foundation previous investigations into automatic generation of elevation data by image correlation. These prior studies, however, have indicated that there is an influence between the image scale, image resolution, mesh size and landscape type on the accuracy of the generated elevation data. This thesis will attempt to fill in the gaps in current academic understanding of the applicability of automatic techniques for elevation data development and to see how this method interacts with Danish landscape types.

An area of typical Danish landscape has been chosen as a test case for this study. The landscape contains five different landscape types, such as open farm fields, forest, villages etc. Aerial images of this test area were taken in 3 different scales. At the start of this study, images had to be scanned in order to digitise them, they were therefore scanned in 3 different resolutions and more than 10,000 reference points were measured. A code was established to differentiate between each landscape type.

To analyse each of the parameters- image scale, image resolution and mesh size- one of the parameters has to be kept constant, while the other two are changing. There have therefore been 3^3 (27) calculations carried out.

The calculation flow for automatically generated elevation data is described. There is also an investigation into the results achieved, how gross errors are detected and eliminated by an iteration method and what accuracy can be obtained after elimination of the gross errors. First the influence of the three different parameters is described, then the influences of the five different landscape types are described.

Finally, the thesis is concluded with a brief description of the calculation experience with the automatic generation method, and what influence of image scale, image resolution, grid size and landscape type has on the accuracy and a few suggestions for future investigations.

At the end of the thesis, a new method to improve the accuracy of the elevations, achieved by automatic generation, is introduced.

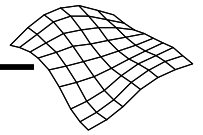
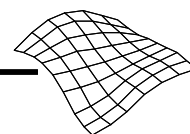


Table of contents:

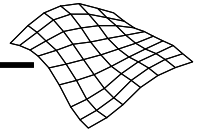
1 Introduction	13
1.2 The motivation for the project	13
1.3 Digital Elevation Models	13
1.3.1 Terrain model or surface model	13
1.4 Standards for Elevation models	14
1.4.1 Accuracy	14
1.4.2 Density	14
1.4.3 Currentness	14
1.5 Danish digital elevation models	14
1.5.1 KMS DTM	14
1.5.2 DDH – Danish Digital Height model	15
1.5.3 Near Future	15
1.6 How to capture terrain data	15
1.6.1 IFSAR - InterFerometric Synthetic Aperture Radar	15
1.6.2 LIDAR – Light Detection And Ranging	16
1.6.3 Automatic correlation within digital photogrammetry	16
1.7 Focus of the thesis	16
1.8 Project delimitation	17
1.9 Choice of method	17
1.10 The structure of the project	17
2 Methods of determining elevation data	21
2.1 SAR	21
2.1.1 Interferometric SAR - IFSAR	22
2.1.2 The accuracy of the IFSAR method	23
2.1.3 The scope of the SAR method	24
2.2 LIDAR	24
2.2.1 The principles of LIDAR	24
2.2.2 The accuracy of LIDAR	26
2.2.3 Pros and cons of LIDAR	26
2.2.4 The scope of the LIDAR method	26
2.3 Photogrammetric determination	27
2.3.1 Socet Set	27
2.3.1.1 Image pyramid	27
2.3.1.2 Orientation	28
2.3.2 Normalisation	28
2.3.3 Correlation and the DTM generation	28
2.3.4 ABM used in Socet Set	29
2.3.5 The edge based method	29
2.3.6 Combination of the methods	29
2.3.7 Correlation and DEM generation	29
2.3.7.1 Accuracy	30
2.3.7.2 Pros and cons in the use of Socet Set	30
2.3.7.3 The scope of Socet Set	30
2.4 Match-T	30
2.4.1 Orientation of Match-T	30
2.4.1.1 Inner orientation	30
2.4.1.2 Absolute orientation	31
2.4.2 The pre-processing of primary data	31
2.4.2.1 Normalisation	31

2.4.2.2 Image pyramid	31
2.4.2.3 Object pyramid	31
2.4.3 Parameters for DEM generation	32
2.4.3.1 Correlation	32
2.4.3.2 The DEM generation	32
2.4.4 Conversion of the grid points	36
2.4.4.1 Accuracy	36
2.4.4.2 Pros and cons of the photogrammetric method	37
2.4.4.3 The scope of the photogrammetric method	37
2.5 Comparison of the three methods	37
2.5.1 Choice of method	38
2.6 Proposal for combining/integrating new z-measurements	38
3 Experience and investigation strategy	43
3.1 Background	43
3.2 A source study of experiences with Match-T	43
3.2.1 Results from the OEEPE-workshop	45
3.2.1.1 The result from Inpho GmbH	46
3.2.1.2 Institut Cartogràfic de Catalunya	46
3.2.1.3 Institut für Photogrammetrie, Stuttgart	46
3.2.1.4 National Geographical Institute, Brussels	46
3.2.1.5 Investigation, Aalborg University	47
3.2.2 Summation of the investigations from the OEEPE workshop	47
3.2.3 Summation of sources and OEEPE workshop	47
3.3 The investigation strategy of this project	49
3.3.1 Accuracy in relation to flight altitude	50
3.3.2 Accuracy in relation to images resolution	50
3.3.3 Accuracy in relation to mesh size	50
3.3.4 Danish landscape types	50
3.4 Selected investigations	50
3.4.1 The influence of the scale	50
3.4.2 The influence of the pixel size	51
3.4.3 The influence of the mesh size	51
3.4.4 The influence of the landscape type	51
3.5 Summation	51
4 The data material	53
4.1 The test area	53
4.2 Aerial photos	54
4.3 Control points	55
4.4 Selection of models	55
4.5 The frame of reference	55
5 Preparation for the grid generation	59
5.1 The set-up of Match-T	59
5.1.1 Image material	60
5.1.2 Geometric data	60
5.1.3 External data	60
5.1.4 Orientation of the model	60
5.1.4.1 Inner orientation	60
5.1.4.2 Absolute orientation	60
5.1.5 Pre-processing of primary data	62
5.1.5.1 Normalisation	62
5.1.5.2 Image pyramid	62
5.1.5.3 Object pyramid	62
5.1.6 The DEM generation	62
5.1.6.1 Correlation	63
5.1.6.2 The finite-element reconstruction	63
5.2 Grid calculation	63



5.2.1.1 Monitor for individual programme steps	63
5.2.1.2 Graphic online/offline	63
5.2.1.3 Online statistics	64
5.2.2 The post-processing	64
5.2.2.1 DEM editing	64
5.2.2.2 DEM analysis	64
5.2.2.3 DEM output	65
5.2.3 Choice of methods for a pre-analysis of data	65
6 Pre-analysis of the generated data	67
6.1 The uniformity of the generated grids	67
6.1.1 The visualisation tool "graphic online/offline"	67
6.1.2 Control of the file sizes	70
6.2 Analysis of the coding of the grid points	70
6.2.1 Summation	72
6.3 Elimination of gross correlation errors	73
6.3.1 The iteration process	74
6.4 Use of codes for identification of gross errors	75
6.5 Partial conclusion	77
7 The investigation	79
7.1 Accuracy before and after elimination of gross errors	80
7.1.1 Accuracy before elimination of gross errors	80
7.1.2 Accuracy after elimination of gross errors	81
7.1.3 Summation	82
7.2 The influence of scale	82
7.2.1 Summation of scale	83
7.3 The influence of pixel size	83
7.3.1 Summation of pixel size	84
7.4 The influence of mesh size	84
7.4.1 Summation of mesh size	85
7.4.2 Common conclusion	85
7.4.3 The pixel size on the ground	85
7.4.4 The number of pixels per mesh size	86
7.5 The influence of the landscape type	88
7.5.1 The accuracy for different landscape types including gross errors	88
7.5.2 The accuracy for different landscape types excluding gross errors	90
7.5.3 Gross errors and the landscape type	91
7.5.4 Summation for the landscape types	92
7.5.5 Correlation errors or objects in the terrain?	92
7.5.6 Summation	96
7.6 Partial conclusion	96
7.6.1 Experiences in table form	97
8 Results on the basis of Chapter 7	99
8.1 Exclusion of the landscape types	99
8.1.1 Results without gross errors	100
8.1.2 Percentage of eliminated points	100
8.1.3 Summation	102
8.2 Method for locating gross errors	102
8.2.1 Object or correlation error	106
8.3 Partial conclusion	107
9 Theory and practice	109
9.1 The scale	109
9.2 The pixel size	110
9.3 The mesh size	110
9.4 The landscape type	111
9.5 Summation	111
9.6 Experiences and currentness	112

10 Conclusion and perspectives	115
10.1 Background	115
10.2 The results achieved	115
10.2.1 The scale and resolution of the images.....	116
10.2.2 The mesh size	116
10.2.3 The landscape type	116
10.2.4 Accuracy.....	116
10.2.5 Eliminated points	116
10.3 Recommendation	116
10.4 Data fusion	117
10.5 Perspectives.....	117
10.5.1 Automatic elimination of problematic areas	117
10.5.2 Automatic localisation and elimination of gross errors	118
10.6 Outlook for future work in this field.....	118
References.....	121
Acknowledgement	127



Appendix A: Image matching techniques

A.1 ABM and FBM	133
A.1.1 Area based matching	134
A.1.1.1 Correlation at pixel level	134
A.1.1.1.1 Correlation coefficient	134
A.1.1.1.2 Mean square	135
A.1.1.2 Correlation at sub pixel level	135
A.1.1.2.1 Fitting in of a polynomial	135
A.1.1.2.2 Least squares matching	136
A.1.2 Feature based matching	138
A.1.2.1 Area	138
A.1.2.2 Line	138
A.1.2.3 Points	139
A.1.2.3.1 The Moravec operator	139
A.1.2.3.2 The Förstner operator	141
A.1.2.3.3 Determination of intersections, corner and end points	141
A.1.2.3.4 Determination of circle points	144
A.1.2.3.5 Quality evaluation of the characteristic points	145
A.1.2.4 The principles of FBM	145
A.1.3 Epipolar geometry	146
A.1.3.1 Resampling	147
A.1.3.2 Normalisation and resampling	148
A.1.3.3 Correlation in one dimension	148
A.1.3.4 ABM in one dimension	148
A.1.4 FBM in one dimension	149
A.1.5 Correlation in one dimension 'on the fly'	149
A.1.6 Image pyramid	149
A.1.7 Object pyramid	150
A.1.8 Pros and cons	151

Appendix B: The data material

B.1 Description of the data material	155
B.1.1 Test area	155
B.1.2 Aerial photos	156
B.1.3 Control points	157
B.1.4 Selection of models and area types	160
B.1.5 Analytically measured points of reference	162
B.2 Data capture	163
B.2.1 Capture of control points	163
B.2.1.1 Planning	163
B.2.1.1.1 Geodetic reference	163
B.2.1.1.2 Equipment	164
B.2.1.2 Grid structure	164
B.2.1.2.1 Measuring method	164
B.2.1.3 Changes during the field survey	165
B.2.1.4 Calculation	165
B.2.1.5 Evaluation	166
B.2.1.5.1 The free adjustment	166
B.2.1.5.2 The retained adjustment	168
B.2.2 Capture of analytically measured elevation data	168

B.2.2.1 Relative orientation.....	168
B.2.2.2 Bundle adjustment.....	169
B.2.2.3 The frame of reference	170
B.2.2.4 The control point list	172

Appendix C: Analysis programme PIL

C.1 Description of the analysis programme PIL	175
C.1.1 Demands on the analysis programme PIL	175
C.1.2 Input files.....	176
C.1.2.1 File format	176
C.1.3 Programme description.....	178
C.1.3.1 The user interface	178
C.1.3.2 Choice of files.....	178
C.1.3.3 Calculation options.....	179
C.1.4 Functionality.....	181
C.1.4.1 Filing of data.....	181
C.1.4.2 Data processing	181
C.1.5 Statistics.....	182
C.1.6 The output files	183

Appendix D: Editing programme

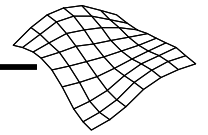
D.1 The editing programme "Klip"	189
--	-----

Appendix E: Bundle adjustment

E.1 Free bundle adjustment of the GPS points.....	193
E.2 Fixed bundle adjustment of the GPS points	196
E.3 The co-ordinate list for the ground control points	199
E.4 Aerotriangulation for images in scale 1:25,000	201
E.4.1 The 'ltera.dat' file from the aerotriangulation for images in 1:25,000	203
E.5 Aerotriangulation for images in scale 1:15,000	204
E.5.1 The 'ltera.dat' file from the aerotriangulation for the images in scale 1:15,000	207
E.6 Aerotriangulation for images in scale 1:5,000	209
E.6.1 The 'ltera.dat' file from the aerotriangulation for the images in scale 1:5,000	217

Appendix F: Graphic online/offline

F.1 Graphic online/offline	227
----------------------------------	-----



Appendix G: Sizes of grid files

G.1 Sizes of grid files	233
-------------------------------	-----

Appendix H: Code specification

H.1 Code specification	237
------------------------------	-----

Appendix I: Analysis calculations

I.1 Analysis calculations	247
---------------------------------	-----

Appendix J: Code specification and error arrows

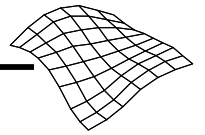
J.1 Code specification and error arrows	299
---	-----

Appendix K: Orthophoto and error arrows

K.1 Orthophoto and error arrows	311
---------------------------------------	-----

Appendix L: STND used as threshold

L.1 STND used as threshold	327
----------------------------------	-----



1 Introduction

The subject of this project is the generation of digital elevation data for the use in map production, among other things. The project originated at Aalborg University, and continued in co-operation with the Danish National Survey and Cadastre. The basis of the project is the automatic correlation models used in the programme package Match-T, as this was accessible at Aalborg University. Furthermore, other quite general methods and problems of generating elevation data are discussed. As the project was done in co-operation with the National Survey and Cadastre, Danish traditions for surveying and mapping are inherent in this investigation.

1.2 The motivation for the project

The use of geo-spatial data has increased dramatically during the last generation. In almost all areas of our society today, geo-spatial data plays a major role. This is valid on a global as well as on a local level. Monitoring pollution and changes of climate are examples of applications where worldwide geo-spatial data is required. At the local level, there is an increased demand for accurate and up-to-date information. Geo-spatial data used in a Geographic Information Systems (GIS) allows for greater possibilities in analysing, planning and decision making.

The technological development of computers with increased computing capacity and speed, in addition to a series of new computer applications, has made it easier to handle and process large amounts of geo-spatial data quicker. This has made geo-spatial analysis more accessible for a broader audience. The increased use is primarily driven by the accelerated development within the digital and technological world, offering new possibilities as regards the use of geo-spatial data on the web, wap, in car navigation systems, cell phones, digital mini calendars etc.

The increased use of geo-spatial data sets new standards for its use, as the end users expect better (more accurate, denser etc.) and more reliable (up to date) data. Geo-spatial data is 3D data. In this project, the emphasis is only on the z-value or, in other words, elevation data.

1.3 Digital Elevation Models

In today's Denmark, digital elevation models play an important role in research, in public administration as well as in private business for a variety of purposes. These include traditional map production (as contour lines), rectification of aerial and satellite photos (true orthophotos), flood analysis, flow simulations, construction planning (new roads, buildings), volume estimates of soil, trace optimisation, 3D animation, 3D graphics, prognosis estimates, accuracy demands, updating demands, data quantity etc. etc. [Larsen, 1996; KMS, 2005].

1.3.1 Terrain model or surface model

When dealing with elevation models, there is a distinction between two types of models: terrain models and surface models.

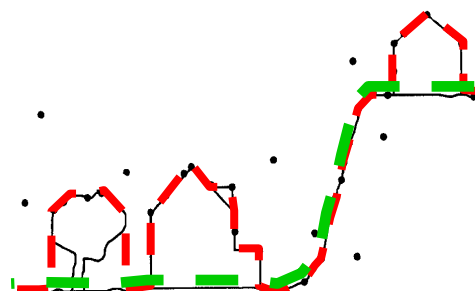


Figure 1.1: The principles of a terrain model (green line) and surface model (red line).

A terrain model reproduces the ground surface without objects such as houses and trees, as illustrated in figure 1.1 with the green line. Terrain models are, among other things, used as grid models for orthophoto rectification, flood analysis, and volume estimation of soil.

A surface model, on the other hand, also describes the elevation of objects, such as houses, trees etc. That is to say, a surface model includes terrain as well as objects. In figure 1.1., the surface model is indicated with the red line. Surface models are used for 3D animation, trace optimisation and true orthophoto rectification, among other applications.

1.4 Standards for Elevation models

Users have required new standards for elevation data based on their uses and applications. These new demands fall into the following three categories:

- Accuracy
- Density
- Currentness

1.4.1 Accuracy

Different users of elevation models have different demands for how accurate the elevation model has to be. Users in the building construction industry and environmental authorities demand an accuracy on the centimetre level.

Users such as 3D animators or 3D graphicers do not require an accuracy on the centimetre level, but can still use an elevation model with a high accuracy.

1.4.2 Density

Accuracy on its own is actually not good enough if the mesh size is too large. What good will it be if, at one point on the mesh, the accuracy is within 10 centimetres and the next point, which is maybe 50 metres away, also has an accuracy within 10 centimetres, but there is no description of the terrain between the mesh points. A grid with a small mesh size represents the terrain better than a grid with a large mesh size. An elevation model described with high accuracy also needs to contain a small mesh size.

1.4.3 Currentness

Elevation models and geo-spatial data in general are only snapshots or a status of the landscape or area they represent. As the landscape changes over time, the elevation model describing the area becomes outdated, corresponding to the degree of change. This yields unreliable data in the elevation model.

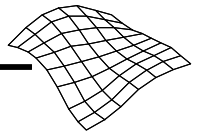
As times goes by, the elevation model slowly degenerates and becomes more and more unreliable, and in analyses where time is a crucial parameter, outdated information will have an effect on the accuracy and reliability of the results obtained from the analysis.

1.5 Danish digital elevation models

In Denmark there are two national digital elevation models in existence; an old one within the framework of the National Survey and Cadastre (25 x 25 m) (KMS DTM), and one within the framework of the firm COWI A/S (2 x 2 m) Danish Digital Height model (DDH). A new, national elevation model within the framework of the National Survey and Cadastre is in production and will be available in the very near future.

1.5.1 KMS DTM

In connection with the production of the national vector atlas TOP10DK in the beginning of the 1990s, the National Survey and Cadastre wanted to add an elevation model. It was decided to produce a new digital elevation model on the basis of the 2.5m contours from the topographic maps in scale 1:25,000 which were scanned and vectored. To achieve an even greater accuracy, the 2.5m contours have been combined with elevation data from different themes from TOP10DK. Examination of the 2.5m contours shows that the accuracy lies in the interval from 1m to 1.5m with a few gross errors up to 2.3 m, in spite of the



expectation that the inclusion of the TOP10DK themes would eliminate gross errors with unknown location [Larsen, 1998].

1.5.2 DDH – Danish Digital Height model

Another national elevation model is established by the firm COWI A/S (www.cowi.dk) by Light Detection And Ranging (LIDAR), and forms part of the so-called DDH, or Denmark's Digital Height model. The elevation model has mesh points of 2 x 2m. This model has not been accessible for this project, and is therefore not dealt with any further.

1.5.3 Near Future

A third national elevation model will come into existence in the very near future. The National Survey and Cadastre has formed a public consortium with the purpose of establishing a national laser scanned elevation model by the beginning of 2009.

The primary characteristics of the future model are, a mesh size of 1.6 x 1.6m and a spatial accuracy on a average of 20cm, but for well defined objects better than 15cm, in all three dimensions.

The establishment of this new elevation model cannot be expected to be retaken within, at least, 20-30 years after being launched. However, there is no doubt that it will degenerate. The question is, how it can be kept updated by using low cost methods?

1.6 How to capture terrain data

The search is for a method to capture terrain data for updating purposes, based on automatic techniques that keep manual work to a minimum. Today, three methods are mainly used for (automatic) capture of large amount of elevation data:

- IFSAR (InterFerometric Synthetic Aperture Radar also called interferometric SAR)
- LIDAR (Light Detection And Ranging also called laser scanning)
- Automatic correlation within digital photogrammetry

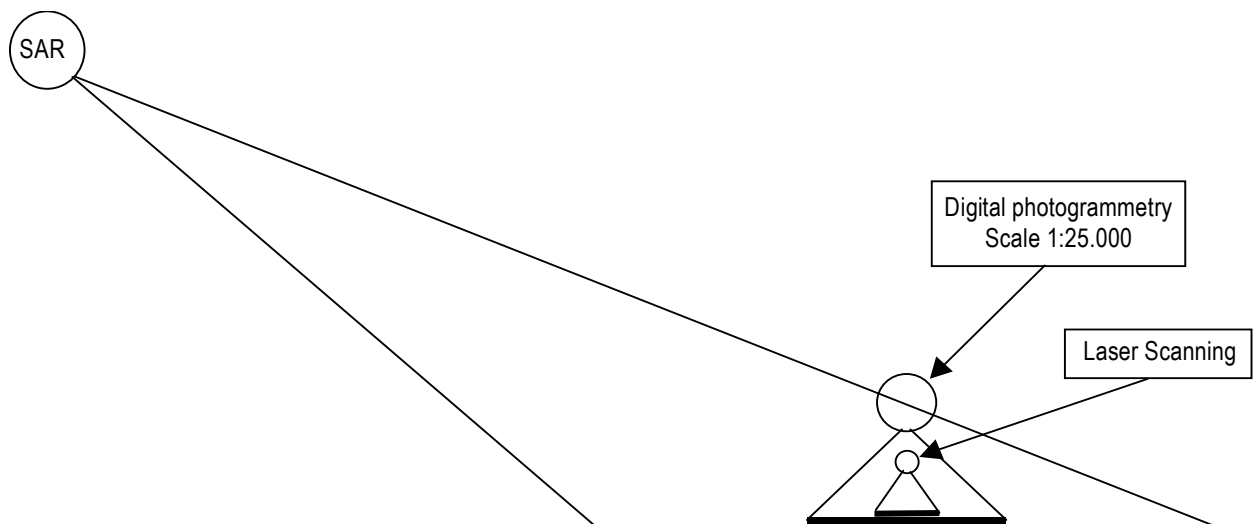


Figure 1.3: Area covered by the three methods of surveying.

As all three methods will be dealt with in detail in chapter 2, they are, therefore, only briefly presented here.

1.6.1 IFSAR - InterFerometric Synthetic Aperture Radar

New SAR methods from overflights, IFSAR - InterFerometric Synthetic Aperture Radar, arrived on the market ten years ago.

In Denmark, this method is still on a trial basis, but it has been used in other countries for elevation data capture. The firm INTERMAP in Canada, for example, has collected elevation data over large parts of North and Central America and some areas in Europe and Asia. Further information can be found at www.intermaptechnologies.com. At www.GLOBALterrain.com an overview of areas covered by INTERMAP elevation data may be found.

A few characteristics of IFSAR should be mentioned here.

Pros:

- IFSAR is an active system and can therefore be used 24 hours per day
- IFSAR covers large areas, compared to other automatic methods for collecting elevation data.

Cons:

- IFSAR suffers from, the so called, shadow effect problems
- IFSAR has a low accuracy compared to other methods

1.6.2 LIDAR – Light Detection And Ranging

Since the beginning of the 1990s, it has also been possible to determine elevations by means of laser scanning, today called LIDAR (Light Detection and Ranging).

A few characteristics of LIDAR should also be mentioned here.

Pros:

- LIDAR is also an active system, like IFSAR, and can, in principal, be used 24 hours per day
- LIDAR has a high accuracy compared to other methods

Cons:

- LIDAR covers a small area and is therefore quite an expensive method if large areas need to be measured.
- LIDAR suffers from the shadow effect, but not to such a degree as does IFSAR.

1.6.3 Automatic correlation within digital photogrammetry

Since the end of the 1980s, possibilities for automatic determination of elevation data, from digital images with digital photogrammetry, have appeared. The method is based on cross correlation in overlapping images, and the method is used today to a greater extent by photogrammetric firms. Various correlation methods are dealt with in Appendix A.

Characteristics of automatic correlation-

Pros:

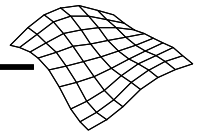
- There is no extra expense because the digital images used for updating the geographical data can also be used for automatic generation of elevations.

Cons:

- The desired accuracy can only be achieved by using high scale images.

1.7 Focus of the thesis

As this search for a method for collecting elevation data where the use of manual work is kept to a minimum, only IFSAR, LIDAR and digital photogrammetry will be dealt with. The manual methods are, therefore, not included in this project. IFSAR and LIDAR will only be briefly described, as they are automatic but demand a flight of their own and are, therefore, expensive.



Today, the Danish national geo-spatial databases have an update cycle of 5 to 10 years. In the future, the update cycle will be 3 to 5 years. The updating process for geographical data will be done using digital images. Aerial images will, therefore, be taken over the whole of Denmark within a cycle of 3 to 5 years. Because the images already exist, it is natural that the next step is to focus on the evaluation of elevation models generated by automatic correlation.

When the method of automatic generation of elevation is chosen, questions of which image scale, image resolution and mesh size would be most beneficial must be asked. Their parameters have to be valued, together with the landscape type which the images cover.

The goal of this thesis is to analyse and value the accuracy that can be achieved by automatic generation in consideration of scale and/or resolution of the digital images, the mesh size in which the grid is determined and to analyse the influence of the landscape types which the images cover.

1.8 Project delimitation

This project will only deal with elevation data for a terrain model. The aim is to find a suitable method for capturing elevation data that satisfies the needs of its users, and to examine the problems and accuracies in different types of landscape. This method must be automatic, require a minimum of manual editing and provide a level of accuracy that meets or nearly meets the precedents set by LIDAR techniques. The landscape type town will not form part of the project, as elevation data of the major part of the town areas are already in existence.

None of the existing Danish terrain models will be used directly in the project. The data analysis uses original data that carries neither preconceived qualifications of its accuracy nor adjustments or improvements.

1.9 Choice of method

The existing methods for automatic determination of elevation data are IFSAR, LIDAR from flights and automatic correlation in digital photogrammetry, where elevation data is generated from digital images.

The principles of IFSAR and LIDAR will only be described briefly in the project. The main focus is laid on the methods used in digital photogrammetry for automatic generation of elevations from digital images. Two applications in particular are used in Denmark: Socet Set (Leica/Helava) and Match-T (Inpho GmbH, Stuttgart). Match-T is sold as an independent application or as a module in the Intergraph package, and as a module in the Zeiss Phodis package. These two programme packages, Socet Set and Match-T, will be described, and the main emphasis will be on Match-T. This choice is due to the fact that Match-T, as a stand alone programme, was available at Aalborg University when the project started. All later studies and analyses in this project are done on the basis of the Match-T programme. IFSAR and the LIDAR are included in the project as possible supplementary methods.

1.10 The structure of the project

Chapter 1: Introduction

The motivation and delimitation of the project is described.

Chapter 2: Methods of determining elevation data

The theory behind different automatic methods for collection of elevation data, including IFSAR, LIDAR and automatic generation of elevation from digital aerial photos, is discussed. As regards the first two methods, only the principles, pros and cons and accuracy are discussed, while the main emphasis is laid on digital photogrammetry. In this section, Socet Set and Match-T are described, Match-T in detail.

The problem of updating data which deals with merging historic, present and future data, as a method for the proposal of combining/integrating new z-measurements, will also be briefly described here.

Chapter 3: Experiences with Match-T and the investigation strategy

A source study of other people's investigations and experiences with Match-T is described. Investigations with Match-T have shown that different parameters can influence the result of automatic generation of elevations from digital images, for instance, the scale of the images, their resolution, the mesh size and the landscape type. On the background of this source study, the investigation strategy of the project is established.

Chapter 4: The data material

A test area is chosen south of Aalborg University. The area is chosen because of its varied terrain and its location close to the university. The area includes open, flat and hilly fields, woods, a residential neighbourhood (suburb), and gravel pits with steep slopes. This small test area represents a broad segment of the kind of landscape types found in Denmark. At the start of this thesis digital cameras did not exist, therefore the area was photographed in three scales, and the images have been scanned in three different resolutions. Further, a description is given of the establishment of the frame of reference for the quality control of the individual tests. The frame of reference consists of elevations that are measured with superior accuracy. Appendix B includes a detailed description of the establishment of the frame of reference, Chapter 4 is a brief summary of this.

Chapter 5: Preparation for grid generation

As preparation for the elevation determination, Match-T is configured. The parameters used are discussed.

Chapter 6: Pre-analysis of the generated grids

Match-T's own modules for the indication of problems with the individual grid points in the automatically generated grids are investigated. Also, a superior evaluation of the completeness of the automatically generated grids is carried out.

Chapter 7: The investigation

The evaluation and analysis of the results from the individual calculations have been done step by step. The first step is a simple determination of the elevation difference between the calculated results and the frame of reference. Another comparison is done after elimination of gross errors. It has been investigated whether the scale, resolution, mesh size and landscape type of the images have had any influence. Possible gross errors have been localised and analysed.

Chapter 8: Results on the basis of Chapter 7

The experiences gained in Chapter 7 are summarised and finalised. Then an elevation model of the test area is generated, where the experiences with the method and the influence of the Danish landscape on the results are discussed, and the accuracy is evaluated. The possibility of eliminating possible gross errors by combining data obtained by the different resolutions has been attempted.

Chapter 9: Theory and practice

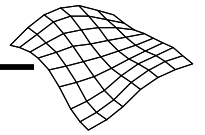
After the analysis of the results, these have been held up to the theory and experience of others. How do theory and practice compare? Where and why are results obtained that do not correspond to the theory? On the basis of the investigations carried out, possible improvements are discussed, and a method for automatic data collection in Denmark is recommended.

Chapter 10: Conclusion and perspectives

The suitability of the automatic correlation method is evaluated in relation to the determination of a nationwide terrain model of Denmark. Furthermore, potential future studies based on the project are discussed.

This thesis also includes an appendix in four parts, A, B, C and D:

- A Correlation techniques
- B The data material



- C Description of the PIL programme
- D Description of the Klip programme

Appendix A: Correlation techniques

In this appendix, the most frequently used correlation techniques in digital photogrammetry are described, both techniques which are directly relevant for understanding the theory used in the project (Match-T), and techniques which are included to give a better background knowledge and understanding of correlation techniques in general.

Appendix B: The data material

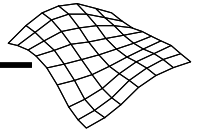
This appendix includes a description of the material used in the project, that is, the test area with typically Danish landscape types, aerial photos from three different altitudes, scanned in three resolutions, control points and the basis for comparison. The appendix is divided into two parts, the first consisting of the description of the material, the second of the description of the process of capturing control points and the basis of comparison, consisting of analytically measured points in a 25 x 25m grid (the frame of reference).

Appendix C: Description of the PIL programme

With a view to the examination and evaluation of automatically generated elevations in relation to a frame of reference, an analytical tool is needed. It has been estimated that there is no commercial programme which fulfils the demands for an analytical tool. Therefore, a programme has been developed specifically for this purpose, called the PIL programme (PIL translated from Danish is "arrow" in English). This programme is described in Appendix C.

Appendix D: The Klip programme

A description of a small programme, called "Klip", used for the cut-out of unwanted rows and columns in the automatically generated grids (Klip translated from Danish is "clip" in English).



2 Methods of determining elevation data

As mentioned earlier, several different methods are used today for the automatic determination of elevation data, among others, IFSAR, laser scanning and digital photogrammetry. In this chapter, the methods are described with the main stress on digital photogrammetry, and Match-T in particular. Each description includes the principles, accuracy, pros and cons, and scope of the individual methods.

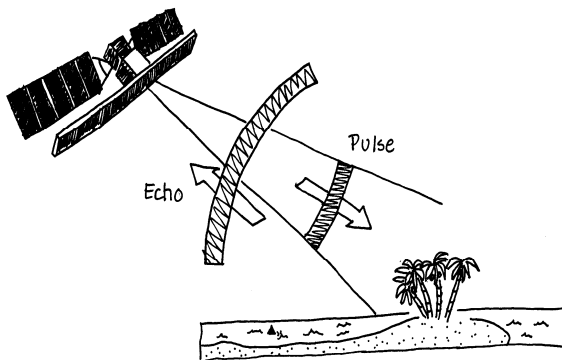


Figure 2.1: The SAR principle shown from a satellite (drawn by B.P. Olsen).



Figure 2.2: Aeroplane with SAR-antenna.

2.1 SAR

In practice, the concept of SAR images is used as a collective concept without distinguishing specifically between the different radar techniques. Radar technology is an active system with an antenna which sends as well as receives an electromagnetic impulse from a high altitude, originally from a satellite, but today also from an aeroplane. Originally, radar technology was called RAR (Real Aperture Radar) and is defined as:

$$L = \frac{\lambda}{D} \cdot R \quad (2.1)$$

where:

- L = The band width
- λ = The wavelength
- D = The length of the antenna
- R = The distance between the band width and the antenna, here the flight altitude

For the RAR method's coverage, the length of the antenna is important, the distance between antenna and band width (determined by flying altitude and the angle of the Impulse) and the frequency of the impulse.

The band width is synonymous with the resolution of the radar images (pixel size) which should be as small as possible. This means that the relationship between wavelength λ and the length of the antenna D (λ/D) should be as small as possible, that is, either the wavelength λ is decreased, or the antenna length D is increased, see formula 2.1. A much used wavelength area is the C band which has a wavelength of approx. 5.7cm. Often a pixel size of maximum 2m is wanted, i.e., that a typical antenna of 10m entails a surveying distance R (the flying altitude) of only ~ 350m. Vice versa, the surveying from a satellite at 800 km altitude will entail a pixel size of ~ 4.5 km!

The example mentioned shows the drawback of RAR. This drawback has formed the basis for the development of SAR. SAR stands for Synthetic Aperture Radar, i.e., that by means of mathematical algorithms an artificially (synthetic) long antenna is created. By adhering to the flying altitude, for instance of a satellite, the pixel size is determined by the λ/D term alone, which has led to the development of mathematical algorithms to decrease this term. The algorithms are based on the Doppler effect, whereby an artificially long antenna L can be calculated.

The background is that every object is included in more than one of the radar measurements and, thereby, registered several times from different positions on the flight path. With the signal which is returned the first time to the radar, an object in the range of vision of the radar beams will have a positive Doppler change which will gradually be decreased to zero, when the plane is at right angles to the object (P). Subsequently, the Doppler change will gradually become more and more negative, see figure 2.3.

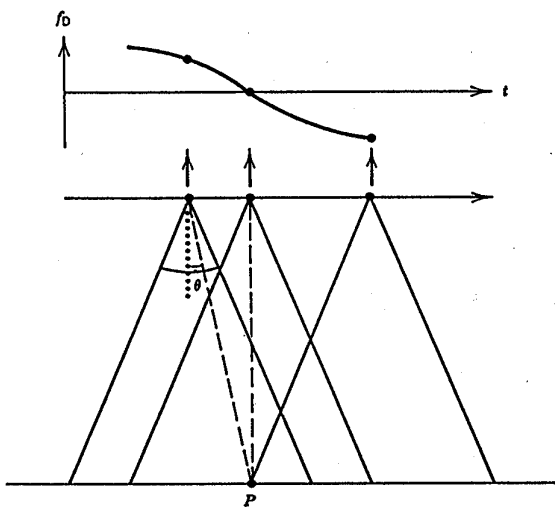


Figure 2.3: Doppler sequence for over flying a point and the impact of the effect on the frequency in different positions [Elachi, 1987].

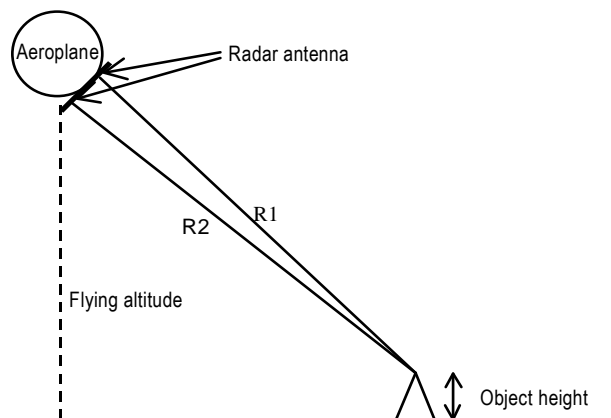


Figure 2.4: The SLAR principle shown from an aeroplane.

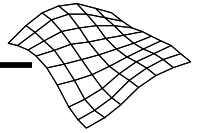
If an antenna is mounted on a plane, it will generally be on the side of the plane, and therefore the radar impulse is sent from the side. This increases the area of coverage. This method is the one used most often in practice., it is called SLAR (Side Looking Aperture Radar), and by far the major part of so-called SAR images are in reality SLAR images and will throughout the project be referred to as SAR, see figure 2.4.

Several factors have an impact on the reflected signal, both in relation to the radar system, and to influences from the surface and the surroundings. In the radar system, the factors are the wavelength used, the angle from which the signal is sent and the polarisation. A surface will reflect the radar signal differently, depending on the structure of the ground surface. The sensitivity of the radar to these influences depends, among other things, on the wavelength and the polarisation. The last circumstance is used in polarimetric SAR which is used for area analysis, among other things, but not for elevation determination, which is why it is not described any further in this project.

2.1.1 Interferometric SAR - IFSAR

The technique of IFSAR consists of registering two data sets over the same area. This can be done by having two antennas mounted on the plane and staggered in relation to each other, so that the distance from the antennas to the object are a little different, see figure 2.4.

The result of IFSAR is an image, called an interferogram. The pixel values in an interferogram are indicated as a fraction of the wavelength, by which the return signal has been staggered. When the position of the satellite/plane, the distance between the antennas, the angle of emission from the two antennas, and the fraction of the wavelength are known, it is possible to determine the elevation of the object on the ground. This form of interferometry is called XTI, "Across-Track Interferometry", see figure 2.4. Alternatively, the two photos can be taken with the same antenna if the plane or the satellite pass the same area twice on staggered flight paths. This form is called RTI "Repeat-Track Interferometry".



The IFSAR system can also be space-borne. An example of that is the IFSAR system onboard the Shuttle Radar Topography Mission flown in Feb. 2000. IFSAR system can also be airborne.

2.1.2 The accuracy of the IFSAR method

Normally, a better elevation determination is obtained by the RTI method than by the XTI method but, on the other hand, the data processing and calibration of the RTI method is more difficult and it demands more manual treatment.

The IFSAR system onboard the Shuttle Radar Topography Mission has been flown in Feb. 2000. From the collected interferometric radar data, a near global digital elevation model covering the Earth's surface in between -56° and $+60^{\circ}$, (which covers 80% of the Earth's landmass) has been made [Kobrick, 2006]. According to [Werner, 2001] the global digital elevation model has an absolute elevation accuracy of $\pm 16\text{m}$. A cover, with a range between -56° and $+60^{\circ}$ means that there will be interferometric radar data over Denmark. It is not known to the author, whether there has been any investigation of the data from the Shuttle Radar Topography Mission over Denmark. The goal for the Shuttle Radar Topography Mission was to process a near as possible global digital elevation model of the planet earth. With this in mind an accuracy of $\pm 16\text{m}$ is good but, from a Danish point of view, we are looking for a method, which gives a better accuracy. In this thesis, the focus will therefore be on air-borne rather than space-borne IFSAR images.

With the RTI method from an aeroplane, an accuracy of $0.2\text{m} - 0.3\text{m}$ horizontally can be obtained, while with the XTI method from an aeroplane, an accuracy of only $5\text{m} - 10\text{m}$ horizontally can be reached. It has been indicated that the vertical accuracy of the XTI method is better than 1m [Skriver et al., 1999]. An investigation from Baden Württemberg shows the elevation differences range between -3.3m and 1.5m and with a standard deviation of $\pm 1\text{m} - \pm 1.3\text{m}$. [Kleusberg et al., 1999]. Clearly, these examples show, that both the RTI and XTI methods are not accurate enough.

Pros and cons of IFSAR:

Among the pros are:

- IFSAR is independent of sunlight, and can therefore also be used during the hours of darkness.
- IFSAR is independent of weather conditions in the atmosphere and on the ground. However, this is not the case if the SAR images are taken after the RTI principle, as the images from one day will not be comparable to the images taken 24 hours later if, for instance, it has been raining.
- Radar wavelengths are longer than visible and infrared light, and if the structure of the ground surface is larger than the wavelength (i.e. approx. 10cm), structure can also be measured.
- Data is born digital, that is, digital mapping can be done on primary data.
- Covers a large area quickly and cheaply.

Among the cons are:

- Poor resolution compared to other methods of elevation determination
- Small scale
- Image disturbances

- Shadow effects in areas with significant variations, see figure 2.5

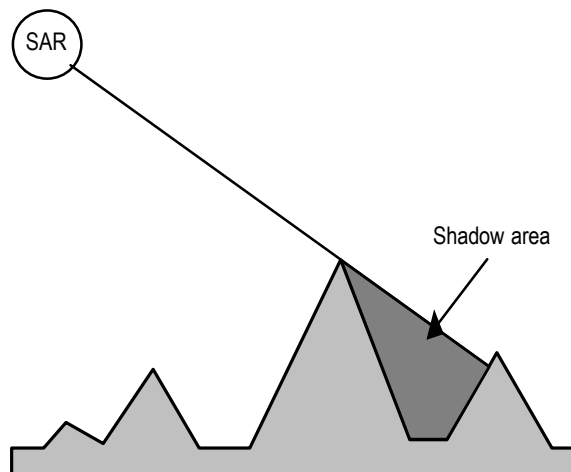


Figure 2.5: Example of the shadow problem.

2.1.3 The scope of the SAR method

The primary strength of the SAR method is that it covers large areas of land quickly. In Denmark, IFSAR from an aeroplane, is still on a trial basis, but it has been used in other countries for elevation data collection, the firm INTERMAP, for example, has collected elevation data over large parts of North and Central America, also some places in Europe and Asia. As mentioned earlier, further information can be found on the internet address www.intermaptechnologies.com. On the internet address www.GLOBALterrain.com, an overview of areas covered by INTERMAP elevation data may be found.

2.2 LIDAR

LIDAR is done from planes at an altitude of approx. 1 km, in special cases, though, from a helicopter at, for instance, an altitude of 350m. The laser system is, like radar, an active system which emits an electromagnetic signal which is reflected from the ground surface. See figure 2.6.

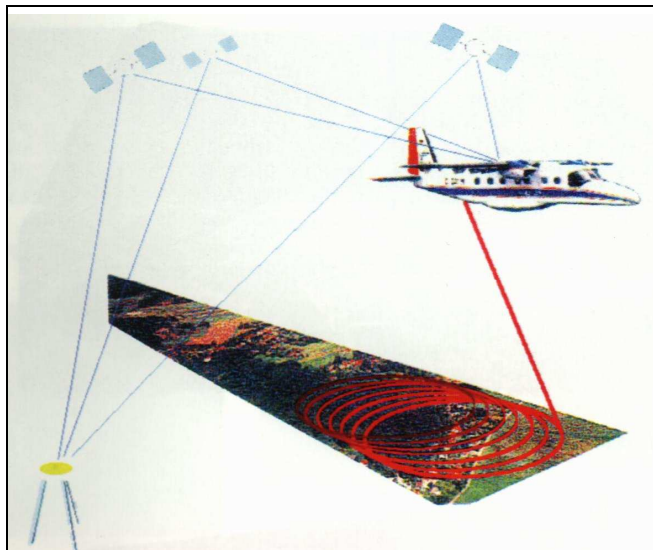


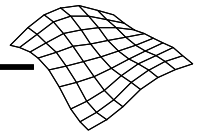
Figure 2.6: An example of laser scanning [Wehr et al., 1999].

2.2.1 The principles of LIDAR

With LIDAR, the distance is determined on the basis of the time difference between the emission of the signal and its reception:

$$R = \frac{1}{2} \cdot c \cdot t \quad (2.2)$$

where: R = the difference between plane and ground surface



c = the speed of light

t = the time difference between the emission of the signal and its reception

$^{1/2}$ = as the time is determined twice over, when the signal moves down and up again

In order to convert this distance to a level, the position and orientation of the plane must be determined at the same time. This is done by means of GPS (Global Positioning System) and INS (Inertial Navigation System). Thus, there are three systems which must be co-ordinated to determine elevation data.

The laser signal can be emitted in different "figures" according to the type of scanner. The most important are oscillating mirror, Palmer scan, rotating mirror and fibre scanner, see figure 2.7.

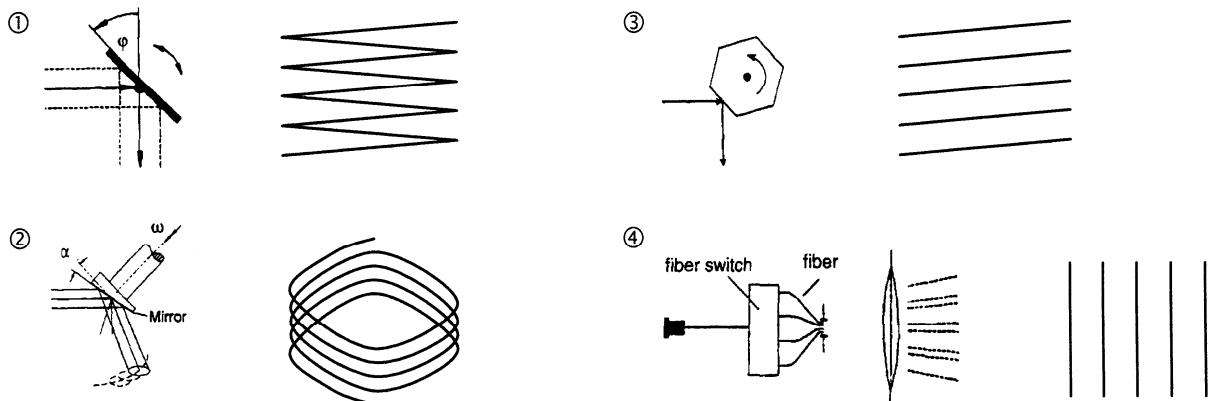


Figure 2.7: Examples of different surveying methods for laser scanning [Rasmussen et al., 2000].

- 1) With the oscillating mirror, a mirror tilts from side to side, thereby creating a zigzag formed grid, created by the plane's forward motion.
- 2) With Palmer scan, a mirror is fastened to an axis with a slight inclination compared to normal. When the axis is rotated, the laser will create an elliptical display, but with the propulsion of the plane, the grid will be displayed as a spiral.
- 3) With a rotating mirror, a mirror polygon rotates, whereby a regular grid is obtained. This method is also called rotating polygon.
- 4) The fibre scanner is built to a slightly different concept than the aforementioned systems. While systems 1 - 3 send the laser beam in a specific direction by means of a mirror, in this case an established optical fibre bundle is used which creates a fan over the landscape. By means of a "Fibre switch" the laser light is sent by turns to the different optical fibres. As the case in point is a static optical fibre bundle, the grid on the ground will be regular. [Rasmussen et al., 2000 and Wehr et al., 1999 b].

The size of the area (the breadth of the strip) which is covered by LIDAR depends on the angle of the laser beam and the flight altitude. To scan broadly is a great advantage as regards the economy of the survey. However, it is not an immediate advantage as, by increased scanning angle, problems of accuracy will occur. By increasing the scanning angle, the angle of impact on the points to be measured will be lower, the longer from the centre line the measuring is done, so, the accuracy of the horizontal determination will be somewhat poorer as regards the outermost measured points. The choice of scanning angle is, therefore, a balance between price and precision. In general, the systems can scan up to a breadth of 1.12 times the flight altitude [Rasmussen et al., 2000].

The strength of the reflected signal depends on the strength of the emitted signal, but also on the type of surface the signal reaches, as a light surface will reflect more than a dark one. Tests have shown that naked earth/sand reflects 10% - 20 %, vegetation 30% - 50% and snow and ice 80% [Wever, 1999, Wever et al., 1999].

2.2.2 The accuracy of LIDAR

The greatest contribution to errors in connection with LIDAR stems from the determination of the plane's position at the time of shooting. Particularly over broken terrain, this may result in gross errors, where a staggering of the x, y-position may result in gross elevation errors. The accuracy of levels determined by means of LIDAR lies between 0.1m and 0.6m with typical values of 0.15m – 0.20m. The deviations on the planimetric co-ordinates is given as lying in the interval between 0.5m and 2m [Rasmussen et al., 2000]. The survey done in Denmark over 73 urban areas have 1m grids with a level accuracy of 0.15m [telephone conversation with P. Nørgaard, COWI A/S, 2004].

2.2.3 Pros and cons of LIDAR

Among the pros are:

- LIDAR is an active system which can be used without regard to sun and light conditions. LIDAR can be performed in all seasons and at any time during day or night [Wever et la., 1999].
- LIDAR is not dependent on the texture of the ground surface, which makes the method suitable for use in wet areas, over ice and snow, along tracks etc. [Wever, 1999].
- LIDAR produces points with a high degree of density.
- A very good degree of level accuracy can be obtained with LIDAR.

Among the cons are:

- Weather conditions in the form of rain, low clouds, fog or ground mist, do not allow the use of LIDAR [Wever et la., 1999]. This is due to the fact that the laser wave cannot be reflected by water, where the signal will be "eaten" [telephone conversation with P. Nørgaard, COWI A/S, 2002].
- LIDAR demands moderate wind conditions, that is, under 10 m/s [telephone conversation with P. Nørgaard, COWI A/S 2002]. The wind conditions have no influence on the LIDAR itself, but on flight navigation, and thereby on the final accuracy of the level determination.
- LIDAR has a shadow problem behind tall objects, but the problem is not very big, as the scanning angle does not deviate much from the vertical axis of the plane.

2.2.4 The scope of the LIDAR method

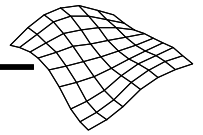
LIDAR is recognised as an accurate and efficient data source for digital surface model generation in urban areas including buildings. Highly accurate models of the surface of urban areas are becoming widely used in applications such as digital orthophoto production, three-dimensional city modelling, and three-dimensional building reconstruction [Stoker et la. 2006].

The LIDAR method has already been used in several countries to create/update a digital terrain model and in special areas where other methods for elevation extractions are not sufficient [Wever et la., 1999]. In the Netherlands, for instance, a nationwide national DTM has been created by means of LIDAR [Vosselman, 2000]. In Denmark a new national elevation model based on the LIDAR method will be completed in the beginning of 2009.

Helicopters are used for low flights and special tasks such as, for instance, determining the elevation of pylons [Lohr et al., 1999].

Other examples for the use of LIDAR are monitoring of coastal erosion, simulation of different areas in order to determine engineering works and simulation of antenna sites or line-of-sight calculations for mobile communication networks [Lohr, 1999].

The signal sent from a laser scanner is reflected by buildings, trees, cars, electric wires and many other objects from either the top, the middle or the bottom [Vosselman, 2000]. When LIDAR is used over woods, it will often result in double reflection, or several reflections from treetops, bushes in the undergrowth and the ground surface respectively [Petzold et al., 2000]. As regards scanning of areas with deciduous trees, there are great differences between summer and winter. The reflection from the forest floor



in summer constitutes 25% - 40% of the total reflection, while the figure in winter is 70% [Ackermann, 1999].

In several tests, LIDAR has been used over built-up areas. As regards establishing a 3D town model, a surface model is needed including, among other things, trees and houses with a point density of approx. one point per 1 m² [Brenner et al., 1999]. According to [MacIntosh et al., 2000] LIDAR is used more and more for determination of a 3D town model.

[Hyypä et al., 2000] describe how the LIDAR method offers good opportunities for estimating tree elevations quickly, and thereby determining tree volume and the biomass of the wood over extensive forest areas. In Finland, an investigation has shown that around 30% of the first signal is reflected directly from the ground surface. By increasing the number of impulses, it is possible to determine every individual tree, and, furthermore, the gap between the trees.

In Denmark, including Greenland, it is interesting to note what accuracy the LIDAR method can offer by determination of elevations over glaciers/ice/snow. Different investigations have shown that it is possible to obtain an elevation accuracy of 0.1m – 0.2m over the Greenland ice cap. The same investigation shows a similar accuracy of 0.1m – 0.2m over a Norwegian glacier [Favey et al., 2000].

2.3 Photogrammetric determination

During the past 10 - 15 years, digital photogrammetry has gained ground in Denmark, and today forms an integral part of the work routines of the photogrammetric firms. Within digital photogrammetry there are several commercial programme packages on offer. In Denmark, the most widespread programmes for automatic generation of elevations are Socet Set and Match-T. Socet Set is a part of the Helava/Leica package. Match-T is an independent programme package which is also sold as a programme module in the Intergraph package and the Zeiss Phodis package respectively under the names TopoSURF or Phodis TS. These two programmes have been chosen for a closer description. Match-T has, furthermore, been chosen to be part of the investigation proper in this project. Match-T is therefore described in detail, while Socet Set is described on a more superficial level.

Common to all the photogrammetric methods are the digital images. These may come from different sources, such as radar images, aerial photos, terrestrial images etc. Some are born digital, whilst others must undergo scanning, before they can be used.

The following specific sections about Socet Set and Match-T respectively are set out to present the methods and principles of the two programme packages, and their anticipated accuracy, pros and cons etc. These descriptions are taken from literature/studies at the beginning of this millennium.

2.3.1 Socet Set

Socet Set has been developed and marketed by Helava/Leica and has found its uses all over the world. At the time of writing, it has not been possible to get details about the correlation principles in use in Socet Set. Contact has been made with the firms and institutions which use Socet Set here in Denmark to obtain information, but they have not been able to furnish sufficient information for a full understanding of the programme. A literary study has also been undertaken to find the mathematics behind the programme, but without success. Helava/Leica Systems have been contacted to get information about specific correlation methods and DTM generation used in Socet Set, again without success. Therefore, it is not possible to present or discuss details concerning the correlation methods and mathematical algorithms used in Socet Set.

In the following, the module for orientation of the images and the module for automatic generation of elevations is described, together with the different calculation possibilities included in the module.

The first step in the Socet Set programme is the build-up of an image pyramid, then the images are orientated, normalised and correlated, the elevation data is determined, and a DTM is generated.

2.3.1.1 Image pyramid

As mentioned previously the first step is the build-up of an image pyramid. The image pyramid can be built according to the principles described in Appendix 1, section A.1.5. The image pyramid is used,

among other things, at the showing of the images in different resolutions by, for instance, the inner orientation.

2.3.1.2 Orientation

Inner orientation

The determination of the inner orientation of the images may be done analogously or fully automatically. By means of the keyed-in camera information and the location of the fiducial marks, Socet Set can determine the inner orientation automatically. The first fiducial mark must be indicated, but it does not have to be very accurate. The correlation for the inner orientation is done by an ordinary area based matching (ABM), where the programme has a fiducial mark library, where the most frequently used fiducial marks are located as a target (see a closer description of ABM in Appendix A, section A.1.2). In general, an analogous description will not give a better determination than the automatic one.

Relative orientation

To determine the relative orientation, Socet Set needs information about overlap and terrain elevation. This information is given by indicating the centre of the images, the flight altitude and a rough indication of the terrain elevation. By means of this information, the programme calculates how big the overlap with the surrounding images is. With the knowledge of the images' inner orientation, their centre and the flight altitude, Socet Set is well informed about the location of the images in relation to each other. Thereby, Socet Set can determine automatically the connecting points by taking a window segment in one image and correlating this with the other image or images, and thus create the relative orientation [Bacher, 1998].

Absolute orientation

The possibilities of automating the absolute orientation is less than for the inner and relative orientation. This is due to the fact that the control points can vary in form and grey level values. With the absolute orientation it is, therefore, necessary to point out the control points manually in the first image and they are then determined automatically in the remaining images, where the control point may be found [Bacher, 1998].

When the orientation of the images is done, they can be normalised, then the correlation and the DTM generation can go forward.

2.3.2 Normalisation

To limit the following correlation from a two-dimensional problem to a one-dimensional one, the images are normalised, that is, the epipolar lines are determined, cf. Appendix A, section A.1.4. Normalisation of the images is done in Socet Set "on the fly" [Zhang et al., 1997]. The dynamic Y parallax sampling algorithm works after the following principles:

- 1) Division of the image into small blocks
- 2) For each block, a number of reliable residuals are determined, Y parallaxes, by searching in two dimensions.
- 3) Use of the residuals from the 2nd principle to compensate the correlation of all images within each block.

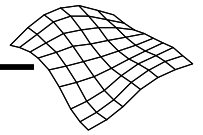
For each area in the image, where a correlation is wanted, the images are normalised, and the correlation is calculated. The result of the normalisation is not kept on the hard disk, but the calculation is done again and again which saves storage capacity.

2.3.3 Correlation and the DTM generation

This part is described superficially, as it has not been possible to obtain information about the mathematical background behind the correlation and the subsequent DTM generation.

In Socet Set the correlation is done according to three different methods:

- The area based matching (ABM)
- Edges used in feature based matching (FBM)



- A combination of the above (the hybrid method)

2.3.4 ABM used in Socet Set

On the basis of the grey level strength of the image, it is possible to correlate conjugating points along conjugating epipolar lines. Such a strategy demands that the points in evidence have the same intensity in each of the images, and that there is a significant intensity variation in both images.

Furthermore, a signal correlation algorithm is used which can choose an approximated window size, dependent on the images' strength of intensity (grey level strength), to reach a precise as well as a stable estimate of a correlation. This method is used to find the correct window size for the correlation [Zhang et al, 1997].

As a method for the ABM the least square matching (LSM) is mentioned [Zhang et al., 1997]. For a more detailed description, see also Appendix A, section A.1.2.3.2.

2.3.5 The edge based method

The edges used in FBM are used to establish correlation between image points by correlating the images' grey level pattern along conjugating epipolar lines. Edges are detected, and the best correlation between these edges intersection with conjugating epipolar lines is sought. Of course, this method will not function well if the image areas have no edges or, if it is difficult to detect the edges precisely, see also Appendix A, section A.1.3.2.

The edges used in FBM have the advantage over the ABM in that it is less influenced by noise in the images.

2.3.6 Combination of the methods

In Socet Set, the two methods are used in combination, so that critical image points are correlated in relation to the representation of the terrain and the frequency of errors is reduced. The combination method uses the intensity value, intensity edges, varying values, varying edges and first and second derived values of the images to find the correct correlation [Zhang et al., 1997].

If a correlation algorithm functions with a high degree of success, it can automatically generate a sufficiently close DEM with very little or no manual editing.

2.3.7 Correlation and DEM generation

The correlation and the DEM generation is done by the so-called Adaptive Automatic Terrain Extradiation (AATE). AATE works on the basis of a "set of rules" consisting of some previously known information. This set of rules is based on three components [Zhang et al., 1997]:

- Rules of thumb and knowledge of the system
- A set of reasonable/logical conclusions
- Applications for interfaces

This information lies in an ASCII-file. The information can be divided into two types:

- Fact rules to define fact values
- Input rules to gather fact values from the user

In AATE, a set of correlation parameters is generated which is a function of terrain types, signal strength, flight altitude and X,Y-parallax.

The concept is based on a set of rules created on the basis of knowledge of how to generate a set of correlation parameters through an intensive theoretical analysis and practical experiments.

2.3.7.1 Accuracy

Tests made over an area in Southern Germany near Stuttgart gave an accuracy of 0.5‰ - 1.2‰ of the flight altitude. A closer investigation of the contribution of the landscape types to errors showed that an accuracy of 0.4‰ – 1.1‰ of the flight altitude could be obtained over all types of landscape, except from the edge of woods, where the accuracy was 1.8‰ of the flight altitude [Bacher, 1998].

Another test done in Norway shows that with the use of the standard setting, an accuracy of 0.6‰ – 1.3‰ of the flight altitude can be obtained without editing [Nilsen, 1998].

2.3.7.2 Pros and cons in the use of Socet Set

As both Socet Set and Match-T are based on photogrammetry, the pros and cons will be the same for the two programmes, and will therefore be described jointly in section 2.4.3.5.

2.3.7.3 The scope of Socet Set

As the scope of the photogrammetric method, and thus for Socet Set is the same as for Match-T, these will be described jointly in section 2.4.3.6.

2.4 Match-T

Like Socet Set, Match-T is a programme package for automatic generation of heights from digital images.

When this project was started the digital images could only be obtained by scanning images. Today images from digital cameras are accessible. DTM generation with digital frame sensors differs little from the use of scanned aerial photographs. The matching strategy has been changed in Match-T 4.0 from a model by model, to a block oriented process [Heuchel, 2005]. Which has had no influence on the results in this project.

The Match-T package is used directly in this investigation and is, therefore, described with a greater degree of detail than the preceding methods.

The process in Match-T can be divided into three parts. First, the images are orientated and various parameters are stated. Then comes the calculation part, which can be divided into calculation of basic facts (pre-processing), the correlation itself, and the DEM generation.

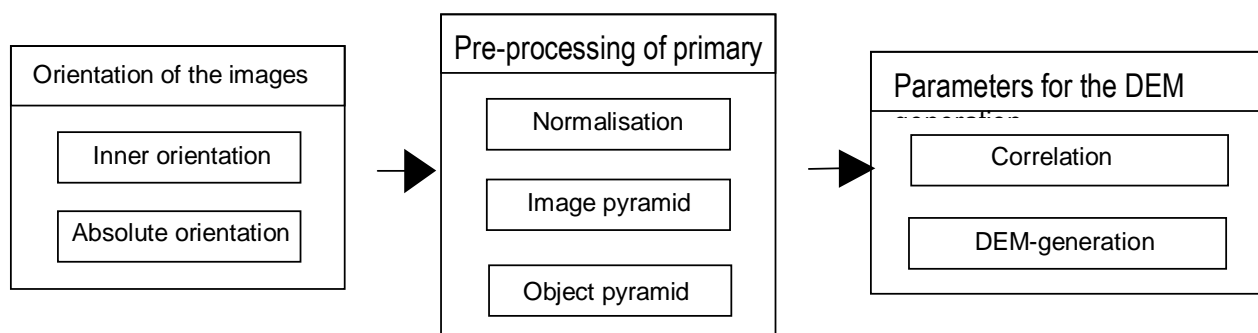
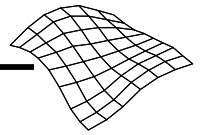


Figure 2.8: The three process parts in a Match-T calculation.

2.4.1 Orientation of Match-T

2.4.1.1 Inner orientation

Today, the inner orientation can be done automatically. The programme must have a target window which can be used for the search. In Match-T, there is a library of target windows for fiducial marks from the most used camera types. If you have used a special camera, where a target window for the used fiducial marks is not yet in existence, it can be supplemented by determining a fiducial mark manually. This fiducial mark will subsequently be used as a target. When using Match-T, two fiducial marks are determined manually, the rest of the fiducial marks are then determined automatically by fitting the target and the search area, in the camera file, on the basis of the given camera data. The orientation is done by fitting in



with the correlation coefficient, see appendix A, section A.1.2.2.1, and then by the principle of least squares, see appendix A, section A.1.2.3.2.

2.4.1.2 Absolute orientation

In the Match-T (version 2.2.0) employed, the relative orientation is not determined, the absolute orientation is started straight away. The possibilities for automating the absolute orientation are much less than for the inner and the relative orientation. This is due to the fact that the location of control points in the image is not necessarily fixed. Furthermore, two types of control points are in use, signalled control points and natural control points. If signalled control points are used, the possibility of doing an absolute orientation is greater. This is because the recognition of the control points is greater, as these are of a fixed size and form. If, on the other hand, natural control points are used, these may vary considerably in form and grey level value. The absolute orientation is, therefore, generally done manually.

When the orientation is determined, the images are ready for the second part of the process, where the pre-processing of primary data will be determined.

2.4.2 The pre-processing of primary data

2.4.2.1 Normalisation

We start out with a quote: *The epipolar line constraint is the strongest constraint in correlation and should be used as soon as available* [Förstner, 1993]. Therefore, the first step in the pre-processing of primary data is the normalisation of the images. This is done to achieve the advantages of the principles of epipolar geometry. The normalisation is done according to the principles described in appendix A, section A.1.4.

2.4.2.2 Image pyramid

The second step is the generation of an image pyramid over the normalised images. The principle of an image pyramid is that temporary values of the terrain heights can be obtained by a process course from coarse to fine resolution/pixel size. In Match-T, the image pyramid is created by use of a binomial filter (the Gaussian function) over, for instance, 5 x 5 pixels (standard Match-T setting). This is called the Gaussian pyramid, see further (Appendix A, section A.2). Between pyramid levels, there is a gap of a factor 4 which for images with a resolution of 15 μm gives an image pyramid of 8 – 9 levels, and for 30 μm images, 7 – 8 levels, ending with an image of minimum 30 x 30 pixels [Inpho a), 1995].

2.4.2.3 Object pyramid

The third step is the build-up of an object pyramid by drawing out objects from each image level in the image pyramid. As the image pyramid is created over normalised images, the withdrawal of objects is done in one dimension, that is, calculation of gradients in the x-direction, see Appendix A, section A.5. The build-up of the object pyramid is done independently for the left and right image, beginning with the topmost level of the image pyramid.

Calculation of gradients is done in the following way [Inpho a), 1995]: The interest point is calculated from the size of a weighted sum of squares on the gradients in the horizontal direction of the chosen window size. The size of the window in which the withdrawal is going on has an impact on the gradients. The bigger the window, the greater the significance of the withdrawn gradients and vice versa.

With a "non maxima suppression", only the most significant objects in the window are included.

- So-called "line spacing" reduces the number of epipolar lines, and subsequently the number of interest points.
- Determination of the direction of the gradient for the centre element in a chosen window determines the sign of the interest point.

An object pyramid is a symbolic description of the image pyramid. The size of an object pyramid corresponds to approx. 80% of the image pyramid. It takes about 20% of the total calculation time to create an object pyramid [Inpho a), 1995].

2.4.3 Parameters for DEM generation

2.4.3.1 Correlation

The starting point of a correlation done in Match-T is a FBM and, as in Socet Set, a combination of ABM and FBM is also used here. Although the algorithms used in Match-T have been in use for more 15 years, there are no alternatives in order to derive DTM's efficiently for large areas [Heuchel, 2005].

The correlation and the DEM generation is done stepwise down through the levels of the pyramid [Inpho a), 1995].

The correlation of the interest points presupposes that the following information is given:

- A temporary indication of the terrain elevation as starting value
- The epipolar geometry
- Delimitation in the row-direction by parallax bound

and the correlation is done on the basis of the following values:

- The existence of a gradient
- The size of the gradient
- The correlation coefficient

The correlation is only done in the x-direction, as the images are normalised. The movement in the x-direction is delimited by the size of the parallax bound. In Match-T, the parallax bound is changed by choice of the landscape type: flat = 3 pixels, hilly = 8 pixels and mountainous = 15 pixels. By choice of, for instance, a mountainous terrain, the fitting in of the correlation can therefore be moved 15 pixels in the x-direction. When the best fit for the correlation is found, taking into consideration the existence of gradients, and the size of these in the two images, a correlation coefficient is calculated, see appendix A, section A.1.2.2.1. The position of the correlation is where the greatest correlation coefficient can be obtained.

By means of the pyramid levels and an approximated starting value for the terrain elevation, a quick and, in principle, independent pre-knowledge of the terrain can be deduced from the preceding pyramid level.

2.4.3.2 The DEM generation

The result of the introductory correlation is a cloud of points on each pyramid level. These clouds of points include gross errors, such as correlation errors, or elevation errors, created by houses, trees, etc. The DEM generation is done stepwise down through the pyramid levels, and the terrain surface is reconstructed by means of the finite element principle. The results for each pyramid level are used as temporary values for the calculation of the next pyramid level, see figure 2.9. The result of a correlation and DEM generation can be seen in figure 2.10.

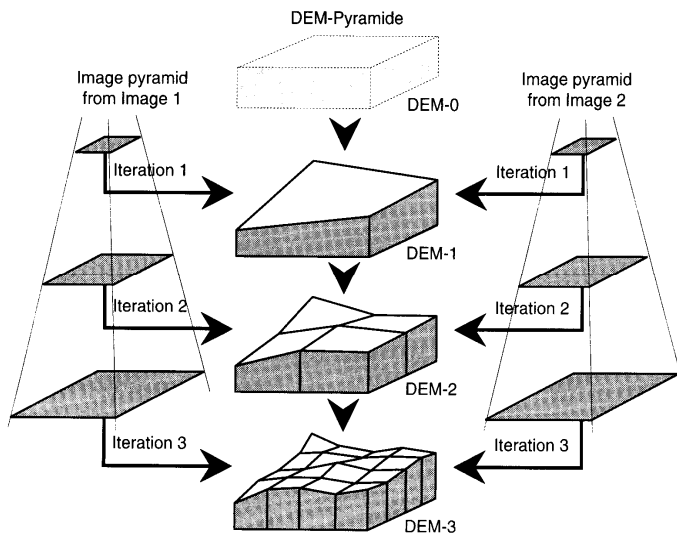
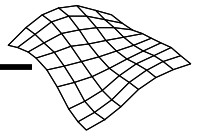


Figure 2.9: The principle of the DEM generation process.



Figure 2.10: A cloud of interest points indicated by green dots, and generated grid points by red dots.

Robust bilinear finite element method

In order to create a regular grid from irregular points and to eliminate gross height errors, like correlation errors, houses, trees, etc., the calculation must be done stepwise. During the process, the prerequisite is that the following conditions are met:

- Grid with a fixed mesh size
- Use of a robust procedure for the elimination of gross errors
- Filtration of DEM
- Smoothing of DEM
- Constrains maximum curvature in the perpendicular direction to regulate the DEM surface
- Constrains maximum torsion to regulate the DEM surface

The mathematical model for the creation of a DEM with $m = n \times m$ grid points is an adjustment called the robust bilinear finite element method and it was presented by [Ebner and Reiss, 1978].

The elements in the model are defined for the height per element of the four neighbouring points, see figure 2.11.

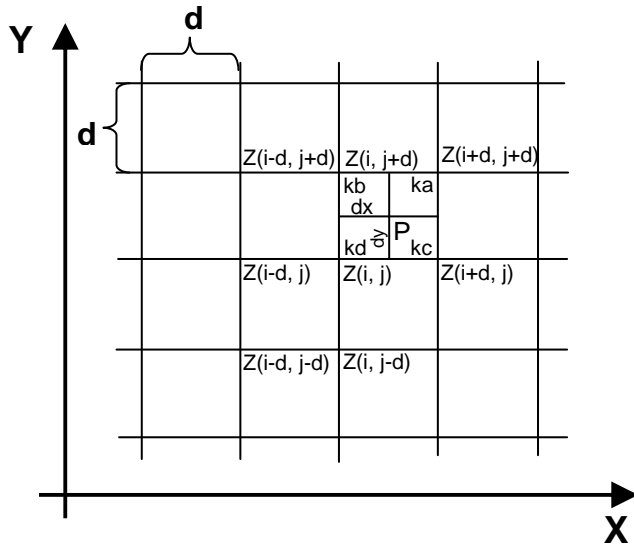


Figure 2.11: Determination of the grid points, [Inpho 1995]

With the following descriptions:

- $k_a := (1-dx)(1-dy)/d^2$
- $k_b := dx(1-dy)/d^2$
- $k_c := (1-dx)dy/d^2$
- $k_d := (dx\ dy)/d^2$

where:

- $dx = x(z_s) - x(z(i,j))$
- $dy = y(z_s) - y(z(i,j))$

and

- $d = \text{mesh size}$

Where k_a , k_b , k_c and k_d are used as weights functions.

The following description is a combination from [Inpho Match-T, Automatic DEM-Generation, Tutorial] and [Intergraph, ImageStation Match-T (ISMT) User's Guide].

Each terrain point is described by:

$$\vec{Z} = \{Z_i : i = 1, k\}$$

where:

Z = vector

Z_i = terrain heights where i runs from 1 to k

k = number of terrain heights

The grid point \vec{Z} can be described as:

$$\vec{Z} = \vec{Z}(x, y) = a_0 + a_1 x + a_2 y$$

The grid also has a curvature and a torsion which is described as follows:

$$\vec{Z}_{xx} = \{Z_{xx}(i, j) : i = 1, n, j = 1, m\}$$

The curvature in the x-direction

$$\vec{Z}_{yy} = \{Z_{yy}(i, j) : i = 1, n, j = 1, m\}$$

The curvature in the y-direction

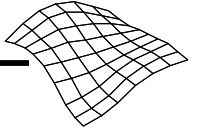
$$\vec{Z}_{xy} = \{Z_{xy}(i, j) : i = 1, n, j = 1, m\}$$

The torsion

The curvature and the torsion apply to $m = n \times m$ grid points for the DEM. For the measured terrain points, curvature and torsion, the following is presumed true:

$$E(\vec{Z}_{xy}) = 0, \quad E(\vec{Z}_{xx}) = 0 \quad \text{and} \quad E(\vec{Z}_{yy}) = 0$$

The following equations refer to the definition of DEM heights for four grid points and a temporary terrain height z_s .



These equations describe a vector for the unknown heights of the grid points.

$$\vec{u}_{\text{part}}^T = \begin{bmatrix} z(i-1, j+1), z(i, j+1), z(i+1, j+1) \\ , z(i-1, j), z(i, j), z(i+1, j) \\ , z(i-1, j-1), z(i, j-1), z(i+1, j-1) \end{bmatrix}$$

The residuals $v_{xx}(i,j)$, $v_{xy}(i,j)$ and v_s for observations are presumed normally distributed.

The vectors \vec{a}_i for $(i=2,3,4)$, which correspond to the nine terrain heights of the four grid meshes in figure 2.11, are multiplied by the coefficient matrices defined as:

$$\vec{a}_2^T := \text{vector}\left(\frac{1}{4} \begin{bmatrix} 1 & -2 & 1 \\ 2 & -4 & 2 \\ 1 & -2 & 1 \end{bmatrix}^T\right) \quad \vec{a}_3^T := \text{vector}\left(\frac{1}{4} \begin{bmatrix} 1 & -2 & 1 \\ -2 & -4 & -2 \\ 1 & -2 & 1 \end{bmatrix}^T\right)$$

$$\vec{a}_4^T := \text{vector}\left(\frac{1}{4} \begin{bmatrix} 1 & 0 & -1 \\ 0 & 0 & 0 \\ -1 & 0 & 1 \end{bmatrix}^T\right)$$

The final mathematical model is finished by setting up the stochastic model:

$$P(\vec{z}_{xx}) = \text{Diag}(D^{-1}(\sigma_{xx}^2))$$

$$P(\vec{z}_{yy}) = \text{Diag}(D^{-1}(\sigma_{yy}^2))$$

$$P(\vec{z}_{xy}) = \text{Diag}(D^{-1}(\sigma_{yx}^2))$$

$$P(\vec{z}) = \text{Diag}(D^{-1}(\sigma_z^2))$$

This stochastic model represents the weight matrix for the temporary observations and their a priori standard deviations. Instead of eliminating the vector for the unknown DEM heights by a linear Gauss-Markoff process by maximising the function:

$$f(\vec{u}, \sigma_{zxx}, \sigma_{zyy}, \sigma_{zxy}) = \vec{v}^T P^{(v)}(\vec{z}) \vec{v} + \vec{v}_{xx}^T P^{(v)}(\vec{z}_{xx}) \vec{v}_{xx} + \vec{v}_{yy}^T P^{(v)}(\vec{z}_{yy}) \vec{v}_{yy} + \vec{v}_{xy}^T P^{(v)}(\vec{z}_{xy}) \vec{v}_{xy}$$

the mathematical model is determined by introducing a weight function with approximated a priori weights for the observations in the stochastic model with a value for their normalised residuals t . As suggested by [Förstner 1989] and [Krarp et al. 1980], the weight functions are:

$$w_2(t) = e^{-(t)^2} \quad \text{and} \quad w_1(t) = \frac{1}{\sqrt{1+(t)^2}}$$

These weight functions are used as the modification for the observation weight in a two-part iterative Gauss-Markoff process by use of the relation:

$$\begin{aligned} P_z^{(v+1)} &= P_z^{(0)} w_j(t_z^{(v)}) & P_{zyy}^{(v+1)} &= P_{zyy}^{(0)} w_j(t_{zyy}^{(v)}) \\ P_{zxx}^{(v+1)} &= P_{zxx}^{(0)} w_j(t_{zxx}^{(v)}) & P_{zxy}^{(v+1)} &= P_{zxy}^{(0)} w_j(t_{zxy}^{(v)}) \end{aligned}$$

Where: v = the iteration step.

Observations with great deviations are weighted low and eliminated, if a given limit for the observation weight is overstepped during the iteration. The minimisation of the following function for each iteration step v gives a solution for the vector \bar{u} for all unknown DTM heights:

$$f(\bar{u}, \sigma_z, \sigma_{z_{xx}}, \sigma_{z_{yy}}, \sigma_{z_{xy}}) = \bar{v}^T P(\bar{z}) \bar{v} + \bar{v}_{xx}^T P(\bar{z}_{xx}) \bar{v}_{xx} + \bar{v}_{yy}^T P(\bar{z}_{yy}) \bar{v}_{yy} + \bar{v}_{xy}^T P(\bar{z}_{xy}) \bar{v}_{xy}$$

The function is minimised, until the estimated values for σ_z (\bar{u} , σ_z , $\sigma_{z_{xx}}$, $\sigma_{z_{yy}}$, $\sigma_{z_{xy}}$) become constant or reach a given limit. The combination of both iteration phases guarantees a "global" convergence, and detection and elimination of height errors.

This mathematical model for the DTM generation is also a "robust filter" process which can deal with areas with insufficient information about the terrain surface (lack of interest points). Because the programme can generate a very large number of measured terrain points, the process is strongly over determined, even if a small mesh size is chosen.

2.4.4 Conversion of the grid points

Further calculation can only be managed in ascii-format. Match-T offers three possibilities when converting the grid file to ascii-format:

- Coded with [X, Y, Z + 8 codes]
- Coded as a mass point [X, Y, Z, 30000000]
- Without codes [X, Y, Z]

Furthermore, it is possible to opt out of points which Match-T considers as being:

- In a bad area
- Interpolated
- Without the stereo-area
- Situated in an excluded area
- Situated without the delimited area

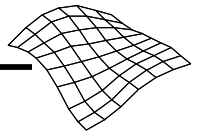
If the grid files are converted with codes, each grid point is furnished with 8 codes:

- Code 1 = the point is OK
- Code 2 = the point is situated without the stereo-area
- Code 3 = the point is situated without the area
- Code 4 = the point is situated within an excluded area
- Code 5 = the point is situated in an area of low accuracy
- Code 6 = the point is situated in an area with a low texture
- Code 7 = the point is situated close to a break line
- Code 8 = the point is not interpolated

These code descriptions are found as headings in the ascii-file, when the conversion is done with code.

2.4.4.1 Accuracy

In the world of photogrammetry, the rule of thumb is that the demand for accuracy in a DTM should be between 0.1‰ and 0.2‰ of the flight altitude. This demand forms the basis of the level of accuracy in Match-T. Here, the demand for accuracy is less than 0.1‰ [Krzystek et al., 1992]. Investigations of Match-T done by Inpho, show that in flat or hilly areas, not only can this demand be met, but elevation data considerably better than 0.1‰ of the flight altitude can be obtained. It should be noted, however, that



the accuracy in mountainous terrain lies between 0.2‰ and 0.35‰ of the flight altitude [Krzystek et al., 1995].

There are other investigations which show that the accuracy is not so good as described previously [Seyfert, 1995], [Thorpe et al., 1996], where accuracies lie between 0.7‰ up to 3‰ of the flight altitude.

An investigation done with images from digital frame cameras shows some very good results with a RMS accuracy in z of 7.2cm, which of the flight altitude is 0.05‰. [Heuchel, 2005].

2.4.4.2 Pros and cons of the photogrammetric method

The greatest advantage of the photogrammetric method, (Socet Set or Match-T), is that the images offer a visual basis for a possible later location of gross errors and thus, an easier editing of the elevation data. Furthermore, the images are already in existence for a possible later mapping or orthophoto production, necessitating only one flight. The photogrammetric method thus offers data in three dimensions which can be used for production of elevation models as well as maps.

The disadvantage is that this method creates very large data collections, which have to be structured and handled and the data collections take up a lot of storage capacity. However, this is offset by the fact that the images may be used for mapping.

2.4.4.3 The scope of the photogrammetric method

The photogrammetric method including Socet Set and Match-T can be used with advantage in areas, where the demand is for elevation data as well as for mapping or orthophotos.

2.5 Comparison of the three methods

IFSAR as well as LIDAR are active systems which emit and receive signals themselves, in contrast to the photogrammetric method which uses a passive collection system. The active systems may be used without regard to sun or light conditions, and independent of the texture of the ground surface. This means that the methods may be used all around the clock and throughout the six months of winter during the leaf free period which gives a much larger degree of usage of the systems.

Studies of comparisons between elevations generated by LIDAR and automatically generated elevations from digital photogrammetry have shown that, as regards images with a low texture and contrast, the photogrammetric method does not offer good results, whereas the LIDAR method is not influenced by such considerations.

IFSAR and LIDAR offer elevation data, but no geographical data. In a possible gross error search, it is therefore necessary to include other data, for instance existing maps. In the photogrammetric method, such information is included as a 'by-product', due to the fact that the elevations are generated from aerial photos. That is, the photogrammetric method offers full information about elevations and geographical material, all at the same time.

If the accuracies of the three methods are compared, the best accuracy is obtained by using LIDAR. The next best accuracy is obtained by the photogrammetric method, while the IFSAR method is the most inaccurate. The opposite is true for the area of coverage, where IFSAR covers the largest area, the next largest area is covered by the photogrammetric method and the smallest area is covered by LIDAR which entails a longer total flight time and, thus, an increase in costs. A more detailed comparison between the photogrammetric method and LIDAR can be found in [Rasmussen et al., 2000].

Also in [Marcer, 2001] the price factor for obtaining elevation data is discussed, see figure 2.11. The elevation accuracy and point density are two of the components driving the cost and applicability of DEM products. In figure 2.11 the unit price (US\$/km²) of DEM products are shown as a function of vertical accuracy. For relative comparison, the relationship between satellite-based DEM products, IFSAR (Radar), LIDAR and aerial photography is shown. Because costs and specifications are often project-specific, there is a broad range for any data type, but the trend is clear.

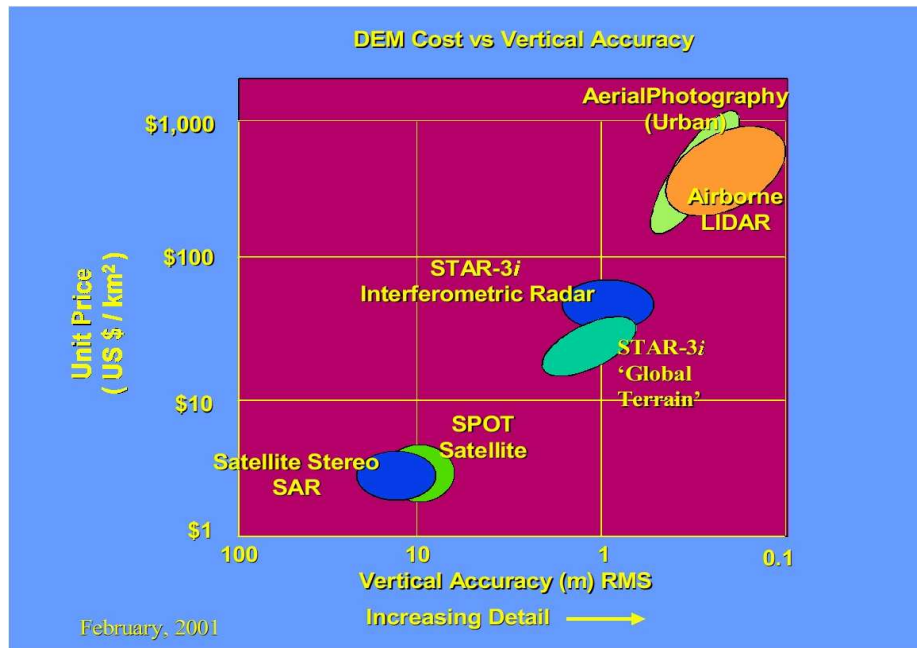


Figure 2.12: The figure illustrates the price factor for obtaining elevation data by different method [Marcer, 2001].

In figure 2.12 it can be seen that the aerial photogrammetry and LIDAR methods, cost and accuracy, works out approximately the same. But because the updating of the geographic data will be performed every 3 to 5 years, the aerial images will therefore already be available for the automatic generation process. This means that there are no expenses for purchasing digital images, only the costs of the calculation process have to be taken into account.

2.5.1 Choice of method

As may be inferred from the aforementioned, all three methods have their pros and cons, but taken the above mentioned considerations it was chosen from the very start to have a closer look at the automatic correlation method, specifically the programme package Match-T. This choice was made as the programme was available at Aalborg University, where the project originated.

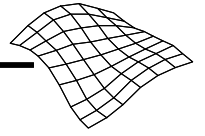
2.6 Proposal for combining/integrating new z-measurements

In Denmark, there are already various elevation models. In the very near future a new nationwide elevation model will be created by the LIDAR method. Only in the first years after the establishment of the new elevation model, can the DEM be considered as updated, because all geo-spatial data degenerates over time and becomes unreliable. It has therefore to be taken into account that the DEM in the future has to be improved with new elevation data.

It must therefore be noted that historical, present and future elevation data must not come from the same sources and/or producers. In this case the updating of the geo-spatial data can, in the future, be done from digital images. It will therefore be straight forward to update the elevation data by using the automatic generation method. This means that the future elevation model will be put together with data from different sources with different accuracies. Furthermore, it can not be expected that the point placement is dispersed equally over the whole area. The points can be randomly spread out and in clusters, here, there and everywhere.

This gives us several situations for combining/integrating new z-measurements:

- unstructured raw elevation data from two or more different sources/producers
- structured elevation data in the grid with the same mesh size or different mesh sizes from different sources and different origo.



- grid and unstructured raw elevation data from different sources/producers

A mathematical model must therefore be established which can handle the problem of historical, present and future elevation data, captured from different sources/producers, with different accuracies and structures (grid or raw elevation data). A solution to this problem, could be the 'multi grid method'. The 'multi grid method' is a highly effective iterative solution strategy which can solve large areas with thinly determined points with the help of an adjustment system. The great advantage with the 'multi grid method' is that the adjustment system is independent of the numbers of unknowns.

The starting point could be: two clouds of structured or unstructured points, where the elevation data is independent and has different accuracies. Should one of the clouds of points consist of grid points, this grid will be looked at, as a non-structural cloud of points.

This is a classic adjustment problem, the solution being, an adjustment is done by means of the least squares measurement principle. (For the readers, who are familiar with least squares measurements, skip the next 1½ pages). The principle of least squares measurement is, that the random values (residuals) (v_i) have to be minimum, which means:

$$v_1^2 + v_2^2 + v_3^2 + \dots + v_m^2 = \sum_{i=1}^m v_i^2 \rightarrow \min$$

When the observations are independent and have different weights the principle of least squares measurement demands that the weight function minimises like:

$$\varphi = c_2 + c_2 v_2^2 + c_3 v_3^2 + \dots + c_m^2 = \sum_{i=1}^m c_i v_i^2 \rightarrow \min$$

This function can be noted as matrix form:

$$\varphi = [v_1 \ v_2 \ v_3 \ \dots \ v_m] \cdot \begin{bmatrix} c_1 & & & \\ & c_2 & & \\ & & c_3 & \\ & & & \ddots \\ & & & & c_m \end{bmatrix} \cdot \begin{bmatrix} v_1 \\ v_2 \\ v_3 \\ \vdots \\ v_m \end{bmatrix}$$

This matrix form can be written more simply as:

$$\varphi = v^T \cdot C \cdot v$$

The equations for the observations can be written in matrix format as:

$$l = A \cdot x - v$$

The above equation can be rewritten as:

$$v = A \cdot x - l$$

and together with equations $\varphi = v^T \cdot C \cdot v$ the equation will be:

$$\begin{aligned} \varphi &= (A \cdot x - l)^T \cdot C \cdot (A \cdot x - l) \\ &= (x^T \cdot A^T \cdot C - l^T \cdot C) \cdot (A \cdot x - l) \\ &= (x^T \cdot A^T \cdot C - l^T \cdot C) \cdot (A \cdot x - l) \\ &= x^T \cdot A^T \cdot C \cdot A \cdot x - l^T \cdot C \cdot A \cdot x - x^T \cdot A^T \cdot C \cdot l + l^T \cdot C \cdot l \end{aligned}$$

Because ϕ is a scalar, every part of the equation is a scalar and because scalars can be transposed over in it self the second and the third part of the equation is the same. This gives:

$$\phi = x^T \cdot (A^T \cdot C \cdot A) \cdot x - 2 \cdot (l^T \cdot C \cdot A \cdot x) + b^T \cdot C \cdot l$$

This is the weight matrix, which has to be minimised according to the principle of least squares measurement.

In the equation, all matrices and vectors are constants, except x , which has to be differential and put to zero. To be able to minimise ϕ , the partial derivatives factor has to be set to zero.

$$\frac{\partial \phi}{\partial x} = 2 \cdot x^T (A^T C A) - 2 \cdot l^T C A = 0$$

By dividing with a factor of 2 and transposing the formula:

$$(A^T C A) x = A^T C \cdot l$$

⇓

$$x = (A^T C A)^{-1} \cdot A^T C \cdot l$$

where: A = the design matrix

C = weight matrix

l = the observations

x = unknown quantities

x is now able to be determined.

As the starting point, an elevation model exists with points described as:

$$P_i(x_i, y_i, z_i) \quad \text{for} \quad \forall i = 0, 1, 2, 3, 4, \dots$$

Where the elevation for z_i ($i = 1 \rightarrow h$) is known and with an accuracy of σ_{z_i} ($i = 1 \rightarrow h$)

The new elevation model is described as:

$$\tilde{P}_i(\tilde{x}_i, \tilde{y}_i, \tilde{z}_i) \quad \text{for} \quad \forall i = 0, 1, 2, 3, 4, \dots$$

Where the elevation for \tilde{z}_i ($i = 1 \rightarrow h$) is known and with an accuracy of $\sigma_{\tilde{z}_i}$ ($i = 1 \rightarrow h$)

For the new elevation data a new equation can be put up as:

$$(z_i + v_{z_i}) - (\tilde{z}_i + v_{\tilde{z}_i}) \rightarrow \text{minimum}$$

Equation $(A^T C A) x = A^T C \cdot l$ is changed to:

$$(A^T \cdot C \cdot A) \cdot z = A^T \cdot C \cdot l$$

where:

$$z = (A^T \cdot C \cdot A)^{-1} \cdot A^T \cdot C \cdot l$$

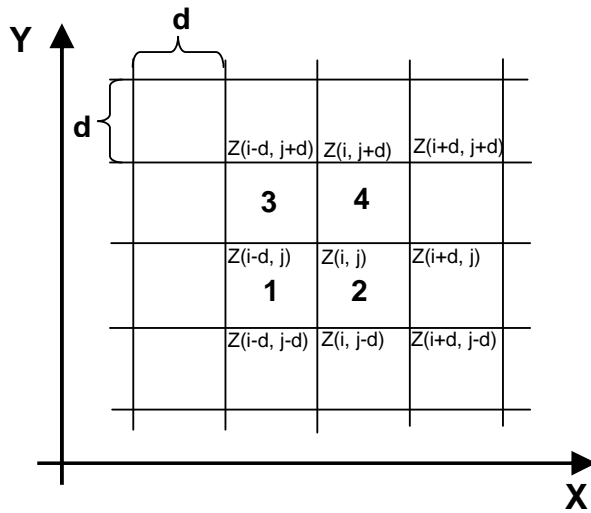
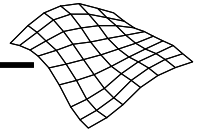


Figure 2.13: Determination of grid points for every mesh.

The adjustment system is now set up, the observation equations have to be defined. For all points placed in the first mesh (1):

$$V_{p1} = k_a \cdot Z_{i-d,j-d} + k_b \cdot Z_{i,j-d} + k_c \cdot Z_{i-d,j} + k_d \cdot Z_{i,j} - Z_{p1}$$

For points placed in the second mesh (2):

$$V_{p2} = k_a \cdot Z_{i,j-d} + k_b \cdot Z_{i+d,j-d} + k_c \cdot Z_{i,j} + k_d \cdot Z_{i+d,j} - Z_{p2}$$

For points placed in the third mesh (3):

$$V_{p3} = k_a \cdot Z_{i-d,j} + k_b \cdot Z_{i,j} + k_c \cdot Z_{i-d,j+d} + k_d \cdot Z_{i,j+d} - Z_{p3}$$

For points placed in the fourth mesh (4):

$$V_{p4} = k_a \cdot Z_{i,j} + k_b \cdot Z_{i+d,j} + k_c \cdot Z_{i,j+d} + k_d \cdot Z_{i+d,j+d} - Z_{p4}$$

As can be seen from figure 2.13 The weights functions according to the Match-T method:

- $k_a = (1-dx)(1-dy)/d^2$
- $k_b = dx(1-dy)/d^2$
- $k_c = (1-dx)dy/d^2$
- $k_d = (dx \cdot dy)/d^2$

where:

- $dx = x(z_s) - x(z(i,j))$
- $dy = y(z_s) - y(z(i,j))$

To be able to determine a 3 x 3 grid we need a minimum of 9 observations to have redundant observations. If there are not enough points to determine a 3 x 3 grid, 6 fictional observations equations can be put up, 3 for the horizontal lines and 3 for the vertical lines:

The horizontal lines are defined by:

$$v_{h1} = z_{i,j} - 2 z_{i+1,j} + z_{i+2,j}$$

$$v_{h2} = z_{i,j+1} - 2 z_{i+1,j+1} + z_{i+2,j+1}$$

$$v_{h3} = z_{i,j+2} - 2 z_{i+1,j+2} + z_{i+2,j+2}$$

The vertical lines are defined by:

$$v_{v1} = z_{i,j} - 2 z_{i,j+1} + z_{i,j+2}$$

$$v_{v2} = z_{i+1,j} - 2 z_{i+1,j+1} + z_{i+1,j+2}$$

$$v_{v3} = z_{i+2,j} - 2 z_{i+2,j+1} + z_{i+2,j+2}$$

An adjustment can now be done and the 9 grid points determined.

This adjustment system can handle any type of point placement and unstructured point clouds, as well as structured grid points.

Points can be determined from different sources and/or producers and can therefore have different accuracies (σ^2). When looking at the updating purposes of the future LIDAR national DEM there are several opportunities: automatically generated elevations from digital images, elevations from the existing 25m x 25m DEM and unknown elevations.

For every observation equation an accuracy of $1/\sigma^2$ has to be put up for the weight matrix. As an example for the different accuracies for possible elevation data including the a adjustment could be:

- LIDAR: 0,15 m
- Automatic generated points: the experience from this thesis
- Old elevations: 1,3 m
- Fictional points: 3 m

All the information is now available in order to solve the problem:

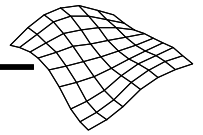
$$x = (A^T C A)^{-1} \cdot A^T C l$$

After determining, the accuracy of the new grid can now be determined:

$$r = A \cdot x - l$$

The only part missing is to take a closer look at what accuracy can be achieved by using the method of automatic generation!

It should be noted that the aforementioned method is only described theoretically and, has not been used in practice. The reason for this is, that there is no LIDAR data available at the moment.



3 Experience and investigation strategy

The purpose of this chapter is to establish a strategy for the investigation of Match-T under Danish conditions. In order to profit from the experience gained from other investigations of Match-T, such investigations and their results are presented. On the basis of this source study, problems and divergent results/statements will be discussed, the problems stressed and listed as "keywords".

In the source study, the terminology of the source has been used, DEM for Digital Elevation Model and DTM for Digital Terrain Model.

3.1 Background

Automatic generation of elevations from digital images has for several years been included as a fixed work routine at the photogrammetric firms in Denmark. In this project, a further investigation of the possibilities and limitations of this method is undertaken, taking the programme package Match-T as point of departure.

For more than 15 years, a series of investigations has been made into the accuracy, completeness and landscape types for automatically generated elevations from digital images. Moreover, OEEPE has conducted a workshop, where the results of automatically generated elevations were presented. On the background of the lessons learned here, areas relevant to a Danish use of Match-T, as regards problems, accuracy versus scale, pixel size, sources of error etc., are estimated. For each source, some central themes will be noted as keywords. The sources are discussed chronologically.

3.2 A source study of experiences with Match-T

In an article about Match-T from 1991 [Krzystek, 1991], 5 tests are presented. These show that with 15 μm images, an accuracy of at least 0.08‰ of the flight altitude can be achieved. Using images with a resolution of 30 μm , an accuracy of 0.1‰ can be achieved. A single one of the five tests gives a poorer result. This is due to the images' content of areas with poor texture. This problem is of immediate importance, both for the automatic and the manual determination of elevations.

Keywords: accuracy, resolution, texture.

In another article [Krzystek et al., 1992], the accuracies of Match-T and control points measured with analogous photogrammetry respectively are compared. This investigation takes as its point of departure the fact that an automatically generated elevation model should have an accuracy of 0.1‰ of the flight altitude. This requires Match-T to automatically find and destroy gross errors which are caused by correlation errors. Moreover, Match-T is expected to eliminate single objects such as trees and houses, and handle areas with a low or insufficient degree of information (none or few interest points). These three problems are handled by Match-T with the same mathematical method, see also Chapter 2, section 2.4.3.2. The investigation also discusses what influence the distance between grid points, that is, the mesh size, has on the result. The smaller the mesh size, the fewer interest points for determination of the grid point. Equally, a large mesh size means a greater number of interest points to determine a grid point. The investigation uses 15 μm and 30 μm images in three different scales (1:7,000 – 1:14,000). The conclusion is obvious: large mesh size, and subsequently, more interest points, give a better result in flat areas. In the case of a steeper terrain, a grid with a large mesh size will reproduce the terrain in considerably less detail, and imply a reduction in accuracy. The accuracy with mesh sizes of over approx. 5m is under 0.1‰ of the flight altitude, regardless of scale or resolution, while the accuracy for 15 μm images is considerably better. The investigation shows that as a whole, Match-T can produce a DTM of high accuracy, and subsequently, handle areas with a low degree of information.

Keywords: accuracy, scale, resolution, mesh size, terrain type.

In another article from 1992 [Ackermann et al., 1992], four different investigations of images in resolutions 15 μm and 30 μm are described. Small built-up areas and wooded areas are excluded in the images, but otherwise the areas are judged suitable for automatic DEM generation, as the remaining areas mostly consist of open country. The areas include sparse vegetation and a few houses which the system should be able to eliminate automatically. Three of the areas are designated as "soft" terrain with images in scale from 1:7,000 to 1:22,600. One of the three test areas is a more "hard" and mountainous terrain in scale 1:22,600. As regards the areas with "soft" terrain, the accuracy was better than 0.1‰ of the flight altitude, regardless of scale. The accuracy of the 15 μm images was 0.04‰ – 0.07‰ of the flight altitude, while the accuracy of the 30 μm images was a little poorer, 0.05‰ – 0.1‰ of the flight altitude. The last investigation was over mountainous terrain in scale of 1:22,600. Here, the accuracy was 0.11‰ – 0.13‰ of the flight altitude for 15 μm images, while for 30 μm images it was 0.14‰ – 0.16‰ of the flight altitude. Conclusion: In "soft" terrain, the accuracy in an automatically generated DEM is extremely good, far better than 0.1‰ of the flight altitude, and the difference between 15 μm and 30 μm images is not all that great.

Keywords: *Accuracy, scale, resolution, terrain type.*

In a third article [Ackermann, 1992], 15 μm and 30 μm images in scale 1:12,000 are used. A grid with 5m and 10m mesh sizes has been determined. The terrain may be designated as moderately hilly with a small housing estate. The result was an accuracy of 0.06‰ of the flight altitude for 15 μm images, and 0.09‰ of the flight altitude for 30 μm images. The conclusion is that an accuracy of 0.1‰ of the flight altitude or better is possible for non-mountainous terrain. Some of the measured points were located on houses, trees and bushes, and Match-T was able to eliminate these "error elevations" automatically.

Keywords: *accuracy, resolution, terrain type, landscape type.*

A Norwegian investigation [Eide et al., 1993] is based on images in scale 1:5,000 with three different resolutions, 15 μm , 30 μm and 60 μm . This investigation shows that the best result is achieved with the resolution 15 μm , while the result for the 30 μm images is a little poorer and the result for the 60 μm images is distinctly poorer. Furthermore, the investigation shows that the accuracy is 0.1‰ of the flight altitude in flat and simple terrain, 0.25‰ of the flight altitude in flat and moderately hilly terrain, and all of 0.55‰ of the flight altitude in mountainous (steep) terrain.

Keywords: *accuracy, resolution, terrain type.*

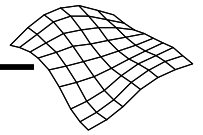
In a later investigation [a) Krzystek et al., 1995] which is also based on images in different scales, various terrain types have been looked at: flat, hilly and mountainous. The investigation is made on the basis of images in resolutions 15 μm and 30 μm . It shows that for images with resolution 15 μm , an accuracy of 0.1‰ of the flight altitude can be achieved for flat as well as hilly terrain types, while there is a small reduction of the accuracy for images with resolution 30 μm . As regards mountainous terrain, the accuracy is 0.2‰ – 0.35‰ of the flight altitude. It has also been tested how well Match-T is able to find and eliminate solitary objects, such as houses and trees, and the "elevation errors" developed in housing estates. The result for housing estates turned out to be promising. However, it must be noted that this conclusion is only valid for images in medium and small scales.

Keywords: *accuracy, scale, resolution, terrain type, landscape type.*

In the article [b) Krzystek et al., 1995], the problem of areas with a lack of texture or areas with buildings/vegetation in combination with images in large scale is investigated. As mentioned earlier, Match-T must be able to handle areas where there is not a sufficient degree of terrain information. Furthermore, Match-T, using the same mathematical model, must be able to edit away correlation errors and solitary objects such as trees and houses automatically. The article describes 10 tests with models in different scales and with different terrain types. Conclusion: In flat and slightly hilly terrain, an accuracy of 0.1‰ of the flight altitude can be achieved. Some of the tests, however, show better results. In mountainous terrain, an accuracy of 0.2‰ to 0.35‰ can be achieved. Moreover, it was confirmed that Match-T is able to edit away solitary objects. The tests show that the said accuracy can be achieved regardless of scale and image resolution.

Keywords: *accuracy, scale, resolution, terrain type, landscape type, texture.*

[Seyfert, 1995] reports an investigation made over densely built-up areas, open country and wooded areas. The accuracy study shows that the type of landscape is crucial. Densely built-up areas give three



times as poor accuracy as open fields. Furthermore, this investigation shows that the same good results as in other investigations have not been achieved here. In this investigation, the accuracy is 0.7‰ of the flight altitude over open land and 2.2‰ of the flight altitude over densely built-up areas. This investigation also shows that it did not matter whether the images were scanned in 15 µm or 30 µm.

Keyword: *accuracy, resolution, type of landscape.*

In the article [Schenk, 1996] it is mentioned briefly that there are problems with large scales and built-up areas.

Keywords: *scale, landscape type.*

In the article [Ackermann, 1996] it is mentioned that the photogrammetric DEM generation in open country will not run into serious problems. However, the automatic method has a few problems in areas with break lines or in areas with low texture. Moreover, areas with vegetation or buildings are a fundamental problem.

Keywords: *texture, terrain type, landscape type.*

The investigation [Thorpe et al., 1996] looks at images with a resolution of 60 µm and scale 1:10,000. The investigation includes built-up areas, where problems are known to arise. In this article, an accuracy of 3.26m is achieved which corresponds to 2.17‰ of the flight altitude without filtration. After filtration, the accuracy was increased to 1.04m which corresponds to 0.69‰ of the flight altitude.

Keywords: *accuracy, landscape type.*

In the article [Heuchel, 2005] the investigation is done by using images taken by digital frame sensors. According to Heuchel, the DEM generation with digital frame sensors differs little from the use of scanned images. The algorithms used in Match-T are still the same now as they were 15 years ago. Two resolutions are investigated 8 and 12 bit data. The images are taken over an open coal mining area. The accuracy is very much the same, 0.05‰ of the flight altitude.

Keywords: *accuracy, scale, resolution, terrain type.*

3.2.1 Results from the OEEPE-workshop

On the basis of several investigations of different programme packages for automatic generation of elevations, a workshop was arranged in 1998 by the University of Stuttgart under the auspices of OEEPE: "OEEPE Experimental Investigations into the Automatic DTM Generation". The purpose was to take a closer look at accuracy, quality and production improvements. The purpose was also to analyse the weaknesses of the DTM generation with regard to pixel size, point density, mesh size and terrain type, taking into consideration covered areas, built-up areas and flat/hilly terrain. The material for this investigation was put at the disposal of Stuttgart University and consisted of two sets of images, over the same area, in scale 1:13,000, scanned in four different resolutions, 7.5 µm, 15 µm, 30 µm and 60 µm. The dataset, from July 1995, concerns an area fully covered by vegetation, while the other set, from October 1996 concerns an area with considerably less vegetation. The reference material consisted of points measured by analytical photogrammetry in a grid with a mesh size of 25 x 25m. The reference material was coded for the different types of growth, so that there was a possibility of later analysing any problems. The most extreme types of landscape, such as woods, gravel pits and waters, were excluded from the material.

Several different institutions and firms took part in the workshop with different programme packages for automatic generation of elevations. The results were presented on 25 – 26 July 1998 and can be found on the web site of "Institut für Photogrammetrie" (<http://www.ifp.uni-stuttgart.de/oeepe/index.htm>).

In this project, only the results achieved with Match-T are summarised. The investigations with Match-T were done by five different institutions:

1. Inpho GmbH, Stuttgart
2. Institut Cartogràfic de Catalunya
3. Institut für Photogrammetrie (ifp), Stuttgart
4. National Geographical Institute, Brussels, presented by ifp

5. The undersigned, Geolab, Aalborg University

Before the results are presented, it should be mentioned briefly that the different investigations have not been done with the same parameter set-ups. An important difference is the choice of terrain type. The terrain type must be chosen before the generation can be done. The choice is between the terrain types: flat, hilly and mountainous. The choice indicates over how many pixels the correlation may be done. If a flat terrain is chosen, the correlation can be done over 3 pixels, if hilly, 8 pixels and in mountainous terrain, 15 pixels. The number of pixels over which the correlation may be done is called parallax bound. Parallax bound may thus be 3, 8 or 15 pixels.

3.2.1.1 The result from Inpho GmbH

Inpho's investigation includes only images with a resolution of 15 μm and 30 μm and a mesh size of 6m. Inpho estimated that the terrain type was "mountainous", and the correlation was then done over 15 pixels. The result for the July images was $\sim 0.25\text{m} - 0.5\text{m}$ which corresponds to $0.13\text{‰} - 0.26\text{‰}$ of the flight altitude, regardless of the resolution of the images. A closer look showed, however, that there are problems with different landscape types. Inpho's result shows clearly that areas with hilly terrain, or with only a little texture gave the greatest problems, while open country and fields gave the best accuracy. It is obvious that images from October with less leaf cover give significantly better results. Here, the improvement is 35% over the July images. It should be noted that the results from Inpho are divided by $\sqrt{2}$, as Inpho assumes that the reference points and the generated elevations have the same accuracy. The conclusion from Inpho is then: the resolution of the images is not very influential. Hilly areas with low texture give problems, whereas open areas give the best result. The result is also better when using images with less leaf cover, that is, October images are better than July images.

Keywords: *accuracy, resolution, terrain type, season.*

3.2.1.2 Institut Cartogràfic de Catalunya

The investigation done by Institut Cartogràfic de Catalunya also uses images with a resolution of 15 μm and 30 μm respectively. In addition, 2.5 x 2.5 m, 5 x 5m and 25 x 25m grids have been used, and the terrain is assumed to be "mountainous". The result for the July images gave a total accuracy of 1.7m which corresponds to 0.9‰ of the flight altitude. Again, the result shows that the resolution of the images does not influence the accuracy much. Moreover, the mesh size has no influence. A closer analysis of the individual landscape types shows that there were problems in built-up or overgrown areas, while open country and fields gave the best result. As regards the images from October, the accuracy was significantly improved by approx. 1.1m over the July result. This is due in particular to an improvement in the landscape type vegetation, from 5.2m to 0.7m. But it is also characteristic of the other landscape types that there is an improvement from the July images to the October images. Conclusion: the resolution of the images and the mesh size have no influence. The problem areas are the landscape types built-up and overgrown. The best result is achieved over open fields. Again, a better result is achieved by using images with less leaf cover, that is, October images rather than July images.

Keywords: *accuracy, resolution, mesh size, landscape type, season.*

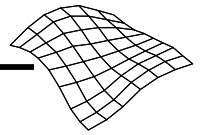
3.2.1.3 Institut für Photogrammetrie, Stuttgart

The investigation done by Institut für Photogrammetrie (ifp), Stuttgart uses July images with a resolution of 15 μm , 30 μm and 60 μm and October images with a resolution of 7.5 μm and 15 μm . In addition, ifp has used positives as well as negatives of the aerial photos. The results from ifp are not presented in table/diagram form and are therefore not directly comparable to the other four results. However, it can be seen that there is no difference between using positive and negative images.

Keywords: *resolution, positive/negative.*

3.2.1.4 National Geographical Institute, Brussels

This investigation has used 15 μm , 30 μm and 60 μm images and 5 x 5 m, 10 x 10 m, 11 x 11m and 23 x 23m grids. Again, the test area has been assumed "mountainous". The accuracy achieved varies between approx. 0.7m and 1.4m ($0.3\text{‰} - 0.7\text{‰}$ of the flight altitude), and the result shows that there is not a great difference between using 15 μm and 30 μm images, or different mesh sizes, while there is a small reduction of the result using 60 μm images. The conclusion is: the accuracy in open country is 0.12‰ of



the flight altitude with a small improvement using 15 μm images. The problem areas are forest edges, built-up areas and areas with dense vegetation of bushes and trees, while the open country needs very little editing. Resolution and mesh size have little or no influence on the accuracy.

Keywords: *accuracy, resolution, mesh size, landscape type.*

3.2.1.5 Investigation, Aalborg University

In the investigation done at Aalborg University, images with the resolution 15 μm , 30 μm and 60 μm , and mesh sizes of 5 x 5 m, 12.5 x 12.5m and 25 x 25m were used. The terrain type was estimated from the elevation difference between the control points which was $\sim 250\text{m}$. This elevation difference was estimated to be neither flat nor mountainous, so the terrain type "hilly" was chosen, which meant that the shift by the correlation could only take place over 8 pixels. The result for the July images was an accuracy of 1m - 2m. In addition, the result showed that neither the resolution of the images nor the mesh size had any great influence on the accuracy. A closer analysis of the individual landscape types showed that problems arose in built-up or overgrown (forest edges) areas, while the open country and fields had an accuracy $< 1\text{m}$ ($< 0.5\%$ of the flight altitude). In the October images, the accuracy was significantly improved by $\sim 0.5\text{m}$ over the July images. Specifically, the result was better in the overgrown areas, as the automatic generation here comes closer to the terrain because of the sparse vegetation in the autumn. Conclusion: Neither the resolution of the images nor the mesh size have any great influence on the accuracy. A better result is achieved by using images with less leaf cover, that is, October images rather than July images.

Keywords: *accuracy, resolution, mesh size, landscape type, season.*

3.2.2 Summation of the investigations from the OEEPE workshop

A common result of the investigations is that image resolution has little influence on accuracy. There are problems in areas with vegetation and buildings, while open fields give the best results. A significantly better result is achieved by using October images rather than July images, as the leaf cover is less in October. If the results of the five investigations are compared, it should be noted that Inpho's investigation is divided by $\sqrt{2}$. Even if Inpho's results are multiplied by $\sqrt{2}$, they are still the best at $\sim 0.35\text{m} - 0.7\text{m}$, whereas the remaining participants get results of between 0.7m and 2m which corresponds to 0.36% - 1.02% of the flight altitude.

3.2.3 Summation of sources and OEEPE workshop

A comparison of the results, from the article sources and the results from the OEEPE investigations leads to the conclusion that there is some divergence. In no way are the same good results achieved in the source material as in the OEEPE investigations. For instance, the accuracy over open, flat terrain varies from 0.04% - 0.07% of the flight altitude in [Ackermann et al., 1992], to 0.7% of the flight altitude in [Seyfert, 1995]. However, several sources show that an accuracy around 0.1% of the flight altitude is realistic [Eide et al., 1993; Brussels, OEEPE, 1998].

Common to several of the articles and the OEEPE results is that the pixel size is estimated to have little or no influence on the accuracy of images in resolution 15 μm and 30 μm , while 60 μm images according to [Eide et al., 1993] and Brussels give a poorer result. However, the OEEPE investigation from Aalborg university shows that even 60 μm images give the same result as images in resolution 15 μm and 30 μm .

The results of all the sources discussed are collated in the following table. For each keyword an indication is made, whether it has an influence (+) or not (/). In cases where the conclusion is ambiguous, this is marked (?).

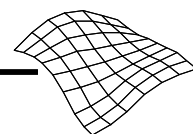
Articles	Accuracy	Resolution	Scale	Landscape type	Terrain type	Mesh size	Texture	Season	Pos./neg. pictures
Krzystek (1991)	X	X (/)					X (+)		
Krzystek, Wild (1992)	X	X (/)	X (/)		X (+)	X (+)			
Ackermann, Schneider, (1992)	X	X (+)	X (/)		X (+)				
Ackermann (1992)	X	X (/)		X (/)	X (+)				
Eide, Mardal (1993)	X	X (+)			X (+)				
Krzystek, Ackermann (1995)	X	X (/)	X (+)	X (+)	X (+)				
Krzystek, Wild, (1995)	X	X (/)	X (+)	X (+)	X (+)		X (+)		
Seyfert (1995)	X	X (/)		X (+)	X (+)				
Schenk (1996)			X (+)	X (+)					
Ackermann (1996)				X (+)	X(?)		X (+)		
Thorpe, Schickler, (1996)	X			X (+)					
Heuchel (2005)	X	X(/)			X				
Inpho (1998)	X	X (/)		X (+)	X (+)		X (+)	X (+)	
Catalunya (1998)	X	X (/)		X (+)		X (/)		X (+)	
lfp Stuttgart (1998)									X (/)
Brussels (1998)	X	X (/)		X (+)		X (/)		X (+)	
Denmark (1998)	X	X (/)		X (+)		X (/)		X (+)	

Table 3.1: The influence of different topics by an automatic generation of elevation data using match-T. X = the topic in question, + = the topic has an influence, / = the topic has no influence and ? = ambiguous conclusion.

On the basis of experiences and results as plotted in table 3.1, the following can be concluded:

Pixel size

The sources disagree about the influence of pixel size on accuracy. Some examples are quoted here; according to [Krzystek et al., 1992], considerably better results are achieved by using 15 µm rather than 30 µm images. On the other hand, a more moderate stand is taken by [Ackermann et al., 1992; Eide et al., 1993; Inpho and Brussels OEEPE, 1998], stating that a little better result is achieved by using 15 µm rather than 30 µm images. [Seyfert, 1995; Catatunya and myself OEEPE, 1998] find that there is no difference. However, the difference is pronounced when 60 µm images are used. Here, the accuracy is somewhat reduced. [Eide et al., 1993; Brussels OEPEE, 1998].



Scale

Opinions also differ about the influence of scale. [Krzystek et al., 1992] shows that the same accuracy can be achieved by different scales, regardless of which scale is in question. However, this is only valid for images in medium or small scale. As regards large scale, it is stated that the landscape type gives problems. [Schenk, 1996]. It can also be seen from the OEEPE presentations that an accuracy of 0.1‰ of the flight altitude cannot always be counted on.

Mesh size

The sources disagree on the influence of mesh size on the accuracy. [Krzystek et al., 1992] mentions that the mesh size has an influence; the greater the mesh size, the better the result, whereas [Catalunya, Brussels and the undersigned OEEPE, 1998] found no such influence.

Landscape type

The sources agree that landscape types pose a fundamental problem. A generation only succeeds in open areas with solitary objects which Match-T can eliminate on its own [Ackermann et al., 1992; a) Krzystek et al., 1995]. In addition, the investigations show [Ackermann, 1992; a) Krzystek et al. 1995] that housing estates appear promising. The investigation [Seyfert, 1995] shows clearly that the landscape type has an influence. Here, it is shown that built-up areas give three times as poor results as open fields. Likewise, [Thorpe et al., 1996] have shown that generation over built-up areas gives a poor result. In addition, the presentations from OEEPE show that there are problems with vegetation and buildings.

Terrain type

The sources agree that the terrain type has an influence. According to [Ackermann et al., 1992; Ackermann 1992; Eide et al., 1993; a) Krzystek et al., 1995], an accuracy of better than 0.1‰ of the flight altitude can be achieved over a flat to slightly hilly landscape with solitary objects, as Match-T according to [Krzystek, 1991; Ackermann 1992; a) Krzystek et al., 1995; b) Krzystek et al., 1995] can handle these objects. [Ackermann, 1996] mentions that photogrammetric DEM generation over open terrain will run into problems. Opinions differ about what accuracy can be achieved over, for instance, mountainous terrain. In the investigation by [Eide et al., 1993], it is shown that in mountainous terrain, an accuracy of 0.55‰ of the flight altitude can be achieved, while, for instance [a) Krzystek et al., 1995], show that an accuracy of between 0.2‰ and 0.35‰ can be achieved.

Texture

The sources agree that poor texture has a negative influence on the accuracy. Several sources [Krzystek 1991; b) Krzystek et al., 1995; Inpho (OEEPE), 1998] mention that there are problems with areas with poor texture, and thus lack of interest points for generation of grid points.

Summation

As seen from the above, there is divergent information about, for instance, the influence of pixel size, scale and mesh size, or the impact of landscape type and texture. This divergent information forms the basis for the choice of topic for the investigation with Match-T under Danish conditions with regard to a nationwide elevation model.

3.3 The investigation strategy of this project

On the basis of finding out how good a result can be achieved by using Match-T, the lessons learned from various investigations and the workshop in Stuttgart, a series of investigations have been set up with relevance to a Danish terrain. The investigations are chosen with regard to optimising the accuracy, and at the same time minimising the data quantity and editing work. The data quantity is evaluated in relation to the scale and resolution (pixel size) of the aerial photos. The editing is evaluated, among other things, on the basis of the influence of landscape type on the accuracy. Furthermore, a closer analysis of the impact of the mesh size has been included.

3.3.1 Accuracy in relation to flight altitude

It appears from the source study that there is a great difference in accuracy in relation to flight altitude. One investigation [Heuchel, 2005] shows that a very good accuracy 0.05‰ of the flight altitude can be achieved. Several other investigations have shown that an accuracy of 0.1‰ of the flight altitude can be achieved, while in a few others, an accuracy of 0.5‰ - 1.0‰ of the flight altitude is achieved, which means that the difference in results may be of the order of a factor 10. This may be due to the fact that in the "good" investigations [Krzystek, 1991; Krzystek et al., 1992; Ackermann et al., 1992; Ackermann 1992; Eide et al., 1993; a) Krzystek et al., 1995; b) Krzystek et al., 1995], possible gross errors and a possible offset have been known and taken into consideration. In the results from OEEPE, on the other hand, it is the "raw" data from which the accuracy is calculated, as no form of editing has been done.

3.3.2 Accuracy in relation to images resolution

The source study and the OEEPE investigation show that opinions differ about the influence of resolution on the result, but several sources [Krzystek, 1991; Krzystek et al., 1992; Ackermann et al., 1992; Ackermann, 1992; Eide et al., 1993] mention that 15 µm images give the best result. At the same time, it is mentioned by [Seyfert, 1995] that no better accuracy is achieved by using 15 µm rather than 30 µm images. It appears from the Norwegian investigation that there is no great difference in accuracy until a resolution of 60 µm, when a relatively poorer result is achieved [Eide et al., 1993].

3.3.3 Accuracy in relation to mesh size

As a factor in the reduction of the data quantity, the mesh size should also be discussed. Small mesh sizes will render the landscape in greater detail, but there will be fewer interest points for the determination of the grid points. On the other hand, using greater mesh sizes means there will be many interest points, facilitating the determination of the grid points. The source [Krzystek et al., 1992] mentions that the mesh size has an influence, while, for instance, the investigation from Aalborg University with the OEEPE material shows that the mesh size has no influence.

3.3.4 Danish landscape types

Taking as point of departure the opinion of [Ackermann et al., 1992; Eide et al., 1993; b) Krzystek et al.; Ackermann, 1996] that the best accuracy is achieved over open flat and slightly hilly terrain, the Danish terrain must be characterised as perfect for the use of Match-T. 70% of the Danish landscape can be described as open, flat, slightly hilly farming land with isolated trees (hedges) and houses (farms). The remaining 30% of the landscape consists of urban and wooded areas and waters. It must therefore be assumed that 70% of the Danish landscape is ideal for automatic generation with Match-T.

It must be taken into consideration, however, that there are large agricultural areas in Denmark which will appear on aerial photos as large uniform planes which, according to [Krzystek, 1991], may pose problems in large-scale images because of a lack of texture.

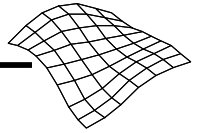
3.4 Selected investigations

The source study has shown that different parameters have an impact on the result of an automatic generation, therefore, the following parameters have been selected for a closer look:

- Scale
- Pixel size
- Mesh size
- Landscape type, including terrain type

3.4.1 The influence of the scale

In this investigation, the influence of the image scale on the accuracy is estimated. Supposedly/empirically seen, the influence of the scale should be linear, but different investigations show that the scale has no influence, except in housing estates, where it has turned out to be problematic to use images in large



scale [Schenk, 1996], while images in medium or small scale give a promising result [b) Krzystek et al., 1992]. In addition, it is investigated whether the optimum scale depends on the chosen landscape type.

3.4.2 The influence of the pixel size

It is investigated, whether it is possible to get a significantly better accuracy in a Danish landscape by using images with a higher resolution. Some investigations [Ackermann et al., 1992; Eide et al., 1993] point to the supposition that the pixel size has an influence on the accuracy, while several others, for instance, [a) & b) Krzystek et al.; all the investigations from OEEPE, 1998] show that pixel size does not have any great influence. The optimum is to operate with as low a resolution as possible with regard to the data quantity.

3.4.3 The influence of the mesh size

On the basis of the difference of opinion of the sources as regards the size of the mesh, an investigation is wanted into the influence of the mesh size in the Danish terrain. Where the mesh size has no influence, the optimum is as large a mesh size as possible, as the calculation time is then shortened, and the grid file is minimised.

3.4.4 The influence of the landscape type

Investigations by, for instance, [a) Krzystek et al., 1995; Seyfert, 1995; Schenk, 1996] show that built-up and overgrown areas pose problems. Furthermore, areas with little or no texture may also give rise to problems by the correlation [Krzystek, 1991]. As Denmark consists of large areas (fields) with low texture, this problem is extremely relevant in large parts of Denmark. An investigation into the usability of the method in the Danish landscape is one of the purposes of this project.

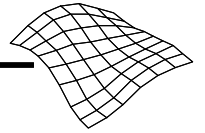
3.5 Summation

These are the investigations which are interesting, and have therefore been selected for inclusion in this project with regard to generating elevation data for a new model or for updating purposes.

In the investigation, the aim is to put up a list in which the necessary scale, resolution and mesh size appear with due consideration of the landscape type and the desired accuracy.

A test area is chosen for use in the investigation, and a frame of reference with superior accuracy is established. Aerial photos are taken over the test area in different scales, and these images are scanned in different resolutions. In addition, grids with different mesh sizes are generated, where the planimetric co-ordinates of the grid points will merge with the planimetric co-ordinates of the frame of reference.

All grids are compared with the frame of reference to examine the accuracy and possible gross errors. Subsequently, an analysis is done of how such gross errors have arisen and why. Is it due to a correlation error, or to objects such as trees and houses? The analysis is done by visualisation of the location of the gross errors on an orthophoto of the test area. Here, it is possible to see whether the error is due to objects or to a correlation error over, for instance, an area with poor texture.



4 The data material

In this chapter the data material of the investigations, in the project, is described, though only briefly. A more detailed description of the data capture, image resolution, accuracy etc. can be found in Appendix B.

All investigations presume that the chosen test area is characteristic of the Danish landscape. In addition, a frame of reference of the test area must be established, and aerial photos in different scales must be taken over the test area. The images will subsequently be scanned in different resolutions.

4.1 The test area

Several areas in Northern Jutland were evaluated, both areas close to Aalborg University and further away. The choice fell on an area of 3.5 km x 4.0 km south of Aalborg University. The area includes a typical Danish landscape with open, flat areas, hilly areas, overgrown areas, built-up areas etc. The choice of area is made on the basis of the literary study's identification of particularly interesting (problematic) landscape and terrain types, that is, areas with vegetation, built-up areas and open areas with low texture. Moreover, in this test area it is possible to take a closer look at other landscape types which are typically Danish and which, according to the literary study, should be ideal landscape types for automatic generation of elevation data.

Five characteristic landscape types are chosen for this investigation:

- Open, flat terrain (fields)
- Gravel pits
- Housing estates (villages)
- Open, hilly terrain (fields)
- Overgrown terrain (woods)

The open, flat terrain is a river valley, where there are no trees, buildings etc. Two gravel pits are included, as these are very hilly and thus, represent steep slopes. The housing estate is an area with one- or one-and-a-half-storey houses surrounded by gardens. In the open, hilly terrain there are a few farms with several buildings and trees around. In addition, there are hedges and such surrounding the fields. This means that the area is not a 100% open area. The last terrain is a wood with both dense and open areas, tall and low vegetation, made up of different species of trees.

The selected areas for the different landscape types are marked on figure 4.1 with colours, so that green shows a typical flat landscape, orange shows the location of the two gravel pits, red marks the village areas, violet the areas with hilly landscape, and blue areas with woods. In addition, the location of the test area is seen in relation to Aalborg University.

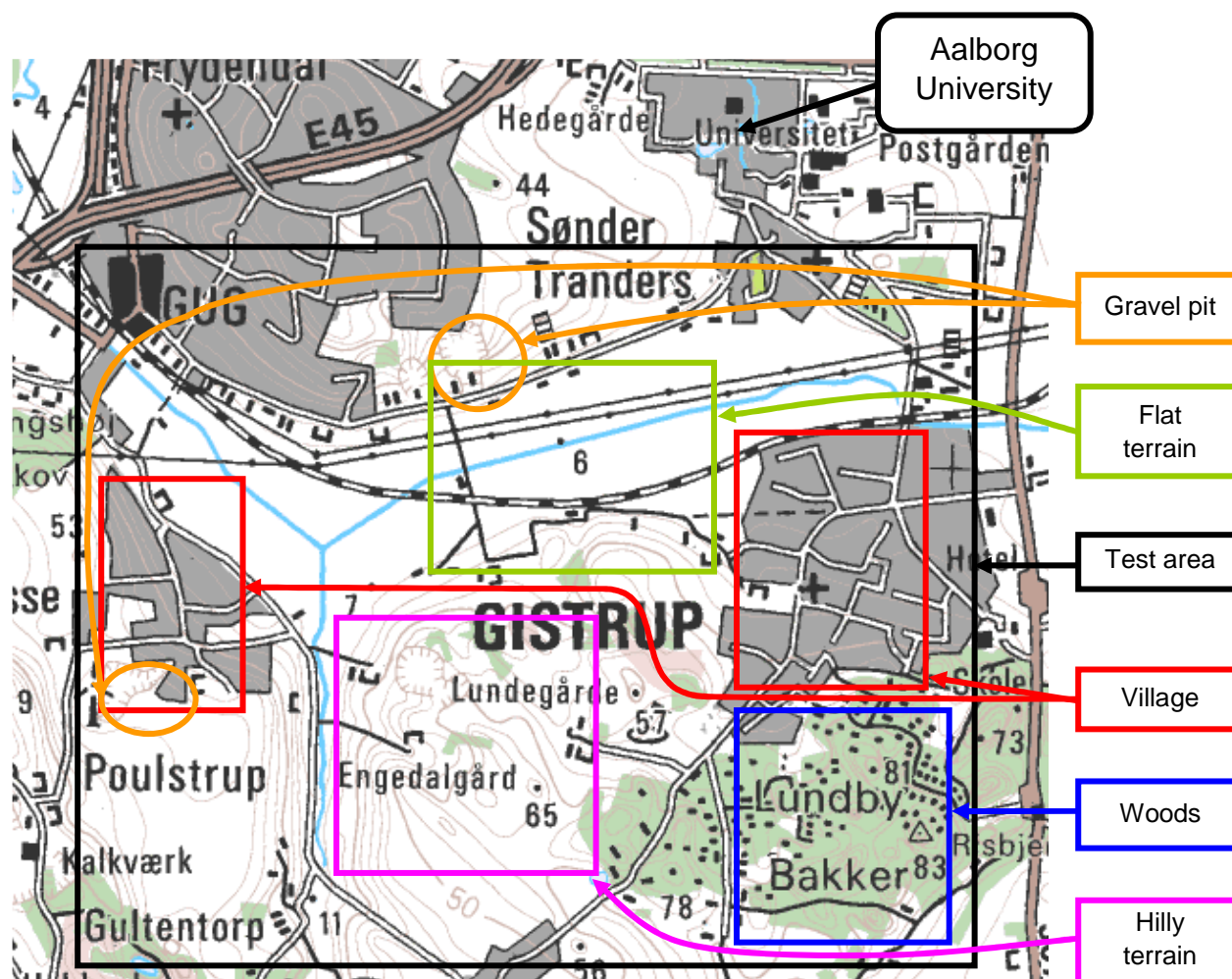


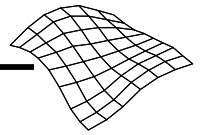
Figure 4.1: The 3.5 km x 4.0 km test area with an indication of the location of the different landscape types.

4.2 Aerial photos

Aerial photos have been taken over the test area in three different flight altitudes producing test material in scales 1:5,000, 1:15,000 and 1:25,000. The point of departure for the choice of these scales is the Danish tradition for shots in scale 1:25,000 for nationwide mapping, and 1:5,000 for detailed projecting. In addition, 1:15,000 has been included in order to decide, whether there is a linear connection between scale and accuracy. The aerial photos of the test area in scales 1:5,000, 1:15,000 and 1:25,000 form 36, 7 and 2 models respectively.

The images were scanned in a PS1 PhotoScan, where the possible resolutions are 7.5 μm , 15 μm , 30 μm , 60 μm and 120 μm . To avoid too many analysis possibilities but, at the same time, keeping the possibility of determining whether the resolution of the images may have a linear influence, it has been decided to look at only three different resolutions. To avoid too great a data quantity, the pixel size 7.5 μm has been excluded. To examine images with a resolution around the traditional 25 μm , the choice has been to scan in 15 μm , 30 μm and 60 μm , excluding the resolution 120 μm .

The shots were to be taken before leafing foliation, but the year 1996, when the images were taken, was a problematic year with late snow and early foliation. As a result, there are some leaves on the trees.



4.3 Control points

This investigation was started back in the mid 90's and at that time the determination of the airplanes position by GPS/INS was not good enough. The orientation of the images is, therefore, done on behalf of ground control points. The selection of control points for the orientation of the images builds on the Danish tradition, where well-defined terrain objects with a good contrast are used. In this project, the selection has therefore included wells, gratings, road markings etc. For the models in 1:25,000 and 1:15,000, a smaller number of control points are in question, while for the 36 models in 1:5,000, a greater number are in question. The measuring has been done with GPS. As the measuring for the 1:5,000 images is very time-consuming, it is supplemented by a bundle adjustment. The location of the control points in the models can be viewed in Appendix B, section B.1.3. Altogether, 77 control points and check points were measured. The result of the GPS calculation and the bundle adjustment can be found in Appendix E. The accuracy of the GPS points is:

$$X = 0.011 \text{ m}$$

$$Y = 0.014 \text{ m}$$

$$Z = 0.015 \text{ m}$$

The 77 control points and check points form part of the bundle adjustments of all the images in the three scales. A discussion of the bundle adjustment can be found in Appendix B, section B.2.2.2.

4.4 Selection of models

All the models in 1:25,000 and 1:15,000 are included, while the number of models in 1:5,000 is reduced to 14 out of the 36 models. The models are selected according to those landscape types which are interesting for this project. The chosen models' approximate location in the test area is shown in figure 4.1.

4.5 The frame of reference

In order to make an analysis, there must be a standard of comparison, a frame of reference. The frame of reference is determined photogrammetrically in an analytical instrument, Planicomp. As the reference points must be compared with automatically generated points, and these are generated in a fixed grid, the reference points should also be determined in the same fixed grid. The reference points are determined with a fixed mesh size of 25 x 25m. For the landscape type gravel pit, however, the mesh size was reduced to 5 x 5m. The planimetric co-ordinates for the reference points are chosen, so that the X- and Y-co-ordinates end on ***00.00, ***25.00, ***50.00 and ***75.00. For the mesh size 5 x 5 m, the planimetric co-ordinates end on ****5.00 or ****0.00. The mesh size was automatically fixed by the PlaniComp. When it was not possible to determine the elevation in the fixed grid, because of trees or houses, the point was moved out, where it was possible to see the terrain. Subsequently, it was moved back to the original grid, where measurements continued.

The measured reference points have been assigned an object code which refer to the different landscape types. The following number of points have been measured within each landscape type:

- Open, flat terrain = 2092 points
- Open, hilly terrain = 2814 points
- Wooded/overgrown terrain = 1223 points
- Village = 1629 points
- Gravel pit = 2429 points

To ensure that the reference points can be used as a basis for the analysis, they must have a superior accuracy. As mentioned earlier, [Krzystek et al., 1992] describe that it is possible to determine elevations automatically with an accuracy of 0.1‰ of the flight altitude. For images in scale 1:5,000, this means that

an accuracy for the generated elevations of approx. 0.075m can be achieved. For images in 1:15,000 and 1:25,000, it should be possible to achieve an accuracy of approx. 0.225m and approx. 0.375m respectively. The reference points should therefore be determined with an accuracy better than 0.075m.

The accuracy of the frame of reference is a combination of the accuracies of the control points, including their measuring and their definition, and the accuracy with which an experienced stereo-operator can measure elevations. The last-mentioned is indicated as 0.06‰ of the flight altitude.

The accuracy of the photogrammetrically measured elevations (the frame of reference) therefore consists of the following three contributions:

$$\sigma_z^2 = ((0.06 \text{ ‰ of } H)^2 + \sigma_{\text{ctrl.pt.}}^2 + \sigma_{\text{def}}^2)$$

Where:

σ_z = the accuracy of the photogrammetrically measured elevations

0.06‰ of H = the empirical experience of how well a professional operator can measure elevation data

H = the flight altitude

$\sigma_{\text{ctrl.pt.}}$ = the accuracy of the control point determination by GPS

σ_{def} = the accuracy of the definition of the control points

In this project, a bundle adjustment has been done. The accuracy of the bundle adjustment includes the accuracy of the control point measurements and the accuracy of their definition. As can be seen from Appendix A, section A.5, the accuracy of the control points in the 1:5,000 images after the bundle adjustment is:

$$x = 0.031 \text{ m}$$

$$y = 0.034 \text{ m}$$

$$z = 0.045 \text{ m}$$

and the accuracy of the tie points after the bundle adjustment is:

$$x = 0.034 \text{ m}$$

$$y = 0.040 \text{ m}$$

$$z = 0.060 \text{ m}$$

If Bingo/Match-T is used on images in scale 1:5,000, the output will include the control point accuracy as well as the accuracy achieved by the bundle adjustment.

This means that the accuracy can be determined as:

$$\sigma_z^2 = (0.06 \text{ ‰})^2 + \sigma_{z \text{ aero + ctrl.pt. + orient}}^2 = 0.045^2 + 0.06^2 = 0.075^2 \text{ m}$$

Where:

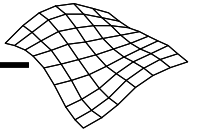
σ_z = the accuracy of the photogrammetrically measured elevations

$\sigma_{z \text{ aero + ctrl.pt. + orient}}$ = the accuracy achieved by the bundle adjustment which is 0.06 m

$\sigma_{\text{measurement}}$ = the accuracy of the measurements of the frame of reference, estimated at 0.045m by error-free control points

As will be seen from the above, the accuracy in the Z-direction is approx. 0.075m.

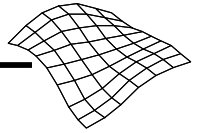
Very few control points have an accuracy poorer than 0.1m after the bundle adjustment. If this accuracy is used as the basis of estimation for the frame of reference, we have:



$$\sigma_z^2 = (0,06 \text{ ‰})^2 + \sigma_{z \text{ aero} + \text{ctrl.pt.} + \text{orient}}^2 = 0,045 \text{ m}^2 + 0,1 \text{ m}^2 = 0,11 \text{ m}^2$$

As there are very few control points which are determined with an accuracy poorer than 0.1 m, the accuracy of the whole frame of reference is, therefore, set at 0.1m. For images in 1:15,000 and 1:25,000, the frame of reference has a superior accuracy. An accuracy of 0.1m is not superior compared to the accuracy which can be achieved by using images in 1:5,000. However, work goes on with this frame of reference and also for images in 1:5,000, as that is the best possible reference that the project can produce. According to Chapter 1, the goal of the project is to analyse and value the accuracy that can be achieved by automatic generation in consideration of, for instance, scale. Images in 1:5,000 will therefore be valued, even though the reference is not superior.

The points of reference were not determined for the whole test area, but only for the models/areas with landscape types which are interesting for the investigations. In order to reduce the error contribution, the frame of reference was determined by an experienced operator. A closer description of the determination of the frame of reference can be found in Appendix B, section B.1.8.3.



5 Preparation for the grid generation

This chapter describes the Match-T set-up which is the basis for all the automatically generated grid calculations which are included in the investigations. The Match-T version employed is version 2.2.0.

5.1 The set-up of Match-T

The use of Match-T demands a series of input data and a choice of parameters. A superior programme menu, "Project Manager" is available to handle the information. A project is defined and organised under "Project Manager" which handles all project-related data, such as image material, geometric data and possible external measurements/data, see figure 5.1.

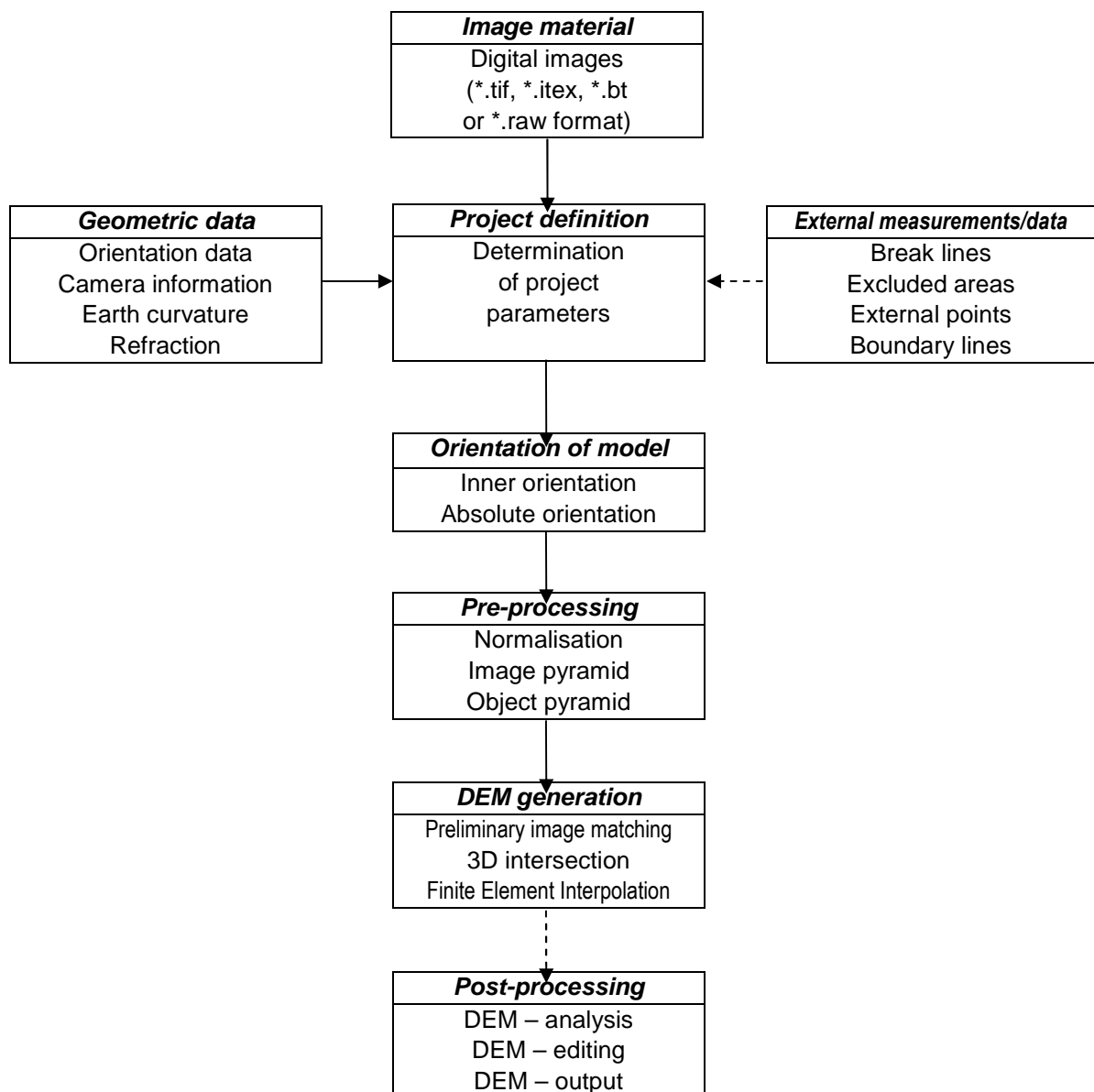


Figure 5.1: The process course in Match-T.

5.1.1 Image material

The location of the digital image material must be indicated with the full path connection. In the Match-T version 2.2.0, the image material must be stored in *.itex, *.tif or *.bt format. For each model, the pair of images must be indicated, and the location of the models in the block must be given.

In this project, the images have the format *.bt or *.itex, and it is noted that aerial photos have been used. Each pair of images and their location paths are given.

5.1.2 Geometric data

Under the heading of geometric data, the terrain type and the mean elevation over the terrain, the calibration report of the camera, control points, earth curvature and refraction are indicated. The information from the calibration report of the camera can be keyed in or transferred per file, if the information lies in Match-T camera format. The co-ordinates of the control points can be keyed in with an indication of whether it is a planimetric control point, a height control point or a fully measured control point, its accuracy, etc. The control point co-ordinates can also lie in a separate control point file to which a reference is given with full path connection. Finally, it must be indicated whether the earth curvature and the refraction must be taken into consideration.

In this project the terrain type is given as flat, the mean elevation as 75 m, the information from the calibration report of the camera is keyed in manually, the control points are keyed in manually and the earth curvature, refraction and lens distortion have been considered.

5.1.3 External data

A generation of elevations can be supported by external data. This is done by including external elevation data as a part of the calculation itself, for instance a grid or as break lines.

However, this possibility has not been used in this project, even though an actual elevation model exists. That is because the purpose is to find out how well Match-T is able to determine elevations without the influence of other data. The existing elevation data will only be included as a standard of comparison.

After the initial set up, the project was chosen. The further calculation process is divided into four steps: orientation of the images, determination of primary data, the DEM generation and, finally, the post-processing.

5.1.4 Orientation of the model

In Match-T, first the inner, then the absolute orientation are determined. The relative orientation is not determined, cf. Chapter 2 part 2.4.1.

5.1.4.1 Inner orientation

In Match-T, the inner orientation can be determined manually or automatically.

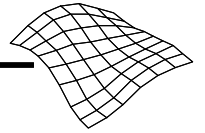
The automatic measuring of the inner orientation was not stable at the start of the project, giving a poorer result than if the orientation had been done manually, therefore, the inner orientation has been done manually.

5.1.4.2 Absolute orientation

Parameters which might have an influence on the absolute orientation are the possibilities of stereo vision and the definition of the control points. The definition of the control points is dependent on among other things, the resolution of the images.

Stereo vision.

The control points in the images are chosen according to those criteria which are used in a stereo system. In the Match-T version 2.2.0, orientation of the images is done, however, in a mono-system, there is no possibility of orientating the images in stereo. The control points in a mono-system must be physical objects which can be recognised in the images. Not all the chosen control points live up to this demand. For example, the height control points are chosen on flat areas, for instance in a field or in the middle of a



courtyard, where it was possible to see in stereo and thus determine the elevation. The determination of the height control points is, therefore, not possible because of the lack of stereo vision in Match-T.

The influence of resolution on the control points.

The control points are chosen in the analogous images. The experience gained in this project shows that control points chosen in analogous images cannot be transferred directly to digital images. The analogous aerial images lose some of their clarity by later scanning which is particularly important to the definition and contrast of the points. The contrast between control points and their surroundings must therefore be greater by digital photogrammetry than by analytical photogrammetry. Their definition in 15 μm images is a little blurred, and even more so in the 30 μm images. As for the 60 μm images, the control points are so blurred that they can only be recognised/localised by an operator who "knows" where the control points are, and therefore can recognise their location in the images.

To avoid that the standard of comparison, of the different image resolutions, vary because of different orientations, it has been decided to "re-use" the same orientation for each image, regardless of resolution. The orientation of the individual images can be achieved by use of different methods. For example, the orientation of 15 μm images can be transferred to the 30 μm and 60 μm images, as the definition of the control points is best in the 15 μm images. However, incomplete elevation orientation caused by lack of stereo vision will still be a problem.

As it has not always been possible to select physical objects as height control points, and to avoid different orientations, it has been decided in this project to orientate all images in a Planicomp, and do a subsequent bundle adjustment in the programme package Bingo. As regards the images in scale 1:5,000, the orientation exists as a consequence of the creation of the frame of reference. As regards images in scale 1:15,000 and 1:25,000, this extra process is done to achieve a uniform orientation of the images. The orientations achieved are then transferred to the respective images, regardless of their resolution. As a result, the orientation of the individual images will be the same, and the orientation will, therefore, not be included as a source of error in the comparison of the individual analyses, or by the evaluation of the method used for automatic generation of elevations in general.

The orientation of the images.

The table below shows the maximum deviation from the absolute orientation in x , y , z , ϕ , ω and κ for images in the different scales achieved in Bingo. The results can be seen in Appendix A, section A.3.

Scale	Accuracy in x (m)	Accuracy in y (m)	Accuracy in z (m)	Max. deviation in ϕ (mgon)	Max. deviation in ω (mgon)	Max. deviation in κ (mgon)
1 : 5,000	0.103	0.108	0.064	7.9	6.7	3.6
1 : 15,000	0.218	0.226	0.152	5.9	5.3	2.6
1 : 25,000	0.277	0.241	0.197	4.6	3.3	1.7

Table 5.1: The accuracy of the absolute orientation in x , y , z , ϕ , ω and κ

Table 5.1 shows that the poorest accuracy is the planimetric, whereas the elevation is somewhat better determined which is important for this project, as it is the elevations which are of interest. If the deviation is expressed in ‰ of the flight altitude, the result is 0.09‰ of the flight altitude for images in scale 1:5,000, 0.07‰ for scale 1:15,000 and 0.05‰ for scale 1:25,000.

The results of the bundle adjustments of the images in 1:5,000, 1:15,000 and 1:25,000 can be found in Appendix A, section A.3 and A.5.

Transfer of the orientation to Match-T

In Match-T, it is possible to transfer the orientation parameters from Bingo automatically. The transfer presupposes, however, that the orientation and scanning of the images are done in the same direction which is not the case in this project. In Planicomp, all the images have been orientated towards south. As regards the scanned images, the greater part is scanned with north upwards. Still, images which were part of a block with several strips were scanned with both north and south upwards. For images in scale 1:15,000, the first strip was scanned with north upwards and the second strip with south upwards. For im-

ages in 1:5,000, the first strip was scanned with north upwards, the second strip with south upwards, the third strip again with north upwards and the last strip with south upwards.

In this project, the orientation parameters are therefore keyed in manually.

5.1.5 Pre-processing of primary data

After the orientation of the images, the pre-processing is carried out. First the images are normalised, then an image pyramid and an object pyramid respectively are created.

5.1.5.1 Normalisation

Each image was normalised, that is, an epipolar geometry was built up according to the principles described in Appendix 1, section A.1.4. These normalised images were then stored on the hard disk.

5.1.5.2 Image pyramid

For each of the normalised images, an image pyramid was built. As standard, the image pyramid was built by the Gaussian function over 5 x 5 pixels. For images with a resolution of 15 μm , 9 levels more than the original image were built. For images with resolution 30 μm , the image pyramid was built with 8 levels, and for the 60 μm images with 7 levels more than the original image. (Cf. Appendix A, section A.1.7).

The standard set-up for Match-T has been chosen for this project.

5.1.5.3 Object pyramid

The object pyramid with interest points is built from the image pyramid. This is done according to the principles described in Appendix A, section A.1.8.

Primary data, that is, the normalised images and the image and object pyramids are not changed by the later correlation or DEM generation. This process is therefore not influenced by changes such as, for instance, a different set up of parameters for the DEM generation. Therefore, primary data is re-used in the subsequent calculations with different mesh sizes. This is done to save calculation time.

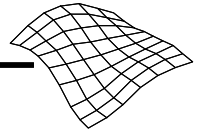
5.1.6 The DEM generation

Input arguments for the grid generation include indication of the calculation area defined by the lower left co-ordinate (lower left, ll) and the upper right co-ordinate (upper right, ur). In addition, a starting point is indicated. This starting point must be located within the model.

In this project, the co-ordinates for (ll) and (ur) are chosen, so that the calculation areas are indicated by means of the corner points in such a way that neighbouring areas adjoin without overlap. This is done to avoid elevations being generated over the same area twice. This is valid for neighbouring models as well as between strips. By avoiding overlapping areas, possible problems arising from such double elevations will not have to be taken into consideration later in the project.

The mesh size is chosen under the parameters for DEM generation. For this project, elevations are generated in a grid with a mesh size of 5 x 5 m, 12.5 x 12.5m and 25 x 25m respectively. As mentioned earlier, the primary data is not re-calculated, it is only the DEM generation itself which is determined for each mesh size.

To achieve the optimum standard of comparison, the automatically generated grids must be coincident with the frame of reference which has a mesh size of 25 x 25m and 5 x 5m respectively. Therefore, the automatic elevations are generated in the same grid as the frame of reference. This means that for the automatically generated grids with the mesh size 25 x 25 m, the same co-ordinate endings are fixed as for the frame of reference, which means that the planimetric co-ordinates X and Y end on ***00.00, ***25.00, ***50.00 and ***75.00. For grids with a mesh size of 12.5 x 12.5 m, the co-ordinate endings are ***00.00, ***12.50, ***25.00, ***37.50, ***50.00 etc. For this mesh size every other grid point will be coincident with a reference point. For automatically generated grids with a mesh size of 5 x 5 m, the planimetric co-ordinates end in ****5.00 or ****0.00. Here each point will be coincident with a reference point in the reference grid of 5 x 5 m, while there will be coincidence in every 5th reference point in the 25 x 25m grid.



5.1.6.1 Correlation

The standard value for the correlation window is 5 x 3 pixels. The threshold value of the correlation coefficient is as a standard value 0.75. The correlation coefficient is described in Appendix A, section A.1.1.1.1. In this project the landscape is considered as flat.

The standard value for the correlation window and the correlation coefficient is selected and fixed. The choice of a flat terrain entails a parallax bound in the x-direction (because of the normalised images) of 3 pixels, see Chapter 2, section 2.4.3.1.

5.1.6.2 The finite-element reconstruction

In the finite-element reconstruction, the values for the curvature, the torsion, the standard deviation etc. are fixed. The standard value of the curvature and torsion is 3, see the description of curvature and torsion in Chapter 2, section 2.4.3.2. The standard value for the standard deviation of the determined terrain points is 0.20m. The iteration process goes through 2 separate phases. The standard value of the first phase is 6 and for the last phase is 4. The last parameter used in the set up in this project is the threshold for the bias, the standard value is 35 %.

All these standard values are fixed. The chosen values are presented in table 5.2:

Function	Parameter	Value	Comments
The image and object pyramid	Gaussian function over 5 x 5 pixels	9 levels	Standard for 15 µm images
The image and object pyramid	Gaussian function over 5 x 5 pixels	8 levels	Standard for 30 µm images
The image and object pyramid	Gaussian function over 5 x 5 pixels	7 levels	Standard for 60 µm images
DEM generation	Window size for convolution	5 x 3 pixels	Standard window size
DEM generation	Parallax bound in row direction	3 pixels	Standard value for flat terrain
DEM generation	Threshold for correlation coefficient	0.75	Standard value
Finite-element	Curvature and torsion	3	Standard value
Finite-element	Standard deviation for grid points	0.20 m	Standard value
Finite-element	First iteration process	6	Standard value
Finite-element	Second iteration process	4	Standard value
Finite-element	Threshold value for bias	35 %	Standard value

Table 5.2: The standard set-up for Match-T for all calculations.

The above parameters are fixed in all automatically generated grid calculations. As described in Chapter 4, there are digital images in three different scales and three different resolutions. In addition, calculations are planned with three different mesh sizes, that is, 27 calculations in all.

5.2 Grid calculation

After setting up Match-T, the calculations are done. In Match-T there are three modules where the grid calculation can be followed online. These modules are called:

- Monitor for individual programme steps
- Graphic online/offline
- Online statistics

5.2.1.1 Monitor for individual programme steps

While the calculation itself is running, the process can be followed in the window, "Monitor for individual programme steps". Here the individual steps for normalisation, pyramid build-up and DEM generation can be followed numerically and in bar form. In this window, the currently used time and the estimated use of time are indicated for each process. Likewise, there is a possibility of interrupting the calculation. In this project the module is only used to follow the calculation and will not be mentioned further.

5.2.1.2 Graphic online/offline

Graphic online/offline is a visualisation function which offers the opportunity to follow the correlation and grid generation process online, where the correlated points and grid points are shown. This function must

be chosen before the calculation is started. The function offers the possibility of doing an a priori evaluation of the generated grid. It shows only a single model calculation at a time, so if the calculation consists of several consecutive models, the visualisation tool must be opened manually when the next model calculation starts. If a graphic result for each model is wanted, the calculations must be followed closely. This has not been done for all calculations in this project because some of the time consuming calculations have been done during the night.

The result of this visualisation is not stored automatically on the hard disk. If the image is to be kept, it must be done by screen dump in a self-elected file. A closer look at some of the results of the graphic online/offline function have been included in the project.

5.2.1.3 Online statistics

In the window "online statistics", the calculation process can also be followed numerically. For instance, the estimated and actually used time, the pyramid level at which the calculation is going on, various information about the calculated grid point and the internal accuracy of the point are shown. In addition, the numerical information is stored in the file 'match_t.log'. This file is changed after each calculation. It is possible that a closer analysis of the information in the match_log file may lead to a greater insight into the quality of the calculations, and thus to the exclusion of doubtful calculations. Such an analysis, however, has not been done in this project.

5.2.2 The post-processing

In [Inpho GmbH,1994] it is stated that it is necessary to do a post-processing in problematic areas like woods, densely built-up areas, in areas where low texture is found in the digital images and in areas in the images with shadows from clouds.

The post-processing can be divided into:

- DEM editing
- DEM analysis
- DEM output

5.2.2.1 DEM editing

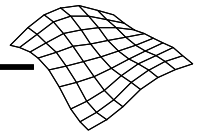
The DEM editing can be done in three ways, and as a combination of these:

- 1) Inclusion of external measuring to support the editing
- 2) Editing of problematic areas
- 3) Manipulation of the automatically generated elevation data without inclusion of external data

In this project, problematic areas will not be edited out. In this project, an examination will be carried out into how a post-processing can be done with the highest degree of accuracy and with a minimum of editing. If the automatic generation is done over a few models, a subsequent editing will be within clear bounds, but when the automatic generation is done over a large block of many km², where several thousand models are included, the post-processing MUST be minimised. External data will not be included. This is due to the fact that users have found errors in the model and to avoid the phenomenon of "garbage in, garbage out", the existing elevation data is excluded. An editing of problematic areas will not be done, the results are viewed for whole models.

5.2.2.2 DEM analysis

Match-T will do an internal quality check of the automatically generated grids. This is done by choosing a threshold value for the whole DEM, and relate this value to the corresponding statistical values from the DEM calculation. This internal quality check can be done for seven different criteria individually or in random combination.



The result of a DEM analysis can be "superimposed" on a digital image. If more differentiated "view" is wanted, the limit of the classification factor can be subdivided into four classes which can be defined as wanted and then shown in different colours.

A test of this analysis option is desired to see whether it can be used quickly and without too much expenditure of time to point out problematic areas.

5.2.2.3 DEM output

The DEM output files exist as binary files. There are three possibilities for converting the grid file to ascii form: with codes, without codes and coded as mass points.

Furthermore, it is possible to exclude points which Match-T estimates as being interpolated without the stereo area etc. In this project all the generated points will be looked at and, therefore, no points have been excluded beforehand. Also, a grid point coded as a mass point has no interest in this project. The generated files will therefore only be converted with or without codes. These codes make it possible to see which grid points Match-T considers to be influenced by error.

5.2.3 Choice of methods for a pre-analysis of data

Options

In this project the visualisation tool and graphic online/offline will be looked at during the calculation itself. This is done to examine whether this method may give a superior first hand impression of problems with the calculation and the subsequent accuracy of the grid.

Also, the ascii file will be examined closer to see whether the codes can be used for a pre-analysis of the individual automatically generated grids. It will be investigated where Match-T finds errors, as opposed to where errors are actually found, when the automatically generated grids are related to the frame of reference.

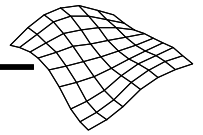
Non-options

Even if many relevant external elevation data exist in Denmark, it has been decided not to include these in the project. In the same way, a closer investigation of the analysis functions might possibly lead to a location of problematic areas but, to delimit the scope of the project, a closer discussion and possible improvement or optimisation of the post-processing has been set apart for a possible subsequent project.

As a post-processing method, Match-T's graphic DEM analysis after calculation has been excluded for several reasons. This analysis was tested to see whether it could be used quickly and without too much expenditure of time to point to problematic areas. It turned out quickly, though, that this analysis function could not be used without a closer and more detailed insight into the programme module which is not immediately accessible. Furthermore, an evaluation of the automatically generated grids down to individual grid points was required, which is not immediately possible as the result is shown graphically. Therefore, this method has been excluded.

The DEM output given in codes will be looked at more closely, as this method renders it possible to evaluate the individual grid points.

Also, the choice has been to maintain focus on the influence of the final result on the parameters chosen in Chapter 3 (scale, resolution, mesh size and landscape type). The influence of the parameters is investigated down to the individual grid point.



6 Pre-analysis of the generated data

In preparation for a thorough analysis of the automatically generated grids, the condition of the grids are examined. First a description of which calculations have been possible to carry out, then a description of one of Match-T's dynamic online visualisation functions, and finally, an evaluation of the ability of Match-T's post-processing application to localise gross errors.

To begin with, the course of the calculations is briefly described. After the generation is finished, a quantity of elevation data is available. This data quantity is expected to include gross errors. These gross errors must be eliminated, before the analysis of the chosen parameters (scale, resolution, mesh size and landscape type) can be done. In Match-T, there are various visualisation tools and post-processing tools. In this chapter, only the visualisation tool "Graphic online/offline" and DEM output with codes will be examined. Can this tool and the output with codes be used to indicate problems with individual grid points? The optimal would be that Match-T was able to point out possible errors on its own. Finally, the iteration process concerning the elimination of gross errors will be discussed.

6.1 The uniformity of the generated grids

The first to be noted is that it has not been possible to generate all the required grids in Match-T. Table 6.1 shows an overview of the calculations.

Resolution	1 : 5,000			1 : 15,000			1 : 25,000		
	5 x 5 m	12.5 x 12.5 m	25 x 25 m	5 x 5 m	12.5 x 12.5 m	25 x 25 m	5 x 5 m	12.5 x 12.5 m	25 x 25 m
15 µm	X	X	X	X	X	X	X	X	X
30 µm	X	X	X	X	X	X	/	X	X
60 µm	X	X	X	/	X	X	/	X	X

Table 6.1: Accomplished calculations shown in green (X) and yellow (x), not accomplished calculations in red (/).

In table 6.1 the accomplished calculations are shown in green (X), calculations which are accomplished, but where the calculation proceeded very slowly is shown in yellow (x), while red (/) indicates that this calculation cannot be carried out. The explanation why some of the calculations cannot be done or have proceeded very slowly is given in Chapter 7.4.

6.1.1 The visualisation tool "graphic online/offline"

By means of Match-T's online visualisation option, the calculation can be followed. The visualisation and possible storing of the result must be done for each individual model. As many of the calculations, especially the time-consuming ones, are done at night, not all the examples from this online visualisation function have been stored. Two examples, figure 6.1 and figure 6.2 are included in this chapter, 11 others are found in Appendix F.

Figure 6.1 (reproduction of figure 2.10) is an image of the dynamic online visualisation function which can be chosen for each calculation. The green dots reproduce correlated interest points, the red dots show the grid points.

A look at figure 6.1 sharpens the attention. Can Match-T deliver a uniform grid? For example, the result shown in figure 6.1 indicates that the grid does not have a uniform mesh size, but is a grid with holes. This phenomenon is not singular. In Appendix G it can be seen that there are many peculiarities which may lead to worries about the ability of Match-T to deliver a uniform grid.

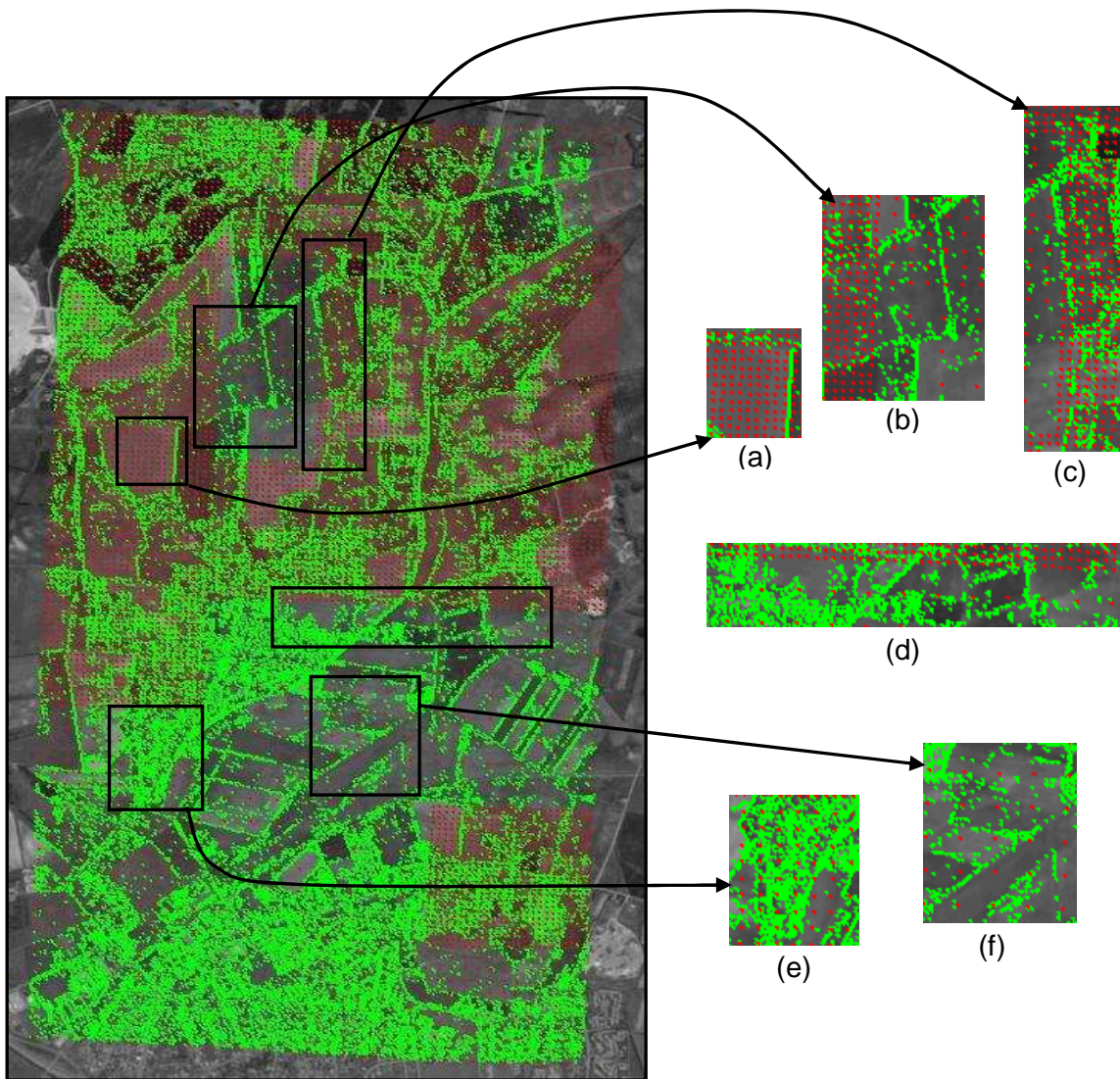


Figure 6.1: The point cloud indicated with green dots is interest points, the red points are the generated grid points. Six interesting areas (a-f) have been extracted for a closer analysis.

In figure 6.1 six interesting areas (a-f) are extracted. These areas will be discussed with a view to a closer investigation of the number of interest points versus generated grid points.

The (a) area: This area shows that Match-T is able to generate grid points, even if the number of interest points is low.

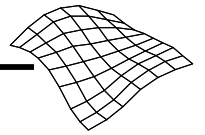
The (b) area: This area shows that within a small area, can be found, both the required number of grid points, and half the number required, and only every fourth grid point.

The (c) and (d) areas: These areas show that the gap between areas with the required number of grid points and areas with few grid points appear in straight lines, both vertically and horizontally. In case the lack of points is due to a random error, it is not very probable that they would appear in such regular patterns. Again, it is seen that the lack of grid points does not necessarily have any connection with the lack of interest points.

The (e) area: This area is an example of an area where there are many interest points, but where only half the number of grid points are being generated. This contradicts the claim that the lack of grid points is due to the lack of points of interest.

The (f) area: In this area one might be tempted to draw the conclusion that Match-T is unable to generate grid points in areas where there are few interest points. Purely intuitively, one would also expect that there would be a lack of grid points in areas where the number of interest points are low.

These six examples show that there is not a systematic connection between the number of grid points and the number of interest points. It can be seen that there are both areas where the generation is done,



even with a small number of interest points (a), and areas where the generation is not done, in spite of the existence of a sufficient number of interest points, for instance area (d), and in particular area (e).

Other results from graphic online functions indicate that some of the calculations are perhaps not finished, but have stopped midway, cf. figure 6.2. It must be emphasised here that figure 6.2 is not a screen dump in the middle of the calculation, but the last image!

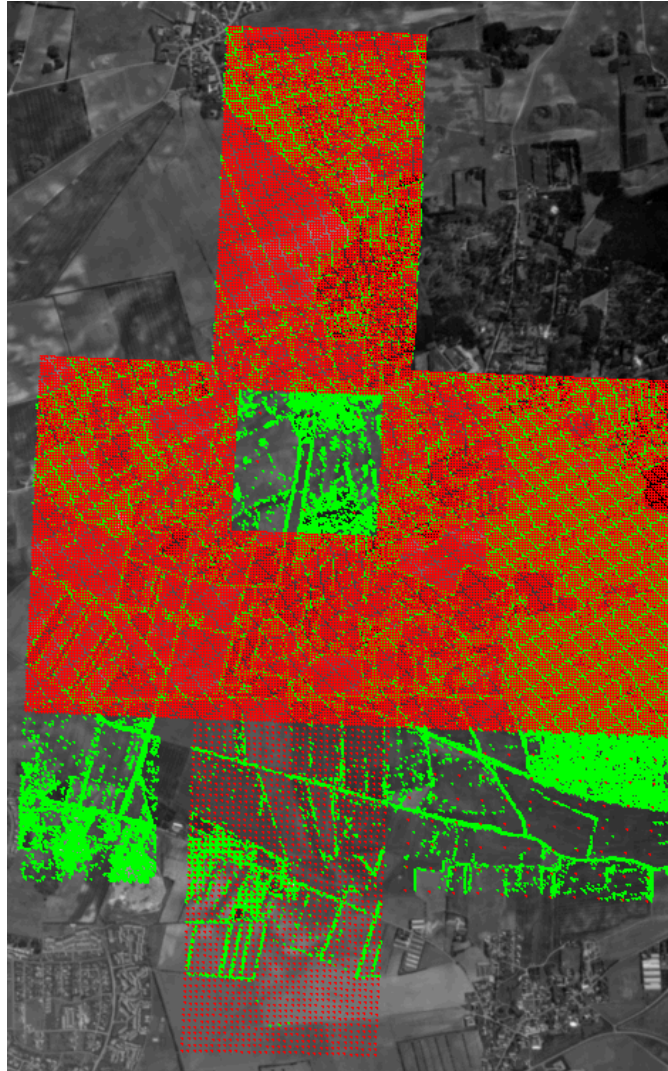


Figure 6.2: The result of the online function for the model 161162 with the resolution $30\ \mu\text{m}$ and mesh size $12.5 \times 12.5\ \text{m}$.

These examples create the suspicion that the generated grids are not always uniform, or that the calculation has stopped in mid-course. If the examples shown are representative of the quality and uniformity of the grids generated automatically by Match-T, there is cause for deep concern.

This leads to an investigation into the uniformity and completeness of the grid files. The files must have the same size, when the same scale and mesh size are used. For example, the files with scale 1:25,000, resolution $15\ \mu\text{m}$ and mesh size $25 \times 25\ \text{m}$ must have the same size as the files with scale 1:25,000, resolution $30\ \mu\text{m}$ and $60\ \mu\text{m}$ and mesh size $25 \times 25\ \text{m}$, as they include the same number of grid points. By comparing the size of the files, it is discovered that those files which were expected to be of equal size, are not necessarily so. Table 6.2 shows the file sizes for scale 1:25,000.

Model and resolution	File size by mesh size		
	5 x 5 m	12.5 x 12.5 m	25 x 25 m
160161_15 μm	Cannot be calculated	2302 Kb	582 Kb
160161_30 μm		2984 Kb	686 Kb
160161_60 μm		2983 Kb	686 Kb
161162_15 μm		3257 Kb	821 Kb
161162_30 μm		3929 Kb	848 Kb
161162_60 μm		3929 Kb	848 Kb

Table 6.2: File sizes for models in scale 1:25,000.

It will be seen, from table 6.2, that the files which are expected to have the same size do not. For model 160161, the file sizes with equal mesh size should be the same, regardless of the resolution, and it appears from the table that this is not the case. Likewise, it will be seen that the file sizes for model 161162 are not the same, regardless of the resolution.

Appendix G includes a table where all the file sizes are indicated, and it is seen here that files expected to have the same size, regardless of scale and resolution, do not fulfil expectations. The different file sizes may have several causes, for instance that the calculation has stopped before it is finished, unequal mesh sizes, or that the generation is done over unequal area sizes.

6.1.2 Control of the file sizes

GeoCAD has been chosen as the visualisation tool for the investigation of whether the individual files are fully calculated and have acquired the wished-for mesh size. (GeoCAD is a Danish developed CAD programme for geometric data). This has entailed that not all results can be shown, as GeoCAD cannot handle very large data quantities. Therefore, there are only 16 plots in Appendix H, as three calculations could not be done, and eight could not be visualised.

It will be seen from the file plots that all calculations are finished, and that the grids have the required mesh sizes, just as they are, apparently, calculated over the required area. As it can thus be demonstrated that the calculations have the expected quality, the conclusion must be that Match-T's visualisation tool is not a reliable representation of the grid calculation, and that it cannot be used other than as a consultative visual indication of how far the calculation has run. This function will therefore not be discussed further in the project.

6.2 Analysis of the coding of the grid points

Can the codes indicate defective grid points?

A grid point is assigned a binary code with up to 8 different combination possibilities, for instance, a point may well be assigned the code 1 (the point is OK), and at the same time the code 6 (the point is located in an area which is supposed by Match-T to have a low texture). A closer description of what the individual codes indicate is found in Chapter 2, section 2.4.4. In the investigation of the usability of the codes to point out gross errors, it was chosen to divide the grid points into three groups:

- Grid points with only code 1 = OK
- Grid points with code 1 and an arbitrarily chosen other code = double code
- Grid points without a code = defective

The result of this analysis is found in Appendix H.

In figure 6.3 the result of the calculation for scale 1:25,000, resolution 15 μm and mesh size 12.5 x 12.5m with codes is shown. The generated grid points with code 1 = OK have been assigned a light grey colour, grid points with double code are shown in medium grey. The grid points which are estimated as defective, and therefore have no code, have been assigned the colour dark grey.

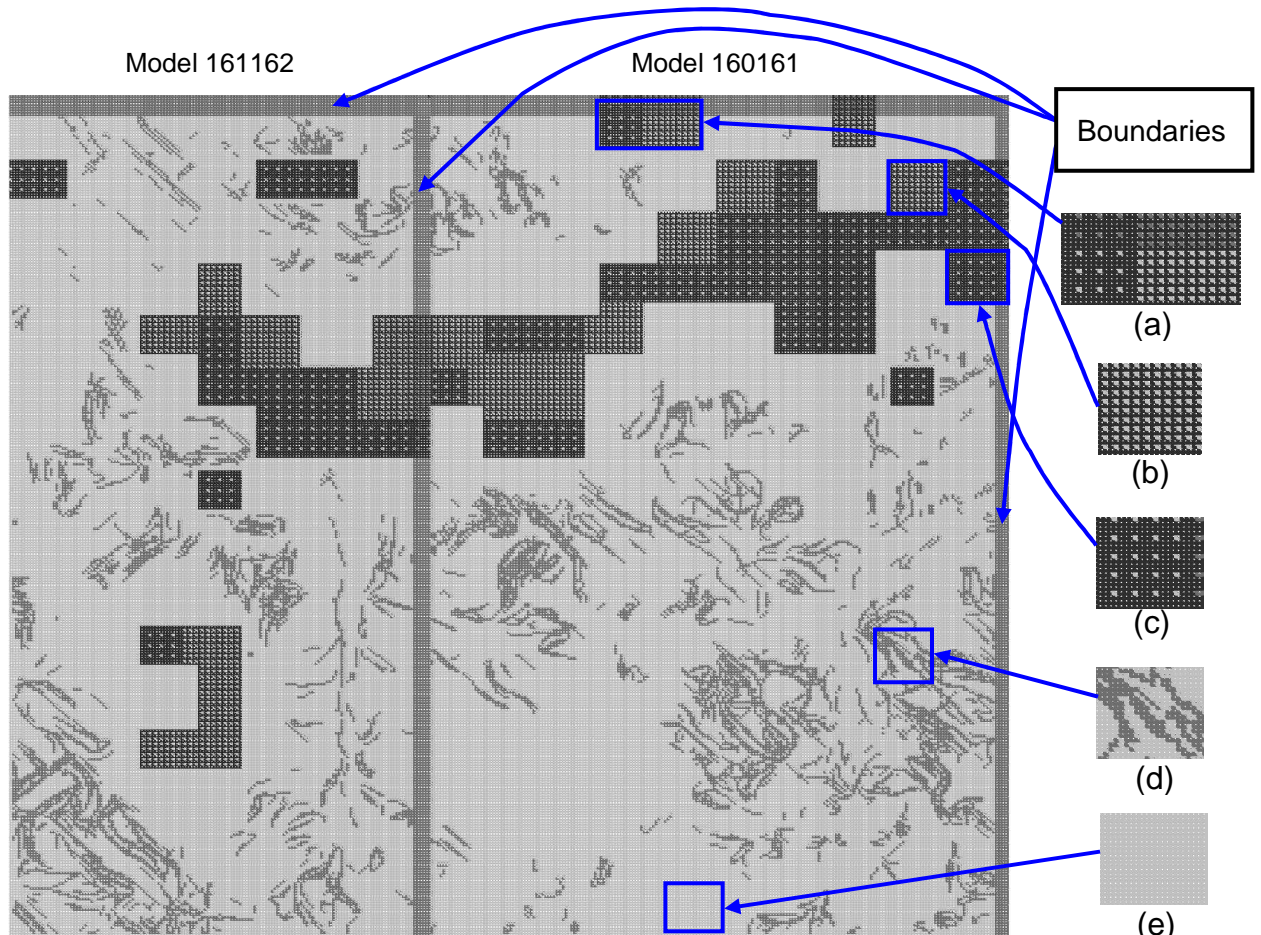
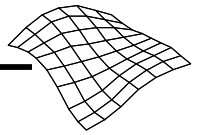


Figure 6.3: The result for 1:25,000, 15 μ m and 12.5 x 12.5 m. Grid points are indicated by codes, light grey = the grid point is OK, medium grey = grid point with double code, dark grey = the grid point is estimated as defective. Six types are emphasised, boundaries and the areas (a) – (e).

Figure 6.3 shows that there are different forms of coding. If figure 6.3 is subjected to a visual overview, four characteristics are demonstrated:

- 1) Boundaries are found along the model limits and along the northern edge.
- 2) The boundaries between points which are estimated as being defective (dark grey) appear in squares with varying interval points, and the boundaries are linear.
- 3) Grid points with a double code (medium grey) appear in a random pattern.
- 4) Areas with grid points estimated as OK are uniformly light grey.

Re 1):

On the background of a visual description, marked elements appear in the form of borders. A closer investigation of the borders between the models and along the northern edge has shown that elevation data in these borders has been assigned the code 3 (outside the area). A further examination showed that the keyed-in LL and UR delimitations have not been observed. This means that the assigned code is correct! But why Match-T has included the points, when these lie outside the limits of the desired area remains uncertain. This phenomenon is not a singular case, but is valid for all the 144 generated files, which are included in this project!

These extra points have also led to an overlap between the models which was not wanted. Therefore, it has been necessary to develop a small programme which cuts out this extra elevation data from the areas again, see Appendix D. After the cut-out of extra points, the file sizes were reduced and rendered uniform.

Re 2):

Grid points which are estimated as being defective (dark grey) appear in squares with varying intervals. Examples of this are shown for the areas (b) and (c). As regards area (b), every second point is estimated as being OK, for area (c), every fourth point is estimated as being OK. The possibility that errors in the data, caused by, for instance, a correlation error due to objects in the terrain, should appear in fixed squares is estimated as improbable. Objects in Denmark do not appear in fixed squares. Furthermore, there are grid points between the points which are defective, likewise in a fixed pattern which does not appear probable either.

In addition, there are areas where every other or every fourth point in a dark area has been assigned a double code. An example of this is seen in (a). Here, it is the code for the boundaries which "shines" through.

Re 3):

Grid points which have been assigned a double code (medium grey) appear in a random pattern. An example of this phenomenon is shown in (d). That grid points with a double code should appear in a random pattern seems probable, as this could, for instance, be a reproduction of objects in the terrain such as hedges, ditches etc.

Re 4):

In area (e), all the points have been estimated as being OK. These areas are as required.

The five different areas (a)-(e) are summed up in table 6.3.

Area	Description	Comments
(a)	Area where both every second and every fourth point have either the code = OK or a double code.	Improbable
(b)	Square where every second grid point has the code = defective and every second point the code = OK.	Improbable
(c)	Square where every fourth grid point has the code = OK, the rest the code = defective.	Improbable
(d)	Area where grid points with a double code appears in a random pattern.	Probable
(e)	Areas where all the points have the code = OK.	Probable

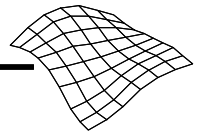
Table 6.3: Comments on the chosen areas.

6.2.1 Summation

In the chosen grid in scale 1:25,000, resolution 15 μ m and mesh size 12.5, there are many and large areas where the coding is improbable (a) – (c). If these codes indicate that there are errors in the grid points, it is grounds for great concern as regards the use of automatic generation of elevation data. Only the areas (d) and (e) show results which are probable, and are wanted by the user.

A look at all the results from Appendix H shows that the number of dark grey squares is diminished, when the mesh size is increased. As regards a few results with mesh size 25 x 25 m, there are no dark grey squares, while with mesh size 12.5 x 12.5 m, there are large areas with dark grey. This indicates that the determination of a grid point is best when a large mesh size is chosen, as there are several interest points to determine the individual grid point, which corresponds with the theory, cf. Chapter 2, section 2.4.3.2.

The next step in the preliminary investigation is to find out whether the assigned codes are actually able to indicate gross errors in the data material. Before this can be done, possible gross errors must be identified and located. For this investigation, the frame of reference and the PIL programme are used. The PIL programme is self-developed specifically for this purpose, a detailed description of the PIL programme is found in Appendix C. By means of the frame of reference, possible gross errors can be identified and located, and thereby isolated.



6.3 Elimination of gross correlation errors

Gross errors in a generated grid can arise for two reasons, because of correlation errors or caused by objects on the ground. In this investigation, there will be no differentiation between the two types of error. The focus in the project is on creating a terrain model, which means that it is regarded as irrelevant whether the question is about a correlation error or a correct correlation which falls, for instance, on a roof. Both situations will be regarded as gross errors in this project.

Apart from the case that the grids may include gross errors, there will probably also be an offset, as the elevations are generated over the terrain. As an example, diagram 6.1. shows the distribution of the deviations between the grid and the frame of reference, calculated on the basis of the images in scale 1:25,000 with resolution 15 μm and mesh size 25 x 25m.

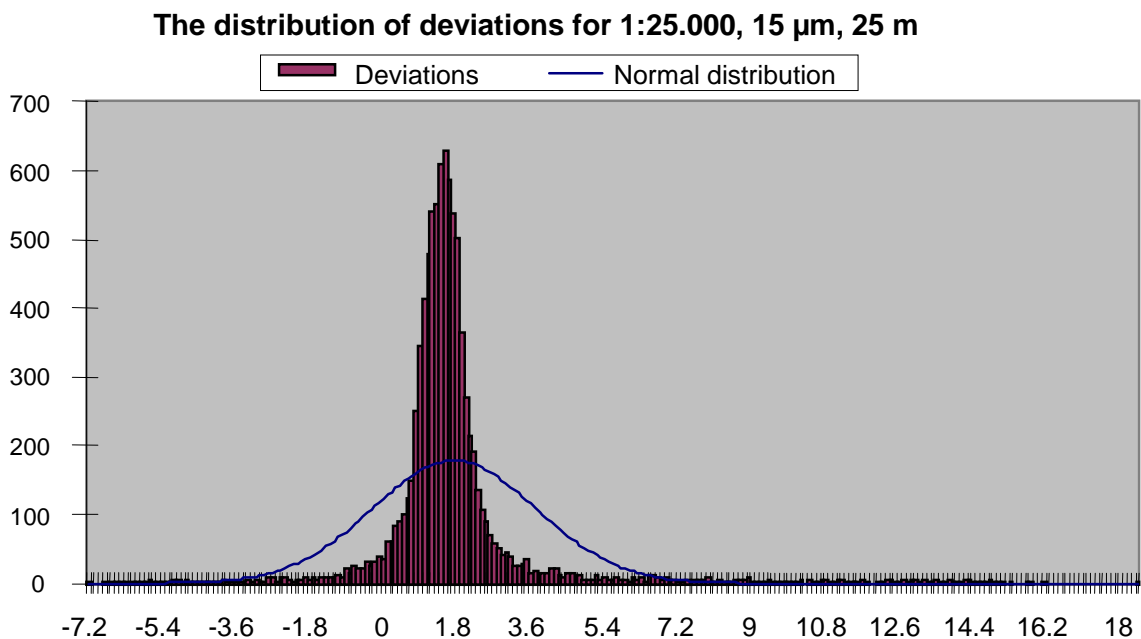


Diagram 6.1: The distribution of the deviations between the frame of reference and the generated grid for images in scale 1:25,000, resolution 15 μm and mesh size 25m with an approximated normal distribution.

As seen from diagram 6.1, the distribution of the deviations has an offset, as the distribution is not placed around zero. It can also be seen that the distribution has "long tails" which means that there are gross errors. The deviations are distributed between -7.2m and 17.8m .

The localisation of gross errors is based on the statistic assumption about normal distribution. If the observations are normally distributed, the following is valid: 68.3% of the points will be located within the 1 x accuracy (1 x Root Mean Square Error or RMSE), 95.4% of the points will be located within the 2 x RMSE, and 99.7% of the points will be located within the 3 x RMSE. If a calculation is normally distributed, a maximum of 0.3% of the good results will be located outside the 3 x RMSE.

The elimination of gross errors is done on the assumption that, if a result is normally distributed, all acceptable results will be located within the 3 x accuracy, and only 0.3% of the good results will be without this limit. This knowledge is used as an argument for the elimination of all deviations which are located outwith the 3 x RMSE. This is done by determining a threshold value, and then eliminating all deviations over the threshold value (numerically).

The elimination runs as an iterative process. At the first calculation, an accuracy is determined over all the deviations, called RMSE(1). At the second run, the threshold value is set at 3 x RMSE(1). At first all the deviations are moved, so that the error distribution is placed around 0. All deviations larger than 3 x RMSE(1) numerically are eliminated. A new accuracy, RMSE(2) is calculated on the basis of the remaining deviations. By the third calculation, the movement is repeated for a possible offset, 3 x RMSE(2) is used as threshold value, and a new accuracy is determined, RMSE(3). This RMSE(3) is used as thresh-

old value at the fourth calculation etc. until the whole process is stabilised, and no better accuracy can be achieved.

The idea was to use the PIL programme to investigate whether the result is normally distributed, and whether there are gross errors. The PIL programme is constructed so that reference points with a greater deviation than 3 x RMSE (level 3) are eliminated (see Appendix C). The chosen threshold value is therefore put in as level 3. By the first calculation in the iterative process, level 3 is chosen so high that all reference points will be included in the calculation. This is done by setting the threshold value (level 3) at 600m. The accuracy achieved from the first calculation is then used in the next calculation etc. etc.

It turned out to be very time-consuming to use the PIL programme for each individual intermediate calculation, so a macro was made in Excel, where the iteration process was run through, until the process was stabilised. The finally achieved 3 x RMSE has then been used as a threshold value in the PIL programme, whereby all the necessary output files are generated for a later analysis.

This process is run through for all the desired combinations as regards scale, resolution and mesh size. As an example of the course of the process, the calculation of images in scale 1:25,000 with the resolution 15 μ m and the mesh size 25 x 25m will be gone through in this chapter.

The remainder of the results are found in Appendix I.

6.3.1 The iteration process

It can be seen from diagram 6.1 that the distribution of the deviations is not normal. There is an offset, and the distribution has "long tails". It appears from a cut from the analysis file, generated by the PIL programme (see table 6.4) that the offset is 1.78m (mean), and the accuracy (RMSE) over all points is 2.68m. This accuracy includes gross errors. It appears from table 6.4 that 8956 points are included in the analysis. The remaining information is found in Appendix I.

1:25,000_15 μ m_25 m	Result from the first iteration done with all points
Mean (m)	1.78 m
RMSE (m)	2.68 m
Number of reference points	8956

Table 6.4: Values from the analysis file for deviations between the frame of reference and the generated grid for images in scale 1:25,000, resolution 15 μ m and mesh size 25 x 25m.

For each calculation in the iterative process (except the first), the values are shifted so that the error distribution is placed around 0.

The values used as threshold value for gross errors are found by taking the numerical value of the accuracy from the previous calculation and multiplying this value by 3 etc., etc. In diagram 6.2, the iteration process is presented graphically.

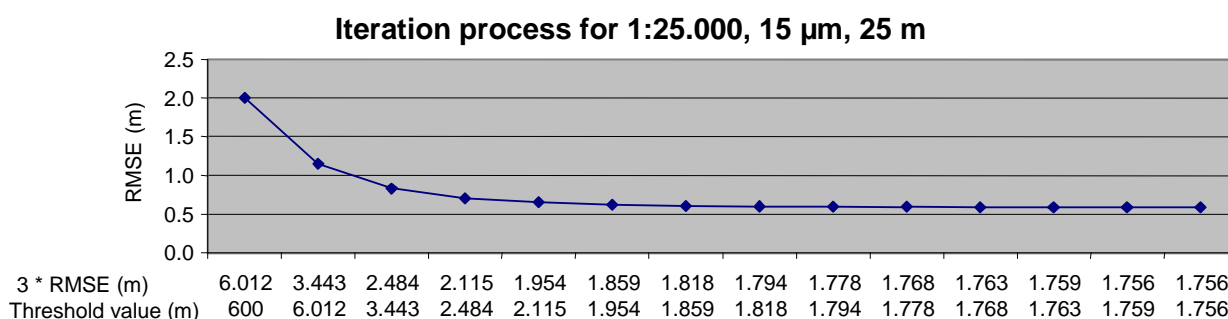


Diagram 6.2: Accuracy and threshold value for the calculations in the iteration process for images in scale 1:25,000, resolution 15 μ m and mesh size 25 x 25 m.

As can be seen from diagram 6.2, the accuracy has not changed between the two last calculations, the iteration has thus stabilised itself, and no more calculations are done. This means that the grid generated on the basis of images in scale 1:25,000, resolution 15 μ m and mesh size 25 x 25m has shifted 1.50m and has an accuracy of 0.585m (1,756m:3), when gross errors are edited out.

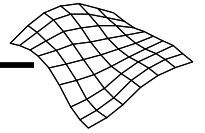


Diagram 6.3 shows the deviations without gross errors between the reference points and the grid with a normal distribution graph determined from the accuracy and the mean value.

Distribution of deviations after elimination of gross errors for image 1:25,000, 15 μm , 25 x 25 m

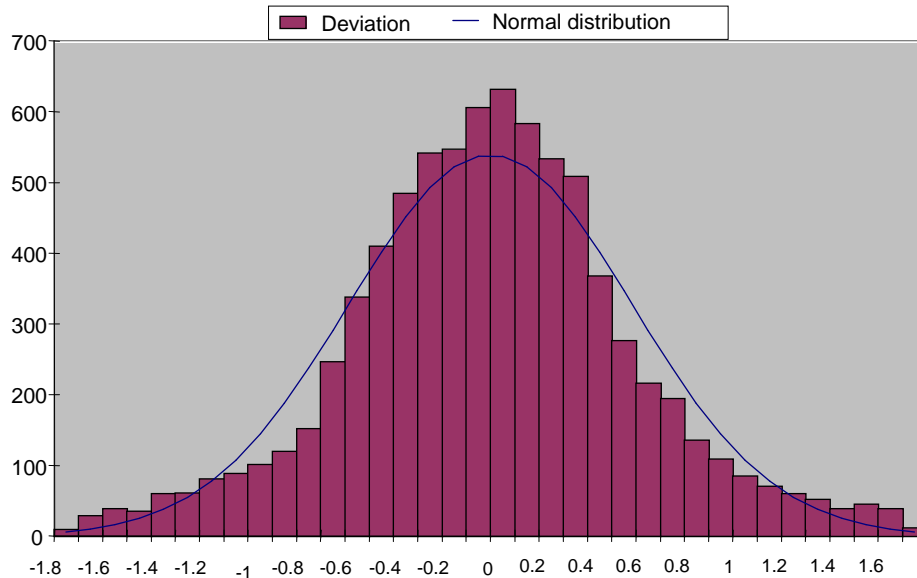


Diagram 6.3: The normal distribution graph for the deviations for images 1:25,000, resolution 15 μm and mesh size 25 x 25m after elimination of gross errors.

As will be seen from diagram 6.3, the result after the iteration process is, approximately, a normal distribution.

In this section only one example of the iterative process has been shown. This process is repeated for all the results from the images in the three different scales, resolutions, and mesh sizes. All in all, 24 processes have been run through, as three calculations could not be accomplished.

This iteration process has shown that there are gross errors. These have been identified and located through the iteration process. Subsequently, it has been investigated whether there is a connection between Match-T's code indication and the location of the gross errors.

6.4 Use of codes for identification of gross errors

As described in Appendix C, the PIL programme generates different output files. Two of these output files can be compared with Match-T's code designations for each grid point. One of these output files includes deviations between the frame of reference and the points from the generated grid which lie within the 3 x RMSE. These deviations are indicated as error arrows, where the location and size of the error arrow indicate the size and location of the deviation. In addition, an output file is generated which includes the eliminated grid points with deviations greater than the 3 x RMSE. These eliminated points are indicated as green crosses. These two files will be used in the investigation of whether the assigned codes indicate problematic grid points (gross errors).

In order to investigate whether there is a connection between the assigned codes and the deviations between the frame of reference and the generated grids, the deviations are visualised over a background with code indications. The deviations within the 3 x RMSE are shown as red arrows, and the eliminated grid points with deviations greater than 3 x RMSE are shown as green crosses. In the example, the background is a reproduction of figure 6.3, the result for scale 1:25,000, resolution 15 μm and mesh size 12.5 x 12.5m where the boundaries are erased.

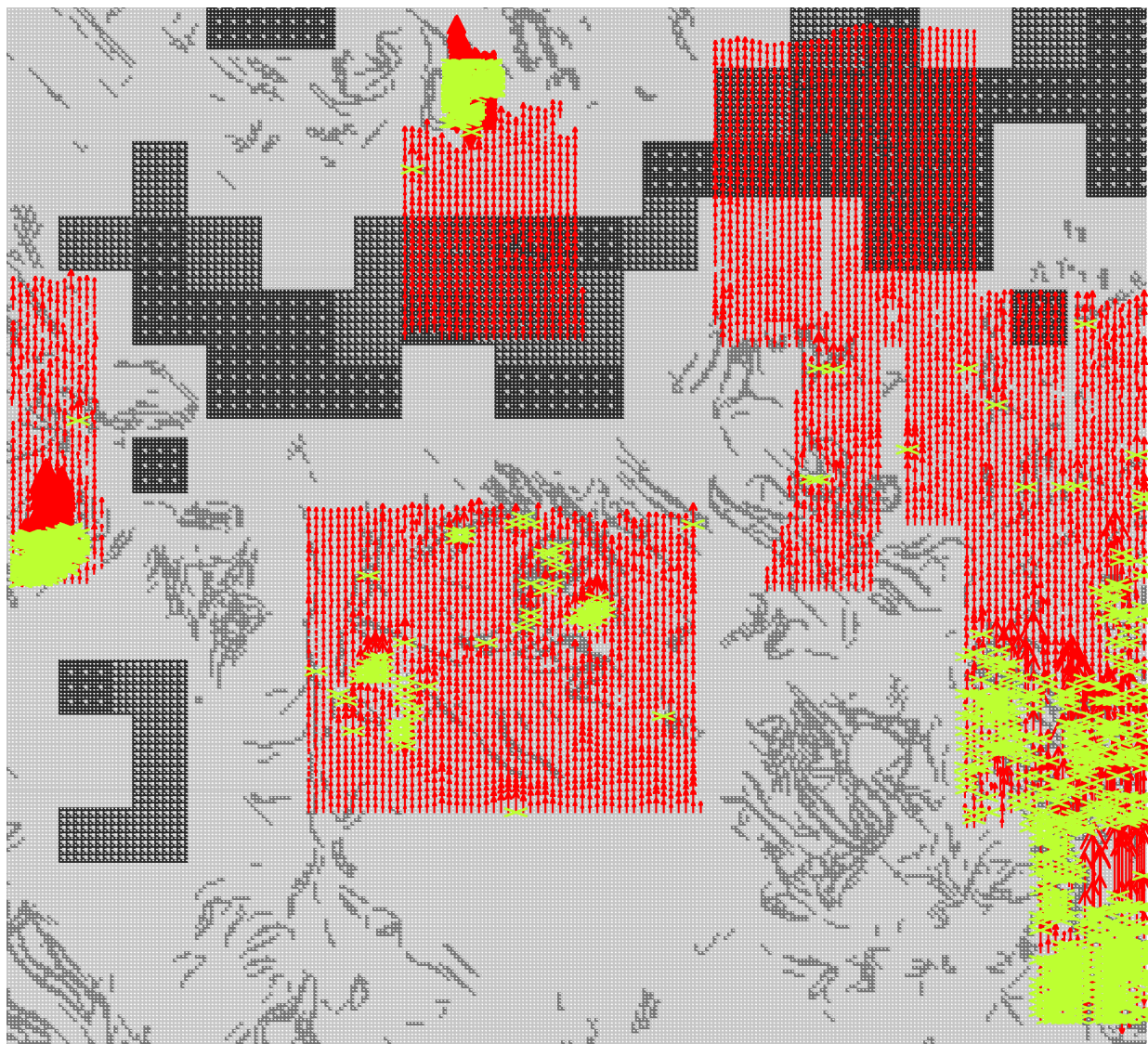
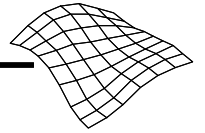


Figure 6.4: The result of the code indication for images in scale 1:25,000, resolution 15 μ m and mesh size 12.5 x 12.5 m, where the error arrows (red) and the eliminated points (green) have been superimposed.

It is quite clear from figure 6.4 that the areas which have been indicated by Match-T as problematic (dark grey), are in fact not so. In these areas, the red error arrows, indicating the deviation, are small, and no grid points are eliminated (green crosses). On the other hand, there are large error arrows and eliminated points (crosses), particularly in three areas which Match-T indicates as being OK (light grey) or OK with code (medium grey).

This investigation has not taken a closer look at the individual codes included in the medium grey colour, but determined that the point has been accepted. These grid points will therefore be treated equally with grid points with the code OK. This choice has been made to limit the investigation and thus make it more easy to assess.

This investigation is done for all the automatic generated grids. The remaining results can be found in Appendix J. It is seen from figure 6.4 and the results in Appendix J that the code indications in their present form are not adequate as editing tools. A closer investigation of how these post-processing tools can be improved is estimated to be a project on its own, as the point of departure for this project is to take a closer look at the accuracy which can be achieved with Match-T.



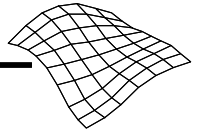
6.5 Partial conclusion

In this chapter a pre-analysis/control of the automatically generated elevation data has been done. The result shows that the chosen tools cannot be used as evaluation tools for the quality/accuracy of the generated grids. The visual tool "graphic online" is not reliable, and can, therefore, only be used as a comfortable indication of how far the calculation has come. But even this must be taken with reservations, as the visual result may well show that the calculation has stopped in mid-process, which later turned out not to be the case, as all calculations, which it has been possible to carry through, have in fact, been carried all the way through. The visual tool can only be used to have "something nice" on the screen, while the calculation runs.

Investigation of the grids showed that the files are complete and have the required mesh size. An examination of the binary codes showed the codes to the grid co-ordinates to be partly useful, as these indicated that unwanted boundaries had been included around each model and these could be located and eliminated. However, the code indication showed that grid points with the code defective appear in fixed squares. This is estimated improbable.

The investigation where the reference grid was included showed that there are gross errors in the generated grids. Unfortunately, the crosses showed that the gross errors are not located where Match-T has given grid points with the code defective. It must be concluded that the coding of the grid points is useful for locating boundaries but not for locating gross errors, thus improving the quality of the generated grids.

In Denmark, a new digital LIDAR elevation model is in the process of being produced but, the problem with the updating of the elevations by the method of automatic generation is still valid. The gross errors are the all-important problem. If the method of generating elevation data automatically from digital images is to be used to create elevation data for updating purposes as good, or nearly as good, as the LIDAR method, the gross errors must be located and eliminated, preferably automatically. The tools which have been examined cannot be used for this, which leaves the investigation in a type of vacuum. Consequently, the original ideas about parameters which might have an influence on the quality and accuracy will be referred to. A closer look will be done into what the influence of scale, pixel size, mesh size and landscape type might have, in order to see whether it is possible to improve the quality and the accuracy by means of these parameters.



7 The investigation

The purpose of this chapter is to examine whether scale, pixel and mesh size and different landscape types have an influence on the accuracy of automatically generated grids.

This whole investigation is concerned with the accuracy of the grid points. These grid points are determined from the interest points, cf. Chapter 2, section 2.4.3.2. The optimal would be to look directly at the elevations of the interest points to estimate whether possible errors are due to a correlation error or an object in the terrain. However, as the interest points are not accessible, it is only the accuracy of the grid points which can be estimated.

In Chapter 6 it turned out that there are gross errors in all the generated grids. Therefore, the results achieved are presented with gross errors, and then after elimination of the gross errors. Furthermore, it is briefly noted, how great a percentage of the grid points it is necessary to eliminate, before the iteration process has stabilised itself.

The investigations proposed in Chapter 3 will be referred to again, to ascertain what influence, the scale, pixel and mesh size have on the final result. As all reference points are coded (cf. Appendix B, section B.1.4), it is also possible to determine which landscape types contribute the most to the gross errors, and the location of such landscape types.

This will occasion altogether four investigations:

- The influence of scale
- The influence of pixel size
- The influence of mesh size
- The influence of landscape type

See also figure 7.1.

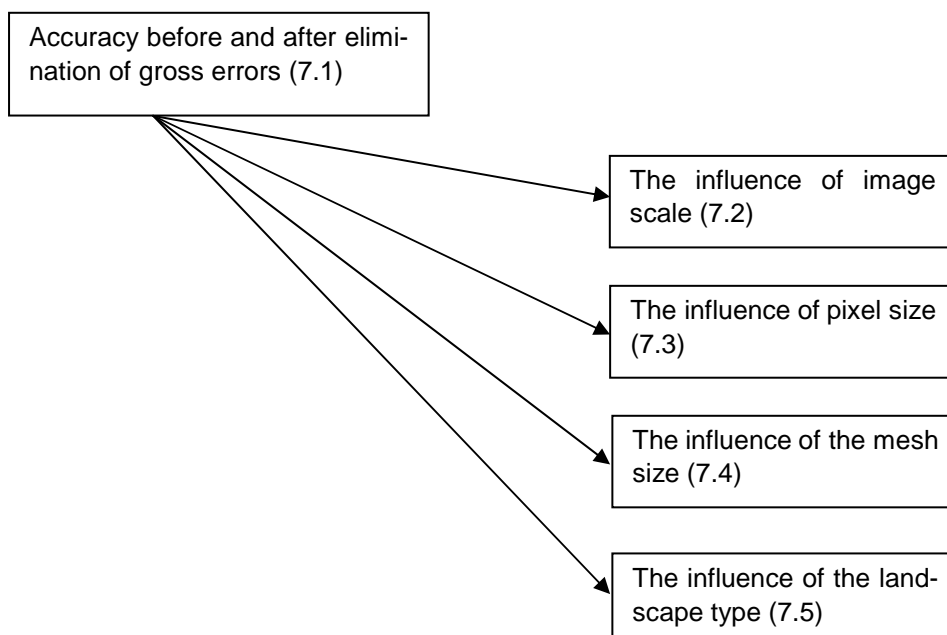


Figure 7.1: Planned investigations.

7.1 Accuracy before and after elimination of gross errors

When the different mesh sizes for the individual calculations were chosen, it was not noted that in Match-T there is a minimum mesh size in relation to scale and resolution. Even if a desired mesh size is keyed in, this size will not be used if it is below the minimum size, and one's attention is not drawn to this fact. Three of the desired grids are therefore not calculated.

These are:

- Scale 1:15,000, resolution 60 μm , mesh size 5 x 5 m
- Scale 1:25,000, resolution 30 μm , mesh size 5 x 5 m
- Scale 1:25,000, resolution 60 μm , mesh size 5 x 5 m

In addition, out of the remaining 24 calculations, 2 were unusually slow, these are:

- Scale 1:15,000, resolution 30 μm , mesh size 5 x 5 m
- Scale 1:25,000, resolution 60 μm , mesh size 12.5 x 12.5 m

As several different parameters are included in this investigation, one must take note that only results with the same parameter set-up can be compared. If, for instance, conclusions are to be drawn on the basis of the scale alone, only those images which have the same resolution and mesh size can be compared. Likewise, if conclusions are to be drawn on the basis of the resolution, only those images which have the same scale and mesh size can be compared.

7.1.1 Accuracy before elimination of gross errors

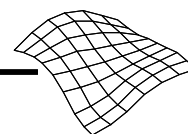
In the tables 7.1 – 7.3 the accuracy and percentage of the flight altitude for the "raw" calculations of the 24 grids are shown. In the "raw" calculation the generation is done over all the image without regard to landscape type or possible lack of texture in the images.

Images scale 1:5,000			
Resolution (μm)	Mesh size (m)	Accuracy (m)	‰ of flight altitude
15 μm	5 x 5 m	2.90 m	3.87‰
	12.5 x 12.5 m	3.23 m	4.30‰
	25 x 25 m	3.29 m	4.39‰
30 μm	5 x 5 m	2.19 m	2.92‰
	12.5 x 12.5 m	2.43 m	3.24‰
	25 x 25 m	2.87 m	3.83‰
60 μm	5 x 5 m	1.65 m	2.20‰
	12.5 x 12.5 m	1.95 m	2.60‰
	25 x 25 m	2.55 m	3.40‰

Table 7.1: The results, included gross errors for images in scale 1:5,000 at the three resolutions and mesh sizes.

Images scale 1:15,000			
Resolution (μm)	Mesh size (m)	Accuracy (m)	‰ of flight altitude
15 μm	5 x 5 m	1.93 m	0.86‰
	12.5 x 12.5 m	1.93 m	0.86‰
	25 x 25 m	2.07 m	0.92‰
30 μm	5 x 5 m	2.17 m	0.97‰
	12.5 x 12.5 m	1.90 m	0.84‰
	25 x 25 m	2.15 m	0.96‰
60 μm	5 x 5 m	Cannot be calculated!	
	12.5 x 12.5 m	1.93 m	0.87‰
	25 x 25 m	1.96 m	0.87‰

Table 7.2: The results, included gross errors for images in scale 1:15,000 at the three resolutions and mesh sizes.



Images scale 1:25,000			
Resolution (μm)	Mesh size (m)	Accuracy (m)	‰ of flight altitude
15 μm	5 x 5 m	1.27 m	0.34‰
	12.5 x 12.5 m	1.86 m	0.50‰
	25 x 25 m	2.00 m	0.53‰
30 μm	5 x 5 m	Cannot be calculated!	
	12.5 x 12.5 m	1.46 m	0.39‰
	25 x 25 m	2.37 m	0.63‰
60 μm	5 x 5 m	Cannot be calculated!	
	12.5 x 12.5 m	1.56 m	0.42‰
	25 x 25 m	1.98 m	0.53‰

Table 7.3: The results, included gross errors for images in scale 1:25,000 at the three resolutions and mesh sizes.

As seen from tables 7.1 – 7.3, the results are not very good, when a "raw" generation of the elevation data from digital images is done. Regardless of scale, pixel size or mesh size, the accuracy lies between approx. 1.3m to approx. 3.5m.

7.1.2 Accuracy after elimination of gross errors

For each calculation in the iterative process, more and more points are eliminated. It is therefore, interesting to see how many points it has been necessary to eliminate, before the iteration has stabilised itself. The gross errors are eliminated according to the principles described in Chapter 6, section 3. In the tables 7.4 – 7.6, the accuracy and the percentage of the flight altitude after elimination is shown, and the numbers of eliminated points are given as percentages.

Images scale 1 : 5,000				
Resolution (μm)	Mesh size (m)	Accuracy (m)	‰ of flight altitude	Eliminated points (%)
15 μm	5 x 5 m	0.11 m	0.14‰	18.7 %
	12.5 x 12.5 m	0.12 m	0.17‰	21.0 %
	25 x 25 m	0.18 m	0.25‰	24.3 %
30 μm	5 x 5 m	0.13 m	0.18‰	18.7 %
	12.5 x 12.5m	0.17 m	0.22‰	21.8 %
	25 x 25 m	0.22 m	0.30‰	22.9 %
60 μm	5 x 5 m	0.24 m	0.32‰	14.3 %
	12.5 x 12.5 m	0.24 m	0.33‰	16.3 %
	25 x 25m	0.31 m	0.41‰	19.8 %

Table 7.4: The results without gross errors for scale 1:5,000 at the three resolutions and mesh sizes. The number of eliminated points is given as a percentage.

Images scale 1 : 15,000				
Resolution (μm)	Mesh size (m)	Accuracy	‰ of flight altitude	Eliminated points (%)
15 μm	5 x 5 m	0.32 m	0.14‰	17.6 %
	12.5 x 12.5 m	0.33 m	0.15‰	18.7 %
	25 x 25 m	0.36 m	0.16‰	19.7 %
30 μm	5 x 5 m	0.53 m	0.24‰	14.0 %
	12.5 x 12.5 m	0.51 m	0.23‰	12.3 %
	25 x 25 m	0.57 m	0.25‰	25.3 %
60 μm	5 x 5 m	Cannot be calculated!		
	12.5 x 12.5 m	0.71 m	0.31‰	10.8 %
	25 x 25 m	0.80 m	0.35‰	10.7 %

Table 7.5: The results without gross errors for scale 1:15,000 at the three resolutions and mesh sizes. The number of eliminated points is given as a percentage.

Images scale 1 : 25,000				
Resolution (μm)	Mesh size (m)	Accuracy (m)	‰ of flight altitude	Eliminated points (%)
15 μm	5 x 5 m	0.53 m	0.14‰	44.1 %
	12.5 x 12.5 m	0.55 m	0.15‰	44.4 %
	25 x 25 m	0.59 m	0.16‰	36.1 %
30 μm	5 x 5 m	Cannot be calculated!		
	12.5 x 12.5 m	0.72 m	0.19‰	21.7 %
	25 x 25 m	0.78 m	0.21‰	20.6 %
60 μm	5 x 5 m	Cannot be calculated!		
	12.5 x 12.5 m	1.06 m	0.28‰	11.7 %
	25 x 25 m	0.93 m	0.25‰	17.9 %

Table 7.6: The results without gross errors for scale 1:25,000 at the three resolutions and mesh sizes. The number of eliminated points is given as a percentage.

7.1.3 Summation

At the "raw" calculation over the whole image, an accuracy is achieved from approx. 1.3m to more than 3 m, regardless of scale and resolution. It must therefore be concluded that there are elements in the data material which are not changed by the use of different scales or pixel sizes. These might, for instance, be objects on the terrain surface such as houses, trees etc. These objects should have been eliminated automatically by means of the principles described in Chapter 2, section 2.4.3.2. As mentioned before, this project will not differentiate between decided correlation errors or a correct correlation over an object in the terrain, such as houses, trees etc. Both kinds are regarded as gross errors. In a later investigation into landscape types, a closer discussion of the cause of the gross errors will be undertaken.

If a "raw" calculation is done without any kind of evaluation or editing in the images, the conclusion is that the flight altitude should be as high as possible, as this gives the best result.

If gross errors are eliminated, it will be seen from the results in tables 7.4 – 7.6 that for images with resolution 15 μm , an accuracy of between 0.14‰ and 0.17‰ of the flight altitude can be achieved regardless of scale, except for one result which is up to 0.25‰ of the flight altitude. For images with resolution 30 μm , the accuracy lies between 0.18‰ and 0.25‰ of the flight altitude regardless of scale. For images with resolution 60 μm , the accuracy lies between 0.25‰ and 0.41‰ of the flight altitude regardless of scale.

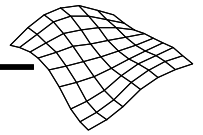
It will be seen that there is a large difference in how great a percentage it has been necessary to eliminate. For images with resolution 15 μm , it has been necessary to eliminate between approx. 14% and approx. 44 %, for 30 μm images approx. 20% are eliminated, whereas for images with resolution 60 μm , it has only been necessary to eliminate between approx. 11% and approx. 18% of the points.

The results in tables 7.4 – 7.6 are presented without any form of analysis of why the results are, as they are. It can, however, be briefly stated that the results have been considerably improved by the iterative process, and that there are quite a few gross errors in the data material. In the source material, included in the literary study of the project, there has been no indications or analyses of how many points must be regarded as gross errors, and consequently cannot be included in an analysis. How many points are in reality eliminated to achieve an accuracy of 0.1‰ of the flight altitude, as described in different sources, is therefore not known.

In the following sections, the results will be discussed more closely with regard to the scale and resolution of the images. In the three calculations which could not be carried out, the chosen mesh size was 5 x 5m. A closer look at the influence of the mesh size will therefore also be undertaken. When it has been investigated which influence the primary parameters (scale, resolution and mesh size) have, a closer look is taken at the cause of the gross errors, and where they are located in relation to the landscape type.

7.2 The influence of scale

One of the primary parameters in the method for automatic generation of elevations is, as mentioned before, the scale of the images. The optimal would be if the accuracy is approximately linear in relation to



the scale. That is, that the accuracy is improved, if images in large scale are used, and, vice versa, that the accuracy is reduced, if an image in a lesser scale is used. The result for images in scale 1:15,000 should theoretically be 3 times poorer than the result for images in scale 1:5,000. The result for images in scale 1:25,000 should be reduced by a factor 5 in relation to the results in scale 1:5,000.

Tables 7.4 – 7.6 show that the accuracy of images in scale 1:5,000 is improved by a factor approx. 2-3 in relation to the scale 1:15,000, whereas the accuracy for images in scale 1:5,000 is improved by a factor approx. 3-5 in relation to the result for images in scale 1:25,000.

The results from tables 7.4 – 7.6 are shown in diagram form in diagram 7.1. As a standard of comparison, the expected accuracy is 0.1‰ of the flight altitude [Krzystek et al., 1992].

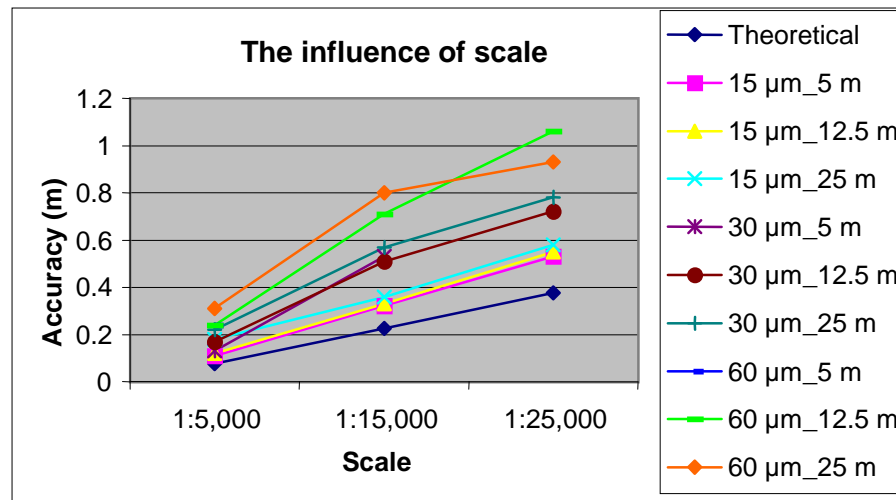


Diagram 7.1: The influence of scale on all calculations and the theoretically promised accuracy.

None of the results come close to the expected accuracy of 0.1‰ of the flight altitude. The results group themselves according to resolution, so that the results with resolutions 15µm, 30µm and 60µm respectively are grouped together.

The results from the use of the 15µm images are linear, and the result is, as expected, approx. 3 times better than the results for the images in scale 1:15,000, and 5 times better than the results from the images in scale 1:25,000. The same tendency can be recognised for images with the resolution 30µm and 60µm, the results are approximately linear, though with a small deflection at scale 1:15,000.

From a superior point of view, the best results are achieved by using a large scale. Likewise, it can be seen that the best results are achieved by using a small resolution, in this case 15µm, then 30µm and poorest by using 60µm, which is not surprising.

7.2.1 Summation of scale

This investigation shows that the scale has the expected influence. The best results are achieved by using images in a large scale, and the accuracy is linearly decreasing with a diminishing scale.

7.3 The influence of pixel size

In digital photogrammetry, aerial photos are scanned in different resolutions. Experience shows that the smaller the pixel size, the greater the accuracy which can be achieved. This is due, of course, to the fact that by using smaller pixel sizes, more details are included, and consequently, the accuracy of the automatically generated elevation model is better. It will be discussed here whether a better accuracy can be achieved by using a higher resolution and whether the improvement is linear.

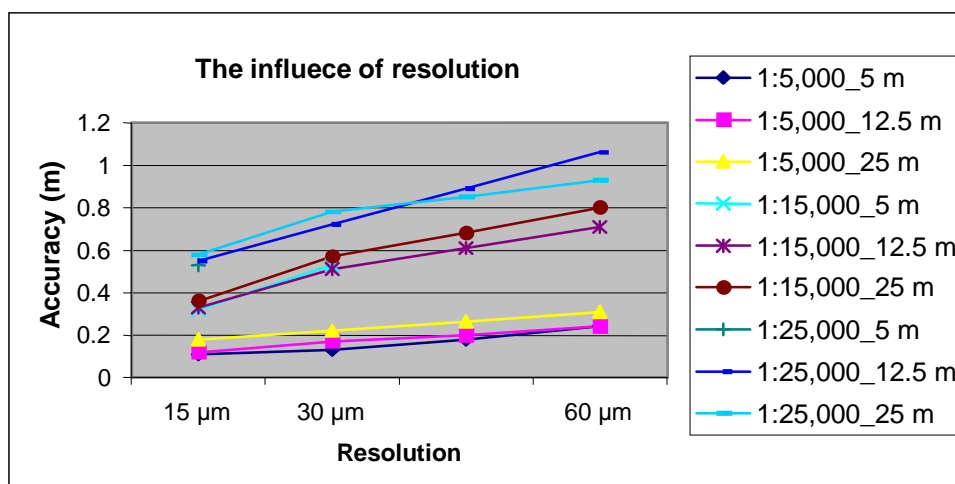


Diagram 7.2: The accuracy with regard to image resolution.

In diagram 7.2 the result can be seen for the three scales 1:5,000, 1:15,000 and 1:25,000 with the image resolutions 15µm, 30µm and 60µm, and the three mesh sizes 5 x 5 m, 12.5 x 12.5 m and 25 x 25m. The results come from tables 7.4 – 7.6.

It will be seen that the results using images in scale 1:5,000 are linear. For scales 1:15,000 and 1:25,000, the same tendencies are found, where the results are approximately linear. In addition, it can be seen that the results again fall into groups of 1:5,000, 1:15,000 and 1:25,000 respectively.

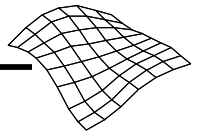
7.3.1 Summation of pixel size

After elimination of gross errors, a twice as good accuracy is achieved by 15µm images compared to 60µm images. To achieve this accuracy, however, it has been necessary to eliminate several more points in resolution 15µm than in resolution 60µm. It holds good for all three scales that significantly more points are eliminated by resolution 15µm than by resolution 60µm. This investigation must conclude that the greater the resolution and the fewer the number of points eliminated, the poorer the accuracy.

7.4 The influence of mesh size

The last of the primary parameters is the mesh size. The elevations of the interest points are determined by the correlation process. From the elevations of the interest points, the elevations of the grid points are interpolated. The determination of the grid points is, therefore, a purely mathematical process which is done on the basis of the elevations of the interest points and has nothing to do with the correlation process itself. The basis (the elevations of the interest points) for the determination of the elevations of the grid points remains unchanged for all mesh sizes.

This means that there should not be any appreciable difference in accuracy, regardless of which mesh size is chosen, taking into consideration the scale and resolution of the images. A grid with mesh size 5 x 5m will reproduce the terrain with more information, while a grid with mesh size 25 x 25m reproduces the terrain more softly. On the other hand, the individual grid points in the 25 x 25m grid are determined with a greater degree of accuracy, as more interest points will be included in the determination of these grid points than by mesh size 5 x 5m.



The influence of mesh size

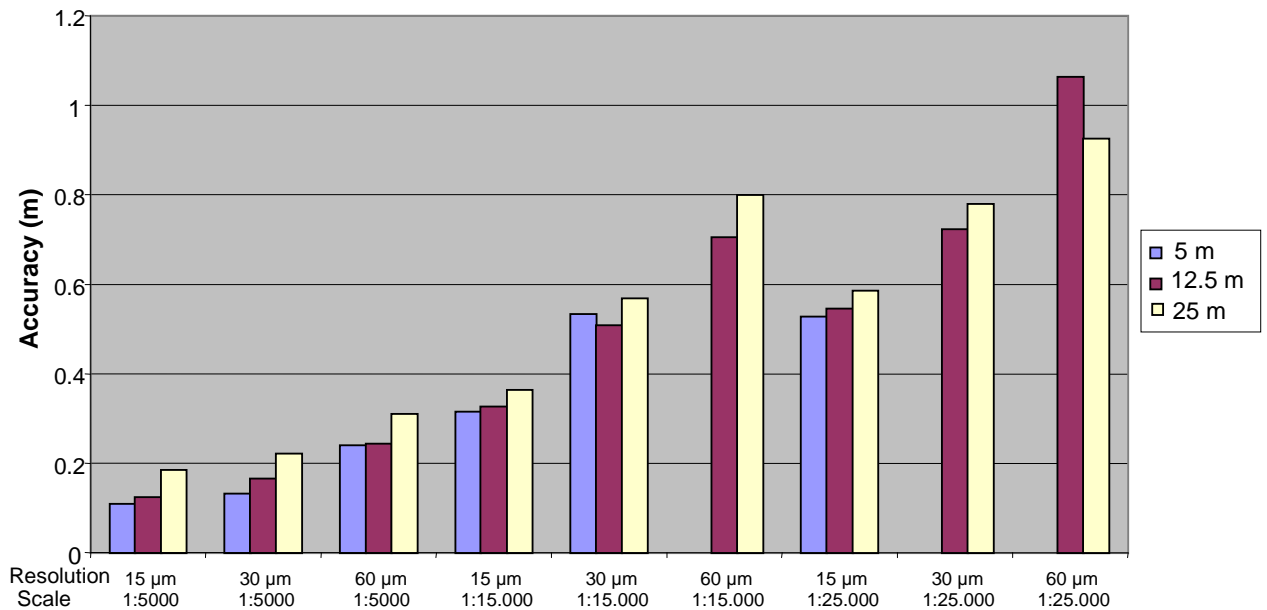


Diagram 7.3: Accuracy with regard to resolution and scale.

In diagram 7.3 the accuracy for the individual mesh sizes is shown. The missing columns in the diagram represent the three grids which could not be calculated. It can be seen that the mesh size has only a small influence, there is only a faint rise when the larger mesh size is chosen. Only two results deviate from this tendency. It is those for 1:15,000, 30µm and 5 x 5 m, and 1:25,000, 60µm and 12.5 x 12.5 m, where the results are poorer than the tendency.

7.4.1 Summation of mesh size

The mesh size does not have a significant influence. However, there is a small reduction in accuracy using a large mesh size. This conforms with expectations. A small mesh size reproduces the terrain with a greater degree of detail than a large mesh size. A grid with large mesh size reproduces the terrain more softly, while the accuracy must be expected to be a little poorer than when using a small mesh size.

7.4.2 Common conclusion

Looking at the results shown in diagram 7.1 and 7.2 where images with different scales and resolution are shown, it can be concluded that the best results are achieved by using a large scale and a small resolution. The results are linear as expected, and they group themselves according to resolution, see diagram 7.1 or according to scale, see diagram 7.2.

The calculations for 1:15,000, 30µm and 5 x 5m and those for 1:25,000, 60µm and 12.5 x 12.5m deviate from the tendency. These two results correspond to these two calculations which ran slower compared to the remaining calculations. This leads to an investigation into whether there is a limit to how few pixels on the ground may be found per mesh size for a calculation to run without hitch.

It is seen again that the scale has an influence, as a better accuracy is achieved by using a small scale and a low resolution than a large scale and a low resolution.

7.4.3 The pixel size on the ground

Approximately the same accuracy is achieved by using a large scale and a low resolution as by using a smaller scale and a higher resolution, for example 1:15,000 and 30µm, and 1:25,000 and 15µm. This suggests that the scale of the images and their resolution should be regarded each on its own, but that the parameters are influenced by each other. This means that it is not the specific scale and resolution of the individual images which are important, but how great an area the individual pixel covers on the ground. This size, henceforth called "pixel size on the ground" is dependent on the scale of the images combined with their resolution.

In table 7.7 the results achieved in relation to the pixel size on the ground are shown.

Scale	Resolution	Pixel size on the ground (m ²)	Accuracy by mesh size		
			5 x 5 m	12.5 x 12.5 m	25 x 25 m
1:5,000	15µm	0.075	0.11 m	0.12 m	0.18 m
	30µm	0.15	0.13 m	0.17 m	0.22 m
	60µm	0.30	0.24 m	0.22 m	0.31 m
1:15,000	15µm	0.225	0.32 m	0.33 m	0.36 m
	30µm	0.45	0.53 m	0.51 m	0.57 m
	60µm	0.90	/	0.71 m	0.80 m
1:25,000	15µm	0.375	0.53 m	0.55 m	0.59 m
	30µm	0.75	/	0.72 m	0.78 m
	60µm	1.50	/	1.06 m	0.93 m

Table 7.7: The results as a function of the pixel size on the ground and the mesh size.

7.4.4 The number of pixels per mesh size

When the investigations are evaluated as to scale, resolution and mesh size, it turns out that there is a connection between the three primary parameters. For instance, it makes no sense to determine an elevation model with the mesh size 5 x 5 m, if a pixel size on the ground covers, for example, 3 x 3m.

The number of pixel sizes on the ground per mesh size is determined thus:

$$\text{number of pixels} = \left(\frac{g}{\mu * M} \right)^2 \quad (7.1)$$

where: number_pixels = the number of pixels on the ground per mesh
g = the mesh size (grid)
µ = the resolution of the images
m = the scale of the images

In tables 7.8 – 7.10, the number of pixels on the ground per mesh is shown. The number is calculated for each scale. The relation is indicated with the colours green, yellow and red. In tables 7.8 – 7.10, the calculations which have gone well are marked with green. The calculations marked with yellow have been done without warning from Match-T that the results deviate from the tendency. It was marked, however, that the calculation, itself, ran slower than expected. Calculations which could not be done are marked with red.

Image scale 1:5,000			
Resolution	5 x 5 m	12.5 x 12.5 m	25 x 25 m
15µm	~ 67 x 67	~ 167 x 167	~ 333 x 333
30µm	~ 33 x 33	~ 83 x 83	~ 167 x 167
60µm	~ 17 x 17	~ 42 x 42	~ 83 x 83

Table 7.8: Number of pixels per mesh by different resolutions and mesh sizes in scale 1:5,000.

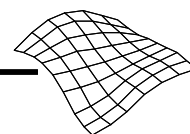


Image scale 1:15,000			
Resolution	5 x 5 m	12.5 x 12.5 m	25 x 25 m
15µm	~ 22 x 22	~ 56 x 56	~ 111 x 111
30µm	~ 11 x 11	~ 28 x 28	~ 56 x 56
60µm	~ 6 x 6	~ 14 x 14	~ 28 x 28

Table 7.9: Number of pixels per mesh by different resolutions and mesh sizes in scale 1:15,000.

Image scale 1:25,000			
Resolution	5 x 5 m	12.5 x 12.5 m	25 x 25 m
15µm	~ 13 x 13	~ 33 x 33	~ 67 x 67
30µm	~ 7 x 7	~ 17 x 17	~ 33 x 33
60µm	~ 3 x 3	~ 8 x 8	~ 17 x 17

Table 7.10: Number of pixels per mesh by different resolutions and mesh sizes in scale 1:25,000.

It will be seen from tables 7.8 – 7.10 that if the number of pixels per mesh size is greater than approx. 13 x 13 pixels, the calculation runs without problems. If the number of pixels per mesh size lies between approx. 8 x 8 pixels, and approx. 11 x 11 pixels, a calculation can be done, but the result deviates from the tendency. If the number of pixels is lower than approx. 8 x 8 pixels per mesh size, a calculation cannot be done. This phenomenon is also confirmed in the sources, where it is mentioned [Inpho, 1994] that a calculation can be expected to run slower if there are less than 30 x 30 pixels per mesh. It is also mentioned by [Baltsavias, 1999] that it is recommended that there are 10 x 10 to 15 x 15 pixels per mesh.

This investigation shows that there should be at least 13 x 13 pixels per mesh size for a calculation to run smoothly, which falls within the recommendation from [Baltsavias, 1999] of $10^2 - 15^2$ pixels. If the minimum of approx. 13 x 13 pixels per mesh size is used, a calculation will run smoothly. However, it is recommended here that 15 x 15 pixels per mesh size is chosen, so that it is certain that a calculation can be done, see table 7.11.

Scale	Pixel size (µm)	Minimum mesh size (m)
1:5,000	15 x 15µm	1.125 x 1.125
1:5,000	30 x 30µm	2.25 x 2.25
1:5,000	60 x 60µm	4.5 x 4.5
1:15,000	15 x 15µm	3.375 x 3.375
1:15,000	30 x 30µm	6.75 x 6.75
1:15,000	60 x 60µm	13.5 x 13.5
1:25,000	15 x 15µm	6.625 x 6.625
1:25,000	30 x 30µm	11.25 x 11.25
1:25,000	60 x 60µm	22.5 x 22.5

Table 7.11: Minimum mesh size considering scale resolution.

The presumption is that with 15 x 15 pixels, Match-T can determine enough interest points to determine the grid points. A closer investigation of this is not possible, as the information concerning the accurate location and elevation of the interest points appear as a binary file. This file has not been accessible in this project. Therefore, it has not been possible to make a closer analysis of, for instance, the lack of interest points for the determination of a small mesh size as opposed to the resolution. The investigation done in this project has shown a tendency as regards which minimum mesh size can be expected to be serviceable with a certain scale and resolution.

If this knowledge is used on any given combination of scale, resolution and mesh size, it can be checked whether the calculation will run correctly, using formula 7.1. It must be noted, however, that even if the number of pixels per mesh size is over 15 x 15, this is no guarantee of a good result, but only of a smooth run of the calculation itself.

In order to come closer to the problem of gross errors, the landscape type will be investigated.

7.5 The influence of the landscape type

In this section the cause of the gross errors will be examined. The test area has been divided into five landscape types. This offers the possibility of investigating whether the gross errors are due to the individual landscape type over which the point is generated, or if the gross error is due to a correlation error. The number of reference points in the five landscape types are indicated here:

- Flat terrain = 2093 points
- Gravel pit = 2429 points
- Village = 1629 points
- Hilly terrain = 2814 points
- Woods = 1223 points

For a further description of the data material, see Chapter 4 and Appendix B.

In [Seyfert, 1995; Ackermann, 1996] it is stated that built-up and overgrown areas give rise to problems. To investigate this claim, a village and a wooded area have been included. In addition, areas with low or no texture may give problems by the correlation [Krzystek, 1991]. Denmark includes large areas of fields with low texture, wherefore this problem may well arise in large parts of the country. The problem will be examined in flat and hilly terrain, as the fields will typically be found here.

To begin with, it is investigated what accuracy can be achieved without any form of editing of the different landscape types. This makes it possible to see which landscape types contribute the largest number of gross errors, and hence which landscape types offer the best and poorest accuracy. Then the iteration process is done for each landscape type, and the accuracy is viewed after elimination of the gross errors. Again, it is investigated which landscape type contributes the best and poorest accuracy respectively. Finally, a closer look is taken at how great a percentage of points it has been necessary to eliminate from the individual landscape types, before the iteration process has stabilised itself.

7.5.1 The accuracy for different landscape types including gross errors

Tables 7.12 – 7.14 show the accuracy including gross errors for the individual landscape types using the three scales, resolutions and mesh sizes.

Image scale 1:5,000						
Resolution	Mesh size	The accuracy for landscape types <u>before</u> elimination of gross errors				
		Flat terrain	Gravel pit	Village	Hilly terrain	Woods
15µm	5 x 5 m	0.11 m	4.58 m	2.34 m	1.27 m	7.58 m
	12.5 x 12.5 m	0.12 m	5.33 m	2.85 m	1.84 m	9.03 m
	25 x 25 m	0.14 m	6.72 m	1.80 m	1.54 m	7.70 m
30µm	5 x 5 m	0.13 m	3.50 m	1.44 m	0.80 m	5.96 m
	12.5 x 12.5 m	0.12 m	4.86 m	1.69 m	1.25 m	4.47 m
	25 x 25 m	0.14 m	5.37 m	2.03 m	1.68 m	6.82 m
60µm	5 x 5 m	0.20 m	0.80 m	1.53 m	0.96 m	6.14 m
	12.5 x 12.5 m	0.19 m	4.46 m	0.72 m	0.61 m	4.37 m
	25 x 25 m	0.19 m	5.03 m	2.01 m	1.47 m	5.16 m

Table 7.12: The accuracy, including gross errors, for the individual landscape types for 1:5,000.

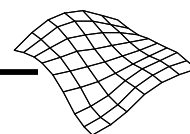


Image scale 1:15,000						
Resolution	Mesh size	The accuracy for landscape types <u>before</u> elimination of gross errors				
		Flat terrain	Gravel pit	Village	Hilly terrain	Woods
15µm	5 x 5 m	0.61 m	1.83 m	0.79 m	2.34 m	3.92 m
	12.5 x 12.5 m	0.59 m	3.05 m	0.68 m	1.02 m	4.02 m
	25 x 25 m	0.61 m	3.86 m	0.69 m	1.27 m	3.12 m
30µm	5 x 5 m	0.60 m	3.14 m	1.08 m	1.77 m	4.48 m
	12.5 x 12.5 m	0.56 m	2.09 m	0.90 m	1.60 m	4.29 m
	25 x 25 m	0.57 m	3.65 m	0.89 m	1.32 m	3.98 m
60µm	5 x 5 m	Cannot be calculated!				
	12.5 x 12.5 m	0.71 m	1.71 m	1.31 m	1.97 m	4.17 m
	25 x 25 m	0.70 m	2.43 m	1.30 m	1.70 m	3.99 m

Table 7.13: Accuracy, including gross errors, for the individual landscape types for scale 1:15,000.

Image scale 1:25,000						
Resolution	Mesh size	The accuracy for landscape types <u>before</u> elimination of gross errors				
		Flat terrain	Gravel pit	Village	Hilly terrain	Woods
15µm	5 x 5 m	1.61 m	1.18 m	1.79 m	1.92 m	4.02 m
	12.5 x 12.5 m	1.53 m	3.85 m	1.59 m	1.78 m	4.39 m
	25 x 25 m	1.53 m	4.21 m	1.56 m	2.01 m	3.87 m
30µm	5 x 5 m	Cannot be calculated!				
	12.5 x 12.5 m	1.50 m	2.49 m	1.90 m	2.00 m	3.93 m
	25 x 25 m	1.49 m	5.26 m	1.81 m	1.93 m	4.29 m
60µm	5 x 5 m	Cannot be calculated!				
	12.5 x 12.5 m	1.79 m	2.74 m	2.20 m	2.01 m	3.95 m
	25 x 25 m	1.76 m	4.38 m	2.14 m	1.96 m	3.76 m

Table 7.14: Accuracy, including gross errors, for the individual landscape types for scale 1:25,000.

In scale 1:5,000, it is obvious that the best results are achieved over open, flat terrain. The landscape types village and hilly terrain give relatively good results, while the landscape type gravel pit and woods give the poorest results.

Again in scale 1:15,000, the best results are achieved for the landscape type open, flat terrain, however, almost as good results are achieved for villages and hilly terrain. Again, it is in the landscape types woods and gravel pit, that the poorest results are achieved.

In scale 1:25,000, the difference in accuracy for the individual landscape types is not so marked as by scales 1:5,000 and 1:15,000. Here, the results are almost equally good over open, flat terrain and villages, closely followed by hilly terrain. Again, it is the landscape types woods and gravel pit, which are problematic.

A comparison of the three scales shows that in scale 1:5,000, either very good or very poor results are achieved. The results for open, flat terrain are very good compared with the results for images in scale 1:15,000 and 1:25,000. Likewise, the results for woods are much poorer in scale 1:5,000 than in 1:15,000 and 1:25,000. For images in scale 1:15,000, differences between the landscape types are evened out a little, and that also applies for the images in scale 1:25,000.

7.5.2 The accuracy for different landscape types excluding gross errors

Tables 7.15 – 7.17 show the accuracy achieved for the individual landscape types after the elimination of all gross errors.

Image scale 1:5,000						
Resolution	Mesh size	The accuracy for landscape types <u>after</u> elimination of gross errors				
		Flat terrain	Gravel pit	Village	Hilly terrain	Woods
15µm	5 x 5 m	0.09 m	0.19 m	0.21 m	0.09 m	0.18 m
	12.5 x 12.5 m	0.10 m	0.24 m	0.20 m	0.11 m	0.18 m
	25 x 25 m	0.12 m	0.27 m	0.24 m	0.19 m	0.30 m
30µm	5 x 5 m	0.11 m	0.25 m	0.14 m	0.11 m	0.24 m
	12.5 x 12.5 m	0.11 m	0.30 m	0.19 m	0.16 m	0.28 m
	25 x 25 m	0.14 m	0.34 m	0.24 m	0.24 m	0.36 m
60µm	5 x 5 m	0.17 m	0.28 m	0.35 m	0.22 m	0.40 m
	12.5 x 12.5 m	0.16 m	0.39 m	0.29 m	0.22 m	0.44 m
	25 x 25 m	0.18 m	0.57 m	0.34 m	0.32 m	0.49 m

Table 7.15: Accuracy for the five landscape types in scale 1:5,000 after elimination of gross errors.

Image scale 1:15,000						
Resolution	Mesh size	The accuracy for landscape types <u>after</u> elimination of gross errors				
		Flat terrain	Gravel pit	Village	Hilly terrain	Woods
15µm	5 x 5 m	0.28 m	0.36 m	0.31 m	0.29 m	0.53 m
	12.5 x 12.5 m	0.25 m	0.42 m	0.28 m	0.30 m	0.48 m
	25 x 25 m	0.27 m	0.51 m	0.31 m	0.35 m	0.44 m
30µm	5 x 5 m	0.36 m	0.64 m	0.55 m	0.46 m	0.82 m
	12.5 x 12.5 m	0.34 m	0.66 m	0.48 m	0.46 m	0.78 m
	25 x 25 m	0.36 m	0.74 m	0.51 m	0.55 m	0.76 m
60µm	5 x 5 m	Cannot be calculated!				
	12.5 x 12.5 m	0.39 m	0.92 m	0.65 m	0.65 m	1.02 m
	25 x 25 m	0.45 m	1.10 m	0.68 m	0.71 m	1.03 m

Table 7.16: Accuracy for the five landscape types in scale 1:15,000 after elimination of gross errors.

Image size 1:25,000						
Resolution	Mesh size	The accuracy for landscape types <u>after</u> elimination of gross errors				
		Flat terrain	Gravel pit	Village	Hilly terrain	Woods
15µm	5 x 5 m	0.42 m	0.51 m	0.51 m	0.53 m	0.69 m
	12.5 x 12.5 m	0.41 m	0.73 m	0.47 m	0.48 m	0.76 m
	25 x 25 m	0.41 m	0.80 m	0.48 m	0.57 m	0.75 m
30µm	5 x 5 m	Cannot be calculated!				
	12.5 x 12.5 m	0.49 m	1.01 m	0.67 m	0.66 m	0.96 m
	25 x 25 m	0.47 m	1.10 m	0.67 m	0.71 m	0.93 m
60µm	5 x 5 m	Cannot be calculated!				
	12.5 x 12.5 m	0.63 m	1.62 m	0.87 m	0.97 m	1.45 m
	25 x 25 m	0.54 m	1.31 m	0.85 m	0.91 m	1.24 m

Table 7.17: Accuracy for the five landscape types in scale 1:25,000 after elimination of gross errors.

Table 7.15 shows that in scale 1:5,000, the condition for achieving nearly the same accuracy, regardless of landscape type, is that gross errors are eliminated. However, the landscape types gravel pit and woods still achieve a slightly poorer result.

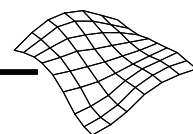


Table 7.16 shows that in scale 1:15,000, after the elimination of gross errors and with resolution 15 μ m, almost the same accuracy can be achieved for the landscape types flat and hilly terrain and village. Woods and gravel pit still achieve a slightly poorer result. For the resolutions 30 μ m and 60 μ m, the results for gravel pit and woods are considerably poorer compared to the three other landscape types.

Table 7.17 shows that with images in scale 1:25,000 and resolution 15 μ m, almost the same accuracy is achieved for four of the five landscape types after elimination of gross errors. Woods, however, still give rise to problems. For resolutions 30 μ m and 60 μ m, the best results are achieved in flat terrain. The accuracy is reduced for gravel pit and woods.

It can thus be concluded that the accuracy achieved is independent of the individual landscape types with resolution 15 μ m after elimination of gross errors. With resolutions 30 μ m and 60 μ m, the results for the landscape types woods and gravel pit are not so good when compared to open, flat terrain.

This means that there are many gross errors for the landscape types gravel pit and woods. It might therefore be interesting to see how great a percentage of the points it has been necessary to eliminate in the individual landscape types, before the iteration process stabilised itself.

7.5.3 Gross errors and the landscape type

Tables 7.18 – 7.20 show the number of points, indicated as a percentage within each landscape type, it has been necessary to eliminate, before the iteration process has stabilised itself.

Image scale 1:5,000						
Resolution	Mesh size	Percentage of eliminated points				
		Flat terrain	Gravel pit	Village	Hilly terrain	Woods
15 μ m	5 x 5 m	1.1 %	41.2 %	23.1 %	4.6 %	85.5 %
	12.5 x 12.5 m	1.0 %	59.3 %	24.3 %	8.7 %	87.8 %
	25 x 25 m	0.6 %	65.2 %	27.5 %	12.8 %	87.8 %
30 μ m	5 x 5 m	1.01 %	36.1 %	27.5 %	4.8 %	86.5 %
	12.5 x 12.5 m	0.2 %	53.3 %	22.7 %	8.8 %	82.4 %
	25 x 25 m	0.1 %	57.6 %	21.6 %	16.0 %	81.8 %
60 μ m	5 x 5 m	0.8 %	14.3 %	29.3 %	6.0 %	74.6 %
	12.5 x 12.5 m	0.5 %	44.9 %	16.4 %	5.3 %	85.0 %
	25 x 25 m	0.1 %	51.1 %	20.9 %	11.1 %	77.2 %

Table 7.18: Percentage of points eliminated by the iteration process for scale 1:5,000 and the landscape types.

Table 7.18 shows clearly that in open, flat and hilly terrain, it has not been necessary to eliminate very many points. For the landscape type village, between 25% and 30% of the points have been eliminated, whereas by far the greatest amount of points for the landscape types gravel pit and woods have had to be eliminated.

Image scale 1:15,000						
Resolution	Mesh size	Percentage of eliminated points				
		Flat terrain	Gravel pit	Village	Hilly terrain	Woods
15 μ m	5 x 5 m	7.5 %	19.6 %	15.4 %	14.7 %	42.7 %
	12.5 x 12.5 m	3.6 %	47.3 %	8.0 %	10.0 %	36.7 %
	25 x 25 m	2.9 %	52.3 %	6.0 %	11.7 %	36.0 %
30 μ m	5 x 5 m	1.3 %	21.3 %	11.2 %	6.6 %	50.0 %
	12.5 x 12.5 m	0.7 %	23.6 %	6.3 %	6.8 %	36.0 %
	25 x 25 m	0.7 %	34.1 %	3.4 %	8.4 %	33.9 %
60 μ m	5 x 5 m	Cannot be calculated!				
	12.5 x 12.5 m	0.9 %	14.4 %	6.6 %	6.0 %	40.1 %
	25 x 25 m	0.5 %	24.1 %	2.4 %	5.8 %	31.5 %

Table 7.19: Percentage of points eliminated by the iteration process for scale 1:15,000 and the landscape types.

Table 7.19 shows that it has not been necessary to eliminate very many points in flat terrain. For the landscape types village and hilly terrain, between approx. 1% and approx. 15% have been eliminated. Again, it has been necessary to eliminate large amounts of points for the landscape types gravel pit and woods, where the percentage lies from approx. 25% to approx. 50 %.

Image scale 1:25,000						
Resolution	Mesh size	Percentage of eliminated points				
		Flat terrain	Gravel pit	Village	Hilly terrain	Woods
15µm	5 x 5 m	42.2 %	14.8 %	48.0 %	54.7 %	47.2 %
	12.5 x 12.5 m	33.7 %	56.5 %	35.2 %	50.0 %	39.4 %
	25 x 25 m	21.4 %	54.5 %	24.0 %	39.8 %	39.3 %
30µm	5 x 5 m	Cannot be calculated!				
	12.5 x 12.5 m	6.8 %	30.6 %	25.9 %	20.4 %	38.0 %
	25 x 25 m	2.8 %	46.5 %	14.7 %	17.2 %	32.3 %
60µm	5 x 5 m	Cannot be calculated!				
	12.5 x 12.5 m	2.0 %	21.3 %	8.1 %	7.2 %	36.8 %
	25 x 25 m	3.4 %	37.7 %	14.6 %	12.0 %	37.1 %

Table 7.20: Percentage of points eliminated by the iteration process for scale 1:25,000 and the landscape types.

Table 7.20 shows that for images in scale 1:25,000 and resolution 15µm, it has been necessary to eliminate markedly more points for all landscape types compared to the two other resolutions. Furthermore, the degree of elimination is the same for all landscape types which is not the case for the other scales and resolution.

7.5.4 Summation for the landscape types

Tables 7.18 – 7.20 show that gross errors mainly occur in those areas where they are expected. In scales 1:5,000 and 1:15,000, the fewest gross errors are found in the landscape type open, flat terrain which is to be expected, as this area is flat without trees or buildings. In scale 1:25,000 and resolution 15µm, it has been necessary to eliminate markedly more points for all landscape types compared to the two other resolutions. It has not been possible to find an explanation for this phenomenon.

In the landscape type open, hilly terrain, quite a few unexpected gross errors occur. The area includes fields, a few hedges, smaller overgrown areas and a couple of farms with vegetation around them. The expectation was that these objects would be eliminated by Match-T.

In the landscape types gravel pit and woods, the largest amount of gross errors are eliminated which was to be expected. In the next section a closer look is taken at the causes of gross errors.

7.5.5 Correlation errors or objects in the terrain?

The PIL programme gives the option of visualising the deviations between the frame of reference and the generated grid as error arrows. Each landscape type has been assigned a colour. These are:

- Flat terrain = green
- Gravel pit = yellow/orange
- Village = red
- Hilly terrain = violet
- Woods = blue

The error arrows are designed so that negative deviations give a dark downwards pointing arrow, and positive deviations give a light upwards pointing arrow, an example is shown in figure 7.2.

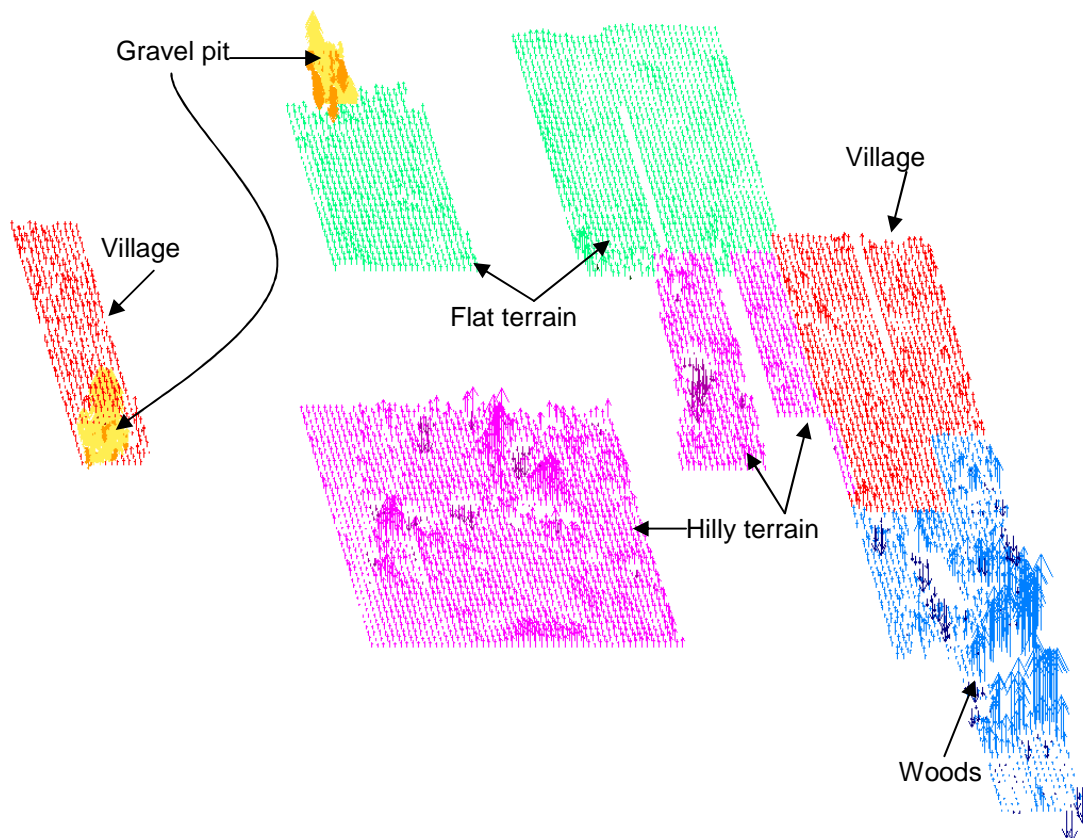
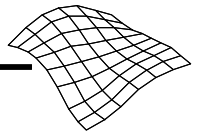


Figure 7.2: The error arrows show the deviation between the frame of reference and the generated grid. Pale colours indicate a positive error, dark colours a negative error. The error arrows are shifted, so that the starting and finishing point for the individual arrows do not adjoin.

Figure 7.2 shows that there are few gross errors in the landscape type open, flat terrain and village, whereas there are relatively many unforeseeable gross errors in the landscape type hilly terrain. There are many positive gross errors in the landscape type woods and a few negative ones.

By means of the error arrows generated by the analysis programme and an orthophoto, it is possible to make a closer analysis of where the errors are located, and whether it is a question of a correlation error or of objects in the terrain. This visualisation does not shift the error arrows, as their location after the shift will not fit in with the orthophotos.

The choice has been to take a closer look at two resolutions of images in scale 1:25,000, namely the results for the resolutions 15 μ m and 60 μ m. The choice is based on the fact that large gaps have appeared within each resolution in the number of points eliminated, and furthermore, that these two results differ from the tendency in the other images.

Tables 7.18 - 7.20 show that there are many gross errors in the landscape types woods, gravel pit and hilly terrain. The gross errors are symbolised by arrows. The arrows are here scaled up by a factor 20, so that they are easier to find. The result for scale 1:25,000, resolution 15 μ m and mesh size 25 x 25m is shown in figure 7.3.

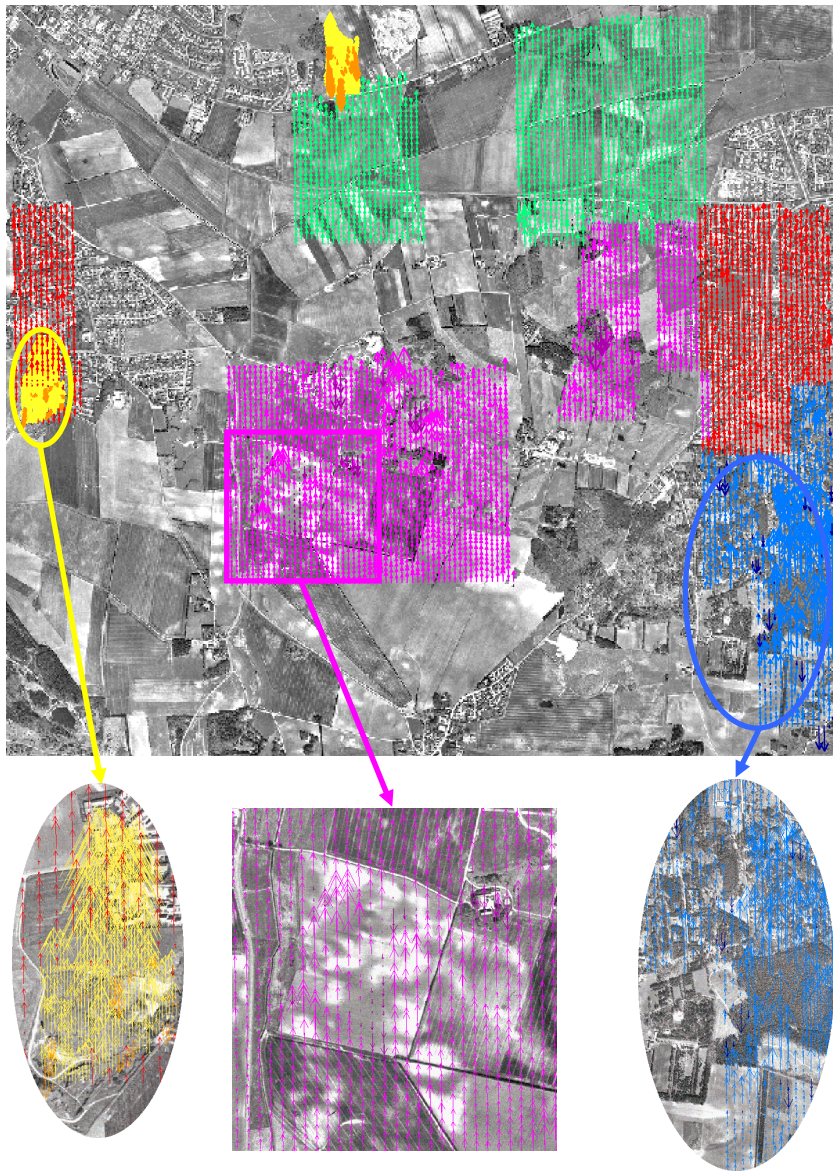


Figure 7.3: The differences between the generated grid in scale 1:25,000, resolution 15 μ m and mesh size 25 x 25m and the frame of reference are shown as arrows. Interesting areas have been extracted.

In figure 7.3 three areas have been extracted, a gravel pit (yellow), a part of the hilly terrain (violet) and a part of the woods (blue). In the chosen gravel pit there are very large error arrows. By far the most of the error arrows are positive, and only a few are negative. Here Match-T has not been able to extend the generation to the bottom of the gravel pit, but has finished by passing it over. In the landscape type hilly terrain there are also many gross errors. After a closer analysis of the error arrows over the orthophoto, it can be seen that a part of the gross errors are due to the farms with outbuildings and vegetation around. Here the automatic generation has not been able to eliminate these objects so that the grid returned to the terrain. Likewise, a field is seen which, due to the soil conditions, has assumed a funny pattern. Match-T regards this pattern as shifts in the terrain, but in reality, it is a gently sloping field without any kind of shifts.

The result of the automatic generation is as expected as regards the landscape type woods. It can be seen from the figure that there are many positive errors (large blue arrows), as the generation must have passed over the treetops.

The same areas as in figure 7.3 have been chosen in figure 7.4.

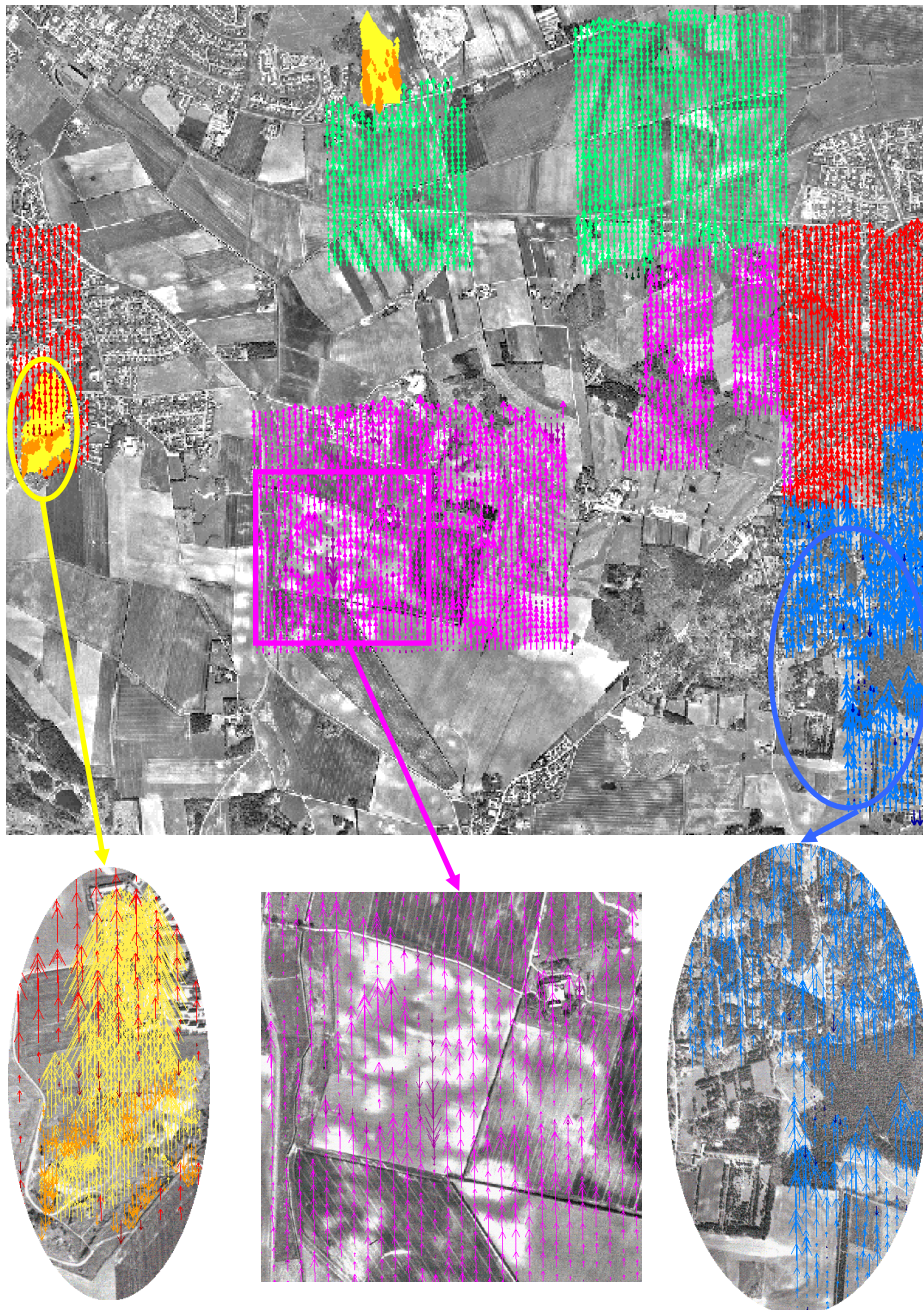
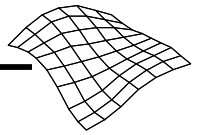


Figure 7.4: The differences between the generated grid in scale 1:25,000, resolution $60\text{ }\mu\text{m}$ and mesh size $25 \times 25\text{m}$ and the frame of reference are shown as arrows. Interesting areas have been extracted.

Figure 7.4 shows that the error arrows generally are much smaller for the whole area.

In the landscape types flat terrain (green), village (red) and hilly terrain (violet), the number of gross errors have fallen compared to the result for images with resolution $15\text{ }\mu\text{m}$ in figure 7.3. This can be seen from the small size of the arrows and from the fact that, in some places, there are holes within the landscape type, where the error arrows are too small to appear.

Generally seen, the error arrows for gravel pits and wooded areas are markedly smaller by resolution $60\text{ }\mu\text{m}$.

In the chosen areas, it will be seen that the error arrows are considerably smaller with a resolution of $60\text{ }\mu\text{m}$ than with $15\text{ }\mu\text{m}$. As regards the gravel pit, there are markedly fewer of the very large error arrows. Furthermore, there are both positive and negative error arrows which indicates that the generated grid in the resolution $60\text{ }\mu\text{m}$ has passed over as well as under the real terrain. In the landscape type woods, there are many positive errors (big blue arrows), as the grid has passed over the treetops as expected.

In general, it can be seen from the figures in Appendix K that the error arrows are large when using a high resolution. These error arrows are reduced by using a lower resolution. For images in scale 1:5,000, it is seen that the same area consisting of village and woods include very large error arrows for all the results, regardless of the image resolution or mesh size. A closer analysis shows that the area is covered by a model. Even if the results from this model are poor, they still show that the deviations are reduced by using a lower resolution.

7.5.6 Summation

A difference between the results for the 15 μ m and the 60 μ m images is seen within the flat area. For the 15 μ m images, all the error arrows are pale green which indicates that the generation passes over the terrain. For the images with resolution 60 μ m, the error arrows are both positive (pale green) and negative (dark green).

Gross errors within the landscape type open, flat terrain must be due to correlation errors, as there are no objects of any kind on the terrain. For images in scale 1:25,000 with resolution 15 μ m, the result is quite wrong. Why the correlation, in these images in particular, has gone wrong is not known.

That gravel pits should give problems is logical, as in this investigation the terrain type flat has been chosen for the whole image, and thereby a parallax bound of 3 pixels is used at the correlation. The gravel pits are very hilly with many steep slopes. If the generation in a gravel pit should have gone well, the terrain type for the generation should have been chosen as mountainous, whereby a parallax bound of 15 pixels would have been used for the correlation.

As regards the landscape type hilly terrain, there are also many gross errors. After a closer analysis of the error arrows over the orthophoto it is seen that there are several farms with outbuildings and vegetation around in the area. Here the automatic generation has not been able to eliminate these objects so that the grid returned to the terrain. This shows that Match-T is not able to eliminate objects if these form a small group, for instance, a farm with outbuildings and trees in a group. Likewise, a field is seen which, due to the soil conditions, appears in a funny pattern. These peculiarities are not foreseeable, and cannot therefore be considered beforehand. They must be characterised as freaks of nature! Match-T regards this pattern as terrain shifts, but in reality, as mentioned earlier, it represents a gently sloping field without any kind of shifts.

In woods there are many positive errors which is natural as the generated grid will pass over the treetops. The holes in, for instance, the landscape type woods are due to the fact that it has not been possible to see the terrain and thus, measure a reference point in a fixed grid, see Appendix B or Chapter 4. The images should have been taken before leafing foliation, but this was not done because of a difficult spring season. The grid therefore passes over not only coniferous but also deciduous trees.

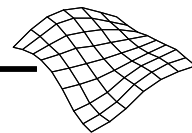
In scales 1:5,000 and 1:15,000, only a few percent of the grid points in the landscape type open, flat terrain are eliminated. This small percentage may be due to correlation errors, as there are no hedges or farms in this area. In scale 1:25,000 and resolution 15 μ m, it has proved necessary to eliminate markedly more points in all landscape types compared to the two other resolutions. It has not been possible to discover the cause of this phenomenon.

7.6 Partial conclusion

This investigation has shown that the Match-T method is not capable of eliminating all objects (trees or buildings) in the terrain. If it is not otherwise possible to eliminate any vegetation or buildings, an accuracy of between approx. 1.5m and 3.5m can be achieved, dependent on the flight altitude and the resolution of the images. If gross errors are not eliminated, there is a tendency that the accuracy improves the higher the altitude. If vegetation and buildings are removed, at best, an accuracy of 0.14‰ of the flight altitude can be achieved with images with resolution 15 μ m and mesh size 5 x 5m.

As a mean, 20% of the grid points must be eliminated to achieve these accuracies, though for images in scale 1:25,000 and resolution 15 μ m, the percentage is 40.

The investigation of the primary parameters have shown that the best results are achieved by using a large scale, and that the result is reduced linearly by using images in smaller scales, when the pixel size is maintained.



The investigation of the resolution shows that the best results are achieved by using a small pixel size. In a high resolution, for instance 15 μ m, a higher degree of detailed information in the images is achieved. This entails a better accuracy, but also more gross errors by the automatic generation of elevation data. A low resolution blurs the images and thus incurs a reduced information basis. This means that the elevation model is more "soft" without so many gross errors as with the 15 μ m images. The accuracy is linearly decreasing with the use of a lower resolution.

The mesh size does not have any significant influence. This concurs with the theory, as the determination of the grid points is a purely mathematical process which is done on the basis of the elevations of the interest points, and has nothing to do with the correlation process itself. The basis (the elevations of the interest points) of the determination of the elevations of the grid points in the elevation model will not be changed by the determination of any mesh size. However, a small mesh size will be determined on the basis of a smaller number of interest points. A grid with a small mesh size will reproduce the terrain with more information, while a grid with a large mesh size will reproduce the terrain more softly. On the other hand, the individual grid points in a large grid will be determined with greater accuracy, as more interest points will be included in the determination of these grid points than by a small mesh size. The essential aspect is the number of pixels on the ground, compared to the desired mesh size. This investigation shows that no less than 15 x 15 pixels per mesh should be used.

The investigation of the landscape types has shown that gross errors arise in the landscape types woods and gravel pit, regardless of the scale or resolution of the images. However, fewer gross errors are generated, when images with resolution 60 μ m rather than with resolution 15 μ m are used. As regards the landscape type gravel pit, there are fewer gross errors with resolution 60 μ m, and they are not so big. This phenomenon is also valid for the landscape type woods, where there are also fewer errors and the error arrows are not so large as by 15 μ m images. For areas within the hilly terrain, there are also "bare" spots, where the error arrows are small. The areas with many gross errors at the generation over the 15 μ m images have become considerably smaller, both in extent and size of the error arrows.

The investigation of the landscape types also shows that elevations automatically generated over gravel pits (steep slopes) or woods cannot be used. These areas should be edited before an automatic generation is done, regardless of scale and resolution. Generations over the landscape type village should not be done in large scales, for instance 1:5,000. In medium and small scales, good results are achieved for the landscape type village.

7.6.1 Experiences in table form

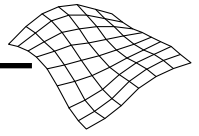
The essential aspect of the landscape type gravel pit is that it consists of steep slopes. To generalise the landscape types used in this project, the type gravel pit is therefore changed to the more generalised designation, steep slopes.

In Denmark, the scale 1:5,000 is traditionally used for technical mapping, and the scale 1:25,000 for nationwide mapping. Furthermore, the scale 1:15,000 has been included in this investigation.

If the experience gained in this project is set on table form in these three scales, the result shows as follows:

Image scale	Resolution	Minimum mesh size (m)	Landscape types				
			Flat Terrain	Steep slope	Village	Hilly terrain	Woods
1:5,000	15µm	1.125 x 1.125	X	/	/	X	/
	30µm	2.25 x 2.25	X	/	/	X	/
	60µm	4.5 x 4.5	X	/	/	X	/
1:15,000	15µm	3.375 x 3.375	X	/	X	X	/
	30µm	6.75 x 6.75	X	/	X	X	/
	60µm	13.5 x 13.5	X	/	X	X	/
1:25,000	15µm	6.625 x 6.625	X	/	X	X	/
	30µm	11.25 x 11.25	X	/	X	X	/
	60µm	22.5 x 22.5	X	/	X	X	/

Table 7.21: Recommended minimum mesh size for a given scale and resolution, and which landscape types can be recommended (x) or not recommended (/) for an automatic generation.



8 Results on the basis of Chapter 7

In this chapter, a closer look will be taken at the accuracy which can be achieved in the calculations, when taking into consideration the lessons learned in Chapter 7.

Even if quite a few gross errors are found in an automatic generation, for instance 30 %, it still means that 70% of the measuring has gone well. This implies that the method of automatic generation of elevations from digital images is still a relevant method for use in the Danish landscape. The question is, how the gross errors can be located. The experience learned from Chapter 7 shows that a part of the gross errors is due to the landscape type over which the automatic generation is done and that, in some of the calculations, there were not enough pixels per mesh. In this chapter, these experiences will be taken into consideration.

The first investigation is into which accuracy can be achieved by using the minimum mesh size, and excluding those landscape types which contribute to the greatest number of gross errors. Then it is investigated whether there are still gross errors in the remaining landscape types.

8.1 Exclusion of the landscape types

It can be concluded from section 7.6 that the landscape types can be divided into three groups. The landscape type open, flat terrain gives the best results, the intermediate group is the landscape types village and open, hilly terrain. The landscape types gravel pit and woods give the poorest results.

In this investigation, a closer look will be taken at which accuracy can be achieved by excluding the landscape types which contribute to the largest errors.

If the desire was only to look at those landscape types where the best results can be achieved, the generation should only be done over the open, flat terrain. Such a narrow choice of landscape types and thus, such a large exclusion of other landscape types, would reduce the area over which an automatic generation can be done. This implies that a great deal of manual editing work must be done in the images before a calculation can be done. Should such a thorough editing of the images be necessary before the automatic generation can be carried out, the method of automatic generation of elevations from digital images can no longer be assessed as a cheap and quick method with a minimum of manual work. If a large part of the image is excluded from the automatic generation, other methods for elevation determination must be included. This complicates and raises the price of the process of determining elevation data.

Gravel pits contribute with very large errors, but as gravel pits cover an insignificant part, and an exclusion of this landscape type is unimportant. If woods are excluded, the area will be reduced by approx. 20% of the total area of Denmark. From the beginning of the project, densely built-up areas and waters have been excluded, which corresponds to approx. 20% of the area of Denmark. This means that the area over which an automatic generation can be done is approx. 60% of the total Danish area.

As mentioned before, the choice has been to take a closer look at which accuracy can be achieved when taking into consideration the experience gained in Chapter 7. The criteria for the subsequent investigations are:

- Only those grids will be included which meet the requirement of a minimum of pixels per mesh size of approx. 15 x 15.
- The landscape types woods and gravel pit are excluded in all three scales. In scale 1:5,000, the landscape type village is also excluded.

The results are presented without gross errors.

8.1.1 Results without gross errors

The data material consists of the landscape types flat and hilly terrain for the images in scale 1:5,000. For the images in scale 1:15,000 and 1:25,000, the data material consists of the landscape types flat and hilly terrain and village. As the same landscape types are not included in all three scales, the results are presented in two tables. The iterative process described in section 6.3 is done to isolate the remaining gross errors. The results are shown in table 8.1 for scale 1:5,000, and in table 8.2 for scales 1:15,000 and 1:25,000 in metres and % of the flight altitude.

Resolution μ m	Mesh size	Accuracy	% of H for 1:5,000
15 μ m	5 x 5 m	0.08 m	0.11
	12.5 x 12.5 m	0.10 m	0.13
	25 x 25 m	0.16 m	0.21
30 μ m	5 x 5 m	0.10 m	0.13
	12.5 x 12.5 m	0.13 m	0.17
	25 x 25 m	0.18 m	0.24
60 μ m	5 x 5 m	0.17 m	0.23
	12.5 x 12.5m	0.17 m	0.23
	25 x 25 m	0.24 m	0.32

Table 8.1: The accuracy without gross errors for scale 1:5,000, the three resolutions and mesh sizes. The landscape types included are flat and hilly terrain.

Resolution	Mesh size	Accuracy for 1:15,000	% of H for 1:15,000	Accuracy for 1:25,000	% of H for 1:25,000
15 μ m	5 x 5 m	0.29 m	0.13 m	Should not be calculated!	
	12.5 x 12.5 m	0.27 m	0.12 m	0.42 m	0.11 m
	25 x 25 m	0.30 m	0.13 m	0.47 m	0.12 m
30 μ m	5 x 5 m	Should not be calculated!		Cannot be calculated!	
	12.5 x 12.5 m	0.41 m	0.18 m	0.59 m	0.16 m
	25 x 25 m	0.46 m	0.21 m	0.60 m	0.16 m
60 μ m	5 x 5 m	Cannot be calculated!		Cannot be calculated!	
	12.5 x 12.5 m	Should not be calculated!		Should not be calculated!	
	25 x 25 m	0.62 m	0.27 m	0.75 m	0.20 m

Table 8.2: The accuracy without gross errors for scale 1:15,000 and 1:25,000, the three resolutions and mesh sizes. The landscape types included are flat terrain, hilly terrain and village.

Table 8.1 and 8.2 show that the best results are achieved by using 15 μ m images in all three scales. Here the accuracy for the landscape type open, flat terrain is close to 0.1% of the flight altitude, if a small mesh size is used. For images with resolution 30 μ m, the accuracy is reduced by a small amount and lies between approx. 0.13% and approx. 0.25% of the flight altitude. For images with resolution 60 μ m, the accuracy is again a little reduced and lies between 0.2% and approx. 0.3% of the flight altitude.

8.1.2 Percentage of eliminated points

After the landscape types gravel pit and woods are no longer part of the data material, and the type village has been excluded in scale 1:5,000, it is now investigated how many points still have to be eliminated during the iteration process. The number of eliminated points is given as a percentage.

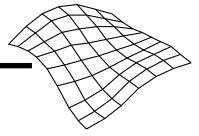


Image scale 1 : 5,000				
Resolution	Mesh sizes	Flat terrain	Hilly terrain	Total
15µm	5 x 5 m	3.25 %	7.69 %	5.95 %
	12.5 x 12.5 m	2.53 %	11.44 %	7.99 %
	25 x 25 m	0.45 %	11.61 %	7.22 %
30µm	5 x 5 m	3.11 %	7.61 %	5.81 %
	12.5 x 12.5 m	0.83 %	11.95 %	7.59 %
	25 x 25 m	0.23 %	19.60 %	11.98 %
60µm	5 x 5 m	2.34 %	10.68 %	7.40 %
	12.5 x 12.5 m	1.67 %	9.65 %	6.52 %
	25 x 25 m	0.45 %	14.16 %	8.77 %

Table 8.3: Number of eliminated points given as a percentage for each landscape type, and for the total number of points in scale 1:5,000.

It will be seen from table 8.3 that very few points have to be eliminated in flat terrain (approx. 0.25% - 3.25 %). In hilly terrain, between approx. 8% and approx. 20% of points have to be eliminated. Of the total number of points, between approx. 6% and approx. 12% are eliminated.

In scale 1:15,000, the landscape types flat and hilly terrain and village are included. The number of eliminated points given as a percentage is shown in table 8.4.

Image scale 1 : 15,000					
Resolution	Mesh sizes	Flat terrain	Village	Hilly terrain	Total
15µm	5 x 5 m	11.97 %	19.69 %	18.16 %	16.62 %
	12.5 x 12.5 m	12.69 %	16.65 %	16.25 %	15.24 %
	25 x 25 m	8.44 %	11.92 %	17.97 %	13.47 %
30µm	5 x 5 m	Should not be calculated!			
	12.5 x 12.5 m	2.04 %	14.01 %	10.91 %	8.90 %
	25 x 25 m	1.49 %	8.81 %	11.56 %	7.72 %
60µm	5 x 5 m	Cannot be calculated!			
	12.5 x 12.5 m	Should not be calculated!			
	25 x 25 m	1.24 %	12.79 %	9.50 %	7.74 %

Table 8.4: Number of eliminated points given as a percentage for each landscape type, and for the total number of points in scale 1:15,000.

Table 8.4 shows that the number of eliminated points in flat terrain is strongly reduced by using a lower resolution from approx. 13% to approx. 1 %. In the landscape types village and hilly terrain, between approx. 10% and 20% of the points are eliminated.

The number of eliminated points given as a percentage in scale 1:25,000.

Image scale 1 : 25,000					
Resolution	Mesh sizes	Flat terrain	Village	Hilly terrain	Total
15µm	5 x 5 m	Should not be calculated!			
	12.5 x 12.5 m	64.40 %	71.44 %	82.25 %	73.91 %
	25 x 25 m	50.62 %	59.09 %	67.81 %	60.16 %
30µm	5 x 5 m	Cannot be calculated!			
	12.5 x 12.5 m	18.3 %	47.3 %	40.6 %	34.7 %
	25 x 25 m	17.02 %	45.64 %	43.29 %	35.15 %
60µm	5 x 5 m	Cannot be calculated!			
	12.5 x 12.5 m	Should not be calculated!			
	25 x 25 m	11.0 %	34.6 %	26.9 %	23.4 %

Table 8.5: Number of eliminated points given as a percentage for each landscape type, and for the total number of points in scale 1:25,000.

Table 8.5 shows that in scale 1:25,000, very many points are still eliminated in the chosen landscape types. With resolution 15 μ m, from 50% to more than 80% are eliminated. With resolution 30 μ m, from approx. 20% to approx. 50% are eliminated. With resolution 60 μ m, from approx. 10% to approx. 35% are eliminated.

8.1.3 Summation

After leaving out the problematic areas and elimination of gross errors, it can be seen from tables 8.1 and 8.2 when compared with the results in Chapter 7, tables 7.4 – 7.6, it can be seen that by excluding the problematic landscape types, an improvement in accuracy of approx. 0.10m to 0.20m can be achieved.

It has turned out in this investigation that there is a very great difference in the number of points it has been necessary to eliminate. Tables 8.3 and 8.4 show that there are still up to 20% gross errors, even if the landscape types which contribute the largest number of gross errors are not included in the investigation. Furthermore, it will be seen that the number of eliminated points vary with the resolution and the mesh size.

Table 8.5 shows that there are still very many gross errors in scale 1:25,000. It should therefore be investigated more closely, why the elevation determination in this scale is so markedly poorer than in the two other scales. Unfortunately this has not been possible as the Match-T programme is no longer available. The results from scale 1:25,000 will still be included in this project, though with an eye on the circumstance that the elimination of gross errors has been very extensive, and therefore deviates from the general tendency.

In scale 1:5,000 in flat terrain, the accuracy without gross errors lies between approx. 0.08 m and 0.24 m, cf. table 8.1. By the elimination process, a maximum of 12% of the points are excluded, cf. table 8.3. This shows that there are few gross errors in this landscape type. This is also valid for the two other scales, though not to such an unambiguous degree. However, it is seen clearly from the tables 8.3 – 8.5 that there are still some gross errors, even if the most problematic landscape types are no longer included in the test material.

Therefore, a method should be found which can locate these gross errors from the existing data material without involving the frame of reference.

8.2 Method for locating gross errors

This project has defined a frame of reference against which all the calculated grids have been held, whereby the gross errors have been located. A frame of reference would not exist, if the survey was done over "virgin" ground. If a frame of reference existed, it would not be necessary to do a new survey, as the elevation data would already be in existence!

It will therefore be investigated whether it is possible, by means of the existing data material, to locate gross errors. The theory and the experience gained in Chapter 7 show that a DEM determined over images with a low resolution, for instance 60 μ m, gives a poorer accuracy, and the grid represents the terrain in soft lines. In resolution 30 μ m, the terrain is represented a little better with a little better accuracy, and again, the images in resolution 15 μ m will represent the terrain even better, and here the best accuracy is achieved. This means that the accuracy is improved by using a higher resolution, and at the same time it turned out that the number and size of the gross errors were likewise increased by using a higher resolution.

In a case where a correlation error caused by, for instance the soil condition generates a hilltop, this error may be found as a small hill in the 60 μ m images, in the 30 μ m images, the hill will have become a little higher, while in the 15 μ m images, it will be shown as a hilltop. Another example could be that Match-T, in a smaller group of objects, generated a medium solution with resolution 60 μ m, a slightly better one with resolution 30 μ m, and a full representation with resolution 15 μ m, see figure 8.1.

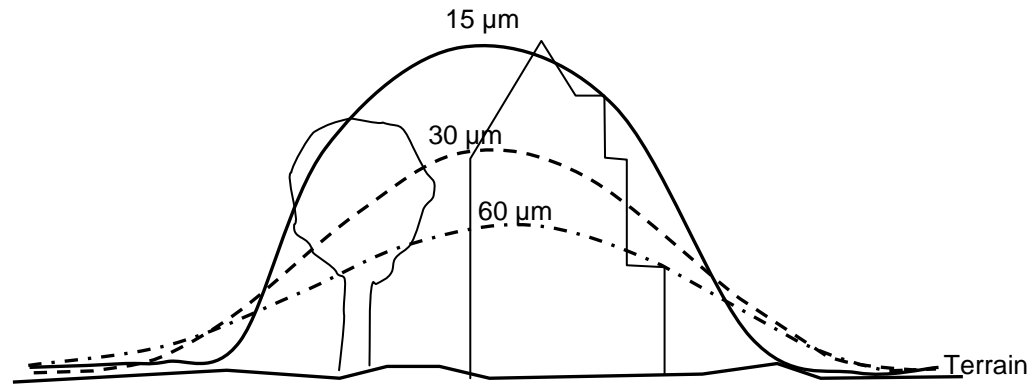
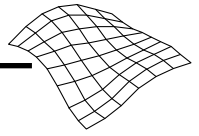


Figure 8.1: Sketch of the results for an object group by different resolutions.

This is the background to the idea of using all three resolutions, 60 μ m, 30 μ m and 15 μ m in combination to locate gross errors in the 15 μ m images. The frame of reference will only be used for an evaluation of the method.

In the investigation, those results are used which fulfil the demand for the minimum of 15 x 15 pixels per mesh size. For each calculation, the scale and the mesh size are maintained. This reduces the investigation to include only six grids. At first, the minimum and maximum deviation, as well as the mean (mean) and accuracy (RMSE) between the frame of reference and the raw data material for the 15 μ m images are regarded. This information stems from the analysis file for the individual calculation, see Appendix L. Again, the results are shown in two tables, as the same landscape types do not appear in scale 1:5,000 as in scales 1:15,000 and 1:25,000.

Table 8.6 shows the results in scale 1:5,000.

Grid	Min. deviation	Max. deviation	Mean	RMSE (m)
1:5,000_15 μ m_5 m	-16.46 m	7.13 m	-0.01 m	0.97 m
1:5,000_15 μ m_12.5 m	-23.28 m	13.04 m	-0.02 m	1.45 m
1:5,000_15 μ m_25 m	-15.87 m	11.76 m	-0.01 m	1.16 m

Table 8.6: Minimum (Min) and maximum (Max) deviation, the mean and Root Mean Squared Error (RMSE) for 1:5,000, 15 μ m and the three mesh sizes.

Table 8.6 shows that there are quite large deviations, with the minimum deviations between approx. –15m down to –23 m, and the maximum deviations between approx. 7m and 13m. In scale 1:5,000, there is almost no offset (mean).

Table 8.7 shows the results for scales 1:15,000 and 1:25,000.

Grid	Min. Deviation	Max. Deviation	Mean	RMSE (m)
1:15,000_15 μ m_12.5 m	-7.43 m	12.68 m	0.54 m	0.83 m
1:15,000_15 μ m_25 m	-4.98 m	11.95 m	0.77 m	1.63 m
1:25,000_15 μ m_25 m	-7.17 m	11.73 m	1.53 m	1.76 m

Table 8.7: Minimum (Min) and maximum (Max) deviation, the mean and RMSE for 1:15,000 and 1:25,000, 15 μ m and the three mesh sizes.

In scales 1:15,000 and 1:25,000, see table 8.7, there is a minimum deviation of approx. –7.5m and a maximum deviation of approx. 13 m, an offset of approx. 0.5m and 0.8m for images in scale 1:15,000. In scale 1:25,000, there is an offset of approx. 1.5m. Regardless of scale, the accuracy lies between approx. 0.8m and approx. 1.75m.

It is to be hoped that the method can locate those grid points where the greatest deviation between the elevation values of the three resolutions is to be found, and that these are also the grid points which contribute with a gross error.

The problematic grid points are determined by means of the standard deviation from the results for the three resolutions, which means that the standard deviation is only determined over three values. This is not optimal, but as no more material exists, use must be made of what does exist.

The analysis of the elevations in the three resolutions and the frame of reference is done in Excel, and therefore appears in one dimension. First, the standard deviation between the individual grid points in the three resolutions is calculated. Then the data material is sorted after the standard deviation to find those grid points, where the standard deviation is largest. This is done to find those grid points, where there is a great difference between the elevations in the different resolutions.

An example of grid points with large standard deviation is the result for scale 1:25,000 and mesh size 25 x 25m. In order to retain an overview, it was chosen to show only the first 100 grid points with the biggest standard deviation. For the sake of readability, the Y-axis has been shifted, so that only the interesting interval is shown.

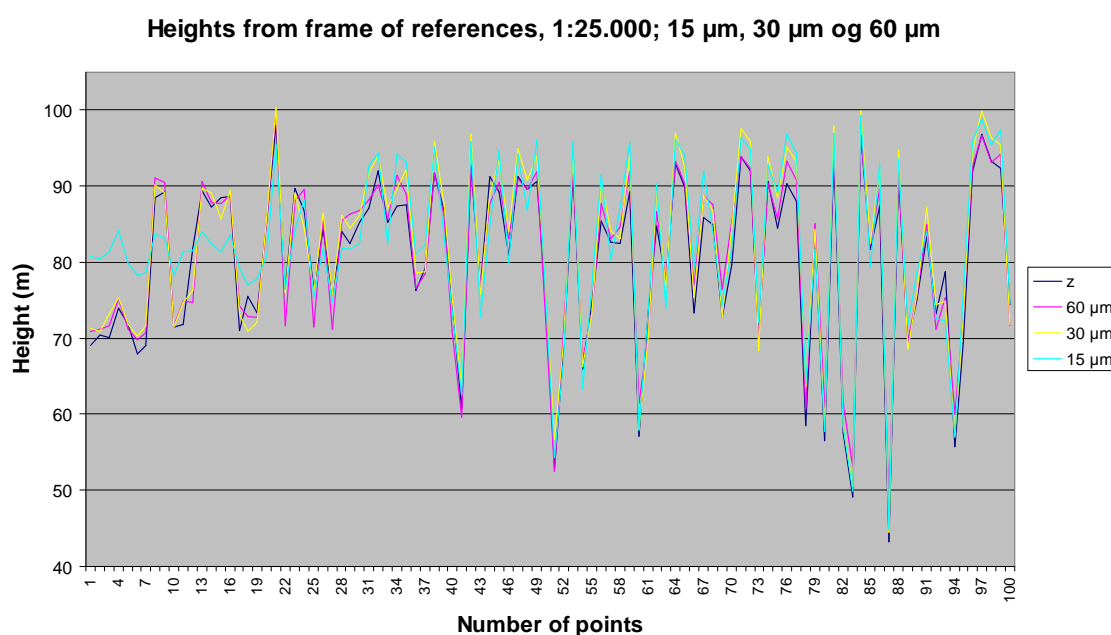


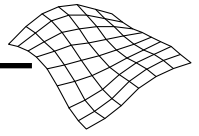
Diagram 8.1: Elevation data in resolution 15 µm, 30 µm and 60 µm in scale 1:25,000 and mesh size 25 x 25 m.

Diagram 8.1 shows that some points follow the results for resolution 30µm and 60µm in the frame of reference nicely, while the results for resolution 15µm deviates appreciably, see points 1-22. By and large, there is a large deviation between 15µm and the frame of reference for the peaks in the diagram. For other grid points, the results for 15µm and the frame of reference follow each other, see the valleys. It is therefore quite clear that if grid points are eliminated by a given standard deviation, correctly as well as wrongly determined grid points will be eliminated.

As the method is investigated for use in the elimination of gross errors in resolution 15µm, the accuracy achieved in Chapter 7 for 15µm images is taken as point of departure for the fixing of a gross error limit for the standard deviation. The gross error limit is determined as the mean per thousand of the flight altitude of all the results for 15µm images achieved in Chapter 7. This value is multiplied by 3 and used as gross error limit for the standard deviation. The result is 0.4‰ of the flight altitude which gives:

- 1:5,000 = 0.3 m
- 1:15,000 = 0.9 m
- 1:25,000 = 1.5 m

The elimination of good grid points is accepted, if the method still finds those grid points which contribute to the really gross errors. It is therefore interesting to see how many grid points are eliminated, how many



of them are correctly determined, and how many are wrongly determined. To get an idea of how much is lost by the elimination of correctly determined grid points, and how much is won by the elimination of wrongly determined points, all deviations are summed up from correctly determined grid points and wrongly determined grid points respectively. All this information is shown for each grid which is included in the investigation, see table 8.8.

Grid	Number of eliminated points	Number of correct points	Number of wrong points	Good metres	Bad metres	Max. Good metres	Max. Bad metres
1:5,000_15 μ m_5 m	158	95	63	10 m	342 m	0.27 m	16.46 m
1:5,000_15 μ m_12.5 m	170	54	116	7 m	632 m	0.29 m	23.28 m
1:5,000_15 μ m_25 m	340	140	200	20 m	597 m	0.30 m	15.87 m

Table:8.8: The number of eliminated points, incl. the number of correct and wrong grid points respectively, the sum of the deviations for the correct points (good m) and for the wrong points (bad m), and the maximum deviation for wrongly and correctly determined grid point in scale 1:5,000.

Grid	Number of eliminated points	Number of correct points	Number of wrong points	Good metres	Bad metres	Max. good metres	Max. Bad metres
1:15,000_15 μ m_12.5 m	199	81	118	38 m	472 m	0.89 m	14.08 m
1:15,000_15 μ m_25 m	177	93	94	39 m	327 m	0.85 m	12.68 m
1:25,000_15 μ m_25 m	70	14	56	11 m	286 m	1.50 m	11.73 m

Table:8.9: The number of eliminated points, incl. the number of correct and wrong grid points respectively, the sum of the deviations for the correct points (good m) and for the wrong points (bad m), and the maximum deviation for wrongly and correctly determined grid point in scale 1:15,000 and 1:25,000.

Table 8.9 shows that in scale 1:5,000 and resolution 15 μ m and mesh size 5 x 5 m, 158 points are eliminated, of which 95 are correctly determined points, and 63 are wrongly determined points. This is the only case where more good than bad points are eliminated. Even in this case, the sum of the deviations for the 95 correctly determined points is only 10 m, whereas the sum of the deviations for the 63 wrongly determined grid points is all of 342 m, of which the largest deviation is 16.5m.

In the remaining grids, more wrongly determined grid points are eliminated than correctly determined ones. Furthermore, it is seen that the sum of the eliminated correctly determined points lies from approx. 7m to approx. 40 m, while the sum of the eliminated wrongly determined grid points lies from approx. 290m to approx. 630m. This shows that even if the method eliminates good grid points, it is clearly an asset in eliminating very gross errors.

Table 8.10 shows how great the minimum and maximum deviations are after the elimination, as well the mean and the accuracy (RMSE). These resolutions are taken from Appendix L.

Grid	Min.	Max.	Mean	RMSE	Std
1:5,000_15 μ m_5 m	-0.92 m	0.82 m	0.07 m	0.12 m	0.10 m
1:5,000_15 μ m_12.5 m	-2.45 m	2.41 m	0.06 m	0.17 m	0.15 m
1:5,000_15 μ m_25 m	-6.03 m	8.52 m	0.04 m	0.47 m	0.46 m

Table 8.10: Min. and max. deviations, mean, RMSE and standard deviation (Std) after the elimination in scale 1:5,000.

Grid	Min.	Max.	Mean	RMSE	Std
1:15,000_15 μ m_12.5 m	-2.93 m	4.11 m	0.53 m	0.64 m	0.36 m
1:15,000_15 μ m_25 m	-3.84 m	4.75 m	0.53 m	0.71 m	0.47 m
1:25,000_15 μ m_25 m	-6.51 m	7.42 m	1.53 m	1.68 m	0.69 m

Table 8.11: Min. and max. deviations, mean, RMSE and Std after the elimination in scale 1:15,000 and 1:25,000.

Table 8.10 shows that in scale 1:5,000 and mesh size 5 x 5 m, the result is quite good with a minimum and maximum of under one metre and a RMSE of 0.12m. In scale 1:5,000 and mesh size 12.5 x 12.5 m,

the result is still good with a minimum of -2.5 m and a maximum of 2.5 m, and a RMSE of 0.17 m. The result for mesh size 25×25 m is a minimum of -6.03 m and a maximum of 8.52 m and the RMSE of 0.47 m.

For the remaining grids, see table 8.11, the result still shows large minimum and maximum deviations, but these are not so large as before the elimination, where the deviations were over 10 m. Furthermore, there is still an offset in the images in scales $1:15,000$ and $1:25,000$. The results are quite good, corresponding to 0.16% – 0.2% of the flight altitude, if this offset is eliminated. And, bearing in mind, in a completely automatic generation process.

8.2.1 Object or correlation error

A drawback to this method is that it is not able to catch gross errors of the same size in all three resolutions. If the gross error is caused by, for instance, an object group, where the correlation is correct, but falls on top of trees or houses, which has happened in all three resolutions, the deviation will not be recognised by this method. It will therefore be investigated whether the remaining gross errors are caused by objects in the terrain. If this is the case, these objects can be located by means of information from map data, in this case by means of TOP10DK data.

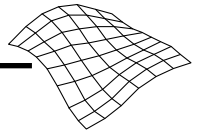
To find out whether the remaining gross errors are due to correlation errors or to objects in the terrain, the grid points with the errors are visualised in an orthophoto over the test area, see figure 8.2.



Figure 8.2: The remaining gross errors after the error elimination using the standard deviation as threshold limit. The gross errors are shown as green crosses.

Figure 8.2 shows that the remaining gross errors are caused not only by objects, but also by correlation errors which are due to soil conditions. These soil conditions are found in all three resolutions. In other cases, the gross error is caused by an object.

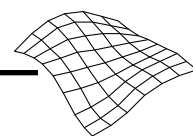
The results for the remaining grids are found in Appendix L.



8.3 Partial conclusion

By choosing the minimum mesh size, it is ensured that the calculation will run without problems, and the result will lie within the tendency. By excluding those landscape types which contribute the largest number of errors, the accuracy is considerably improved, but there are still quite a few gross errors in the remaining landscape types. In scales 1:5,000 and 1:15,000, the number of gross errors is 0.20 %, while in scale 1:25,000, very many gross errors are still eliminated.

By using the results from the three resolutions, the largest gross errors are located, and the result improved considerably. However, there is still an offset in the scales 1:15,000 and 1:25,000. If this offset can be removed, the result is quite good.



9 Theory and practice

The purpose of this chapter is to compare the results from Chapter 7 and 8 with the theory from Chapter 2 and with the experience of others, as appears in the source study in Chapter 3. It will be discussed here, whether there are discrepancies between the results achieved, the theory and the experience of others.

The individual parameters which are included in this project will be treated individually. First, the scale is described, then the pixel size, the mesh size, and finally the landscape type. For each subject, the theory is described first, then the source study, and finally the results. To round off, possible accordance's are discussed.

In this project, the results appear on several levels, results for all landscape types with and without gross errors (Chapter 7), results for selected landscape types with and without gross errors, and results achieved by use of the standard deviation between the resolutions 15 μ m, 30 μ m and 60 μ m as gross error limit. (Chapter 8).

9.1 The scale

Theory: The accuracy of the elevations is presented as ‰ of the flight altitude which shows that the flight altitude and thus the scale have a linear influence on the accuracy. Therefore, one should be able to achieve a better accuracy with images in a large scale, where there are far more details than in images in a small scale.

Source: Several articles discuss what accuracy can be achieved with Match-T as function of the flight altitude. One investigation shows that an accuracy better than 0.1‰ of the flight altitude, down to 0.08‰ of the flight altitude is possible [Krzystek, 1991]. Another article shows that an even better accuracy can be achieved, down to between 0.04‰ and 0.1‰ of the flight altitude dependent on the resolution of the images and the landscape type [Ackermann et al., 1992]. A Norwegian investigation [Eide, et al., 1993] also shows that an accuracy of 0.1‰ of the flight altitude in flat and simple terrain, 0.25‰ in flat and moderately hilly terrain and 0.55‰ of the flight altitude in mountainous (steep) terrain can be achieved.

In none of the described articles has it been discussed whether there is linearity between the different flight altitudes, or how many points have possibly been eliminated to achieve these results.

Practice: The investigations undertaken in this project show that not very good results are achieved when a "raw" generation is done over all landscape types. The results lie between 1.5m and 3.5m regardless of scale. After the elimination of gross errors, investigations show that if accuracy is regarded from a centimetre point of view, the best results are achieved by using images in large scale and the poorest by using images in small scale. This result is as expected.

If the results achieved are transformed into ‰ of the flight altitude, the best results are achieved by using images with resolution 15 μ m. Here, the accuracy is approx. 0.15‰ of the flight altitude, for the 30 μ m images, the accuracy lies between approx. 0.2‰ and 0.3‰ of the flight altitude, and between 0.3‰ and 0.4‰ of the flight altitude for the 60 μ m images.

Furthermore, the investigation shows that with resolution 15 μ m, the accuracy is by and large linearly dependent of the scale, whereas there is a small deflection in scale 1:15,000 with the resolutions 30 μ m and 60 μ m.

It has also turned out that it has not been possible to achieve the accuracy of 0.1‰ of the flight altitude, regardless of the scale or resolution of the images, if the elevation data is generated over all landscape types. If problematic landscape types are excluded, the results are considerably improved. The accuracy then lies between 0.5m and 1.5m.

An accuracy of 0.1‰ of the flight altitude can only be achieved for images with resolution 15µm and without problematic landscape types and gross errors in the remaining landscape types. In this investigation, the accuracy lies between 0.1‰ and 0.2‰ of the flight altitude for the 15µm images, between 0.15‰ and 0.25‰ of the flight altitude for the 30µm images and around 0.2‰ to 0.25‰ of the flight altitude for the 60µm images.

9.2 The pixel size

Theory: Theoretically seen, the best results should be achieved by using images with a high resolution, as a small pixel size means that far more information is included in the images, than when they are scanned with a low resolution, where the images become more blurred.

Source: In an article by [Krzystek, et al., 1992] images with resolutions 15µm and 30µm have been used. This investigation shows that the accuracy for the 15µm images is considerably better than for the 30µm images. In another article [Ackermann, 1992], 15µm and 30µm images have also been used. The result was 0.06‰ of the flight altitude for the 15µm images and 0.09‰ of the flight altitude for the 30µm images. A Norwegian investigation [Eide, et al., 1993] is based on images with 3 different resolutions, 15µm, 30µm and 60µm. This investigation shows that the best result was achieved with the resolution 15µm, while the result for the 30µm images was a little poorer, and the result for the 60µm images was clearly poorer. The articles mentioned show that the image resolution has an influence, on the other hand, the results from the OEEPE workshop where for instance, the results from Inpho GmbH, Institut Cartogràfic de Catalunya or the Aalborg University OEEPE investigation show that resolution has no influence.

Practice: The results from the "raw" generation show that the resolution has no influence. After the elimination of gross errors, the best results are achieved by using a high resolution, and the results are approximately linear.

The results achieved in this project show that the best accuracy is achieved by using the 15µm images. At the same time, a high resolution entails many gross errors. The images with resolution 60µm gives a poorer accuracy, but at the same time contains fewer gross errors.

9.3 The mesh size

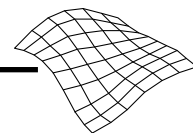
Theory: The grid heights are determined mathematically from the elevations of the interest points. The elevations of the interest points are determined by the correlation process itself. After having determined the elevations of a group of interest points, the grid heights are determined from the elevations of the interest points. The determination of the different mesh sizes is, therefore, done on the same basis, from the elevations of the same interest points. Theoretically, the mesh size should, therefore, not have any appreciable influence on the result. However, with a large mesh size there will be more interest points elevations as a basis for the determination of the grid point than with a small mesh size. Furthermore, a grid with a small mesh size will reproduce the terrain with a greater degree of detail, while a grid with a large mesh size will reproduce the terrain more softly. This should form part of the reflections when a large and small mesh size over the same area is compared. A 100% similar result cannot be expected with different mesh sizes, even if the basis is the same.

In each calculation, Match-T itself suggests a mesh size. Under which conditions this mesh size is determined, is not known in this project.

Source: In the article [Krzystek, et al., 1992] the conclusion is clear: large mesh size, and thus more interest points, gives a better result in flat areas. In the case of steeper terrain, a grid with a large mesh size will entail a reduction in the accuracy. The accuracy for mesh sizes over approx. 5m is better than 0.1‰ of the flight altitude, regardless of scale or resolution. Other investigations from OEEPE workshop [Institut Cartogràfic de Catalunya; National Geographical Institute, Bruxelles; the Aalborg University investigation] show that the mesh size has no influence.

[Inpho, 1995] points to the rule of thumb that the mesh size should be covered by approx. 30 x 30 pixels in the digital image. If the mesh size is reduced drastically and it relates to this rule of thumb, the calculation time will increase considerably. The mesh size can be calculated by means of the following formula:

The mesh size = 30 x pixels x the scale.



However, this is only a rough recommendation and may be ignored [Inpho, 1995].

It is also stated by [Baltsavias, 1999] that there should be a minimum of $10^2 - 15^2$ pixels per mesh.

Practice: This project has shown that the mesh size has an influence. It has turned out that there is a lower limit to how small a mesh size the programme can handle in relation to the scale and resolution of the images. The influence is probably due to a lack of interest points. The experience gained in this project says that if one wishes to use a mesh size which is smaller than 15×15 pixels per mesh, calculation problems may arise, and it may even be impossible to calculate a grid. This corresponds well with the sizes suggested by [Baltsavias, 1999].

If this minimum demand for the number of pixels per mesh is observed, the mesh size does not have any great influence, the accuracy is reduced very little by using a large mesh size.

9.4 The landscape type

Theory: If the problems surrounding landscape types are regarded theoretically, they must be divided into two superior areas, open country and areas with objects (houses, trees etc.). Theoretically seen, 100% of the open country without any form of objects should not give rise to problems. Areas with objects can be subdivided into areas with solitary objects, sparsely built-up areas (housing estates, woods with clearings etc.) and densely built-up areas or closely wooded areas. Match-T should be able to eliminate solitary objects by use of the mathematics for smoothing the grid. This method will not be very successful in densely built-up or closely wooded areas. Here, the grid will pass over the objects.

Source: The sources agree that landscape types pose a fundamental problem. Only in open areas with solitary objects, which Match-T can eliminate itself, does the generation go immediately well [Ackermann et al., 1992; a) Krzystek et al., 1995]. The article [b) Krzystek et al., 1995] shows that Match-T is also able to handle areas with a lack of texture, and therefore not sufficient terrain information. The investigation by [Seyfert, 1995] shows that densely built-up areas yield three times as poor a result as fields. Likewise, [Thorpe, 1996] has shown that generation over built-up areas gives poor results. Furthermore, the presentations from the OEEPE workshop show that there are problems with vegetation and buildings.

Practice: In this project five landscape types have been included. The type flat, open terrain is without objects, while open, hilly terrain was not quite without objects. In this area there are hedges, solitary trees and a few farms/houses. These objects were estimated to be without problems. The problem areas are gravel pits, the housing estate and the woods.

The investigation showed that the same results are achieved regardless of landscape type after elimination of gross errors. Regardless of scale, resolution and mesh size, only a few gross errors are found in flat terrain. In hilly terrain and village in scale 1:15,000, there are between 2% and 15% gross errors and between 7% and approx. 25% for images in scale 1:25,000. It must be noted, however, that images with resolution $15\mu\text{m}$ have been excluded, as these involve an unusual amount of errors.

Most deviations are found in the landscape types gravel pit and woods which was to be expected. In the housing estate area, it was surprising to see how well Match-T was able to handle this area, particularly in scales 1:15,000 and 1:25,000, a conclusion which was also reached in [Krzystek et al., 1995]. It was to be expected that this area would give large deviations. If the influence of this result is regarded by the creation of elevation models for updating purposes, the result is even more gratifying, as changes in the Danish terrain is usually caused by the building of new housing estates. On the other hand, it has been a surprise to find so many gross errors in the hilly terrain.

The conclusion is that the landscape type has a great influence on the result, and that gravel pits and woods should not be included, regardless of the scale of the images. Furthermore, villages should not be included for images in a large scale. If a higher accuracy is required, problematic areas can be edited away before the generation. Even if this is done, one must still calculate with a deal of editing work after the generation.

9.5 Summation

If the experience gained in this project is summed up, it has turned out that the accuracy, by and large, is linear with the scale or the pixel size. It has not been possible to achieve an accuracy of 0.1‰ of the flight

altitude, regardless of the scale or resolution of the images, if the elevation data is generated over all landscape types. The mesh size has an influence, as it has been found that there are lower limits to how small a mesh size the programme can handle in relation to the scale and resolution of the images. An experience gained in this project is that, if one wishes to use a mesh size smaller than 15 x 15 pixels per mesh size, calculation problems may arise or, it may even be impossible to calculate a grid. This corresponds to the sizes suggested by [Baltsavias, 1999]. If this minimum demand for number of pixels per mesh size is observed, the mesh size does not have any great influence, the accuracy is only reduced very little by the use of a large mesh size.

A summation of the results for the landscape types showed that open, flat and hilly terrain can be included regardless of scale and resolution. The greatest deviations are found in the landscape types gravel pit and woods which is as expected. In general, the landscape types gravel pit and woods should be eliminated. As regards the housing estate area, it is surprising to see how well Match-T could handle this area, in particular for images in scale 1:15,000 and 1:25,000, as it was to be expected that this landscape type would offer larger deviations.

These experiences are summed up, and the recommendation concerning minimum mesh size is indicated in table 9.2.

Landscape type	Image scale 1:5,000			Image scale 1:15,000			Image scale 1:25,000		
	15µm	30µm	60µm	15µm	30µm	60µm	15µm	30µm	60µm
Flat terrain	+	+	+	+	+	+	+	+	+
Gravel pit	/	/	/	/	/	/	/	/	/
Village	/	/	/	+	+	+	+	+	+
Hilly terrain	+	+	+	+	+	+	+	+	+
Woods	/	/	/	/	/	/	/	/	/
Mesh sizes (m ²)	> 1.125	> 2.25	> 4.5	> 3.375	> 6.75	> 13.5	> 6.625	> 11.25	> 22,5

Table 9.2: Recommendation of the landscape types over which generation can be done in different scales and resolutions, and the minimum mesh size. (+)=recommendation, (/)=no recommendation.

9.6 Experiences and currentness

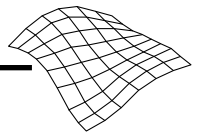
If the experience gained is used in the preparation for a method of an updating routine of elevation data, so that the nationwide elevation model will keep its currentness, the following factors must be taken into consideration:

1. New elevation data for updating purposes, the accuracy must be nearly as good as the upcoming LIDAR model
2. The burden of work must be minimised

Re 1: If new elevation data is generated for updating purposes with an accuracy nearly as good as the LIDAR model, the accuracy must be better than 0.5m. In order to achieve this, problematic areas will have to be excluded, and gross errors in the remaining landscape types must be eliminated.

Re. 2: The burden of work must be minimised which means that the localisation and elimination of problematic areas and elimination of gross errors in the landscape types included must be done automatically. Gravel pits and larger wooded areas can be found by means of map data (TOP10DK). The largest gross errors in the chosen landscape types may, for instance, be eliminated by use of the standard deviation determined between images in different resolutions over the same area as the gross error limit, as done in Chapter 8.

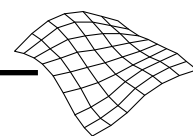
The results achieved in this project, where a minimum of 15 x 15 pixels per mesh size is found in the calculation, where scales 1:15,000 or 1:25,000 are used, where gravel pit and woods are not included, and where the standard deviation as the gross error limit is used for elimination of the remaining gross errors, are shown in table 9.3.



Scale	Resolution_Mesh size	Mean	RMSE (m)	Stnd (m)
1:5,000	15µm _5 m	0.07 m	0.12 m	0.10 m
	15µm _12.5 m	0.06 m	0.17 m	0.15 m
	15µm _25 m	0.04 m	0.47 m	0.46 m
1:15,000	15µm _12.5 m	0.53 m	0.64 m	0.36 m
	15µm _25 m	0.53 m	0.71 m	0.47 m

Table 9.3: Accuracy for images in scales 1:5,000 and 1:15,000 without problematic landscape types, and with the largest gross errors eliminated.

Table 9.3 shows that elevation data can be created by using images in scale 1:5,000 and 1:15,000 in which the accuracy (standard deviation, std) is better than 0.5 metre, even if there is an offset of approx. 0.5m. If the offset is eliminated, really good results can be achieved.



10 Conclusion and perspectives

In this chapter, the project as a whole is summed up and a conclusion is reached on the basis of the results achieved. On the basis of these results, a recommendation is offered as to how elevation data may be generated by automatic generation. There will be a brief formulation of the perspectives inherent in the ideas to improve accuracy, although these have not been tested in this project. There will also be a consideration of how the data fusion problem between old and new data can be solved. The chapter concludes with some perspectives and hopes for the future.

10.1 Background

The background/motivation for this project has been that the use of geo-spatial data has increased dramatically during the last generation. In this thesis, the focus has been on elevation data. In addition, the technological options will offer existing and future users unimaginable possibilities for the use of elevation data. Today, elevation data is increasingly used for a range of evaluation and analysis purposes. With this increase, end users have set new standards for the quality of data they are willing to accept, in relation to, the accuracy, density and viability of data, regarding how up to date it is.

The goal was to analyse and value the accuracy which can be achieved by automatic generation, in consideration of scale and/or resolution of the digital images, the mesh size in which the grid is determined and to analyse the influence of the landscape types which the images covers.

For the acquisition and capture of elevation data, three methods have been discussed in the project: IF-SAR, LIDAR and automatic correlation of digital images. The choice was to carry out a detailed investigation on the basis of automatic correlation of digital images with the programme package Match-T.

The specific purpose of this project has thus been to investigate, with what accuracy it is possible to capture elevation data with Match-T with a minimum of manual editing work. Several different investigations were carried out to determine the influence of the scale and resolution of the images on the accuracy, the influence of the mesh size from the automatically generated grid and the influence of the landscape type. These themes have been treated by others through time, but the reported results have been divergent. These divergences have formed the basis of the investigations in this project.

A test area was chosen for use in the investigations. This test area included ordinary landscape types found in Denmark. A frame of reference was established with over 10,000 points. All results achieved in this project have been compared with this frame of reference.

The automatically generated grids have all been generated with the standard set-up for Match-T. Before the detailed analysis was done, a pre-analysis of the generated grids was done, to see whether they included the required mesh size and were generated over the required area. The grids included the required mesh size, but none of the grids were generated over the required area, wherefore all the grids had to be trimmed before the detailed analysis could be done.

10.2 The results achieved

The investigations in this project have shown that it is possible to determine terrain data with an accuracy close to 10 cm by using automatic correlation by means of the Match-T programme.

The investigations have also shown that a great deal of gross errors arise by the automatic generation of elevations. It is therefore necessary to identify and eliminate gross errors wholly or partly. Two types of gross errors arise, the one created by problematic landscape types such as woods or areas with steep slopes, for instance, a gravel pit. The other type of gross error is correlation errors that arise for more diffuse reasons, such as lack of texture or the programme misunderstands information in the images etc.

These errors are found in the landscape types flat and hilly and at the same time, they are difficult to anticipate and therefore to handle, as they cannot immediately be located.

10.2.1 The scale and resolution of the images

The results in this project show that scale and resolution have a linear influence on the accuracy, which means that a large scale and a high resolution give the best results. However, this is only valid if the gross errors are eliminated. Even after the gross errors were eliminated, it has not been possible to achieve the expected accuracy of 0.1‰ of the flight altitude, regardless of the scale or resolution of the images, when the elevation data is generated over all landscape types.

10.2.2 The mesh size

It has turned out in this project that there is a minimum limit to how small a mesh size the programme can handle in relation to the scale and resolution of the images. The lesson learned here is that if the requirement is to use a mesh size which is covered by less than 15 x 15 pixels per mesh, calculation problems may arise, or it may even be impossible to calculate a grid. If this minimum requirement for the number of pixels per mesh is observed, the mesh size does not have any great influence. The accuracy is only reduced by a fraction when using a large mesh size.

10.2.3 The landscape type

This project has shown that landscape type has a very large influence on accuracy. The landscape types that represent the greatest part of the Danish landscape are open fields which are either flat or hilly. The best results are achieved by generation over a flat terrain. The second best results are achieved in hilly terrain and villages, but only for images in medium or small scales. The investigations showed that woods and gravel pit landscapes give great problems, regardless of the scale or resolution of the images. This was expected. Likewise, the landscape type village gives problems for images in a large scale, such as 1:5,000.

10.2.4 Accuracy

It has been mentioned in several sources that an accuracy of 0.1‰ of flight altitude or better can be achieved by automatic generation of elevation data. Investigations in this project show that when problem areas are excluded, and the gross errors in the remaining landscape types are eliminated, accuracies close to 0.1‰ of the flight altitude can be achieved.

The best results are achieved by using images with a resolution of 15µm and over the landscape type open, flat terrain.

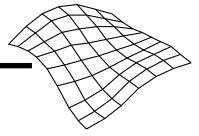
10.2.5 Eliminated points

If elevations are generated over an area without regard to landscape type, it must be calculated that approximately 25% of the generated points must be eliminated due to their poor quality, and in individual cases, up to 45% of these points. If the generation is only done over open, flat or hilly terrain, up to 15% of the points must be eliminated.

10.3 Recommendation

In this project, three methods for automatic determination of elevation data have been discussed. The method IFSAR cannot be recommended for the determination of elevation data over Denmark. The accuracy achieved using this method will not contribute to a new and better elevation model than the existing one. The method LIDAR gives a much higher accuracy, but is expensive, and cannot therefore be immediately recommended either. Automatic generation of elevation data by use of Match-T can be recommended for the creation of elevation data for updating the laser scanned nationwide elevation model. This is based on the fact that the greater part of Denmark consists of flat or hilly terrain, where the method for automatic generation of elevations functions well. If the gross error elimination method which is described in Chapter 8 is included, this accuracy may even be achieved with an acceptable manual editing effort.

The process of elevation data capture could, for example, run parallel with the updating of other existing map material, for instance, the nationwide map TOP10DK. TOP10DK is updated today every 5 years, in



the future every 3 years, from images at the scale of 1:25,000 which means that image material is already in existence and can be used for the generation of elevation data. For example, an operator could digitise maps in the daytime, and the computer could generate elevation data over the same images at night. The problematic areas must be eliminated before the generation, and to optimise the process, the elimination should be carried out automatically, for instance from TOP10DK data. The elevation determination of these areas must then be carried out in other ways. This can be done by different means:

- Manually, on an analytical instrument by an operator in the already orientated images
- Supplemented by LIDAR data for these specific areas which means, however, that an extra flight must be done
- Inclusion of existing elevation data

Not all landscape types have been represented in the test area. For example, a dense midtown area has not been included in this investigation. At this point in time a new national LIDAR elevation model will cover this area. With updating purposes in mind, the changes will be more pronounced in the outlying areas of towns and cities, where it is usual for industrial sites and housing estates to be developed.

Should other problematic areas in open country, such as areas with woods and steep slopes be covered by means of an automatic survey, LIDAR would be the best alternative.

10.4 Data fusion

Only over “virgin land”, where no geo-spatial data already exists, does the combining of old data with new data not come into question. Over an old country like Denmark, ‘tons’ of geo-spatial data, including elevation models, exist at different qualities. In this thesis, the method “data fusion” is chosen as the answer to how to mix existing elevation data with new measured elevation data.

10.5 Perspectives

During the work on this project, new ideas/perspectives have turned up which might be interesting to explore. On account of the scope of the project, these ideas have not been further investigated. Two ideas are mentioned here:

- Automatic elimination of problematic areas
- Automatic localisation and elimination of gross errors

10.5.1 Automatic elimination of problematic areas

The experience of this project has been that an automatic generation does not run well over overgrown areas (woods), and areas with slopes (gravel pit). It has also turned out that the generation does not run well, if, for example, a farm reaches a certain size and is surrounded by trees. According to theory, Match-T should be able to eliminate solitary objects. The first step in this investigation would, therefore, be to confirm how well Match-T is able to eliminate solitary objects, and at what size of area, Match-T is no longer able to cope on its own.

The obvious solution would be to investigate whether it is possible to automatically eliminate areas such as woods, gravel pits or other areas with slopes, dense urban areas etc. Likewise to investigate the possibility of eliminating smaller mixed areas, such as farms surrounded by a group of trees, on the basis of the existing map material, before an automatic generation is done. Denmark is covered by nationwide maps built up geologically, and wooded areas of a certain size are registered as coherent objects. The same goes for urban mid-town areas. Furthermore, all buildings over a certain size are registered. It would, therefore, be interesting to investigate whether it is possible to eliminate problem areas automatically in the images, before an automatic generation of elevation data is done.

This is obviously a good idea, as this data already exists, but the necessarily limited scope of this project has made it impossible to include this theme in the investigations.

10.5.2 Automatic localisation and elimination of gross errors

Another idea for further investigation is how gross errors can be eliminated individually by use of the existing image material. If there is not, as in the case of this project, an existing elevation model or other data material, it is necessary to localise and eliminate the gross errors in other ways.

It has been found in this project that the smallest number of points is eliminated by the use of a low resolution, and at the same time the accuracy is the poorest. This gave the idea of determining the standard deviation between the three image resolutions which existed in this project. However, this is a difficult and lengthy process. The optimal solution would be if this process could be done as an internal process in Match-T. The process is carried out by means of the three last levels in the pyramid.

A poorer accuracy is achieved by using images in resolution 60 μ m, but the investigations show clearly that there are also far fewer gross errors in this resolution. A higher resolution gives a greater degree of detail in the images, and thus a better accuracy, but also far more gross errors.

Instead of repeating the process in the project, where a standard deviation is calculated between the results from the 15 μ m, 30 μ m and 60 μ m images, this is done over the results from the three last levels in the pyramid process. A standard deviation for the Z-co-ordinates is determined between the grid points with the same planimetric co-ordinates in the last level. If this standard deviation is larger than 0.4‰ of the flight altitude, this point is cut out. The result is a grid with holes. There are two possibilities of filling out these holes:

1. The missing grid points are interpolated from the surrounding grid points
2. The missing grid points are determined manually

See figure 10.1

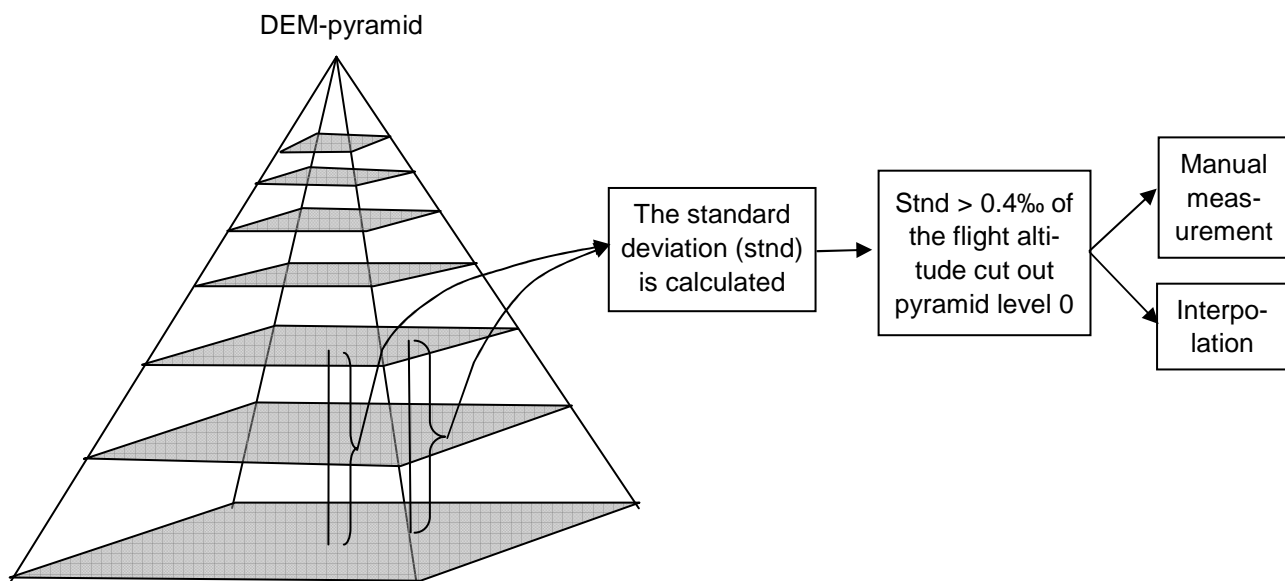


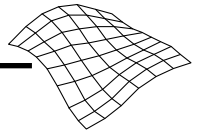
Figure 10.1: The course of process in an investigation where generated elevation data from three levels in the pyramid are used.

10.6 Outlook for future work in this field

This project has given the author a deep insight into the methods for automatic determination of elevation data and, in particular, into the methods for automatic correlation.

Firstly, the author has had to accept that the proverb *In theory, theory and practice are the same; in practice, they never are!* is true.

The author would also like to include some words from Anton Schenk [Schenk, 1996] Even though the words are over 10 years old, the author still believes that they are valid, even today. *"Ever since computers became available, researchers have tried to generate DEMs automatically. Despite considerable progress, the problem is still not entirely solved. Consider a large-scale, urban area, for example. No sys-*



tem exists today which would generate a DEM automatically. The problem has been underestimated, like so many other attempts, which try to mimic the mental faculty of seeing. What a human operator solves without conscious effort does not mean the task is easy.

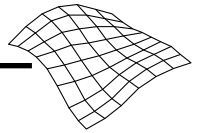
With automatic generation of DEMs, one would expect that the computer performs the same task that is usually assigned to an operator. Today's systems are not autonomous and will not be in the foreseeable future.

A computer can calculate, estimate and classify in accordance with the algorithms and calculation methods it is predisposed to. These types of operations it carries out precisely and tirelessly, but it cannot interpret image data, and can only recognise patterns in images to the extent that it has been programmed for. On the contrary, the human eye and sight can spot and recognise large and complex patterns which are created by physical structures, landscapes or urban areas, of which we have concrete or general experience in the physical world. A human being can, without problems, recognise an urban area, a golf course or a wood in a photo. A computer will only perceive the difference between the wood and the surrounding open country as a grey level difference which it has been trained to perceive as a shift in the terrain.

Therefore, the “automatic” in “automatic generation”, should be taken with a grain of salt, and it should not be expected that automatic procedures can run without problems. For the most part, there will be several gross errors, and the final elevations can only be determined after subsequent editing work.

There is hardly any doubt that the work towards a more automated generation of elevations has to continue. Among other things, through a refining of the mathematical descriptions which make the computer calculations possible. It is hoped that this project has contributed to the general understanding of the complexity that characterises work with automatic generation. And perhaps in that way opened up new vistas for future work within this field. It is the understanding of the author that the investigation and results have contributed to confirm and solve some of the existing problems, and that the project has thus brought us a step higher up on the ladder towards automatic generation with less subsequent editing.

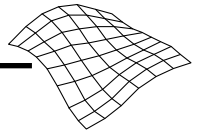
Furthermore, it is hoped that interest in further investigation has been aroused, in one or both of the ideas put forward in the section on perspectives, or a combination of both as inspiration for the future.



References

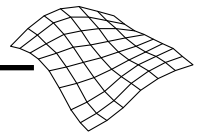
- Ackermann, F., (1984): Digital image correlation: Performance and potential application in photogrammetry, *Photogrammetric Record*, vol. 11(64), October, pp. 429 – 439.
- Ackermann, F., (1992): Automatic generation of digital elevation models.
- Ackermann, F. and Schneider, W., (1992): Experience with Automated DEM Generation. *Int. Archives of Photogrammetry and Remote Sensing*, ISPRS Congress 1992, Washington, Vol. XXIX, part B4, pp. 986 - 989.
- Ackermann, F., (1996): Techniques and strategies for DEM generation. *Digital Photogrammetry, An Addendum to the Manual of Photogrammetry*. Published by American Society for Photogrammetry and Remote Sensing. Cliff Greve (ed.) pp. 135 – 141.
- Ackermann, F., (1999): Airborne laser scanning – present status and future expectations, *ISPRS Journal of Photogrammetry & Remote Sensing* 54 (1999) pp. 64 - 67.
- ASHTech, (1992): ASHTech FILLNET User's manual, AshtechTM Document number 600089, Ashtech, Inc. 1170 Kifer Road, Sunnyvale, CA 94086, USA.
- Bacher, U., (1998): Experimental studies into automated DTM generation on the DPW770, Universität der Bundeswehr Muenchen. *GIS-Between Visions and Application*, ISPRS Commission Symposium, volume 32 Part 4, sep. 7 – 10, pp. 35 - 41.
- Baltsavias, E. P., (1991): Multiphoto Geometrically Constrained matching, Institut für Geodäsie und Photogrammetrie and der Eidg. Technischen Hochschule Zürich, ETH Hönggerberg, Zürich.
- Baltsavias, E. P., (1999): A comparison between photogrammetry and laser scanning, Institute of Geodesy and Photogrammetry, Swiss Federal Institute of Technology, ETH-Hoenggerberg, CH-8093 Zurich, Switzerland, *ISPRS Journal of Photogrammetry & Remote Sensing* 54 (1999) pp. 83 - 94.
- Binzer, J. og Tscherning, C. C., Geodætisk Institut, Frederiksen, L. og Krüger, J. C., Matrikeldirektoratet, (1982): Etablering af en digital højdedatabase for Danmark, *Landinspektøren*, 5. hæfte, 1982, udgivet af Den danske Landinspektørforening. (*Danish Journal for Mapping and Land-use*), pp. 289 - 297.
- Brande-Lavridsen, O., (1987): Theory/Practice about a Danish DEM. *ISPRS, proceedings of the international colloquium PROGRESS IN TERRAIN MODELLING*, Technical University of Denmark, 1987, pp. 49 - 54.
- Brande-Lavridsen, O., (1993): *Fotogrammetri*, 9. udgave, Laboratoriet for Fotogrammetri og Landmåling, Aalborg Universitetscenter, Danmark.
- Brenner, C. and Haala, N., (1999): Rapid production of virtual reality city models, *GIS, Geo-Informationssysteme, Zeitschrift für raumbezogene Informationen und Entscheidungen*, volume 12, 2/99, Wichmann, pp. 22 - 28.
- Cederholm, P., (1995): Øvelse i detailmåling med GPS/PNAV, Institut for Samfundsudvikling og Planlægning, Laboratoriet for Fotogrammetri og Landmåling, Aalborg Universitet, Danmark.
- Dahl, P. H. S., Lassen, A. G. og Christensen, K. R., (1995): Ajourføring af tekniske kort med monoplottning, 9. Sem., *Geoinformatik*, Aalborg Universitetscenter, Danmark.

- Ebner, H. and Reiss P., (1978): Height interpolation by the Method of Finite Elements. Proc. DTM Symp. St. Louis, pp. 241-254
- Eggers, O., Ellegaard, S., Hølleddig, L. og Norvin, P., (1989): Fra kurveplaner til digital højdemodel, Afgangsprojekt på landinspektørstudiet, Aalborg Universitet, Aalborg Universitetsbibliotek.
- Eide, O. R. og Mardal L., (1993): Digital Fotogrammetri, Test av Intergraph's Image Station, Diploma Thesis, Ås, Norway. Unpublished.
- Elachi, C., (1987): Introduction to the physics and techniques of remote sensing, California Institute of Technology, Earth and Space Sciences Divisions, Jet Propulsion Laboratory, Pasadena, California, editor Jin Au Kong, A Wiley-Interscience Publication John Wiley & Sons.
- Favey, E., Pateraki, M., Baltsavias, E., Bauder, A. and Bösch, H., (2000): Surface modelling for alpine glacier monitoring by airborne laser scanning and digital photogrammetry, International Archives of Photogrammetry and Remote Sensing. Vol. XXXIII, Part B4, Amsterdam 2000, pp. 269 - 277.
- Frederiksen P., (1987): A digital elevation model for Radio Communication. ISPRS, proceedings of the international colloquium PROGRESS IN TERRAIN MODELLING, Technical University of Denmark, 1987, pp. 127-133.
- Frederiksen, P., (1993): Instituttet for Landmåling og Fotogrammetri, DTH: Digitale højdedatabaser i Danmark, Landinspektøren, nr. 2-93, 36. Bind, 102 årgang, 1993. Udgivet af Den danske Landinspektørforening (Danish Journal for mapping and land-use).
- Förstner, W., (1986): A feature based correspondence algorithm for image matching, International Archives of Photogrammetry and Remote Sensing, vol. 26, part 3 Rovaniemi, 1986.
- Förstner, W., and Gülch, E., (1987): A fast operator for detection and precise location of distinct points, corners and centres of circular features, University Stuttgart, Institute of Photogrammetry, Proceedings ISPRS Intercommission Conference on Fast Processing of Photogrammetric Data, Interlaken, Switzerland, 1987, pp. 281 - 305.
- Förstner W. (1989): A Feature Based Correspondence Algorithm for Image Matching and Least Squares Matching. International Archives of Photogrammetry and Remote Sensing, Vol. 26, Part 3, Rovanieme, 1989.
- Förstner, W., (1991): Statistische verfahren für die automatische Bildanalyse und ihre Bewertung bei der Objekterkennung und –vermessung, Deutsche Geodätische Kommission bei der Bayerischen Akademie der Wissenschaften, Dissertationen, Heft nr. 370, München 1991, verlag der Bayerischen Akademie der Wissenschaften en Kommission bei der C. H. Beck'schen Verlagsbuchhandlung München.
- Förstner, W., (1993): Image Matching, chapter 16 in Computer and Robot Vision, volume II, edited by R. Haralick and L. Shapiro, University of Washington, printed by Addison-Wesley publishing company.
- Geodætisk Institut (1978): Geodætisk Institut 1928-1978, København, red. Sørensen, E., Arentzen, E. S., trykt ved Geodætisk Institut 1978.
- Geodæsidivisionen, (1992): Signalerings-vejledning, Kort- og Matrikelstyrelsen, Rentemestervej 8, (DK) 2400 København NV.
- Hahn, M., (1989): Automatic measurement of digital Terrain Models by means of Image Matching Techniques. Proceedings of 42nd Photogrammetric Week, Stuttgart, pp. 141 - 151.



- Hansen, M., Mølgaard, M. S. og Overby, S., Weje, P. N., (1995): Stråleudjævningsprogrammet BINGO – anvendt på statue. Aalborg Universitet, Landinspektøruddannelsen, 8. semester, Teknisk måling, Gruppe TM2 – Juni 1995.
- Haralick, R. M. and Shapiro, L. G. (1992): Computer and Robot Vision, volume 1, University of Washington, printed by Addison-Wesley Publishing Company.
- Heipke, C., (1996): Overview of image matching techniques, European Organization for experimental Photogrammetric Research, proceedings of the OEEPE- WORKSHOP on application of digital photogrammetric workstations, official publication No 33, Lausanne, 1996, editor O. Kölbl, pp. 173 – 189.
- Heuchel, T. (2005): Experience in Applying Matching Techniques Using Images from Digital Cameras. Proceedings of the 50th Photogrammetric Week, Stuttgart. Dieter Fritsch (eds.). Wichman Verlag Heidelberg, pp. 181-188.
- Holm, M., Permes, E., Andersson, K., and Vuorela, A., (1995): A nation wide automatic satellite image registration system, SPIE Aerosense '95, Conference on integrating Photogrammetric Techniques with scene analysis and machine vision II, Orlando, Florida, USA, 17 – 21 April 1995, SPIE vol. 2486 – 18, pp. 156 – 167.
- Hyypä, J., Hyypä, H. and Ruppert, G., (2000): Automatic derivation of features related to forest stand attributes using laser scanner, International Archives of Photogrammetry and Remote Sensing. Vol. XXXIII, Part B3, Amsterdam 2000, pp. 421 - 428.
- Intergraph (1994): ImageStation Match-T (ISMT) User's guide, appendix B: Mathematical Model for DTM Generation.
- Inpho GmbH, Stuttgart, (1994): Match-T, Automatic DEM Generation, User Manual, Version 1.3.1.
- Inpho Stuttgart, (1995): Match-T, Automatic DEM – Generation, Tutorial, Inpho Stuttgart, Photogrammetric Information Processing, Smaragdweg 1, D-70174 Stuttgart, Germany.
- Johansen, N. P., (1927): Danmarks Topografiska Kartläggning, Foredrag holdt i "Kartografiska Sällskapet" i Stockholm 7. marts 1927, Stockholm 1927, A. Börtzells Tryckeri A-B.
- Kleusberg, A. and Klaedtke, H-G., (1999): Accuracy assessment of a digital height model derived from airborne synthetic aperture radar measurements. Proceedings of the 47th Photogrammetric Week, Stuttgart. Fritsch/Spiller (eds.). Wichman Verlag Heidelberg, pp. 139-143.
- Kobrick, M., (2006): On the Toes of Giants – How SRTM was Born. Photogrammetric Engineering and Remote Sensing, March 2006, Volume 72, Number 3, pp 207-210.
- Kort- og Matrikelstyrelsen, (1989): Danmarks Geografiske Referencenet, Brugervejledning, Matrikelstyrelsen, Rentemestervej 8, (DK) 2400 København NV.
- Kort- og Matrikelstyrelsen, Geodæsidivisionen, (1992): Signalerings-Vejledning, Kort- og Matrikelstyrelsen, Rentemestervej 8, (DK) 2400 København NV.
- KMS, (2005): Forslag om etablering af en nøjagtig højdemodel over Danmark, note.
- Krarup, T., Kubik, K. and Juhl, J., (1980): Goetterdaemmerung over least squares adjustment. Int Arch Photogram XXIII, Part B3, Commission III, Proc. 14th Congress of ISP, Hamburg, 1980, pp. 369-378.
- Kraus, K., (1990): Fernerkundung, Band 2, Auswertung photographischer und digitaler bilder, Institut für photogrammetrie und fernerkundung der Technischen Universität Wien, Ferd. Dümmlers verlag, Bonn.

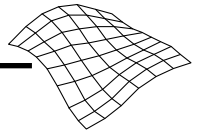
- Kraus, K., (1993): Photogrammetry, Volume 1, Fundamentals and Standard Processes, Institute for Photogrammetry, Vienna University of Technology, contributions by P. Waldhäusl, translated by P. Stewardson, Ferd. Dümmlers verlag, Bonn.
- Kraus, K., (1997): Photogrammetry, Volume 2, Advanced Methods and Applications, Institute for Photogrammetry and Remote Sensing, Vienna University of Technology, contributions by J. Jansa and H. Kager, translated by P. Stewardson, Ferd. Dümmlers verlag, Bonn.
- Kruck, E., (1995): BINGO – User's Manual, Hannover 1995.
- Krzystek, P., (1991): Fully automatic measurement of digital elevation models. Proceedings of the 43rd Photogrammetric Week, Stuttgart. Ackermann/Plietker (ed.). pp. 203 – 214.
- Krzystek, P. and Wild, D., (1992) (a): Experimental accuracy analysis of automatically measured digital terrain models. Robust Computer Vision. Quality of Vision Algorithms. Förstner/Ruwiedel (ed), Wichmann Verlag, Karlsruhe, pp. 372 - 390.
- Krzystek, P. and Ackermann, F., (1995): New investigations into the practical performance of automatic DEM generation, Technical Papers ACSM/ASPRA Annual Convention and Exposition, Charlotte, Feb. 27th - March 2nd, 1995, vol. 2 pp. 488 - 499.
- Krzystek, P. and Wild, D., (1995): Automatic Generation of Elevation Models. Second Course on Digital Photogrammetry, University Bonn, Institute for Photogrammetry and Remote Sensing and LVA NRW
- Krzystek, P., (1995): Automatic Generation of Elevation Models. Third Course in Digital Photogrammetry, University Bonn, Institute for Photogrammetry and Remote Sensing and LVA NRW
- Larsen, J. N., (1996): Fra højdemodel mod terrænmodel, Forbedring af Digitale Højdemodeller ved tilføjelse af ekstra data, Afgangsprøjet, Institut for Planlægning, Danmarks Tekniske Universitet, Faggruppe Landmåling.
- Larsen, J. N., (1998): Improving a DEM by integrating data, ISPRS volume XXXII, part 2, Commission II, proceedings of the commission II symposium, Data integration: Systems and techniques, Cambridge, UK, pp. 177 - 183.
- Lemmens, M. J. P. M., (1988): A Survey on stereo Matching Techniques, Proceedings of 16th ISPRS. In IAPRS, vol. 27 / B8, pp. 11 – 23.
- Lohr, U., (1999): High Resolution Laserscanning, not only for 3D-City Models. Proceedings of the 47th Photogrammetric Week, Stuttgart, Fritsch/Spiller (eds.). Wichman Verlag Heidelberg, pp. 133-138.
- Lohr, U. und Schaller, J., (1999): Trassenbefliegungen mit dem TopoSys Laserscanner, GIS, Geo-Informationssysteme, Zeitschrift für raumbezogene Informationen und Entscheidungen, volume 12, 2/99, Wichmann, pp. 3 - 5.
- McIntosh, K., Krupnik, A. and Schenk, T., (2000): Improvement of automatic DSM generation over urban areas using airborne laser scanner data, International Archives of Photogrammetry and Remote Sensing. Vol. XXXIII, Part B3, Amsterdam 2000, pp. 563 - 570.
- Mercer, B., (2001): Combining LIDAR and IfSAR: What can you expect? Proceedings of the 48th Photogrammetric Week 01', Stuttgart, Fritsch/Spiller (eds.). Wichman Verlag Heidelberg, pp. 227-237.
- Nilsen, B., (1998): Nøyaktighet av automatisk genererte digitale terrengmodeller, Kart og Plan 1-98, pp. 35 – 44.



- Nørgård, P., (2001): Præcisionshøjdemodeller – med luftbåren laserskanner, *Geologisk Nyt* 3/01, pp. 26 - 27.
- Petzold, B. and Axelsson, P., (2000): Results of the OEEPE WG on laser data acquisition, *International Archives of Photogrammetry and Remote Sensing*. Vol. XXXIII, Part B3, Amsterdam 2000, pp. 718 - 723.
- Rasmussen, J. K. og Flatman, A. C., (2000): Laserskanning - En kvalitetsvurdering, afgangprojekt fra Aalborg Universitet, Landinspektøruddannelse, Fibigerstræde 11, Aalborg, Danmark.
- Seyfert, E., (1995): Erste Erfahrungen bei der automatischen Generierung von digitalen Höhenmodellen in Siedlungsgebieten. *Proceedings of the 45th Photogrammetric Week*, Stuttgart. Fritsch/Hobbie (ed.). Wichman Verlag. pp. 269 – 276.
- Schenk, A. F., (1996): Automatic Generation of DEM's, *Digital Photogrammetry*, An addendum to the *Manual of Photogrammetry*, Published by American Society for Photogrammetry and Remote Sensing, edited by Cliff Greve, pp. 145 – 150.
- Schenk, T., Li, J.-C., and Toth, C., (1991): Towards an Autonomous System for Orienteering Digital Stereopairs, Department of Geodetic Science and Surveying, The Ohio State University, Columbus, *Photogrammetric Engineering and Remote Sensing*, vol. 57, no. 8, August 1991, pp. 1057 – 1064.
- Skriver, H., Dall, J. og Madsen, S. N., (1999): Kortlægning med billeddannende radar, Institut for Elektromagnetiske Systemer, Danmarks Tekniske Universitet, *Landinspektøren Tidsskrift for kortlægning og areal forvaltning*, No. 2-99, pp. 336 - 341.
- Stoker, J. M., Greenlee, S. K., Gesch, D. B. and Menig, J. C. (2006): Click: The new USGS Center for Li-dar Information Coordination and Knowledge. *Photogrammetric Engineering and Remote Sensing*, June 2006, Volume 72, Number 6, pp 613-616.
- Thorpe, J. A. and Schickler, W., (1996): New automated procedures for creating large scale digital orthophotography in urban areas, *ISPRS Congress 1996*, Vienna, *International Archives of Photogrammetry and Remote Sensing*, Vol. XXXI, part B4, pp. 868 – 873.
- Vosselman, G., (2000): Slope based filtering of laser altimetry data, Working Group III/2, *International Archives of Photogrammetry and Remote Sensing*. Vol. XXXIII, Part B3, Amsterdam 2000, pp. 935 - 942.
- Wehr, A. und Hug, C., (1999): Topographische Geländeaufnahme mit ScaLARS, GIS, Geo-Informationssysteme, *Zeitschrift für raumbezogene Informationen und Entscheidungen*, volume 12, 2/99, Wichmann, pp. 6 - 11.
- Wehr, A. and Lohr, U., (1999): Airborne laser scanning – an introduction and overview, *ISPRS Journal of Photogrammetry & Remote Sensing* 54 (1999) pp. 68 - 82.
- Werner, M. (2001): Status of the SRTM data processing: when will the world-wide 30m DTM data be available? *Proceedings of the 48th Photogrammetric Week 01'*, Stuttgart, Fritsch/Spiller (eds.). Wichman Verlag Heidelberg, pp. 159-165.
- Wever, C., (1999): Laserscannermessungen – ein Verfahren setzt sich durch, GIS, Geo-Informationssysteme, *Zeitschrift für raumbezogene Informationen und Entscheidungen*, volume 12, 2/99, Wichmann, pp. 12 - 17.
- Wever, C. and Lindenberger, J., (1999): Experiences of 10 years laser scanning. *Proceedings of the 47th Photogrammetric Week*, Stuttgart, Fritsch/Spiller (eds.). Wichman Verlag Heidelberg, pp. 125-132.

Zhang, B. and Miller, S., (1997): Adaptive automatic terrain extraction, Proceedings of SPIE – The International society for Optical Engineering, Integrating Photogrammetric Techniques with Scene analysis and Machine Vision III, volume 3072, Orlando, Florida, pp. 27 – 36.

Aarestrup, M. og Villadsen S. S. (1994): Koordinatsystemer i Danmark, GIS i Danmark, red. ved Balstrøm, T. et al., 1. udgave, 1. oplag, Teknisk Forlag A/S, 1994, pp 31-43.



Acknowledgement

This project original started at Aalborg University under the supervision of Prof. J. Höhle. The project continued in my spare time and in co-operation with the National Survey and Cadastre in Copenhagen and Institut für Photogrammetrie (ifp) at Stuttgart University. Special thanks go to Prof. J. Höhle for originating the idea and helping with starting the project, also thanks to the National Survey and Cadastre for the time I have been given to work on the project, and to Prof. D. Fritsch for his interest and support during the course of my time at ifp and later comments and discussions.

Special thanks go to Associate Professors Jens Juhl and Poul Frederiksen for their interest, and the countless discussions which have spread much light at difficult times. Also thanks for the loan of the GeoCAD programme.

Thanks to all ifp colleagues in Stuttgart for the time I spent with you. You made my stay in Stuttgart interesting both on and off campus. Also thanks to Inpho colleagues Frank Petran and Dietmar Wild for our good discussions about professional as well as cultural life.

During the long course of this project, I have had much support and felt a large degree of commitment from my family, the close as well as the larger one, and from friends and acquaintances. Special thanks go to my husband Ian and my brother Kaj for their unstinting support during the years, humanly as well as professionally. Also special thanks to my parents for their hospitality that made it possible to work at their home, while the two of you and my brother Ole looked after the girls.

Also thanks to Ina, Mette, Marie, Bjarke, Stefan and Keld.

Thanks to all of you who have not been mentioned in this acknowledgement, but who have, during the years, helped or shown professional interest. I remember your help and interest in the project and I am deeply grateful.

Ishøj June 2008

Marianne Wind



Appendices

Appendix A: Correlation techniques

Appendix B: The data material

Appendix C: Analysis programme

Appendix D: Editing programme

Appendix E: Bundle adjustment

Appendix F: Graphic online/offline

Appendix G: Sizes of grid files

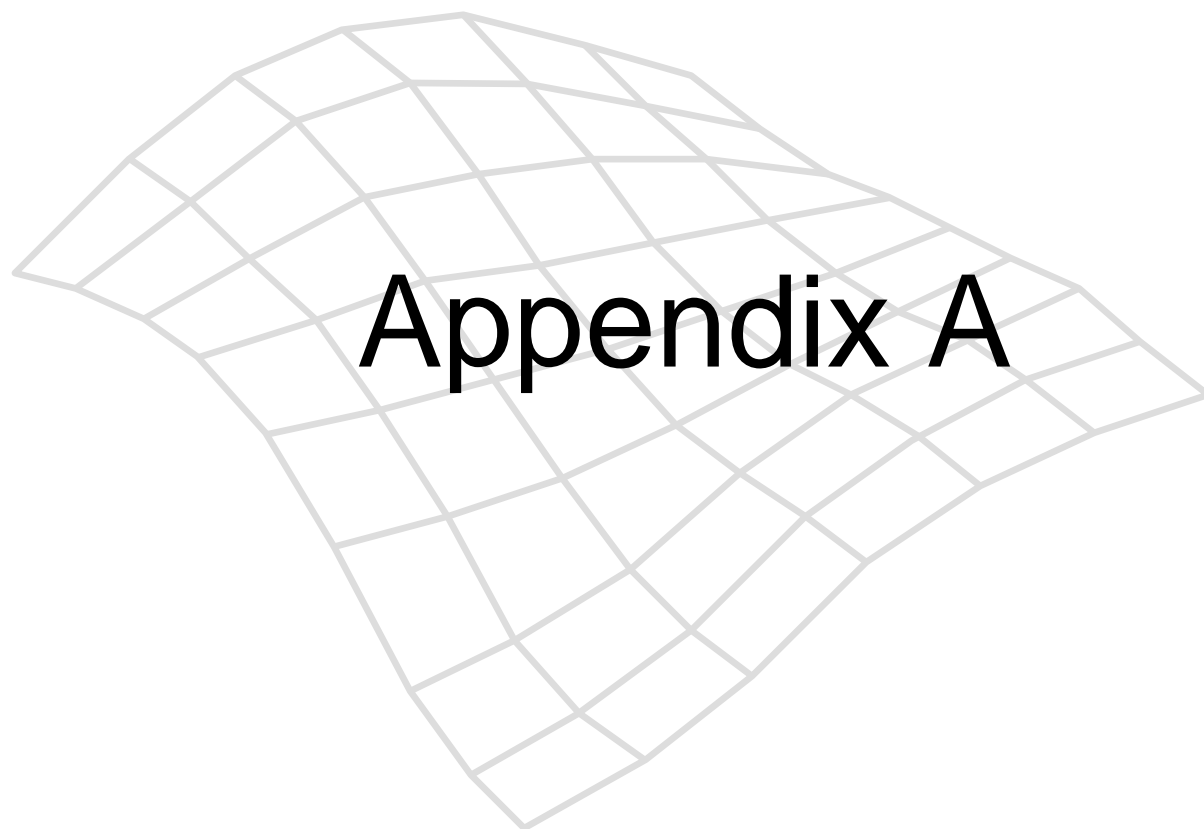
Appendix H: Code specification

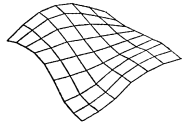
Appendix I: Analysis calculations

Appendix J: Code specification and error arrows

Appendix K: Orthophoto and error arrows

Appendix L: STND used as threshold





Appendix A: Correlation techniques

In this appendix, the most frequently used correlation techniques in digital photogrammetry are described, both techniques which are directly relevant for the understanding of the theory used in the project (Match-T), and other techniques which are included here to give a better background knowledge and understanding of correlation techniques in general.

A.1 ABM and FBM

Photogrammetric correlation may be defined as the establishment of coherence between two images [Heipke, 1996]. The aim of correlation is to determine the position where the concordance between the two images is at its best. That corresponds to making an orientation of the images in analogous photogrammetry. The method for digital photogrammetry is based, however, on image processing theory rather than optical/mechanical theory. In the following, the most frequently used correlation techniques used in digital photogrammetry are described in connection with, among other things, orientation, aerotriangulation and determination of an elevation model.

In general, the purpose of the correlation technique is to make two digital images, or rather image patches correlate, that is, find corresponding points by means of the grey level values of the images' pixels or image features. A correlation which is done over the whole image at once will be practically impossible in terms of the large quantity of data, therefore, an image segment of, for instance, 7 x 7 pixels is selected to work in. In one image, a segment is selected which is used as the target in the search for the best correlation. In the other image, an image segment, the search area, is selected, where the search itself is done. The search area is moved consecutively, so that the whole search image is covered. The purpose of the use of selected segments is minimisation of error possibilities, search time and the demand for calculation capacity.

In general terms, there are two correlation methods in digital photogrammetry. One is known as Area Based Matching (ABM), where the grey level values in the digital image are the basis of the correlation. The ABM method is described in Appendix A.1.1. The present description includes two types of ABM: correlation coefficient and least squares matching. The other method is known as Feature Based Matching (FBM). With this method, the image features, such as lines, points and areas, are extracted from the images, and the correlation is done by means of the image features. The FBM method is described in Appendix A.1.2.

In a correlation, the fitting in must be done in the row as well as the column direction of the pixels, that is, in two dimensions. By use of the normalisation method, epipolar geometry may be achieved, and the correlation problem reduced to a one-dimensional problem. This method is described in Appendix A.1.3.

According to each correlation principle, the correlation may be done at pixel level or sub pixel level, that is, the co-ordinates of the corresponding point are indicated as whole pixels or fractions of pixels, and thus, the accuracy can be determined on two levels: whole pixel level and sub pixel level or pixel fraction level. The last mentioned is the most accurate of the two indications. By transformation/adaptation, image 1 (the target area) is moved a whole number of pixels, or a whole and a fraction number of pixels over image 2 (the search area). If the movement is only wanted after a whole number of pixels, correlation calculations will suffice. If the adaptation is to be better than at whole pixel level, the correlation calculation must be followed by, for instance, an adjustment.

In order to achieve good results by a correlation, temporary co-ordinates must be available. These can be found by means of the pyramid technique described in Appendix A.1.6 and A.1.7.

Appendix A concludes with a discussion of the pros and cons of the use of ABM and FBM respectively (A.1.8).

A.1.1 Area based matching

Area based matching (ABM) is the most straightforward type of correlation, as the images are used without previous processing and interpretation. This correlation method has a high degree of accuracy in areas with a good structure [Ackermann, 1984], where there are grey level gaps, for instance, boundaries in the images. Areas with poor structure and subsequent poor contrast present a higher risk of errors, and subsequent poorer accuracy. Boundaries may, for instance, be differences between road and ditch, cultivation boundaries, or rooves and surroundings etc. On the other hand, the method is sensitive to changes in the grey level value between the images.

The accuracy of ABM can be divided into an accuracy at pixel level and one at sub pixel level. The first-mentioned will find the best whole pixel position for a correlation.

A.1.1.1 Correlation at pixel level

Correlation at pixel level is done by means of correlation calculations, and in the following, different algorithms will be discussed. The difference between these algorithms lies mainly in the reliability of the correlation value and the speed. Speed is often an important factor in the choice of which correlation function should be used [Kraus, 1990].

Here, two will be mentioned: correlation coefficient and mean square of the grey level differences, as it is these which have acquired the greatest importance.

A.1.1.1.1 Correlation coefficient

The correlation coefficient is an expression of the quality of the concordance between two images or image segments. The correlation coefficient (c) is determined on the basis of the standard deviation for the grey level values in the two images, or image segments, and the mutual co-variance matrix.

$$\sigma_T = \sqrt{\sum (g_T - \mu_T)^2} \quad A(1.1)$$

$$\sigma_S = \sqrt{\sum (g_S - \mu_S)^2} \quad A(1.2)$$

$$\sigma_{TS} = \sum (g_T - \mu_T)(g_S - \mu_S) \quad A(1.3)$$

where:

σ_T = the standard deviation in the target area

σ_S = the standard deviation in the search area

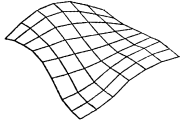
g_T = the individual grey level values in the target area

g_S = the individual grey level values in the search area

μ_T = the mean of the grey level values in the target area

μ_S = the mean of the grey level values in the search area

calculated for the same position as the target segment.



The correlation coefficient may then be described as [Kraus, 1993]:

$$c = \frac{\sigma_{TS}}{\sigma_T \cdot \sigma_S} = \frac{\sum (g_T - \mu_T)(g_S - \mu_S)}{\sqrt{\sum (g_T - \mu_T)^2} \cdot \sqrt{\sum (g_S - \mu_S)^2}} \quad A(1.4)$$

The correlation coefficient is often used as a criterion for confirmation of a correlation. The correlation coefficient can vary between -1 and 1 . The correlation is best when the coefficient is 1 . For example, the programme package Match-T uses a minimum value for the coefficient, which as point of departure is 0.85 [Inpho GmbH, 1994]. The correlation coefficient is a measure of the quality of the correlation at pixel level. Calculation of the correlation coefficient for a series of search areas may form the basis of the selection of the best correlation at pixel level.

A.1.1.1.2 Mean square

Another measure of the quality of the correlation is the mean square which is calculated in the following way:

$$\sqrt{\frac{\sum (g_T - g_S)^2}{n}} \quad A(1.5)$$

where:
 g_T = the grey level value in the target area
 g_S = the grey level value in the search area
 n = the number of pixels used

By an optimal correlation, the mean square is 0 .

The correlation coefficient has, as its most important advantage, its reliability, but it still results in a longer calculation time. On the other hand, the mean square of the grey level differences is easy to calculate and implement, but cannot handle differences in image scale.

Correlation with a greater accuracy than at pixel level can be achieved by means of other methods which indicate positions at sub pixel level.

Often a better determination of the position than at whole pixel level is desirable. Therefore, sub pixel level is used as well, and here two of the most important types of ABM at sub pixel level, polynomial correlation [Schenk et al., 1991; Kraus, 1997] and least squares matching [Ackermann, 1984] are treated.

A.1.1.2 Correlation at sub pixel level

Correlation at sub pixel level can be done by means of 1) fitting in a polynomial, or 2) least squares matching. Both methods presuppose temporary co-ordinates at pixel level which can be produced by iterative use of correlation calculations, as, for instance, a calculation of the correlation coefficient or the mean square which is repeated for each pixel in a given area.

A.1.1.2.1 Fitting in of a polynomial

As it is wished to find the best fitting in at sub pixel level, the surrounding pixel co-ordinates are also regarded, for instance, in a segment of 3×3 pixels. The segment is placed so that the pixel position with the optimal correlation value is in the centre of the segment. The nine correlation values are used as observations for a better determination of a polynomial. A second degree polynomial is suitable for this purpose [Schenk et al., 1991; Kraus, 1997].

$$a_0 + ra_1 + sa_2 + rsa_3 + r^2a_4 + s^2a_5 = p(r, s) + v \quad A(1.6)$$

where: r and s are the integer pixel co-ordinates
 a_0, \dots, a_5 are the parameters which are determined by the adjustment
 $p_i(r,s)$ = the individual correlation coefficients within the window
 v = the residuals

If this equation is used as an observation equation, the coefficients a_i for the polynomial can be found by an adjustment. The following equation system is set up:

$$I + v = A \cdot x \quad A(1.7)$$

which means:

$$v = A \cdot x - I$$

where: I = the observations
 v = random values (the residuals)
 A = the design matrix
 x = unknown quantities

If $I = g_T(x,y)$, $x = r_0$ it follows that:

$$v(x,y) = g_S \cdot r_0 \cdot \left(\begin{bmatrix} a_1 x + a_2 y \\ a_4 x + a_5 y \end{bmatrix} + \begin{bmatrix} a_3 \\ a_6 \end{bmatrix} \right) + r_1 - g_M(x,y) \quad A(1.8)$$

where: $a_1, a_2, a_3, a_4, a_5, a_6, r_0$ og r_1 = temporary values
 $v(x,y)$ = the residuals

The turning point of the polynomial (the sub pixel position) can then be found by differentiating. A sub pixel position can then be achieved by:

$$r_{\text{sub}} = \frac{a_2 a_3 - 2a_1 a_5}{4a_4 a_5 - a_3^2} \quad A(1.9)$$

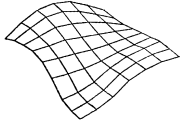
$$s_{\text{sub}} = \frac{-2a_2 a_4 + a_1 a_3}{4a_4 a_5 - a_3^2} \quad A(1.10)$$

[Schenk et al., 1991]. This method offers a sub pixel accuracy of $1/4$ pixel [Kraus, 1997].

A.1.1.2.2 Least squares matching

To find the best correlation at sub pixel level, the least squares matching, which consists of two transformations, is often used. The best correlation between two images can be regarded as an affine transformation between the images. By affine transformation, we have 6 geometric unknown quantities: 2 moves, 2 twists and 2 scalings. Furthermore, we have 2 unknown corrections for the contrast in grey level strength. Altogether, 8 unknown quantities.

Therefore, the transformation parameters are calculated during the process, but it is only the co-ordinates of the corresponding point in the search image which are of interest.



If the correlation is done by means of least squares matching, there is, as mentioned, 8 unknown quantities, 6 corrections for the approximated value of the move, and 2 corrections for the contrast in grey level strength:

- The move in grey level values
- The change in scale
- The x-co-ordinate for the target area (g_T)
- The y-co-ordinate for the target area (g_T)
- The x-co-ordinate for the search area (g_S)
- The y-co-ordinate for the search area (g_S)
- The grey level values in the target area (g_T)
- The grey level values in the search area (g_S)

Least squares matching in two dimensions consists of:

1) The radiometric transformation:

$$\begin{array}{ccc} g_T(x,y) & = & r_0 \cdot g_S(u,v) + r_1 \\ \uparrow & & \uparrow \\ \text{Target area} & & \text{Search area} \end{array} \quad \text{A(1.11)}$$

where:

g_T = the grey level values for the target area

x = x-position for the target area

y = y-position for the target area

r_0 = estimated correction for the scaling factor in the grey levels

g_S = the grey level values for the search area

u = the x-position in the search area

v = the y-position in the search area

r_1 = estimated correction for the shift of the grey level values

2) The geometric transformation:

$$\begin{pmatrix} u \\ v \end{pmatrix} = \begin{pmatrix} a_1 & a_2 \\ a_4 & a_5 \end{pmatrix} \begin{pmatrix} x \\ y \end{pmatrix} + \begin{pmatrix} a_3 \\ a_6 \end{pmatrix} \quad \text{A(1.12)}$$

where:

a_1, a_2, a_4, a_5 = the affinity divided into 2 scalings and 2 twists

a_3, a_6 = the shift in the x- and y-direction

If the radiometric and the geometric transformation are put together, the following applies:

$$g_T(x,y) = r_0 \cdot g_S \left(\begin{bmatrix} a_{1x}x + a_{2y} \\ a_{4x}x + a_{5y} \end{bmatrix} + \begin{bmatrix} a_3 \\ a_6 \end{bmatrix} \right) + r_1 \quad \text{A(1.13)}$$

By assigning the target random errors (v), there will be:

$$g_T(x, y) + v = r_0 \cdot g_S \left(\begin{bmatrix} a_1 x + a_2 y \\ a_4 x + a_5 y \end{bmatrix} + \begin{bmatrix} a_3 \\ a_6 \end{bmatrix} \right) + r_1 \quad A(1.14)$$

To solve this problem, an adjustment is used again by means of the least squares principle. The equation system seen in A(1.7) and A(1.8) is set up, and repeated here for clarity:

$$l + v = A \cdot x$$

which means:

$$v = A \cdot x - l$$

where:

l = the observations

v = random values (the residuals)

A = the design matrix

x = unknown quantities

If $l = g_T(x, y)$, $x = r_0$ it follows that:

$$v(x, y) = g_S \left(\begin{bmatrix} a_1 x + a_2 y \\ a_4 x + a_5 y \end{bmatrix} + \begin{bmatrix} a_3 \\ a_6 \end{bmatrix} \right) \cdot r_0 + r_1 - g_T(x, y) \quad A(1.15)$$

where:

$a_1, a_2, a_3, a_4, a_5, a_6, r_0$ og r_1 = estimated values

$v(x, y)$ = the residuals

A.1.2 Feature based matching

The feature based matching (FBM), in contrast to ABM, uses image features as background for the correlation. The first step is to extract image features, which is done by means of a so-called operator. Dependent on the operator, the image features may be areas, lines or points. These image features' position and attributes are stored in a list. This extract is done for both images in an image pair. The second step is the correlation itself, where the features on the two lists are investigated with regard to coincidence.

A.1.2.1 Area

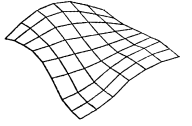
An example of the use of areas as features in a FBM is done on the background of satellite images. Lakes and islands were chosen as features. This is due to the fact that these are easy to extract automatically by setting up a limit in the histogram for the near-infrared channel. The correlation can, for instance, be done between an orientated satellite image, and a non-orientated satellite image. The features are extracted from each satellite image. The method can also be used between a digital topographical map in raster form and a satellite image, where the same features are extracted, here lakes and islands.

As attributes for the area features, the size of the area is registered, both as area (km^2), by the length and shoreline, and as to type, including whether it is land (island) or water (lake). For the determination of the sub pixel position of the area, its centre of gravity is used. These attributes were considered in the correlation.

The accuracy of this method has turned out to be at least as good as a traditional measuring of control points [Holm et al., 1995].

A.1.2.2 Line

Human vision is, to a large degree, based on the correlation between distinct, well-defined lines rather than on the grey level values themselves. Such distinct lines and edges can be derived from the grey



level values (edge detection) by calculating the differences from the neighbouring grey level values. The grey level variations are further emphasised in the image by taking the second-derived differences. This process is also called the Laplace operator.

It has turned out that there is an advantage to filtering the image for noise (random errors) before edges can be detected. A known operator which both filters and emphasises edges is the LoG operator (**L**aplacian of **G**aussian zero-crossing edge detector) [Haralick et al., 1992]. As the name LoG operator indicates, it is the Laplace operator combined with a 3D Gaussian distribution.

The LoG operator is found by double differentiation of the Gaussian bell function. The derivation itself appears from [Kraus, 1992].

$$\text{LoG}(r, c) = \frac{r^2 + c^2 - 2\sigma^2}{2\pi\sigma^6} e^{-\left(\frac{r^2 + c^2}{2\sigma^2}\right)} \quad \text{A(1.16)}$$

where: r = rows
 c = columns

The value σ is the only eligible parameter. A small σ gives a transformed image with many zero points. If you want to choose points for an orientation, it is reasonable to use a large value for σ .

This operator is used with a view to extraction of lines for, for instance, a relative orientation [Schenk et al., 1991].

The edges are found in locations where $\text{LoG}(r, c) = 0$. For the linking together of the edges found, the chain code principle is used. Of course, edges will be found in one image, which are either not found in the other image, or which deviate as regards form or linking together. Therefore, the problem of finding corresponding edges must be formulated very generally. Reasonable correlation criteria are that the lines have a certain concordance as regards length, form, derived gradients and location in both images. These attributes are independent of rotation or scale difference between the images.

This investigation indicates that the method (the use of edges) may be quite serviceable for the solution of correlation problems in connection with, for instance, correlation between two images, or between images and maps.

A.1.2.3 Points

It has turned out that if the correlation of the images is to be used later for measuring, and not only for analysis purposes, points are the best image features [Baltsavias, 1991].

Other criteria, such as robustness, point density, the demand for a temporary value, and in some cases also, the question of the calculation speed, can play a part in the evaluation of whether an operator is the optimal one. The most precise operators use points as image features, and thus offer a closer result while, at the same time, the calculation runs quicker. The operator is, however, sensitive to noise in the images which adds to the risk of faulty correlation because of ambiguity. The point operators need better temporary co-ordinates than operators which use lines and areas.

Over time, different operators have been developed. One of the oldest and most used operators is the Moravec operator (1980). Another much used operator is the Förstner operator (1987), both will be discussed in the following two paragraphs. A long series of operators are compared by [Baltsavias, 1991].

A.1.2.3.1 The Moravec operator

The Moravec operator determines the change in grey level value in the four directions, row, column and the two diagonals. The change in the grey level value is determined as the sum of the grey level differences between neighbouring pixels squared. The original Moravec operator is defined as a 5 x 5 window:

$$M_1(r, c) = \frac{1}{20} \cdot \sum_{k=-2}^2 \sum_{l=-2}^1 [g(r+k, c+l) - g(r+k, c+l+1)]^2 \quad \text{A(1.17)}$$

$$M_2(r, c) = \frac{1}{20} \cdot \sum_{k=-2}^1 \sum_{l=-2}^2 [g(r+k, c+l) - g(c+k+1, c+l)]^2 \quad A(1.18)$$

$$M_3(r, c) = \frac{1}{16} \cdot \sum_{k=-2}^1 \sum_{l=-2}^1 [g(r+k, c+l) - g(r+k+1, c+l+1)]^2 \quad A(1.19)$$

$$M_4(r, c) = \frac{1}{16} \cdot \sum_{k=-2}^1 \sum_{l=-2}^1 [g(r+k, c+l+1) - g(r+k+1, c+l)]^2 \quad A(1.20)$$

where: r = rows
 c = columns

The definition of the Moravec operator (M) is: $M = \min (M_i)$ for $i = 1, 2, 3, 4$

If M reaches a certain limit, the point will be included as a characteristic point. In order to choose only the clearly separate points, the thinning out is then done. The advantage of this method is that it is easy to implement, but there are also the following drawbacks [Lemmens, 1988]:

- Points are determined which do not relate to real points, but only to grey level differences
- The operator is sensitive to features with a poor resolution, for instance, small points will give a larger operator signal
- The operator is not rotation-independent

It has turned out that the Moravec operator has certain weaknesses as regards precise determinations of corners [Förstner, 1993].

As regards achieving the greatest number of extracted points, the Förstner operator is preferable, as it is able not only to extract corners, but also the centre of circles, intersections, points where the structure is marked in relation to the surroundings, end points of lines etc. [Förstner, 1991; Förstner, 1993]. The operator is good at using an image with little variation in the grey level values, which results in a general high degree of point density.

Other operators can only extract some of the mentioned image features, and the density of the extracted features is therefore lower. Furthermore, investigations have shown that for images with noise, the Förstner operator is also the best in every sense [Baltsavias, 1991].

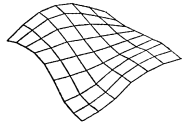
Förstner has stated a series of demands for the extraction of image features [Förstner, 1986]. Characteristic image features are corners, intersections, points with a high contour gradient, and end points for lines, and centres of circles. Common to all these features are that they fulfil the following demands:

Clear separation: The points must be clearly separated from the immediately neighbouring points. This demand is valid locally, that is, in the immediate surroundings of the interest points. This demand excludes points on the same line. Clearly separated points may be corners, round features etc.

Rare/unique: The points must be rare or unique within the image, so that recognition of a point by comparison of the two images' lists becomes quicker. That way, the speed of the correlation is increased, which also ensures a better result.

Stable/unchangeable: The image features must be recognisable in the other image. The features must be stable at the selection, grey level wise as well as geometrically. The stability has a direct influence on the accuracy of the correlation, and thus on the reliability of the later processes.

According to [Förstner, 1991 and 1993], it is only the Förstner operator which in practice can deliver the points which live up to the aforementioned demands.



A.1.2.3.2 The Förstner operator

In 1986, another FBM algorithm was presented by W. Förstner. This is the algorithm which later became known as the Förstner operator. The algorithm is presented as being an operator which extracts points with greater accuracy, and thus with a total better accuracy. This operator has later been described in detail in [Förstner et al., 1987 & 1993], which also forms the basis of the description in the following.

The Förstner operator really consists of several part processes: determination of gradients, determination of corner and end points, intersections, points with a high contour gradient, circle points, quality calculation and build-up of a point list.

The gradient image

A gradient image consists of derived grey level values, which are calculated separately in the pixels' row and column direction. The gradients are determined by means of, for instance, a Roberts operator or a Sobel operator. If the Roberts operator is used, the image must first be smoothed by means of a "low-pass" filter [Förstner, 1986]. Therefore, the Sobel operator is used more often, as the smoothing is done there during the calculation of the gradients. A Sobel operator is described thus:

For the pixel rows

$$\begin{bmatrix} -1 & 0 & 1 \\ -2 & 0 & 2 \\ -1 & 0 & 1 \end{bmatrix}$$

For the pixel columns

$$\begin{bmatrix} -1 & -2 & -1 \\ 0 & 0 & 0 \\ 1 & 2 & 1 \end{bmatrix}$$

The calculation of the gradients may, for instance, begin in the upper left corner of the image. The operator moves from pixel to pixel and line to line (row) until gradients are calculated over the whole image. This is done for the row operator as well for the column operator. Of course, there will be problems along the edge of the image, as the operator will not be able to find pixel points for the whole size of the operator here. This edge problem may be solved in different ways.

- 1) The choice is to go on working with only a reduced gradient image, where the incorrect gradients are not included
- 2) For an operator of 3 x 3 pixels, 2 extra columns and 2 extra rows are added along the edge with the grey level value 0
- 3) The outermost rows and columns outside the image have to be copied

First when the Sobel operator is in the position second row and second column, will there be pixel values for a correct gradient determination. The result of this will be 2 gradient images, one including the gradients in the x-direction, and the other the gradients in the y-direction.

The gradients are used in the later processes where the search is for intersections, corner, end and circle points. These points may be designated as characteristic points in the digital image.

A.1.2.3.3 Determination of intersections, corner and end points

As the determination of intersections, corner and end points is done in the same way, these are treated as one.

Let it be presumed that in a fixed window, for example of 7 x 7 pixels, there will be an intersection, corner, or end point. Before this point can be determined, line segments must first be determined. These are determined by means of gradient lines. The line segments are defined as the line which passes through the middle of the pixel, and runs perpendicular to the gradient. [Förstner, 1991]. For each pixel, a gradient line is determined, and for each gradient line, a line segment is determined.

A line segment in pixel position (r, c) is defined as:

$$G: \quad l(r,c) = r \cdot \cos \phi + c \cdot \sin \phi \quad A(1.21)$$

Where: l = the distance to origin for the (r,c) position
 ϕ = the direction found by means of the gradient ($\cos \phi = g_r/|\Delta g|$)
 where: g_r = the grey level value for the row
 $|\Delta g|$ = the length of the gradient

see figure A.1.1.

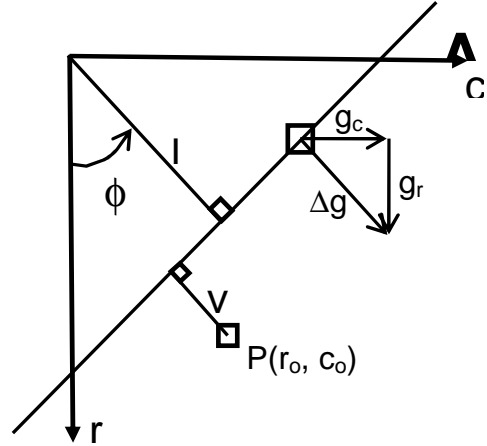


Figure A.1.1: Designation of the line segment with gradient.

When the line segment is given, the distance (v) to an intersection, corner or end point $P(r_0, c_0)$ is given by:

$$v = r \cdot \cos \phi + c \cdot \sin \phi - l \quad A(1.22)$$

A so-called characteristic point is the position from which the distance to all the line segments is the shortest. Generally, the work is done within a smaller window of, for instance, 7×7 pixels. For each window, the position is determined, from which the distance to all lines in this window is the shortest. For the solution of this problem, an adjustment is used. An intersection, corner or end point can therefore be determined from the following equation for each of the surrounding gradient lines:

$$l(r,c) = r_0 \cdot \cos \phi(r,c) + c_0 \cdot \sin \phi(r,c) + v(r,c) \quad A(1.23)$$

where $v(r,c)$ is the distance to be minimised.

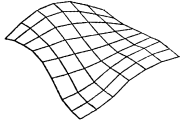
In figures A.1.2 and A.1.3 examples are shown of a corner situation, for instance, a house corner, and an end situation, for instance, the end of a road or a hedge.

The equation A(1.23) is used as an observation equation at an adjustment by the least squares method. In an $n \times n$ window (for example 5×5 or 7×7), there are n^2 edge elements, and thus n^2 observation equations of the type:

$$v_i = r_0 \cdot \cos \phi_i + c_0 \cdot \sin \phi_i - l_i \quad A(1.24)$$

Thereby this is the case:

1. The equation for all line segments within a window, set up as in equation A(1.23)
2. The determination of the point P which is in the position, where the distance to all lines is the shortest



This is done by an adjustment by the least squares method.

On the background of the equation A(1.24), n^2 normal equations are set up:

$$v_i = r_0 \cdot \cos \phi_i + c_0 \cdot \sin \phi_i - l_i$$

where the position of the characteristic point is (r_0, c_0) and r_0 and c_0 are the unknown quantities.

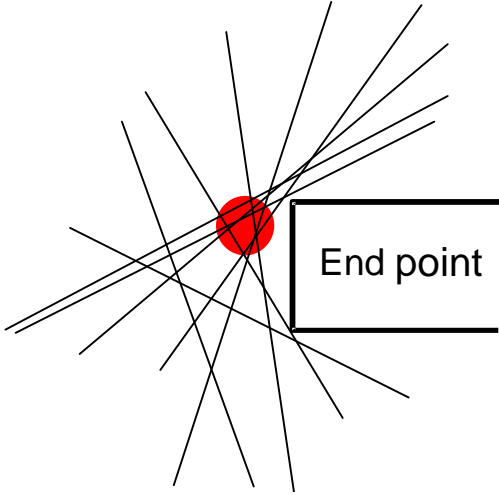


Figure A.1.2: Determination of an end point

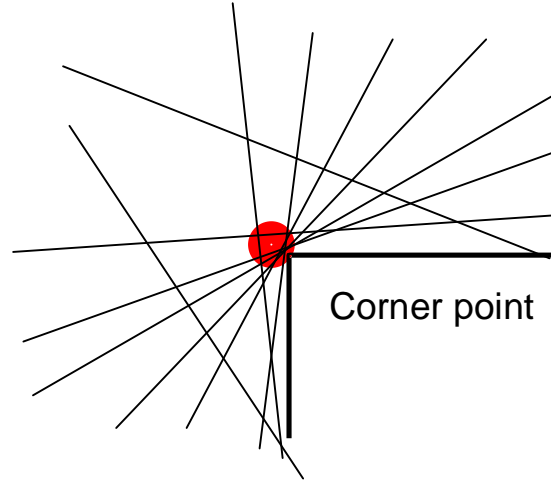


Figure A.1.3: Determination of a corner point

The normal equation system:

$$A^T P A x = A^T P b \quad A(1.25)$$

Translates to:

$$A = \begin{bmatrix} \cos \phi_1 & \cdots & \sin \phi_1 \\ \vdots & \ddots & \vdots \\ \cos \phi_n & \cdots & \sin \phi_n \end{bmatrix} \quad P = \begin{bmatrix} |\nabla g_1|^2 & \cdots & 0 \\ \vdots & \ddots & \vdots \\ 0 & \cdots & |\nabla g_n|^2 \end{bmatrix} \quad A(1.26)$$

By using the normal equation system, this is the formula:

$$N = A^T P A = \begin{bmatrix} \sum \cos^2 \phi_i \cdot |\nabla g_i|^2 & \sum \cos \phi_i \cdot \sin \phi_i \cdot |\nabla g_i|^2 \\ \sum \cos \phi_i \cdot \sin \phi_i \cdot |\nabla g_i|^2 & \sum \sin^2 \phi_i \cdot |\nabla g_i|^2 \end{bmatrix} \quad A(1.27)$$

If $\cos \phi = \frac{g_r}{|\nabla g|}$ and $\sin \phi = \frac{g_c}{|\nabla g|}$ is set

this is obtained:

$$N = \begin{bmatrix} \sum g_r^2 & \sum g_r \cdot g_{c_i} \\ \sum g_r \cdot g_{c_i} & \sum g_{c_i}^2 \end{bmatrix} \quad A(1.28)$$

$$A^T P I = \begin{bmatrix} \sum \cos \varphi_i \cdot |g_i|^2 \cdot l_i \\ \sum \sin \varphi_i \cdot |g_i|^2 \cdot l_i \end{bmatrix} = \begin{bmatrix} \sum \cos \varphi_i \cdot |g_i|^2 \cdot (r_i \cdot \cos \varphi + c_i \cdot \sin \varphi_i) \\ \sum \sin \varphi_i \cdot |g_i|^2 \cdot (r_i \cdot \cos \varphi + c_i \cdot \sin \varphi_i) \end{bmatrix} = \begin{bmatrix} \sum g_{r_i}^2 \cdot r_i + \sum g_{r_i} g_{c_i} \cdot c_i \\ \sum g_{r_i} g_{c_i} \cdot r_i + \sum g_{c_i}^2 \cdot c_i \end{bmatrix} \quad A(1.29)$$

A.1.2.3.4 Determination of circle points

Circle points are defined as the centre of circular features, that is, rings and round surfaces. The point of departure is gradients, determined as described in section 1.2.3.2. The gradient lines have the same direction as the gradients. As the gradient lines by circular features are turned 90°, a line designation is indicated as:

$$l(r, c) = -\sin \phi(r, c) + \cos \phi(r, c) + v(r, c) \quad A(1.30)$$

⇓

$$r \cdot (-\sin \phi(r, c)) + c \cdot \cos \phi(r, c) - l(r, c) = 0$$

The circle point is determined as the position from which the distance to all the gradient lines in the window is the shortest possible. See figure A.1.4.

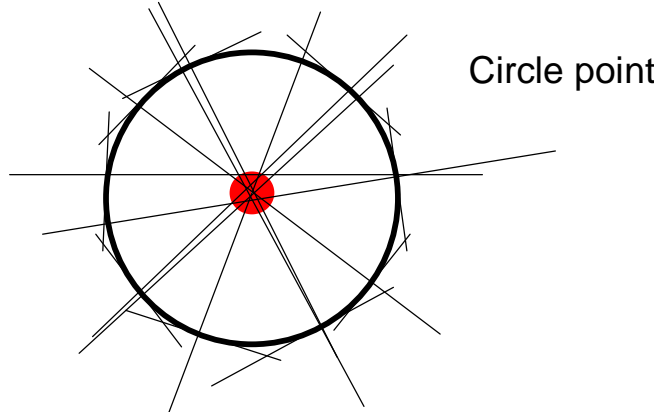


Figure A.1.4: Determination of a circle point from a circle element

As for intersections, corner and end points, the adjustment is done by the least squares method.

This gives:

$$v_i = r_0 \cdot (-\sin \varphi_i) + c_0 \cdot \cos \varphi_i - l_i \quad A(1.31)$$

where:

$$l_i = r_i \cdot (-\sin \varphi_i) + c_i \cdot \cos \varphi_i$$

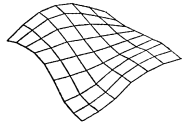
and thus the normal equations:

$$A^T P A x = A^T P b$$

⇓

$$\begin{bmatrix} \sum g_{c_i}^2 & -\sum g_{r_i} g_{c_i} \\ -\sum g_{r_i} g_{c_i} & \sum g_{r_i}^2 \end{bmatrix} \cdot \begin{bmatrix} r_0 \\ c_0 \end{bmatrix} = \begin{bmatrix} \sum g_{c_i}^2 \cdot r_i - \sum g_{r_i} \cdot g_{c_i} \cdot c_i \\ -\sum g_{r_i} \cdot g_{c_i} \cdot r_i + \sum g_{r_i}^2 \cdot c_i \end{bmatrix} \quad A(1.32)$$

By iterative use of the equations for corner and circle points respectively, the points are identified which will then be registered with co-ordinates at sub pixel level in a list.



A.1.2.3.5 Quality evaluation of the characteristic points

The first time around, the Förstner operator has identified a long series of points, but the quality may be very varied, therefore a closer evaluation can exclude the points with the poorest determination. For each point, an error ellipsis and its size (w) and roundness (q) is determined, which is used as a measure of the quality of the determination of the point. The size and roundness of the error ellipsis can be expressed as:

$$w = \frac{\det N}{\frac{1}{2}\text{tr } N} \quad \text{A(1.33)}$$

$$q = \frac{4\det N}{\text{tr}^2 N} \quad \text{A(1.34)}$$

where: $\det N$ = the determinant for the normal equation matrix
 $\text{tr } N$ = the trace for the normal equation matrix

By means of w and q , the best determined points are chosen, which are also the most suitable as temporary co-ordinates. The size of the error ellipsis should not exceed a certain value. A maximum value for w may be found in the following way: The mean of the w values is calculated for a segment of the image. Tests have shown that 2/3 times the mean is a suitable minimum limit [Kraus, 1997]. These points are the so-called interest points which are stored in a list.

At the same time, the error ellipsis should be approximately round, that is, q close to 1. Practical experience has shown that a minimum limit of 0.75 is suitable for q [Kraus, 1997].

A selection criterion for a point could be that the w value as well as the q value of the point should keep within the limit. But if a common limit for w and q is set for the whole image, it may result in the inclusion only of points which are determined in areas with a good structure and which, therefore, achieve a good determination. By the later correlation, it is therefore only possible to correlate over these areas.

To avoid this problem, the non-maximum principle (the thinning out principle) is often used. Within a window of, for instance, 7×7 pixels, only the point with the best determination is chosen. The w value and q value of the remaining points are set at zero [Förstner, 1993].

Because of the ability of the Förstner operator to eliminate points in areas with low contrast, the chosen points will be well defined, and thus form the basis of a final correlation with a high accuracy. The drawback, however, is that in areas with low texture, no points will be chosen.

A.1.2.4 The principles of FBM

The correlation is started with the selection of point pairs in lists of the extracted points from the two images. For each point in one list, the most suitable candidate from the other list is nominated. Together, the two points constitute a point pair.

The selection of points for a point pair may be done in different ways [Förstner, 1993]:

- 1) The point pair must meet a demand for a certain homogeneity as regards the attributes w and q .
- 2) For an image pair, a parallax can be interpolated. Between chosen points, a uniform "parallax field" must be filled. An expected parallax can be used to exclude improbable point pairs. This expected parallax may be the result of using the image pyramid principle (section A.1.6), where the results from the one level is used as the temporary values for the next pyramid level.
- 3) A third criterion might be that the points must be unique, that is, that uniform points must not lie close to each other. This is done separately for both images by eliminating uniform points within a window.

- 4) Finally, the nomination of the candidate point may be done by combining with a criterion about concordance between the immediate surroundings of the points. For this comparison, an ABM can be used, for instance, correlation coefficient or least squares matching [Kraus, 1997].

The result of a selection is a list with $\{(r_1, c_1), (r_2, c_2), w\}$ of a candidate pair with their co-ordinates for left and right image, and their size as attributes.

The position of the selected points is indicated at sub pixel level. In case the accuracy on the background of the above Förstner operator is not sufficient, it can be supplemented by an ABM, for instance, least squares matching [Kraus, 1997].

A.1.3 Epipolar geometry

A quotation by Förstner is a good starting point: *The epipolar line constraint is the strongest constraint in image matching and should be used as soon as available* [Förstner, 1993].

The correlation problem between images can be markedly simplified if the relative orientation is known. The two-dimensional search area can thereby be reduced to a one-dimensional problem by means of the so-called epipolar geometry [Förstner 1993]. To achieve epipolar geometry, a mathematical process, also called normalisation of the images, is done.

The reduction from two to one dimension is done by elimination of the vertical parallaxes (the y-parallaxes). The two normalised images deviate geometrically only along the horizontal parallaxes (the x-parallaxes).

To determine the epipolar geometry, it requires the relative orientation or the whole outer orientation to be known. x_1, y_1 and x_2, y_2 are the image co-ordinates in the two original images, and x'_1, y'_1 and x'_2, y'_2 are the image co-ordinates in the corresponding normalised images. Furthermore, it is determined that origin for the local co-ordinate system is placed in the projection centre of image (O_1), and that the x-axis passes through the projection centre of image (O_2). The z-direction is in concordance with the shooting direction of the first normally shot image, that is, $\kappa_1 = \phi_1 = \omega_1 = 0$. The y-axis is perpendicular to the xz-plane, see figure A.1.5.

The original image co-ordinates may be expressed as:

$$x = -c \frac{r_{11}x' + r_{12}y' - r_{31}c'}{r_{13}x' + r_{23}y' - r_{33}c'} \quad A(1.35)$$

$$y = -c \frac{r_{12}x' + r_{22}y' - r_{32}c'}{r_{13}x' + r_{23}y' - r_{33}c'} \quad A(1.36)$$

The normalised image co-ordinates may be expressed as:

$$x' = -c' \frac{r_{11}x + r_{12}y - r_{13}c}{r_{31}x + r_{32}y - r_{33}c} \quad A(1.37)$$

$$y' = -c' \frac{r_{21}x + r_{22}y - r_{23}c}{r_{31}x + r_{32}y - r_{33}c} \quad A(1.38)$$

where: c = the camera constant
 c' = the camera constant for the normalised images
 x' = the x-co-ordinate in the normalised image
 y' = the y-co-ordinate in the normalised image
 r_{ij} = the elements in rotation matrix R

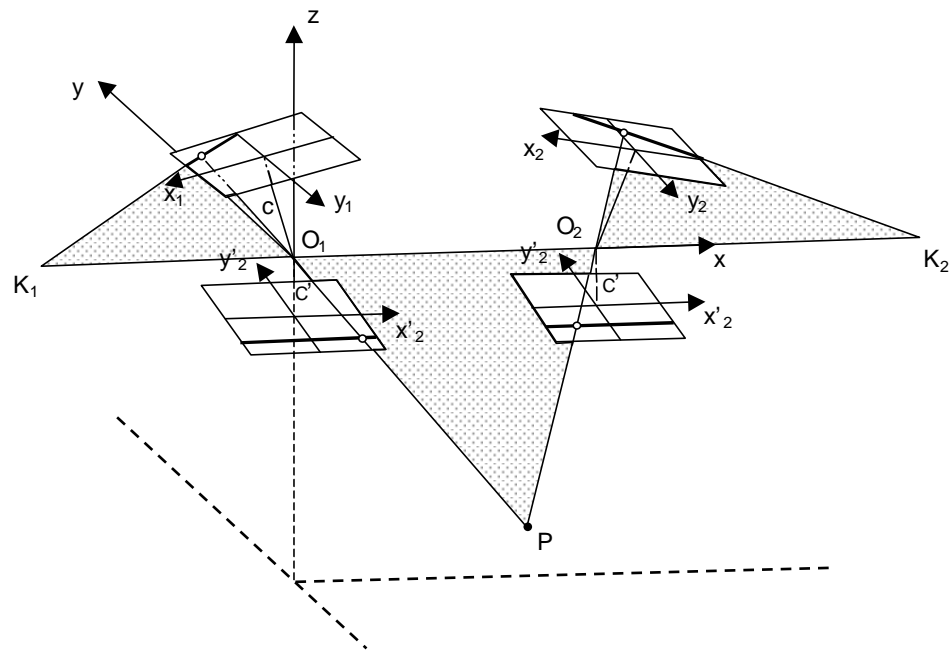
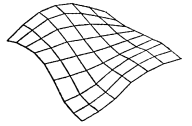


Figure A.1.5: Epipolar geometry

By means of the formulas A(1.37) and A(1.38) it is now possible to make a conversion of the original digital images into normalised images. For the normalisation process, a value for the camera constant c is chosen. This must be somewhat larger than the original camera constant to ensure that all the image features from the original image are included. The pixel size is the same as in the original image. A pixel position in the normalised image does not normally correspond directly to a pixel position in the original image, but often falls on a sub pixel position.

The grey level value of each pixel in the normalised image may be transferred directly from the original image.

A.1.3.1 Resampling

If the grey level value is transferred directly, the result will rarely be a harmonious image. To minimise this problem, resampling can be used. By means of the equations A(1.37) and A(1.38), a pixel position in the normalised image is transferred to a position in the original image, see figure A.1.6. An adapted grey level value is interpolated from the grey levels in an area in the original image by using, for instance, a bi-linear interpolation [Kraus, 1993], or a bi-cubic interpolation [Krzystek, 1995].

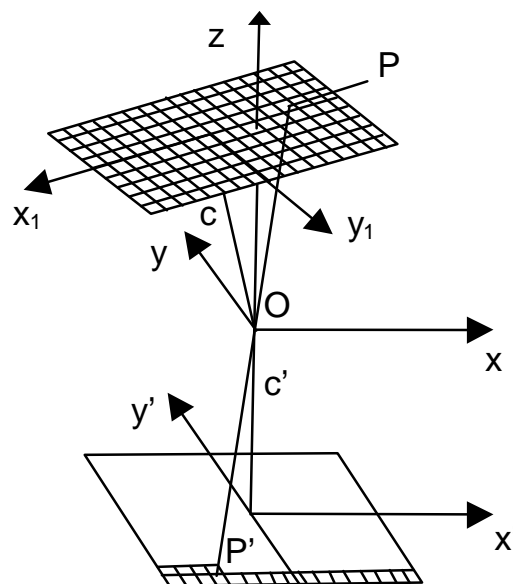


Figure A.1.6: The resampling principle

A.1.3.2 Normalisation and resampling

If epipolar geometry and resampling are combined, it can be done as an independent process, where the whole normalised image is stored on the hard disk, or the process can run concurrently during the correlation process. The process of normalisation and resampling of a whole image is quite time-consuming. Time may therefore be saved by only normalising and resampling those pixels which are necessary for the correlation. The last-mentioned can be regarded as a one-dimensional correlation in the original images.

A.1.3.3 Correlation in one dimension

As described, the correlation problem is reduced from a two-dimensional problem to a one-dimensional one by using the normalisation principle. In the following, the correlation principles for ABM and FBM are described in one dimension.

A.1.3.4 ABM in one dimension

The methods described for the determination of a position at pixel level (see section A.1.1.1) may be used directly in one dimension. As an example, the least squares matching is described here to find the best correlation at sub pixel level. If the pixel position on an integer is designated (α) and the small shift (β), the fitting in between the position for the two normalised images I_1 and I_2 can be expressed in the following way:

$$g_T(\alpha) = g_S(\alpha + \beta) \quad A(1.39)$$

where g_T = the grey level values for the target area
 g_S = the grey level values for the search area

As described in section A.1.1.2.2, the target area and the search area do not only diverge from each other in position, but also in grey level values. Therefore, the grey level values for the target, g_T , are assigned random values v . g_S is supplied with systematic correlations, such as a scale factor r_0 and a shift r_1 for the grey level values:

$$g_T(\alpha) + v = r_0 g_S(\alpha + \beta) + r_1 \quad A(1.40)$$

By using the least squares method for the adjustment, the square sum of the random values v is minimised, and the elements β , r_0 and r_1 are determined. For this purpose, the equations must first be linearised. As β is a small element, the equation can be expressed thus:

$$g_T(\alpha) + v = r_0 (g_S(\alpha) + g_T'(\alpha) \beta) + r_1 \quad A(1.41)$$

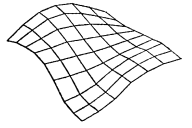
After a change of the terms, finally the searched-for error equation for an element adjustment with the unknown quantities (r_0 , β), r_0 and r_1 is obtained:

$$v = [r_0 (g_S(\alpha) + g_T'(\alpha) \beta) + r_1] - g_T(\alpha) \quad A(1.42)$$

where: $g_T(\alpha)$ and $g_S(\alpha)$ are corresponding grey levels in the two images. The number of grey level pairs is usually given by the size of the target area.

and where: $g_T'(\alpha)$ is the inclination of the grey level profile for the first image for a given pixel position, that is, $g'(\alpha) = \nabla g / \nabla \alpha$. For the first pixel, we put $\nabla g = g_S - g_T$, for the last, the n^{th} , $\nabla g = g_n - g_{n-1}$; for pixels between $1 < i < n$, the suitable choice is $\nabla g = g_{i+1} - g_{i-1}$.

The accuracy of the position determination is in the order of a tenth of a pixel size.



A.1.4 FBM in one dimension

An example of the use of FBM in one dimension is in the programme package Match-T. The Förstner operator is, as mentioned before, originally an operator, where corners and circular features are extracted, and their "sub pixel position" is determined (see section 1.3.3.2). This is done in two dimensions. Match-T first converts images into normalised images. In these normalised images, the Förstner operator is specified, so that only squared gradients in the row direction are summed up within a window size, determined beforehand. The assumption of the location of a point within the window is fundamentally a Gauss-Markoff process [Krzystek 1995]:

$$\left(\sum g_r^2\right)x = \sum g_r^2 \cdot r \quad \text{A(1.43)}$$

with: g_r = the gradient in the row direction in the window
 r = the number of column co-ordinates in the window
 x = the location of the point in the window

In specific cases of epipolar geometry, the operator is a pure edge operator which is very sensitive to vertical edges [Krzystek 1995]. By means of the principle of non-maxima suppression, the list of feature points (gradients) is thinned out. Then, only the most significant points remain. The final correlation of corresponding points is geometrically delimited by the epipolar lines (the image rows), and by a parallax bound between the correlation candidates. In addition, a symbol and the size of the "interest" value as well as the correlation coefficient in a defined window are used as frame of comparison for the correlation. A list of "interest" candidates (gradients), which are not unique after an introductory correlation, is cleared of discrepancies by a robust affine transformation.

A.1.5 Correlation in one dimension 'on the fly'

The procedure for finding corresponding points by means of kernel rays in the two original images is as follows: an arbitrary point $P_1(x_1, y_1)$ in the original image is chosen. This point P_1 and the kernel point K_1 define a kernel ray in the first image. $P_1(x_1, y_1)$ is transformed in the corresponding, normalised image by the equations A(1.37), A(1.38) into $P_1'(x_1', y_1')$. This point may then be used to define the point P_2' in the other normalised image. Finally, this $P_2'(x_2', y_2', c')$ is transformed into the other original image by the equations A(1.35) and A(1.36). P_2' and K_2 determine the kernel beam in image 2 which corresponds with the kernel beam in the first original image, determined by the points P_1 and K_1 .

A.1.6 Image pyramid

ABM may be supplemented by the build-up of a so-called image pyramid. An image pyramid consists of different resolutions of the same image, where the top level has the lowest resolution, and thus the smallest number of pixels. The method is also known as the multi-resolution or coarse to fine resolution, as the pyramid is used beginning at the upper, coarse level. The image pyramid can be regarded as image information presented in a series, where the resolution increases, when moving downwards in the pyramid.

There are different methods of building up an image pyramid. Typically however, the number of pixels is changed by a factor 4 between two neighbouring levels in the pyramid. Here, some of the methods employed most often are indicated:

- For a group of four pixels, the grey level value for the lower left pixel is transferred. The remaining three pixels are not transferred.
- Every second row and column are eliminated.
- The mean grey level value for 2 x 2 pixels is calculated and transferred to the next level.
- Binomial filter (for instance the Gaussian function) in a window of, for instance, 5 x 5 pixels.
- Interpolation, for instance bi-linear, over four neighbouring pixels.

The levels over the original image will altogether fill 33 % of the original image. An example of an image pyramid is seen in figure A.1.7. The individual pyramid levels are determined by calculating the mean grey level value for 2 x 2 pixels, and transferring it to the next pyramid level.

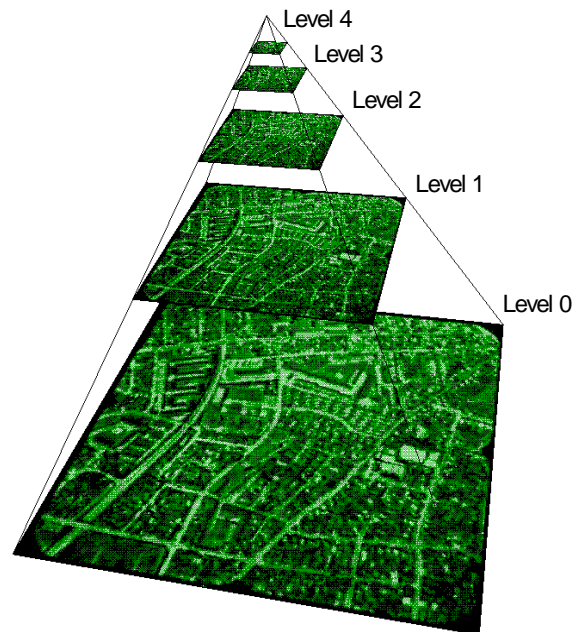


Figure A.1.7: Image pyramid

The purpose of an image pyramid is to achieve temporary values for correlation. The first correlation is done with data from the upper level of the pyramid, and the result is then used as temporary values on the next (finer) pyramid level. The use of the image pyramid is very effective in the search for temporary values, and at the same time quick and certain. There are three valuable qualities in the use of the image pyramid [Ackermann & Hahn, 1991]:

- The area over which the correlation is done may be broadened, as there is only need for a coarse, temporary value at the upper pyramid level.
- The total expense of time for the correlation is minimised.
- Greater certainty of achieving a correct correlation.

Back in the beginning of the 1990s, many, if not all correlation algorithms were based on the image pyramid principle [Ackermann & Hahn, 1991].

A.1.7 Object pyramid

If the requirement is to transfer the pyramid principle to FBM, an object pyramid must be built up. The point of departure is an image pyramid, where for each level features are extracted by means of an operator which is described in section 1.2. In contrast to the image pyramid, the object pyramid is built from the top, and independent of the previous levels, see figure A.1.8.

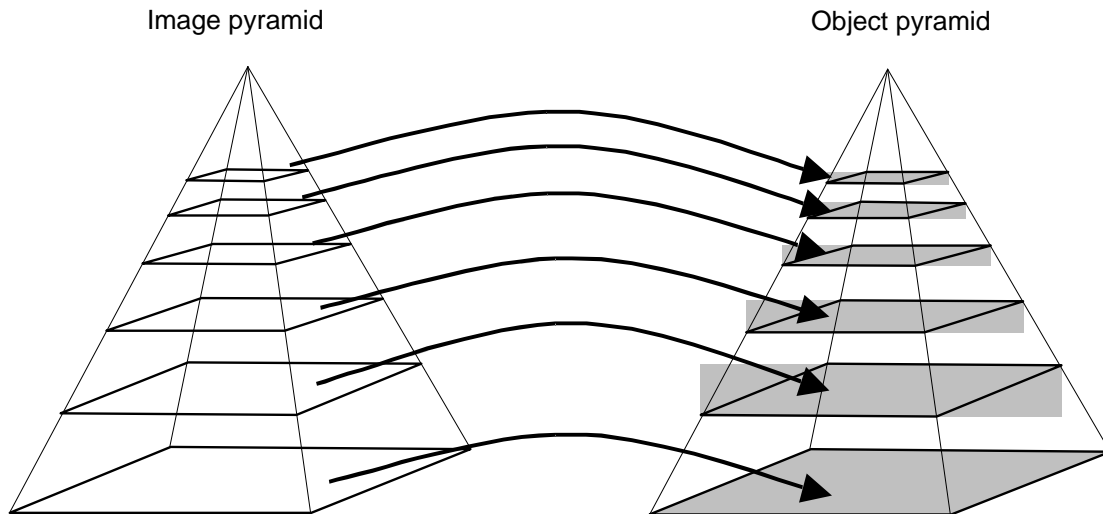
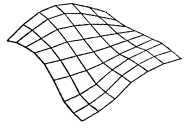


Figure A.1.8: Creation of the object pyramid from the image pyramid

An FBM can then proceed down through the object pyramid by means of the results from the previous pyramid level as temporary values.

A.1.8 Pros and cons

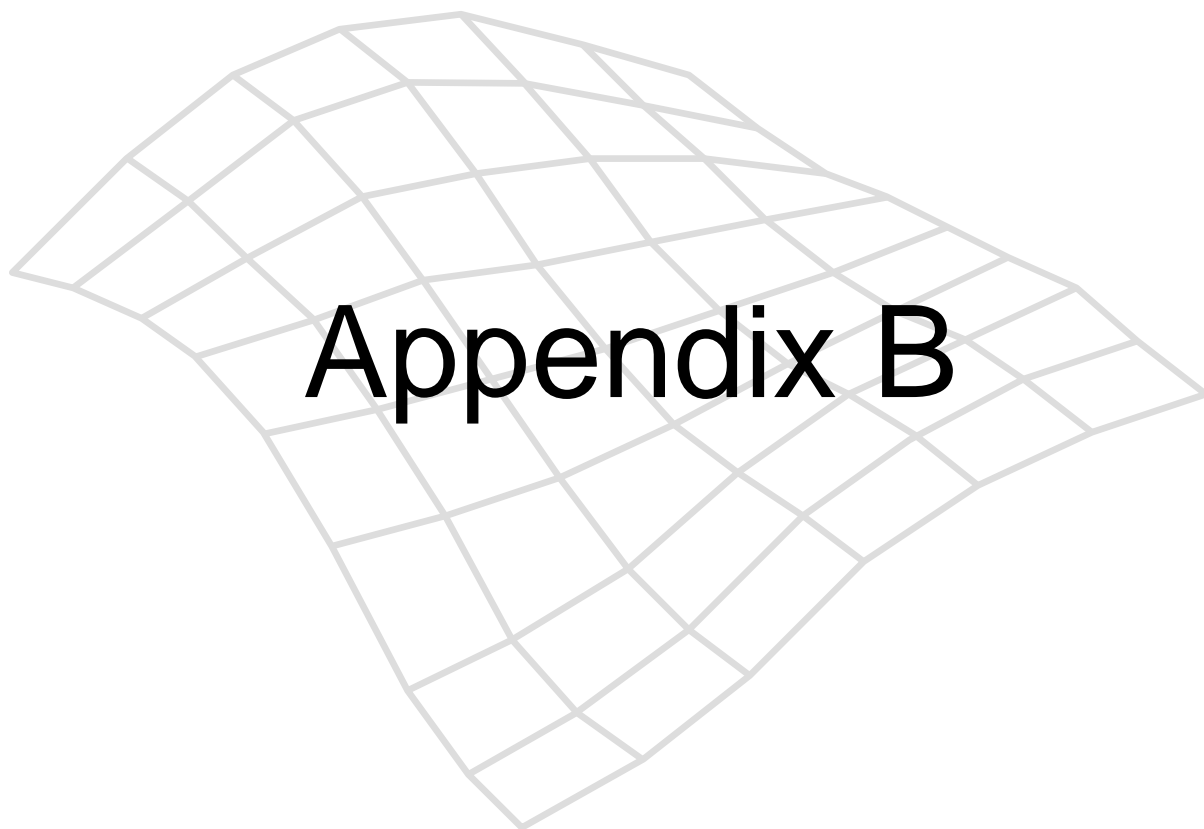
FBM is often discussed as an alternative to ABM. In reality, both methods have their advantages and drawbacks [Baltsavias, 1991]. FBM is superior for correlation as regards speed and possibilities [Förstner 1986], and does not require such good temporary values as ABM [Krzystek, 1995; Baltsavias, 1991]. FBM is generally less sensitive to geometric and radiometric deformations [Baltsavias, 1991], but, on the other hand, it gives a poorer accuracy (1.5 pixels) and more scattered results.

ABM poses problems when the images have been shot from very different positions, when they have a low signal structure, or are very different and incoherent [Baltsavias, 1991].

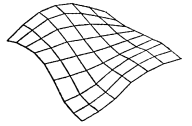
The end result for the final correlation with FBM, however, is not as good as with an ABM, where an accuracy of 0.1 pixel can be achieved [Kraus, 1997]. One of the drawbacks of an ABM, for instance the least squares matching, is that it requires good temporary values to achieve a good result. Furthermore, the calculation process of least squares matching is demanding, both as regards the calculation time and the calculation capacity.

FBM is, in general, a superior correlation method as regards speed and versatility. Likewise, when comparing least squares matching, FBM is better as regards convergence, speed and versatility.

The optimal would therefore be to combine the two methods. FBM is used to achieve good temporary values, and the least squares matching in ABM is used to find sub pixel level with an accuracy of 1/10 of a pixel [Kraus, 1997].



Appendix B



Appendix B: The data material

This appendix includes a description of the data material which is used in the project, that is, test area, aerial photos, control points and frame of comparison. The appendix is divided into two parts, in the first part the data material itself is described. The second part includes a description of the process of acquiring control points, and the frame of comparison, consisting of analytically measured points in a 25 x 25 m grid (the frame of reference). The second part is concluded with the final control point list.

B.1 Description of the data material

The structure of this part of appendix B, is as follows: The chosen test area with typically Danish landscape types is described in section B.1.1. The shooting and scanning of aerial photos, shot at three different flight altitudes are discussed in section B.1.2. Section B.1.3 includes a presentation of control points, chosen for use at the orientation of the aerial photos. In section B.1.4, a description is given of the models chosen as background for the frame of reference. Section B.1.5 describes the frame of reference, and the existing elevation models are described in section B.1.6.

B.1.1 Test area

With a view to the purpose of the project, a test area is required which is representative of Danish conditions, that is, including open, flat areas, hilly areas, overgrown areas, built-up areas etc. Of particular interest are area types such as woods and buildings, as earlier investigations [Hahn, 1989; Ackermann et al., 1992; Krzystek et al., 1992] have proved problems with automatic generation of elevation data over these areas in particular. For practical reasons, proximity to Aalborg University (AAU) has also been stressed.

The result of the search was an area of 3.5 x 4 km situated immediately south of the university. The area includes two villages, flat and hilly fields, gravel pits and part of a wood. With the chosen test area, more than 70 % of the area types in Denmark are represented. Only densely built-up areas and waters are not represented. Urban areas are a landscape type which [Seyfert, 1995; Thorpe et al., 1996] have taken a closer look at. Their investigation shows that this kind of landscape type poses problems. For natural reasons, no correlation is possible over sea or lakes, and these are therefore not interesting for this investigation.

The location of the test area is shown in figure B.1.1.

B.1.2 Aerial photos

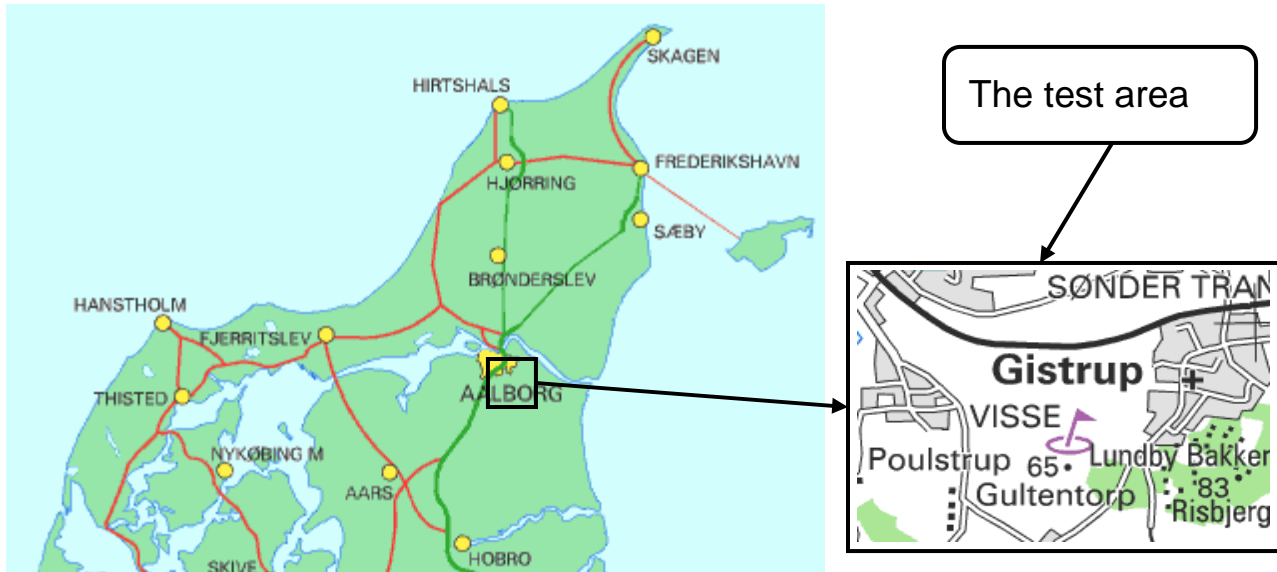


Figure B.1.1: The location of the test area in relation to Aalborg/Northern Jutland.

For use in the analysis, digital aerial photos are necessary. When this investigation was started, digital cameras did not exist. This investigation is therefore done on scanned aerial photos. As the photogrammetric system Match-T cannot handle colour photos, the aerial photos were shot in black/white.

Earlier investigations, for instance [Ackermann et al., 1992; Eide et al., 1993; Krzystek et al., 1995], show that the scale and resolution of the images have an influence on the accuracy by automatic generation. The aerial photos are therefore shot at 3 different flight altitudes, and so test material in scales 1:5,000, 1:15,000 and 1:25,000 is available. The point of departure for these scales is that shots in scale 1:25,000 are the basis of the nationwide atlas TOP10DK, and scale 1:5,000 is used for detailed projecting. 1:15,000 has been included in order to determine, whether there is a linear connection between scale and accuracy. The aerial photos of the test area in scales 1:5,000, 1:15,000 and 1:25,000 are covered by 36, 7 and 2 models respectively.

The images were scanned in a PS1 PhotoScan, where the possible resolutions are 7.5 μm , 15 μm , 30 μm , 60 μm and 120 μm . Traditionally, images have been scanned for many years in the pixel size 21 μm . To avoid too many analysis options, and to investigate whether the resolution of the images by any chance, has a linear influence, the choice has been to look at only three different resolutions. To avoid too large data quantities, the pixel size 7.5 μm has been excluded. In order to investigate images with a resolution around the traditional 21 μm , the choice has been to scan in 15 μm , 30 μm and 60 μm , thus excluding the resolution 120 μm .

Figure B.1.2 shows the flight paths for the photo shot of the images in scale 1:5,000.

The requirements for the shooting of the images were that these should live up to the general demands for images for photogrammetric mapping. The images in scales 1:5,000 and 1:15,000 meet the demands, while the images in scale 1:25,000 are hazy. The point of departure for the images was that they would be shot before leafing foliage. The year 1996, however, was a problematic year, where the snow disappeared late, and the trees were out early. Therefore, it may be expected that the trees are in leaf.

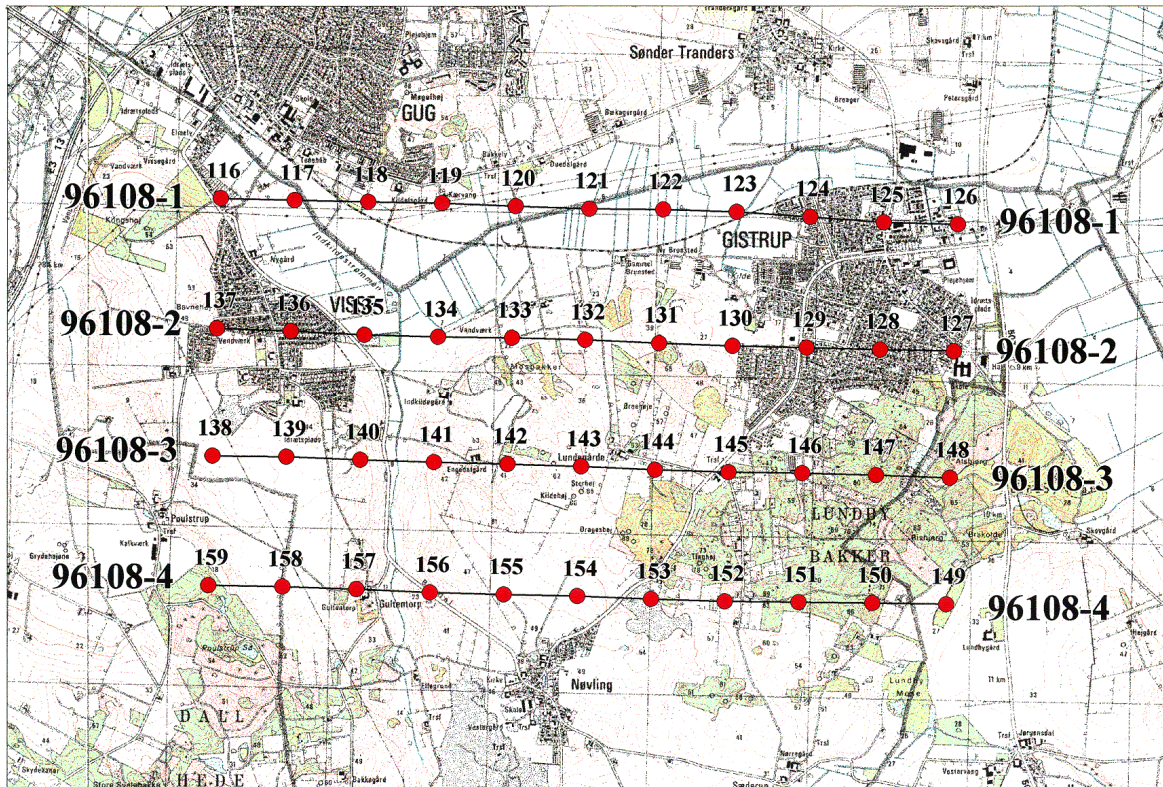
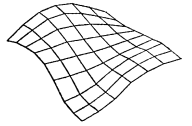


Figure B.1.2: The flight paths for the shooting of images in 1:5,000.

B.1.3 Control points

When this investigation was started the position of the airplane determined by GPS/INS was not as trustworthy as it is today. The images have therefore been orientated by the old traditional way of using control points.

The number of control points for the models in scales 1:25,000 and 1:15,000 is small, while for the 36 models in scale 1:5,000, a larger number of points is in question. The number of control points takes as point of departure the recommendation of 4 PP and 6HP per model [Brande-Lavridsen, 1993]. Measuring by means of GPS was time-consuming in the middle of the 1990s, and might therefore, with advantage, be supplemented with a bundle adjustment. Determination of control points by photogrammetric methods, furthermore ensures good coherence and uniform accuracy. For this purpose, the distance between the elevation control points should be 2 times the basis over the whole block, while as regards the planimetric control points, the distance between them should be 4 times the basis along the edge of the block [Brande-Lavridsen, 1993]. For practical reasons, the control points from the models in 1:25,000 are as far as possible reused for the models in 1:15,000, cf. for example point 500 or 506, see figure B.1.4 and B.1.5. Where the models cover more than the test area, the control points are chosen, so that they primarily surround the test area, but not necessarily most of the model, see figure B.1.4.

The selection of control points builds on the Danish tradition of using terrain objects as control points. Truly well-defined terrain objects are wells, gratings and road markings, wherefore such points are used in this project. The use of natural control points requires a good contrast between the point and the surroundings. As regards the size of the control points, the National Survey and Cadastre has laid down signalling guidelines for the size of signal plates for use in traditional analogue photogrammetry for models in scale 1:5,000 at between 25-30 cm x 25-30 cm [The Geodesy division, 1992]. This size of signal plane corresponds to 50 μ m - 60 μ m in the image. The guidelines are valid for scales down to 1:12,000, but if the size 60 μ m is transferred to the models in scale 1:15,000 and 1:25,000, it corresponds to point sizes

of 75 –90 x 90 cm and 125-150 x 150 cm respectively. In the middle of the 1990s, there existed no specific guidelines for digital photogrammetry in Denmark, or for that matter, guidelines for the size of natural control points, therefore the aforementioned guidelines were adhered to.

With a view to a later comparison with other data, the control points were linked to the GI grid, and the co-ordinates were given in System34 Jutland/DNN.

As the control points are used for the generation of elevation data as well as for the production of the analytically measured elevation data, the strictest demand for accuracy by the automatic generation of elevation data has been taken as point of departure. That is, better than 0.1 % of the flight altitude for images in scale 1:5,000, which means a final accuracy requirement for the frame of reference better than 0.075 m. This entails a demand on the GPS measurement of 0.015 m in all three directions (see the later section B.1.5).

As mentioned before, control points of the types gratings, wells and road markings have primarily been used in this project. For the models in scales 1:15,000 and 1:25,000, however, objects such as sand boxes and flower beds have also been used. More supplementary planimetric control points have been measured than prescribed, to improve the accuracy of the whole model. The total number of points (geodetic reference points and control points) is 119, and the maximum co-ordinate deviation is:

$$x = 0.011 \text{ m}$$

$$y = 0.014 \text{ m}$$

$$z = 0.015 \text{ m}$$

See also section B.2.8.4.2 and Appendix E.2 and E.3.

An example of a terrain object used as control point is shown in figure B.1.3.



Figure B.1.3: Grating used as control point.

The chosen control points and the location of the test area for the models in scale 1:25,000 are shown in the following figure B.1.4.

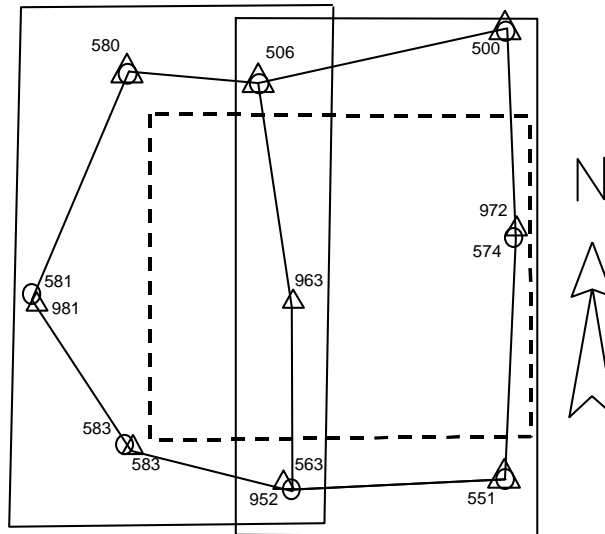
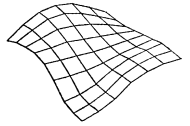


Figure B.1.4: Tracing for 1:25,000.

The control points and the location of the test area for images in scale 1:15,000 are shown in figure B.1.5.

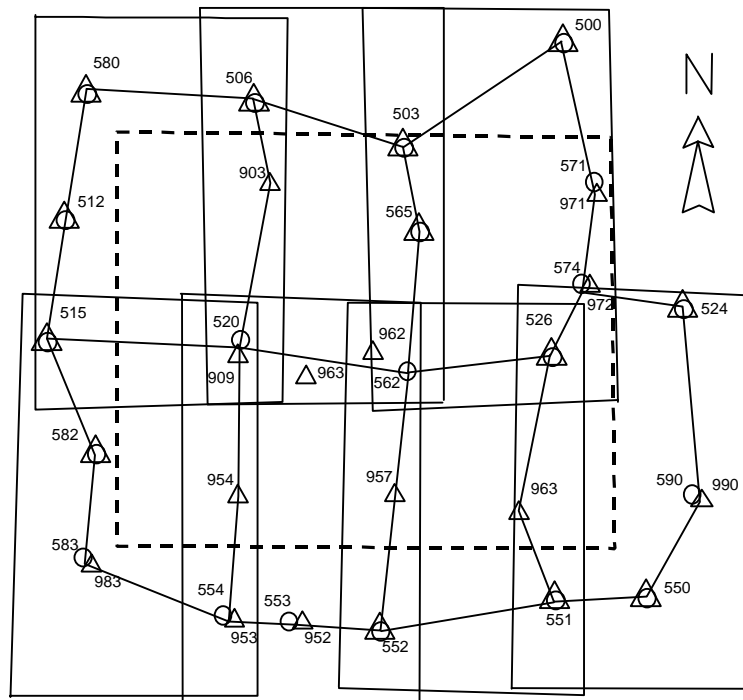


Figure B.1.5: Tracing for scale 1:15,000.

As mentioned earlier, as regards the images in scale 1:5,000, only the number of control points necessary to do a bundle adjustment has been chosen. The location of these control points is shown in figure B.1.6. As the models in scale 1:5,000 are all situated within the test area, this has not been delineated in figure B.1.6.

As may be seen from the tracing, plane control points for 4 times the basis in the middle of the model have also been chosen, even if this is not strictly necessary.

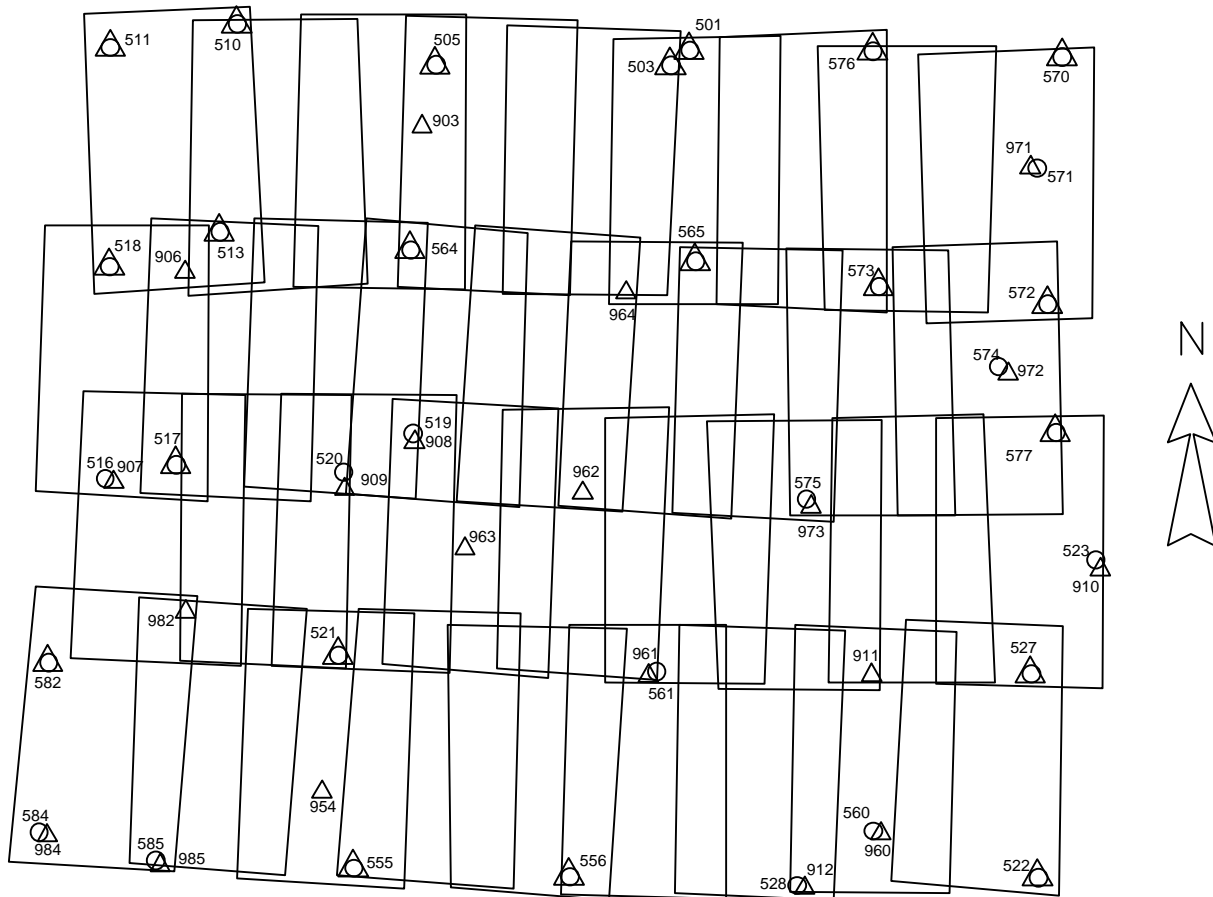


Figure B.1.6: Tracing for scale 1:5,000

The control determination has been described in more detail in another part of Appendix B.

B.1.4 Selection of models and area types

Not all models in scale 1:5,000 are included in the investigation. The selection of models is done on the following basis: the quality of the control points and the landscape types represented in the model. Interesting area types are flat and hilly areas, wooded/overgrown areas, built-up areas and gravel pits.

As it will appear from figure B.2.7 (see section B.2.2.1), the control points in the corners of the test area are not so well determined as in the rest of the block. It has therefore been the aim to select models which were not corner models. The 14 models were chosen to represent the test basis in scale 1:5,000, and it is also those models which are the basis of the frame of reference. The selected models, and thus the location of the frame of reference in the test area are shown in figure B.1.7. The individual landscape types are represented by colours, where red is village, blue is woods, green is flat fields, violet is hilly fields, and orange is gravel pits.

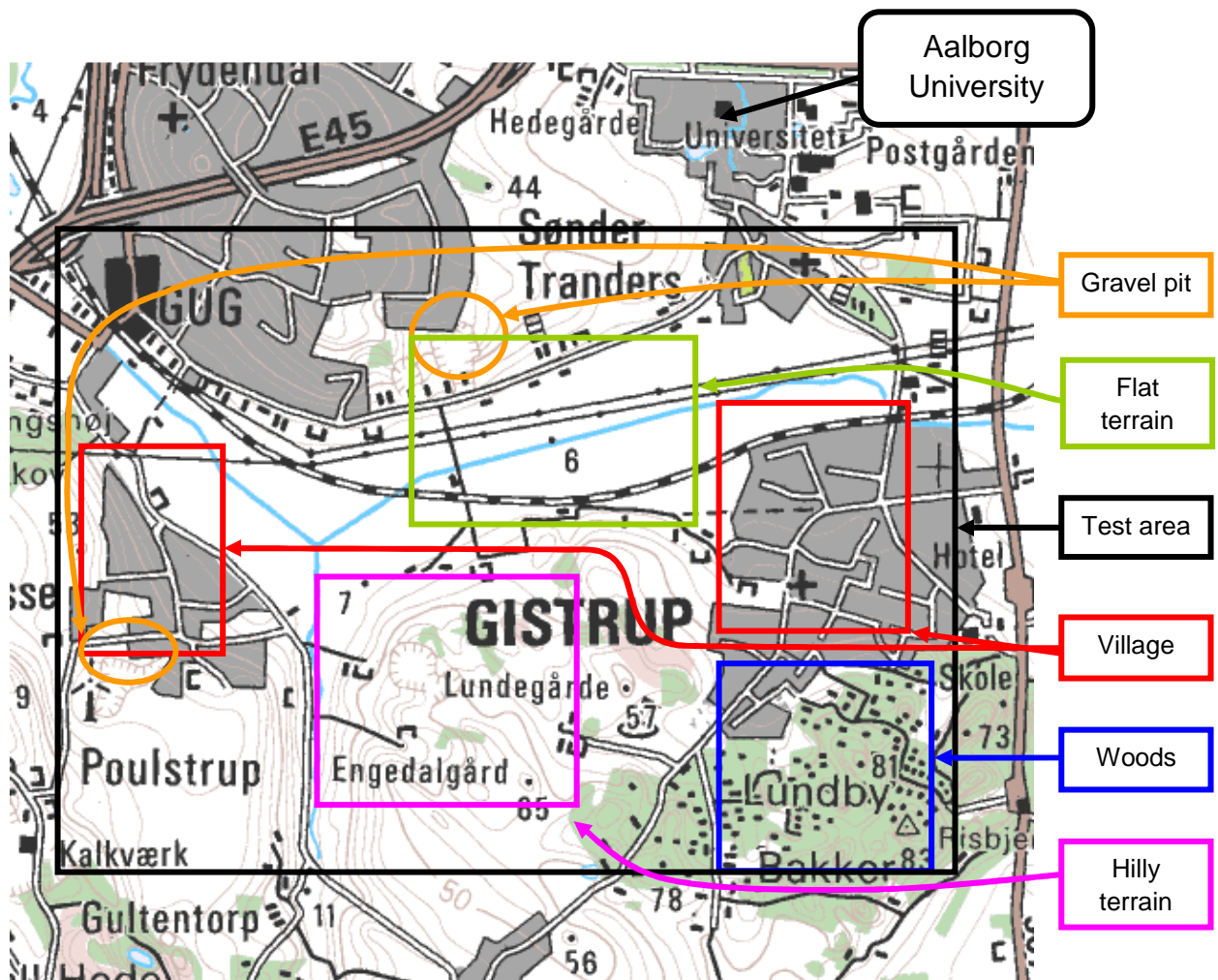
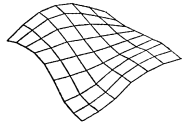


Figure B.1.7: The location of the landscape types in the 3.5 x 4.0 km large test area.

The measured points of reference have been assigned an object code which refers to the different landscape types. The number of points of reference for the different landscape types are distributed as follows:

Code 12	= Flat terrain:	2092 points
Code 34	= Gravel pits:	2429 points
Code 56	= Village:	1629 points
Code 78	= Hilly terrain:	2814 points
Code 90	= Woods/vegetation:	1223 points
Total:		10.188 points

The points of reference are measured in a grid with a fixed mesh size of 25 x 25 m. However, in the landscape type gravel pit, the measured grid has a mesh size of 5 x 5 m. This is due to the fact that this landscape type is steeper than the others. Furthermore, this landscape type covers a somewhat smaller area than the others, and to get a sufficient number of points for the statistical material, the mesh size must be smaller. It is seen that there is a sufficient number of points for a statistically representative frame of reference.

B.1.5 Analytically measured points of reference

In order to make an analysis of elevation data determined in different ways over an area, a frame of reference over this area must be available. This frame of reference may be established in different ways. The elevations may be determined by levelling, or, for instance, by use of GPS or by photogrammetry etc. In this project, the choice has been to determine the frame of reference photogrammetrically in an analytical instrument, on the basis of the same aerial photos and control points which are used for the automatic generation of elevation data. The point set is thus independent of the method for automatic generation of elevation data itself, but takes the same data as point of departure. As the automatic generation is done in a fixed grid without break lines (cf. Chapter 2, section 2.4.3.2), the best basis of comparison is a grid, that is, with identical plane co-ordinates. The chosen mesh size in Match-T is 25 x 25 m, 12.5 x 12.5 m and 5 x 5 m respectively.

The original idea was that the analytically measured elevation data should be compared with the automatically generated elevation data as well as with existing elevation models. Therefore, the points were co-ordinated in System34 Jutland/DNN. If the existing elevation model was not to be included directly, but only used as frame of comparison for the accuracy demands of the method, the analytical determination of the points could be done in a local system, and thus be quite uninfluenced by existing grid tensions.

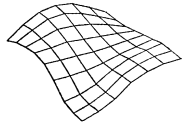
In order to be able to use the analytically measured elevation data as frame of reference, these points must have a superior accuracy. It is stated in the literature that it is possible to determine elevation data automatically with an accuracy of 0.1 ‰ of the flight altitude [Krzystek et al., 1992]. Images in scale 1:5,000 are shot at a flight altitude of 750 m, which means that by automatic generation of elevation data, an accuracy of approx. 0.075 m should be possible to achieve. For images in scale 1:15,000, an accuracy of approx. 0.225 m should thus be possible, while for images in scale 1:25,000, the accuracy might be approx. 0.375 m.

If the analytically measured elevation data is to have a superior accuracy in relation to the automatically generated elevation data, the point deviation must not exceed 0.03 m – 0.04 m, because of the high degree of accuracy, which may be expected in scale 1:5,000. However, this cannot be achieved, as the expected accuracy of the result of an aerotriangulation with use of images in scale 1:5,000 is better than 0.05 m in the planimetric, and 0.05 m – 0.10 m in elevation. As the largest error contribution traditionally arises from the photogrammetric part, the accuracy demand for the GPS measurement of the control points is less than 0.015 m in all three dimensions.

For the production of the frame of reference, an analytical instrument of the type Planicomp was available for the project. To minimise the error contribution from the manual measuring of the analytically measured elevation data, an experienced stereo operator did the work.

The provision of the analytically measured elevation points is described in more detail in section B.2.2.

As it will appear later from section B.2.2.2, the accuracy of the aerotriangulation has not turned out so well as expected. To this must be added the error contribution from the analytical measuring, after which the total accuracy of the analytically measured points is estimated to be 0.10 m (see the later section B.2.2.3). This accuracy is not superior for models in 1:5,000, as the literature [Krzystek et al., 1992; Krzystek et al., 1995] prescribes that an accuracy of 0.075 m can be achieved here. This means that the frame of reference must be used with caution for the evaluation of the result of automatically generated elevation data in scale 1:5,000. For images in scale 1:15,000 or 1:25,000, the accuracy achieved will still be superior in relation to 0.225 m and 0.375 m respectively, which may be achieved by automatic generation of elevation data.



B.2 Data capture

The second part includes section B.2.1 about control point capture, and section B.2.2 about capture of the analytically measured elevation data which are used as frame of comparison, called the frame of reference.

B.2.1 Capture of control points

With point of departure in the requirements of the control points mentioned in section B.1.3, the process of capturing the control point co-ordinates will be described here.

B.2.1.1 Planning

B.2.1.1.1 Geodetic reference

The control points must be measured in relation to the nationwide, superior net, the Geodetic reference net, as a later comparison with other elevation data may then be possible. The connection to the Geodetic reference net has, furthermore, the advantage that it is possible to control the measurement, as both elevation and planimetric reference points are included. Thus, gross errors can be detected, and a possible repeat measurement can be planned optimally. Reference points are selected, so that they are

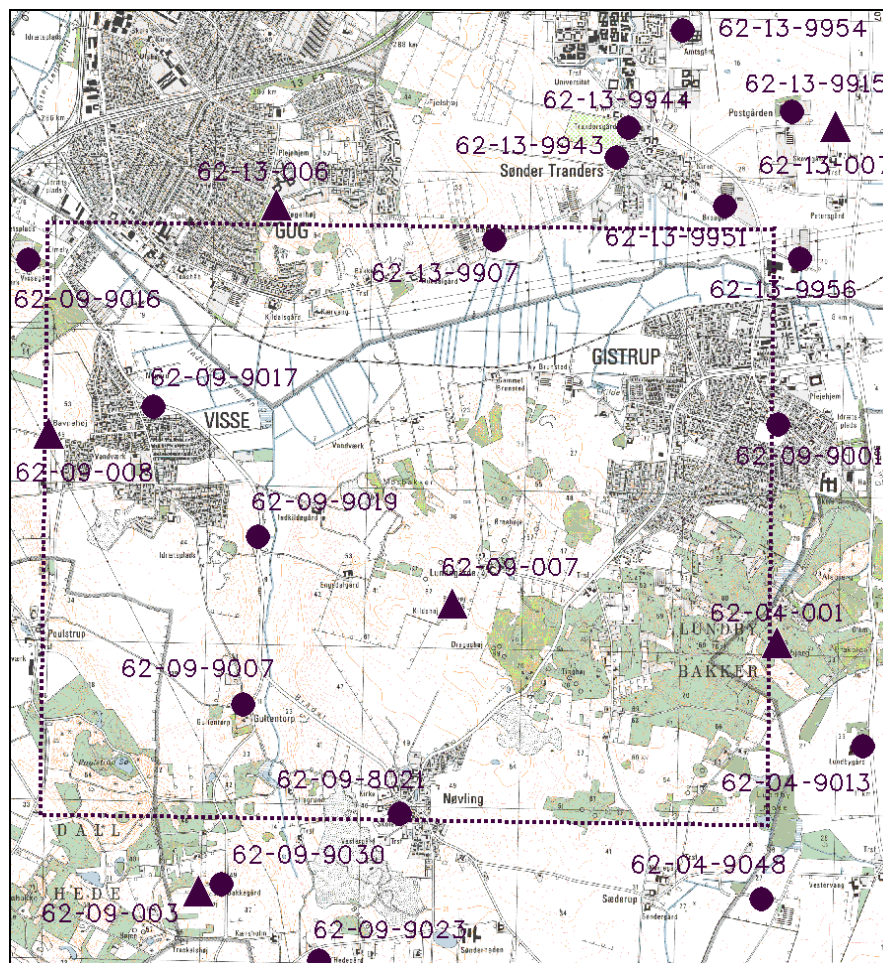


Figure B.2.1: The location of the geodetic reference points in relation to the test area.

dispersed evenly and cover the whole area, see figure B.2.1.

To satisfy the demand for accuracy in the control points, these are measured with GPS. As the elevation reference points are often placed on, for instance, house walls, a moving-out/establishment of the offset point is necessary, which is then determined by means of levelling. These offset points are then measured with GPS. Where possible, these offset points are included as elevation control points as well.

B.2.1.1.2 Equipment

At the disposal of the measurement were two-frequency Ashtech Z12 receivers with the matching programme package called PRISM. The calculation of the vectors was done with PNAV, a calculation module in the Ashtech programme package, and the subsequent adjustment was done with the module Fillnet.

B.2.1.2 Grid structure

The optimal location of the master station is in a point with free horizon. The reach of the measuring method in the mid 1990s was a maximum of 10 km, therefore, the master station should be located within a radius of 10 km. Furthermore, it was required that the point where the master station was placed, was a point where all three co-ordinates were known.

Two points were chosen for the master set-ups. One was a point located on the wall of a building at Aalborg University called 0011. This point was chosen, as there is a free horizon, and it is situated in such a way that the point could be under surveillance, while the field measurements were done. In addition, the geodetic reference point 62-09-007 on Storhøj was chosen. Storhøj is a tumulus with free horizon in the middle of the test area. While the point at Aalborg University was known with co-ordinates in all three planes, the 62-09-007 point was only known in the x, y plane, but as the point was situated in the middle of the test area, and therefore was of optimum use, its elevation was determined for the occasion.



Figure B.2.2: The masterstation on the wall of Fibigerstræde 11, Aalborg University and on Storhøj, geodetic reference point GI 62-09-007.

Planimetric control points and fully measured points are assigned numbers from 500-599. The elevation control points are assigned numbers from 600 and up.

B.2.1.2.1 Measuring method

The GPS measurement was done as a cinematic measurement called "stop and go". The chosen surveying method can be used for both real-time positioning and for post-processing. The last mentioned is chosen for this measuring task because of the greater accuracy which is expected at cm level [Cederholm, 1995].

At the "stop and go" survey, data is captured continuously in both rover and master. When the rover is moved between the points, the contact to the satellites must be preserved. In that way, the measuring

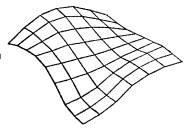


Figure B.2.3: Example of the rover on the move



Figure B.2.4: An example of a rover position

time is reduced, as it is not required to initialise (make contact with the satellites) for each new point. Initialising is only done in the first point, and if the contact is lost in the course of the process. A first time initialisation takes approx. 10 minutes, while an initialisation on the way is a little shorter. To achieve good results, contact to a minimum of 5 satellites is required, and also that PDOP is less than 4 [Cederholm, 1995].

The Rover antenna is mounted on a Kern telescope tripod which can be moved fairly easily while, at the same time, the contact to the satellite is maintained. Likewise, a stable set-up is secured, where the centering is maintained during the whole of the survey. The antenna elevation is not meant to be fixed during the whole process, but changed so that there is always the best possible contact with the satellites. This means that the antenna elevation must be registered for each set-up.

Over-determination is achieved by measurement of two vectors for each point. This can be done, either by simultaneous measuring to two master stations, or by two separate measurements, each with one master. By using two master stations at the same time, a wrongly indicated antenna elevation will not be discovered, wherefore the choice has been to use two separate measurements.

B.2.1.3 Changes during the field survey

During the course of the process, it turned out to be necessary to extend the numbering system. Extra or re-measured points were assigned four-digit numbers by adding 6, 7, 8 or 9 respectively in front of the original number. As the elevation control points are not well-defined horizontally, and therefore cannot be re-measured in precisely the same place, they received a 9xx number at the first measurement, and at the second measurement one of the above-mentioned four-digit numbers. At the assignment of four-digit numbers, no difference was made between a required measurement and a re-measurement.

B.2.1.4 Calculation

With the co-ordinate calculation by the PNAV module, there are two methods to choose between. Data can be calculated from the beginning in the order in which they have been measured, or a double calculation can be done beginning from the end and then from the beginning. The last-mentioned method closes a part of the cycle slips which may have arisen during the measurements, and it is therefore chosen for this project.

According to how good a solution the programme achieves, the solution for the vector of the point is assigned the designation "fixed" or "floating". By a "fixed" solution, the determination of the whole number of

wavelengths is an integer. With a "floating" solution, the determination of the whole number of wavelengths is approximately solved. Only points with the designation "fixed" were used in the further process, whereas the points with the designation "floating" were measured again.

The subsequent adjustment in the module Fillnet was done both freely and quickly.

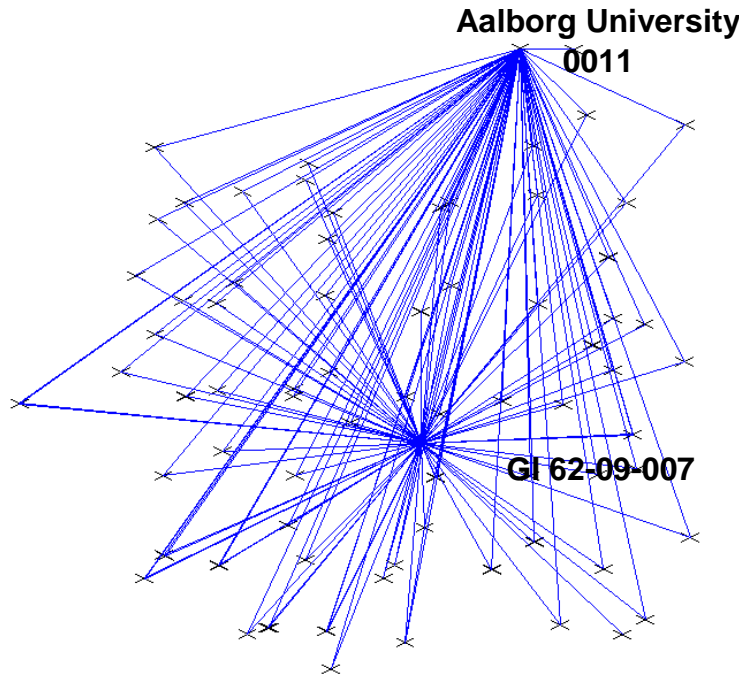


Figure B.2.5: The grid sketch

The grid sketch in figure B.2.5 shows that the grid is harmonious, and that there are two vectors to almost all points. For a single point, two vectors from 0011 have been measured instead of one from 0011 and one from GI 62-09-007. Other points originally had one vector from 0011 and one vector from 007 was measured, but the vector from 0011 was poor because of a bad connection to the satellites. This vector has therefore been taken out of the calculation, and the vector has not been re-measured, as the point is an elevation reference point, and not a control point.

B.2.1.5 Evaluation

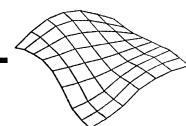
119 points were measured, and the result of the free adjustment is shown in Appendix E.1. The fixed adjustment is shown in Appendix E.2.

B.2.1.5.1 The free adjustment

The calculation programme PNAV requires that a minimum of one point is fixed. A free adjustment over all the points can therefore not be done. The closest you can come to a free adjustment is by fixing only one point. With a free adjustment the aim is that the standard deviation of the weight unity is around 1. By using Fillnet's standard a priori values, the standard deviation on the weight unit was approx. 1.8 [Ashtech, 2002]. Fillnet's standard a priori values for latitude, longitude and elevation of 0.003, 0.005 and 0.005 respectively were estimated as too narrow by the measuring of natural control points, where the point definition cannot assert that accuracy. These a priori values were therefore increased to the double size of 0.006, 0.010 and 0.010. After this, the standard deviation on the weight unit fell to 1.015. The greatest deviations are seen for points determined by a single vector, that is, the elevation control points. For the remaining points, the deviation is less than one centimetre in all three directions.

It may be seen from Appendix E.1 that the maximum co-ordinate deviation of the points by the free adjustment is:

$$x = 0.011 \text{ m}$$



$$y = 0.011 \text{ m}$$

$$z = 0.011 \text{ m}$$

For the evaluation of the measurement, the co-ordinates to the reference points from the free adjustment can be compared with the co-ordinates from the National Survey and Cadastre.

The point fixed in the adjustment is point GI 62-07-007. Table B.1 shows the given and the calculated co-ordinate for the plane reference points plus the deviation.

Point number	Given co-ordinates		Measured co-ordinates		Deviations	
	X (m)	Y (m)	X (m)	Y (m)	ΔX (m)	ΔY (m)
62-04-001	-233063.37	283824.09	-233063.375	283824.088	0.005	0.002
62-09-003	-236757.47	282257.20	-236757.439	282257.179	-0.031	0.021
62-09-007	-235111.88	284064.85	-235111.880	284064.850	0.000	0.000
62-09-008	-237630.91	285102.78	-237630.916	285102.741	-0.006	0.039
62-13-006	-236203.02	286570.39	-236203.059	286570.339	-0.057	0.051
62-13-007	-232601.67	287097.65	-232601.632	287097.668	0.038	-0.018

Table B.1: Given and calculated X, Y-co-ordinates and the deviation between these by fixing point GI 62-13-007.

Table B.1 shows that the deviations for point 62-13-006 is somewhat larger than for the other points. It is assumed that the measurement is normally distributed, and that there may appear points with a deviation of 3 times the standard deviation. If the accuracy of the planimetric geodetic reference point is set at 0.015 m, a deviation of up to 0.045 m is acceptable. The deviation for point 62-13-006 therefore exceeds 3 times the standard deviation. The deviation may be due to damage to the point, which is not the case, however. As point 62-09-007 is fixed, the deviation might also be due to damage to point 62-09-007, which is not the case either. What really causes the deviation is uncertain, as both points are situated optimally on an open Viking burial mound, and thus offer the very best conditions for receiving. Point 62-13-006 has not been included in the final calculation.

The same comparison is done for the geodetic reference elevation points. Here, it is the elevation from the offset points and a single fully measured reference point which are compared with the measured elevations.

Point No.	Given elevations (m)	Measured elevations (m)	Deviations (m)
62-13-007	45.749	45.755	-0.006
501	48.117	48.107	0.010
570	46.285	46.301	-0.016
901	48.786	48.788	-0.002
902	47.777	47.735	0.042
905	47.337	47.335	0.002
906	48.014	48.010	0.004
909	48.844	48.833	0.011
950	69.037	69.038	-0.001
951	61.753	61.737	0.016
953	85.843	85.835	0.008
954	61.146	61.144	0.002
955	80.140	80.143	-0.003
970	50.175	50.180	-0.005
990	70.531	70.522	0.009

Table B.2: Given and measured z-co-ordinates and the deviation between them.

It can be seen in table B.2 that the greatest deviation between a given elevation and the measured elevation is in point 902, where the deviation is 0.042 m. The offset point 902 was not optimally placed for measuring with GPS, as there were many trees, which caused many cycle slips. These may have caused the point to have been poorly determined. As regards the remaining points, the deviation is less than 0.016 m. Point 902 is, likewise, not included in the final calculation.

It may be seen from both table B.1 and B.2 that the results of the measurements are satisfactory.

B.2.1.5.2 The retained adjustment

[NS&C, 1989] has stated that the neighbouring accuracy of the planimetric geodetic reference points is better than 2 cm per km. As shown in table 1, there are great tensions at reference point 62-13-006. This point has, therefore, not been included in the final adjustment. As for the remaining reference points, there have not been greater deviations than the stated standard deviation from the National Survey and Cadastre times 3, these are therefore retained, which means that 5 planimetric and 14 elevation reference points have been retained.

As seen in Appendix E.2, the maximum co-ordinate deviation is:

$$x = 0.011 \text{ m}$$

$$y = 0.014 \text{ m}$$

$$z = 0.015 \text{ m}$$

The measurement thus meets the accuracy requirement of 0.015 m determined in section B.1.3.

The points were transformed from WGS 84 to System34 Jutland. Furthermore, the y- and x-columns were exchanged, and the x-co-ordinates multiplied by -1 . This was done so that the co-ordinates might be included in a bundle adjustment in the programme packages Bingo and Match-T.

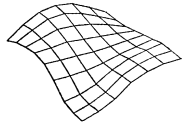
B.2.2 Capture of analytically measured elevation data

A superior accuracy of 0.03 m – 0.04 m as discussed in section B.1.5 can only be achieved by GPS measurement or by levelling. These measuring methods, on the other hand, are time-consuming, and it is difficult to determine the elevation data in a uniform square grid. Photogrammetric determination in images in scale 1:5,000, in comparison, cannot quite meet the accuracy requirements, but is far quicker and easier for this task. Seen in the time frame of this project, the choice therefore fell on photogrammetric determination.

The photogrammetric process of determining elevation data in a square grid consists of several parts, of which the first is the relative orientation (section B.2.2.1). In the orientated images, the image co-ordinates are measured, and then a bundle adjustment is done (section B.2.2.2), and finally, the reference points are measured in an analytical instrument (section B.2.2.3). To achieve the best total accuracy, the aim is for each of these parts to result in as small a standard deviation as possible.

B.2.2.1 Relative orientation

The relative orientation is done in an analytical instrument, Planicomp. In connection with the relative orientation, a fixed numbering system was chosen, so that all point numbers are four-digit numbers. The first number refers to the flight path, while the next numbers refer to the model number. A minimum of 5 points must be determined in order to solve the relative orientation [Brande-Lavridsen, 1993]. In practice, more points are always measured to achieve over-determination, so that adjustments may be done, and poorly determined points may be excluded. For each model, 12 tie points were measured together with the control points which might be in the model. As regards the tie points between the flight paths, sketches were drawn, so that it was possible to recover these in the neighbouring flight path.



The accuracy requirement for the individual orientation over 12 tie points for each model is set at max. 5 μm . Only a few models do not meet this demand fully, in spite of re-measurements. These models are included anyway.

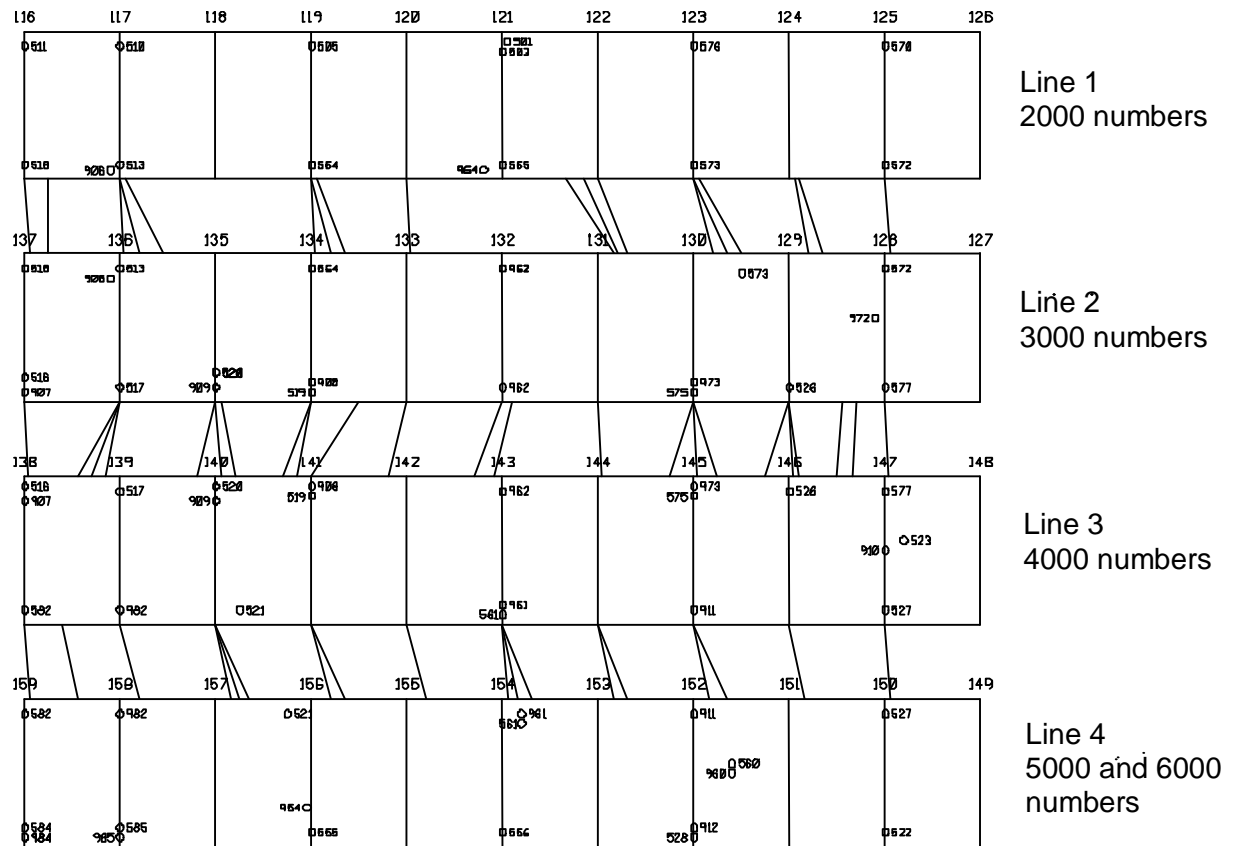


Figure B.2.6: Model overview of the relative orientation with ties between the flight lines.

The image co-ordinates from the relative orientation are now ready for use in a bundle adjustment.

B.2.2.2 Bundle adjustment

The bundle adjustment was done with the programme Bingo developed by Hannover University. The image co-ordinates to the tie and control points from the relative orientation were transferred from the analytical instrument Planicomp to Bingo.

As part of the programme, Bingo helps the user, on the way, as regards detecting gross errors. As 12 tie points were measured with the points determined in pairs, points with large residuals could be eliminated, but only one point per pair. Bingo eliminates automatically the points with the poorest determination. Furthermore, the less good points are indicated with an asterisk system, where the poorest points are indicated with 4 asterisks, less poor points with 3 asterisks etc. The good points have no asterisk.

In Bingo, the control points must be indicated with a point deviation. Experiences from [Hansen et al., 1995] show that an a priori value for the point deviation of 0.04 m is suitable in order for an adjustment iteration to start. As a priori value for the image co-ordinates from the relative orientation, Bingo's standard value of 4 μm is used [Kruck, 1995].

Figure B.2.7 shows the result of the bundle adjustment.

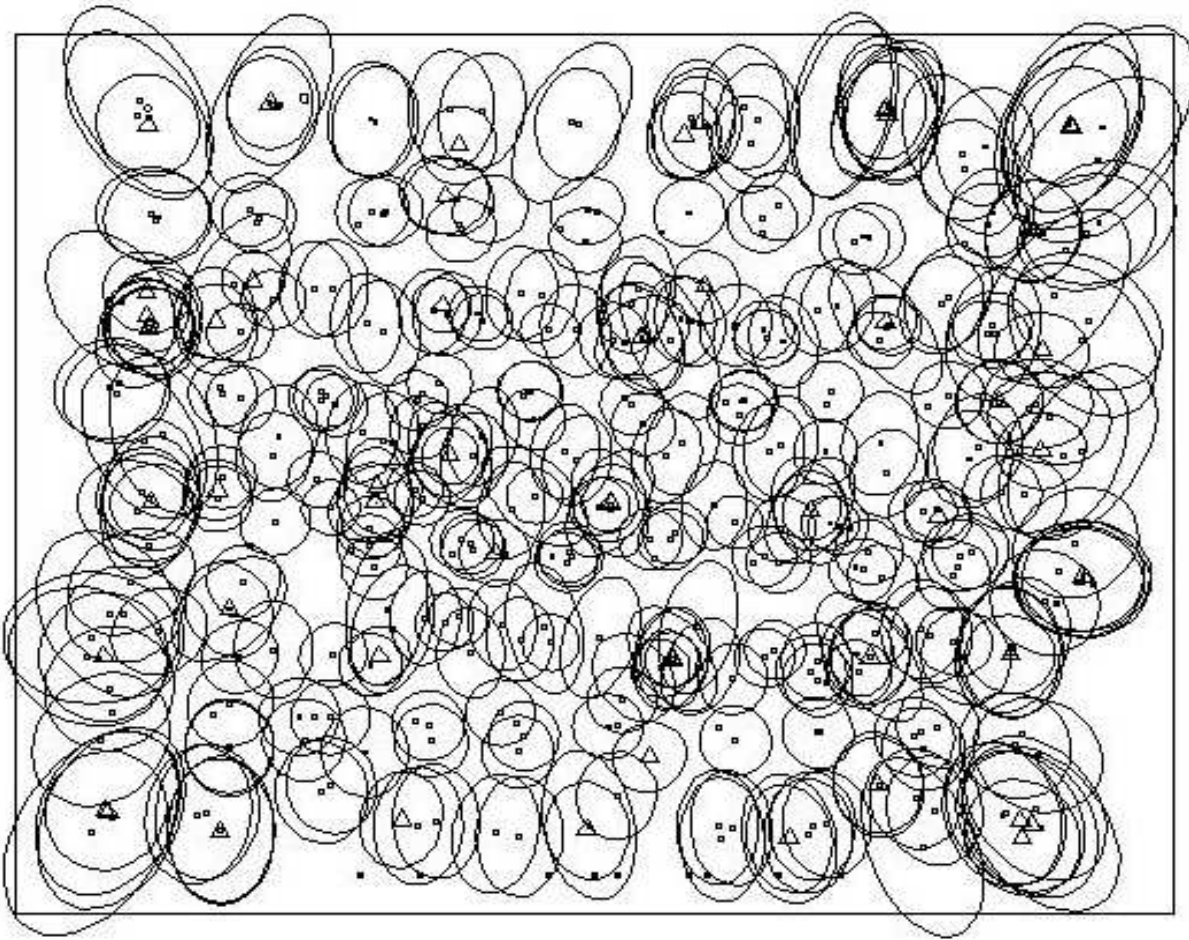


Figure B.2.7: The error ellipses from Bingo for the images in scale i 1:5,000.

As will be seen from figure B.2.7, some of the points are less well determined, in particular, the points in the corners.

The use of Bingo's standard value for an a priori value of $4\text{ }\mu\text{m}$ must be reckoned too narrow, as the demand for accuracy of the model measurement at the relative orientation was set at $5\text{ }\mu\text{m}$. This may also be concluded from the fact that the accuracy of the adjustment of all the models was $5.64\text{ }\mu\text{m}$.

It is also seen that the relation between a posteriori and a priori values is 1.41, while the value aimed for was 1.

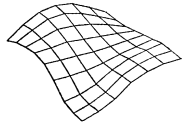
The result of the bundle adjustment was an accuracy of 0.06 m, see Appendix E.6.

B.2.2.3 The frame of reference

Before the reference points can be determined, the images must be orientated absolutely. This was done in the analytical instrument, Planicomp. The co-ordinates of control points and tie points were transferred to the Planicomp, and subsequently a transformation was done in the analytical instrument. Thereby, the images are orientated absolutely, and the reference points can then be determined.

The reference points were not determined for the whole test area, but only for models/areas with landscape types which were interesting for the investigation. At the selection of the models, the accuracy of the control points was also considered. 14 models were selected. The frame of reference was determined by an experienced operator to lessen the error contribution.

The accuracy of the frame of reference is a combination of the standard deviations of the control points, including their measuring and definition, and an experience contribution of 0.06 % of the flight altitude which indicates how well an experienced operator can measure elevation data.



The standard deviation of the photogrammetrically measured elevation data (the frame of reference) therefore consists of these three contributions:

$$\sigma_z^2 = ((0.06 \text{ ‰})^2 + \sigma_{\text{ctrp}} + \sigma_{\text{def}}$$

where:

σ_z = The standard deviation of the photogrammetrically measured elevation data

0.06 ‰ = The empirical experience of how well a professional operator can measure elevation data

σ_{ctrp} = The standard deviation of the control point determination by GPS

σ_{def} = The standard deviation of the control point definition

A bundle adjustment has been done in this project. In the standard deviation of this bundle adjustment, the standard deviation of the measurement and definition of the control points are included. As may be seen from Appendix E.6, the standard deviation for the control points after the aerotriangulation is:

$$x = 0.031 \text{ m}$$

$$y = 0.034 \text{ m}$$

$$z = 0.045 \text{ m}$$

and the standard deviation for the tie points after the aerotriangulation is:

$$x = 0.034 \text{ m}$$

$$y = 0.040 \text{ m}$$

$$z = 0.060 \text{ m}$$

For Bingo/Match-T used on images in scale 1:5,000, it applies that the output includes the control point deviation as well as the aerotriangulation deviation. Furthermore, the estimated accuracy of the measurement of elevation data also includes the deviation of the orientation of the images. To lessen the error contribution from the measurement of the reference points, this part has been done by an experienced operator.

This means that the accuracy can be determined as:

$$\sigma_z^2 = ((0.06 \text{ ‰})^2 + \sigma_{\text{aero} + \text{ctrp} + \text{orient}}^2 = 0.045^2 + 0.06^2 = 0.075 \text{ m}$$

where:

σ_z = the standard deviation of the photogrammetrically measured elevation data

$\sigma_{\text{aero} + \text{ctrp} + \text{orient}}$ = the standard deviation of the aerotriangulation which is 0.06 m

0.06 ‰ = the empirical experience of how well a professional operator can measure elevation data

As will be seen from the above, the accuracy in the z-direction is around 0.075 m.

Very few control points have a standard deviation after the bundle adjustment larger than 0.1 m. If this deviation is used as evaluation basis for the frame of reference, we have:

$$\sigma_z^2 = ((0.06 \text{ ‰})^2 + \sigma_{\text{aero} + \text{ctrp} + \text{orient}}^2 = 0.045^2 + 0.1^2 = 0.11 \text{ m}$$

The accuracy of the whole frame of reference is therefore set at 0.1 m. An accuracy of 0.1 m is not superior compared to the accuracy which may be achieved by use of images in scale 1:5,000. For images in scales 1:15,000 and 1:25,000, the frame of reference has a superior accuracy.

The points of reference are determined with a fixed mesh size of 25 x 25 m. For the landscape type gravel pit, the mesh size was reduced to 5 x 5 m. The mesh size was fixed automatically by the Plani-comp. When it proved impossible to determine elevation data in the fixed mesh grid, for instance because of trees or houses, the point was moved out to an area, where it was possible to see the ground, and here the elevation and the corresponding x- and y-co-ordinates were registered. Then it was moved back to the original grid, where the measurement continued. The planimetric co-ordinates to the reference points with the mesh size 25 x 25 m were chosen so that the x- and y-co-ordinates ended in ***00.00, ***25.00, ***50.00 and ***75.00. For the mesh size 5 x 5 m, the plane co-ordinates fell on ****5.00 or ****0.00.

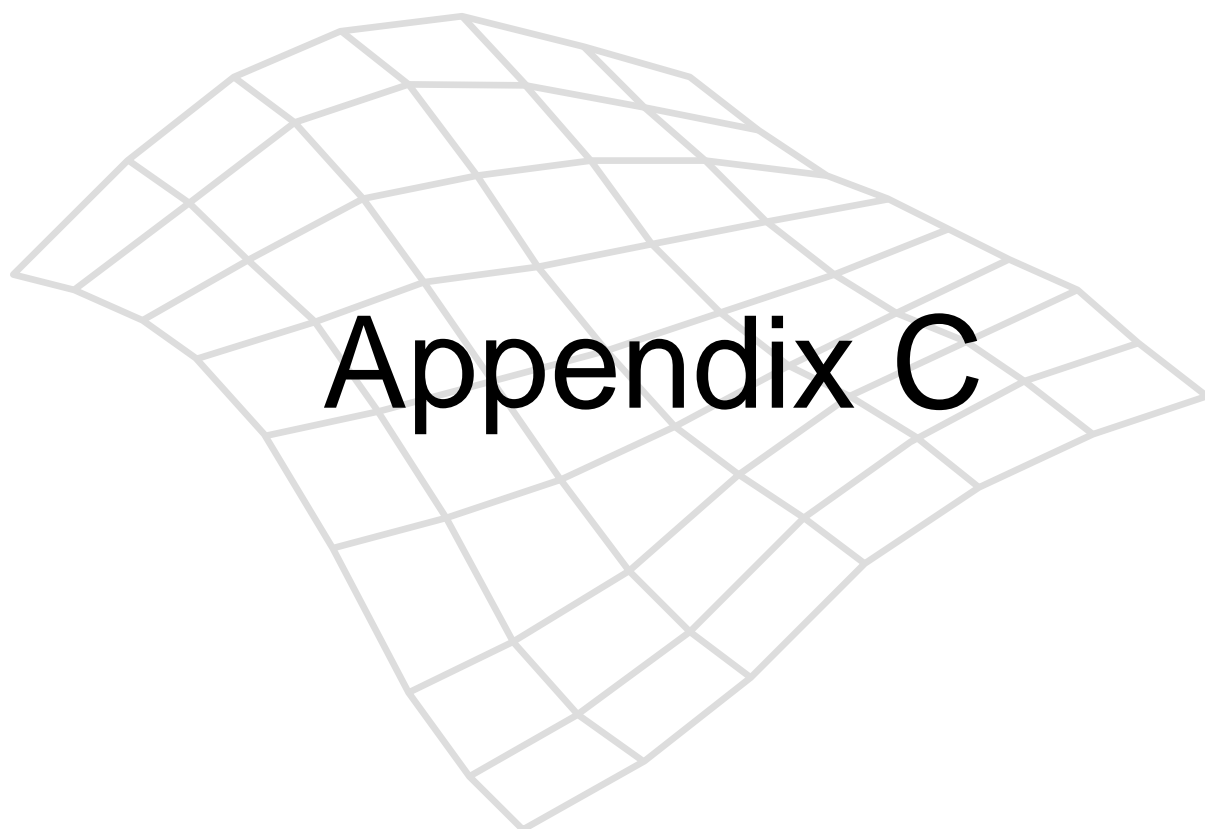
All in all, 10188 points were registered, distributed with 2092 points in open, flat fields, 2814 points in hilly fields, 12123 points in woods, 1629 points in village and 2429 points in the gravel pit.

B.2.2.4 The control point list

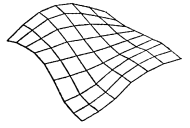
The control point list consists of the 119 control points determined by GPS, see Appendix E.3. These points are included in the bundle adjustments, see Appendix E.

As mentioned earlier, the elevation control points have been determined by means of a minimum of two independent vectors. The first was assigned a point number 9***, the next the numbers 9***, 8*** or 7*** in the number series. An elevation mean over these points was determined after the bundle adjustment, and used in the final co-ordinate list.

Those reference points and offset points which are not suitable as elevation control points have been taken out of the control point list, as they are no longer to be used.



Appendix C



Appendix C: Analysis programme PIL

With regard to investigation and evaluation of automatically generated elevation data in relation to a frame of reference, an analytical tool is required. The actual investigation evaluates elevation data generated by the programme package Match-T, used in a selected test area (cf. Chapter 4 and Appendix B).

C.1 Description of the analysis programme PIL

C.1.1 Demands on the analysis programme PIL

One of the basic demands on an analysis tool is complete insight into method and data. The analysis tool must be able to present various statistical data calculated on the basis of the differences between reference data and generated elevation data, such as the maximum (max) and minimum (min) deviation, mean (mean), the standard deviation (Stnd), the Root Mean Square Error (RMSE) etc. It must be possible to do these calculations separately according to landscape type. It must also be possible to cut out points, where the difference exceeds a chosen limit. Furthermore, the programme must be able to take a possible offset into consideration, here calculated as the mean (mean).

The input format must be able to handle Match-T files. The output files from the programme must be flexible as regards the presentation of result file and method. One demand to the output files is that they must be in GeoCAD format, so that it is possible to use GeoCAD for visualisation of the results. GeoCAD is a CAD programme developed in Denmark.

The point of departure is that there are two elevation models in existence over an area, for example, a new elevation model and a frame of reference. The programme is built up so that the one elevation model is regarded as frame of reference, and the other is the model under investigation, for instance by Match-T. There are thus one set of reference data and one set of test data in operation.

In this project, the elevation model, which is automatically generated in Match-T, is regarded as test data, and it is compared to the frame of reference determined in the Planicomp.

It was estimated that there was not a commercial programme on the market, which could fulfil the wishes of an analysis tool. Therefore, a programme was developed specifically for this purpose. A programme developed by the author also has the advantage that it can be changed or the analysis possibilities can be broadened. The analysis programme has been named PIL, as the deviations between the reference data and the generated elevation data is shown as "pile" (arrows).

The demands on the user interface in the PIL programme are that it must be intuitively built up, and easily accessible. Furthermore, it must be clear and have a short path of access to all functions. There must be the possibility of correcting the keyed-in information, and the option of breaking off the programme, both during the set-up, during the calculation itself, and after the calculation.

Data flow diagram for the programmes modules

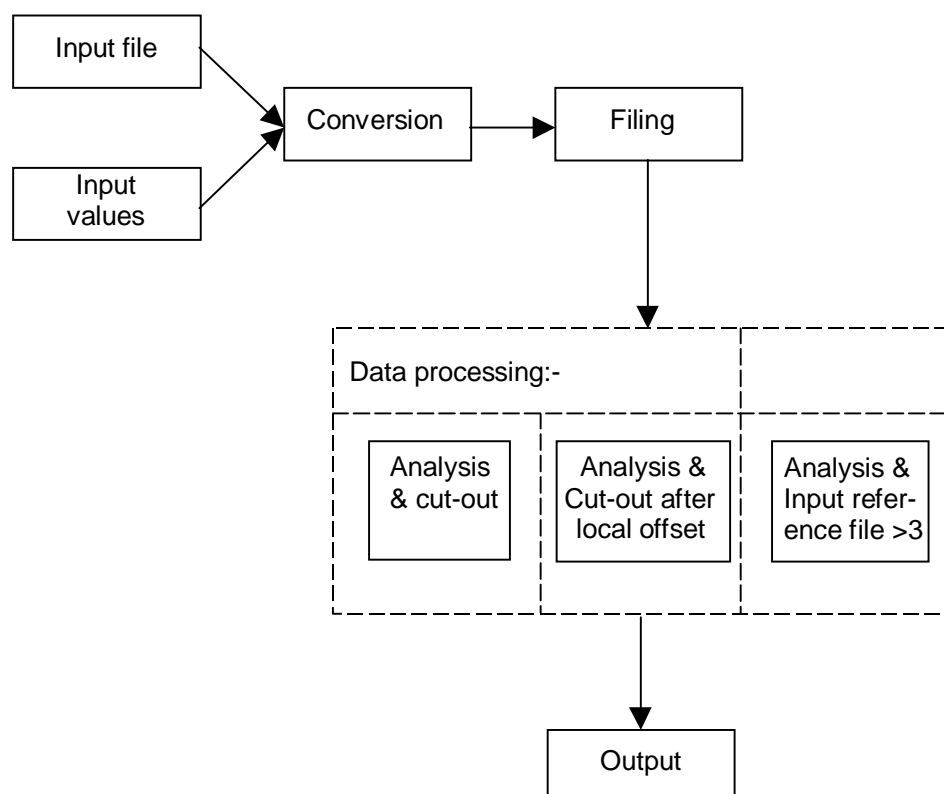


Figure C.1.1: Data flow diagram for the analysis program PIL

To optimise the analysis process, the programme must be able to optimise the search, so that the calculation time is minimised, as the data quantities included in the process are very large.

The development of the PIL programme has been a long process, where new options have been included during the whole course of the project.

Figure C.1.1 shows a dataflow diagram for the programme modules.

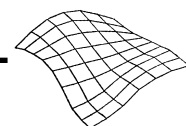
C.1.2 Input files

Input files consist of a reference file and a test file respectively. The reference file includes analytically determined elevation data. The test file is automatically generated elevation data from Match-T.

C.1.2.1 File format

Reference file(s)

The reference file must be in ascii and column format. The first column includes a possible code for the landscape type, the second column is the x-co-ordinate, the third column is the y-co-ordinate, and the fourth column is the z-co-ordinate. As the landscape type is identified from the code, each point must have a code. The codes for the landscape type are described in Appendix B, section 1.4. The PIL programme can handle a file format for the reference file, which consists only of three columns (x, y and z), which is to say that there is no code for the points. If the points do not have a code from the start, they are automatically assigned the code 00 for unknown landscape type. If decimals are included, the decimal separation must be made with a full stop.



An example of the format of the reference file, code, x-co-ordinate, y-co-ordinate and z-co-ordinate:

12	-235800	286025	49.808
12	-235800	286050	52.891
34	-235834	286125	63.017
34	-235834	286130	64.777
56	-233552.419	284697.242	65.093
56	-233551.245	284675.049	65.205
78	-234475	284700	80.079
78	-234475	284725	78.676
90	-233925	284025	77.845
90	-233924.783	284006.829	77.579

Test file(s)

The format of the test file must also be in ascii and column format. The PIL programme can handle test files both with and without codes. The individual codes are described in Chapter 5, section 5.9.3 and Appendix B, section 1.4.

The PIL programme examines how many columns the test file contains. If the test file contains the x-co-ordinate as the first column, then a column with the y-co-ordinate, and finally a column with the z-co-ordinate, it means that the test files do not include codes, and all grid points are therefore assigned the code 00.

If there are more than 3 columns, the test file includes codes, and the individual codes are identified.

Again, if decimals are included, the decimal separation must be done with a full stop.

An example of the format of a test file without codes, x-co-ordinate, y-co-ordinate, z-co-ordinate:

```
-237725.0000 282775.0000 75.8301
-237700.0000 282775.0000 75.6937
-237675.0000 282775.0000 75.3046
-237650.0000 282775.0000 75.3496
-237625.0000 282775.0000 75.3223
-237600.0000 282775.0000 74.3945
-237575.0000 282775.0000 74.6186
-237550.0000 282775.0000 75.6875
-237525.0000 282775.0000 75.7793
```

If co-ordinates given in SYSTEM34 are used, these must be fitted in by exchanging the x- and y- co-ordinate, and multiplying the x-co-ordinate by -1 before they are used in the PIL programme. For both the reference file and the test file, the division of columns must be done with space (ASCII 32), tab (ASCII 9) or comma (ASCII 44).

Both the reference files and the test files are examined by the PIL programme to see whether they contain the prescribed formats. If the files have the wrong format, the PIL programme draws attention to this, and the programme stops without updating.

C.1.3 Programme description

C.1.3.1 The user interface

The PIL programme is run in a Windows format, and is therefore built up as a typical user interface for the Windows standard, see figure C.1.2

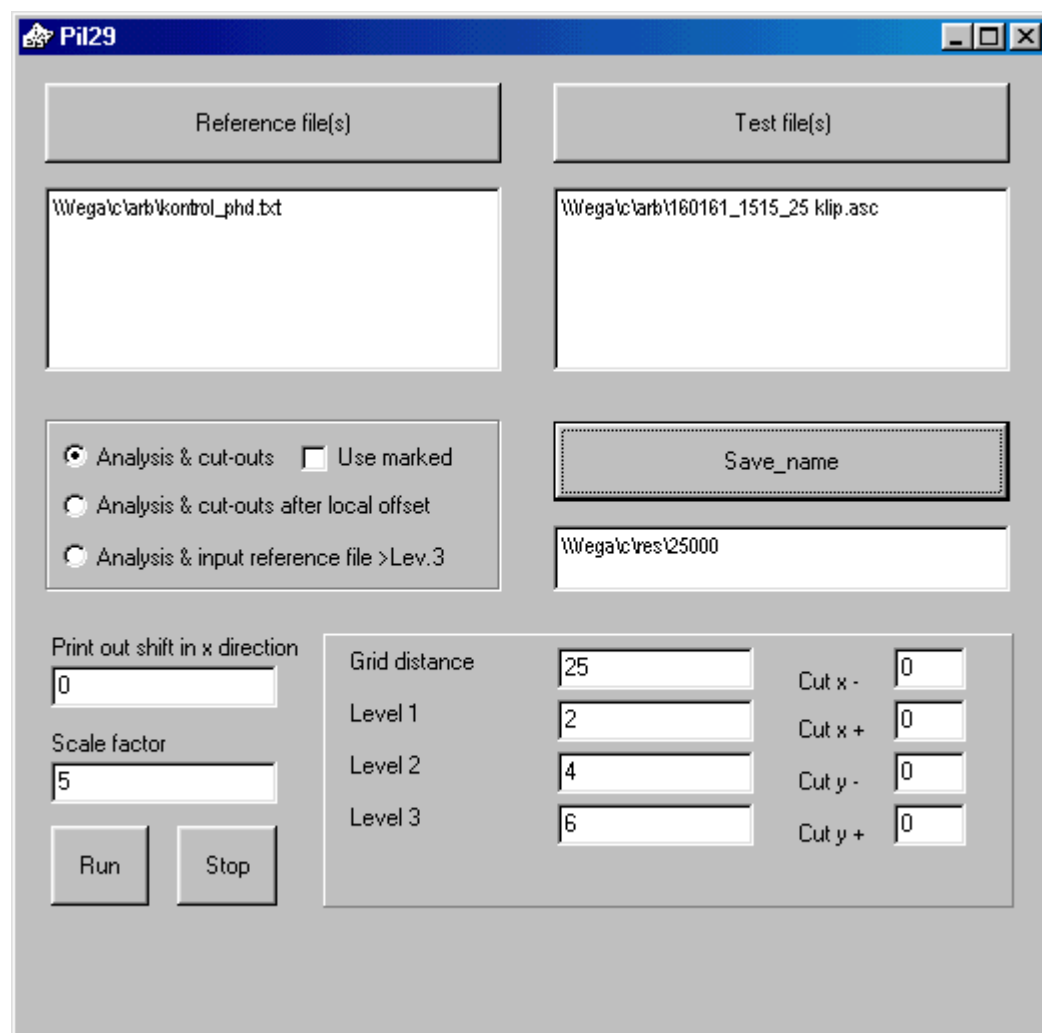


Figure C.1.2: The programme window for the analysis programme PIL.

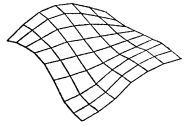
C.1.3.2 Choice of files

Reference file(s)

The reference file is indicated by clicking on Reference file(s), see figure C.1.2. The file is found by clicking in the normal way in a Windows format. After acceptance of the file, it is shown in the window with the whole of its path indication. There is a choice between several files. These are listed under each other. The file list can be edited by means of the "delete" button.

Test file(s)

The test file or files is chosen by clicking on Test file(s). The files are found by clicking in the Windows format. After the choice of file, this is shown with the path indication. Several files may be chosen at a time. These are listed under each other, see figure C.1.2. The file list may be edited by means of the "delete" button.



C.1.3.3 Calculation options

To make the programme run, a work directory c:/work, and a result directory c:/res must be established.

There are three different calculation options in the programme. The wanted calculation is chosen by the user by marking:

- 1) Analysis and cut-out
- 2) Analysis and cut-out after local offset
- 3) Analysis and input reference file > level 3

1) Analysis and cut-out

With the calculation option "Analysis and cut-out", a differential calculation is done, and the statistical data is calculated. All differences, which numerically exceed the gross error limit determined in level 3, are cut out. If this calculation method is chosen, the cut-outs are done numerically without regard to a possible offset.

If all points are to be included, the gross error limit in level 3 is set so high that there will be no differences larger than this value.

2) Analysis and cut-out after local offset

If the choice is to do the calculation with the option "Analysis and cut-out after local offset", a possible offset is determined first, and the cut-out is then done numerically from this offset.

If all points are to be included, level 3 is set higher than the greatest difference.

3) Analysis and input reference file > level 3

If this calculation option is chosen, the elevation differences are determined. Points, where the elevation differences are numerically larger than the gross error limit indicated in level 3 after shift of offset, are taken out, and elevation data from the reference file is put in instead of the grid point from the test file. For example, a new, generated elevation model (test file) may be compared to an existing model (reference file), and in case there is a difference in elevations greater than the value in level 3, elevation data from the existing elevation model are put in. As reference file, the existing elevation model from the National Survey and Cadastre might be used.

In case the two grids are not coincident, a bi-linear interpolation is done to move the grid points from the reference file to the grid position for the test file.

A new grid file is generated which includes the automatically generated points plus put-in points. The new grid file is placed in c:/work. It is then possible to compare this new grid file with the analytically determined reference file. This offers an opportunity of analysing how good an accuracy can be achieved, if grid points from an existing elevation model are included.

If, for example, a poor accuracy is achieved by the inclusion of the NS&C elevations, it is still possible to avoid putting in the NS&S elevation data by using calculation option 2). This results in a grid full of holes, where the cut-out points lie in the file "Udklip.txt" or by self-chosen indication with the ending "*ukl.txt.". In the files "Udklip.txt" or "*ukl.txt", the cut-out points are found in list format. In the file "Dummy.asc", the points in GeoCAD format are found. The external points will be assigned the landscape code 00 in here.

It is then possible to re-measure these points.

Use marked

For all three calculations options, it is possible to add "use marked". If an interpolation is included, the grid point out of the four, which has an elevation difference larger than the one chosen in level 3, is cut out (marked by the computer). This point will not be included in the interpolation of the neighbouring point. If

"use marked" is chosen, the marked (cut-out) grid points will be used anyway by the interpolation of a neighbouring point.

Save_name

As point of departure, the output files will be stored in c:/res. Under "save_name", the path indication of the output files may be indicated plus another first name on the files. The output files will then be stored here with the chosen names, while the output files with the standard names will still be placed in c:/res as safety copy. The standard names are described in section C.1.7.

Grid distance

The mesh size used in the test file is indicated as grid distance. This value limits the search radius according to the surrounding grid points, unless there is a direct merging of points, an interpolation is then necessary. Only grid points which lie within the mesh size plus one meter are included in a possible calculation.

Level 1, 2, 3

The elevation differences are sorted according to size into four levels, divided by three level limits which may be indicated by the user:

- Level 1: the difference smaller than the 1st level limit
- Level 2: the difference between the 1st and 2nd level limit
- Level 3: the difference between the 2nd and 3rd level limit
- Cut-out: differences exceeding the 3rd level limit

The standard values for the level limits are 2 m, 4 m and 6 m. If these values are used, it means that:

- Level 1: the difference < 2 m
- Level 2: $2 \text{ m} \leq \text{the difference} < 4 \text{ m}$
- Level 3: $4 \leq \text{the difference} < 6 \text{ m}$
- Cut-out: $6 \text{ m} \leq \text{the difference}$

The level limits keyed-in by users may be arbitrary figures. If decimals are used, they must be divided by a full stop. Furthermore, the following must be observed: Level limit 1 should always be smaller than level limit 2, which again must be smaller than level limit 3. If the individual level classifications are not observed, the PIL programme will stop without updating. Differences exceeding, for instance 6 m, are cut out and transferred to the "cut-out file".

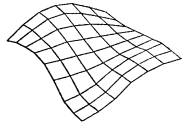
Cut x -, cut x cut y – and cut y +

This function gives the option of excluding an integer number of rows or columns, which is not required to be included in the analysis calculation of the test grid. This function is developed in order to handle unwanted columns or rows in the automatically generated grids.

The keyed-in figure must be an integer. This figure indicates how many rows or columns are to be ignored. For example, the keyed-in number of columns from the east is ignored by using klip x+, and from the west by using klip x-. By using klip y- and klip y+, the keyed-in number of rows from the south and the north respectively are ignored.

Scale factor

By means of the scale factor, the user may indicate a factor for the size of the error arrows. To make possible a clearer view of the elevation differences, all elevation differences may be multiplied with this self-



chosen factor. This facilitates the analysis of where the large errors have arisen. The standard value is 5, see figure C.1.2.

Print-out shift in the x-direction

Some of the elevation differences are so great that the individual arrows overlap. That means that it is impossible to see, how large the individual arrows are, as these start and end on top of other error arrows. By "Print-out shift in the x-direction" it is possible to shift the arrows in relation to each other, so that the arrow in the row underneath does not overlap the starting point of the arrow in the row above.

Run

The choice of "run" starts the calculation process.

Stop

The choice of "stop" breaks the programme without dialogue box for the user, and without saving data.

C.1.4 Functionality

C.1.4.1 Filing of data

As large data quantities are often in question, the calculations take a long time. To optimise the calculation time, it is of great importance to optimise the search routine. In order for the search to run more easily, data is filed in both files. This is done by first filing data according to the y-co-ordinate, then according to the x-co-ordinate. This filing makes the programme able to handle "chaos" files, for instance, unstructured files, or files where there is an overlap between files as well as files which are not in grid format etc. If there is an overlap between the elevation data, and these are coincident, these data are put next to each other in the filing.

The elevation models do not need to have coincident grid positions, that is, the same plane co-ordinates. This is handled by the interpolation. Both, different mesh sizes and a possible twist between the elevation models can be handled by the programme. This is due to the filing, which ensures that the elevation data is structured after the filing process. After the filing, the data is put in storage.

When the files are filed, the search is further refined by means of a pointer.

C.1.4.2 Data processing

The automatically generated elevation data is placed in a grid with a fixed mesh size. However, it has not been possible to place all the reference points in a corresponding grid, but they have been determined as close to the mesh position as possible. (cf. Appendix B, section B.2.9.3). An interpolation would give an error contribution, wherefore the points, as far as possible, should coincide, that is, have the same plane co-ordinates in the two files. Thus, a direct comparison point to point may be done, without an error contribution from the interpolation.

In case the planimetric co-ordinates to the points in the two files do not coincide, and the deviation is greater than 0.01 m, a new elevation for the reference point's x- and y-position will be interpolated by means of the bi-linear interpolation calculation between four neighbouring points:

$$h(x, y) = ax + by + cx + d \quad \text{C(1.1)}$$

where h = the interpolated elevation.

See figure C.1.3.

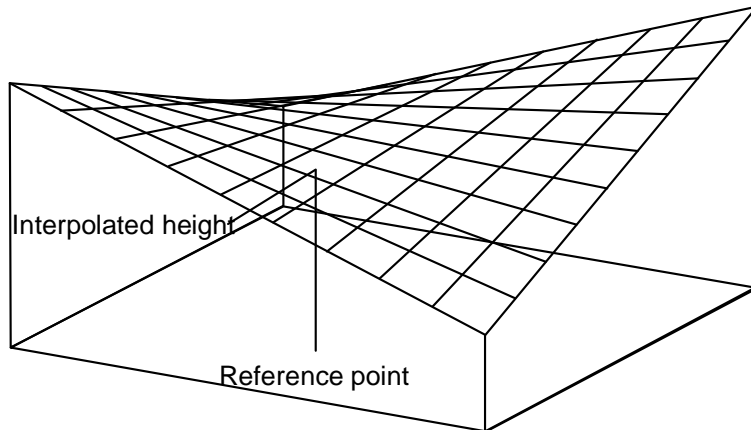


Figure C.1.3: The principle of the bi-linear interpolation.

When the points are located precisely in the fixed grid, that is, the points in the test file(s) and the frame of reference file(s) have the same x- and y- co-ordinates, a simple difference calculation is done with the formula:

$$\text{diff} = 'z'\text{test} - 'z'\text{ref} \quad \text{C(1.2)}$$

where:
 diff = the elevation difference
 'z'test = the elevation from the test file
 'z'ref = the elevation from the reference file

Only one interpolated elevation is determined if there are four surrounding grid points. The search for the grid points is limited by the value, which is indicated in the mesh distance in the main menu of the PIL programme.

C.1.5 Statistics

Various statistical calculations are done on the located differences. These calculations are done, both on all the differences as a whole, and for each landscape type. The data determined is the minimum difference (min.), the maximum difference (max.), the mean (mean), the standard deviation (stnd) and the Root Mean Square Error (RMSE).

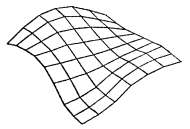
The RMSE is determined according to the formula:

$$\text{RMSE} = \sqrt{\frac{\sum_{i=1 \rightarrow n} x_i^2}{n}} \quad \text{C(1.3)}$$

where:
 RMSE = the Root Mean Square Error
 x_i = the deviation between frame of reference and the generated grid
 n = the number of points

The standard deviation is determined according to the formula:

$$\text{stnd} = \sqrt{\frac{\sum_{i=1 \rightarrow n} (x_i - \bar{x})^2}{n}} \quad \text{C(1.4)}$$



where:

- stnd = the standard deviation
- x_i = the elevation deviation between frame of reference and the generated grid
- \bar{x} = the mean of all deviations
- n = the number of points

The total number of points included in the analysis is indicated, as well as the number of points for the individual landscape types. The number of differences falling within the four different level classifications (level '1', level '2', level '3', udklip.pkt) are indicated. The total area, and the area of each landscape type for each of the four levels (level '1', level '2', level '3', udkl.areas) are calculated, see figure C.1.6.

Offset

In the offset calculation, a possible offset is determined for elevation differences and the individual landscape types. All the elevation differences are deducted from the total offset, and the offset from the individual landscape types is deducted from the individual landscape types, and new min., max, mean, Stnd and RMSE are calculated for all the points in one, and for the individual landscape types each on its own.

The cut-out

In the first editions of the programme, the reference point was cut out, if there was a difference larger than level 3. Later, this was changed, so that the cut-out was done in the test file. This change was caused by the fact that, basically seen, it is not the reference point which contributes to the error, but on the contrary, the grid point in the test file. If the problem is regarded from the point of view of a production course, it would be the grid point which should be registered for a possible re-measurement, not the reference point! If an interpolation is included, the grid point out of the four, which has an elevation difference larger than the one chosen in level 3, is cut out. This point will only be included in the interpolation of the neighbouring point.

After the cut-out, new values are calculated for min., max., mean, Stnd and RMSE for all points, and for the individual landscape types.

The cut-out + offset

In this category, cut-outs are done under consideration of possible offsets, and new min., max., mean, Stnd and RMSE are calculated for all points, and for the individual landscape types.

C.1.6 The output files

The PIL programme is meant to be an intermediate link between the calculated elevation differences and the visualisation by means of the graphic programme GeoCAD. The PIL programme does not only calculate elevation differences, but also converts data, so that they appear in the GeoCAD format.

The following files are generated as a result of a calculation. The standard file names are:

- Differens.txt
- Differens_max.txt
- Analyse.txt
- Udklip.txt
- Resultat.asc
- Resultat_max.asc
- Dummy.asc
- Remu.acs

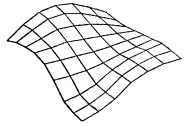
The first four files are for analysis purposes and, therefore, are in ordinary list format, the last are in GeoCAD format, and are used for visualisation. The difference file includes four columns consisting of the x-, y- and z-co-ordinates of the frame of reference file, plus a difference column with sign. This file includes all the differences. The Differens_max file includes four columns consisting of the x-, y- and z-co-ordinates of the frame of reference file, plus a difference column with sign. This file includes only the differences which remain after the cut-out of points with a difference exceeding the threshold value chosen in level 3. The analysis file includes the result of the statistical analysis, such as the maximum and minimum elevation difference, the mean, the standard deviation, the deviation, the number of points per landscape type and the area calculation. The analysis file consists of a table as shown in figure C.1.6.

	Total	Fladt A 12	Grusgrav 34	Landsby 56	Bakket A 78	Skov 90	Ukendt 00
Min	-8.42	-1.07	-6.94	-1.12	-8.42	-7.55	0.00
Max	17.52	6.17	15.66	3.96	11.18	17.52	0.00
Gns	1.64	1.33	2.20	1.29	1.60	1.78	0.00
Std	2.12	0.48	3.60	0.52	1.33	3.02	0.00
RMSE	2.68	1.41	4.22	1.39	2.08	3.50	0.00
Antal	9187	2093	1805	1287	2785	1217	0
Niv'2.0'	7311	1977	1065	1203	2133	933	0
Niv'4.0'	1276	110	405	84	540	137	0
Niv'500'	600	6	335	0	112	147	0
Udklip.pkt	0	0	0	0	0	0	0
Areal	708431.4	72232.5	47688.3	262563.3	95402.3	230544.9	0.00
Niv'2.0'	570979.2	66003.3	28698.6	242590.7	72517.2	161169.4	0.00
Niv'4.0'	88703.3	6229.2	10572.8	19972.6	18412.4	33516.3	0.00
Niv'500'	48748.99	0.0	8416.9	0.0	4472.7	35859.3	0.00
Udklip.pkt	0	0	0	0	121705.6	101715.0	0.0
Udkl. i %	6.40	0.62	9.35	0.00	6.99	16.01	0
Offset	Gns 1.64	1.33	2.20	1.29	1.60	1.78	0.00
Min	-10.02	-2.40	-9.13	-2.41	-10.02	-9.33	0.00
Max	15.74	4.84	13.46	2.67	9.58	15.74	0.00
Gns	0.00	0.00	0.00	0.00	0.00	0.00	0.00
Std	2.09	0.48	3.60	0.52	1.33	3.02	0.00
RMSE	2.09	0.48	3.60	0.52	1.33	3.02	0.00
Udklippet							
Min	-8.42	-1.07	-6.94	-1.12	-8.42	-7.55	0.00
Max	17.52	6.17	15.66	3.96	11.18	17.52	0.00
Gns	1.64	1.33	2.20	1.29	1.60	1.78	0.00
Std	2.12	0.48	3.60	0.52	1.33	3.02	0.00
RMSE	2.68	1.41	4.22	1.39	2.08	3.50	0.00
Udklippet + Offset							
Min	-10.02	-2.40	-9.13	-2.41	-10.02	-9.33	0.00
Max	15.74	4.84	13.46	2.67	9.58	15.74	0.00
Gns	0.00	0.00	0.00	0.00	0.00	0.00	0.00
Std	2.09	0.48	3.60	0.52	1.33	3.02	0.00
RMSE	2.09	0.48	3.60	0.52	1.33	3.02	0.00

Figure C.1.6: Analysis file generated by the programme PIL. A translated format can be found in Appendix L on page 331.

The cut-out file includes the x- and y-co-ordinates of the cut-out grid points from the test file(s). This file may be used as a guide to a possible re-measurement.

The last four files (*.asc) are in GeoCAD format. The result file includes the elevation differences which are shown as arrows by means of GeoCAD. If the elevation difference is positive, the arrow points up-



wards, while it points downwards if the difference is negative. The length of the arrow (plus possibly the scale used) indicates the size of the elevation difference. Furthermore, each arrow has a colour, which indicates the landscape type. If the elevation difference is positive, the colour is light, if the difference is negative, the colour is dark. For instance, the arrows which represent the landscape type woods have been assigned the colour blue, light blue arrows for positive elevation differences, and dark blue arrows for negative elevation differences. The result file can be drawn into GeoCAD for visualisation, see figure C.1.7.

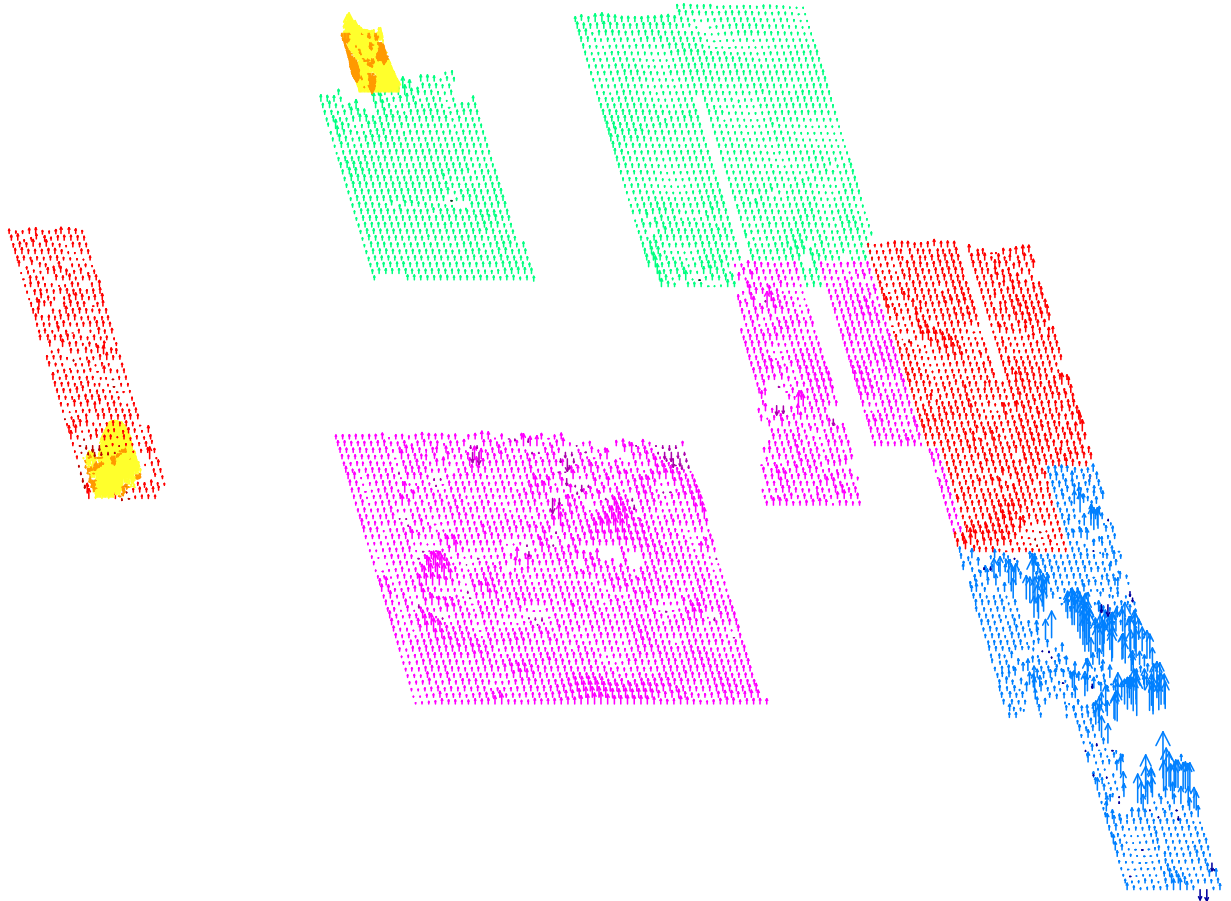
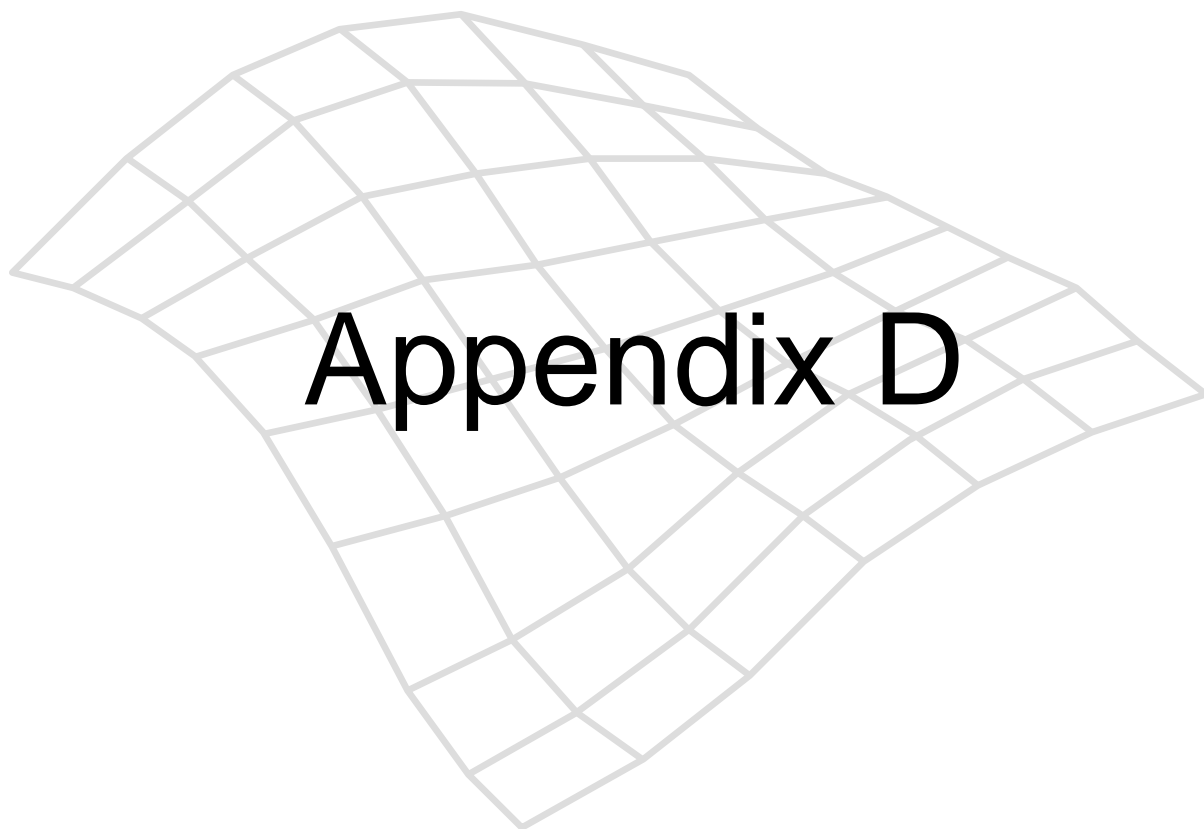


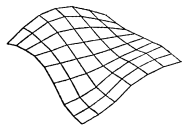
Figure C.1.7: The result in GeoCAD format with the elevation difference indicated as arrows.

The Resultat_max file includes those elevation differences which remain after cutting out those elevation differences which are larger than the threshold value in level 3. Here, the differences are also shown by means of GeoCAD as arrows, as described above. The Dummy file includes the same points as the file Cut-out, but in GeoCAD format, so that they can be drawn directly into GeoCAD with a view to visualisation. Remu.asc is an abbreviation of Result minus cut-out. This file, however, like the Resultat.asc' file, is without those arrows, which fall above level 3, and are thus cut out.

No matter which calculation is chosen, all eight files are generated. The standard files are put in c:/res as copy. These files are copied at each calculation.



Appendix D



Appendix D: Editing programme

This appendix includes a brief description of a small programme for cutting out unwanted data.

D.1 The editing programme "Klip"

With different investigations of the automatically generated grids, it turned out that in none of the grids were the keyed-in corner indications, "lower left, LL" and "upper right, UR" observed. It has therefore been necessary to develop a small programme called "Klip" for cutting out the unwanted columns or rows. The Klip programme is also run in a Windows format, and is therefore built up with user interface in Windows standard, see figure D.1.

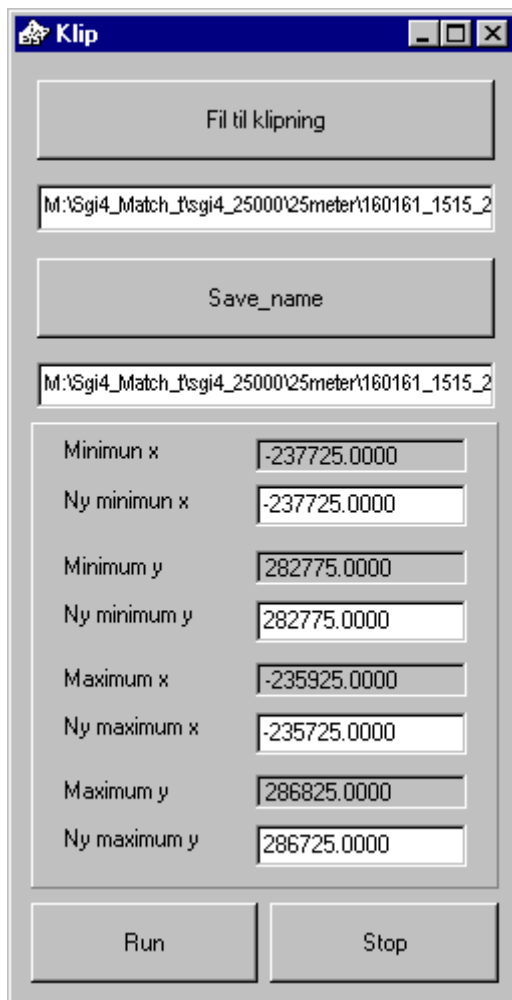


Figure D.1: Programme window for the 'klip' programme.

Input file

The input file is one of the generated files from Match-T. The input file is indicated by clicking on "Fil til klipning" and then continue as in a normal Windows format.

During the input of the input file, max. and min. for the x- and y-co-ordinates are found, and these are indicated by the programme in the grey areas for Minimum x, Minimum y, Maximum x and Maximum y.

The wanted corner co-ordinates are keyed-in in the white areas. Co-ordinates must be indicated in all the white areas. Should a corner co-ordinate shown in the grey area turn out to be correct, this co-ordinate is keyed-in again in the white area below, see figure D.1 "New minimum x" and "New minimum y".

Output file

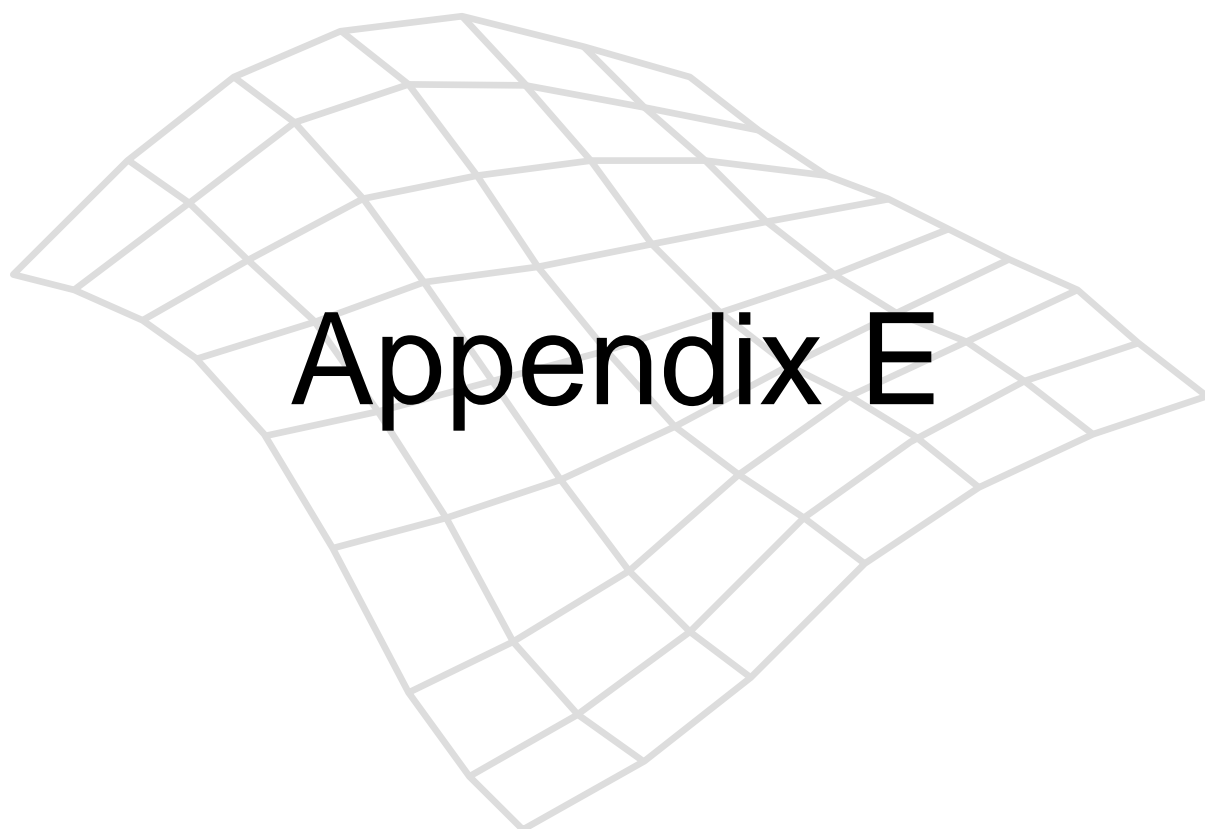
The name of the output file is indicated by clicking on "save_name". Here a new name for the output file is chosen with the whole path indication.

Run

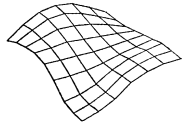
By 'run', the Klip programme cuts out the surplus columns or rows according to the co-ordinates indicated in the white areas.

Stop

By 'stop', the programme is broken off without dialogue box for the user, and without saving data.



Appendix E



Appendix E: Bundle adjustment

E.1 Free bundle adjustment of the GPS points

This Appendix contains a cut out of the results from the free bundle adjustment of the GPS measured points calculated by Fillnet. The programme Fillnet demands that one point is fixed. In this case number 007 is fixed.

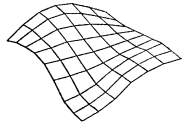
S.E. OF UNIT WEIGHT = 1.082

NUMBER OF -
 OBS. EQUATIONS 565
 UNKNOWNNS 358
 DEGREES OF FREEDOM 207
 ITERATIONS 1

ADJUSTED POSITIONS:

		LAT.		LON.		ELEV.	STD. ERRORS (m)		
1	0007	56 59 3.44834	-	9 57 44.07348		103.306	0.000	0.000	0.000
2	0001	56 58 56.04333	-	9 59 45.45155		122.449	0.007	0.007	0.007
3	0522	56 58 25.26783	-	9 59 27.10754		81.467	0.007	0.007	0.007
4	0910	56 59 6.51531	-	9 59 42.96724		82.283	0.009	0.009	0.009
5	0523	56 59 6.69497	-	9 59 43.02594		83.349	0.007	0.007	0.007
6	0526	56 59 15.74958	-	9 59 4.01221		72.036	0.006	0.006	0.006
7	0527	56 58 54.25855	-	9 59 23.60839		95.449	0.007	0.007	0.007
8	0580	57 0 33.98310	-	9 55 13.44922		46.663	0.007	0.007	0.007
9	0590	56 58 35.11809	-	10 0 15.79015		71.525	0.007	0.007	0.007
10	0911	56 58 53.67167	-	9 58 45.66613		91.007	0.009	0.009	0.009
11	0990	56 58 35.11899	-	10 0 15.84213		70.531	0.009	0.009	0.009
12	0954	56 58 38.16479	-	9 56 30.05689		61.144	0.007	0.007	0.007
13	0555	56 58 27.54789	-	9 56 39.85560		52.569	0.007	0.007	0.007
14	0955	56 58 22.08493	-	9 57 23.61907		80.144	0.007	0.007	0.007
15	0556	56 58 26.07140	-	9 57 29.93424		80.770	0.007	0.007	0.007
16	0557	56 58 37.68781	-	9 57 46.51392		89.002	0.007	0.007	0.007
17	0550	56 58 9.76669	-	9 59 50.90095		70.203	0.007	0.007	0.007
18	0951	56 57 54.07683	-	9 56 54.47313		61.737	0.007	0.007	0.007
19	0553	56 58 5.59602	-	9 56 51.95006		53.858	0.007	0.007	0.007
20	8952	56 58 5.68627	-	9 56 51.79459		53.410	0.011	0.011	0.011
21	0003	56 58 4.68166	-	9 56 7.31426		97.627	0.007	0.007	0.007
22	0953	56 58 6.71316	-	9 56 19.92651		85.836	0.007	0.007	0.007
23	0011	57 1 5.02833	-	9 58 38.70234		52.851	0.002	0.002	0.002
24	0515	56 59 24.87107	-	9 54 55.36688		65.768	0.007	0.007	0.007
25	0518	56 59 46.90183	-	9 55 30.22926		68.213	0.007	0.007	0.007
26	0552	56 58 2.28243	-	9 57 35.94176		64.658	0.011	0.011	0.011
27	0577	56 59 26.40894	-	9 59 31.66847		67.413	0.006	0.006	0.006
28	7960	56 58 33.46197	-	9 58 48.25761		98.324	0.010	0.010	0.010
29	7985	56 58 25.65730	-	9 55 51.22989		68.133	0.011	0.011	0.011
30	7973	56 59 16.71027	-	9 58 29.50883		78.356	0.010	0.010	0.010
31	0560	56 58 33.50432	-	9 58 48.38307		99.536	0.007	0.007	0.007
32	8960	56 58 33.46642	-	9 58 48.28979		98.278	0.010	0.010	0.010
33	0528	56 58 24.89181	-	9 58 24.36103		84.476	0.006	0.006	0.006
34	8912	56 58 24.96555	-	9 58 24.35376		83.952	0.010	0.010	0.010
35	0561	56 58 53.05819	-	9 57 52.61057		98.071	0.007	0.007	0.007

36	8961	56 58	53.27097	-	9 57	52.49404	98.019	0.010	0.010	0.010
37	0562	56 59	12.68138	-	9 57	54.79421	83.371	0.006	0.006	0.006
38	8962	56 59	17.79172	-	9 57	35.44830	86.645	0.010	0.010	0.010
39	8963	56 59	9.83119	-	9 57	4.68741	72.020	0.010	0.010	0.010
40	0519	56 59	25.16743	-	9 56	52.40897	54.126	0.006	0.006	0.006
41	8908	56 59	25.17191	-	9 56	52.35891	52.872	0.010	0.010	0.010
42	0564	56 59	48.84901	-	9 56	50.00526	44.554	0.006	0.006	0.006
43	0565	56 59	52.05976	-	9 58	0.86240	46.804	0.006	0.006	0.006
44	8964	56 59	43.93181	-	9 57	43.79598	57.377	0.009	0.009	0.009
45	7504	57 0	15.88004	-	9 57	54.71038	46.007	0.009	0.009	0.009
46	0554	56 58	6.52883	-	9 56	18.54113	88.129	0.006	0.006	0.006
47	0576	57 0	20.02245	-	9 58	48.74222	45.473	0.005	0.005	0.005
48	6902	57 0	35.18329	-	9 58	46.16635	47.684	0.009	0.009	0.009
49	0505	57 0	14.10700	-	9 56	54.11391	65.293	0.006	0.006	0.006
50	0903	57 0	6.13631	-	9 56	50.91242	55.223	0.006	0.006	0.006
51	0500	57 0	44.76893	-	9 59	16.16652	57.978	0.006	0.006	0.006
52	0570	57 0	17.71620	-	9 59	38.96836	46.301	0.006	0.006	0.006
53	0571	57 0	1.04166	-	9 59	29.03586	44.750	0.006	0.006	0.006
54	8971	57 0	1.15316	-	9 59	28.83524	44.535	0.009	0.009	0.009
55	0573	56 59	46.55132	-	9 58	49.46301	47.445	0.006	0.006	0.006
56	0575	56 59	16.63363	-	9 58	29.81030	79.293	0.006	0.006	0.006
57	0107	57 0	41.95236	-	10 0	11.75041	45.755	0.007	0.007	0.007
58	0970	56 59	40.48010	-	9 59	49.46954	50.180	0.006	0.006	0.006
59	0572	56 59	42.26675	-	9 59	31.70807	47.932	0.006	0.006	0.006
60	0574	56 59	34.03980	-	9 59	20.17309	57.010	0.006	0.006	0.006
61	8972	56 59	34.00350	-	9 59	20.35496	56.868	0.009	0.009	0.009
62	0901	57 1	4.84263	-	9 59	8.84128	48.788	0.006	0.006	0.006
63	0581	56 59	15.03204	-	9 53	58.56395	49.065	0.007	0.007	0.007
64	8981	56 59	15.00601	-	9 53	58.74243	48.251	0.011	0.011	0.011
65	0582	56 58	53.01182	-	9 55	19.55301	56.167	0.007	0.007	0.007
66	8982	56 59	0.76025	-	9 55	52.93278	82.327	0.010	0.010	0.010
67	0583	56 58	21.66405	-	9 55	9.46612	75.529	0.007	0.007	0.007
68	8983	56 58	21.46327	-	9 55	9.49124	75.183	0.011	0.011	0.011
69	0584	56 58	28.77778	-	9 55	20.26470	70.295	0.007	0.007	0.007
70	8984	56 58	28.41458	-	9 55	21.04573	71.074	0.011	0.011	0.011
71	0585	56 58	25.70175	-	9 55	51.45826	68.808	0.007	0.007	0.007
72	8985	56 58	25.63672	-	9 55	51.17518	68.191	0.011	0.011	0.011
73	8990	56 58	35.11860	-	10 0	15.83156	70.512	0.010	0.010	0.010
74	0981	56 59	15.00581	-	9 53	58.73292	48.275	0.010	0.010	0.010
75	0982	56 59	0.76074	-	9 55	52.93294	82.268	0.009	0.009	0.009
76	0985	56 58	25.66081	-	9 55	51.17433	68.179	0.009	0.009	0.009
77	0984	56 58	28.42713	-	9 55	21.06665	71.083	0.009	0.009	0.009
78	0983	56 58	21.45583	-	9 55	9.52484	75.177	0.009	0.009	0.009
79	0912	56 58	24.96456	-	9 58	24.35440	83.961	0.009	0.009	0.009
80	0961	56 58	53.27122	-	9 57	52.49300	98.023	0.009	0.009	0.009
81	0962	56 59	17.75529	-	9 57	35.51212	86.697	0.009	0.009	0.009
82	0963	56 59	9.84135	-	9 57	4.64887	72.004	0.009	0.009	0.009
83	0908	56 59	25.17125	-	9 56	52.35552	52.877	0.009	0.009	0.009
84	0964	56 59	43.93539	-	9 57	43.83105	57.428	0.009	0.009	0.009
85	0008	56 59	36.49145	-	9 55	14.50841	87.309	0.007	0.007	0.007
86	0512	56 59	54.47244	-	9 55	3.65495	81.585	0.007	0.007	0.007
87	0516	56 59	17.58075	-	9 55	31.98712	83.793	0.007	0.007	0.007
88	0907	56 59	17.55986	-	9 55	32.02004	83.534	0.009	0.009	0.009
89	0517	56 59	19.43405	-	9 55	49.61569	83.741	0.007	0.007	0.007
90	0501	57 0	17.81273	-	9 57	59.54135	48.107	0.005	0.005	0.005
91	6502	57 0	15.95924	-	9 57	54.58831	46.082	0.006	0.006	0.006
92	6503	57 0	15.92834	-	9 57	54.77953	46.011	0.006	0.006	0.006
93	0551	56 58	8.01914	-	9 59	3.00450	69.896	0.005	0.005	0.005
94	0950	56 58	5.16469	-	9 59	37.89795	69.038	0.009	0.009	0.009
95	0952	56 58	5.68908	-	9 56	51.78993	53.421	0.009	0.009	0.009
96	0521	56 58	53.49245	-	9 56	33.75730	46.618	0.007	0.007	0.007
97	0906	56 59	46.14614	-	9 55	48.97606	48.010	0.007	0.007	0.007
98	0511	57 0	17.06665	-	9 55	30.44647	44.868	0.007	0.007	0.007
99	0520	56 59	20.23476	-	9 56	32.78459	47.624	0.007	0.007	0.007
100	0513	56 59	52.57720	-	9 55	59.00737	44.532	0.007	0.007	0.007
101	0905	57 0	11.94038	-	9 55	15.54437	47.335	0.007	0.007	0.007
102	0510	57 0	20.63732	-	9 56	3.14322	56.885	0.007	0.007	0.007
103	0006	57 0	24.23163	-	9 56	38.53673	105.948	0.006	0.006	0.006
104	0506	57 0	29.28496	-	9 56	40.19745	101.481	0.006	0.006	0.006
105	0971	57 0	1.15962	-	9 59	28.92980	44.588	0.009	0.009	0.009



106	0973	56	59	16.63304	-	9	58	29.63436	78.188	0.009	0.009	0.009
107	0972	56	59	33.98641	-	9	59	20.34750	56.900	0.009	0.009	0.009
108	0524	56	59	29.19443	-	10	0	11.96634	53.496	0.007	0.007	0.007
109	9902	57	0	35.18306	-	9	58	46.16601	47.787	0.009	0.009	0.009
110	0502	57	0	15.88264	-	9	57	54.72306	46.007	0.009	0.009	0.009
111	0503	57	0	15.98193	-	9	57	54.73038	46.125	0.009	0.009	0.009
112	9502	57	0	15.88309	-	9	57	54.72129	45.991	0.009	0.009	0.009
113	0504	57	0	15.95727	-	9	57	54.58648	46.089	0.009	0.009	0.009
114	8907	56	59	17.56018	-	9	55	32.02028	83.518	0.010	0.010	0.010
115	9908	56	59	25.17363	-	9	56	52.35534	52.874	0.010	0.010	0.010
116	8909	56	59	17.72413	-	9	56	32.30671	48.833	0.010	0.010	0.010
117	8910	56	59	6.51028	-	9	59	42.96292	82.276	0.010	0.010	0.010
118	8911	56	58	53.67216	-	9	58	45.66500	90.997	0.010	0.010	0.010
119	9912	56	58	24.96534	-	9	58	24.35214	83.963	0.010	0.010	0.010

E.2 Fixed bundle adjustment of the GPS points

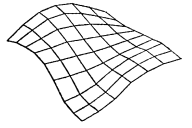
This Appendix contains a cut out of the results from the fixed bundle adjustment of the GPS measured points calculated by Fillnet. The adjustment is done on behalf of 2 full control points, 3 planimetric control points and 14 height control points.

S.E. OF UNIT WEIGHT = 1.166

NUMBER OF -
 OBS. EQUATIONS 561
 UNKNOWNNS 337
 DEGREES OF FREEDOM 224
 ITERATIONS 1

ADJUSTED POSITIONS:

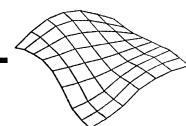
		LAT.		LON.		ELEV.	STD.	ERRORS	(m)
1	0007	56 59 3.44834	-	9 57 44.07348		103.306	0.000	0.000	0.000
2	0001	56 58 56.04341	-	9 59 45.45179		122.446	0.000	0.000	0.008
3	0522	56 58 25.26736	-	9 59 27.10756		81.464	0.006	0.008	0.008
4	0910	56 59 6.51494	-	9 59 42.96779		82.280	0.007	0.010	0.009
5	0523	56 59 6.69453	-	9 59 43.02732		83.353	0.007	0.010	0.009
6	0526	56 59 15.74936	-	9 59 4.01276		72.034	0.005	0.007	0.007
7	0527	56 58 54.25822	-	9 59 23.60871		95.446	0.005	0.007	0.007
8	0580	57 0 33.98410	-	9 55 13.44930		46.671	0.010	0.012	0.012
9	0590	56 58 35.11743	-	10 0 15.79037		71.527	0.008	0.010	0.010
10	0911	56 58 53.67143	-	9 58 45.66629		91.005	0.006	0.009	0.009
11	0990	56 58 35.11839	-	10 0 15.84249		70.531	0.008	0.010	0.000
12	0954	56 58 38.16494	-	9 56 30.05625		61.146	0.005	0.007	0.000
13	0555	56 58 27.54791	-	9 56 39.85490		52.566	0.005	0.008	0.007
14	0955	56 58 22.08483	-	9 57 23.61852		80.140	0.005	0.007	0.000
15	0556	56 58 26.07150	-	9 57 29.93373		80.773	0.005	0.007	0.007
16	0557	56 58 37.68779	-	9 57 46.51371		89.003	0.006	0.009	0.009
17	0550	56 58 9.76605	-	9 59 50.90096		70.198	0.007	0.009	0.008
18	0951	56 57 54.07676	-	9 56 54.47214		61.737	0.007	0.008	0.008
19	0553	56 58 5.59598	-	9 56 51.94921		53.859	0.006	0.008	0.008
20	8952	56 58 5.68622	-	9 56 51.79373		53.410	0.012	0.013	0.013
21	0003	56 58 4.68169	-	9 56 7.31319		97.626	0.007	0.008	0.008
22	0953	56 58 6.71324	-	9 56 19.92553		85.843	0.006	0.008	0.000
23	0011	57 1 5.02873	-	9 58 38.70387		52.852	0.006	0.005	0.004
24	0515	56 59 24.87184	-	9 54 55.36635		65.772	0.007	0.009	0.008
25	0518	56 59 46.90248	-	9 55 30.22915		68.217	0.006	0.008	0.008
26	0552	56 58 2.28223	-	9 57 35.94106		64.657	0.012	0.013	0.013
27	0577	56 59 26.40874	-	9 59 31.66922		67.412	0.005	0.007	0.007
28	7960	56 58 33.46167	-	9 58 48.25755		98.322	0.010	0.012	0.012
29	7985	56 58 25.65754	-	9 55 51.22898		68.135	0.011	0.013	0.013
30	7973	56 59 16.71023	-	9 58 29.50915		78.355	0.008	0.011	0.010
31	0560	56 58 33.50397	-	9 58 48.38302		99.534	0.005	0.007	0.007
32	8960	56 58 33.46612	-	9 58 48.28974		98.275	0.010	0.012	0.012
33	0528	56 58 24.89146	-	9 58 24.36078		84.472	0.005	0.006	0.006
34	8912	56 58 24.96529	-	9 58 24.35351		83.950	0.010	0.012	0.012
35	0561	56 58 53.05817	-	9 57 52.61048		98.072	0.004	0.007	0.007
36	8961	56 58 53.27094	-	9 57 52.49395		98.019	0.009	0.011	0.011
37	0562	56 59 12.68132	-	9 57 54.79445		83.371	0.004	0.007	0.007
38	8962	56 59 17.79185	-	9 57 35.44840		86.645	0.008	0.011	0.011
39	8963	56 59 9.83138	-	9 57 4.68730		72.021	0.009	0.011	0.011
40	0519	56 59 25.16772	-	9 56 52.40898		54.128	0.005	0.007	0.007
41	8908	56 59 25.17221	-	9 56 52.35890		52.874	0.008	0.011	0.011



42	0564	56 59 48.84941	-	9 56 50.00548	44.555 0.005 0.007 0.007
43	0565	56 59 52.05994	-	9 58 0.86298	46.804 0.005 0.007 0.007
44	8964	56 59 43.93202	-	9 57 43.79640	57.377 0.007 0.010 0.010
45	7504	57 0 15.88032	-	9 57 54.71120	46.008 0.007 0.010 0.010
46	0554	56 58 6.52886	-	9 56 18.54015	88.130 0.006 0.007 0.007
47	0576	57 0 20.02263	-	9 58 48.74332	45.473 0.005 0.006 0.006
48	6902	57 0 35.18349	-	9 58 46.16760	47.685 0.008 0.011 0.010
49	0505	57 0 14.10746	-	9 56 54.11447	65.296 0.005 0.006 0.006
50	0903	57 0 6.13686	-	9 56 50.91274	55.228 0.005 0.006 0.006
51	0500	57 0 44.76913	-	9 59 16.16805	57.979 0.009 0.011 0.011
52	0570	57 0 17.71611	-	9 59 38.96976	46.285 0.008 0.011 0.000
53	0571	57 0 1.04171	-	9 59 29.03716	44.752 0.008 0.010 0.010
54	8971	57 0 1.15309	-	9 59 28.83584	44.533 0.008 0.012 0.012
55	0573	56 59 46.55106	-	9 58 49.46365	47.443 0.006 0.009 0.009
56	0575	56 59 16.63339	-	9 58 29.81072	79.305 0.005 0.009 0.009
57	0107	57 0 41.95293	-	10 0 11.75027	45.749 0.000 0.000 0.000
58	0970	56 59 40.47959	-	9 59 49.47029	50.175 0.007 0.010 0.000
59	0572	56 59 42.26630	-	9 59 31.70910	47.930 0.007 0.010 0.010
60	0574	56 59 34.03967	-	9 59 20.17358	57.013 0.007 0.009 0.009
61	8972	56 59 34.00341	-	9 59 20.35532	56.866 0.008 0.012 0.012
62	0901	57 1 4.84288	-	9 59 8.84305	48.786 0.008 0.010 0.000
63	0581	56 59 15.03283	-	9 53 58.56296	49.061 0.010 0.012 0.012
64	8981	56 59 15.00661	-	9 53 58.74200	48.258 0.011 0.014 0.015
65	0582	56 58 53.01238	-	9 55 19.55215	56.168 0.007 0.010 0.010
66	8982	56 59 0.76055	-	9 55 52.93248	82.331 0.009 0.013 0.013
67	0583	56 58 21.66442	-	9 55 9.46490	75.524 0.008 0.011 0.010
68	8983	56 58 21.46359	-	9 55 9.49055	75.188 0.011 0.014 0.014
69	0584	56 58 28.77800	-	9 55 20.26393	70.291 0.008 0.010 0.010
70	8984	56 58 28.41490	-	9 55 21.04511	71.079 0.010 0.014 0.014
71	0585	56 58 25.70204	-	9 55 51.45726	68.814 0.007 0.010 0.010
72	8985	56 58 25.63696	-	9 55 51.17460	68.195 0.010 0.014 0.014
73	8990	56 58 35.11825	-	10 0 15.83159	70.531 0.010 0.013 0.000
74	0981	56 59 15.00658	-	9 53 58.73206	48.280 0.010 0.012 0.012
75	0982	56 59 0.76108	-	9 55 52.93243	82.271 0.006 0.010 0.009
76	0985	56 58 25.66101	-	9 55 51.17343	68.180 0.007 0.010 0.010
77	0984	56 58 28.42743	-	9 55 21.06565	71.085 0.008 0.010 0.010
78	0983	56 58 21.45614	-	9 55 9.52371	75.180 0.008 0.011 0.010
79	0912	56 58 24.96426	-	9 58 24.35416	83.959 0.006 0.009 0.009
80	0961	56 58 53.27115	-	9 57 52.49293	98.022 0.005 0.009 0.009
81	0962	56 59 17.75538	-	9 57 35.51224	86.698 0.005 0.009 0.009
82	0963	56 59 9.84151	-	9 57 4.64877	72.005 0.005 0.009 0.009
83	0908	56 59 25.17151	-	9 56 52.35552	52.879 0.006 0.009 0.009
84	0964	56 59 43.93557	-	9 57 43.83148	57.429 0.006 0.009 0.009
85	0008	56 59 36.49272	-	9 55 14.50871	87.305 0.000 0.000 0.000
86	0512	56 59 54.47319	-	9 55 3.65478	81.591 0.006 0.008 0.007
87	0516	56 59 17.58125	-	9 55 31.98678	83.797 0.005 0.007 0.007
88	0907	56 59 17.56034	-	9 55 32.01961	83.538 0.007 0.010 0.010
89	0517	56 59 19.43449	-	9 55 49.61537	83.744 0.005 0.007 0.006
90	0501	57 0 17.81316	-	9 57 59.54220	48.117 0.004 0.005 0.000
91	6502	57 0 15.95956	-	9 57 54.58913	46.083 0.005 0.007 0.007
92	6503	57 0 15.92863	-	9 57 54.78034	46.012 0.005 0.007 0.007
93	0551	56 58 8.01867	-	9 59 3.00420	69.891 0.005 0.006 0.006
94	0950	56 58 5.16408	-	9 59 37.89782	69.037 0.008 0.010 0.000
95	0952	56 58 5.68899	-	9 56 51.78908	53.421 0.007 0.010 0.009
96	0521	56 58 53.49265	-	9 56 33.75685	46.619 0.005 0.006 0.006
97	0906	56 59 46.14672	-	9 55 48.97599	48.014 0.005 0.007 0.000
98	0511	57 0 17.06747	-	9 55 30.44664	44.869 0.006 0.007 0.007
99	0520	56 59 20.23508	-	9 56 32.78476	47.623 0.004 0.006 0.006
100	0513	56 59 52.57786	-	9 55 59.00745	44.534 0.005 0.007 0.006
101	0905	57 0 11.94115	-	9 55 15.54451	47.337 0.006 0.008 0.000
102	0510	57 0 20.63801	-	9 56 3.14363	56.887 0.006 0.007 0.006
103	0006	57 0 24.23220	-	9 56 38.53736	105.951 0.005 0.007 0.006
104	0506	57 0 29.28554	-	9 56 40.19808	101.483 0.006 0.007 0.006
105	0971	57 0 1.15953	-	9 59 28.93087	44.586 0.008 0.010 0.010
106	0973	56 59 16.63296	-	9 58 29.63470	78.187 0.005 0.009 0.009
107	0972	56 59 33.98623	-	9 59 20.34824	56.898 0.007 0.009 0.009
108	0524	56 59 29.19393	-	10 0 11.96723	53.488 0.005 0.007 0.006
109	9902	57 0 35.18330	-	9 58 46.16725	47.786 0.006 0.007 0.007
110	0502	57 0 15.88296	-	9 57 54.72387	46.008 0.005 0.007 0.007
111	0503	57 0 15.98225	-	9 57 54.73119	46.126 0.005 0.007 0.007

Bundle adjustment

112	9502	57	0	15.88341	-	9	57	54.72210	45.991	0.005	0.007	0.007
113	0504	57	0	15.95759	-	9	57	54.58728	46.090	0.005	0.007	0.007
114	8907	56	59	17.56070	-	9	55	32.01984	83.521	0.007	0.009	0.009
115	9908	56	59	25.17393	-	9	56	52.35533	52.875	0.006	0.008	0.008
116	8909	56	59	17.72446	-	9	56	32.30654	48.834	0.006	0.008	0.008
117	8910	56	59	6.50996	-	9	59	42.96346	82.273	0.009	0.011	0.011
118	8911	56	58	53.67196	-	9	58	45.66515	90.995	0.009	0.011	0.011
119	9912	56	58	24.96509	-	9	58	24.35189	83.961	0.010	0.012	0.012
120	0957	56	58	37.68778	-	9	57	46.51364	89.001	0.005	0.007	0.007
121	0960	56	58	33.52460	-	9	58	48.13771	97.051	0.006	0.009	0.009
123	6551	56	58	8.01899	-	9	59	3.00407	71.786	0.011	0.013	0.013
124	7503	57	0	15.96169	-	9	57	54.72101	44.005	0.007	0.010	0.010
125	8523	56	59	6.69473	-	9	59	43.02551	83.604	0.009	0.011	0.011



E.3 The co-ordinate list for the ground control points

This Appendix contains the co-ordinate list for the ground control points which are used in the following aerotriangulations.

In total 119 vectors are measured. In this list, geometric reference points are deleted. The height control points are determined by two individual vectors. The average of the Z-co-ordinates is determined and one of the vectors is deleted. The list now only contains relevant ground control points, in total 77 points with accuracies.

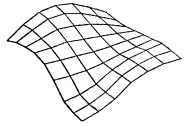
X- and Y-co-ordinates are original WGS'84 co-ordinates. These are transferred over to System34 Jutland/DNN (System34 is the official Danish Datum). The accuracy for X, Y, Z in metres is placed in the last three columns. The accuracy has to be taken with reservation because there have to be minor corrections due to the transference. The accuracy of the Z-co-ordinates is correct.

All accuracies over 0.01 m are highlighted.

500	-233539.136	287189.892	57.979	0.006	0.009	0.009
501	-234837.086	286363.522	48.117	0.005	0.007	0.000
503	-234919.569	286305.927	46.879	0.008	0.012	0.012
505	-235942.096	286255.562	65.309	0.006	0.009	0.009
506	-236174.048	286726.49	101.483	0.006	0.009	0.009
510	-236801.153	286462.969	56.877	0.006	0.009	0.010
511	-237353.676	286355.987	44.815	0.007	0.009	0.010
512	-237810.480	285660.147	81.591	0.007	0.009	0.010
513	-236876.458	285595.415	44.577	0.006	0.009	0.009
515	-237956.482	284745.466	65.772	0.007	0.009	0.010
516	-237339.559	284515.894	83.534	0.006	0.009	0.009
517	-237041.524	284571.290	83.720	0.006	0.009	0.009
518	-237363.396	285423.054	68.141	0.006	0.009	0.010
519	-235980.163	284741.915	54.107	0.006	0.009	0.009
520	-236312.473	284591.484	48.182	0.006	0.009	0.009
521	-236301.284	283764.202	46.654	0.006	0.009	0.009
522	-233378.467	282873.829	81.333	0.006	0.009	0.009
523	-233102.511	284153.771	83.216	0.006	0.009	0.009
524	-232610.071	284847.067	53.488	0.006	0.009	0.009
526	-233759.808	284437.601	72.046	0.006	0.009	0.009
527	-233432.576	283770.938	95.378	0.006	0.009	0.009
528	-234438.501	282868.186	84.240	0.005	0.008	0.008
550	-232979.141	282392.155	70.198	0.007	0.009	0.010
551	-233788.621	282342.592	69.891	0.005	0.007	0.008
552	-235260.560	282173.715	64.657	0.010	0.014	0.014
553	-236003.170	282280.737	53.859	0.006	0.009	0.009
554	-236567.420	282313.115	88.130	0.006	0.009	0.009
555	-236203.228	282961.065	53.121	0.006	0.009	0.009
556	-235357.638	282910.106	80.788	0.006	0.009	0.009
557	-235075.449	283267.723	89.012	0.006	0.009	0.009
560	-234030.714	283131.978	98.544	0.006	0.009	0.009
561	-234969.605	283742.595	97.901	0.005	0.009	0.009
562	-234929.141	284349.365	83.371	0.005	0.009	0.009
564	-236016.279	285474.800	44.591	0.006	0.009	0.009
565	-234819.461	285566.792	46.788	0.005	0.009	0.009
570	-233159.003	286350.914	46.021	0.006	0.009	0.000
571	-233329.343	285836.161	44.708	0.006	0.009	0.009
572	-233287.552	285255.139	47.621	0.006	0.009	0.009
573	-234000.004	285391.701	47.427	0.005	0.009	0.009
574	-233483.647	285001.785	56.888	0.006	0.009	0.009
575	-234337.117	284468.167	78.919	0.005	0.009	0.009

Bundle adjustment

576	-234006.225	286427.026	45.494	0.005	0.008	0.007
577	-233290.934	284764.615	67.004	0.006	0.009	0.009
580	-237637.107	286881.183	46.671	0.007	0.010	0.010
581	-238917.674	284447.618	49.061	0.008	0.010	0.011
582	-237554.347	283757.393	56.158	0.007	0.010	0.010
583	-237731.321	282788.805	75.524	0.007	0.010	0.010
584	-237547.518	283007.617	70.654	0.007	0.009	0.010
585	-237021.134	282909.262	68.805	0.007	0.009	0.010
590	-232554.462	283174.045	71.527	0.007	0.009	0.010
903	-235997.773	286009.151	55.278	0.007	0.009	0.000
905	-237606.224	286199.132	47.337	0.007	0.009	0.000
906	-237046.166	285396.913	48.032	0.006	0.009	0.000
907	-237338.731	284514.254	83.463	0.008	0.012	0.012
908	-235981.383	284741.966	52.951	0.007	0.012	0.012
909	-236320.798	284513.924	48.853	0.009	0.013	0.013
910	-233102.948	284149.274	82.209	0.008	0.012	0.012
911	-234073.623	283756.103	91.001	0.007	0.012	0.012
912	-234438.496	282869.983	84.017	0.007	0.012	0.012
950	-233199.601	282251.011	69.037	0.006	0.009	0.010
952	-236005.858	282283.630	53.421	0.008	0.012	0.012
953	-236543.979	282318.671	85.843	0.006	0.009	0.000
954	-236366.495	283292.343	61.084	0.006	0.009	0.000
957	-235075.449	283267.723	89.012	0.005	0.007	0.007
960	-234033.786	283131.455	98.275	0.006	0.009	0.000
961	-234971.648	283748.946	98.080	0.007	0.012	0.012
962	-235254.598	284509.749	86.660	0.007	0.012	0.012
963	-235775.678	284266.188	72.075	0.007	0.012	0.012
964	-235110.072	285316.600	57.468	0.007	0.012	0.012
970	-232988.010	285198.205	50.175	0.006	0.009	0.000
971	-233332.349	285838.927	44.555	0.008	0.012	0.012
972	-233481.254	285000.952	56.838	0.008	0.012	0.012
973	-234342.630	284470.555	78.289	0.009	0.013	0.014
981	-238914.824	284446.786	48.280	0.009	0.013	0.014
982	-236986.745	283991.389	82.298	0.008	0.012	0.012
983	-237730.370	282782.356	75.180	0.008	0.012	0.013
984	-237534.169	282997.628	71.038	0.008	0.012	0.013
985	-237024.678	282907.587	68.189	0.008	0.012	0.000
990	-232553.581	283174.079	70.531	0.008	0.012	0.000



E.4 Aerotriangulation for images in scale 1:25,000

This Appendix contains a cut out of the results from the aerotriangulation for the images in the scale 1:25,000 calculated by Bingo.

The co-ordinate list 'ltera.dat' file from the aerotriangulation can be found in section 4.1.

BINGO-F - VERS. 3.3 / 12.96 10:27:32 Monday, 07 February 2000
=====

RESULTS OF ADJUSTMENT SIGMA 0 = 4.24 (1/1000)
=====

EXTERIOR ORIENTATION DATA

TYPE	PHOTO	X +- S (1/1000)	Y	Z	PHI	OMEGA	KAPPA
A	60	-238430.755	284695.965	3809.087	0.1108	1.0431	197.3096
	+-	277.	241.	197.	4.6	3.3	1.7
A	62	-233826.896	284522.027	3796.847	-0.9418	0.1314	198.4115
	+-	260.	231.	140.	4.1	3.3	1.4
A	61	-236129.459	284617.439	3805.005	0.2995	1.2819	198.2017
	+-	212.	201.	102.	3.2	3.0	1.1

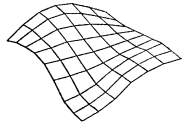
CAMERA DATA

CAMERA NO. 1
NO UNKNOWN PARAMETERS

COORDINATES OF OBJECT POINTS

POINT NO.	X	Y	Z	+- S X (1 / 1 0 0 0)	S Y	S Z
580	-237637.036	286881.216	46.703	78.	87.	135.
981	-238915.398	284447.722	48.191	134.	107.	143.
581	-238917.635	284447.615	47.796	89.	80.	262.
506	-236174.183	286726.584	101.651	68.	76.	120.
520	-236312.494	284591.399	49.258	63.	63.	150.
963	-235775.530	284266.746	72.122	105.	90.	137.
952	-236006.679	282282.887	53.479	87.	116.	128.
583	-237731.410	282788.866	75.032	78.	89.	234.
1194	-235887.516	282242.084	59.917	88.	127.	178.
983	-237725.151	282787.200	75.062	104.	135.	140.
1111	-236108.543	284380.039	53.837	75.	77.	149.
1100	-236500.127	284781.888	55.894	77.	77.	152.
1106	-236131.840	287181.344	93.056	87.	131.	184.

1105	-236256.222	287004.740	102.184	86.	124.	180.
1124	-238546.221	282220.624	93.288	147.	205.	304.
1123	-238590.831	282177.872	93.335	150.	209.	306.
1121	-238908.525	284897.477	52.421	152.	108.	295.
1120	-238856.131	284504.035	49.851	149.	106.	293.
1126	-238660.464	287183.299	48.902	155.	215.	320.
1125	-238528.880	287293.175	47.826	149.	222.	319.
551	-233788.733	282342.616	69.765	81.	87.	137.
526	-233759.568	284437.529	72.269	75.	72.	133.
574	-233483.637	285001.741	57.227	85.	74.	230.
500	-233539.299	287189.782	57.706	82.	90.	140.
9963	-235775.917	284267.075	75.440	101.	89.	256.
553	-236003.093	282280.655	53.983	77.	91.	206.
1113	-235727.089	282127.007	56.271	108.	195.	283.
1096	-233339.146	287202.214	57.966	160.	217.	310.
1095	-233478.460	287229.890	55.438	152.	218.	307.
1094	-233765.007	282354.567	76.256	134.	183.	290.
1093	-233831.065	282287.281	69.863	132.	187.	291.
1091	-233550.847	284934.634	59.931	134.	98.	275.
1090	-233655.927	284747.147	64.215	128.	95.	272.
Mean squared precision of object points:				113.	136.	231.
Mean squared precision of control points:				78.	82.	135.



E.4.1 The 'Itera.dat' file from the aerotriangulation for images in 1:25,000

ORIA	160	-238430.755	284695.965	3809.087	0.1108	1.0431	197.3096	1
ORIA	161	-236129.459	284617.439	3805.005	0.2995	1.2819	198.2017	1
ORIA	162	-233826.896	284522.027	3796.847	-0.9418	0.1314	198.4115	1
CORD	500	-233539.299	287189.782	57.706	0.082	0.090	0.140	
CORD	506	-236174.183	286726.584	101.651	0.068	0.076	0.120	
CORD	520	-236312.494	284591.399	49.258	0.063	0.063	0.150	
CORD	526	-233759.568	284437.529	72.269	0.075	0.072	0.133	
CORD	551	-233788.733	282342.616	69.765	0.081	0.087	0.137	
CORD	553	-236003.093	282280.655	53.983	0.077	0.091	0.206	
CORD	574	-233483.637	285001.741	57.227	0.085	0.074	0.230	
CORD	580	-237637.036	286881.216	46.703	0.078	0.087	0.135	
CORD	581	-238917.635	284447.615	47.796	0.089	0.080	0.262	
CORD	583	-237731.410	282788.866	75.032	0.078	0.089	0.234	
CORD	952	-236006.679	282282.887	53.479	0.087	0.116	0.128	
CORD	963	-235775.530	284266.746	72.122	0.105	0.090	0.137	
CORD	981	-238915.398	284447.722	48.191	0.134	0.107	0.143	
CORD	983	-237725.151	282787.200	75.062	0.104	0.135	0.140	
CORD	1090	-233655.927	284747.147	64.215	0.128	0.095	0.272	
CORD	1091	-233550.847	284934.634	59.931	0.134	0.098	0.275	
CORD	1093	-233831.065	282287.281	69.863	0.132	0.187	0.291	
CORD	1094	-233765.007	282354.567	76.256	0.134	0.183	0.290	
CORD	1095	-233478.460	287229.890	55.438	0.152	0.218	0.307	
CORD	1096	-233339.146	287202.214	57.966	0.160	0.217	0.310	
CORD	1100	-236500.127	284781.888	55.894	0.077	0.077	0.152	
CORD	1105	-236256.222	287004.740	102.184	0.086	0.124	0.180	
CORD	1106	-236131.840	287181.344	93.056	0.087	0.131	0.184	
CORD	1111	-236108.543	284380.039	53.837	0.075	0.077	0.149	
CORD	1113	-235727.089	282127.007	56.271	0.108	0.195	0.283	
CORD	1120	-238856.131	284504.035	49.851	0.149	0.106	0.293	
CORD	1121	-238908.525	284897.477	52.421	0.152	0.108	0.295	
CORD	1123	-238590.831	282177.872	93.335	0.150	0.209	0.306	
CORD	1124	-238546.221	282220.624	93.288	0.147	0.205	0.304	
CORD	1125	-238528.880	287293.175	47.826	0.149	0.222	0.319	
CORD	1126	-238660.464	287183.299	48.902	0.155	0.215	0.320	
CORD	1194	-235887.516	282242.084	59.917	0.088	0.127	0.178	
CORD	9963	-235775.917	284267.075	75.440	0.101	0.089	0.256	

END

E.5 Aerotriangulation for images in scale 1:15,000

This Appendix contains a cut out of the results from the aerotriangulation for the images in scale 1:15,000 calculated by Bingo.

The co-ordinate list 'ltera.dat'-file from the aerotriangulation can be found in section A.5.1.

```
BINGO-F - VERS. 3.3 / 12.96          10:26:45  Monday, 07 February 2000
=====
```

```
RESULTS OF ADJUSTMENT          SIGMA 0 =          4.90 (1/1000)
=====
```

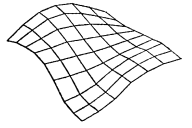
EXTERIOR ORIENTATION DATA

TYPE	PHOTO	X	Y	Z	PHI	OMEGA	KAPPA
	+- S (1/1000)						
A	50	-237724.848	285806.445	2330.373	-1.4139	-0.6494	198.5242
	+-	205.	226.	140.	5.2	5.1	2.6
A	59	-237939.897	283472.478	2327.585	0.3645	-0.7929	197.2592
	+-	196.	205.	135.	5.1	4.7	2.3
A	58	-236557.157	283416.057	2327.377	0.4164	-1.4382	196.7872
	+-	131.	166.	71.	3.3	4.2	1.5
A	51	-236343.692	285770.199	2331.093	-0.2055	2.8972	199.1731
	+-	144.	191.	81.	3.4	4.9	1.8
A	55	-232419.404	283242.176	2337.560	0.1449	-0.5721	195.2690
	+-	218.	206.	152.	5.9	4.7	2.4
A	57	-235177.282	283354.397	2333.829	0.2893	-1.1086	196.5917
	+-	116.	151.	54.	2.8	4.0	1.2
A	56	-233797.720	283315.066	2334.663	0.5206	-0.3600	195.7568
	+-	147.	165.	77.	3.7	4.2	1.5
A	53	-233582.516	285648.282	2336.727	-0.2777	2.8198	199.7259
	+-	214.	214.	126.	5.6	5.3	2.2
A	52	-234964.014	285682.564	2330.803	-0.6651	1.9315	199.1407
	+-	147.	175.	71.	3.4	4.6	1.5

CAMERA DATA

```
-----
CAMERA NO. 1
NO UNKNOWN PARAMETERS
```

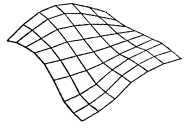
COORDINATES OF OBJECT POINTS



POINT NO.	X	Y	Z	+ - S X (1 / 1 0 0 0)	S Y	S Z
580	-237636.945	286881.304	46.043	111.	125.	189.
903	-235997.359	286008.974	55.277	87.	65.	127.
512	-237810.138	285660.737	81.322	90.	89.	127.
515	-237956.507	284745.480	65.167	68.	63.	125.
1034	-237853.987	284295.895	53.334	108.	147.	223.
1032	-237745.793	284534.407	65.752	97.	128.	210.
1033	-237635.627	284451.113	82.657	91.	131.	208.
1031	-237969.724	285655.504	79.736	110.	94.	198.
1036	-237939.667	286995.714	41.316	135.	147.	235.
1035	-237860.817	287129.996	41.541	134.	156.	239.
1126	-236480.364	287107.404	101.314	99.	143.	216.
506	-236174.067	286726.504	101.438	65.	68.	108.
520	-236312.537	284591.399	48.419	38.	37.	84.
1023	-236259.218	284417.870	44.924	39.	38.	85.
909	-236322.553	284496.517	48.998	43.	41.	82.
1024	-236312.856	284491.159	46.918	40.	38.	84.
1025	-236451.671	287412.363	97.020	89.	120.	165.
1020	-236508.666	285869.832	48.200	58.	57.	107.
582	-237554.522	283757.394	55.987	60.	65.	123.
983	-237728.781	282782.309	75.093	81.	86.	129.
583	-237731.449	282788.782	74.561	72.	75.	188.
1086	-237720.110	284787.355	83.352	81.	127.	203.
1085	-238060.766	284640.805	48.519	100.	124.	212.
1084	-237853.088	281770.423	76.234	112.	168.	235.
1083	-238004.465	282139.546	92.020	113.	137.	224.
1081	-238025.103	283314.029	68.198	96.	82.	200.
1080	-238087.010	283407.552	72.296	99.	82.	200.
1071	-236429.968	283408.897	56.873	50.	50.	102.
554	-236567.429	282313.131	87.663	55.	67.	124.
1070	-236554.020	283433.781	61.064	50.	51.	102.
954	-236366.481	283292.382	61.247	50.	50.	88.
1076	-236550.799	284892.647	47.072	55.	79.	128.
1075	-236631.650	285015.363	45.886	57.	84.	133.
1074	-236951.777	281955.028	87.914	72.	96.	145.
1073	-236817.835	281945.441	88.054	69.	96.	144.
952	-236006.005	282283.492	53.431	66.	90.	125.
1061	-235498.720	283136.675	84.979	64.	59.	174.
553	-236003.062	282280.747	53.536	59.	81.	168.
953	-236543.645	282315.811	85.998	77.	90.	126.
1060	-235164.424	283618.446	88.484	47.	47.	102.
1063	-235024.851	282075.554	62.134	60.	81.	132.
1064	-235397.310	282157.306	65.669	60.	78.	130.
1066	-234976.536	284745.566	69.336	52.	76.	128.
1065	-235279.228	284620.937	83.105	50.	70.	122.
552	-235260.507	282173.982	64.915	54.	64.	105.
561	-234969.559	283742.575	98.025	45.	45.	102.
962	-235254.393	284502.971	86.861	49.	62.	100.
562	-234929.064	284349.408	83.205	46.	55.	112.
963	-235775.945	284265.741	72.068	57.	100.	123.
9501	-234841.575	286362.191	48.278	85.	75.	129.
503	-234919.573	286305.946	46.856	58.	57.	124.
565	-234819.414	285566.756	47.033	49.	47.	90.
9962	-235252.808	284506.074	86.883	60.	87.	122.
1026	-236494.372	287031.781	103.355	110.	136.	218.
1016	-235030.468	286505.559	62.079	66.	70.	133.
1015	-234772.551	287100.882	65.330	79.	102.	162.
1013	-234859.336	284303.474	77.580	39.	39.	85.
1021	-236552.956	285900.917	41.191	97.	66.	191.
9960	-234029.661	283133.045	98.195	78.	60.	123.
560	-234031.046	283132.072	99.519	74.	55.	165.
551	-233788.727	282342.569	69.689	56.	63.	101.
550	-232979.126	282392.157	69.885	68.	75.	125.
990	-232553.563	283174.327	70.456	81.	78.	128.
590	-232554.500	283174.039	70.361	72.	69.	192.

Bundle adjustment

524	-232610.069	284846.958	52.791	73.	92.	168.
1054	-233662.026	281947.678	63.725	68.	92.	137.
1053	-233688.937	281809.200	63.765	70.	99.	143.
1051	-233844.034	283698.732	86.298	51.	53.	103.
1050	-234056.540	283250.121	93.589	52.	50.	103.
1056	-233786.171	284735.575	62.096	57.	81.	130.
1055	-233914.621	284901.448	60.103	89.	150.	214.
1046	-232049.045	284369.939	46.916	123.	125.	228.
1045	-232062.869	284326.151	48.082	121.	122.	226.
1043	-232635.363	281892.199	85.343	101.	142.	221.
1044	-232610.433	281736.181	89.563	106.	156.	227.
1040	-232250.242	283257.493	69.320	103.	84.	206.
526	-233759.670	284437.502	71.985	43.	45.	83.
1004	-233428.478	284443.588	89.806	53.	56.	99.
1003	-233417.951	284270.398	100.549	53.	56.	100.
960	-234029.597	283133.019	98.508	64.	60.	120.
1155	-233693.960	284814.069	61.031	88.	134.	207.
1014	-234745.498	284273.670	76.900	43.	42.	91.
972	-233480.722	285000.859	56.886	78.	78.	123.
574	-233483.648	285001.768	56.957	66.	66.	118.
971	-233331.959	285838.318	44.629	93.	77.	128.
571	-233329.487	285836.159	44.210	81.	68.	183.
500	-233539.069	287190.133	56.457	116.	157.	237.
501	-234841.655	286362.198	48.207	78.	77.	129.
9562	-234928.901	284349.078	83.014	74.	119.	195.
1006	-233478.242	287230.326	54.093	123.	167.	250.
1005	-233339.227	287202.267	57.091	132.	166.	252.
1001	-233364.589	285718.132	45.455	101.	75.	196.
1000	-233378.997	285600.573	48.776	99.	74.	193.
Mean squared precision of object points:				80.	93.	160.
Mean squared precision of control points:				69.	75.	128.

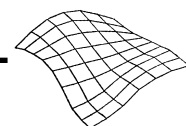


E.5.1 The 'ltera.dat' file from the aerotriangulation for the images in scale 1:15,000

ORIA	150	-237724.848	285806.445	2330.373	-1.4139	-0.6494	198.5242	1
ORIA	151	-236343.692	285770.199	2331.093	-0.2055	2.8972	199.1731	1
ORIA	152	-234964.014	285682.564	2330.803	-0.6651	1.9315	199.1407	1
ORIA	153	-233582.516	285648.282	2336.727	-0.2777	2.8198	199.7259	1
ORIA	155	-232419.404	283242.176	2337.560	0.1449	-0.5721	195.2690	1
ORIA	156	-233797.720	283315.066	2334.663	0.5206	-0.3600	195.7568	1
ORIA	157	-235177.282	283354.397	2333.829	0.2893	-1.1086	196.5917	1
ORIA	158	-236557.157	283416.057	2327.377	0.4164	-1.4382	196.7872	1
ORIA	159	-237939.897	283472.478	2327.585	0.3645	-0.7929	197.2592	1
CORD	500	-233539.069	287190.133	56.457	0.116	0.157	0.237	
CORD	501	-234841.655	286362.198	48.207	0.078	0.077	0.129	
CORD	503	-234919.573	286305.946	46.856	0.058	0.057	0.124	
CORD	506	-236174.067	286726.504	101.438	0.065	0.068	0.108	
CORD	512	-237810.138	285660.737	81.322	0.090	0.089	0.127	
CORD	515	-237956.507	284745.480	65.167	0.068	0.063	0.125	
CORD	520	-236312.537	284591.399	48.419	0.038	0.037	0.084	
CORD	524	-232610.069	284846.958	52.791	0.073	0.092	0.168	
CORD	526	-233759.670	284437.502	71.985	0.043	0.045	0.083	
CORD	550	-232979.126	282392.157	69.885	0.068	0.075	0.125	
CORD	551	-233788.727	282342.569	69.689	0.056	0.063	0.101	
CORD	552	-235260.507	282173.982	64.915	0.054	0.064	0.105	
CORD	553	-236003.062	282280.747	53.536	0.059	0.081	0.168	
CORD	554	-236567.429	282313.131	87.663	0.055	0.067	0.124	
CORD	560	-234031.046	283132.072	99.519	0.074	0.055	0.165	
CORD	561	-234969.559	283742.575	98.025	0.045	0.045	0.102	
CORD	562	-234929.064	284349.408	83.205	0.046	0.055	0.112	
CORD	565	-234819.414	285566.756	47.033	0.049	0.047	0.090	
CORD	571	-233329.487	285836.159	44.210	0.081	0.068	0.183	
CORD	574	-233483.648	285001.768	56.957	0.066	0.066	0.118	
CORD	580	-237636.945	286881.304	46.043	0.111	0.125	0.189	
CORD	582	-237554.522	283757.394	55.987	0.060	0.065	0.123	
CORD	583	-237731.449	282788.782	74.561	0.072	0.075	0.188	
CORD	590	-232554.500	283174.039	70.361	0.072	0.069	0.192	
CORD	903	-235997.359	286008.974	55.277	0.087	0.065	0.127	
CORD	909	-236322.553	284496.517	48.998	0.043	0.041	0.082	
CORD	952	-236006.005	282283.492	53.431	0.066	0.090	0.125	
CORD	953	-236543.645	282315.811	85.998	0.077	0.090	0.126	
CORD	954	-236366.481	283292.382	61.247	0.050	0.050	0.088	
CORD	960	-234029.597	283133.019	98.508	0.064	0.060	0.120	
CORD	962	-235254.393	284502.971	86.861	0.049	0.062	0.100	
CORD	963	-235775.945	284265.741	72.068	0.057	0.100	0.123	
CORD	971	-233331.959	285838.318	44.629	0.093	0.077	0.128	
CORD	972	-233480.722	285000.859	56.886	0.078	0.078	0.123	
CORD	983	-237728.781	282782.309	75.093	0.081	0.086	0.129	
CORD	990	-232553.563	283174.327	70.456	0.081	0.078	0.128	
CORD	1000	-233378.997	285600.573	48.776	0.099	0.074	0.193	
CORD	1001	-233364.589	285718.132	45.455	0.101	0.075	0.196	
CORD	1003	-233417.951	284270.398	100.549	0.053	0.056	0.100	
CORD	1004	-233428.478	284443.588	89.806	0.053	0.056	0.099	
CORD	1005	-233339.227	287202.267	57.091	0.132	0.166	0.252	
CORD	1006	-233478.242	287230.326	54.093	0.123	0.167	0.250	
CORD	1013	-234859.336	284303.474	77.580	0.039	0.039	0.085	

Bundle adjustment

CORD	1014	-234745.498	284273.670	76.900	0.043	0.042	0.091
CORD	1015	-234772.551	287100.882	65.330	0.079	0.102	0.162
CORD	1016	-235030.468	286505.559	62.079	0.066	0.070	0.133
CORD	1020	-236508.666	285869.832	48.200	0.058	0.057	0.107
CORD	1021	-236552.956	285900.917	41.191	0.097	0.066	0.191
CORD	1023	-236259.218	284417.870	44.924	0.039	0.038	0.085
CORD	1024	-236312.856	284491.159	46.918	0.040	0.038	0.084
CORD	1025	-236451.671	287412.363	97.020	0.089	0.120	0.165
CORD	1026	-236494.372	287031.781	103.355	0.110	0.136	0.218
CORD	1031	-237969.724	285655.504	79.736	0.110	0.094	0.198
CORD	1032	-237745.793	284534.407	65.752	0.097	0.128	0.210
CORD	1033	-237635.627	284451.113	82.657	0.091	0.131	0.208
CORD	1034	-237853.987	284295.895	53.334	0.108	0.147	0.223
CORD	1035	-237860.817	287129.996	41.541	0.134	0.156	0.239
CORD	1036	-237939.667	286995.714	41.316	0.135	0.147	0.235
CORD	1040	-232250.242	283257.493	69.320	0.103	0.084	0.206
CORD	1043	-232635.363	281892.199	85.343	0.101	0.142	0.221
CORD	1044	-232610.433	281736.181	89.563	0.106	0.156	0.227
CORD	1045	-232062.869	284326.151	48.082	0.121	0.122	0.226
CORD	1046	-232049.045	284369.939	46.916	0.123	0.125	0.228
CORD	1050	-234056.540	283250.121	93.589	0.052	0.050	0.103
CORD	1051	-233844.034	283698.732	86.298	0.051	0.053	0.103
CORD	1053	-233688.937	281809.200	63.765	0.070	0.099	0.143
CORD	1054	-233662.026	281947.678	63.725	0.068	0.092	0.137
CORD	1055	-233914.621	284901.448	60.103	0.089	0.150	0.214
CORD	1056	-233786.171	284735.575	62.096	0.057	0.081	0.130
CORD	1060	-235164.424	283618.446	88.484	0.047	0.047	0.102
CORD	1061	-235498.720	283136.675	84.979	0.064	0.059	0.174
CORD	1063	-235024.851	282075.554	62.134	0.060	0.081	0.132
CORD	1064	-235397.310	282157.306	65.669	0.060	0.078	0.130
CORD	1065	-235279.228	284620.937	83.105	0.050	0.070	0.122
CORD	1066	-234976.536	284745.566	69.336	0.052	0.076	0.128
CORD	1070	-236554.020	283433.781	61.064	0.050	0.051	0.102
CORD	1071	-236429.968	283408.897	56.873	0.050	0.050	0.102
CORD	1073	-236817.835	281945.441	88.054	0.069	0.096	0.144
CORD	1074	-236951.777	281955.028	87.914	0.072	0.096	0.145
CORD	1075	-236631.650	285015.363	45.886	0.057	0.084	0.133
CORD	1076	-236550.799	284892.647	47.072	0.055	0.079	0.128
CORD	1080	-238087.010	283407.552	72.296	0.099	0.082	0.200
CORD	1081	-238025.103	283314.029	68.198	0.096	0.082	0.200
CORD	1083	-238004.465	282139.546	92.020	0.113	0.137	0.224
CORD	1084	-237853.088	281770.423	76.234	0.112	0.168	0.235
CORD	1085	-238060.766	284640.805	48.519	0.100	0.124	0.212
CORD	1086	-237720.110	284787.355	83.352	0.081	0.127	0.203
CORD	1126	-236480.364	287107.404	101.314	0.099	0.143	0.216
CORD	1155	-233693.960	284814.069	61.031	0.088	0.134	0.207
CORD	9501	-234841.575	286362.191	48.278	0.085	0.075	0.129
CORD	9562	-234928.901	284349.078	83.014	0.074	0.119	0.195
CORD	9960	-234029.661	283133.045	98.195	0.078	0.060	0.123
CORD	9962	-235252.808	284506.074	86.883	0.060	0.087	0.122
END							



E.6 Aerotriangulation for images in scale 1:5,000

This Appendix contains a cut out of the results from the aerotriangulation for the images in scale 1:5,000 calculated by Bingo.

The co-ordinate list 'Itera-dat' file from the aerotriangulation can be found in section A.6.1.

```

BINGO-F - VERS. 3.3 / 12.96                      17:37:23 Friday, 13 June 1997
=====
RESULTS OF ADJUSTMENT          SIGMA 0 =          5.64 (1/1000)
=====

EXTERIOR ORIENTATION DATA

TYPE  PHOTO      X      Y      Z      PHI      OMEGA      KAPPA
      +- S (1/1000)
-----
A      25  -233179.216  285745.958  852.126  -0.5397  2.9245  0.4688
      +-      103.      94.      64.      7.9      5.4      3.2

A      24  -233637.218  285778.321  846.394  -0.9264  3.3689  0.3643
      +-      74.      64.      38.      5.0      4.0      2.0
A      23  -234096.980  285811.615  842.376  -0.7450  3.1955  0.9883
      +-      55.      62.      32.      3.6      4.0      1.6

A      22  -234557.542  285826.807  840.822  -0.6096  1.5624  1.5186
      +-      53.      54.      34.      3.4      3.6      1.5

A      28  -233346.155  284966.369  846.695  0.4905  -0.8700  -2.8712
      +-      96.      77.      58.      7.5      5.0      2.7

A      29  -233807.007  284978.145  846.696  0.1334  -0.6853  -2.6454
      +-      56.      62.      34.      3.9      4.2      1.5

A      47  -233215.748  284179.148  848.918  -0.6165  1.7285  -0.7529
      +-      88.      80.      58.      6.6      5.0      3.0

A      50  -233375.137  283383.390  835.308  0.4113  -0.3104  -2.1485
      +-      95.     101.      58.      7.7      6.4      3.1

A      46  -233674.833  284192.486  848.576  -0.1593  1.4757  -0.7465
      +-      57.      66.      34.      4.0      4.4      1.9

A      51  -233835.694  283387.231  831.605  0.2399  -0.8748  -1.8160
      +-      63.      67.      35.      4.4      4.7      2.1

A      30  -234267.289  284987.450  848.212  0.6982  -1.2703  -1.8252
      +-      48.      56.      32.      3.3      3.9      1.2

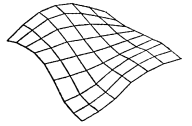
A      45  -234137.416  284200.401  849.873  -0.6427  0.9059  -0.9229
      +-      49.      59.      30.      3.3      4.3      1.4

A      52  -234296.811  283392.882  831.894  0.4037  -1.6701  -1.5609
      +-      56.      67.      34.      4.0      4.8      1.8

```

Bundle adjustment

A	44	-234597.462	284214.869	847.518	-0.7318	1.1641	-0.8227
	+-	45.	55.	29.	3.0	4.0	1.3
A	31	-234726.972	285005.292	847.792	1.0107	-2.1772	-1.8911
	+-	46.	53.	31.	2.9	3.7	1.2
A	53	-234756.815	283407.806	830.036	0.9576	-2.2953	-1.5895
	+-	61.	66.	37.	4.5	4.9	1.6
A	43	-235055.798	284234.716	850.143	-0.4898	1.6250	-0.7681
	+-	47.	55.	30.	3.2	4.0	1.2
A	54	-235215.156	283423.867	830.885	1.0449	-1.9683	-1.4650
	+-	57.	62.	35.	4.0	4.6	1.7
A	21	-235016.779	285832.133	844.607	-0.3232	1.5418	1.3886
	+-	55.	60.	34.	3.5	3.9	1.4
A	32	-235185.959	285024.143	846.497	0.7617	-1.9123	-1.8986
	+-	52.	55.	32.	3.5	3.8	1.3
A	42	-235515.687	284251.581	850.102	-0.2895	0.8219	-0.5635
	+-	46.	52.	28.	3.0	3.8	1.1
A	55	-235675.349	283433.840	834.141	1.3325	-1.6600	-1.4489
	+-	61.	65.	39.	4.4	4.7	1.6
A	20	-235478.377	285846.227	844.075	-0.7417	1.9825	1.1766
	+-	53.	56.	30.	3.1	3.7	1.5
A	33	-235646.174	285033.569	844.193	0.4681	-1.6560	-1.6280
	+-	50.	53.	29.	3.3	3.6	1.2
A	19	-235938.893	285864.748	843.860	-1.0137	1.5901	1.3236
	+-	54.	62.	32.	3.6	4.0	1.6
A	56	-236135.452	283448.501	834.874	1.1969	-2.4428	-1.7624
	+-	65.	69.	43.	4.7	4.9	1.8
A	34	-236106.032	285039.190	842.027	0.5885	-2.0339	-1.5793
	+-	48.	51.	28.	3.2	3.5	1.2
A	41	-235975.280	284263.367	852.039	-0.2524	1.1511	-0.6252
	+-	48.	55.	28.	3.2	4.0	1.2
A	40	-236433.678	284278.458	855.376	-0.5436	1.6036	-0.5884
	+-	49.	58.	29.	3.2	4.1	1.3
A	57	-236596.001	283468.255	835.142	0.7732	-2.3852	-1.8457
	+-	66.	69.	40.	4.5	5.0	2.1
A	58	-237054.566	283479.872	839.904	1.1973	-1.9727	-1.6910
	+-	71.	77.	43.	4.9	5.4	2.3
A	59	-237516.804	283487.318	841.266	0.8795	-1.6951	-1.2705
	+-	90.	108.	63.	6.7	6.7	3.6
A	39	-236892.603	284296.914	855.320	-0.2433	1.2525	-0.4415
	+-	52.	62.	33.	3.4	4.2	1.6
A	38	-237353.784	284305.809	857.948	-0.0370	-0.1739	-0.2144
	+-	75.	78.	55.	5.7	4.9	2.7
A	37	-237482.584	285093.060	841.018	0.9637	-2.4814	-2.0346
	+-	82.	83.	53.	6.4	4.7	2.9
A	35	-236563.528	285055.529	840.315	0.8977	-3.0431	-1.9596
	+-	48.	53.	27.	3.2	3.5	1.3
A	16	-237319.673	285893.592	849.076	-0.8618	0.1705	2.4667



	+-	72.	79.	43.	5.1	4.5	2.5
A	17	-236859.041	285881.673	849.567	-0.8425	0.9451	1.1708
	+-	55.	62.	29.	3.5	3.8	1.7
A	36	-237023.137	285076.503	840.804	0.8952	-2.7507	-2.0233
	+-	57.	59.	28.	4.1	3.6	1.7
A	18	-236398.040	285873.118	846.771	-0.5826	0.5119	1.2708
	+-	52.	54.	28.	3.1	3.6	1.4

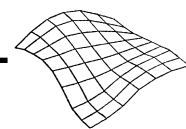
CAMERA DATA

CAMERA NO. 1
NO UNKNOWN PARAMETERS

COORDINATES OF OBJECT POINTS

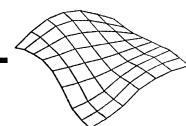
POINT NO.	X	Y	Z	+- S X	S Y	S Z
	(1 / 1 0 0 0)					
611	-233148.535	286345.001	46.165	52.	68.	49.
610	-233159.069	286346.880	46.200	52.	68.	49.
2087	-233509.667	285338.157	49.670	36.	53.	91.
971	-233332.349	285838.927	44.555	36.	41.	47.
571	-233329.343	285836.161	44.708	36.	41.	84.
570	-233159.003	286350.914	46.021	43.	48.	79.
2096	-233081.082	285397.772	46.391	56.	56.	100.
2095	-233105.727	285306.524	47.910	56.	62.	102.
2094	-233010.817	286344.573	47.119	69.	82.	97.
2083	-233653.908	286209.900	41.710	44.	64.	100.
2093	-233036.334	286187.146	44.317	62.	66.	93.
2092	-233171.473	286361.887	46.084	54.	81.	92.
2091	-233029.318	285877.418	42.978	57.	50.	92.
2090	-233083.874	285831.732	43.236	52.	47.	91.
2089	-233550.034	286249.782	42.599	37.	47.	58.
2080	-233536.712	285866.289	45.405	31.	34.	53.
2088	-233641.126	286136.469	41.483	33.	41.	57.
2081	-233516.570	285925.938	44.960	32.	35.	53.
572	-233287.552	285255.139	47.621	35.	30.	62.
2085	-233513.990	285375.146	48.400	30.	27.	51.
2086	-233531.890	285334.487	49.454	30.	27.	51.
600	-233992.593	286435.707	44.997	38.	58.	48.
601	-233989.049	286406.416	44.694	37.	56.	48.
576	-234006.225	286427.026	45.494	31.	39.	50.
2073	-233972.020	286429.833	44.576	35.	50.	53.
2071	-234143.695	285786.276	44.125	26.	27.	49.
2070	-234074.782	285809.838	43.528	26.	27.	48.
2076	-233984.964	285375.775	48.420	24.	23.	44.
2075	-234027.544	285304.822	47.198	24.	23.	44.
573	-234000.004	285391.701	47.427	23.	22.	39.
8601	-233989.027	286406.721	44.671	42.	53.	48.
8600	-233992.533	286435.816	44.999	42.	55.	48.
2077	-234000.836	285363.146	47.845	42.	52.	86.
2074	-234179.488	286431.534	43.563	39.	71.	86.
2072	-234202.295	286453.191	44.598	38.	74.	87.
2062	-234579.660	286379.703	45.636	31.	45.	62.
2063	-234639.036	286442.242	47.538	32.	50.	64.
2066	-234463.392	285298.833	63.996	26.	37.	56.
2065	-234554.492	285354.966	57.699	23.	23.	43.
2061	-234561.842	285897.992	43.221	26.	27.	52.
2064	-234615.271	286262.234	45.968	30.	39.	59.
2060	-234489.539	285960.091	43.408	27.	28.	53.
2068	-234538.868	285312.117	61.795	24.	24.	44.
2067	-234543.779	285311.591	61.973	24.	24.	44.
501	-234837.120	286363.528	48.120	30.	38.	46.

565	-234819.461	285566.792	46.788	26.	29.	46.
2053	-234869.683	286358.185	48.124	31.	45.	64.
2052	-234879.111	286387.856	48.905	31.	47.	64.
2051	-234891.580	285926.590	43.146	27.	27.	55.
503	-234919.569	286305.927	46.879	28.	35.	59.
2055	-234930.562	285407.204	48.293	26.	36.	57.
2054	-234890.815	285394.385	51.998	26.	36.	57.
972	-233481.254	285000.952	56.838	32.	33.	47.
574	-233483.647	285001.785	56.888	33.	33.	82.
3081	-233254.466	284923.584	59.626	46.	37.	86.
3082	-233233.207	285526.877	47.314	57.	69.	100.
3080	-233312.642	284993.871	56.159	42.	36.	85.
3086	-233469.470	284557.690	77.091	30.	30.	49.
3085	-233371.524	284555.871	80.947	32.	32.	52.
577	-233290.934	284764.615	67.004	33.	31.	58.
3074	-233715.293	285517.308	46.788	33.	42.	67.
3073	-233748.182	285478.710	47.310	32.	39.	66.
3072	-233715.257	285036.496	57.657	27.	27.	51.
3075	-233766.681	284475.596	70.582	25.	24.	38.
526	-233759.808	284437.601	72.046	25.	24.	35.
3076	-233830.308	284469.000	69.532	25.	25.	39.
8973	-234342.154	284470.864	78.345	33.	42.	47.
575	-234337.117	284468.167	78.919	22.	23.	38.
3066	-234215.201	284399.100	69.065	23.	23.	38.
3065	-234252.296	284410.364	69.820	22.	22.	36.
3063	-234310.211	285450.398	47.556	27.	36.	62.
3064	-234220.527	285475.939	43.016	28.	37.	63.
3062	-234249.627	285053.336	60.297	24.	25.	49.
3061	-234272.826	284758.111	71.251	24.	26.	45.
4097	-233425.015	283778.995	100.445	39.	52.	80.
8523	-233102.461	284153.754	83.079	51.	44.	84.
910	-233102.948	284149.274	82.209	46.	44.	48.
4096	-233274.351	284025.828	102.329	41.	42.	78.
4095	-233439.305	283776.735	93.978	38.	53.	81.
4094	-233192.391	284743.310	63.818	49.	67.	94.
4093	-233107.713	284756.561	61.930	56.	71.	97.
4092	-233136.944	284313.405	96.856	47.	44.	81.
4091	-233126.539	284120.250	84.203	49.	44.	83.
4090	-233105.215	284124.870	81.327	51.	44.	84.
527	-233432.576	283770.938	95.378	33.	32.	41.
4083	-233578.605	284782.427	63.033	34.	42.	63.
4082	-233694.969	284158.889	81.294	28.	29.	45.
4086	-233688.651	283833.289	88.322	29.	28.	39.
4085	-233636.732	283753.396	85.862	33.	38.	53.
4081	-233613.523	284274.189	84.347	29.	30.	47.
4084	-233617.417	284724.459	64.158	32.	40.	60.
4080	-233664.343	284252.825	79.977	28.	29.	46.
620	-233340.719	282939.845	75.721	51.	59.	48.
621	-233385.805	282955.554	75.384	48.	57.	48.
622	-233468.889	282986.782	78.317	45.	58.	80.
522	-233378.467	282873.829	81.333	43.	46.	76.
6097	-233452.627	282995.787	77.588	45.	57.	80.
6096	-233290.856	282921.004	73.450	59.	67.	86.
6095	-233318.814	283017.947	80.256	53.	58.	82.
6093	-233420.858	283812.956	94.726	43.	54.	81.
6091	-233410.776	283325.867	82.118	42.	43.	75.
6090	-233307.630	283276.992	88.120	49.	46.	77.
6087	-233777.158	283007.299	87.659	37.	44.	60.
6085	-233861.687	283065.907	83.381	35.	41.	60.
6083	-233793.794	283863.146	81.151	31.	39.	56.
6082	-233869.470	283367.810	97.386	30.	32.	49.
6081	-233763.278	283413.998	88.980	31.	33.	48.
6084	-233837.359	283893.633	80.934	31.	40.	57.
6080	-233828.214	283309.083	90.606	31.	33.	50.
911	-234073.623	283756.103	91.001	31.	41.	46.
4077	-234129.049	283772.664	94.162	27.	34.	48.
4076	-234121.379	283683.524	87.250	25.	26.	40.
4075	-234049.027	283870.585	87.145	24.	25.	38.
4074	-233993.752	284653.035	62.881	28.	35.	56.
4073	-234022.130	284798.518	63.248	29.	42.	61.



4072	-234105.001	284182.420	73.421	25.	25.	45.
4071	-234012.683	284147.764	73.700	26.	26.	45.
4070	-234076.862	284269.229	68.328	25.	26.	46.
960	-234033.786	283131.455	98.275	34.	38.	45.
560	-234030.714	283131.978	98.544	34.	42.	73.
8911	-234073.484	283756.013	91.032	29.	38.	45.
6086	-233832.182	282827.482	84.194	46.	72.	91.
6077	-234333.755	282931.182	88.808	32.	43.	59.
6076	-234352.849	282884.688	87.491	33.	46.	61.
6075	-234267.942	282940.984	92.990	33.	43.	58.
6072	-234309.555	283644.375	102.779	26.	29.	50.
6074	-234337.164	283683.121	103.551	26.	30.	51.
6073	-234313.874	283734.209	103.000	27.	31.	53.
6070	-234307.990	283388.509	96.726	27.	29.	49.
973	-234342.630	284470.555	78.289	29.	43.	46.
3056	-234778.631	284498.385	86.870	24.	36.	50.
3055	-234685.251	284416.106	87.120	21.	21.	36.
3054	-234683.067	285379.543	57.667	27.	33.	60.
3052	-234639.367	285011.644	78.667	25.	24.	50.
3051	-234650.367	285005.857	77.294	25.	24.	50.
3050	-234665.605	284942.704	76.387	24.	24.	49.
7911	-234073.651	283756.167	91.014	40.	51.	79.
7973	-234342.330	284470.384	78.283	28.	32.	46.
4066	-234503.087	283791.482	91.692	23.	24.	40.
4065	-234549.433	283754.792	91.662	23.	24.	40.
4064	-234532.480	284759.244	81.746	27.	39.	58.
4063	-234476.318	284789.939	76.735	28.	41.	60.
4062	-234472.076	284380.280	72.486	25.	26.	49.
4061	-234484.454	284217.159	77.012	25.	24.	47.
4060	-234550.854	284250.780	76.972	24.	24.	46.
912	-234438.496	282869.983	84.017	36.	52.	48.
528	-234438.501	282868.186	84.240	32.	43.	71.
6067	-234762.381	282927.093	87.971	30.	46.	61.
6066	-234701.009	282921.748	86.223	31.	46.	61.
6065	-234743.770	282866.974	83.506	31.	50.	64.
6062	-234693.435	283649.505	104.252	26.	29.	52.
6060	-234682.797	283350.225	86.536	26.	28.	51.
961	-234971.648	283748.946	98.080	28.	41.	46.
561	-234969.605	283742.595	97.901	21.	22.	39.
4056	-235023.494	283701.107	94.413	22.	23.	40.
4055	-234985.444	283748.332	96.538	21.	23.	39.
4054	-234996.648	284743.061	68.954	26.	38.	59.
4053	-234925.965	284799.412	71.116	28.	41.	61.
4052	-235070.589	284335.680	80.740	24.	24.	47.
4050	-234956.966	284363.274	79.182	24.	25.	48.
4051	-234978.093	284330.287	78.612	24.	24.	47.
8962	-235254.609	284509.551	86.631	33.	43.	47.
7964	-235108.434	285317.508	57.550	32.	42.	86.
3046	-235300.483	284492.711	81.698	23.	23.	38.
3045	-235254.349	284502.744	86.892	21.	22.	35.
3044	-235236.745	285302.409	52.684	26.	31.	55.
3043	-235152.489	285480.178	48.676	27.	39.	61.
3042	-235126.624	285550.632	46.397	28.	43.	63.
3041	-235102.196	284895.010	72.675	24.	25.	47.
3040	-235150.987	284993.936	64.818	24.	24.	48.
7961	-234971.030	283749.814	98.283	27.	41.	73.
557	-235075.449	283267.723	89.012	28.	28.	45.
5054	-235145.046	283657.587	88.181	31.	35.	76.
6063	-234840.701	283709.278	98.863	30.	38.	74.
6064	-234852.122	283901.309	90.756	30.	53.	80.
5056	-235221.454	283078.824	85.528	30.	35.	58.
5051	-235197.131	283547.130	95.231	26.	27.	53.
5050	-235261.534	283417.466	91.161	26.	26.	53.
3053	-235595.390	284541.686	72.086	39.	40.	86.
8961	-234971.647	283748.790	97.977	33.	42.	46.
7962	-235253.287	284507.975	86.671	27.	31.	45.
4045	-235522.737	283826.836	97.323	22.	23.	41.
4042	-235452.219	284220.527	83.882	24.	24.	47.
4044	-235403.326	284720.026	73.285	26.	36.	55.
4043	-235460.155	284764.605	70.461	26.	38.	56.

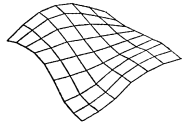
4041	-235441.877	284269.948	90.581	24.	24.	46.
4040	-235430.076	284245.297	88.000	24.	24.	47.
4046	-235552.275	283900.335	93.229	29.	53.	81.
5055	-235349.472	282935.084	80.747	35.	60.	86.
556	-235357.638	282910.106	80.788	31.	39.	47.
5053	-235297.236	283852.356	96.074	30.	49.	82.
5046	-235773.738	282895.939	78.297	33.	48.	73.
5045	-235665.741	282880.927	82.650	32.	48.	72.
5044	-235741.584	283913.846	93.259	26.	37.	61.
5043	-235662.255	283843.284	96.286	25.	34.	59.
5042	-235670.852	283293.861	77.370	27.	29.	58.
5041	-235751.785	283485.499	80.694	26.	27.	56.
5040	-235644.385	283370.521	82.523	26.	28.	56.
964	-235110.072	285316.600	57.468	30.	45.	48.
2056	-234979.930	285300.536	55.485	37.	63.	88.
2045	-235408.701	285353.408	48.547	26.	37.	55.
2043	-235398.393	286363.041	71.212	32.	45.	63.
2041	-235365.578	285790.090	42.846	27.	26.	53.
2040	-235356.231	285939.708	44.317	28.	27.	55.
2046	-235529.509	285352.109	47.112	22.	22.	38.
8964	-235108.294	285317.414	57.453	35.	34.	47.
962	-235254.598	284509.749	86.660	29.	44.	46.
3036	-235700.099	284477.741	76.897	25.	39.	52.
3034	-235565.236	285521.387	44.228	27.	37.	56.
3033	-235654.683	285534.571	43.776	27.	38.	57.
3032	-235621.782	285059.111	58.187	24.	24.	47.
3031	-235615.084	285057.039	57.688	24.	24.	47.
3030	-235599.840	284918.757	64.654	24.	24.	46.
3035	-235595.473	284541.719	71.954	21.	22.	36.
963	-235775.678	284266.188	72.075	26.	27.	45.
7908	-235981.352	284741.983	52.847	32.	42.	47.
519	-235980.163	284741.915	54.107	21.	23.	40.
4036	-235887.238	283775.554	82.136	26.	36.	56.
4035	-236006.258	283926.624	68.174	22.	23.	43.
4037	-235942.955	283951.720	77.058	22.	23.	42.
4034	-235831.912	284833.759	63.778	26.	40.	54.
4031	-235883.669	284310.741	68.265	24.	24.	46.
4033	-235873.172	284737.925	63.560	25.	35.	51.
4032	-235873.247	284282.756	67.308	24.	24.	46.
4030	-235927.472	284329.735	65.005	24.	24.	46.
555	-236203.228	282961.065	53.121	31.	38.	75.
5036	-236043.164	282955.135	67.865	33.	46.	78.
5035	-236125.730	282933.174	55.913	33.	47.	79.
5033	-236092.877	283946.676	60.899	27.	37.	63.
5031	-236067.761	283349.768	65.078	28.	29.	61.
5030	-236078.472	283422.526	57.725	27.	28.	60.
8903	-235997.764	286008.978	55.216	35.	32.	46.
2044	-235426.619	286367.785	71.245	45.	64.	91.
505	-235942.096	286255.562	65.309	28.	31.	39.
2039	-235852.280	285435.350	43.848	23.	22.	37.
2038	-235830.905	285393.948	43.682	23.	22.	38.
2037	-235977.195	286433.826	89.909	32.	47.	54.
2036	-235834.700	286423.069	82.396	33.	47.	55.
564	-236016.279	285474.800	44.591	22.	22.	33.
2034	-235930.074	285845.075	47.279	26.	26.	47.
2033	-235797.045	285942.468	44.591	28.	27.	48.
908	-235981.383	284741.966	52.951	28.	33.	46.
3025	-236107.173	284533.597	58.861	21.	22.	37.
3026	-236142.566	284575.023	47.140	21.	22.	37.
3024	-235988.852	285432.833	43.948	26.	33.	57.
3023	-236058.266	285447.788	43.877	26.	34.	56.
3022	-236028.423	285097.610	44.266	24.	24.	50.
3021	-236131.132	285009.283	43.714	24.	24.	49.
3020	-236110.590	284881.961	44.153	24.	25.	48.
903	-235997.773	286009.151	55.278	32.	31.	46.
2031	-236360.262	285386.437	44.170	26.	40.	59.
2025	-236279.590	285343.615	44.061	27.	42.	61.
2030	-236320.466	286368.840	80.701	32.	45.	59.
2024	-236342.183	286386.796	82.016	32.	46.	59.
2028	-236275.052	285935.736	50.875	28.	28.	53.



2022	-236332.834	285935.828	50.401	27.	28.	52.
5034	-236268.284	283988.613	47.090	31.	60.	92.
954	-236366.495	283292.343	61.084	32.	36.	83.
5032	-236243.173	283892.802	50.016	31.	52.	88.
5026	-236521.411	283130.113	67.604	34.	39.	66.
5025	-236565.144	283097.488	69.763	34.	41.	66.
5022	-236643.820	283351.571	71.763	31.	33.	60.
5021	-236665.698	283466.543	71.973	30.	31.	59.
5020	-236526.393	283462.116	61.387	30.	30.	59.
4025	-236341.525	283719.441	51.259	24.	25.	45.
521	-236301.284	283764.202	46.654	23.	24.	40.
909	-236320.798	284513.924	48.853	28.	44.	47.
520	-236312.473	284591.484	48.182	25.	38.	68.
3016	-236582.876	284624.469	70.494	22.	23.	36.
3015	-236523.930	284488.517	69.337	22.	22.	35.
3014	-236593.372	285553.828	44.318	27.	39.	59.
3013	-236515.476	285557.035	44.140	27.	39.	60.
3012	-236502.351	284986.513	45.799	24.	25.	49.
3011	-236542.681	285030.346	45.017	24.	25.	49.
3010	-236567.665	285010.562	44.287	24.	25.	49.
7909	-236320.979	284513.824	48.910	29.	31.	46.
8908	-235981.253	284742.154	52.831	31.	41.	47.
4026	-236512.324	283768.234	68.809	25.	26.	45.
4024	-236378.177	284851.855	49.008	27.	40.	58.
4023	-236288.155	284817.639	44.039	27.	39.	57.
4022	-236324.359	284192.729	50.436	25.	25.	47.
4021	-236343.025	284388.453	48.332	25.	25.	47.
4020	-236347.324	284304.687	47.938	25.	25.	46.
8982	-236987.046	283991.963	82.303	43.	42.	83.
8909	-236320.837	284513.753	48.821	35.	31.	47.
4016	-236782.220	283792.989	80.491	29.	39.	57.
4015	-236937.588	283759.791	78.978	29.	29.	46.
4011	-236918.305	284127.431	84.557	27.	29.	48.
4014	-236784.222	284737.342	62.637	29.	36.	57.
4012	-236775.812	284416.678	82.643	26.	27.	47.
4013	-236759.060	284832.629	56.117	30.	41.	62.
5016	-237087.012	282999.161	61.091	39.	54.	59.
5015	-237125.676	282988.274	60.259	40.	56.	60.
5012	-236987.307	283322.685	84.192	33.	38.	51.
5011	-236981.154	283529.039	80.378	32.	34.	53.
985	-237024.678	282907.587	68.142	40.	58.	48.
585	-237021.134	282909.262	68.805	40.	60.	61.
5010	-236986.564	283311.356	84.081	33.	38.	51.
582	-237554.347	283757.393	56.158	48.	52.	49.
984	-237534.169	282997.628	71.038	54.	66.	50.
584	-237547.518	283007.617	70.654	45.	48.	84.
5002	-237612.423	283849.168	64.530	60.	60.	94.
5004	-237628.237	283757.756	55.783	59.	56.	93.
5001	-237529.038	283603.554	62.899	49.	49.	85.
5006	-237519.390	282971.541	72.458	55.	73.	90.
5005	-237613.867	282896.359	75.074	65.	82.	97.
5003	-237527.026	283967.521	64.230	55.	67.	95.
5000	-237568.469	283353.984	61.070	52.	53.	86.
4006	-237304.426	283882.138	73.927	36.	35.	56.
4005	-237464.049	283966.963	68.466	44.	39.	63.
982	-236986.745	283991.389	82.298	33.	38.	46.
8907	-237338.862	284514.415	83.524	37.	39.	47.
4004	-237282.199	284841.943	75.152	41.	63.	87.
4003	-237374.464	284813.250	81.141	47.	62.	87.
4001	-237429.879	284126.548	75.859	47.	43.	84.
4000	-237403.702	284472.467	87.542	44.	41.	80.
3006	-237036.699	284529.596	84.928	26.	26.	37.
517	-237041.524	284571.290	83.720	25.	25.	33.
516	-237339.559	284515.894	83.534	31.	30.	47.
3007	-237016.604	284635.557	74.741	25.	25.	36.
3005	-237380.495	284563.967	88.774	34.	36.	54.
632	-237358.996	285540.407	64.087	33.	32.	32.
631	-237349.471	285366.589	67.869	32.	31.	31.
8630	-237350.419	285365.281	67.875	35.	38.	45.
3009	-236958.300	285572.048	44.093	41.	58.	86.

Bundle adjustment

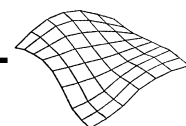
3004	-237522.931	285505.019	84.251	48.	55.	78.
907	-237338.731	284514.254	83.463	36.	52.	47.
8906	-237046.158	285396.886	48.065	28.	30.	36.
518	-237363.396	285423.054	68.141	31.	30.	31.
2010	-237322.836	285381.904	68.691	34.	43.	74.
3003	-236930.384	285017.786	54.404	26.	26.	44.
3001	-237495.644	285042.254	82.485	40.	40.	75.
3008	-237348.126	284529.707	82.712	37.	63.	81.
2004	-237347.170	285370.582	67.754	34.	32.	38.
3002	-237014.405	285047.277	56.464	26.	27.	43.
3000	-237524.125	285069.908	85.471	42.	40.	75.
2011	-236936.669	285341.916	46.627	24.	24.	32.
2005	-236782.938	285501.515	44.251	24.	24.	34.
513	-236876.458	285595.415	44.577	24.	24.	30.
630	-237350.457	285365.379	67.930	39.	48.	46.
906	-237046.166	285396.913	48.032	31.	43.	46.
2003	-236801.100	286463.105	56.698	47.	72.	92.
2008	-237399.757	286404.094	44.546	54.	68.	94.
2002	-237394.584	286475.477	45.235	56.	75.	97.
2006	-237336.096	285923.015	47.638	42.	38.	80.
511	-237353.676	286355.987	44.815	38.	41.	47.
2000	-237310.868	285905.567	47.875	40.	37.	80.
510	-236801.153	286462.969	56.877	32.	37.	43.
2007	-236893.754	285940.661	45.875	28.	29.	47.
2001	-236850.632	285904.200	45.191	28.	28.	46.
2009	-236786.499	286450.696	57.168	34.	48.	58.
Mean squared precision of object points:				34.	40.	60.
Mean squared precision of control points:				31.	34.	45.



E.6.1 The 'ltera.dat' file from the aerotriangulation for the images in scale 1:5,000

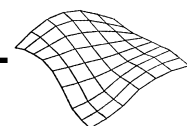
ORIA	116	-237319.673	285893.592	849.076	-0.8618	0.1705	2.4667	1
ORIA	117	-236859.041	285881.673	849.567	-0.8425	0.9451	1.1708	1
ORIA	118	-236398.040	285873.118	846.771	-0.5826	0.5119	1.2708	1
ORIA	119	-235938.893	285864.748	843.860	-1.0137	1.5901	1.3236	1
ORIA	120	-235478.377	285846.227	844.075	-0.7417	1.9825	1.1766	1
ORIA	121	-235016.779	285832.133	844.607	-0.3232	1.5418	1.3886	1
ORIA	122	-234557.542	285826.807	840.822	-0.6096	1.5624	1.5186	1
ORIA	123	-234096.980	285811.615	842.376	-0.7450	3.1955	0.9883	1
ORIA	124	-233637.218	285778.321	846.394	-0.9264	3.3689	0.3643	1
ORIA	125	-233179.216	285745.958	852.126	-0.5397	2.9245	0.4688	1
ORIA	128	-233346.155	284966.369	846.695	0.4905	-0.8700	-2.8712	1
ORIA	129	-233807.007	284978.145	846.696	0.1334	-0.6853	-2.6454	1
ORIA	130	-234267.289	284987.450	848.212	0.6982	-1.2703	-1.8252	1
ORIA	131	-234726.972	285005.292	847.792	1.0107	-2.1772	-1.8911	1
ORIA	132	-235185.959	285024.143	846.497	0.7617	-1.9123	-1.8986	1
ORIA	133	-235646.174	285033.569	844.193	0.4681	-1.6560	-1.6280	1
ORIA	134	-236106.032	285039.190	842.027	0.5885	-2.0339	-1.5793	1
ORIA	135	-236563.528	285055.529	840.315	0.8977	-3.0431	-1.9596	1
ORIA	136	-237023.137	285076.503	840.804	0.8952	-2.7507	-2.0233	1
ORIA	137	-237482.584	285093.060	841.018	0.9637	-2.4814	-2.0346	1
ORIA	138	-237353.784	284305.809	857.948	-0.0370	-0.1739	-0.2144	1
ORIA	139	-236892.603	284296.914	855.320	-0.2433	1.2525	-0.4415	1
ORIA	140	-236433.678	284278.458	855.376	-0.5436	1.6036	-0.5884	1
ORIA	141	-235975.280	284263.367	852.039	-0.2524	1.1511	-0.6252	1
ORIA	142	-235515.687	284251.581	850.102	-0.2895	0.8219	-0.5635	1
ORIA	143	-235055.798	284234.716	850.143	-0.4898	1.6250	-0.7681	1
ORIA	144	-234597.462	284214.869	847.518	-0.7318	1.1641	-0.8227	1
ORIA	145	-234137.416	284200.401	849.873	-0.6427	0.9059	-0.9229	1
ORIA	146	-233674.833	284192.486	848.576	-0.1593	1.4757	-0.7465	1
ORIA	147	-233215.748	284179.148	848.918	-0.6165	1.7285	-0.7529	1
ORIA	150	-233375.137	283383.390	835.308	0.4113	-0.3104	-2.1485	1
ORIA	151	-233835.694	283387.231	831.605	0.2399	-0.8748	-1.8160	1
ORIA	152	-234296.811	283392.882	831.894	0.4037	-1.6701	-1.5609	1
ORIA	153	-234756.815	283407.806	830.036	0.9576	-2.2953	-1.5895	1
ORIA	154	-235215.156	283423.867	830.885	1.0449	-1.9683	-1.4650	1
ORIA	155	-235675.349	283433.840	834.141	1.3325	-1.6600	-1.4489	1
ORIA	156	-236135.452	283448.501	834.874	1.1969	-2.4428	-1.7624	1
ORIA	157	-236596.001	283468.255	835.142	0.7732	-2.3852	-1.8457	1
ORIA	158	-237054.566	283479.872	839.904	1.1973	-1.9727	-1.6910	1
ORIA	159	-237516.804	283487.318	841.266	0.8795	-1.6951	-1.2705	1
CORD	501	-234837.120	286363.528	48.120	0.030	0.038	0.046	
CORD	503	-234919.569	286305.927	46.879	0.028	0.035	0.059	
CORD	505	-235942.096	286255.562	65.309	0.028	0.031	0.039	
CORD	510	-236801.153	286462.969	56.877	0.032	0.037	0.043	
CORD	511	-237353.676	286355.987	44.815	0.038	0.041	0.047	
CORD	513	-236876.458	285595.415	44.577	0.024	0.024	0.030	
CORD	516	-237339.559	284515.894	83.534	0.031	0.030	0.047	
CORD	517	-237041.524	284571.290	83.720	0.025	0.025	0.033	
CORD	518	-237363.396	285423.054	68.141	0.031	0.030	0.031	
CORD	519	-235980.163	284741.915	54.107	0.021	0.023	0.040	
CORD	520	-236312.473	284591.484	48.182	0.025	0.038	0.068	
CORD	521	-236301.284	283764.202	46.654	0.023	0.024	0.040	

CORD	522	-233378.467	282873.829	81.333	0.043	0.046	0.076
CORD	526	-233759.808	284437.601	72.046	0.025	0.024	0.035
CORD	527	-233432.576	283770.938	95.378	0.033	0.032	0.041
CORD	528	-234438.501	282868.186	84.240	0.032	0.043	0.071
CORD	555	-236203.228	282961.065	53.121	0.031	0.038	0.075
CORD	556	-235357.638	282910.106	80.788	0.031	0.039	0.047
CORD	557	-235075.449	283267.723	89.012	0.028	0.028	0.045
CORD	560	-234030.714	283131.978	98.544	0.034	0.042	0.073
CORD	561	-234969.605	283742.595	97.901	0.021	0.022	0.039
CORD	564	-236016.279	285474.800	44.591	0.022	0.022	0.033
CORD	565	-234819.461	285566.792	46.788	0.026	0.029	0.046
CORD	570	-233159.003	286350.914	46.021	0.043	0.048	0.079
CORD	571	-233329.343	285836.161	44.708	0.036	0.041	0.084
CORD	572	-233287.552	285255.139	47.621	0.035	0.030	0.062
CORD	573	-234000.004	285391.701	47.427	0.023	0.022	0.039
CORD	574	-233483.647	285001.785	56.888	0.033	0.033	0.082
CORD	575	-234337.117	284468.167	78.919	0.022	0.023	0.038
CORD	576	-234006.225	286427.026	45.494	0.031	0.039	0.050
CORD	577	-233290.934	284764.615	67.004	0.033	0.031	0.058
CORD	582	-237554.347	283757.393	56.158	0.048	0.052	0.049
CORD	584	-237547.518	283007.617	70.654	0.045	0.048	0.084
CORD	585	-237021.134	282909.262	68.805	0.040	0.060	0.061
CORD	600	-233992.593	286435.707	44.997	0.038	0.058	0.048
CORD	601	-233989.049	286406.416	44.694	0.037	0.056	0.048
CORD	610	-233159.069	286346.880	46.200	0.052	0.068	0.049
CORD	611	-233148.535	286345.001	46.165	0.052	0.068	0.049
CORD	620	-233340.719	282939.845	75.721	0.051	0.059	0.048
CORD	621	-233385.805	282955.554	75.384	0.048	0.057	0.048
CORD	622	-233468.889	282986.782	78.317	0.045	0.058	0.080
CORD	630	-237350.457	285365.379	67.930	0.039	0.048	0.046
CORD	631	-237349.471	285366.589	67.869	0.032	0.031	0.031
CORD	632	-237358.996	285540.407	64.087	0.033	0.032	0.032
CORD	903	-235997.773	286009.151	55.278	0.032	0.031	0.046
CORD	906	-237046.166	285396.913	48.032	0.031	0.043	0.046
CORD	907	-237338.731	284514.254	83.463	0.036	0.052	0.047
CORD	908	-235981.383	284741.966	52.951	0.028	0.033	0.046
CORD	909	-236320.798	284513.924	48.853	0.028	0.044	0.047
CORD	910	-233102.948	284149.274	82.209	0.046	0.044	0.048
CORD	911	-234073.623	283756.103	91.001	0.031	0.041	0.046
CORD	912	-234438.496	282869.983	84.017	0.036	0.052	0.048
CORD	954	-236366.495	283292.343	61.084	0.032	0.036	0.083
CORD	960	-234033.786	283131.455	98.275	0.034	0.038	0.045
CORD	961	-234971.648	283748.946	98.080	0.028	0.041	0.046
CORD	962	-235254.598	284509.749	86.660	0.029	0.044	0.046
CORD	963	-235775.678	284266.188	72.075	0.026	0.027	0.045
CORD	964	-235110.072	285316.600	57.468	0.030	0.045	0.048
CORD	971	-233332.349	285838.927	44.555	0.036	0.041	0.047
CORD	972	-233481.254	285000.952	56.838	0.032	0.033	0.047
CORD	973	-234342.630	284470.555	78.289	0.029	0.043	0.046
CORD	982	-236986.745	283991.389	82.298	0.033	0.038	0.046
CORD	984	-237534.169	282997.628	71.038	0.054	0.066	0.050
CORD	985	-237024.678	282907.587	68.142	0.040	0.058	0.048
CORD	2000	-237310.868	285905.567	47.875	0.040	0.037	0.080
CORD	2001	-236850.632	285904.200	45.191	0.028	0.028	0.046
CORD	2002	-237394.584	286475.477	45.235	0.056	0.075	0.097
CORD	2003	-236801.100	286463.105	56.698	0.047	0.072	0.092
CORD	2004	-237347.170	285370.582	67.754	0.034	0.032	0.038



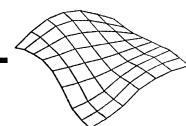
CORD	2005	-236782.938	285501.515	44.251	0.024	0.024	0.034
CORD	2006	-237336.096	285923.015	47.638	0.042	0.038	0.080
CORD	2007	-236893.754	285940.661	45.875	0.028	0.029	0.047
CORD	2008	-237399.757	286404.094	44.546	0.054	0.068	0.094
CORD	2009	-236786.499	286450.696	57.168	0.034	0.048	0.058
CORD	2010	-237322.836	285381.904	68.691	0.034	0.043	0.074
CORD	2011	-236936.669	285341.916	46.627	0.024	0.024	0.032
CORD	2022	-236332.834	285935.828	50.401	0.027	0.028	0.052
CORD	2024	-236342.183	286386.796	82.016	0.032	0.046	0.059
CORD	2025	-236279.590	285343.615	44.061	0.027	0.042	0.061
CORD	2028	-236275.052	285935.736	50.875	0.028	0.028	0.053
CORD	2030	-236320.466	286368.840	80.701	0.032	0.045	0.059
CORD	2031	-236360.262	285386.437	44.170	0.026	0.040	0.059
CORD	2033	-235797.045	285942.468	44.591	0.028	0.027	0.048
CORD	2034	-235930.074	285845.075	47.279	0.026	0.026	0.047
CORD	2036	-235834.700	286423.069	82.396	0.033	0.047	0.055
CORD	2037	-235977.195	286433.826	89.909	0.032	0.047	0.054
CORD	2038	-235830.905	285393.948	43.682	0.023	0.022	0.038
CORD	2039	-235852.280	285435.350	43.848	0.023	0.022	0.037
CORD	2040	-235356.231	285939.708	44.317	0.028	0.027	0.055
CORD	2041	-235365.578	285790.090	42.846	0.027	0.026	0.053
CORD	2043	-235398.393	286363.041	71.212	0.032	0.045	0.063
CORD	2044	-235426.619	286367.785	71.245	0.045	0.064	0.091
CORD	2045	-235408.701	285353.408	48.547	0.026	0.037	0.055
CORD	2046	-235529.509	285352.109	47.112	0.022	0.022	0.038
CORD	2051	-234891.580	285926.590	43.146	0.027	0.027	0.055
CORD	2052	-234879.111	286387.856	48.905	0.031	0.047	0.064
CORD	2053	-234869.683	286358.185	48.124	0.031	0.045	0.064
CORD	2054	-234890.815	285394.385	51.998	0.026	0.036	0.057
CORD	2055	-234930.562	285407.204	48.293	0.026	0.036	0.057
CORD	2056	-234979.930	285300.536	55.485	0.037	0.063	0.088
CORD	2060	-234489.539	285960.091	43.408	0.027	0.028	0.053
CORD	2061	-234561.842	285897.992	43.221	0.026	0.027	0.052
CORD	2062	-234579.660	286379.703	45.636	0.031	0.045	0.062
CORD	2063	-234639.036	286442.242	47.538	0.032	0.050	0.064
CORD	2064	-234615.271	286262.234	45.968	0.030	0.039	0.059
CORD	2065	-234554.492	285354.966	57.699	0.023	0.023	0.043
CORD	2066	-234463.392	285298.833	63.996	0.026	0.037	0.056
CORD	2067	-234543.779	285311.591	61.973	0.024	0.024	0.044
CORD	2068	-234538.868	285312.117	61.795	0.024	0.024	0.044
CORD	2070	-234074.782	285809.838	43.528	0.026	0.027	0.048
CORD	2071	-234143.695	285786.276	44.125	0.026	0.027	0.049
CORD	2072	-234202.295	286453.191	44.598	0.038	0.074	0.087
CORD	2073	-233972.020	286429.833	44.576	0.035	0.050	0.053
CORD	2074	-234179.488	286431.534	43.563	0.039	0.071	0.086
CORD	2075	-234027.544	285304.822	47.198	0.024	0.023	0.044
CORD	2076	-233984.964	285375.775	48.420	0.024	0.023	0.044
CORD	2077	-234000.836	285363.146	47.845	0.042	0.052	0.086
CORD	2080	-233536.712	285866.289	45.405	0.031	0.034	0.053
CORD	2081	-233516.570	285925.938	44.960	0.032	0.035	0.053
CORD	2083	-233653.908	286209.900	41.710	0.044	0.064	0.100
CORD	2085	-233513.990	285375.146	48.400	0.030	0.027	0.051
CORD	2086	-233531.890	285334.487	49.454	0.030	0.027	0.051
CORD	2087	-233509.667	285338.157	49.670	0.036	0.053	0.091
CORD	2088	-233641.126	286136.469	41.483	0.033	0.041	0.057
CORD	2089	-233550.034	286249.782	42.599	0.037	0.047	0.058
CORD	2090	-233083.874	285831.732	43.236	0.052	0.047	0.091

CORD	2091	-233029.318	285877.418	42.978	0.057	0.050	0.092
CORD	2092	-233171.473	286361.887	46.084	0.054	0.081	0.092
CORD	2093	-233036.334	286187.146	44.317	0.062	0.066	0.093
CORD	2094	-233010.817	286344.573	47.119	0.069	0.082	0.097
CORD	2095	-233105.727	285306.524	47.910	0.056	0.062	0.102
CORD	2096	-233081.082	285397.772	46.391	0.056	0.056	0.100
CORD	3000	-237524.125	285069.908	85.471	0.042	0.040	0.075
CORD	3001	-237495.644	285042.254	82.485	0.040	0.040	0.075
CORD	3002	-237014.405	285047.277	56.464	0.026	0.027	0.043
CORD	3003	-236930.384	285017.786	54.404	0.026	0.026	0.044
CORD	3004	-237522.931	285505.019	84.251	0.048	0.055	0.078
CORD	3005	-237380.495	284563.967	88.774	0.034	0.036	0.054
CORD	3006	-237036.699	284529.596	84.928	0.026	0.026	0.037
CORD	3007	-237016.604	284635.557	74.741	0.025	0.025	0.036
CORD	3008	-237348.126	284529.707	82.712	0.037	0.063	0.081
CORD	3009	-236958.300	285572.048	44.093	0.041	0.058	0.086
CORD	3010	-236567.665	285010.562	44.287	0.024	0.025	0.049
CORD	3011	-236542.681	285030.346	45.017	0.024	0.025	0.049
CORD	3012	-236502.351	284986.513	45.799	0.024	0.025	0.049
CORD	3013	-236515.476	285557.035	44.140	0.027	0.039	0.060
CORD	3014	-236593.372	285553.828	44.318	0.027	0.039	0.059
CORD	3015	-236523.930	284488.517	69.337	0.022	0.022	0.035
CORD	3016	-236582.876	284624.469	70.494	0.022	0.023	0.036
CORD	3020	-236110.590	284881.961	44.153	0.024	0.025	0.048
CORD	3021	-236131.132	285009.283	43.714	0.024	0.024	0.049
CORD	3022	-236028.423	285097.610	44.266	0.024	0.024	0.050
CORD	3023	-236058.266	285447.788	43.877	0.026	0.034	0.056
CORD	3024	-235988.852	285432.833	43.948	0.026	0.033	0.057
CORD	3025	-236107.173	284533.597	58.861	0.021	0.022	0.037
CORD	3026	-236142.566	284575.023	47.140	0.021	0.022	0.037
CORD	3030	-235599.840	284918.757	64.654	0.024	0.024	0.046
CORD	3031	-235615.084	285057.039	57.688	0.024	0.024	0.047
CORD	3032	-235621.782	285059.111	58.187	0.024	0.024	0.047
CORD	3033	-235654.683	285534.571	43.776	0.027	0.038	0.057
CORD	3034	-235565.236	285521.387	44.228	0.027	0.037	0.056
CORD	3035	-235595.473	284541.719	71.954	0.021	0.022	0.036
CORD	3036	-235700.099	284477.741	76.897	0.025	0.039	0.052
CORD	3040	-235150.987	284993.936	64.818	0.024	0.024	0.048
CORD	3041	-235102.196	284895.010	72.675	0.024	0.025	0.047
CORD	3042	-235126.624	285550.632	46.397	0.028	0.043	0.063
CORD	3043	-235152.489	285480.178	48.676	0.027	0.039	0.061
CORD	3044	-235236.745	285302.409	52.684	0.026	0.031	0.055
CORD	3045	-235254.349	284502.744	86.892	0.021	0.022	0.035
CORD	3046	-235300.483	284492.711	81.698	0.023	0.023	0.038
CORD	3050	-234665.605	284942.704	76.387	0.024	0.024	0.049
CORD	3051	-234650.367	285005.857	77.294	0.025	0.024	0.050
CORD	3052	-234639.367	285011.644	78.667	0.025	0.024	0.050
CORD	3053	-235595.390	284541.686	72.086	0.039	0.040	0.086
CORD	3054	-234683.067	285379.543	57.667	0.027	0.033	0.060
CORD	3055	-234685.251	284416.106	87.120	0.021	0.021	0.036
CORD	3056	-234778.631	284498.385	86.870	0.024	0.036	0.050
CORD	3061	-234272.826	284758.111	71.251	0.024	0.026	0.045
CORD	3062	-234249.627	285053.336	60.297	0.024	0.025	0.049
CORD	3063	-234310.211	285450.398	47.556	0.027	0.036	0.062
CORD	3064	-234220.527	285475.939	43.016	0.028	0.037	0.063
CORD	3065	-234252.296	284410.364	69.820	0.022	0.022	0.036
CORD	3066	-234215.201	284399.100	69.065	0.023	0.023	0.038

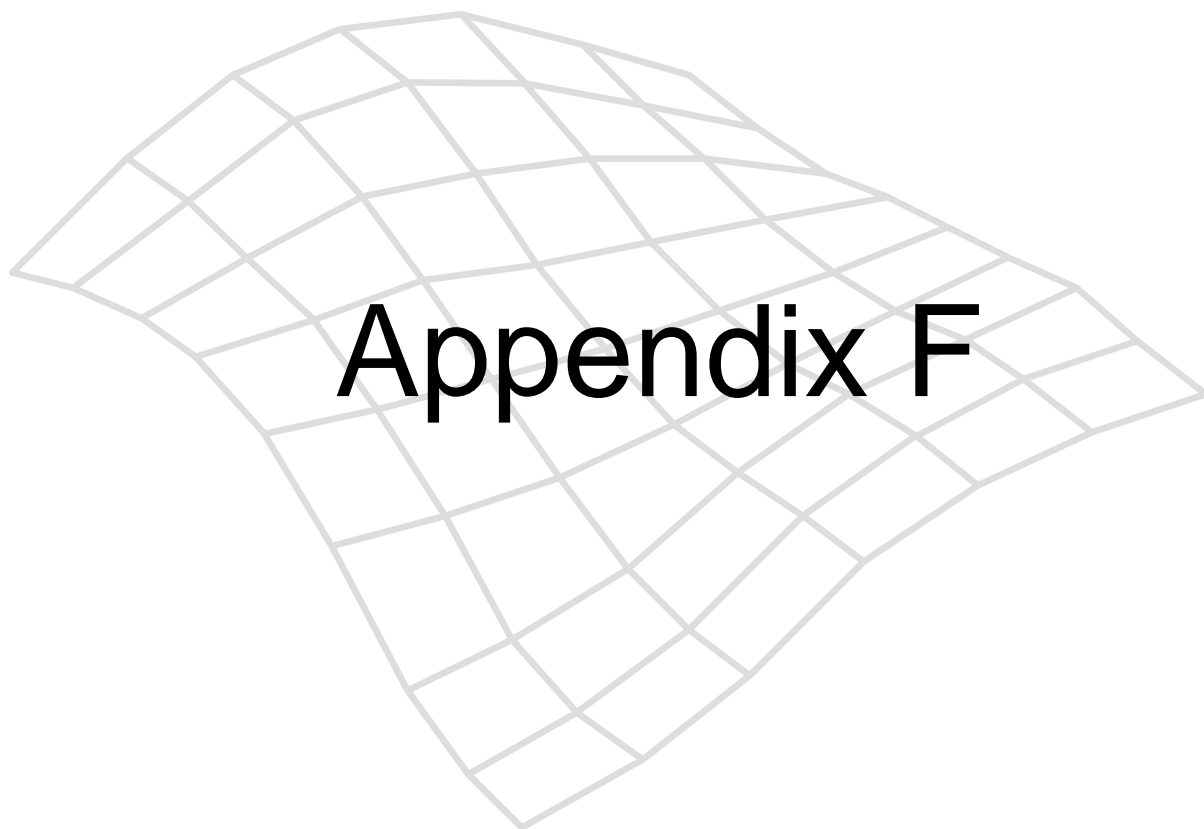


CORD	3072	-233715.257	285036.496	57.657	0.027	0.027	0.051
CORD	3073	-233748.182	285478.710	47.310	0.032	0.039	0.066
CORD	3074	-233715.293	285517.308	46.788	0.033	0.042	0.067
CORD	3075	-233766.681	284475.596	70.582	0.025	0.024	0.038
CORD	3076	-233830.308	284469.000	69.532	0.025	0.025	0.039
CORD	3080	-233312.642	284993.871	56.159	0.042	0.036	0.085
CORD	3081	-233254.466	284923.584	59.626	0.046	0.037	0.086
CORD	3082	-233233.207	285526.877	47.314	0.057	0.069	0.100
CORD	3085	-233371.524	284555.871	80.947	0.032	0.032	0.052
CORD	3086	-233469.470	284557.690	77.091	0.030	0.030	0.049
CORD	4000	-237403.702	284472.467	87.542	0.044	0.041	0.080
CORD	4001	-237429.879	284126.548	75.859	0.047	0.043	0.084
CORD	4003	-237374.464	284813.250	81.141	0.047	0.062	0.087
CORD	4004	-237282.199	284841.943	75.152	0.041	0.063	0.087
CORD	4005	-237464.049	283966.963	68.466	0.044	0.039	0.063
CORD	4006	-237304.426	283882.138	73.927	0.036	0.035	0.056
CORD	4011	-236918.305	284127.431	84.557	0.027	0.029	0.048
CORD	4012	-236775.812	284416.678	82.643	0.026	0.027	0.047
CORD	4013	-236759.060	284832.629	56.117	0.030	0.041	0.062
CORD	4014	-236784.222	284737.342	62.637	0.029	0.036	0.057
CORD	4015	-236937.588	283759.791	78.978	0.029	0.029	0.046
CORD	4016	-236782.220	283792.989	80.491	0.029	0.039	0.057
CORD	4020	-236347.324	284304.687	47.938	0.025	0.025	0.046
CORD	4021	-236343.025	284388.453	48.332	0.025	0.025	0.047
CORD	4022	-236324.359	284192.729	50.436	0.025	0.025	0.047
CORD	4023	-236288.155	284817.639	44.039	0.027	0.039	0.057
CORD	4024	-236378.177	284851.855	49.008	0.027	0.040	0.058
CORD	4025	-236341.525	283719.441	51.259	0.024	0.025	0.045
CORD	4026	-236512.324	283768.234	68.809	0.025	0.026	0.045
CORD	4030	-235927.472	284329.735	65.005	0.024	0.024	0.046
CORD	4031	-235883.669	284310.741	68.265	0.024	0.024	0.046
CORD	4032	-235873.247	284282.756	67.308	0.024	0.024	0.046
CORD	4033	-235873.172	284737.925	63.560	0.025	0.035	0.051
CORD	4034	-235831.912	284833.759	63.778	0.026	0.040	0.054
CORD	4035	-236006.258	283926.624	68.174	0.022	0.023	0.043
CORD	4036	-235887.238	283775.554	82.136	0.026	0.036	0.056
CORD	4037	-235942.955	283951.720	77.058	0.022	0.023	0.042
CORD	4040	-235430.076	284245.297	88.000	0.024	0.024	0.047
CORD	4041	-235441.877	284269.948	90.581	0.024	0.024	0.046
CORD	4042	-235452.219	284220.527	83.882	0.024	0.024	0.047
CORD	4043	-235460.155	284764.605	70.461	0.026	0.038	0.056
CORD	4044	-235403.326	284720.026	73.285	0.026	0.036	0.055
CORD	4045	-235522.737	283826.836	97.323	0.022	0.023	0.041
CORD	4046	-235552.275	283900.335	93.229	0.029	0.053	0.081
CORD	4050	-234956.966	284363.274	79.182	0.024	0.025	0.048
CORD	4051	-234978.093	284330.287	78.612	0.024	0.024	0.047
CORD	4052	-235070.589	284335.680	80.740	0.024	0.024	0.047
CORD	4053	-234925.965	284799.412	71.116	0.028	0.041	0.061
CORD	4054	-234996.648	284743.061	68.954	0.026	0.038	0.059
CORD	4055	-234985.444	283748.332	96.538	0.021	0.023	0.039
CORD	4056	-235023.494	283701.107	94.413	0.022	0.023	0.040
CORD	4060	-234550.854	284250.780	76.972	0.024	0.024	0.046
CORD	4061	-234484.454	284217.159	77.012	0.025	0.024	0.047
CORD	4062	-234472.076	284380.280	72.486	0.025	0.026	0.049
CORD	4063	-234476.318	284789.939	76.735	0.028	0.041	0.060
CORD	4064	-234532.480	284759.244	81.746	0.027	0.039	0.058
CORD	4065	-234549.433	283754.792	91.662	0.023	0.024	0.040

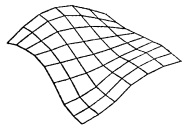
CORD	4066	-234503.087	283791.482	91.692	0.023	0.024	0.040
CORD	4070	-234076.862	284269.229	68.328	0.025	0.026	0.046
CORD	4071	-234012.683	284147.764	73.700	0.026	0.026	0.045
CORD	4072	-234105.001	284182.420	73.421	0.025	0.025	0.045
CORD	4073	-234022.130	284798.518	63.248	0.029	0.042	0.061
CORD	4074	-233993.752	284653.035	62.881	0.028	0.035	0.056
CORD	4075	-234049.027	283870.585	87.145	0.024	0.025	0.038
CORD	4076	-234121.379	283683.524	87.250	0.025	0.026	0.040
CORD	4077	-234129.049	283772.664	94.162	0.027	0.034	0.048
CORD	4080	-233664.343	284252.825	79.977	0.028	0.029	0.046
CORD	4081	-233613.523	284274.189	84.347	0.029	0.030	0.047
CORD	4082	-233694.969	284158.889	81.294	0.028	0.029	0.045
CORD	4083	-233578.605	284782.427	63.033	0.034	0.042	0.063
CORD	4084	-233617.417	284724.459	64.158	0.032	0.040	0.060
CORD	4085	-233636.732	283753.396	85.862	0.033	0.038	0.053
CORD	4086	-233688.651	283833.289	88.322	0.029	0.028	0.039
CORD	4090	-233105.215	284124.870	81.327	0.051	0.044	0.084
CORD	4091	-233126.539	284120.250	84.203	0.049	0.044	0.083
CORD	4092	-233136.944	284313.405	96.856	0.047	0.044	0.081
CORD	4093	-233107.713	284756.561	61.930	0.056	0.071	0.097
CORD	4094	-233192.391	284743.310	63.818	0.049	0.067	0.094
CORD	4095	-233439.305	283776.735	93.978	0.038	0.053	0.081
CORD	4096	-233274.351	284025.828	102.329	0.041	0.042	0.078
CORD	4097	-233425.015	283778.995	100.445	0.039	0.052	0.080
CORD	5000	-237568.469	283353.984	61.070	0.052	0.053	0.086
CORD	5001	-237529.038	283603.554	62.899	0.049	0.049	0.085
CORD	5002	-237612.423	283849.168	64.530	0.060	0.060	0.094
CORD	5003	-237527.026	283967.521	64.230	0.055	0.067	0.095
CORD	5004	-237628.237	283757.756	55.783	0.059	0.056	0.093
CORD	5005	-237613.867	282896.359	75.074	0.065	0.082	0.097
CORD	5006	-237519.390	282971.541	72.458	0.055	0.073	0.090
CORD	5010	-236986.564	283311.356	84.081	0.033	0.038	0.051
CORD	5011	-236981.154	283529.039	80.378	0.032	0.034	0.053
CORD	5012	-236987.307	283322.685	84.192	0.033	0.038	0.051
CORD	5015	-237125.676	282988.274	60.259	0.040	0.056	0.060
CORD	5016	-237087.012	282999.161	61.091	0.039	0.054	0.059
CORD	5020	-236526.393	283462.116	61.387	0.030	0.030	0.059
CORD	5021	-236665.698	283466.543	71.973	0.030	0.031	0.059
CORD	5022	-236643.820	283351.571	71.763	0.031	0.033	0.060
CORD	5025	-236565.144	283097.488	69.763	0.034	0.041	0.066
CORD	5026	-236521.411	283130.113	67.604	0.034	0.039	0.066
CORD	5030	-236078.472	283422.526	57.725	0.027	0.028	0.060
CORD	5031	-236067.761	283349.768	65.078	0.028	0.029	0.061
CORD	5032	-236243.173	283892.802	50.016	0.031	0.052	0.088
CORD	5033	-236092.877	283946.676	60.899	0.027	0.037	0.063
CORD	5034	-236268.284	283988.613	47.090	0.031	0.060	0.092
CORD	5035	-236125.730	282933.174	55.913	0.033	0.047	0.079
CORD	5036	-236043.164	282955.135	67.865	0.033	0.046	0.078
CORD	5040	-235644.385	283370.521	82.523	0.026	0.028	0.056
CORD	5041	-235751.785	283485.499	80.694	0.026	0.027	0.056
CORD	5042	-235670.852	283293.861	77.370	0.027	0.029	0.058
CORD	5043	-235662.255	283843.284	96.286	0.025	0.034	0.059
CORD	5044	-235741.584	283913.846	93.259	0.026	0.037	0.061
CORD	5045	-235665.741	282880.927	82.650	0.032	0.048	0.072
CORD	5046	-235773.738	282895.939	78.297	0.033	0.048	0.073
CORD	5050	-235261.534	283417.466	91.161	0.026	0.026	0.053
CORD	5051	-235197.131	283547.130	95.231	0.026	0.027	0.053



CORD	5053	-235297.236	283852.356	96.074	0.030	0.049	0.082
CORD	5054	-235145.046	283657.587	88.181	0.031	0.035	0.076
CORD	5055	-235349.472	282935.084	80.747	0.035	0.060	0.086
CORD	5056	-235221.454	283078.824	85.528	0.030	0.035	0.058
CORD	6060	-234682.797	283350.225	86.536	0.026	0.028	0.051
CORD	6062	-234693.435	283649.505	104.252	0.026	0.029	0.052
CORD	6063	-234840.701	283709.278	98.863	0.030	0.038	0.074
CORD	6064	-234852.122	283901.309	90.756	0.030	0.053	0.080
CORD	6065	-234743.770	282866.974	83.506	0.031	0.050	0.064
CORD	6066	-234701.009	282921.748	86.223	0.031	0.046	0.061
CORD	6067	-234762.381	282927.093	87.971	0.030	0.046	0.061
CORD	6070	-234307.990	283388.509	96.726	0.027	0.029	0.049
CORD	6072	-234309.555	283644.375	102.779	0.026	0.029	0.050
CORD	6073	-234313.874	283734.209	103.000	0.027	0.031	0.053
CORD	6074	-234337.164	283683.121	103.551	0.026	0.030	0.051
CORD	6075	-234267.942	282940.984	92.990	0.033	0.043	0.058
CORD	6076	-234352.849	282884.688	87.491	0.033	0.046	0.061
CORD	6077	-234333.755	282931.182	88.808	0.032	0.043	0.059
CORD	6080	-233828.214	283309.083	90.606	0.031	0.033	0.050
CORD	6081	-233763.278	283413.998	88.980	0.031	0.033	0.048
CORD	6082	-233869.470	283367.810	97.386	0.030	0.032	0.049
CORD	6083	-233793.794	283863.146	81.151	0.031	0.039	0.056
CORD	6084	-233837.359	283893.633	80.934	0.031	0.040	0.057
CORD	6085	-233861.687	283065.907	83.381	0.035	0.041	0.060
CORD	6086	-233832.182	282827.482	84.194	0.046	0.072	0.091
CORD	6087	-233777.158	283007.299	87.659	0.037	0.044	0.060
CORD	6090	-233307.630	283276.992	88.120	0.049	0.046	0.077
CORD	6091	-233410.776	283325.867	82.118	0.042	0.043	0.075
CORD	6093	-233420.858	283812.956	94.726	0.043	0.054	0.081
CORD	6095	-233318.814	283017.947	80.256	0.053	0.058	0.082
CORD	6096	-233290.856	282921.004	73.450	0.059	0.067	0.086
CORD	6097	-233452.627	282995.787	77.588	0.045	0.057	0.080
CORD	7908	-235981.352	284741.983	52.847	0.032	0.042	0.047
CORD	7909	-236320.979	284513.824	48.910	0.029	0.031	0.046
CORD	7911	-234073.651	283756.167	91.014	0.040	0.051	0.079
CORD	7961	-234971.030	283749.814	98.283	0.027	0.041	0.073
CORD	7962	-235253.287	284507.975	86.671	0.027	0.031	0.045
CORD	7964	-235108.434	285317.508	57.550	0.032	0.042	0.086
CORD	7973	-234342.330	284470.384	78.283	0.028	0.032	0.046
CORD	8523	-233102.461	284153.754	83.079	0.051	0.044	0.084
CORD	8600	-233992.533	286435.816	44.999	0.042	0.055	0.048
CORD	8601	-233989.027	286406.721	44.671	0.042	0.053	0.048
CORD	8630	-237350.419	285365.281	67.875	0.035	0.038	0.045
CORD	8903	-235997.764	286008.978	55.216	0.035	0.032	0.046
CORD	8906	-237046.158	285396.886	48.065	0.028	0.030	0.036
CORD	8907	-237338.862	284514.415	83.524	0.037	0.039	0.047
CORD	8908	-235981.253	284742.154	52.831	0.031	0.041	0.047
CORD	8909	-236320.837	284513.753	48.821	0.035	0.031	0.047
CORD	8911	-234073.484	283756.013	91.032	0.029	0.038	0.045
CORD	8961	-234971.647	283748.790	97.977	0.033	0.042	0.046
CORD	8962	-235254.609	284509.551	86.631	0.033	0.043	0.047
CORD	8964	-235108.294	285317.414	57.453	0.035	0.034	0.047
CORD	8973	-234342.154	284470.864	78.345	0.033	0.042	0.047
CORD	8982	-236987.046	283991.963	82.303	0.043	0.042	0.083
END							



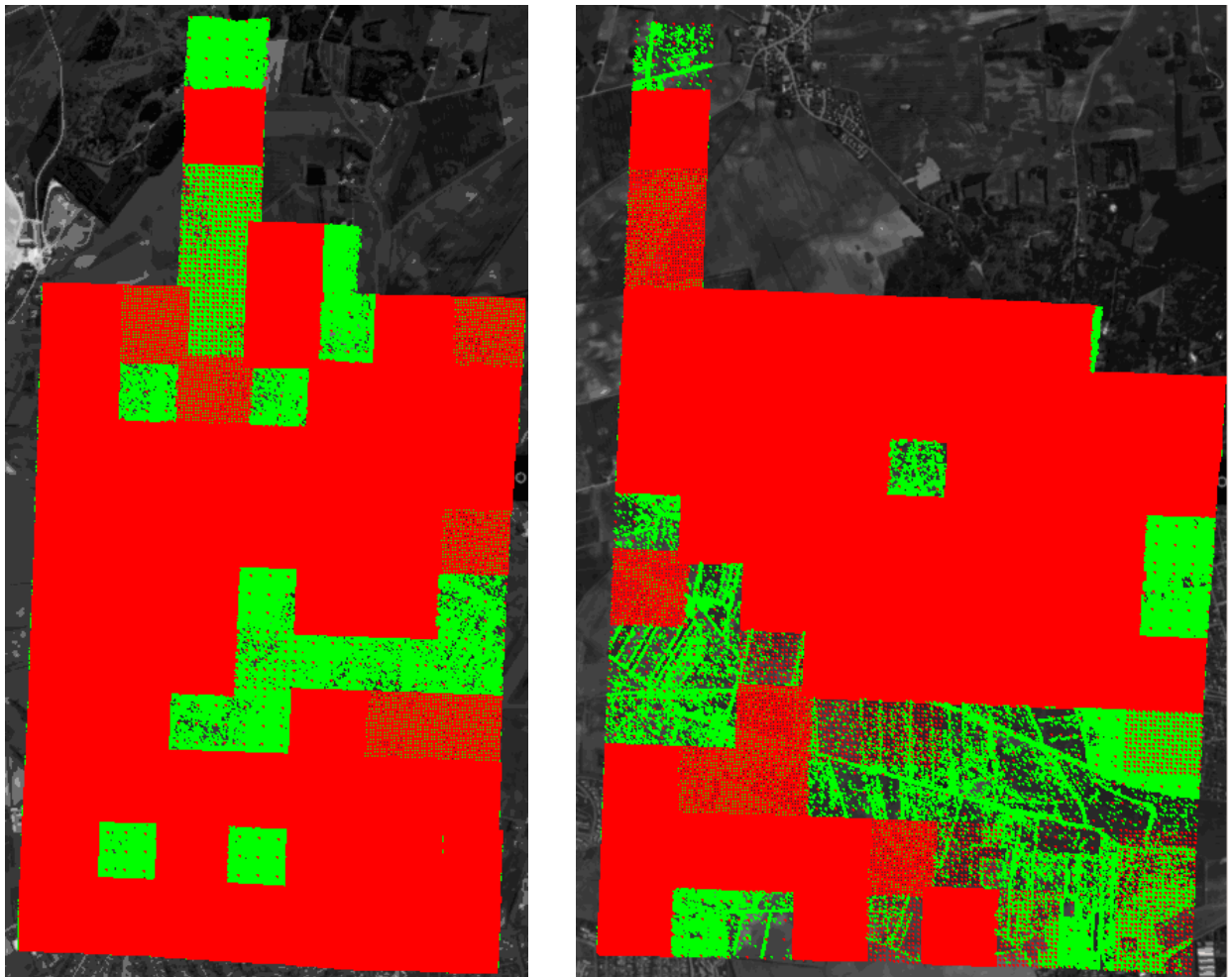
Appendix F



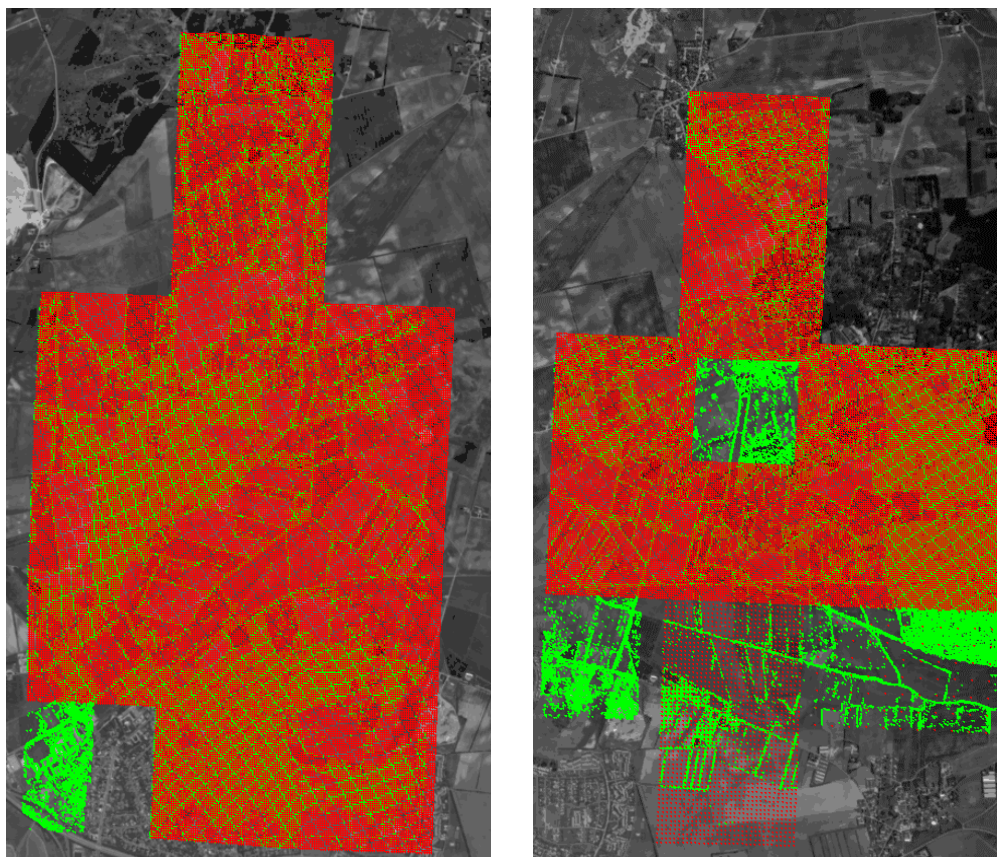
Appendix F: Graphic online/offline

F.1 Graphic online/offline

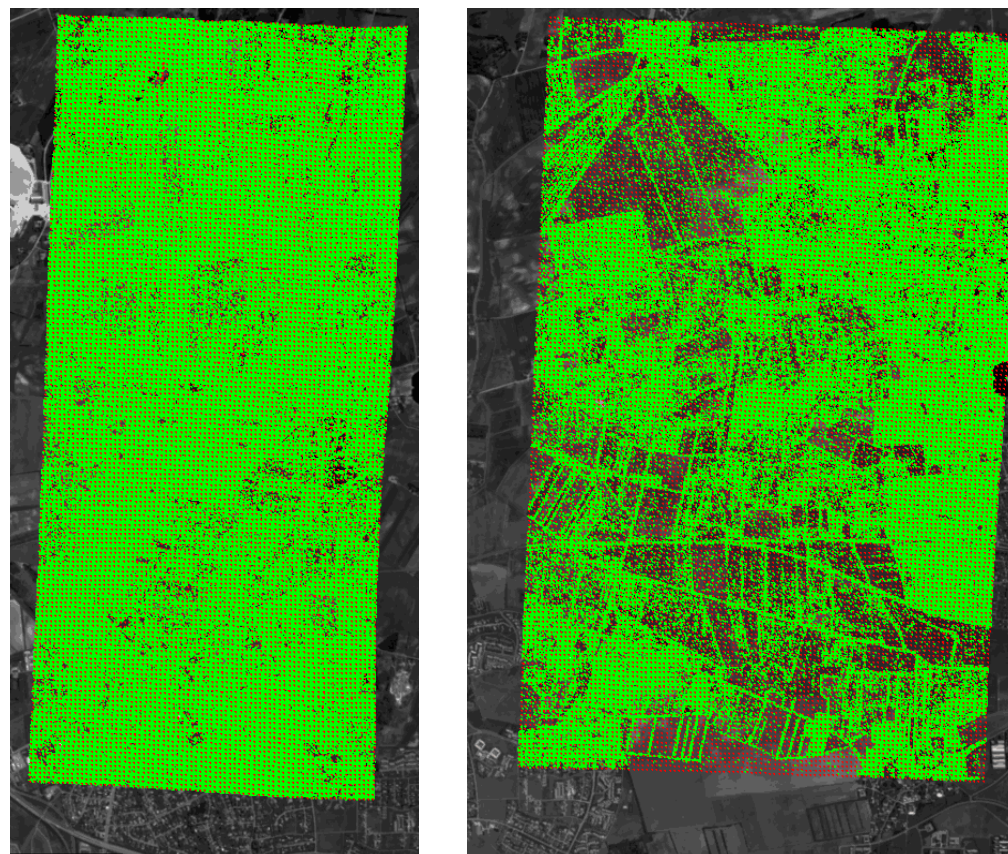
Appendix F contains 11 examples of the visualisation tool graphic online/offline. All these examples are in scale 1:25,000. The reason for this, is that the window for the graphic online/offline has to be open for each model calculation. The block of images in scale 1:25,000 consists of 2 models, while the block for images in 1:15,000 and 1:5,000 consists of several models. It has therefore been easier to follow the calculations for the images in 1:25,000 than the images in 1:15,000 and 1:5,000.



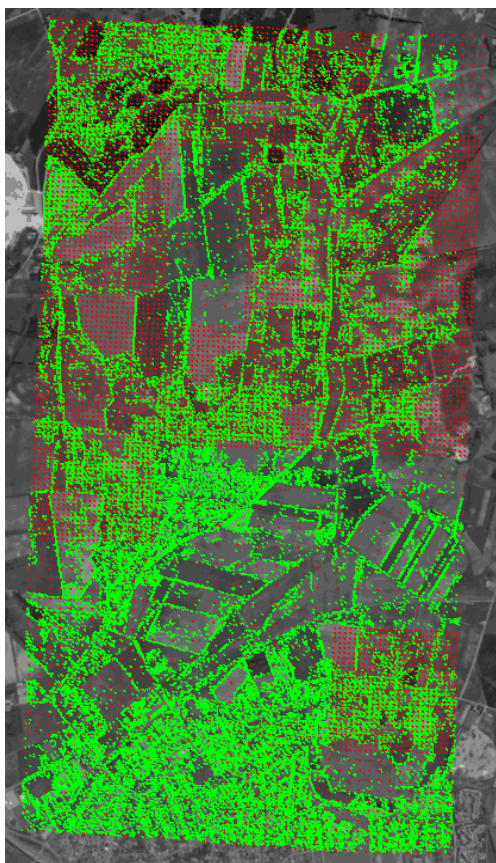
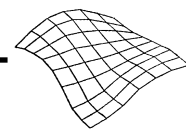
Graphic online/offline for scale 1:25,000, resolution 15 μ m and mesh size 5 x 5 m. Green dots symbolises interest points, red dots symbolises grid points.



Graphic online/offline for scale 1:25,000, resolution 15 μ m and mesh size 12.5 x 12.5 m. Green dots symbolises interest points, red dots symbolises grid points.



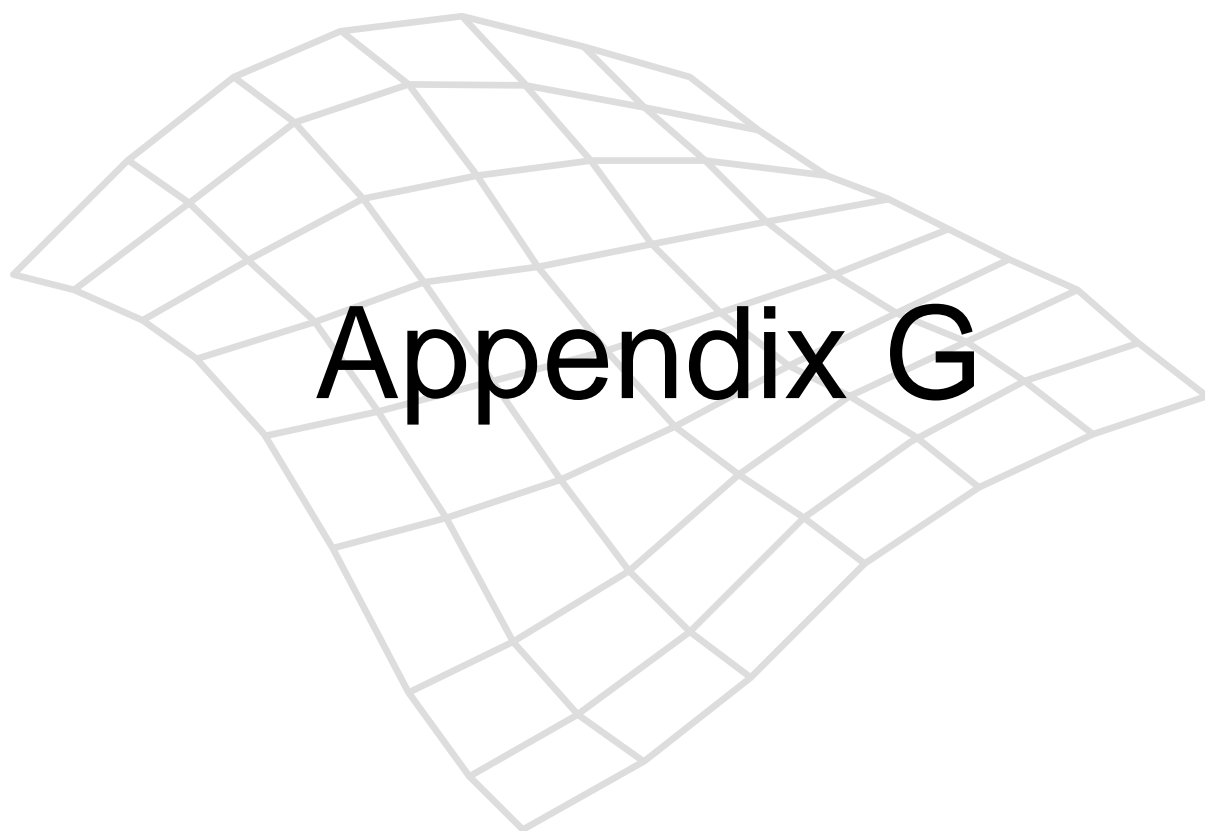
Graphic online/offline for scale 1:25,000, resolution 15 μ m and mesh size 25 x 25 m. Green dots symbolises interest points, red dots symbolises grid points.



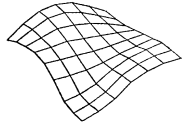
Graphic online/offline for scale 1:25,000, resolution 60 μm and mesh size 25 x 25 m. Green dots symbolises interest points, red dots symbolises grid points.



Graphic online/offline for scale 1:25,000, resolution 30 μm and mesh size 25 x 25 m. Green dots symbolises interest points, red dots symbolises grid points.



Appendix G



Appendix G: Sizes of grid files

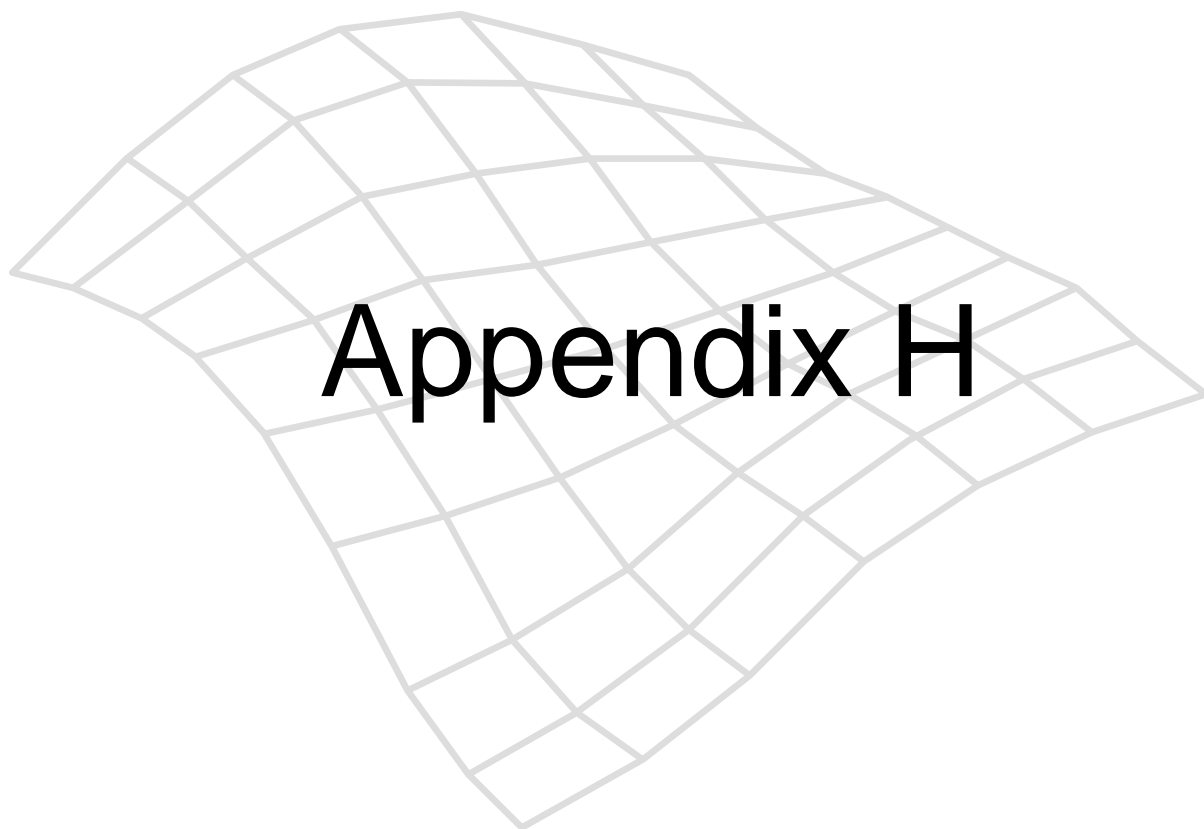
G.1 Sizes of grid files

This Appendix contains a table with the file sizes of all models in the project. The file sizes of the models in scale 1:5,000 are on this page and the file sizes of the models in the scales 1:15,000 and 1:25,000 are shown on the following page.

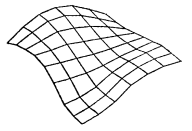
Scale	Model and resolution	Sizes of grid files after generation for each mesh size		
		5 x 5 m (kB)	12.5 x 12.5 m (kB)	25 x 25 m (kB)
1:5,000	121122_15μm	570	115	37
	121122_30μm	570	103	37
	121122_60μm	570	60	37
	122123_15μm	813	153	43
	122123_30μm	746	124	46
	122123_60μm	813	59	46
	128129_15μm	691	95	137
	128129_30μm	558	98	29
	128129_60μm	558	76	29
	136137_15μm	845	169	53
	136137_30μm	845	179	53
	136137_60μm	845	179	53
	140141_15μm	813	153	46
	140141_30μm	813	153	46
	140141_60μm	813	153	46
	141142_15μm	525	153	46
	141142_30μm	525	153	46
	141142_60μm	525	153	46
	142143_15μm	813	144	53
	142143_30μm	813	176	43
	142143_60μm	813	153	43
	146147_15μm	597	126	46
	146147_30μm	597	107	46
	146147_60μm	597	66	50

Scale	Model and resolution	Sizes of grid files after generation for each mesh size		
		5 x 5 m (kB)	12.5 x 12.5 m (kB)	25 x 25 m (kB)
1:15,000	150151_15μm	3535	623	172
	150151_30μm	1831	462	172
	150151_60μm	---	204	172
	151152_15μm	2618	465	125
	151152_30μm	2031	360	125
	151152_60μm	---	238	125
	152153_15μm	3159	608	172
	152153_30μm	2167	423	172
	152153_60μm	---	245	172
	155156_15μm	2118	337	89
	155156_30μm	2043	305	89
	155156_60μm	---	278	89
	156157_15μm	4235	756	196
	156157_30μm	3848	767	197
	156157_60μm	---	669	197
	157158_15μm	3848	559	142
	157158_30μm	3496	538	142
	157158_60μm	---	33	142
	158159_15μm	4115	747	196
	158159_30μm	3375	696	196
	158159_60μm	---	545	196
1:25,000	160161_15μm	---	2302	582
	160161_30μm		2984	686
	160161_60μm		2983	686
	161162_15μm	---	3257	821
	161162_30μm		3929	848
	161162_60μm		3929	848

Appendix G: Sizes of grid files for each of the models.



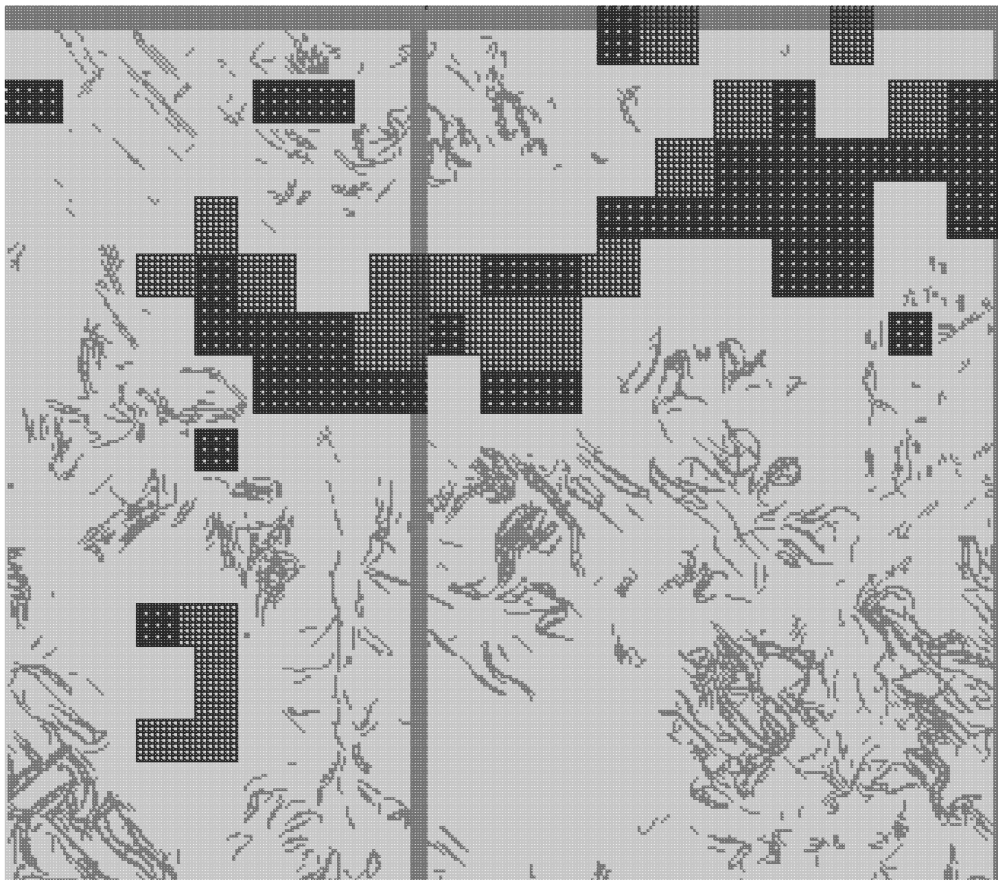
Appendix H



Appendix H: Code specification

H.1 Code specification

This Appendix contains 16 examples of the grid points placement and their code specification.



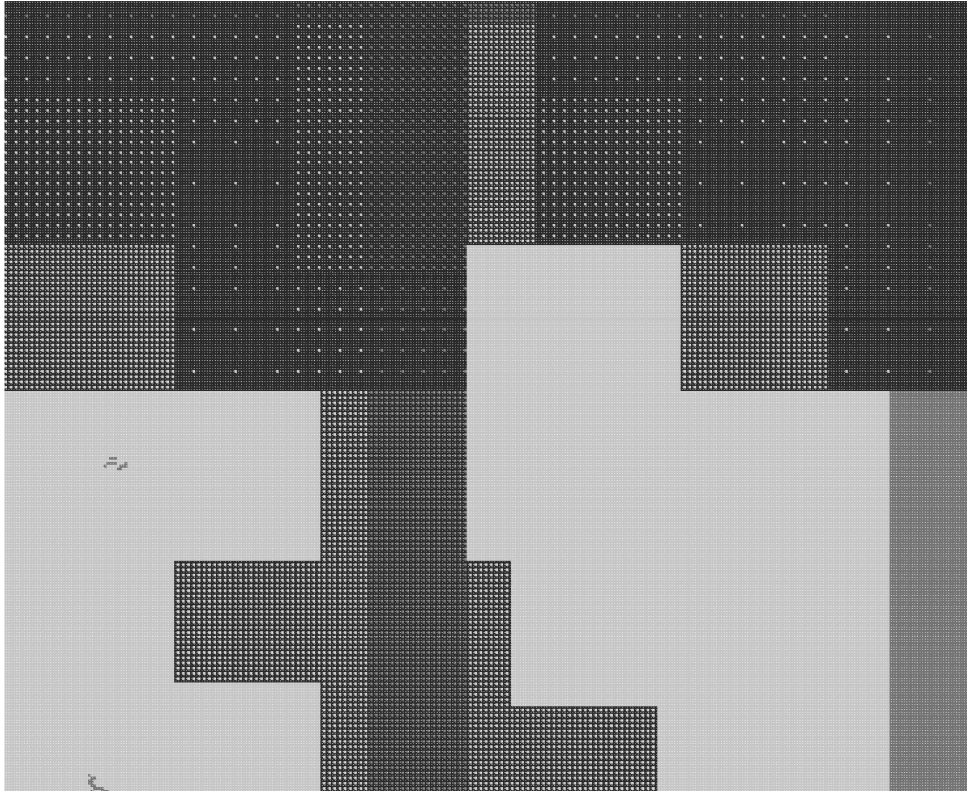
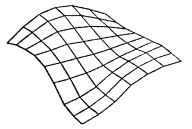
Code specification for image in scale 1:25,000, resolution 15 μ m and mesh size 25 x 25 m. Light grey = grid point is OK, medium grey = grid point with double code, dark grey = grid point is defective.



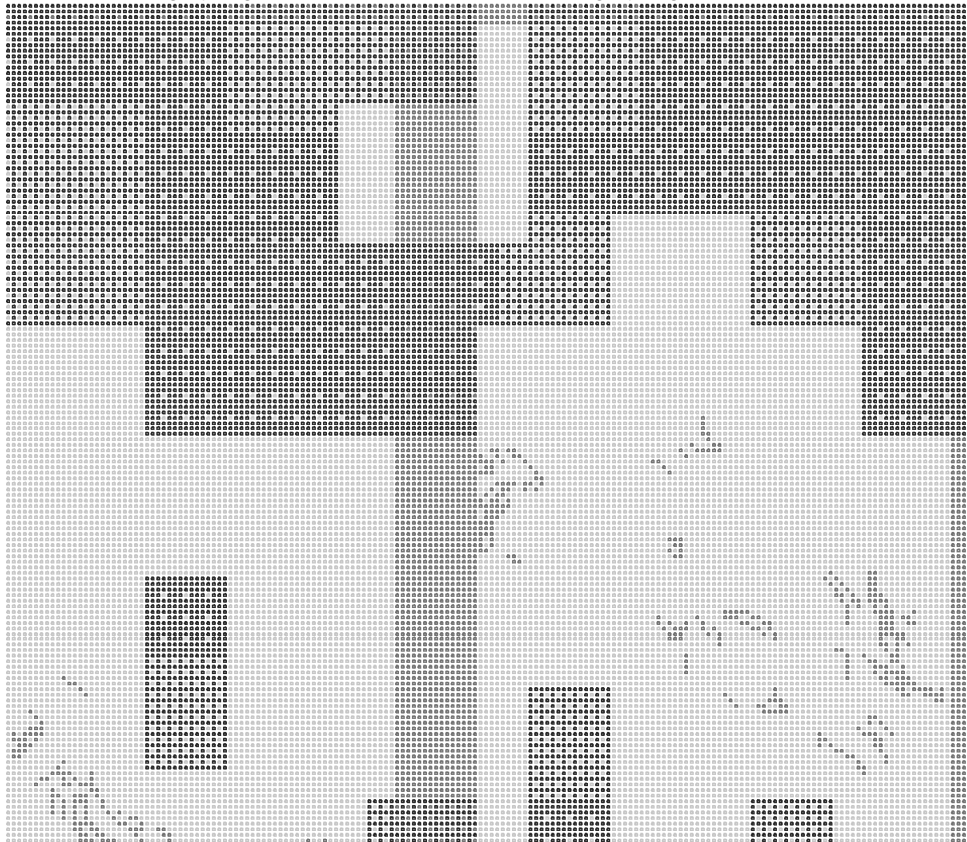
Code specification for image in scale 1:25,000, resolution 30 μm and mesh size 12.5 x 12.5 m. Light grey = grid point is OK, medium grey = grid point with double code, dark grey = grid point is defective.



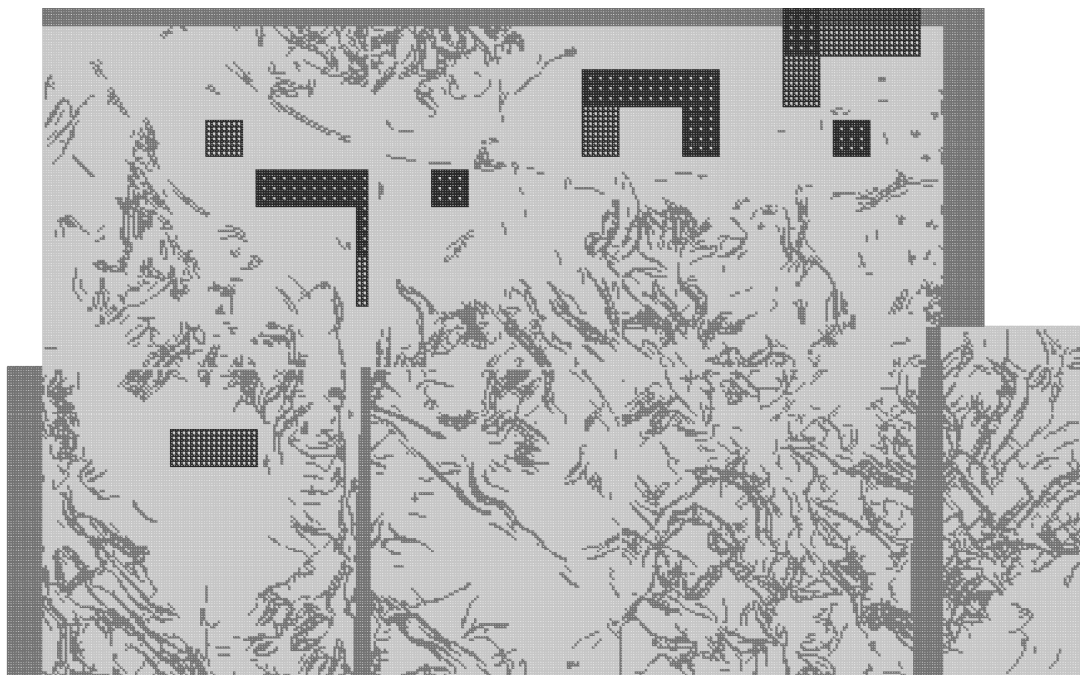
Code specification for image in scale 1:25,000, resolution 30 μm and mesh size 25 x 25 m. Light grey = grid point is OK, medium grey = grid point with double code, dark grey = grid point is defective.



Code specification for image in scale 1:25,000, resolution 15 μm and mesh size 12.5 x 12.5 m. Light grey = grid point is OK, medium grey = grid point with double code, dark grey = grid point is defective.



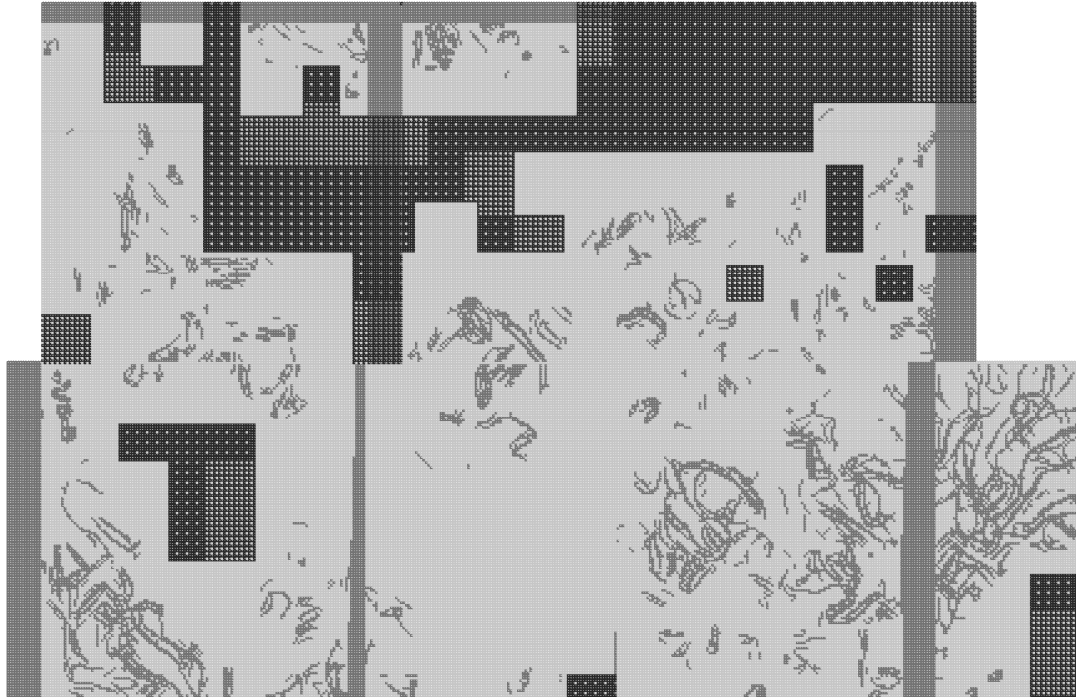
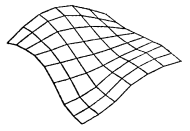
Code specification for image in scale 1:25,000, resolution 60 μm and mesh size 25 x 25 m. Light grey = grid point is OK, medium grey = grid point with double code, dark grey = grid point is defective.



Code specification for image in scale 1:15,000, resolution 15 μ m and mesh size 12.5 x 12.5 m. Light grey = grid point is OK, medium grey = grid point with double code, dark grey = grid point is defective.



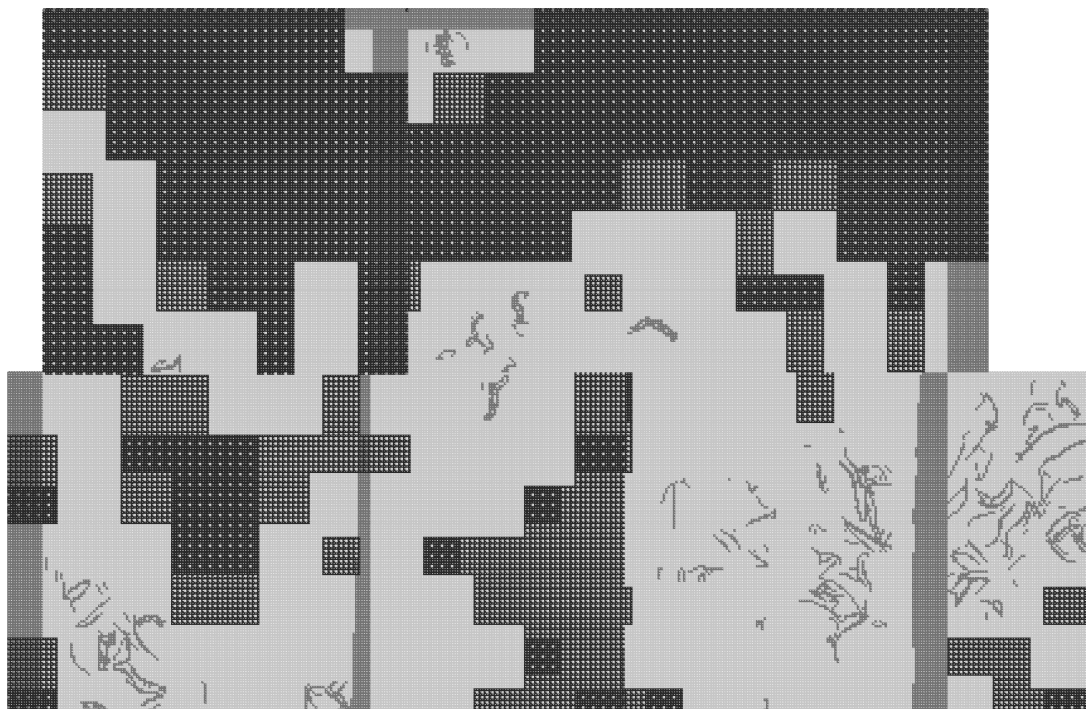
Code specification for image in scale 1:15,000, resolution 15 μ m and mesh size 25 x 25 m. Light grey = grid point is OK, medium grey = grid point with double code, dark grey = grid point is defective.



Code specification for image in scale 1:15,000, resolution 30 μm and mesh size 12.5 x 12.5 m. Light grey = grid point is OK, medium grey = grid point with double code, dark grey = grid point is defective.



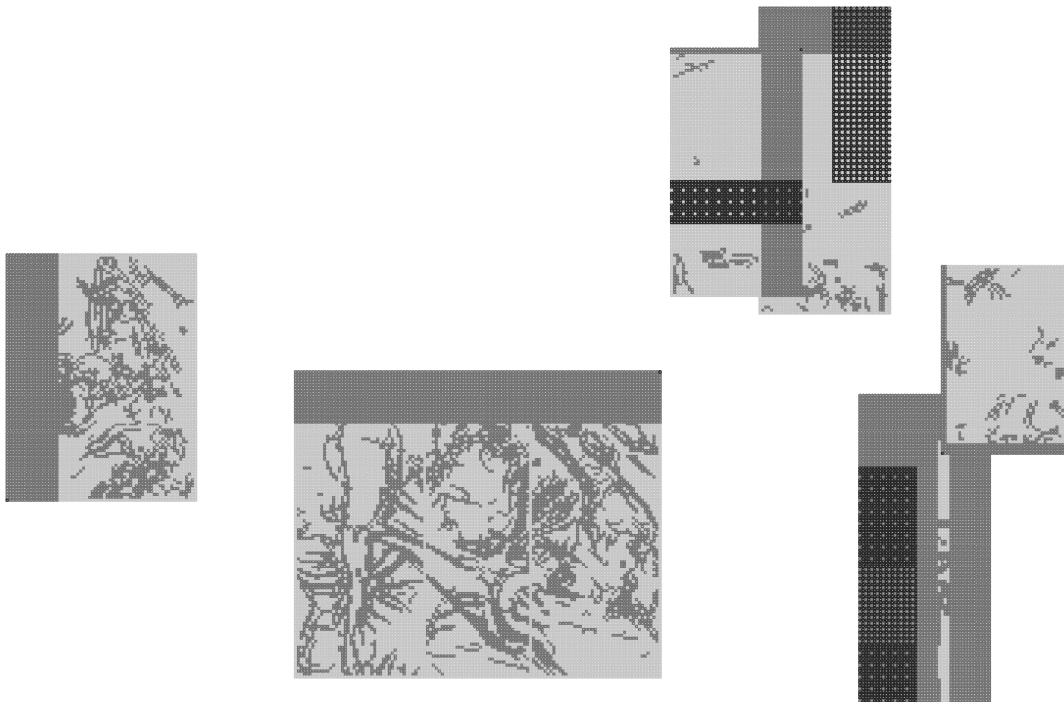
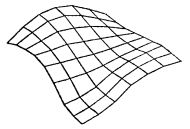
Code specification for image in scale 1:15,000, resolution 30 μm and mesh size 25 x 25 m. Light grey = grid point is OK, medium grey = grid point with double code, dark grey = grid point is defective.



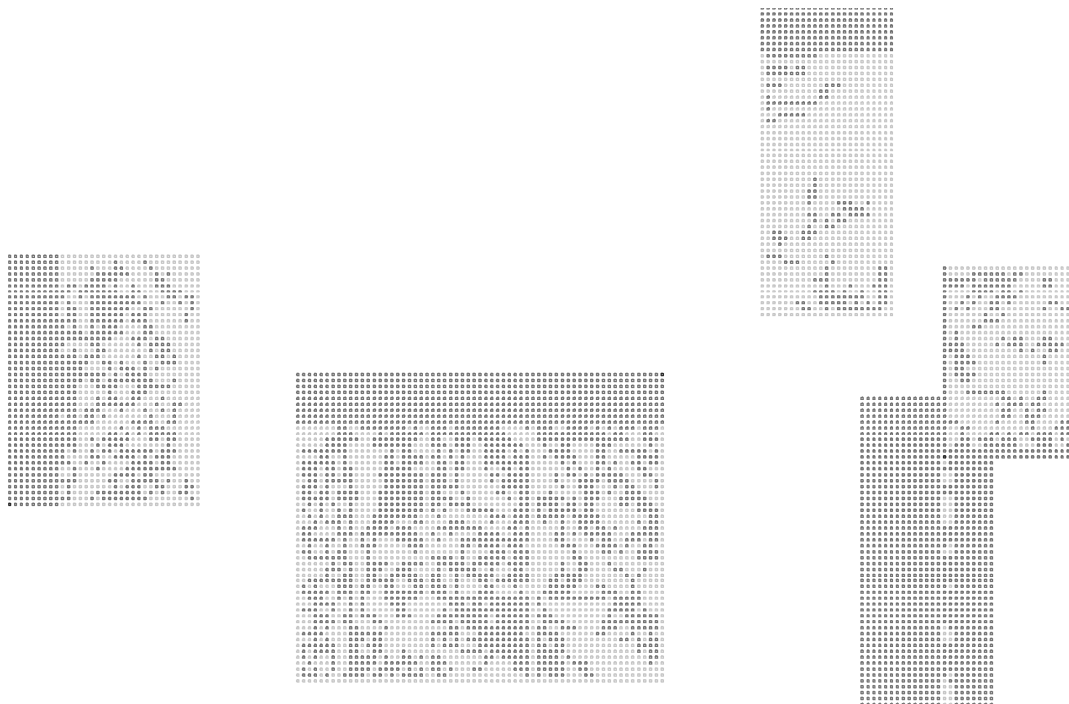
Code specification for image in scale 1:15,000, resolution 60 μm and mesh size 12.5 x 12.5 m. Light grey = grid point is OK, medium grey = grid point with double code, dark grey = grid point is defective.



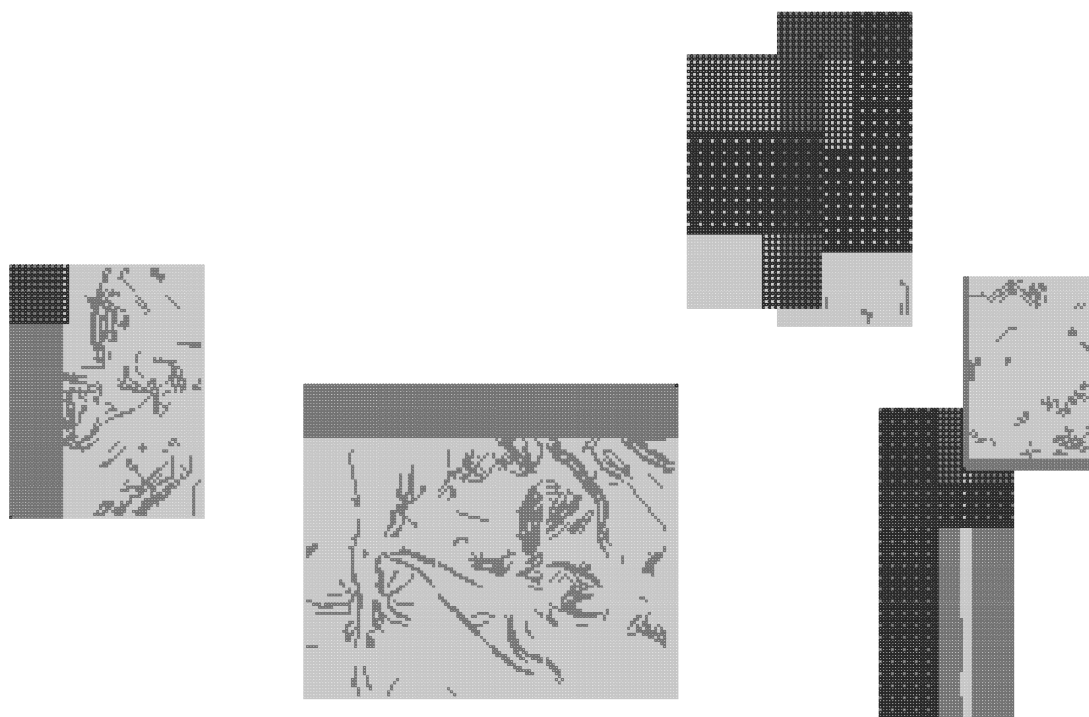
Code specification for image in scale 1:15,000, resolution 60 μm and mesh size 25 x 25 m. Light grey = grid point is OK, medium grey = grid point with double code, dark grey = grid point is defective.



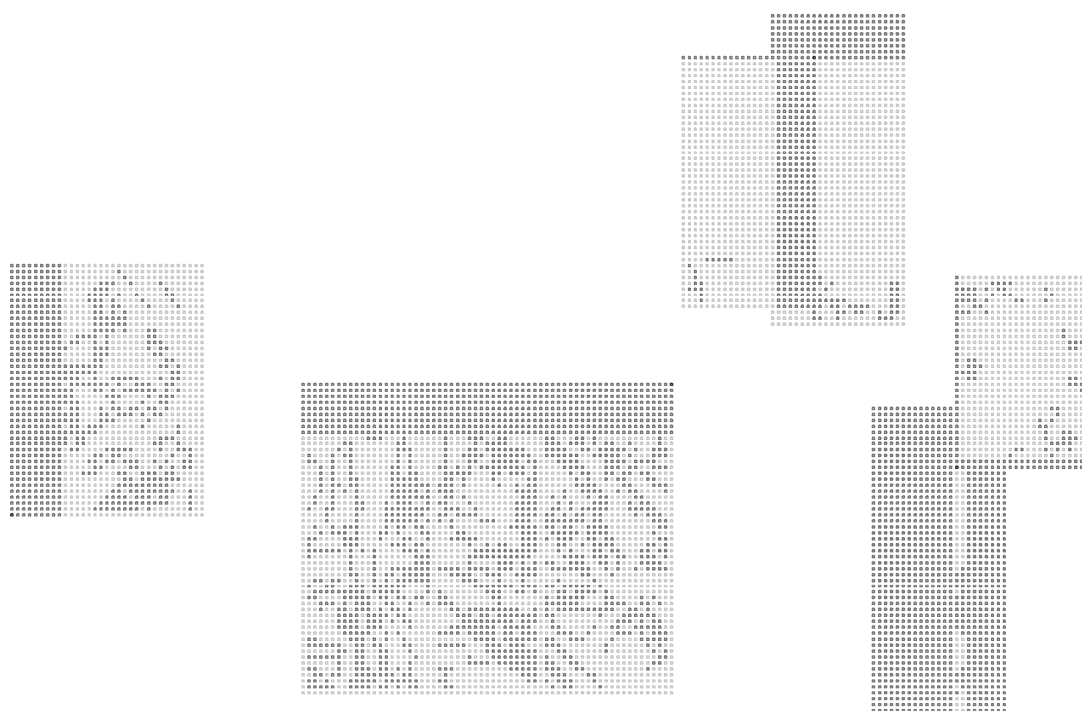
Code specification for image in scale 1:5,000, resolution 30 μ m and mesh size 12.5 x 12.5 m. Light grey = grid point is OK, medium grey = grid point with double code, dark grey = grid point is defective.



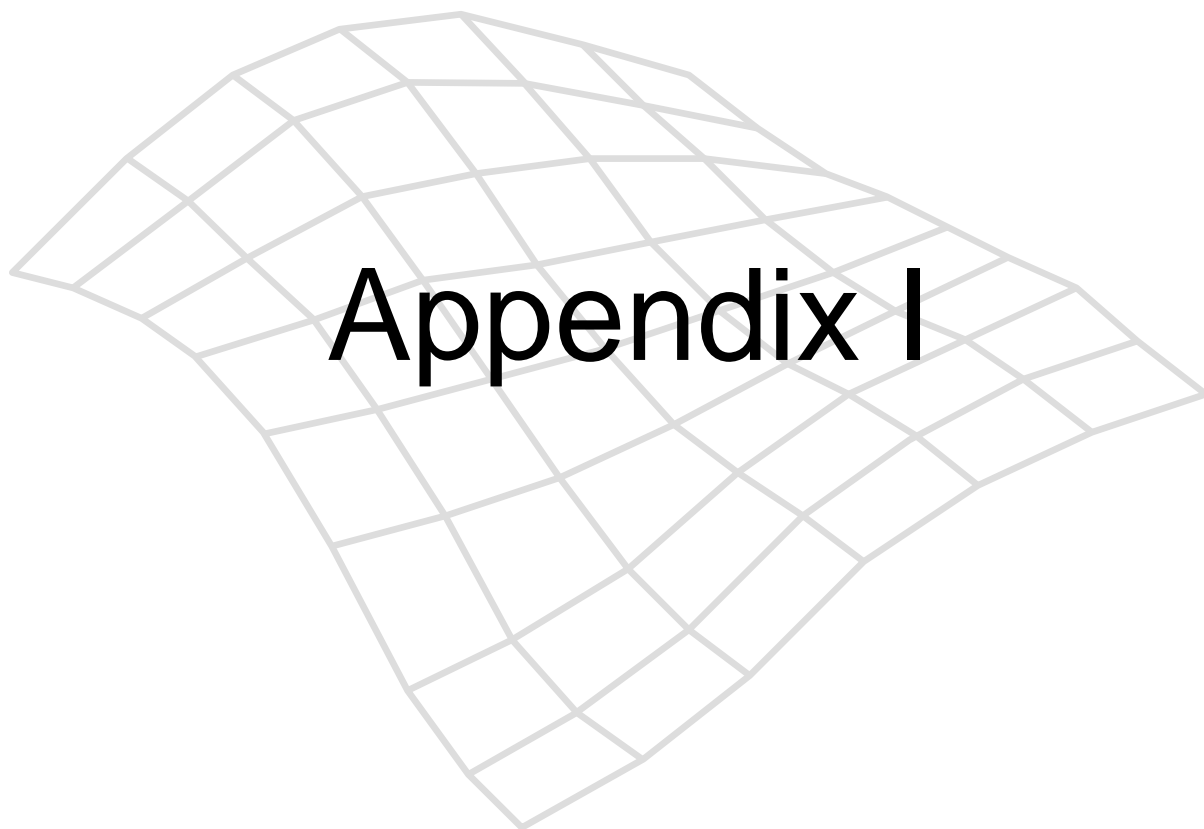
Code specification for image in scale 1:5,000, resolution 30 μ m and mesh size 25 x 25 m. Light grey = grid point is OK, medium grey = grid point with double code, dark grey = grid point is defective.



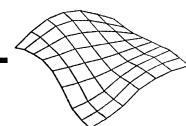
Code specification for image in scale 1:5,000, resolution 60 μm and mesh size 12.5 x 12.5 m. Light grey = grid point is OK, medium grey = grid point with double code, dark grey = grid point is defective.



Code specification for image in scale 1:5,000, resolution 60 μm and mesh size 25 x 25 m. Light grey = grid point is OK, medium grey = grid point with double code, dark grey = grid point is defective.



Appendix I



Appendix I: Analysis calculations

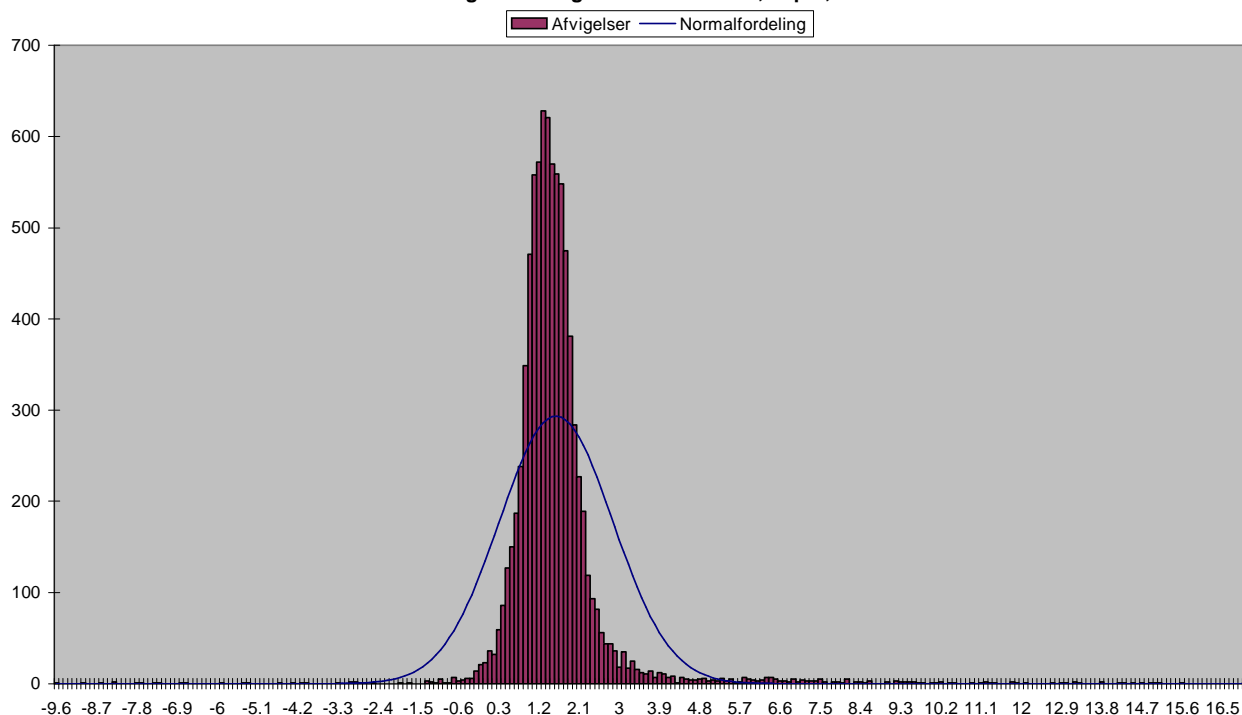
I.1 Analysis calculations

This Appendix contains the deviation between the frame of reference and the automatically generated grid in diagram format for each of the 24 calculations. Following, is a print out of the analysis file generated by the PIL program belonging to each diagram.

In order to be able to compare the results of the before and after iteration, the results are placed with the before results on the left hand page and the after results on the right hand page for the same image scale, resolution and mesh size.

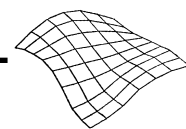
The language in this Appendix is Danish with a translation into English on an A3 page, which can be found after Appendix L (page 331). This can be folded out.

Fordelingen af afvigelser for 1:25.000, 15µm, 5 m.

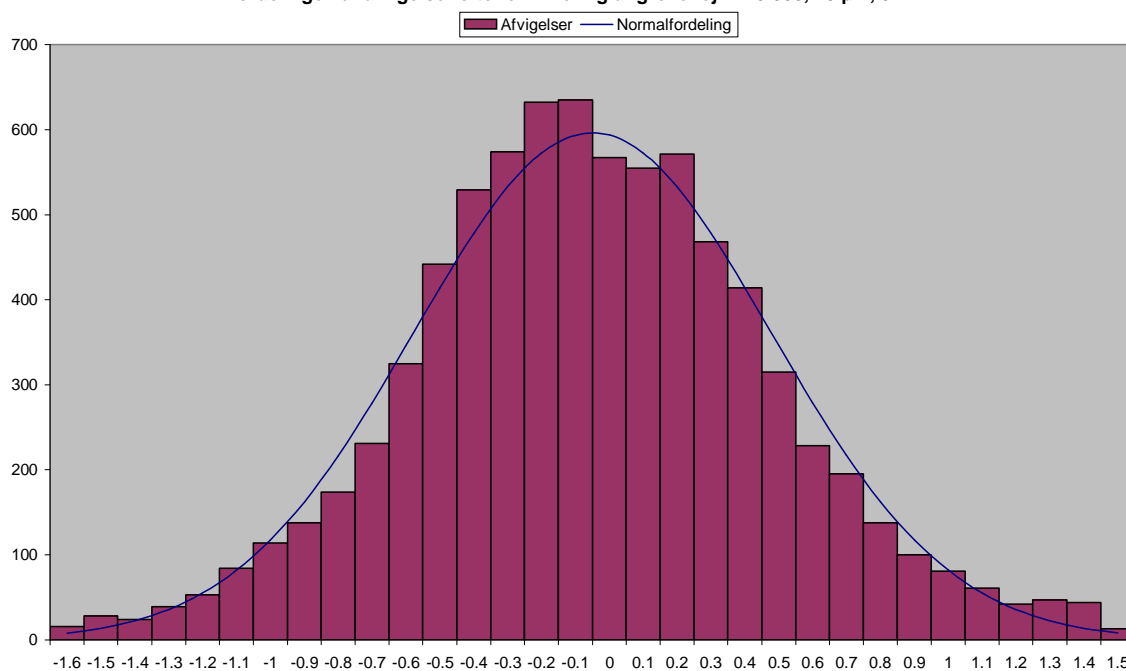


	Total	Fladt A 12	Grusgrav 34	Landsby 56	Bakket A 78	Skov 90	Ukendt 00
Min	-9.51	-0.07	-0.98	0.06	-2.73	-9.51	0
Max	17.13	4.65	2.89	6.98	8.40	17.13	0
Gns	1.64	1.55	1.05	1.65	1.70	2.39	0
Stnd	1.27	0.45	0.54	0.68	0.89	3.22	0
Sprd	2.07	1.61	1.18	1.79	1.92	4.02	0
Antal	8342	2092	1168	1410	2811	861	0
Niv'200.0'	8342	2092	1168	1410	2811	861	0
Niv'400.0'	0	0	0	0	0	0	0
Niv'600.0'	0	0	0	0	0	0	0
Udklip.pkt	0	0	0	0	0	0	0
Areal	202.0	0.0	107.3	0.0	0.0	94.6	0.0
Niv'200.0'	202.0	0.0	107.3	0.0	0.0	94.6	0.0
Niv'400.0'	0.0	0.0	0.0	0.0	0.0	0.0	0.0
Niv'600.0'	0.0	0.0	0.0	0.0	0.0	0.0	0.0
Udklip.pkt	0.0	0.0	0.0	0.0	0.0	0.0	0.0
Udkl. i %	0.00	0.00	0.00	0.00	0.00	0.00	-0-
Offset gns.	1.64	1.55	1.05	1.65	1.70	2.39	-0-
Min	-11.90	-1.62	-2.03	-1.59	-4.43	-11.90	0
Max	14.73	3.10	1.83	5.33	6.70	14.73	0
Gns	-0.00	0.00	0.00	0.00	-0.00	0.00	0
Stnd	1.23	0.45	0.54	0.68	0.89	3.22	0
Sprd	1.23	0.45	0.54	0.68	0.89	3.22	0
Udklippet							
Min	-9.51	-0.07	-0.98	0.06	-2.73	-9.51	0
Max	17.13	4.65	2.89	6.98	8.40	17.13	0
Gns	1.64	1.55	1.05	1.65	1.70	2.39	0
Stnd	1.27	0.45	0.54	0.68	0.89	3.22	0
Sprd	2.07	1.61	1.18	1.79	1.92	4.02	0
Udklippet + Offset							
Min	-	-1.62	-2.03	-1.59	-4.43	-11.90	0
Max	-	3.10	1.83	5.33	6.70	14.73	0
Gns	-	0.00	0.00	0.00	-0.00	0.00	0
Stnd	-	0.45	0.54	0.68	0.89	3.22	0
Sprd	-	0.45	0.54	0.68	0.89	3.22	0

Analysefilen for 1:25,000, opløsningen 15 µm og maskestørrelsen 5 m. før iterationsprocessen.



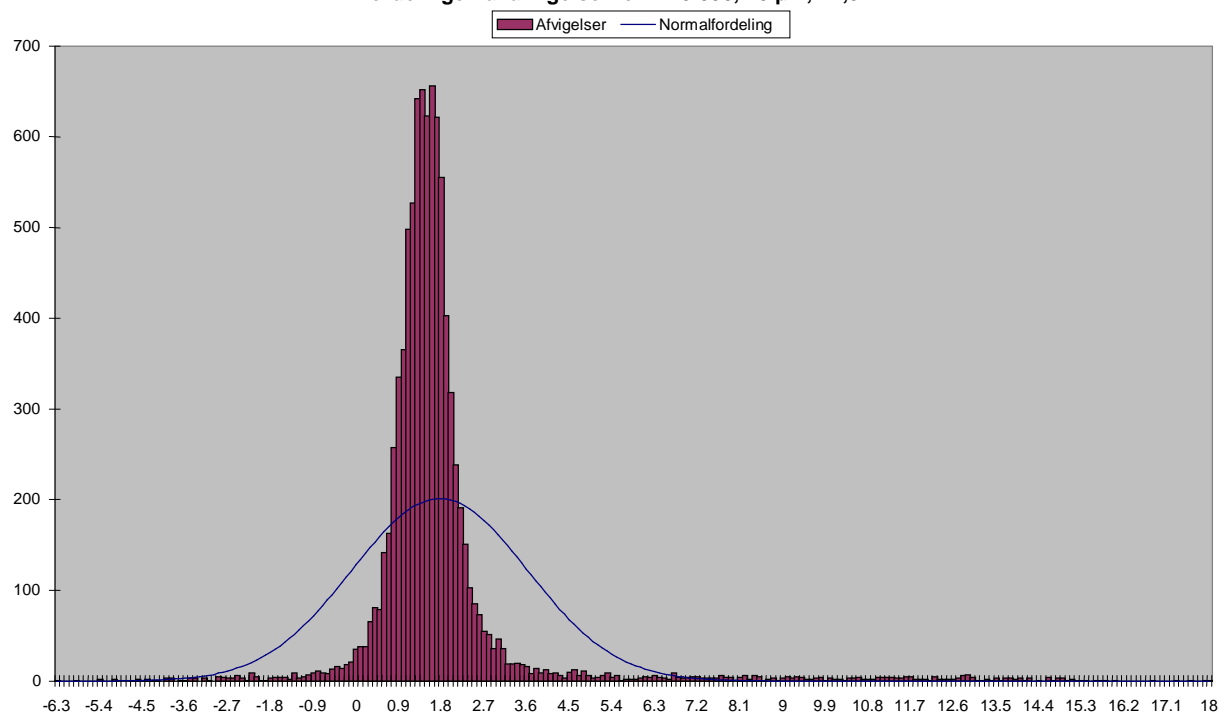
Fordelingen af afvigelser efter eliminering af grove fejl 1:25.000, 15 µm, 5 m.



	Total	Fladt A 12	Grusgrav 34	Landsby 56	Bakket A 78	Skov 90	Ukendt 00
Min	-9.51	-0.07	-0.98	0.06	-2.73	-9.51	0
Max	17.13	4.65	2.89	6.98	8.40	17.13	0
Gns	1.64	1.55	1.05	1.65	1.70	2.39	0
Stnd	1.27	0.45	0.54	0.68	0.89	3.22	0
Sprd	2.07	1.61	1.18	1.79	1.92	4.02	0
Antal	8342	2092	1168	1410	2811	861	0
Niv'0.5'	324	11	172	11	91	39	0
Niv'1.1'	1308	206	431	181	312	178	0
Niv'1.6'	3033	987	392	552	857	245	0
Udclip.pkt	3677	888	173	666	1551	399	0
Areal	202.0	0.0	107.3	0.0	0.0	94.6	0.0
Niv'0.5'	0.0	0.0	0.0	0.0	0.0	0.0	0.0
Niv'1.1'	34.2	0.0	34.2	0.0	0.0	0.0	0.0
Niv'1.6'	20.2	0.0	20.2	0.0	0.0	0.0	0.0
Udclip.pkt	147.5	0.0	52.9	0.0	0.0	94.6	0.0
Udcl. i %	44.08	42.45	14.81	47.23	55.18	46.34	-0-
Offset gns.	1.64	1.55	1.05	1.65	1.70	2.39	-0-
Min	-11.90	-1.62	-2.03	-1.59	-4.43	-11.90	0
Max	14.73	3.10	1.83	5.33	6.70	14.73	0
Gns	-0.00	0.00	0.00	0.00	-0.00	0.00	0
Stnd	1.23	0.45	0.54	0.68	0.89	3.22	0
Sprd	1.23	0.45	0.54	0.68	0.89	3.22	0
Udclippet							
Min	-0.42	0.10	-0.42	0.13	0.12	0.82	0
Max	3.96	3.13	2.60	3.22	3.28	3.96	0
Gns	1.51	1.54	1.05	1.58	1.62	1.66	0
Stnd	0.55	0.42	0.51	0.51	0.53	0.70	0
Sprd	1.61	1.59	1.17	1.66	1.71	1.80	0
Udclippet + Offset							
Min	-	-1.43	-1.46	-1.45	-1.50	-0.84	0
Max	-	1.59	1.55	1.64	1.66	2.31	0
Gns	-	0.00	0.00	0.00	-0.00	-0.00	0
Stnd	-	0.42	0.51	0.51	0.53	0.70	0
Sprd	-	0.42	0.51	0.51	0.53	0.70	0

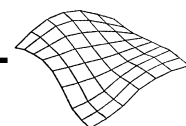
Analysefilen for 1:25,000, opløsningen 15 µm og maskestørrelsen 5 m. efter iterationsprocessen.

Fordelingen af afvigelser for 1:25.000, 15 µm, 12,5 m.

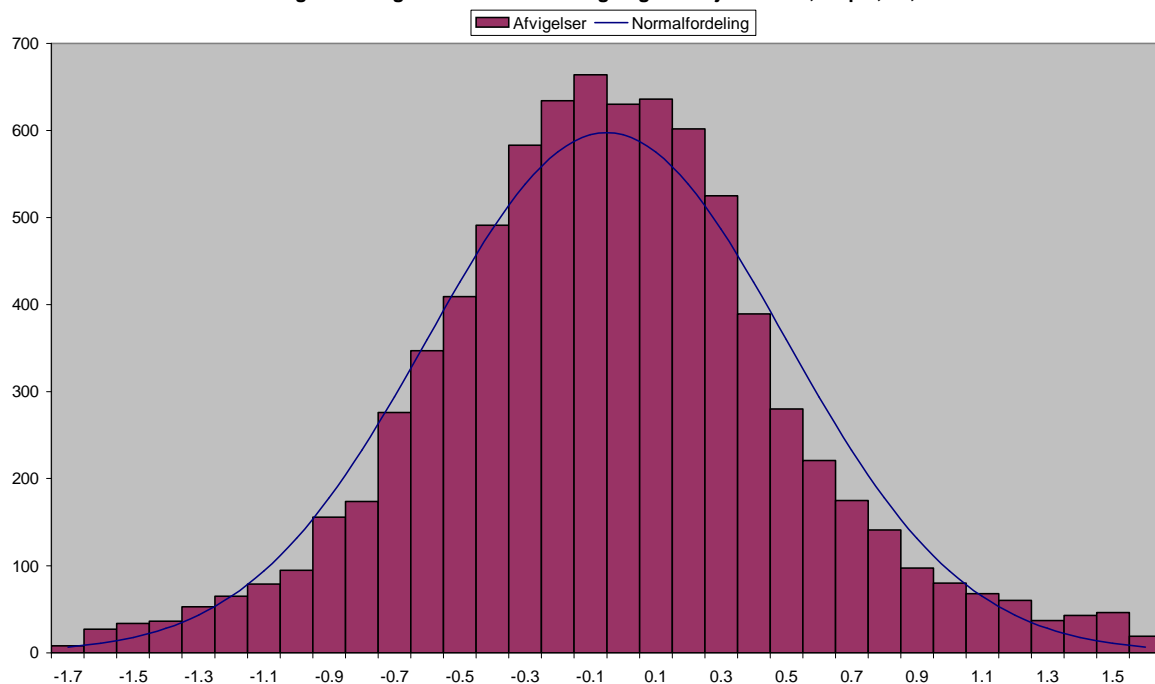


	Total	Fladt A 12	Grusgrav 34	Landsby 56	Bakket A 78	Skov 90	Ukendt 00
Min	-6.20	0.13	-6.20	-0.32	-3.42	-2.76	0
Max	18.07	3.93	15.41	4.43	6.19	18.07	0
Gns	1.82	1.47	2.28	1.51	1.67	2.69	0
Stnd	1.86	0.42	3.10	0.49	0.63	3.47	0
Sprd	2.60	1.53	3.85	1.59	1.78	4.39	0
Antal	8929	2087	1802	1392	2805	843	0
Niv'200.0'	8929	2087	1802	1392	2805	843	0
Niv'400.0'	0	0	0	0	0	0	0
Niv'600.0'	0	0	0	0	0	0	0
Udklip.pkt	0	0	0	0	0	0	0
Areal	52611.6	721.7	45759.7	1261.2	0.0	4868.9	0.0
Niv'200.0'	52611.6	721.7	45759.7	1261.2	0.0	4868.9	0.0
Niv'400.0'	0.0	0.0	0.0	0.0	0.0	0.0	0.0
Niv'600.0'	0.0	0.0	0.0	0.0	0.0	0.0	0.0
Udklip.pkt	0.0	0.0	0.0	0.0	0.0	0.0	0.0
Udkl. i %	0.00	0.00	0.00	0.00	0.00	0.00	-0-
Offset gns.	1.82	1.47	2.28	1.51	1.67	2.69	-0-
Min	-8.48	-1.34	-8.48	-1.83	-5.09	-5.45	0
Max	15.38	2.47	13.14	2.92	4.52	15.38	0
Gns	-0.00	0.00	-0.00	-0.00	0.00	-0.00	0
Stnd	1.81	0.42	3.10	0.49	0.63	3.47	0
Sprd	1.81	0.42	3.10	0.49	0.63	3.47	0
Udklippet							
Min	-6.20	0.13	-6.20	-0.32	-3.42	-2.76	0
Max	18.07	3.93	15.41	4.43	6.19	18.07	0
Gns	1.82	1.47	2.28	1.51	1.67	2.69	0
Stnd	1.87	0.42	3.10	0.49	0.63	3.47	0
Sprd	2.60	1.53	3.85	1.59	1.78	4.39	0
Udklippet + Offset							
Min	-	-1.34	-8.48	-1.83	-5.09	-5.45	0
Max	-	2.47	13.14	2.92	4.52	15.38	0
Gns	-	0.00	-0.00	-0.00	0.00	-0.00	0
Stnd	-	0.42	3.10	0.49	0.63	3.47	0
Sprd	-	0.42	3.10	0.49	0.63	3.47	0

Analysefilen for 1:25,000, opløsningen 15 µm og maskestørrelsen 12.5 m. før iterationsprocessen.



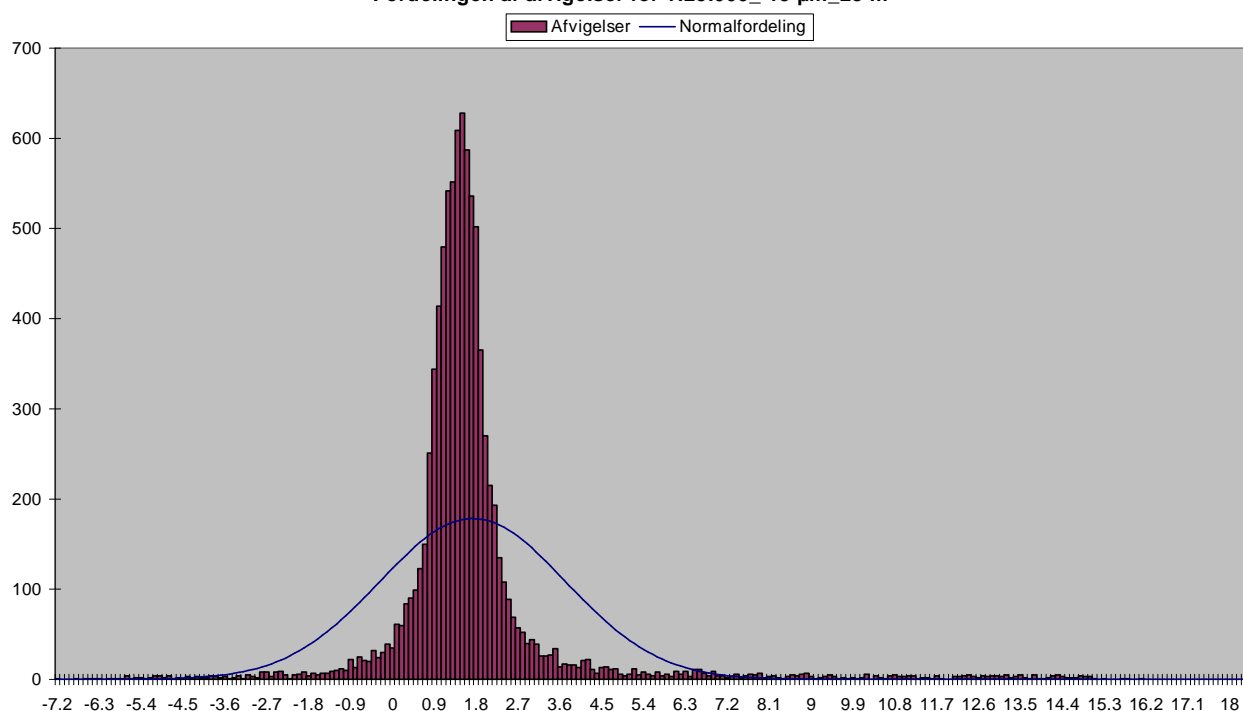
Fordelingen af afvigelser efter eliminering af grove fejl 1:25.000, 15 µm, 12,5 m.



	Total	Fladt A 12	Grusgrav 34	Landsby 56	Bakket A 78	Skov 90	Ukendt 00
Min	-6.20	0.13	-6.20	-0.32	-3.42	-2.76	0
Max	18.07	3.93	15.41	4.43	6.19	18.07	0
Gns	1.82	1.47	2.28	1.51	1.67	2.69	0
Stnd	1.86	0.42	3.10	0.49	0.63	3.47	0
Sprd	2.60	1.53	3.85	1.59	1.78	4.39	0
Antal	8929	2087	1802	1392	2805	843	0
Niv'0.6'	382	10	232	30	46	64	0
Niv'1.1'	1347	370	274	221	248	234	0
Niv'1.6'	3237	982	278	664	1096	217	0
Udklip.pkt	3963	725	1018	477	1415	328	0
Areal	52611.6	721.7	45759.7	1261.2	0.0	4868.9	0.0
Niv'0.6'	6446.9	0.0	5927.2	372.4	0.0	147.3	0.0
Niv'1.1'	8100.5	0.0	6914.1	343.2	0.0	843.2	0.0
Niv'1.6'	7660.0	0.0	6940.1	197.1	0.0	522.8	0.0
Udklip.pkt	30404.1	721.7	25978.3	348.5	0.0	3355.6	0.0
Udkl. i %	44.38	34.74	56.49	34.27	50.45	38.91	-0-
Offset gns.	1.82	1.47	2.28	1.51	1.67	2.69	-0-
Min	-8.48	-1.34	-8.48	-1.83	-5.09	-5.45	0
Max	15.38	2.47	13.14	2.92	4.52	15.38	0
Gns	-0.00	0.00	-0.00	-0.00	0.00	-0.00	0
Stnd	1.81	0.42	3.10	0.49	0.63	3.47	0
Sprd	1.81	0.42	3.10	0.49	0.63	3.47	0
Udklippet							
Min	-0.03	0.13	0.65	-0.03	0.06	1.05	0
Max	4.24	3.06	3.92	3.11	3.31	4.24	0
Gns	1.59	1.47	2.08	1.49	1.65	1.78	0
Stnd	0.50	0.41	0.47	0.45	0.48	0.73	0
Sprd	1.66	1.52	2.13	1.56	1.72	1.93	0
Udklippet + Offset							
Min	-	-1.34	-1.42	-1.53	-1.59	-0.73	0
Max	-	1.59	1.84	1.61	1.66	2.46	0
Gns	-	0.00	0.00	0.00	0.00	0.00	0
Stnd	-	0.41	0.47	0.45	0.48	0.73	0
Sprd	-	0.41	0.47	0.45	0.48	0.73	0

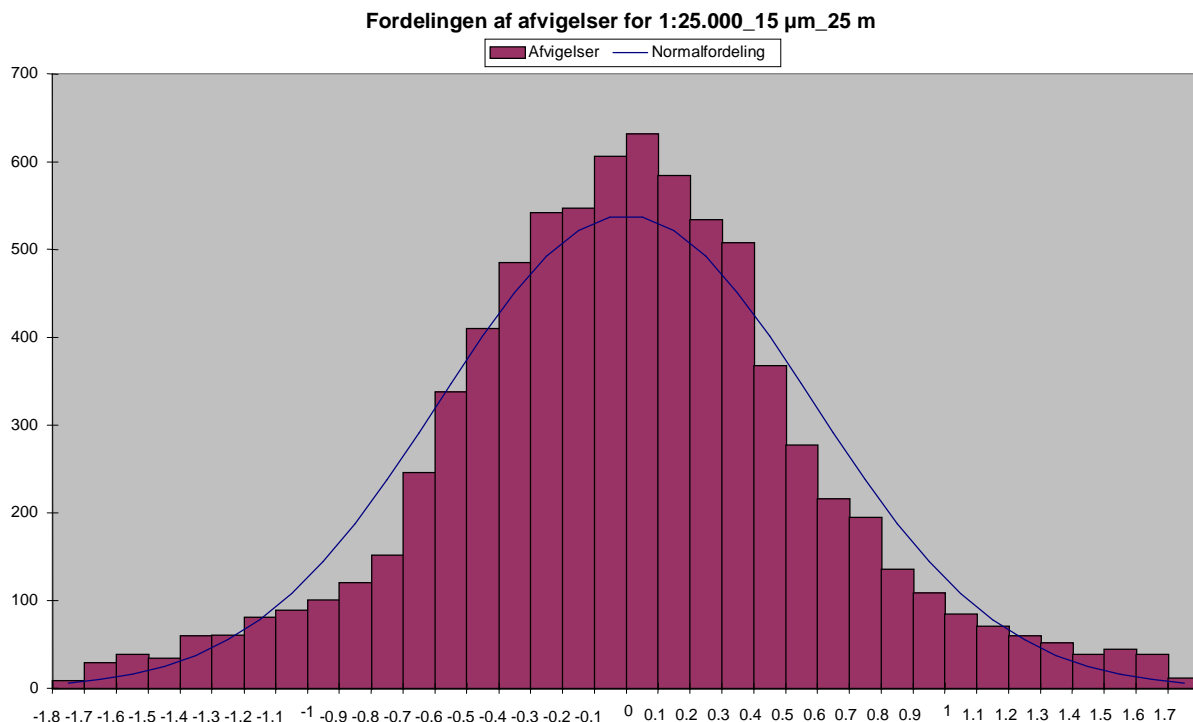
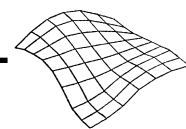
Analysefilen for 1:25,000, opløsningen 15 µm og maskestørrelsen 12.5 m. efter iterationsprocessen.

Fordelingen af afvigelser for 1:25.000_15 µm_25 m



	Total	Fladt A 12	Grusgrav 34	Landsby 56	Bakket A 78	Skov 90	Ukendt 00
Min	-7.17	-1.29	-6.73	-1.04	-7.17	-6.36	0
Max	18.48	4.78	15.39	4.32	11.73	18.48	0
Gns	1.78	1.45	2.34	1.46	1.64	2.35	0
Stnd	2.00	0.47	3.50	0.53	1.16	3.07	0
Sprd	2.68	1.53	4.21	1.56	2.01	3.87	0
Antal	8956	2092	1805	1401	2811	847	0
Niv'200.0'	8956	2092	1805	1401	2811	847	0
Niv'400.0'	0	0	0	0	0	0	0
Niv'600.0'	0	0	0	0	0	0	0
Udklip.pkt	0	0	0	0	0	0	0
Areal	645893.3	72222.3	47670.5	262049.5	95868.7	168082.3	0.0
Niv'200.0'	645893.3	72222.3	47670.5	262049.5	95868.7	168082.3	0.0
Niv'400.0'	0.0	0.0	0.0	0.0	0.0	0.0	0.0
Niv'600.0'	0.0	0.0	0.0	0.0	0.0	0.0	0.0
Udklip.pkt	0.0	0.0	0.0	0.0	0.0	0.0	0.0
Udkl. i %	0.00	0.00	0.00	0.00	0.00	0.00	-0-
Offset gns.	1.78	1.45	2.34	1.46	1.64	2.35	-0-
Min	-9.07	-2.74	-9.07	-2.50	-8.80	-8.70	0
Max	16.13	3.33	13.05	2.86	10.09	16.13	0
Gns	-0.00	-0.00	-0.00	0.00	-0.00	-0.00	0
Stnd	1.97	0.47	3.50	0.53	1.16	3.07	0
Sprd	1.97	0.47	3.50	0.53	1.16	3.07	0
Udklippet							
Min	-7.17	-1.29	-6.73	-1.04	-7.17	-6.36	0
Max	18.48	4.78	15.39	4.32	11.73	18.48	0
Gns	1.78	1.45	2.34	1.46	1.64	2.35	0
Stnd	2.02	0.47	3.50	0.53	1.16	3.07	0
Sprd	2.68	1.53	4.21	1.56	2.01	3.87	0
Udklippet + Offset							
Min	-	-2.74	-9.07	-2.50	-8.80	-8.70	0
Max	-	3.33	13.05	2.86	10.09	16.13	0
Gns	-	-0.00	-0.00	0.00	-0.00	-0.00	0
Stnd	-	0.47	3.50	0.53	1.16	3.07	0
Sprd	-	0.47	3.50	0.53	1.16	3.07	0

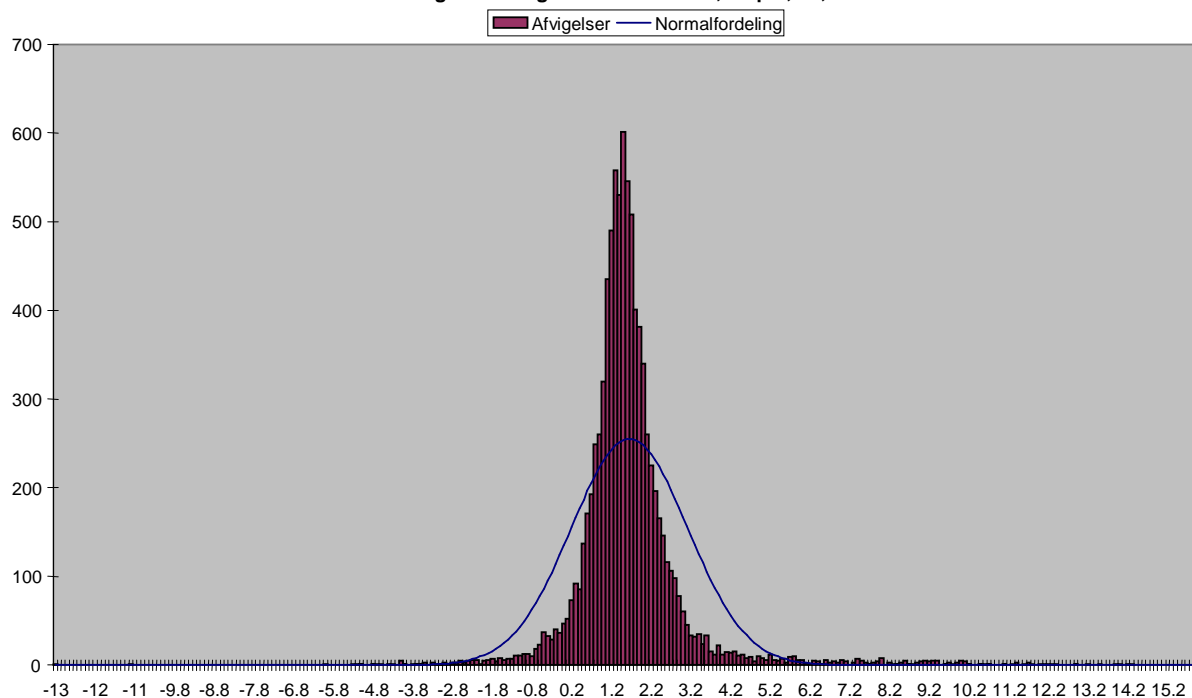
Analysefilen for 1:25,000, opløsningen 15 µm og maskestørrelsen 25 m. før iterationsprocessen.



	Total	Fladt A 12	Grusgrav 34	Landsby 56	Bakket A 78	Skov 90	Ukendt 00
Min	-7.17	-1.29	-6.73	-1.04	-7.17	-6.36	0
Max	18.48	4.78	15.39	4.32	11.73	18.48	0
Gns	1.78	1.45	2.34	1.46	1.64	2.35	0
Stnd	2.00	0.47	3.50	0.53	1.16	3.07	0
Sprd	2.68	1.53	4.21	1.56	2.01	3.87	0
Antal	8956	2092	1805	1401	2811	847	0
Niv'0.6'	587	30	269	64	126	98	0
Niv'1.2'	1782	559	273	312	430	208	0
Niv'1.8'	3358	1037	280	697	1128	216	0
Udklip.pkt	3229	466	983	328	1127	325	0
Areal	645893.3	72222.3	47670.5	262049.5	95868.7	168082.3	0.0
Niv'0.6'	38660.5	1640.1	7292.8	12604.1	4576.8	12546.8	0.0
Niv'1.2'	111099.5	13775.0	7570.8	47735.8	13722.0	28296.0	0.0
Niv'1.8'	257798.6	36900.8	7445.0	127785.3	36825.2	48842.3	0.0
Udklip.pkt	238334.6	19906.3	25361.9	73924.3	40744.7	78397.3	0.0
Udkl. i %	36.05	22.28	54.46	23.41	40.09	38.37	-0-
Offset gns.	1.78	1.45	2.34	1.46	1.64	2.35	-0-
Min	-9.07	-2.74	-9.07	-2.50	-8.80	-8.70	0
Max	16.13	3.33	13.05	2.86	10.09	16.13	0
Gns	-0.00	-0.00	-0.00	0.00	-0.00	-0.00	0
Stnd	1.97	0.47	3.50	0.53	1.16	3.07	0
Sprd	1.97	0.47	3.50	0.53	1.16	3.07	0
Udklippet							
Min	-0.27	-0.18	1.70	-0.27	-0.12	0.59	0
Max	4.07	3.16	2.83	3.13	3.38	4.07	0
Gns	1.52	1.44	2.23	1.45	1.62	1.51	0
Stnd	0.52	0.42	0.24	0.47	0.56	0.68	0
Sprd	1.61	1.50	2.25	1.53	1.71	1.66	0
Udklippet + Offset							
Min	-	-1.63	-0.53	-1.72	-1.73	-0.92	0
Max	-	1.72	0.60	1.68	1.77	2.56	0
Gns	-	-0.00	0.00	0.00	-0.00	0.00	0
Stnd	-	0.42	0.24	0.47	0.56	0.68	0
Sprd	-	0.42	0.24	0.47	0.56	0.68	0

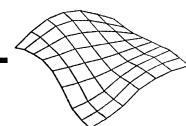
Analysefilen for 1:25,000, opløsningen 15 µm og maskestørrelsen 25 m. efter iterationsprocessen.

Fordelingen af afvigelser for 1:25.000, 30 µm, 12,5 m.

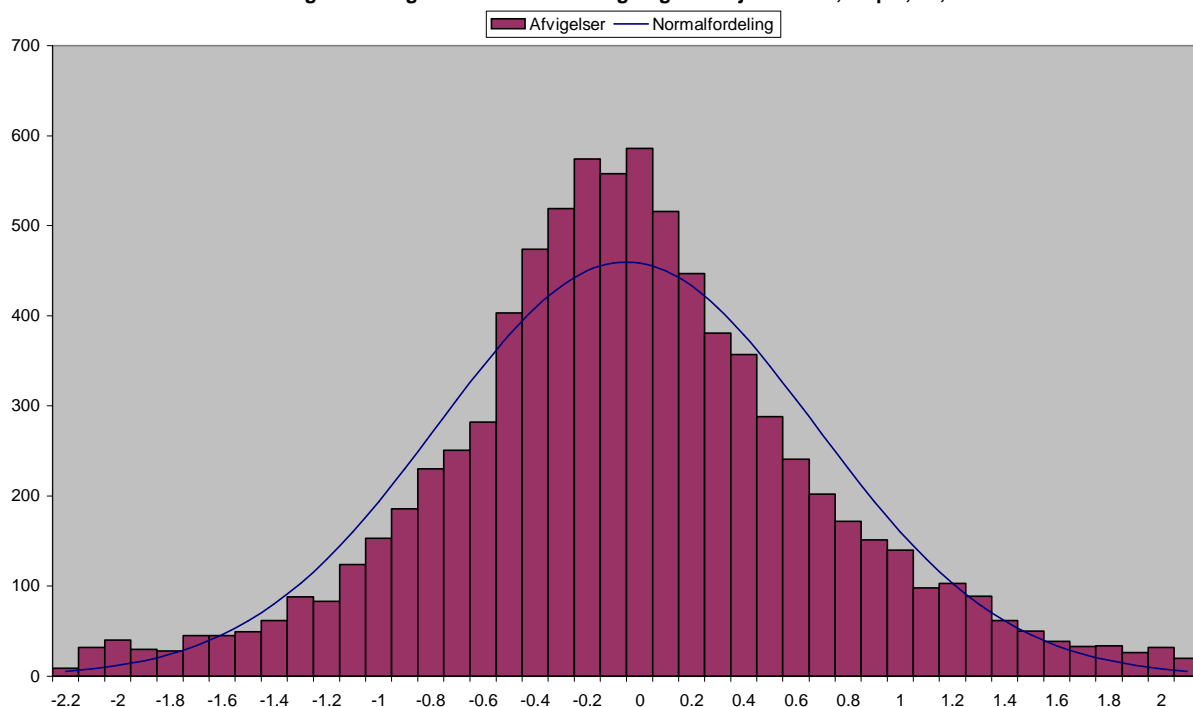


	Total	Fladt A 12	Grusgrav 34	Landsby 56	Bakket A 78	Skov 90	Ukendt 00
Min	-12.77	-0.65	-4.61	-0.69	-12.77	-1.03	0
Max	16.12	4.43	12.98	5.10	7.95	16.12	0
Gns	1.70	1.40	1.59	1.76	1.65	2.79	0
Stnd	1.46	0.52	1.92	0.71	1.12	2.77	0
Sprd	2.25	1.50	2.49	1.90	2.00	3.93	0
Antal	8929	2087	1802	1392	2805	843	0
Niv'200.0'	8929	2087	1802	1392	2805	843	0
Niv'400.0'	0	0	0	0	0	0	0
Niv'600.0'	0	0	0	0	0	0	0
Udklip.pkt	0	0	0	0	0	0	0
Areal	52611.6	721.7	45759.7	1261.2	0.0	4868.9	0.0
Niv'200.0'	52611.6	721.7	45759.7	1261.2	0.0	4868.9	0.0
Niv'400.0'	0.0	0.0	0.0	0.0	0.0	0.0	0.0
Niv'600.0'	0.0	0.0	0.0	0.0	0.0	0.0	0.0
Udklip.pkt	0.0	0.0	0.0	0.0	0.0	0.0	0.0
Udkl. i %	0.00	0.00	0.00	0.00	0.00	0.00	-0-
Offset gns.	1.70	1.40	1.59	1.76	1.65	2.79	-0-
Min	-14.42	-2.05	-6.19	-2.45	-14.42	-3.83	0
Max	13.32	3.02	11.39	3.34	6.30	13.32	0
Gns	-0.00	-0.00	0.00	0.00	-0.00	-0.00	0
Stnd	1.42	0.52	1.92	0.71	1.12	2.77	0
Sprd	1.42	0.52	1.92	0.71	1.12	2.77	0
Udklippet							
Min	-12.77	-0.65	-4.61	-0.69	-12.77	-1.03	0
Max	16.12	4.43	12.98	5.10	7.95	16.12	0
Gns	1.70	1.40	1.59	1.76	1.65	2.79	0
Stnd	1.46	0.52	1.92	0.71	1.12	2.77	0
Sprd	2.25	1.50	2.49	1.90	2.00	3.93	0
Udklippet + Offset							
Min	-	-2.05	-6.19	-2.45	-14.42	-3.83	0
Max	-	3.02	11.39	3.34	6.30	13.32	0
Gns	-	-0.00	0.00	0.00	-0.00	-0.00	0
Stnd	-	0.52	1.92	0.71	1.12	2.77	0
Sprd	-	0.52	1.92	0.71	1.12	2.77	0

Analysefilen for 1:25,000, opløsningen 30 µm og maskestørrelsen 12.5 m. før iterationsprocessen.



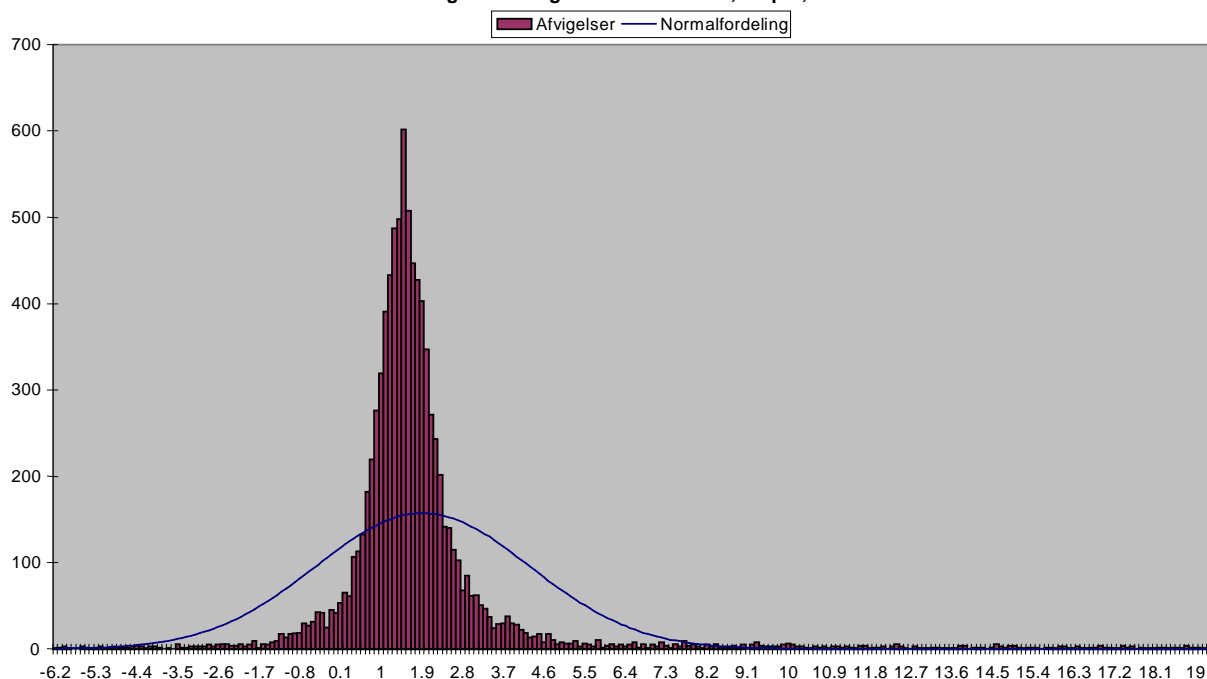
Fordelingen af afvigelser efter eliminering af grove fejl 1:25.000, 30 µm, 12,5 m.



	Total	Fladt A 12	Grusgrav 34	Landsby 56	Bakket A 78	Skov 90	Ukendt 00
Min	-12.77	-0.65	-4.61	-0.69	-12.77	-1.03	0
Max	16.12	4.43	12.98	5.10	7.95	16.12	0
Gns	1.70	1.40	1.59	1.76	1.65	2.79	0
Stnd	1.46	0.52	1.92	0.71	1.12	2.77	0
Sprd	2.25	1.50	2.49	1.90	2.00	3.93	0
Antal	8929	2087	1802	1392	2805	843	0
Niv'0.7'	919	173	403	68	199	76	0
Niv'1.4'	2766	992	393	408	741	232	0
Niv'2.2'	3309	772	454	571	1293	219	0
Udklip.pkt	1935	150	552	345	572	316	0
Areal	52611.6	721.7	45759.7	1261.2	0.0	4868.9	0.0
Niv'0.7'	11225.6	0.0	10161.0	544.9	0.0	519.8	0.0
Niv'1.4'	11205.0	200.8	9955.2	342.9	0.0	706.1	0.0
Niv'2.2'	12469.8	90.8	11409.3	138.2	0.0	831.5	0.0
Udklip.pkt	17711.1	430.0	14234.2	235.3	0.0	2811.6	0.0
Udkl. i %	21.67	7.19	30.63	24.78	20.39	37.49	-0-
Offset gns.	1.70	1.40	1.59	1.76	1.65	2.79	-0-
Min	-14.42	-2.05	-6.19	-2.45	-14.42	-3.83	0
Max	13.32	3.02	11.39	3.34	6.30	13.32	0
Gns	-0.00	-0.00	0.00	0.00	-0.00	-0.00	0
Stnd	1.42	0.52	1.92	0.71	1.12	2.77	0
Sprd	1.42	0.52	1.92	0.71	1.12	2.77	0
Udklippet							
Min	-0.65	-0.65	-0.58	-0.36	-0.52	0.63	0
Max	4.95	3.54	3.74	3.88	3.80	4.95	0
Gns	1.61	1.39	1.57	1.73	1.66	1.89	0
Stnd	0.70	0.50	0.90	0.65	0.66	0.94	0
Sprd	1.75	1.48	1.81	1.85	1.78	2.12	0
Udklippet + Offset							
Min	-	-2.04	-2.14	-2.10	-2.18	-1.27	0
Max	-	2.15	2.17	2.14	2.14	3.06	0
Gns	-	0.00	-0.00	0.00	-0.00	0.00	0
Stnd	-	0.50	0.90	0.65	0.66	0.94	0
Sprd	-	0.50	0.90	0.65	0.66	0.94	0

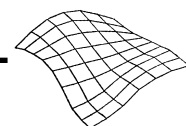
Analysefilen for 1:25,000, opløsningen 30 µm og maskestørrelsen 12.5 m. efter iterationsprocessen.

Fordelingen af afvigelser for 1:25.000, 30 µm, 25 m.

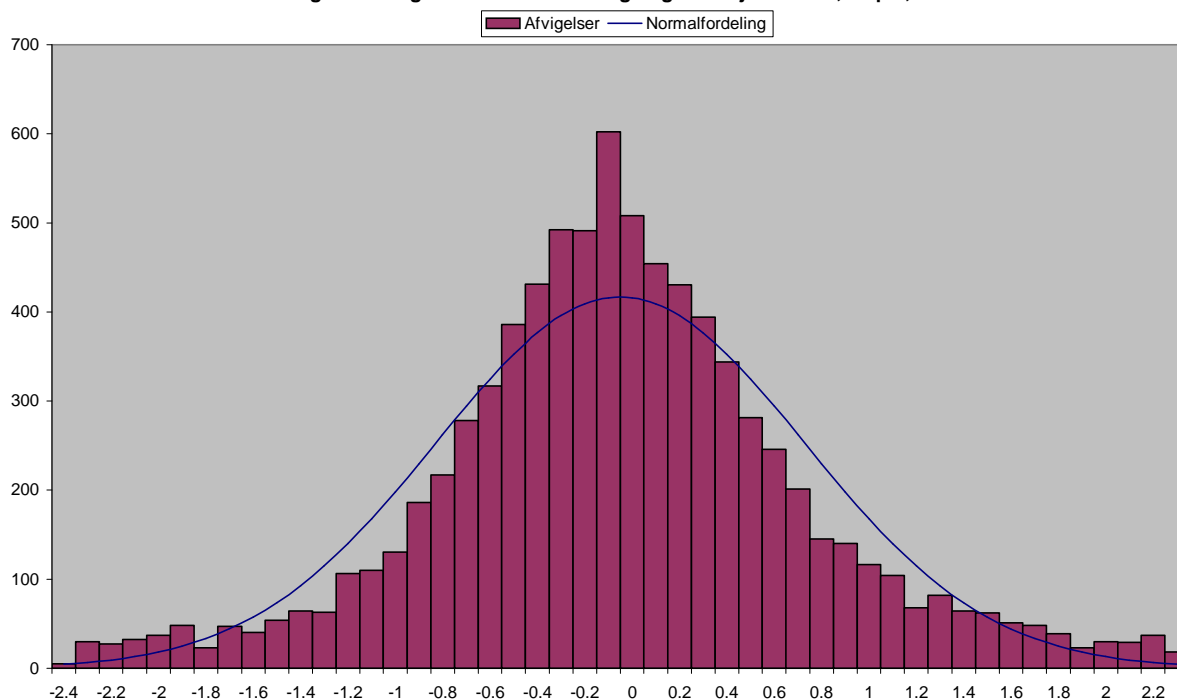


	Total	Fladt A 12	Grusgrav 34	Landsby 56	Bakket A 78	Skov 90	Ukendt 00
Min	-6.13	-0.14	-6.13	-2.30	-5.52	-4.33	0
Max	19.42	4.11	19.42	4.56	6.50	17.51	0
Gns	1.97	1.41	2.89	1.66	1.70	2.81	0
Stnd	2.37	0.49	4.39	0.72	0.91	3.24	0
Sprd	3.08	1.49	5.26	1.81	1.93	4.29	0
Antal	8956	2092	1805	1401	2811	847	0
Niv'0.8'	983	177	332	116	232	126	0
Niv'1.6'	3118	1168	301	466	931	252	0
Niv'2.3'	3007	682	332	624	1166	203	0
Udklip.pkt	1848	65	840	195	482	266	0
Areal	645893.3	72222.3	47670.5	262049.5	95868.7	168082.3	0.0
Niv'0.8'	52064.4	2797.9	9775.5	16109.8	6610.4	16770.8	0.0
Niv'1.6'	187048.7	36341.5	7733.0	67952.2	35422.0	39600.1	0.0
Niv'2.3'	254480.3	28912.1	8614.2	132124.7	39997.8	44831.5	0.0
Udklip.pkt	152300.0	4170.9	21547.8	45862.9	13838.5	66879.9	0.0
Udkl. i %	20.63	3.11	46.54	13.92	17.15	31.40	-0-
Offset gns.	1.97	1.41	2.89	1.66	1.70	2.81	-0-
Min	-9.02	-1.55	-9.02	-3.97	-7.22	-7.14	0
Max	16.53	2.70	16.53	2.90	4.80	14.70	0
Gns	-0.00	-0.00	-0.00	0.00	0.00	0.00	0
Stnd	2.30	0.49	4.39	0.72	0.91	3.24	0
Sprd	2.30	0.49	4.39	0.72	0.91	3.24	0
Udklippet							
Min	-0.63	-0.14	0.70	-0.49	-0.63	0.47	0
Max	4.87	3.59	3.69	3.93	3.96	4.87	0
Gns	1.62	1.41	2.63	1.69	1.71	1.72	0
Stnd	0.67	0.48	0.53	0.65	0.70	0.87	0
Sprd	1.75	1.49	2.68	1.82	1.85	1.93	0
Udklippet + Offset							
Min	-	-1.54	-1.93	-2.18	-2.33	-1.25	0
Max	-	2.18	1.06	2.24	2.25	3.15	0
Gns	-	-0.00	-0.00	0.00	0.00	0.00	0
Stnd	-	0.48	0.53	0.65	0.70	0.87	0
Sprd	-	0.48	0.53	0.65	0.70	0.87	0

Analysefilen for 1:25,000, opløsningen 30 µm og maskestørrelsen 25 m. før iterationsprocessen.



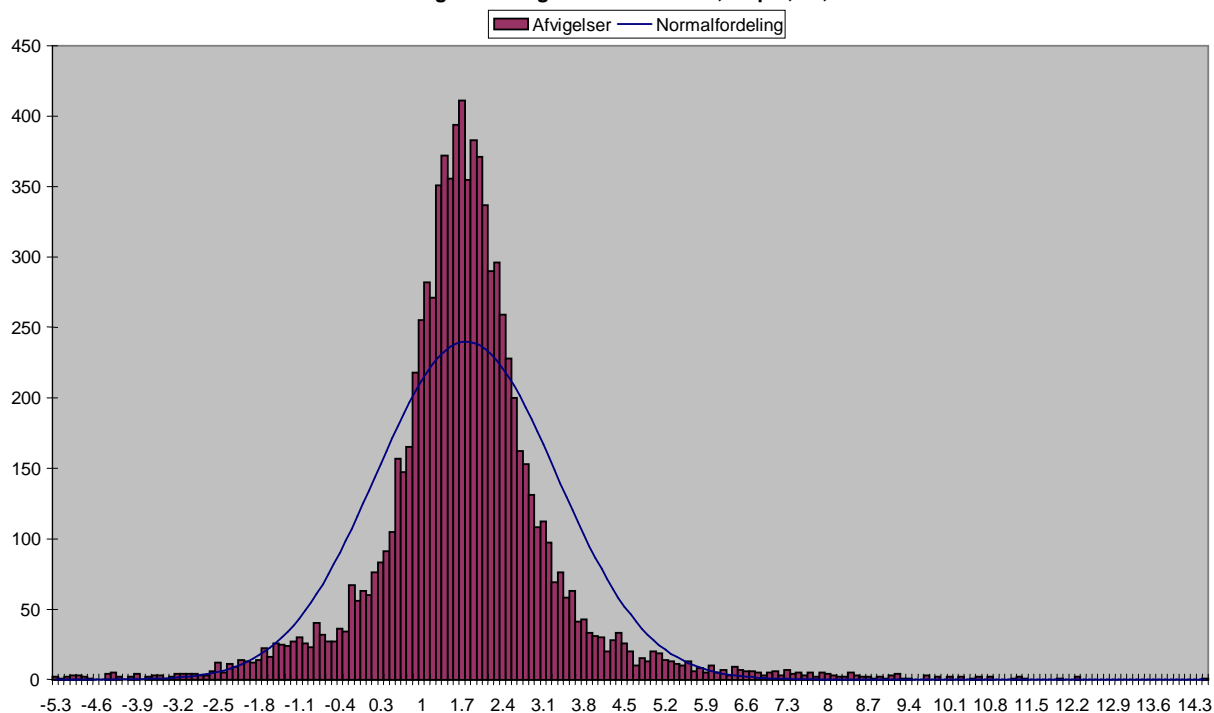
Fordelingen af afvigelser efter eliminering af grove fejl 1:25.000, 30 µm, 25 m.



	Total	Fladt A 12	Grusgrav 34	Landsby 56	Bakket A 78	Skov 90	Ukendt 00	
Min	-6.13	-0.14	-6.13	-2.30	-5.52	-4.33	0	
Max	19.42	4.11	19.42	4.56	6.50	17.51	0	
Gns	1.97	1.41	2.89	1.66	1.70	2.81	0	
Stnd	2.37	0.49	4.39	0.72	0.91	3.24	0	
Sprd	3.08	1.49	5.26	1.81	1.93	4.29	0	
Antal	8956	2092	1805	1401	2811	847	0	
Niv'0.8'	983	177	332	116	232	126	0	
Niv'1.6'	3118	1168	301	466	931	252	0	
Niv'2.3'	3007	682	332	624	1166	203	0	
Udklip.pkt	1848	65	840	195	482	266	0	
Areal	645893.3	72222.3	47670.5	262049.5	95868.7	168082.3	0.0	
Niv'0.8'	52064.4	2797.9	9775.5	16109.8	6610.4	16770.8	0.0	
Niv'1.6'	187048.7	36341.5	7733.0	67952.2	35422.0	39600.1	0.0	
Niv'2.3'	254480.3	28912.1	8614.2	132124.7	39997.8	44831.5	0.0	
Udklip.pkt	152300.0	4170.9	21547.8	45862.9	13838.5	66879.9	0.0	
Udkl. i %	20.63	3.11	46.54	13.92	17.15	31.40	-0-	
Offset gns.	1.97	1.41	2.89	1.66	1.70	2.81	-0-	
Min	-9.02	-1.55	-9.02	-3.97	-7.22	-7.14	0	
Max	16.53	2.70	16.53	2.90	4.80	14.70	0	
Gns	-0.00	-0.00	-0.00	0.00	0.00	0.00	0	
Stnd	2.30	0.49	4.39	0.72	0.91	3.24	0	
Sprd	2.30	0.49	4.39	0.72	0.91	3.24	0	
Udklippet								
Min	-0.63	-0.14	0.70	-0.49	-0.63	0.47	0	
Max	4.87	3.59	3.69	3.93	3.96	4.87	0	
Gns	1.62	1.41	2.63	1.69	1.71	1.72	0	
Stnd	0.67	0.48	0.53	0.65	0.70	0.87	0	
Sprd	1.75	1.49	2.68	1.82	1.85	1.93	0	
Udklippet + Offset								
Min	-	-1.54	-1.93	-2.18	-2.33	-1.25	0	
Max	-	2.18	1.06	2.24	2.25	3.15	0	
Gns	-	-0.00	-0.00	0.00	0.00	0.00	0	
Stnd	-	0.48	0.53	0.65	0.70	0.87	0	
Sprd	-	0.48	0.53	0.65	0.70	0.87	0	

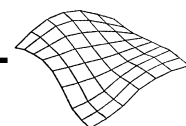
Analysefilen for 1:25,000, opløsningen 30 µm og maskestørrelsen 25 m. efter iterationsprocessen.

Fordelingen af afvigelser for 1:25.000, 60 µm, 12,5 m.

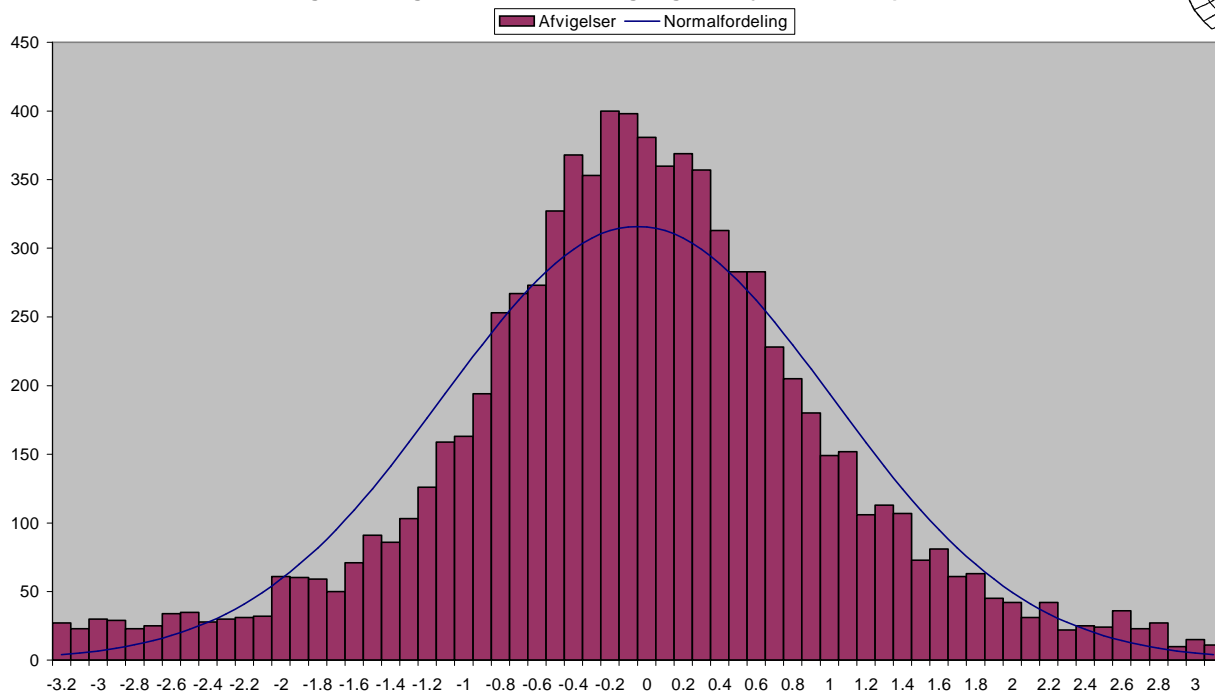


	Total	Fladt A 12	Grusgrav 34	Landsby 56	Bakket A 78	Skov 90	Ukendt 00
Min	-5.22	-1.57	-5.22	-2.49	-3.65	-3.16	0
Max	14.55	4.03	11.30	5.32	5.63	14.55	0
Gns	1.83	1.67	1.41	1.99	1.72	3.17	0
Stnd	1.56	0.64	2.34	0.94	1.03	2.36	0
Sprd	2.40	1.79	2.74	2.20	2.01	3.95	0
Antal	8929	2087	1802	1392	2805	843	0
Niv'200.0'	8929	2087	1802	1392	2805	843	0
Niv'400.0'	0	0	0	0	0	0	0
Niv'600.0'	0	0	0	0	0	0	0
Udklip.pkt	0	0	0	0	0	0	0
Areal	52611.6	721.7	45759.7	1261.2	0.0	4868.9	0.0
Niv'200.0'	52611.6	721.7	45759.7	1261.2	0.0	4868.9	0.0
Niv'400.0'	0.0	0.0	0.0	0.0	0.0	0.0	0.0
Niv'600.0'	0.0	0.0	0.0	0.0	0.0	0.0	0.0
Udklip.pkt	0.0	0.0	0.0	0.0	0.0	0.0	0.0
Udkl. i %	0.00	0.00	0.00	0.00	0.00	0.00	-0-
Offset gns.	1.83	1.67	1.41	1.99	1.72	3.17	-0-
Min	-6.63	-3.24	-6.63	-4.48	-5.37	-6.34	0
Max	11.38	2.36	9.88	3.33	3.91	11.38	0
Gns	0.00	0.00	0.00	-0.00	-0.00	0.00	0
Stnd	1.48	0.64	2.34	0.94	1.03	2.36	0
Sprd	1.48	0.64	2.34	0.94	1.03	2.36	0
Udklippet							
Min	-5.22	-1.57	-5.22	-2.49	-3.65	-3.16	0
Max	14.55	4.03	11.30	5.32	5.63	14.55	0
Gns	1.83	1.67	1.41	1.99	1.72	3.17	0
Stnd	1.56	0.64	2.34	0.94	1.03	2.36	0
Sprd	2.40	1.79	2.74	2.20	2.01	3.95	0
Udklippet + Offset							
Min	-	-3.24	-6.63	-4.48	-5.37	-6.34	0
Max	-	2.36	9.88	3.33	3.91	11.38	0
Gns	-	0.00	0.00	-0.00	-0.00	0.00	0
Stnd	-	0.64	2.34	0.94	1.03	2.36	0
Sprd	-	0.64	2.34	0.94	1.03	2.36	0

Analysefilen for 1:25,000, opløsningen 60 µm og maskestørrelsen 12.5 m. før iterationsprocessen.

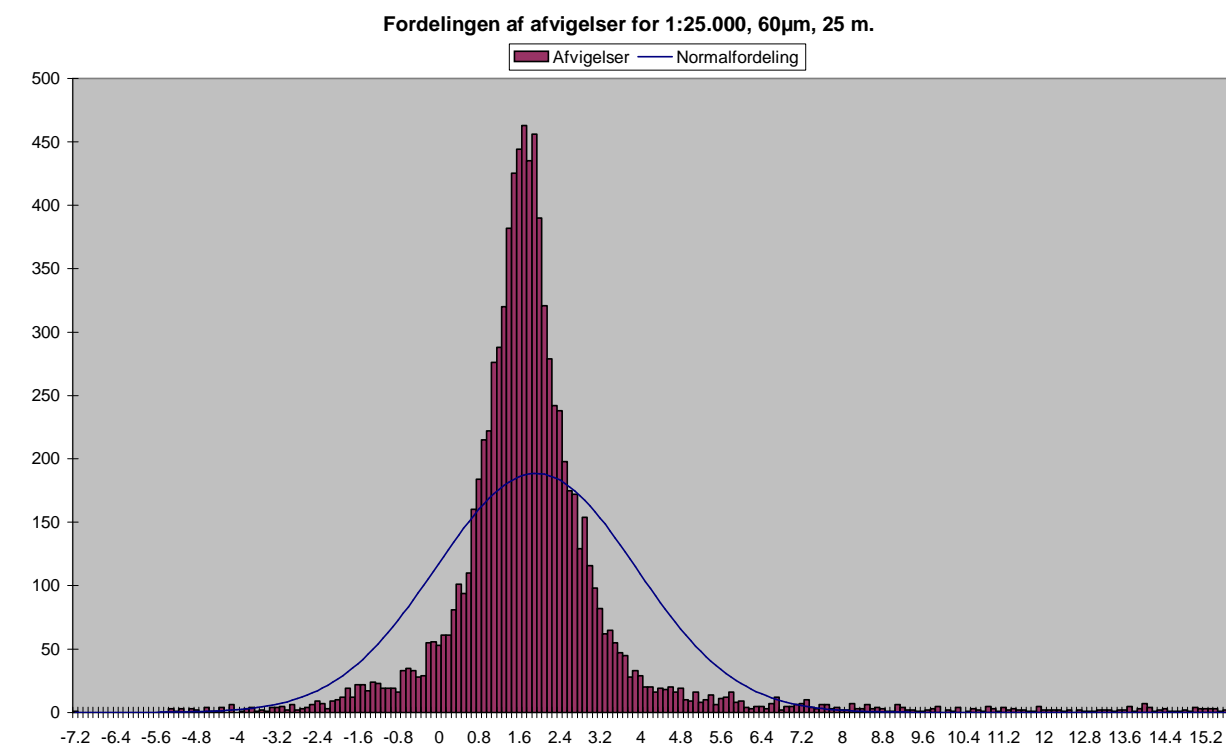


Fordelingen af afvigelser efter eliminering af grove fejl 1:25.000, 60 µm, 12,5 m.



	Total	Fladt A 12	Grusgrav 34	Landsby 56	Bakket A 78	Skov 90	Ukendt 00
Min	-5.22	-1.57	-5.22	-2.49	-3.65	-3.16	0
Max	14.55	4.03	11.30	5.32	5.63	14.55	0
Gns	1.83	1.67	1.41	1.99	1.72	3.17	0
Stnd	1.56	0.64	2.34	0.94	1.03	2.36	0
Sprd	2.40	1.79	2.74	2.20	2.01	3.95	0
Antal	8929	2087	1802	1392	2805	843	0
Niv'1.1'	1698	304	543	163	591	97	0
Niv'2.1'	3913	1351	470	597	1265	230	0
Niv'3.2'	2275	389	405	525	749	207	0
Udklip.pkt	1043	43	384	107	200	309	0
Areal	52611.6	721.7	45759.7	1261.2	0.0	4868.9	0.0
Niv'1.1'	14702.7	0.0	13713.8	490.6	0.0	498.2	0.0
Niv'2.1'	12969.0	401.7	11833.6	325.0	0.0	408.7	0.0
Niv'3.2'	11401.8	100.0	10497.9	348.5	0.0	455.4	0.0
Udklip.pkt	13538.2	220.0	9714.4	97.1	0.0	3506.6	0.0
Udkl. i %	11.68	2.06	21.31	7.69	7.13	36.65	-0-
Offset gns.	1.83	1.67	1.41	1.99	1.72	3.17	-0-
Min	-6.63	-3.24	-6.63	-4.48	-5.37	-6.34	0
Max	11.38	2.36	9.88	3.33	3.91	11.38	0
Gns	0.00	0.00	0.00	-0.00	-0.00	0.00	0
Stnd	1.48	0.64	2.34	0.94	1.03	2.36	0
Sprd	1.48	0.64	2.34	0.94	1.03	2.36	0
Udklippet							
Min	-1.73	-1.41	-1.73	-1.18	-1.40	-0.01	0
Max	6.28	4.03	4.49	5.15	4.84	6.28	0
Gns	1.83	1.67	1.50	2.02	1.74	2.61	0
Stnd	1.04	0.63	1.45	0.86	0.97	1.41	0
Sprd	2.10	1.79	2.08	2.20	1.99	2.96	0
Udklippet + Offset							
Min	-	-3.08	-3.22	-3.20	-3.14	-2.62	0
Max	-	2.36	3.00	3.13	3.10	3.68	0
Gns	-	0.00	0.00	0.00	-0.00	-0.00	0
Stnd	-	0.63	1.45	0.86	0.97	1.41	0
Sprd	-	0.63	1.45	0.86	0.97	1.41	0

Analysefilen for 1:25,000, opløsningen 60 µm og maskestørrelsen 12.5 m. efter iterationsprocessen.



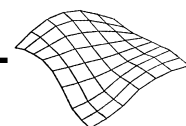
	Total	Fladt A 12	Grusgrav 34	Landsby 56	Bakket A 78	Skov 90	Ukendt 00
Min	-7.13	-1.29	-5.28	-1.47	-7.13	-3.05	0
Max	15.64	4.34	15.64	4.81	5.60	14.63	0
Gns	1.98	1.66	2.42	1.97	1.64	2.93	0
Stnd	2.00	0.55	3.65	0.90	1.07	2.48	0
Sprd	2.82	1.75	4.38	2.16	1.96	3.84	0
Antal	9041	2092	1805	1435	2811	898	0
Niv'200.0'	9041	2092	1805	1435	2811	898	0
Niv'400.0'	0	0	0	0	0	0	0
Niv'600.0'	0	0	0	0	0	0	0
Udklip.pkt	0	0	0	0	0	0	0
Areal	667180.5	72222.3	47670.5	272829.8	95868.7	178589.3	0.0
Niv'200.0'	667180.5	72222.3	47670.5	272829.8	95868.7	178589.3	0.0
Niv'400.0'	0.0	0.0	0.0	0.0	0.0	0.0	0.0
Niv'600.0'	0.0	0.0	0.0	0.0	0.0	0.0	0.0
Udklip.pkt	0.0	0.0	0.0	0.0	0.0	0.0	0.0
Udkl. i %	0.00	0.00	0.00	0.00	0.00	0.00	-0-

Offset	gns.	1.98	1.66	2.42	1.97	1.64	2.93	-0-
Min		-8.77	-2.95	-7.69	-3.44	-8.77	-5.98	0
Max		13.22	2.68	13.22	2.85	3.95	11.70	0
Gns		0.00	0.00	-0.00	0.00	0.00	0.00	0
Stnd		1.95	0.55	3.65	0.90	1.07	2.48	0
Sprd		1.95	0.55	3.65	0.90	1.07	2.48	0

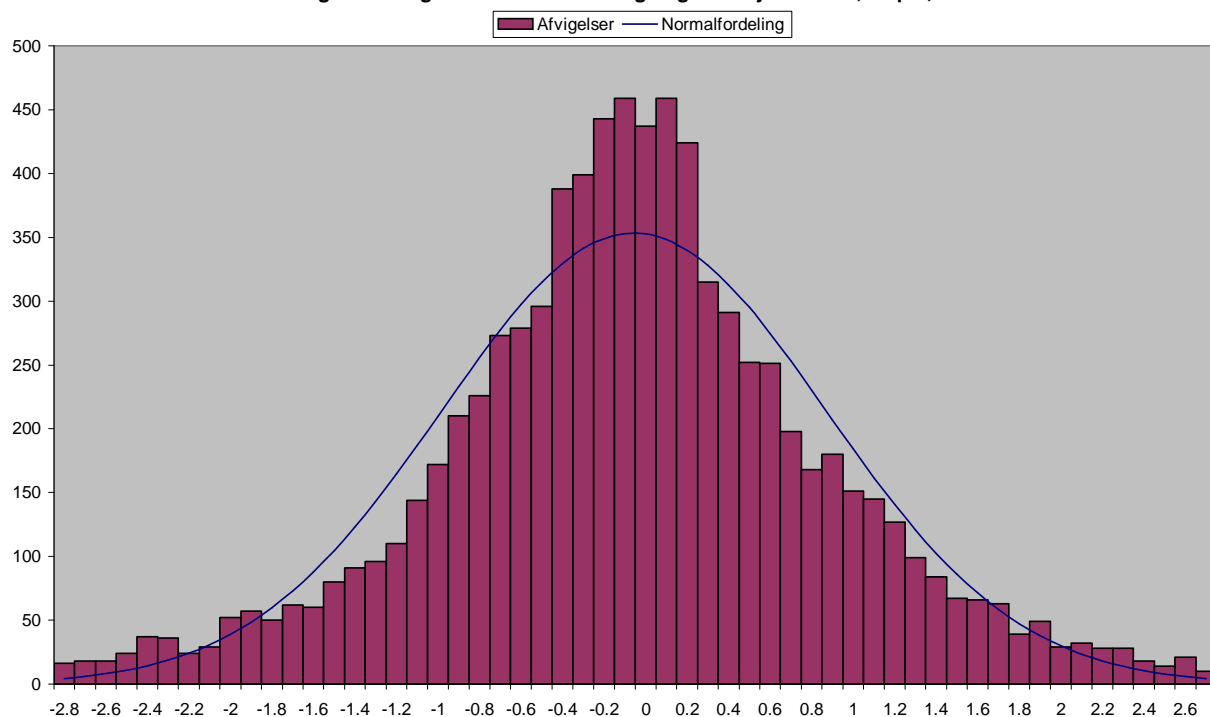
Udklippet							
Min	-7.13	-1.29	-5.28	-1.47	-7.13	-3.05	0
Max	15.64	4.34	15.64	4.81	5.60	14.63	0
Gns	1.98	1.66	2.42	1.97	1.64	2.93	0
Stnd	2.00	0.55	3.65	0.90	1.07	2.48	0
Sprd	2.82	1.75	4.38	2.16	1.96	3.84	0

Udklippet + Offset							
Min	-	-2.95	-7.69	-3.44	-8.77	-5.98	0
Max	-	2.68	13.22	2.85	3.95	11.70	0
Gns	-	0.00	-0.00	0.00	0.00	0.00	0
Stnd	-	0.55	3.65	0.90	1.07	2.48	0
Sprd	-	0.55	3.65	0.90	1.07	2.48	0

Analysefilen for 1:25,000, opløsningen 60 µm og maskestørrelsen 25 m. før iterationsprocessen.



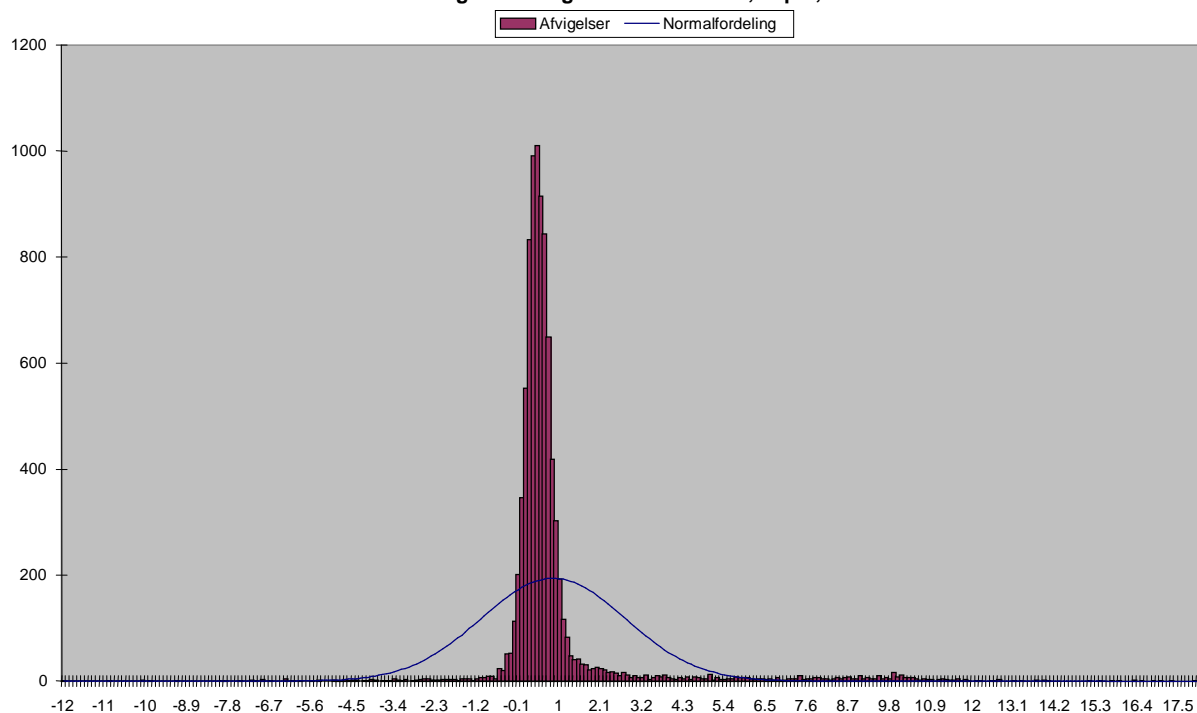
Fordelingen af afvigelser efter eliminering af grove fejl 1:25.000, 60 µm, 25 m.



	Total	Fladt A 12	Grusgrav 34	Landsby 56	Bakket A 78	Skov 90	Ukendt 00
Min	-7.13	-1.29	-5.28	-1.47	-7.13	-3.05	0
Max	15.64	4.34	15.64	4.81	5.60	14.63	0
Gns	1.98	1.68	2.42	1.95	1.67	2.89	0
Stnd	1.98	0.55	3.65	0.89	1.03	2.40	0
Sprd	2.80	1.76	4.38	2.14	1.96	3.76	0
Antal	8956	2092	1805	1401	2811	847	0
Niv'0.9'	1276	151	373	144	503	105	0
Niv'1.9'	3411	1274	406	425	1092	214	0
Niv'2.8'	2670	591	345	637	877	220	0
Udklip.pkt	1599	76	681	195	339	308	0
Areal	645893.3	72222.3	47670.5	262049.5	95868.7	168082.3	0.0
Niv'0.9'	73731.0	4320.7	10505.7	31187.2	16075.7	11641.6	0.0
Niv'1.9'	195446.0	41326.9	10661.9	73885.3	33358.0	36214.0	0.0
Niv'2.8'	228815.9	19630.4	8876.0	124250.7	31329.0	44729.8	0.0
Udklip.pkt	147900.4	6944.3	17626.9	32726.4	15105.9	75496.9	0.0
Udkl. i %	17.85	3.63	37.73	13.92	12.06	36.36	-0-
Offset gns.	1.98	1.68	2.42	1.95	1.67	2.89	-0-
Min	-8.80	-2.96	-7.69	-3.42	-8.80	-5.95	0
Max	13.22	2.66	13.22	2.87	3.93	11.74	0
Gns	-0.00	-0.00	-0.00	0.00	-0.00	0.00	0
Stnd	1.94	0.55	3.65	0.89	1.03	2.40	0
Sprd	1.94	0.55	3.65	0.89	1.03	2.40	0
Udklippet							
Min	-1.10	-0.91	0.56	-0.79	-1.10	0.13	0
Max	5.64	4.34	4.44	4.70	4.44	5.64	0
Gns	1.81	1.68	2.60	1.98	1.71	2.18	0
Stnd	0.85	0.54	0.62	0.83	0.90	1.14	0
Sprd	1.99	1.76	2.67	2.14	1.93	2.46	0
Udklippet + Offset							
Min	-	-2.59	-2.04	-2.76	-2.81	-2.05	0
Max	-	2.66	1.85	2.73	2.73	3.46	0
Gns	-	-0.00	-0.00	0.00	-0.00	-0.00	0
Stnd	-	0.54	0.62	0.83	0.90	1.14	0
Sprd	-	0.54	0.62	0.83	0.90	1.14	0

Analysefilen for 1:25,000, opløsningen 60 µm og maskestørrelsen 25 m. efter iterationsprocessen.

Fordelingen af afvigelser for 1:15.000, 15 µm, 5 m.



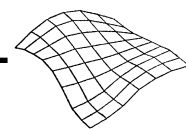
	Total	Fladt A 12	Grusgrav 34	Landsby 56	Bakket A 78	Skov 90	Ukendt 00
Min	-12.12	-1.07	-3.89	-0.75	-4.98	-12.12	0
Max	18.34	1.53	9.25	2.98	11.95	18.34	0
Gns	0.89	0.54	0.79	0.65	1.00	1.60	0
Stnd	1.93	0.29	1.65	0.45	2.11	3.58	0
Sprd	2.12	0.61	1.83	0.79	2.34	3.92	0
Antal	8766	1980	1168	1611	2811	1196	0
Niv'200.0'	8766	1980	1168	1611	2811	1196	0
Niv'400.0'	0	0	0	0	0	0	0
Niv'600.0'	0	0	0	0	0	0	0
Udklip.pkt	0	0	0	0	0	0	0
Areal	202.0	0.0	107.3	0.0	0.0	94.6	0.0
Niv'200.0'	202.0	0.0	107.3	0.0	0.0	94.6	0.0
Niv'400.0'	0.0	0.0	0.0	0.0	0.0	0.0	0.0
Niv'600.0'	0.0	0.0	0.0	0.0	0.0	0.0	0.0
Udklip.pkt	0.0	0.0	0.0	0.0	0.0	0.0	0.0
Udkl. i %	0.00	0.00	0.00	0.00	0.00	0.00	-0-

Offset	gns.	0.89	0.54	0.79	0.65	1.00	1.60	-0-
Min		-13.72	-1.61	-4.68	-1.40	-5.99	-13.72	0
Max		16.74	0.99	8.47	2.33	10.94	16.74	0
Gns		-0.00	0.00	0.00	0.00	-0.00	0.00	0
Stnd		1.90	0.29	1.65	0.45	2.11	3.58	0
Sprd		1.90	0.29	1.65	0.45	2.11	3.58	0

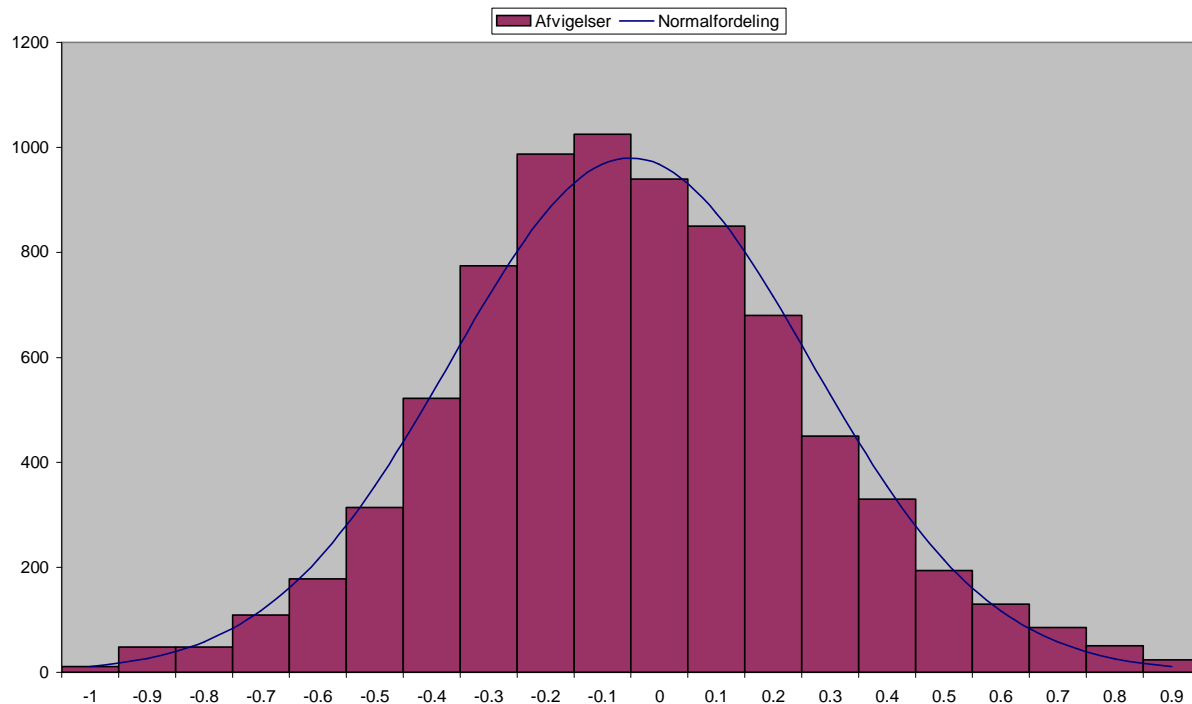
Udklippet							
Min	-12.12	-1.07	-3.89	-0.75	-4.98	-12.12	0
Max	18.34	1.53	9.25	2.98	11.95	18.34	0
Gns	0.89	0.54	0.79	0.65	1.00	1.60	0
Stnd	1.93	0.29	1.65	0.45	2.11	3.58	0
Sprd	2.12	0.61	1.83	0.79	2.34	3.92	0

Udklippet + Offset							
Min	-	-1.61	-4.68	-1.40	-5.99	-13.72	0
Max	-	0.99	8.47	2.33	10.94	16.74	0
Gns	-	0.00	0.00	0.00	-0.00	0.00	0
Stnd	-	0.29	1.65	0.45	2.11	3.58	0
Sprd	-	0.29	1.65	0.45	2.11	3.58	0

Analysefilen for 1:15,000, opløsningen 15 µm og maskestørrelsen 5 m. før iterationsprocessen.



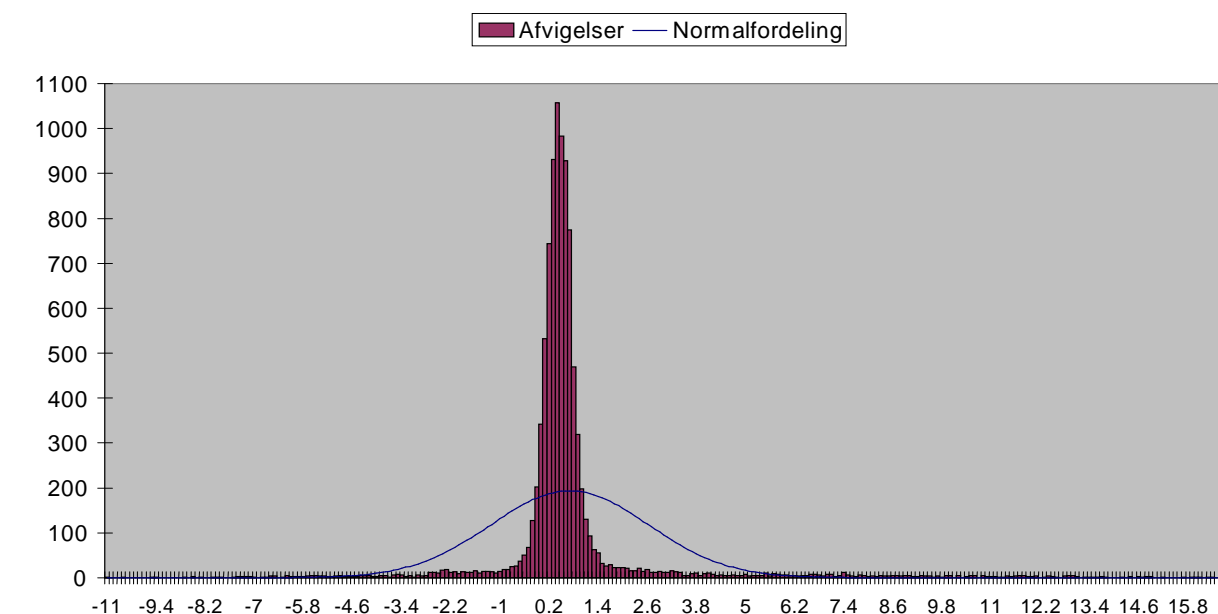
Fordelingen af afvigelser efter eliminering af grove fejl 1:15.000, 15 µm, 5 m.



	Total	Fladt A 12	Grusgrav 34	Landsby 56	Bakket A 78	Skov 90	Ukendt 00
Min	-12.12	-1.07	-3.89	-0.75	-4.98	-12.12	0
Max	18.34	1.53	9.25	2.98	11.95	18.34	0
Gns	0.89	0.54	0.79	0.65	1.00	1.60	0
Stnd	1.93	0.29	1.65	0.45	2.11	3.58	0
Sprd	2.12	0.61	1.83	0.79	2.34	3.92	0
Antal	8766	1980	1168	1611	2811	1196	0
Niv'0.3'	2298	394	484	287	766	367	0
Niv'0.6'	3172	870	333	655	1090	224	0
Niv'0.9'	1758	579	122	421	544	92	0
Udklip.pkt	1538	137	229	248	411	513	0
Areal	202.0	0.0	107.3	0.0	0.0	94.6	0.0
Niv'0.3'	54.4	0.0	54.4	0.0	0.0	0.0	0.0
Niv'0.6'	33.5	0.0	14.8	0.0	0.0	18.7	0.0
Niv'0.9'	38.1	0.0	38.1	0.0	0.0	0.0	0.0
Udklip.pkt	75.9	0.0	0.0	0.0	0.0	75.9	0.0
Udkl. i %	17.55	6.92	19.61	15.39	14.62	42.89	-0-
Offset gns.	0.89	0.54	0.79	0.65	1.00	1.60	-0-
Min	-13.72	-1.61	-4.68	-1.40	-5.99	-13.72	0
Max	16.74	0.99	8.47	2.33	10.94	16.74	0
Gns	-0.00	0.00	0.00	0.00	-0.00	0.00	0
Stnd	1.90	0.29	1.65	0.45	2.11	3.58	0
Sprd	1.90	0.29	1.65	0.45	2.11	3.58	0
Udklippet							
Min	-0.39	-0.39	-0.16	-0.25	0.06	0.65	0
Max	2.53	1.48	1.73	1.58	1.84	2.53	0
Gns	0.55	0.54	0.40	0.58	0.52	1.34	0
Stnd	0.35	0.28	0.36	0.31	0.28	0.53	0
Sprd	0.65	0.61	0.54	0.65	0.59	1.44	0
Udklippet + Offset							
Min	-	-0.93	-0.57	-0.83	-0.47	-0.69	0
Max	-	0.94	1.33	1.00	1.32	1.19	0
Gns	-	-0.00	-0.00	0.00	-0.00	-0.00	0
Stnd	-	0.28	0.36	0.31	0.28	0.53	0
Sprd	-	0.28	0.36	0.31	0.28	0.53	0

Analysefilen for 1:15,000, opløsningen 15 µm og maskestørrelsen 5 m. efter iterationsprocessen.

Fordelingen af afvigelser for 1:15.000, 15 µm, 12,5 m.



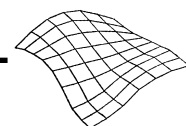
	Total	Fladt A 12	Grusgrav 34	Landsby 56	Bakket A 78	Skov 90	Ukendt 00
Min	-10.56	-0.85	-7.72	-1.69	-7.43	-10.56	0
Max	16.69	1.85	13.31	3.36	12.68	16.69	0
Gns	0.75	0.54	1.12	0.56	0.52	1.38	0
Stnd	1.93	0.25	2.84	0.38	0.88	3.77	0
Sprd	2.07	0.59	3.05	0.68	1.02	4.02	0
Antal	9355	1975	1802	1592	2805	1181	0
Niv'200.0'	9355	1975	1802	1592	2805	1181	0
Niv'400.0'	0	0	0	0	0	0	0
Niv'600.0'	0	0	0	0	0	0	0
Udklip.pkt	0	0	0	0	0	0	0
Areal	57434.9	721.7	45759.7	1800.3	0.0	9153.1	0.0
Niv'200.0'	57434.9	721.7	45759.7	1800.3	0.0	9153.1	0.0
Niv'400.0'	0.0	0.0	0.0	0.0	0.0	0.0	0.0
Niv'600.0'	0.0	0.0	0.0	0.0	0.0	0.0	0.0
Udklip.pkt	0.0	0.0	0.0	0.0	0.0	0.0	0.0
Udkl. i %	0.00	0.00	0.00	0.00	0.00	0.00	-0-

Offset	gns. 0.75	0.54	1.12	0.56	0.52	1.38	-0-
Min	-11.94	-1.39	-8.84	-2.25	-7.95	-11.94	0
Max	15.31	1.32	12.20	2.80	12.16	15.31	0
Gns	-0.00	0.00	0.00	-0.00	-0.00	0.00	0
Stnd	1.90	0.25	2.84	0.38	0.88	3.77	0
Sprd	1.90	0.25	2.84	0.38	0.88	3.77	0

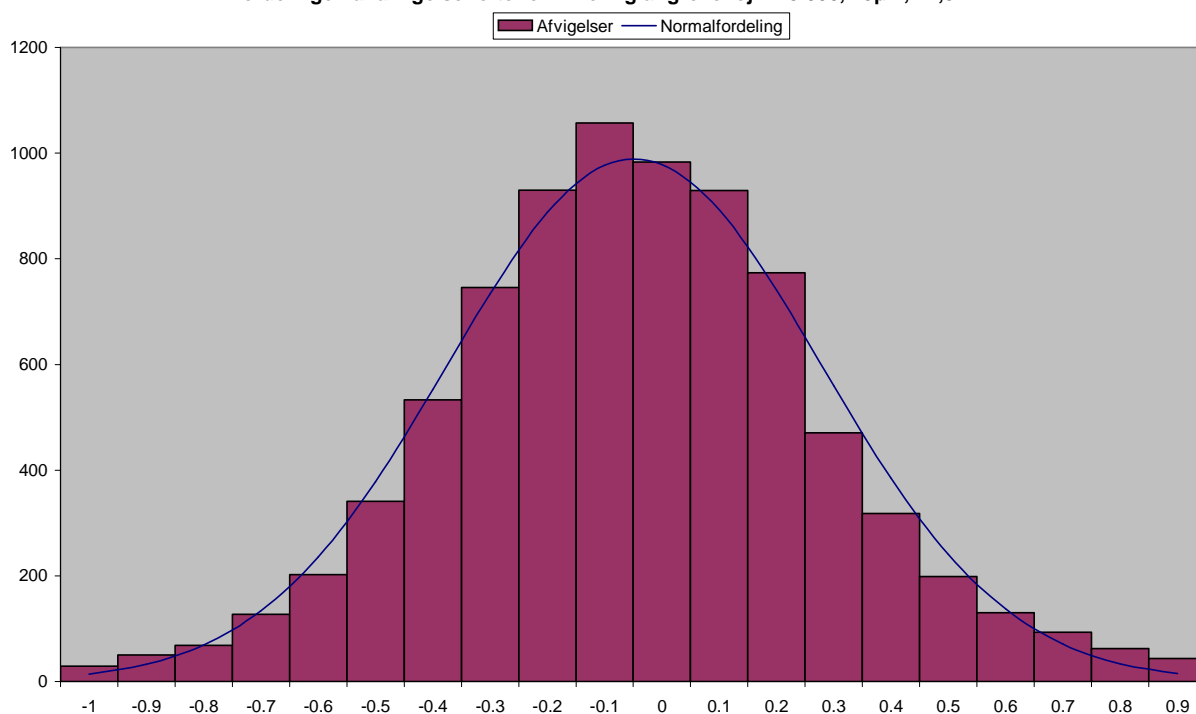
Udklippet							
Min	-10.56	-0.85	-7.72	-1.69	-7.43	-10.56	0
Max	16.69	1.85	13.31	3.36	12.68	16.69	0
Gns	0.75	0.54	1.12	0.56	0.52	1.38	0
Stnd	1.94	0.25	2.84	0.38	0.88	3.77	0
Sprd	2.07	0.59	3.05	0.68	1.02	4.02	0

Udklippet + Offset							
Min	-	-1.39	-8.84	-2.25	-7.95	-11.94	0
Max	-	1.32	12.20	2.80	12.16	15.31	0
Gns	-	0.00	0.00	-0.00	-0.00	0.00	0
Stnd	-	0.25	2.84	0.38	0.88	3.77	0
Sprd	-	0.25	2.84	0.38	0.88	3.77	0

Analysefilen for 1:15,000, opløsningen 15 µm og maskestørrelsen 12.5 m. før iterationsprocessen.



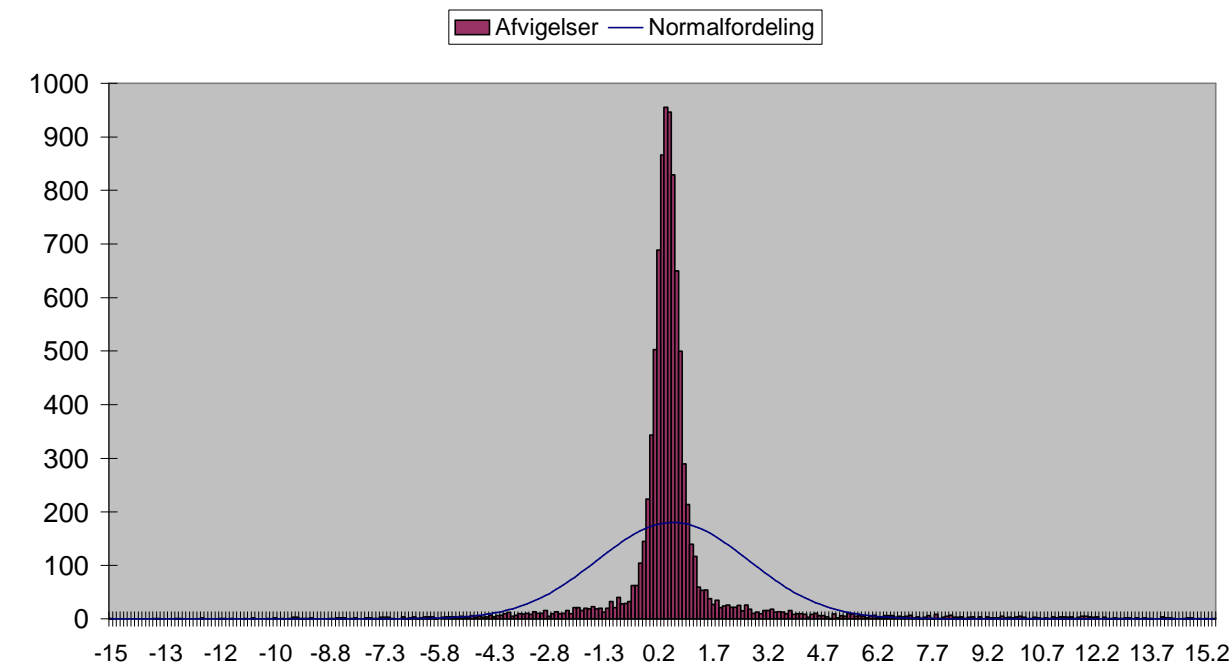
Fordelingen af afvigelser efter eliminerings af grove fejl: 1:15.000, 15µm, 12,5 m.



	Total	Fladt A 12	Grusgrav 34	Landsby 56	Bakket A 78	Skov 90	Ukendt 00	
Min	-10.56	-0.85	-7.72	-1.69	-7.43	-10.56	0	
Max	16.69	1.85	13.31	3.36	12.68	16.69	0	
Gns	0.75	0.54	1.12	0.56	0.52	1.38	0	
Stnd	1.93	0.25	2.84	0.38	0.88	3.77	0	
Sprd	2.07	0.59	3.05	0.68	1.02	4.02	0	
Antal	9355	1975	1802	1592	2805	1181	0	
Niv'0.3'	2300	397	311	333	872	387	0	
Niv'0.6'	2274	619	194	489	799	173	0	
Niv'1.0'	3028	897	445	642	858	186	0	
Udklip.pkt	1753	62	852	128	276	435	0	
Areal	57434.9	721.7	45759.7	1800.3	0.0	9153.1	0.0	
Niv'0.3'	9487.3	0.0	7918.7	544.9	0.0	1023.7	0.0	
Niv'0.6'	6177.2	0.0	4898.2	487.7	0.0	791.3	0.0	
Niv'1.0'	13825.3	520.8	11468.5	625.0	0.0	1211.0	0.0	
Udklip.pkt	27945.1	200.8	21474.3	142.9	0.0	6127.1	0.0	
Udkl. i %	18.74	3.14	47.28	8.04	9.84	36.83	-0-	
Offset	gns.	0.75	0.54	1.12	0.56	0.52	1.38	-0-
Min	-11.94	-1.39	-8.84	-2.25	-7.95	-11.94	0	
Max	15.31	1.32	12.20	2.80	12.16	15.31	0	
Gns	-0.00	0.00	0.00	-0.00	-0.00	0.00	0	
Stnd	1.90	0.25	2.84	0.38	0.88	3.77	0	
Sprd	1.90	0.25	2.84	0.38	0.88	3.77	0	
Udklippet								
Min	-0.45	-0.40	0.20	-0.39	-0.45	0.40	0	
Max	2.35	1.45	1.66	1.54	1.50	2.35	0	
Gns	0.54	0.53	0.82	0.54	0.48	0.87	0	
Stnd	0.31	0.24	0.28	0.28	0.30	0.48	0	
Sprd	0.62	0.59	0.87	0.61	0.56	0.99	0	
Udklippet + Offset								
Min	-	-0.93	-0.63	-0.93	-0.92	-0.46	0	
Max	-	0.91	0.83	1.00	1.02	1.49	0	
Gns	-	-0.00	-0.00	-0.00	-0.00	0.00	0	
Stnd	-	0.24	0.28	0.28	0.30	0.48	0	
Sprd	-	0.24	0.28	0.28	0.30	0.48	0	

Analysefilen for 1:15,000, opløsningen 15 µm og maskestørrelsen 12.5 m. efter iterationsprocessen.

Fordelingen af afvigelse for 1:15.000, 15µm, 25 m.



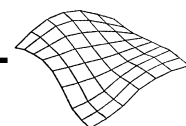
	Total	Fladt A 12	Grusgrav 34	Landsby 56	Bakket A 78	Skov 90	Ukendt 00
Min	-14.71	-0.60	-7.22	-1.79	-9.50	-14.71	0
Max	15.46	4.54	15.46	3.65	14.08	12.09	0
Gns	0.64	0.53	1.48	0.54	0.50	0.05	0
Stnd	2.07	0.29	3.57	0.43	1.17	3.12	0
Sprd	2.17	0.61	3.86	0.69	1.27	3.12	0
Antal	9370	1980	1775	1611	2811	1193	0
Niv'200.0'	9370	1980	1775	1611	2811	1193	0
Niv'400.0'	0	0	0	0	0	0	0
Niv'600.0'	0	0	0	0	0	0	0
Udklip.pkt	0	0	0	0	0	0	0
Areal	803020.7	70567.2	46920.5	331645.2	95868.7	258019.2	0.0
Niv'200.0'	803020.7	70567.2	46920.5	331645.2	95868.7	258019.2	0.0
Niv'400.0'	0.0	0.0	0.0	0.0	0.0	0.0	0.0
Niv'600.0'	0.0	0.0	0.0	0.0	0.0	0.0	0.0
Udklip.pkt	0.0	0.0	0.0	0.0	0.0	0.0	0.0
Udkl. i %	0.00	0.00	0.00	0.00	0.00	0.00	-0-

Offset	gns. 0.64	0.53	1.48	0.54	0.50	0.05	-0-
Min	-14.75	-1.13	-8.70	-2.33	-10.00	-14.75	0
Max	13.98	4.00	13.98	3.11	13.59	12.05	0
Gns	-0.00	0.00	-0.00	0.00	0.00	-0.00	0
Stnd	2.03	0.29	3.57	0.43	1.17	3.12	0
Sprd	2.03	0.29	3.57	0.43	1.17	3.12	0

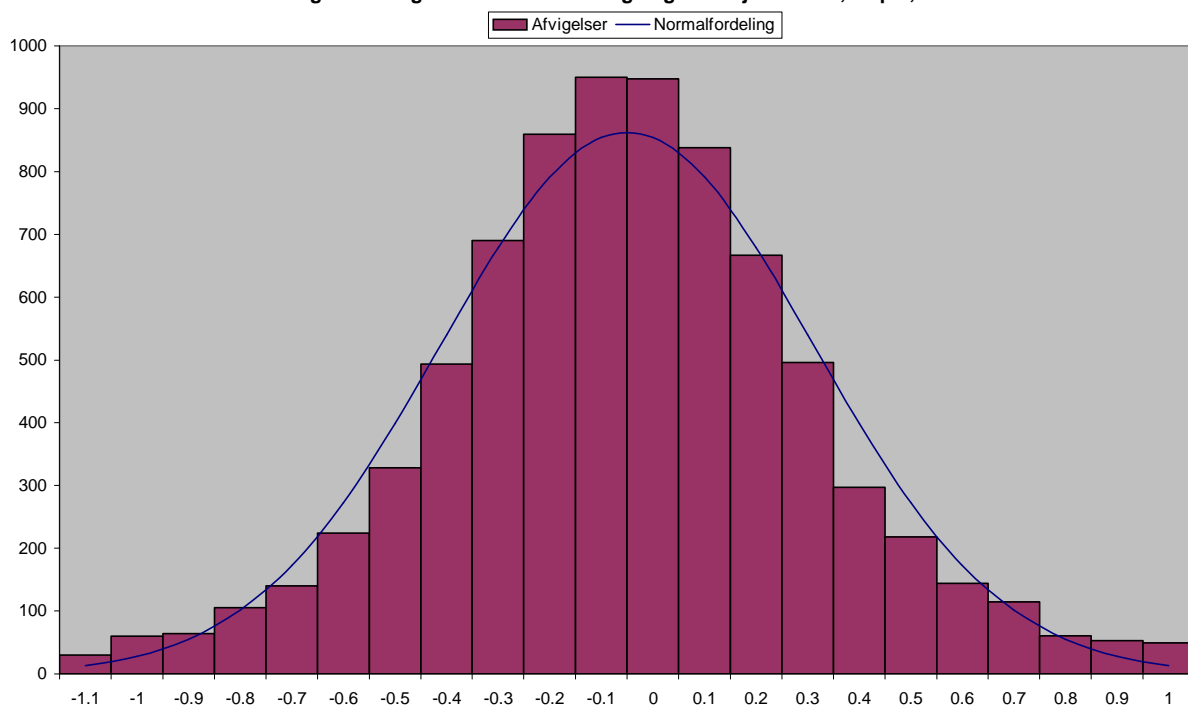
Udklippet							
Min	-14.71	-0.60	-7.22	-1.79	-9.50	-14.71	0
Max	15.46	4.54	15.46	3.65	14.08	12.09	0
Gns	0.64	0.53	1.48	0.54	0.50	0.05	0
Stnd	2.07	0.29	3.57	0.43	1.17	3.12	0
Sprd	2.17	0.61	3.86	0.69	1.27	3.12	0

Udklippet + Offset							
Min	-	-1.13	-8.70	-2.33	-10.00	-14.75	0
Max	-	4.00	13.98	3.11	13.59	12.05	0
Gns	-	0.00	-0.00	0.00	0.00	-0.00	0
Stnd	-	0.29	3.57	0.43	1.17	3.12	0
Sprd	-	0.29	3.57	0.43	1.17	3.12	0

Analysefilen for 1:15,000, opløsningen 15 µm og maskestørrelsen 25 m. før iterationsprocessen.

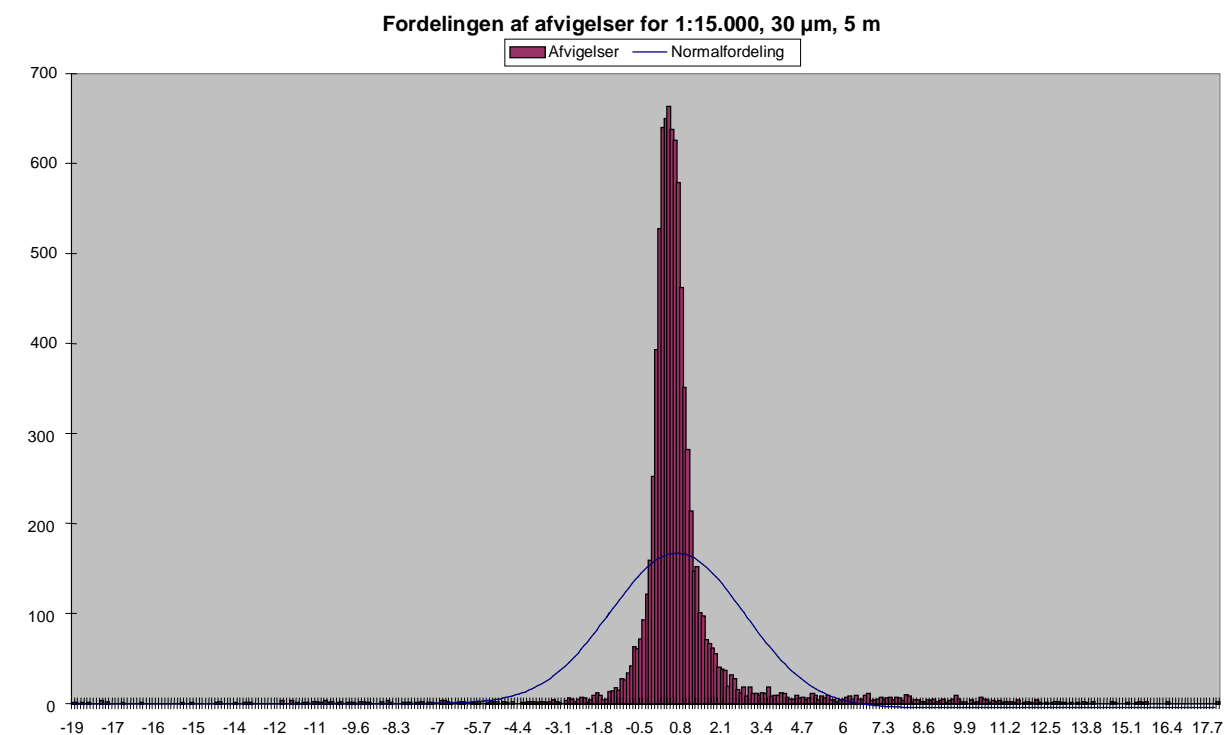


Fordelingen af afvigelser efter eliminering af grove fejl 1:15.000, 15 µm, 25 m.



	Total	Fladt A 12	Grusgrav 34	Landsby 56	Bakket A 78	Skov 90	Ukendt 00
Min	-14.71	-0.60	-7.22	-1.79	-9.50	-14.71	0
Max	15.46	4.54	15.46	3.65	14.08	12.09	0
Gns	0.64	0.53	1.48	0.54	0.50	0.05	0
Stnd	2.07	0.29	3.57	0.43	1.17	3.12	0
Sprd	2.17	0.61	3.86	0.69	1.27	3.12	0
Antal	9370	1980	1775	1611	2811	1193	0
Niv'0.4'	2519	504	251	434	963	367	0
Niv'0.7'	3408	1038	310	760	1034	266	0
Niv'1.1'	1614	388	289	321	486	130	0
Udklip.pkt	1829	50	925	96	328	430	0
Areal	803020.7	70567.2	46920.5	331645.2	95868.7	258019.2	0.0
Niv'0.4'	174978.0	14495.4	7462.4	79145.5	21113.6	52761.1	0.0
Niv'0.7'	300108.7	37244.3	8161.4	151541.7	39500.7	63660.6	0.0
Niv'1.1'	145980.1	15048.9	7593.0	74137.6	20266.2	28934.5	0.0
Udklip.pkt	181953.9	3778.7	23703.7	26820.4	14988.1	112662.9	0.0
Udkl. i %	19.52	2.53	52.11	5.96	11.67	36.04	-0-
Offset gns.	0.64	0.53	1.48	0.54	0.50	0.05	-0-
Min	-14.75	-1.13	-8.70	-2.33	-10.00	-14.75	0
Max	13.98	4.00	13.98	3.11	13.59	12.05	0
Gns	-0.00	0.00	-0.00	0.00	0.00	-0.00	0
Stnd	2.03	0.29	3.57	0.43	1.17	3.12	0
Sprd	2.03	0.29	3.57	0.43	1.17	3.12	0
Udklippet							
Min	-0.98	-0.49	0	-0.51	-0.59	-0.98	0
Max	1.58	1.57	0	1.58	1.58	1.13	0
Gns	0.48	0.53	0	0.52	0.47	0.25	0
Stnd	0.34	0.27	0	0.31	0.35	0.41	0
Sprd	0.58	0.59	0	0.61	0.59	0.48	0
Udklippet + Offset							
Min	-	-1.01	0	-1.03	-1.06	-1.23	0
Max	-	1.04	0	1.06	1.11	0.88	0
Gns	-	-0.00	0	0.00	-0.00	-0.00	0
Stnd	-	0.27	0	0.31	0.35	0.41	0
Sprd	-	0.27	0	0.31	0.35	0.41	0

Analysefilen for 1:15,000, opløsningen 15 µm og maskestørrelsen 25 m. efter iterationsprocessen.



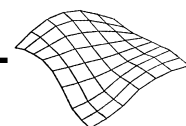
	Total	Fladt A 12	Grusgrav 34	Landsby 56	Bakket A 78	Skov 90	Ukendt 00
Min	-18.62	-0.51	-1.95	-2.70	-18.62	-14.83	0
Max	18.09	3.50	13.90	4.45	6.14	18.09	0
Gns	0.80	0.47	1.30	0.84	0.30	1.96	0
Stnd	2.17	0.37	2.86	0.67	1.75	4.03	0
Sprd	2.31	0.60	3.14	1.08	1.77	4.48	0
Antal	8766	1980	1168	1611	2811	1196	0
Niv'200.0'	8766	1980	1168	1611	2811	1196	0
Niv'400.0'	0	0	0	0	0	0	0
Niv'600.0'	0	0	0	0	0	0	0
Udklip.pkt	0	0	0	0	0	0	0
Areal	202.0	0.0	107.3	0.0	0.0	94.6	0.0
Niv'200.0'	202.0	0.0	107.3	0.0	0.0	94.6	0.0
Niv'400.0'	0.0	0.0	0.0	0.0	0.0	0.0	0.0
Niv'600.0'	0.0	0.0	0.0	0.0	0.0	0.0	0.0
Udklip.pkt	0.0	0.0	0.0	0.0	0.0	0.0	0.0
Udkl. i %	0.00	0.00	0.00	0.00	0.00	0.00	-0-

Offset	gns.	0.80	0.47	1.30	0.84	0.30	1.96	-0-
Min		-18.92	-0.98	-3.25	-3.53	-18.92	-16.79	0
Max		16.13	3.03	12.60	3.62	5.84	16.13	0
Gns		0.00	0.00	-0.00	-0.00	-0.00	0.00	0
Stnd		2.10	0.37	2.86	0.67	1.75	4.03	0
Sprd		2.10	0.37	2.86	0.67	1.75	4.03	0

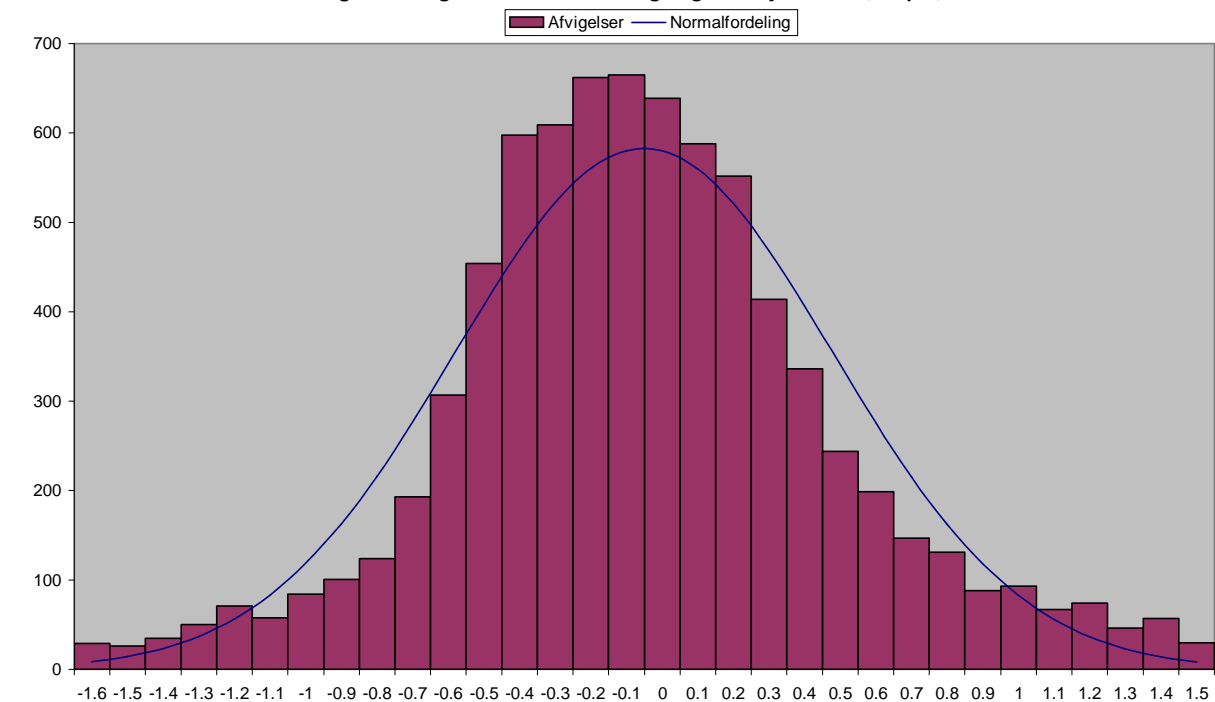
Udklippet								
Min		-18.62	-0.51	-1.95	-2.70	-18.62	-14.83	0
Max		18.09	3.50	13.90	4.45	6.14	18.09	0
Gns		0.80	0.47	1.30	0.84	0.30	1.96	0
Stnd		2.17	0.37	2.86	0.67	1.75	4.03	0
Sprd		2.31	0.60	3.14	1.08	1.77	4.48	0

Udklippet + Offset								
Min	-		-0.98	-3.25	-3.53	-18.92	-16.79	0
Max	-		3.03	12.60	3.62	5.84	16.13	0
Gns	-		0.00	-0.00	-0.00	-0.00	0.00	0
Stnd	-		0.37	2.86	0.67	1.75	4.03	0
Sprd	-		0.37	2.86	0.67	1.75	4.03	0

Analysefilen for 1:15,000, opløsningen 30 µm og maskestørrelsen 5 m. før iterationsprocessen.



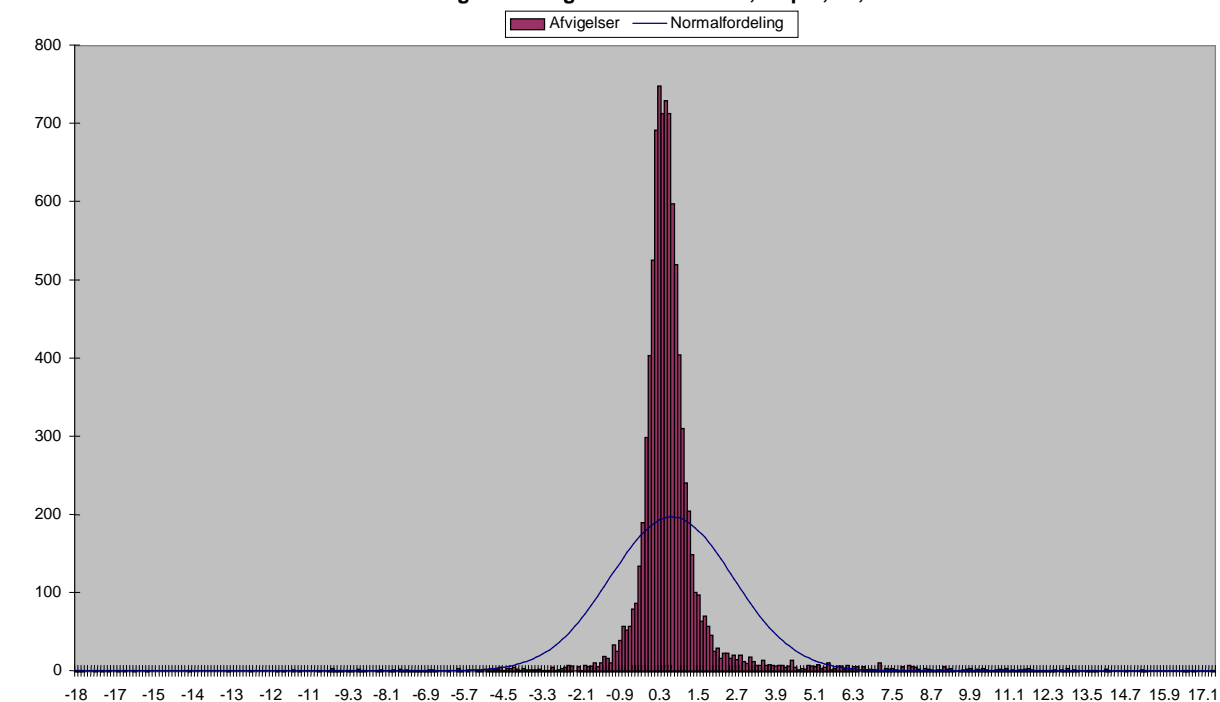
Fordelingen af afvigelser efter eliminering af grove fejl 1:15.000, 30 µm, 5 m.



	Total	Fladt A 12	Grusgrav 34	Landsby 56	Bakket A 78	Skov 90	Ukendt 00
Min	-18.62	-0.51	-1.95	-2.70	-18.62	-14.83	0
Max	18.09	3.50	13.90	4.45	6.14	18.09	0
Gns	0.80	0.47	1.30	0.84	0.30	1.96	0
Stnd	2.17	0.37	2.86	0.67	1.75	4.03	0
Sprd	2.31	0.60	3.14	1.08	1.77	4.48	0
Antal	8766	1980	1168	1611	2811	1196	0
Niv'0.5'	3783	1158	528	465	1433	199	0
Niv'1.1'	2864	721	261	656	953	273	0
Niv'1.6'	890	82	130	310	242	126	0
Udklip.pkt	1229	19	249	180	183	598	0
Areal	202.0	0.0	107.3	0.0	0.0	94.6	0.0
Niv'0.5'	54.4	0.0	54.4	0.0	0.0	0.0	0.0
Niv'1.1'	52.9	0.0	52.9	0.0	0.0	0.0	0.0
Niv'1.6'	3.3	0.0	0.0	0.0	0.0	3.3	0.0
Udklip.pkt	91.3	0.0	0.0	0.0	0.0	91.3	0.0
Udkl. i %	14.02	0.96	21.32	11.17	6.51	50.00	-0-
Offset gns.	0.80	0.47	1.30	0.84	0.30	1.96	-0-
Min	-18.92	-0.98	-3.25	-3.53	-18.92	-16.79	0
Max	16.13	3.03	12.60	3.62	5.84	16.13	0
Gns	0.00	0.00	-0.00	-0.00	-0.00	0.00	0
Stnd	2.10	0.37	2.86	0.67	1.75	4.03	0
Sprd	2.10	0.37	2.86	0.67	1.75	4.03	0
Udklippet							
Min	-1.30	-0.51	-0.30	-0.73	-1.30	0.38	0
Max	3.55	1.99	2.88	2.43	1.89	3.55	0
Gns	0.63	0.47	0.54	0.82	0.49	1.37	0
Stnd	0.60	0.35	0.64	0.55	0.46	0.82	0
Sprd	0.86	0.59	0.84	0.99	0.68	1.60	0
Udklippet + Offset							
Min	-	-0.98	-0.83	-1.56	-1.79	-1.00	0
Max	-	1.52	2.35	1.60	1.40	2.18	0
Gns	-	-0.00	0.00	-0.00	-0.00	0.00	0
Stnd	-	0.35	0.64	0.55	0.46	0.82	0
Sprd	-	0.35	0.64	0.55	0.46	0.82	0

Analysefilen for 1:15,000, opløsningen 30 µm og maskestørrelsen 5 m. efter iterationsprocessen.

Fordelingen af afvigelser for 1:15.000, 30 µm, 12,5 m.



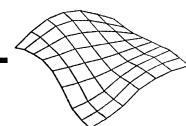
	Total	Fladt A 12	Grusgrav 34	Landsby 56	Bakket A 78	Skov 90	Ukendt 00
Min	-17.68	-0.56	-6.57	-1.80	-17.68	-12.26	0
Max	17.42	2.16	12.00	4.36	5.25	17.42	0
Gns	0.73	0.44	0.81	0.71	0.35	2.01	0
Stnd	1.90	0.34	1.92	0.55	1.56	3.79	0
Sprd	2.03	0.56	2.09	0.90	1.60	4.29	0
Antal	9355	1975	1802	1592	2805	1181	0
Niv'200.0'	9355	1975	1802	1592	2805	1181	0
Niv'400.0'	0	0	0	0	0	0	0
Niv'600.0'	0	0	0	0	0	0	0
Udklip.pkt	0	0	0	0	0	0	0
Areal	57434.9	721.7	45759.7	1800.3	0.0	9153.1	0.0
Niv'200.0'	57434.9	721.7	45759.7	1800.3	0.0	9153.1	0.0
Niv'400.0'	0.0	0.0	0.0	0.0	0.0	0.0	0.0
Niv'600.0'	0.0	0.0	0.0	0.0	0.0	0.0	0.0
Udklip.pkt	0.0	0.0	0.0	0.0	0.0	0.0	0.0
Udkl. i %	0.00	0.00	0.00	0.00	0.00	0.00	-0-

Offset	gns. 0.73	0.44	0.81	0.71	0.35	2.01	-0-
Min	-18.03	-1.00	-7.37	-2.51	-18.03	-14.27	0
Max	15.41	1.72	11.19	3.65	4.90	15.41	0
Gns	0.00	0.00	-0.00	-0.00	0.00	-0.00	0
Stnd	1.82	0.34	1.92	0.55	1.56	3.79	0
Sprd	1.82	0.34	1.92	0.55	1.56	3.79	0

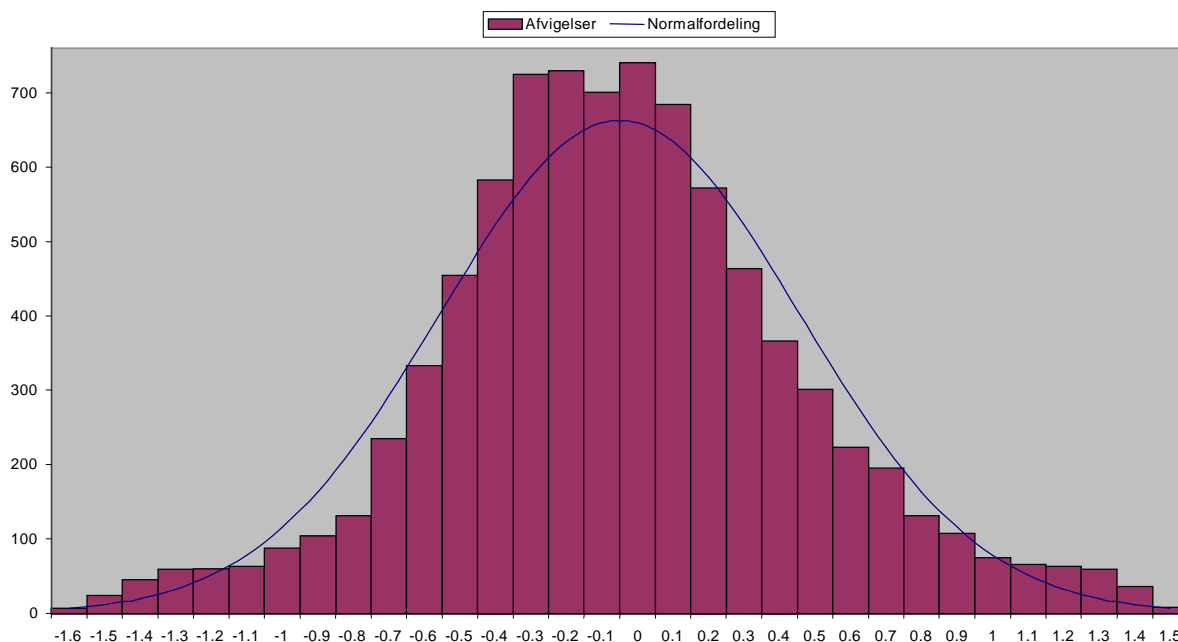
Udklippet							
Min	-17.68	-0.56	-6.57	-1.80	-17.68	-12.26	0
Max	17.42	2.16	12.00	4.36	5.25	17.42	0
Gns	0.73	0.44	0.81	0.71	0.35	2.01	0
Stnd	1.90	0.34	1.92	0.55	1.56	3.79	0
Sprd	2.03	0.56	2.09	0.90	1.60	4.29	0

Udklippet + Offset							
Min	-	-1.00	-7.37	-2.51	-18.03	-14.27	0
Max	-	1.72	11.19	3.65	4.90	15.41	0
Gns	-	0.00	-0.00	-0.00	0.00	-0.00	0
Stnd	-	0.34	1.92	0.55	1.56	3.79	0
Sprd	-	0.34	1.92	0.55	1.56	3.79	0

Analysefilen for 1:15,000, opløsningen 30 µm og maskestørrelsen 12.5 m. før iterationsprocessen.



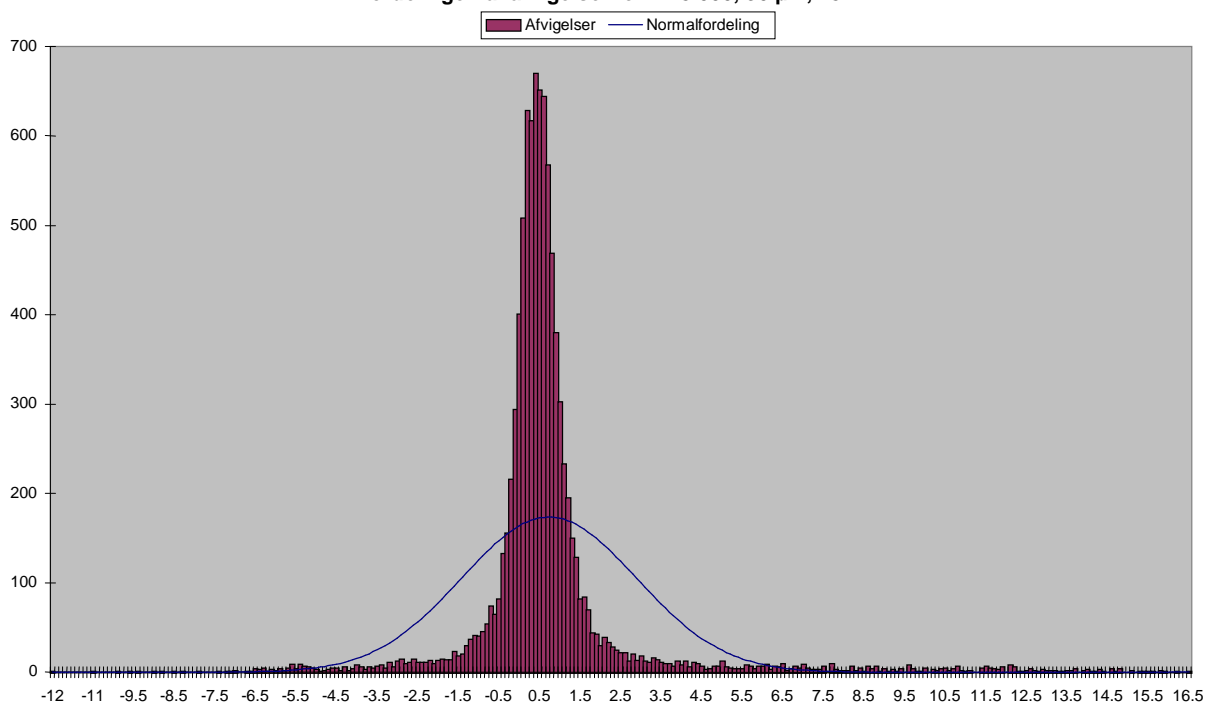
Fordelingen af afvigelser efter eliminering af grove fejl: 15.000, 30 µm, 12,5 m.



	Total	Fladt A 12	Grusgrav 34	Landsby 56	Bakket A 78	Skov 90	Ukendt 00
Min	-17.68	-0.56	-6.57	-1.80	-17.68	-12.26	0
Max	17.42	2.16	12.00	4.36	5.25	17.42	0
Gns	0.73	0.44	0.81	0.71	0.35	2.01	0
Stnd	1.90	0.34	1.92	0.55	1.56	3.79	0
Sprd	2.03	0.56	2.09	0.90	1.60	4.29	0
Antal	9355	1975	1802	1592	2805	1181	0
Niv'0.5'	3947	1165	513	529	1393	347	0
Niv'1.0'	3192	721	567	677	955	272	0
Niv'1.5'	1066	80	297	285	266	138	0
Udklip.pkt	1150	9	425	101	191	424	0
Areal	57434.9	721.7	45759.7	1800.3	0.0	9153.1	0.0
Niv'0.5'	15066.0	0.0	12926.9	692.0	0.0	1447.0	0.0
Niv'1.0'	17006.2	501.7	14585.8	515.3	0.0	1403.4	0.0
Niv'1.5'	9036.7	220.0	7526.9	593.1	0.0	696.8	0.0
Udklip.pkt	16326.0	0.0	10720.1	0.0	0.0	5605.9	0.0
Udkl. i %	12.29	0.46	23.58	6.34	6.81	35.90	-0-
Offset gns.	0.73	0.44	0.81	0.71	0.35	2.01	-0-
Min	-18.03	-1.00	-7.37	-2.51	-18.03	-14.27	0
Max	15.41	1.72	11.19	3.65	4.90	15.41	0
Gns	0.00	0.00	-0.00	-0.00	0.00	-0.00	0
Stnd	1.82	0.34	1.92	0.55	1.56	3.79	0
Sprd	1.82	0.34	1.92	0.55	1.56	3.79	0
Udklippet							
Min	-1.16	-0.56	-0.71	-0.75	-1.16	0.50	0
Max	3.53	1.90	1.91	2.21	1.86	3.53	0
Gns	0.59	0.44	0.64	0.70	0.50	1.28	0
Stnd	0.52	0.33	0.47	0.48	0.46	0.76	0
Sprd	0.78	0.55	0.79	0.85	0.68	1.49	0
Udklippet + Offset							
Min	-	-1.00	-1.35	-1.45	-1.66	-0.78	0
Max	-	1.46	1.27	1.51	1.37	2.25	0
Gns	-	-0.00	-0.00	-0.00	-0.00	0.00	0
Stnd	-	0.33	0.47	0.48	0.46	0.76	0
Sprd	-	0.33	0.47	0.48	0.46	0.76	0

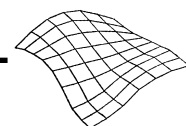
Analysefilen for 1:15,000, opløsningen 30 µm og maskestørrelsen 12.5 m. efter iterationsprocessen.v

Fordelingen af afvigelser for 1:15.000, 30 µm, 25 m.

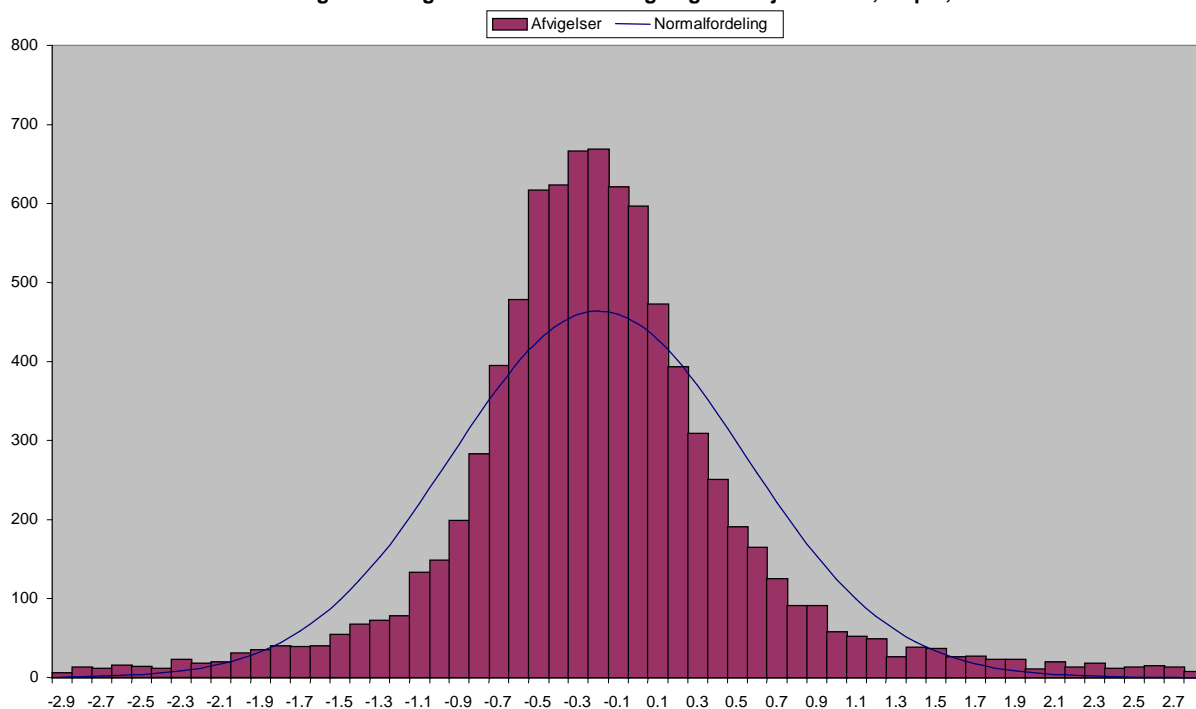


	Total	Fladt A 12	Grusgrav 34	Landsby 56	Bakket A 78	Skov 90	Ukendt 00
Min	-11.49	-1.00	-7.09	-2.17	-8.99	-11.49	0
Max	16.55	2.40	15.13	3.50	13.98	16.55	0
Gns	0.79	0.44	1.24	0.69	0.49	1.53	0
Stnd	2.15	0.36	3.43	0.56	1.23	3.67	0
Sprd	2.29	0.57	3.65	0.89	1.32	3.98	0
Antal	9370	1980	1775	1611	2811	1193	0
Niv'200.0'	9370	1980	1775	1611	2811	1193	0
Niv'400.0'	0	0	0	0	0	0	0
Niv'600.0'	0	0	0	0	0	0	0
Udklip.pkt	0	0	0	0	0	0	0
Areal	803020.7	70567.2	46920.5	331645.2	95868.7	258019.2	0.0
Niv'200.0'	803020.7	70567.2	46920.5	331645.2	95868.7	258019.2	0.0
Niv'400.0'	0.0	0.0	0.0	0.0	0.0	0.0	0.0
Niv'600.0'	0.0	0.0	0.0	0.0	0.0	0.0	0.0
Udklip.pkt	0.0	0.0	0.0	0.0	0.0	0.0	0.0
Udkl. i %	0.00	0.00	0.00	0.00	0.00	0.00	-0-
Offset gns.	0.79	0.44	1.24	0.69	0.49	1.53	-0-
Min	-13.02	-1.44	-8.33	-2.85	-9.48	-13.02	0
Max	15.02	1.96	13.90	2.81	13.49	15.02	0
Gns	-0.00	-0.00	-0.00	-0.00	0.00	0.00	0
Stnd	2.12	0.36	3.43	0.56	1.23	3.67	0
Sprd	2.12	0.36	3.43	0.56	1.23	3.67	0
Udklippet							
Min	-11.49	-1.00	-7.09	-2.17	-8.99	-11.49	0
Max	16.55	2.40	15.13	3.50	13.98	16.55	0
Gns	0.79	0.44	1.24	0.69	0.49	1.53	0
Stnd	2.16	0.36	3.43	0.56	1.23	3.67	0
Sprd	2.29	0.57	3.65	0.89	1.32	3.98	0
Udklippet + Offset							
Min	-	-1.44	-8.33	-2.85	-9.48	-13.02	0
Max	-	1.96	13.90	2.81	13.49	15.02	0
Gns	-	-0.00	-0.00	-0.00	0.00	0.00	0
Stnd	-	0.36	3.43	0.56	1.23	3.67	0
Sprd	-	0.36	3.43	0.56	1.23	3.67	0

Analysefilen for 1:15,000, opløsningen 30 µm og maskestørrelsen 25 m. før iterationsprocessen.



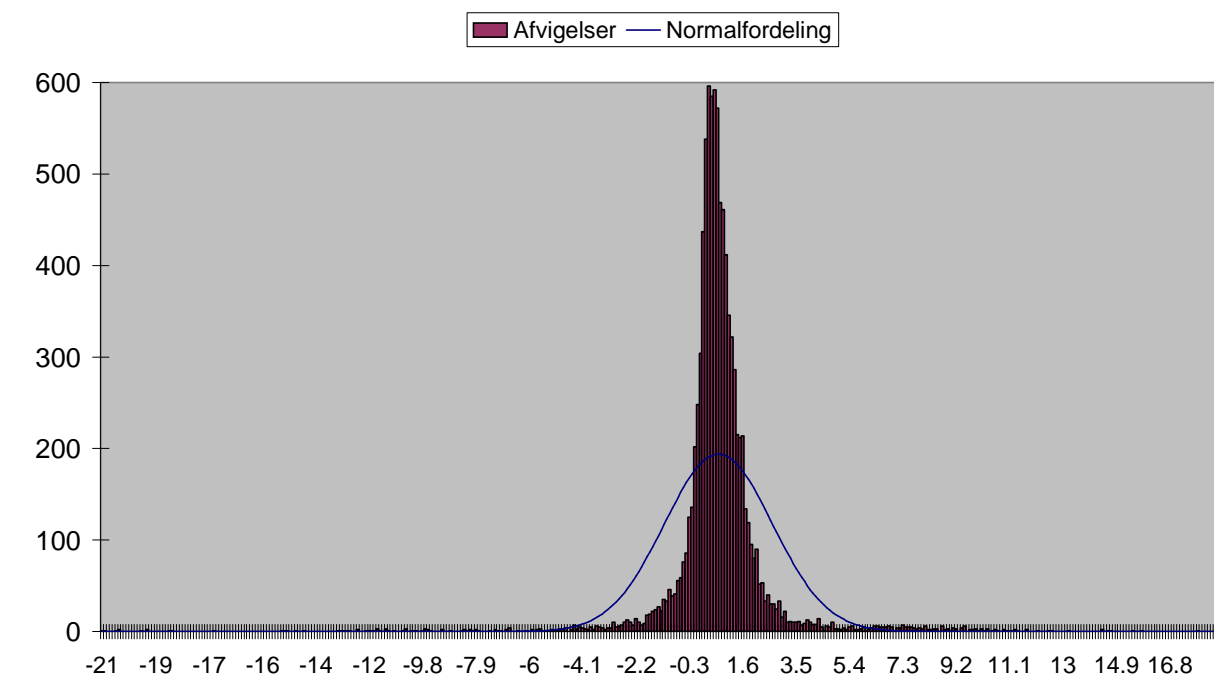
Fordelingen af afvigelser efter eliminering af grove fejl 1:15.000, 30 µm, 25 m.



	Total	Fladt A 12	Grusgrav 34	Landsby 56	Bakket A 78	Skov 90	Ukendt 00
Min	-11.49	-1.00	-7.09	-2.17	-8.99	-11.49	0
Max	16.55	2.40	15.13	3.50	13.98	16.55	0
Gns	0.79	0.44	1.24	0.69	0.49	1.53	0
Stnd	2.15	0.36	3.43	0.56	1.23	3.67	0
Sprd	2.29	0.57	3.65	0.89	1.32	3.98	0
Antal	9370	1980	1775	1611	2811	1193	0
Niv'0.4'	2657	845	271	326	961	254	0
Niv'0.7'	2624	729	320	514	846	215	0
Niv'1.1'	1715	334	299	425	481	176	0
Udklip.pkt	2374	72	885	346	523	548	0
Areal	803020.7	70567.2	46920.5	331645.2	95868.7	258019.2	0.0
Niv'0.4'	140158.5	23863.0	7599.9	43783.6	25842.5	39069.6	0.0
Niv'0.7'	207176.4	29466.9	8480.0	94440.3	34425.7	40363.5	0.0
Niv'1.1'	177752.6	11990.1	7897.2	100526.0	18715.3	38624.1	0.0
Udklip.pkt	277933.2	5247.3	22943.4	92895.3	16885.2	139962.0	0.0
Udkl. i %	25.34	3.64	49.86	21.48	18.61	45.93	-0-
Offset	gns. 0.79	0.44	1.24	0.69	0.49	1.53	-0-
Min	-13.02	-1.44	-8.33	-2.85	-9.48	-13.02	0
Max	15.02	1.96	13.90	2.81	13.49	15.02	0
Gns	-0.00	-0.00	-0.00	-0.00	0.00	0.00	0
Stnd	2.12	0.36	3.43	0.56	1.23	3.67	0
Sprd	2.12	0.36	3.43	0.56	1.23	3.67	0
Udklippet							
Min	-0.61	-0.61	0.38	-0.40	-0.60	0.44	0
Max	2.60	1.53	1.43	1.77	1.57	2.60	0
Gns	0.53	0.43	0.96	0.68	0.46	1.05	0
Stnd	0.46	0.33	0.26	0.42	0.45	0.53	0
Sprd	0.69	0.54	0.99	0.80	0.64	1.17	0
Udklippet + Offset							
Min	-	-1.04	-0.58	-1.08	-1.06	-0.60	0
Max	-	1.10	0.47	1.09	1.10	1.55	0
Gns	-	0.00	-0.00	-0.00	-0.00	0.00	0
Stnd	-	0.33	0.26	0.42	0.45	0.53	0
Sprd	-	0.33	0.26	0.42	0.45	0.53	0

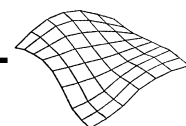
Analysefilen for 1:15,000, opløsningen 30 µm og maskestørrelsen 25 m. efter iterationsprocessen.

Fordelingen af afvigelser for 1:15.000, 60µm, 12,5 m.

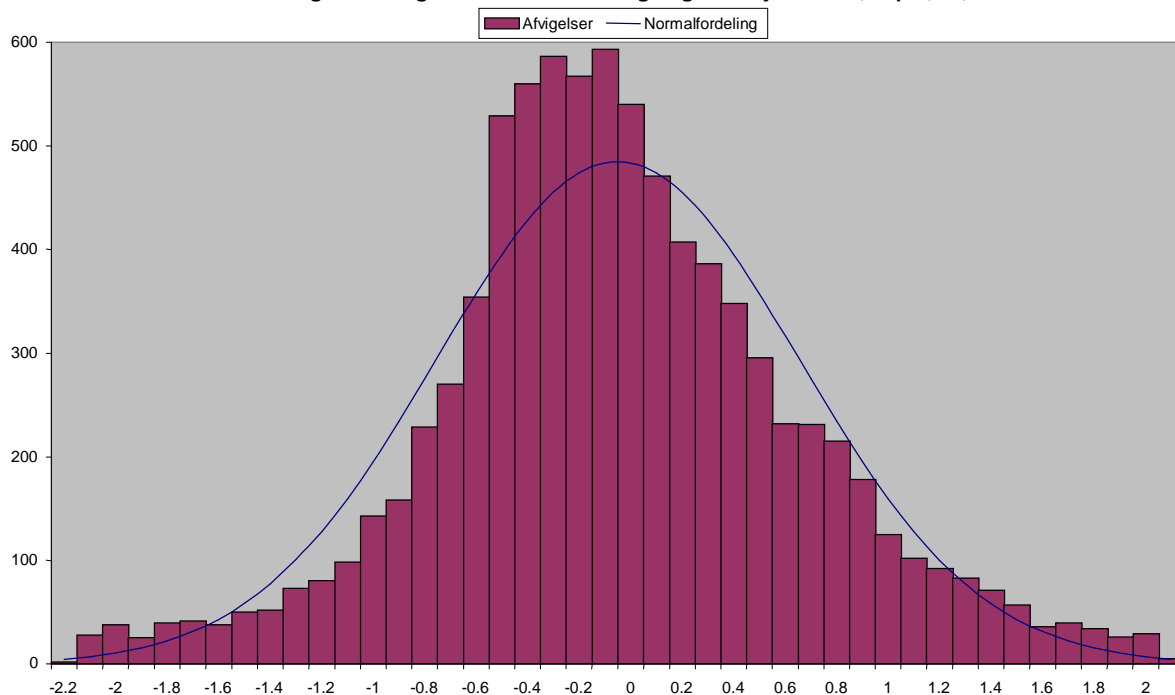


	Total	Fladt A 12	Grusgrav 34	Landsby 56	Bakket A 78	Skov 90	Ukendt 00
Min	-21.11	-1.03	-5.86	-2.52	-21.11	-14.77	0
Max	18.53	2.98	11.43	3.62	4.84	18.53	0
Gns	0.79	0.59	0.48	1.10	0.45	1.97	0
Stnd	1.93	0.39	1.64	0.71	1.92	3.67	0
Sprd	2.08	0.71	1.71	1.31	1.97	4.17	0
Antal	9355	1975	1802	1592	2805	1181	0
Niv'200.0'	9355	1975	1802	1592	2805	1181	0
Niv'400.0'	0	0	0	0	0	0	0
Niv'600.0'	0	0	0	0	0	0	0
Udklip.pkt	0	0	0	0	0	0	0
Areal	57434.9	721.7	45759.7	1800.3	0.0	9153.1	0.0
Niv'200.0'	57434.9	721.7	45759.7	1800.3	0.0	9153.1	0.0
Niv'400.0'	0.0	0.0	0.0	0.0	0.0	0.0	0.0
Niv'600.0'	0.0	0.0	0.0	0.0	0.0	0.0	0.0
Udklip.pkt	0.0	0.0	0.0	0.0	0.0	0.0	0.0
Udkl. i %	0.00	0.00	0.00	0.00	0.00	0.00	-0-
Offset gns.	0.79	0.59	0.48	1.10	0.45	1.97	-0-
Min	-21.56	-1.63	-6.34	-3.62	-21.56	-16.75	0
Max	16.56	2.39	10.95	2.52	4.40	16.56	0
Gns	-0.00	0.00	0.00	0.00	-0.00	-0.00	0
Stnd	1.86	0.39	1.64	0.71	1.92	3.67	0
Sprd	1.86	0.39	1.64	0.71	1.92	3.67	0
Udklippet							
Min	-21.11	-1.03	-5.86	-2.52	-21.11	-14.77	0
Max	18.53	2.98	11.43	3.62	4.84	18.53	0
Gns	0.79	0.59	0.48	1.10	0.45	1.97	0
Stnd	1.94	0.39	1.64	0.71	1.92	3.67	0
Sprd	2.08	0.71	1.71	1.31	1.97	4.17	0
Udklippet + Offset							
Min	-	-1.63	-6.34	-3.62	-21.56	-16.75	0
Max	-	2.39	10.95	2.52	4.40	16.56	0
Gns	-	0.00	0.00	0.00	-0.00	-0.00	0
Stnd	-	0.39	1.64	0.71	1.92	3.67	0
Sprd	-	0.39	1.64	0.71	1.92	3.67	0

Analysefilen for 1:15,000, opløsningen 60 µm og maskestørrelsen 12.5 m. før iterationsprocessen.



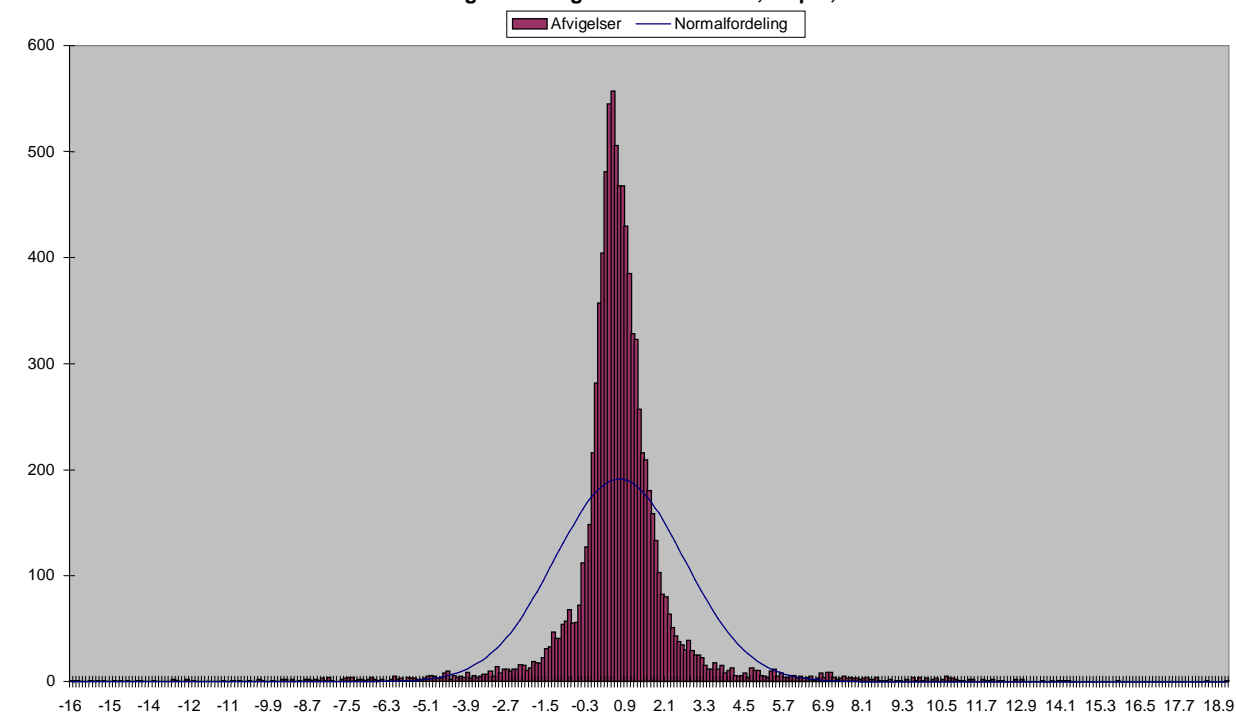
Fordelingen af afvigelser efter eliminering af grove fejl: 1:15.000, 60µm, 12,5 m.



	Total	Fladt A 12	Grusgrav 34	Landsby 56	Bakket A 78	Skov 90	Ukendt 00
Min	-21.11	-1.03	-5.86	-2.52	-21.11	-14.77	0
Max	18.53	2.98	11.43	3.62	4.84	18.53	0
Gns	0.79	0.59	0.48	1.10	0.45	1.97	0
Stnd	1.93	0.39	1.64	0.71	1.92	3.67	0
Sprd	2.08	0.71	1.71	1.31	1.97	4.17	0
Antal	9355	1975	1802	1592	2805	1181	0
Niv'0.7'	4105	1339	676	404	1392	294	0
Niv'1.4'	3047	574	605	669	943	256	0
Niv'2.1'	1190	54	262	414	302	158	0
Udklip.pkt	1013	8	259	105	168	473	0
Areal	57434.9	721.7	45759.7	1800.3	0.0	9153.1	0.0
Niv'0.7'	18436.8	291.7	17045.7	565.6	0.0	533.8	0.0
Niv'1.4'	17746.9	210.0	15558.6	466.6	0.0	1511.7	0.0
Niv'2.1'	7952.2	220.0	6623.4	407.7	0.0	701.0	0.0
Udklip.pkt	13299.0	0.0	6532.0	360.3	0.0	6406.6	0.0
Udkl. i %	10.83	0.41	14.37	6.60	5.99	40.05	-0-
Offset gns.	0.79	0.59	0.48	1.10	0.45	1.97	-0-
Min	-21.56	-1.63	-6.34	-3.62	-21.56	-16.75	0
Max	16.56	2.39	10.95	2.52	4.40	16.56	0
Gns	-0.00	0.00	0.00	0.00	-0.00	-0.00	0
Stnd	1.86	0.39	1.64	0.71	1.92	3.67	0
Sprd	1.86	0.39	1.64	0.71	1.92	3.67	0
Udklippet							
Min	-1.65	-1.03	-1.60	-0.98	-1.65	-0.12	0
Max	4.08	2.57	2.52	3.13	2.54	4.08	0
Gns	0.80	0.59	0.59	1.12	0.67	1.35	0
Stnd	0.74	0.38	0.72	0.65	0.64	1.00	0
Sprd	1.07	0.71	0.93	1.29	0.93	1.69	0
Udklippet + Offset							
Min	-	-1.62	-2.19	-2.10	-2.32	-1.47	0
Max	-	1.98	1.93	2.01	1.87	2.73	0
Gns	-	0.00	-0.00	-0.00	0.00	0.00	0
Stnd	-	0.38	0.72	0.65	0.64	1.00	0
Sprd	-	0.38	0.72	0.65	0.64	1.00	0

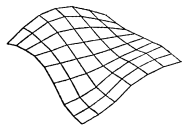
Analysefilen for 1:15,000, opløsningen 60 µm og maskestørrelsen 12.5 m. efter iterationsprocessen.

Fordelingen af afvigelser for 1:15.000, 60 µm, 25 m.

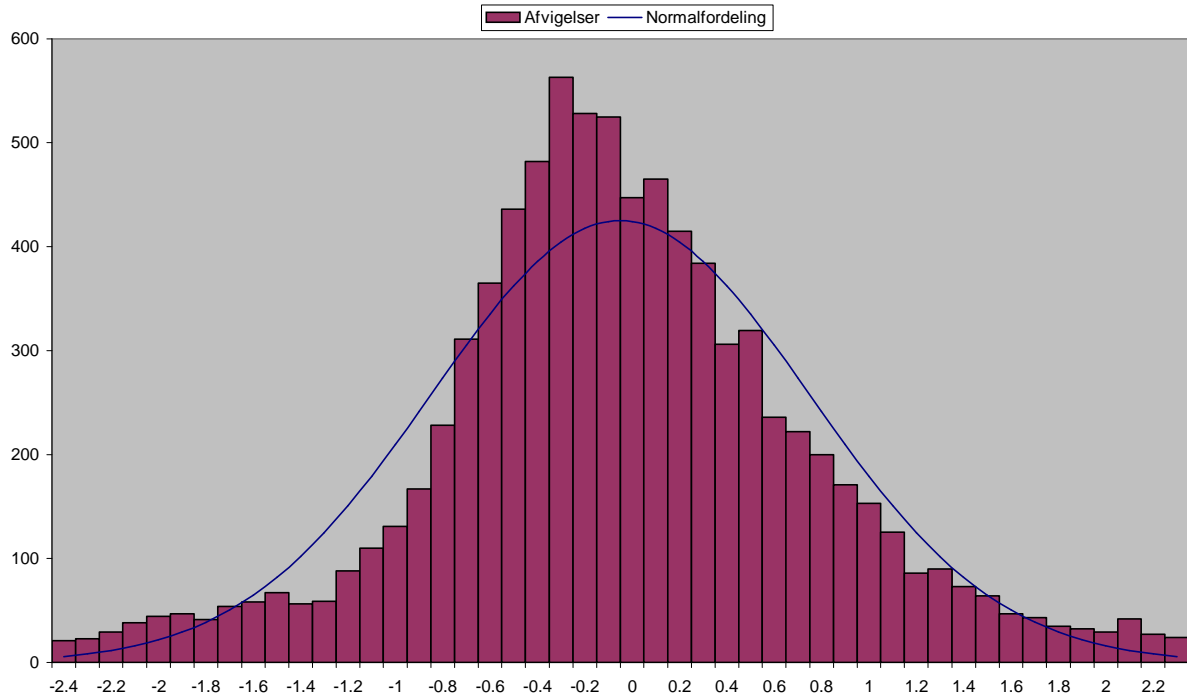


	Total	Fladt A 12	Grusgrav 34	Landsby 56	Bakket A 78	Skov 90	Ukendt 00
Min	-15.89	-1.73	-12.71	-1.98	-15.89	-13.86	0
Max	19.16	2.69	9.82	3.14	5.50	19.16	0
Gns	0.76	0.54	0.43	1.09	0.53	1.72	0
Stnd	1.96	0.45	2.39	0.70	1.61	3.60	0
Sprd	2.10	0.70	2.43	1.30	1.70	3.99	0
Antal	9370	1980	1775	1611	2811	1193	0
Niv'200.0'	9370	1980	1775	1611	2811	1193	0
Niv'400.0'	0	0	0	0	0	0	0
Niv'600.0'	0	0	0	0	0	0	0
Udklip.pkt	0	0	0	0	0	0	0
Areal	803020.7	70567.2	46920.5	331645.2	95868.7	258019.2	0.0
Niv'200.0'	803020.7	70567.2	46920.5	331645.2	95868.7	258019.2	0.0
Niv'400.0'	0.0	0.0	0.0	0.0	0.0	0.0	0.0
Niv'600.0'	0.0	0.0	0.0	0.0	0.0	0.0	0.0
Udklip.pkt	0.0	0.0	0.0	0.0	0.0	0.0	0.0
Udkl. i %	0.00	0.00	0.00	0.00	0.00	0.00	-0-
Offset gns.	0.76	0.54	0.43	1.09	0.53	1.72	-0-
Min	-16.42	-2.27	-13.14	-3.07	-16.42	-15.58	0
Max	17.44	2.15	9.39	2.04	4.97	17.44	0
Gns	-0.00	0.00	-0.00	-0.00	-0.00	-0.00	0
Stnd	1.91	0.45	2.39	0.70	1.61	3.60	0
Sprd	1.91	0.45	2.39	0.70	1.61	3.60	0
Udklippet							
Min	-15.89	-1.73	-12.71	-1.98	-15.89	-13.86	0
Max	19.16	2.69	9.82	3.14	5.50	19.16	0
Gns	0.76	0.54	0.43	1.09	0.53	1.72	0
Stnd	1.97	0.45	2.39	0.70	1.61	3.60	0
Sprd	2.10	0.70	2.43	1.30	1.70	3.99	0
Udklippet + Offset							
Min	-	-2.27	-13.14	-3.07	-16.42	-15.58	0
Max	-	2.15	9.39	2.04	4.97	17.44	0
Gns	-	0.00	-0.00	-0.00	-0.00	-0.00	0
Stnd	-	0.45	2.39	0.70	1.61	3.60	0
Sprd	-	0.45	2.39	0.70	1.61	3.60	0

Analysefilen for 1:15,000, opløsningen 60 µm og maskestørrelsen 25 m. før iterationsprocessen.



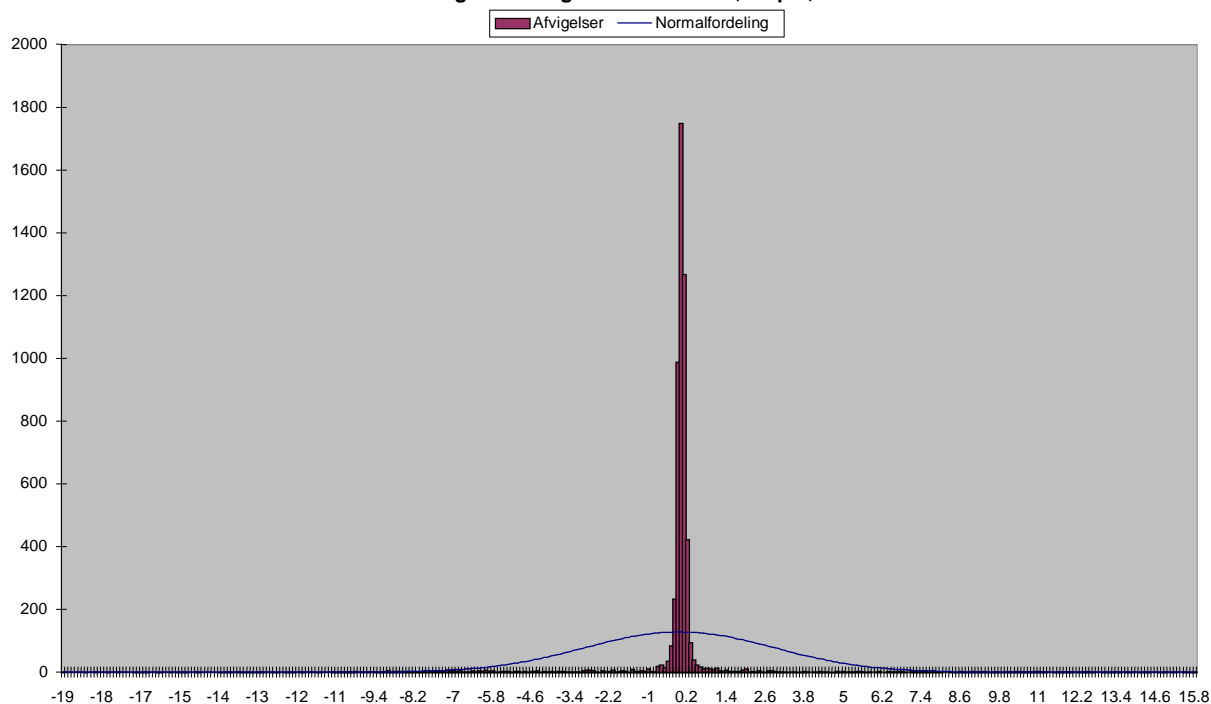
Fordelingen af afvigelser efter eliminering af grove fejl 1:15.000, 60 µm, 25 m.



	Total	Fladt A 12	Grusgrav 34	Landsby 56	Bakket A 78	Skov 90	Ukendt 00
Min	-15.89	-1.73	-12.71	-1.98	-15.89	-13.86	0
Max	19.16	2.69	9.82	3.14	5.50	19.16	0
Gns	0.76	0.54	0.43	1.09	0.53	1.72	0
Stnd	1.96	0.45	2.39	0.70	1.61	3.60	0
Sprd	2.10	0.70	2.43	1.30	1.70	3.99	0
Antal	9370	1980	1775	1611	2811	1193	0
Niv'0.8'	4454	1536	577	488	1496	357	0
Niv'1.6'	2943	393	563	746	933	308	0
Niv'2.4'	973	48	210	339	220	156	0
Udklip.pkt	1000	3	425	38	162	372	0
Areal	803020.7	70567.2	46920.5	331645.2	95868.7	258019.2	0.0
Niv'0.8'	238385.9	50969.9	15765.6	61667.4	52000.6	57982.4	0.0
Niv'1.6'	292787.3	16714.5	15028.0	164750.5	33718.5	62575.8	0.0
Niv'2.4'	151125.9	2882.8	5454.4	93137.4	8614.2	41037.2	0.0
Udklip.pkt	120721.6	0.0	10672.5	12089.9	1535.3	96423.8	0.0
Udkl. i %	10.67	0.15	23.94	2.36	5.76	31.18	-0-
Offset	gns. 0.76	0.54	0.43	1.09	0.53	1.72	-0-
Min	-16.42	-2.27	-13.14	-3.07	-16.42	-15.58	0
Max	17.44	2.15	9.39	2.04	4.97	17.44	0
Gns	-0.00	0.00	-0.00	-0.00	-0.00	-0.00	0
Stnd	1.91	0.45	2.39	0.70	1.61	3.60	0
Sprd	1.91	0.45	2.39	0.70	1.61	3.60	0
Udklippet							
Min	-1.87	-1.73	-1.54	-1.27	-1.87	-0.66	0
Max	4.08	2.69	1.72	3.14	2.92	4.08	0
Gns	0.78	0.54	0.79	1.11	0.67	1.10	0
Stnd	0.76	0.45	0.57	0.67	0.71	0.97	0
Sprd	1.06	0.70	0.97	1.30	0.98	1.47	0
Udklippet + Offset							
Min	-	-2.27	-2.33	-2.38	-2.54	-1.76	0
Max	-	2.15	0.93	2.03	2.25	2.98	0
Gns	-	0.00	-0.00	-0.00	-0.00	-0.00	0
Stnd	-	0.45	0.57	0.67	0.71	0.97	0
Sprd	-	0.45	0.57	0.67	0.71	0.97	0

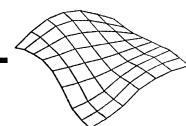
Analysefilen for 1:15,000, opløsningen 60 µm og maskestørrelsen 25 m. efter iterationsprocessen.

Fordelingen af afvigelser for 1:5.000, 15 µm, 5 m.

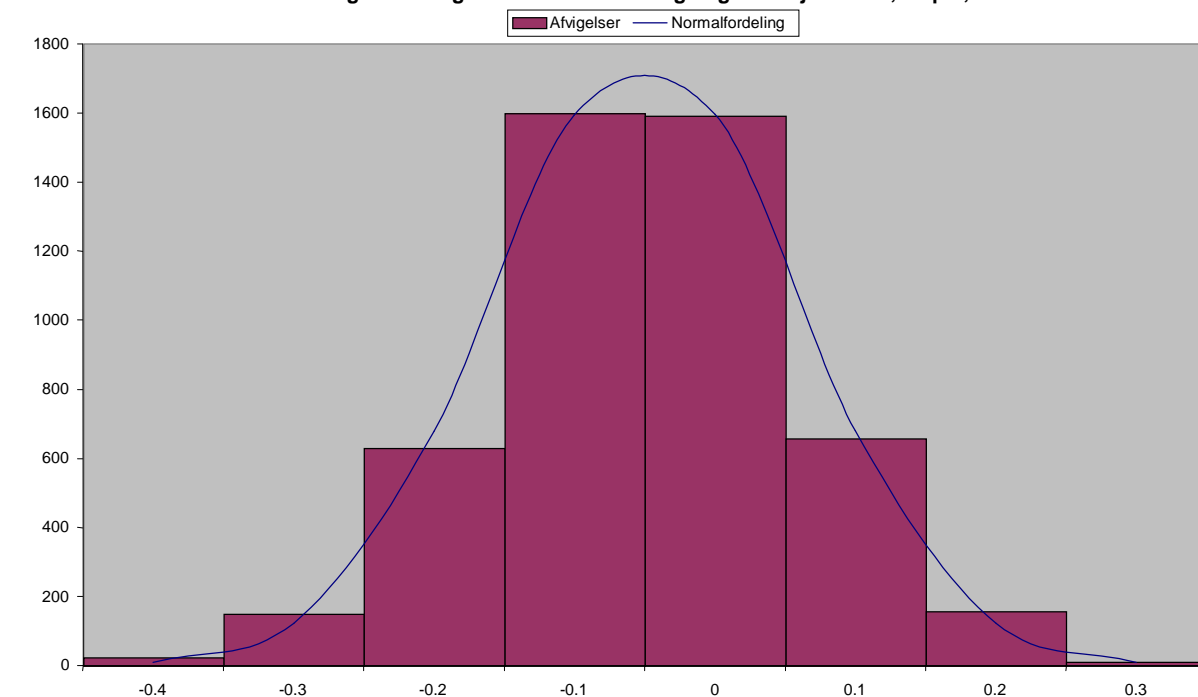


	Total	Fladt A 12	Grusgrav 34	Landsby 56	Bakket A 78	Skov 90	Ukendt 00
Min	-18.97	-0.43	-2.34	-13.56	-16.46	-18.97	0
Max	15.87	0.66	15.87	2.55	7.39	1.89	0
Gns	0.01	0.05	2.16	-0.70	-0.04	-5.62	0
Stnd	2.90	0.10	4.03	2.23	1.27	5.08	0
Sprd	2.90	0.11	4.58	2.34	1.27	7.58	0
Antal	5914	1323	1143	1121	2041	286	0
Niv'200.0'	5914	1323	1143	1121	2041	286	0
Niv'400.0'	0	0	0	0	0	0	0
Niv'600.0'	0	0	0	0	0	0	0
Udklip.pkt	0	0	0	0	0	0	0
Areal	37.4	0.0	0.0	0.0	0.0	37.4	0.0
Niv'200.0'	37.4	0.0	0.0	0.0	0.0	37.4	0.0
Niv'400.0'	0.0	0.0	0.0	0.0	0.0	0.0	0.0
Niv'600.0'	0.0	0.0	0.0	0.0	0.0	0.0	0.0
Udklip.pkt	0.0	0.0	0.0	0.0	0.0	0.0	0.0
Udkl. i %	0.00	0.00	0.00	0.00	0.00	0.00	-0-
Offset gns.	0.01	0.05	2.16	-0.70	-0.04	-5.62	-0-
Min	-16.41	-0.48	-4.50	-12.86	-16.41	-13.35	0
Max	13.71	0.61	13.71	3.25	7.43	7.51	0
Gns	0.00	-0.00	0.00	-0.00	0.00	0.00	0
Stnd	2.43	0.10	4.03	2.23	1.27	5.08	0
Sprd	2.43	0.10	4.03	2.23	1.27	5.08	0
Udklippet							
Min	-18.97	-0.43	-2.34	-13.56	-16.46	-18.97	0
Max	15.87	0.66	15.87	2.55	7.39	1.89	0
Gns	0.01	0.05	2.16	-0.70	-0.04	-5.62	0
Stnd	2.95	0.10	4.03	2.23	1.27	5.08	0
Sprd	2.90	0.11	4.58	2.34	1.27	7.58	0
Udklippet + Offset							
Min	-	-0.48	-4.50	-12.86	-16.41	-13.35	0
Max	-	0.61	13.71	3.25	7.43	7.51	0
Gns	-	-0.00	0.00	-0.00	0.00	0.00	0
Stnd	-	0.10	4.03	2.23	1.27	5.08	0
Sprd	-	0.10	4.03	2.23	1.27	5.08	0

Analysefilen for 1:5,000, opløsningen 15 µm og maskestørrelsen 5 m. før iterationsprocessen.



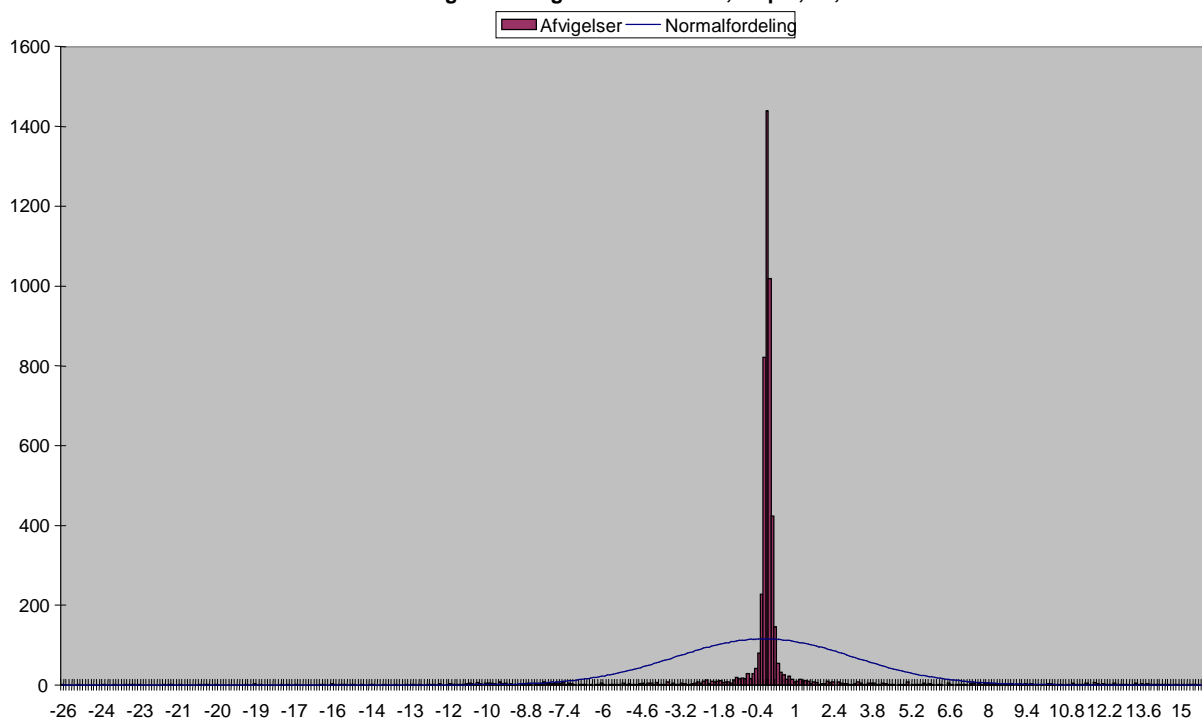
Fordelingen af afvigelser efter eliminering af grove fejl 1:5.000, 15 µm, 5 m.



	Total	Fladt A 12	Grusgrav 34	Landsby 56	Bakket A 78	Skov 90	Ukendt 00
Min	-18.97	-0.43	-2.34	-13.56	-16.46	-18.97	0
Max	15.87	0.66	15.87	2.55	7.39	1.89	0
Gns	0.01	0.05	2.16	-0.70	-0.04	-5.62	0
Stnd	2.90	0.10	4.03	2.23	1.27	5.08	0
Sprd	2.90	0.11	4.58	2.34	1.27	7.58	0
Antal	5914	1323	1143	1121	2041	286	0
Niv'0.1'	2952	992	431	354	1166	9	0
Niv'0.2'	1467	273	159	356	667	12	0
Niv'0.3'	390	44	82	148	108	8	0
Udklip.pkt	1105	14	471	263	100	257	0
Areal	37.4	0.0	0.0	0.0	0.0	37.4	0.0
Niv'0.1'	0.0	0.0	0.0	0.0	0.0	0.0	0.0
Niv'0.2'	0.0	0.0	0.0	0.0	0.0	0.0	0.0
Niv'0.3'	0.0	0.0	0.0	0.0	0.0	0.0	0.0
Udklip.pkt	37.4	0.0	0.0	0.0	0.0	37.4	0.0
Udkl. i %	18.68	1.06	41.21	23.46	4.90	89.86	-0-
Offset gns.	0.01	0.05	2.16	-0.70	-0.04	-5.62	-0-
Min	-16.41	-0.48	-4.50	-12.86	-16.41	-13.35	0
Max	13.71	0.61	13.71	3.25	7.43	7.51	0
Gns	0.00	-0.00	0.00	-0.00	0.00	0.00	0
Stnd	2.43	0.10	4.03	2.23	1.27	5.08	0
Sprd	2.43	0.10	4.03	2.23	1.27	5.08	0
Udklippet							
Min	-5.94	-0.28	1.92	-1.00	-0.35	-5.94	0
Max	2.47	0.36	2.47	-0.41	0.29	-5.33	0
Gns	0.05	0.05	2.15	-0.70	0.07	-5.66	0
Stnd	0.42	0.09	0.19	0.21	0.09	0.21	0
Sprd	0.41	0.10	2.15	0.73	0.12	5.66	0
Udklippet + Offset							
Min	-	-0.32	-0.22	-0.30	-0.43	-0.28	0
Max	-	0.32	0.32	0.29	0.21	0.33	0
Gns	-	-0.00	-0.00	-0.00	-0.00	0.00	0
Stnd	-	0.09	0.19	0.21	0.09	0.21	0
Sprd	-	0.09	0.19	0.21	0.09	0.21	0
	Total	Fladt A 12	Grusgrav 34	Landsby 56	Bakket A 78	Skov 90	Ukendt 00

Analysefilen for 1:5.000, opløsningen 15 µm og maskestørrelsen 5 m. efter iterationsprocessen.

Fordelingen af afvigelser for 1:5.000, 15 µm, 12,5 m.



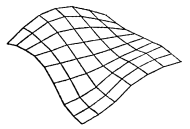
Min	-25.60	-0.49	-2.87	-20.25	-23.28	-25.60	0
Max	16.23	0.88	16.23	3.45	11.68	1.88	0
Gns	-0.05	0.05	2.67	-0.75	-0.07	-6.64	0
Stnd	3.23	0.11	4.61	2.75	1.84	6.12	0
Sprd	3.23	0.12	5.33	2.85	1.84	9.03	0
Antal	5265	1265	764	1059	1957	220	0
Niv'200.0'	5265	1265	764	1059	1957	220	0
Niv'400.0'	0	0	0	0	0	0	0
Niv'600.0'	0	0	0	0	0	0	0
Udklip.pkt	0	0	0	0	0	0	0
Areal	22293.4	0.0	19316.5	1800.3	0.0	1176.5	0.0
Niv'200.0'	22293.4	0.0	19316.5	1800.3	0.0	1176.5	0.0
Niv'400.0'	0.0	0.0	0.0	0.0	0.0	0.0	0.0
Niv'600.0'	0.0	0.0	0.0	0.0	0.0	0.0	0.0
Udklip.pkt	0.0	0.0	0.0	0.0	0.0	0.0	0.0
Udkl. i %	0.00	0.00	0.00	0.00	0.00	0.00	-0-

Offset	gns.	-0.05	0.05	2.67	-0.75	-0.07	-6.64	-0-
Min		-23.21	-0.54	-5.54	-19.50	-23.21	-18.96	0
Max		13.56	0.83	13.56	4.20	11.75	8.51	0
Gns		-0.00	-0.00	-0.00	-0.00	0.00	0.00	0
Stnd		2.72	0.11	4.61	2.75	1.84	6.12	0
Sprd		2.72	0.11	4.61	2.75	1.84	6.12	0

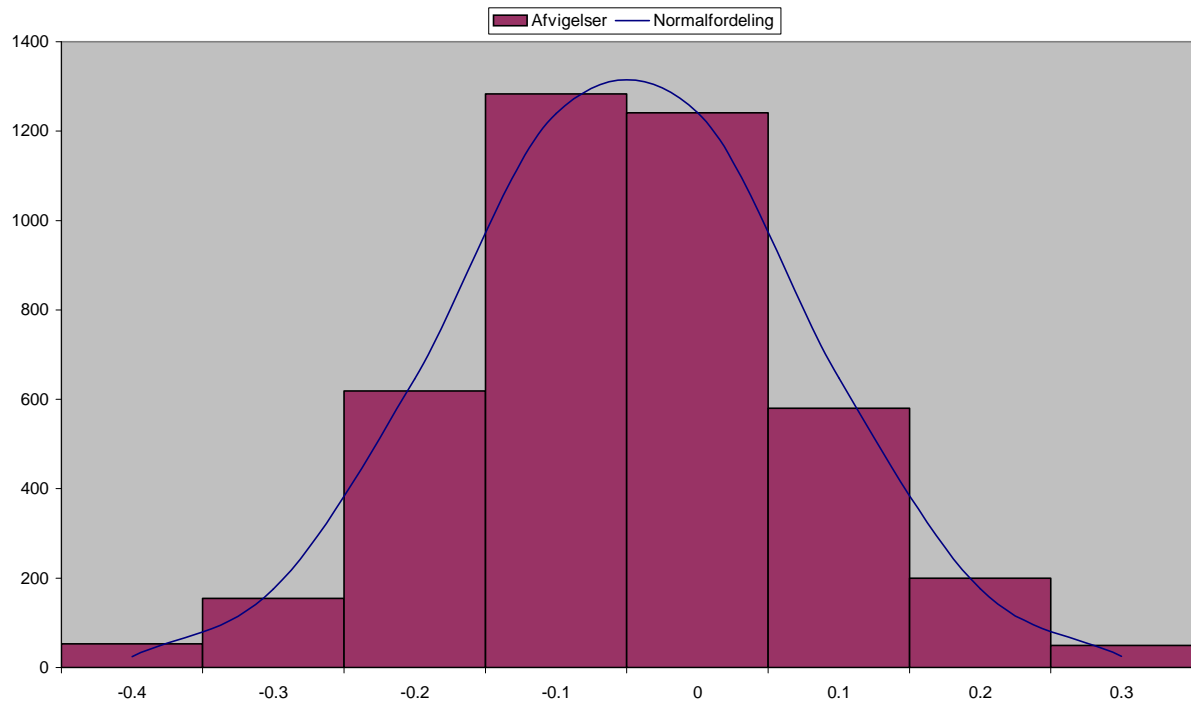
Udklippet								
Min		-25.60	-0.49	-2.87	-20.25	-23.28	-25.60	0
Max		16.23	0.88	16.23	3.45	11.68	1.88	0
Gns		-0.05	0.05	2.67	-0.75	-0.07	-6.64	0
Stnd		3.27	0.11	4.61	2.75	1.84	6.12	0
Sprd		3.23	0.12	5.33	2.85	1.84	9.03	0

Udklippet + Offset								
Min	-	-	-0.54	-5.54	-19.50	-23.21	-18.96	0
Max	-	-	0.83	13.56	4.20	11.75	8.51	0
Gns	-	-	-0.00	-0.00	-0.00	0.00	0.00	0
Stnd	-	-	0.11	4.61	2.75	1.84	6.12	0
Sprd	-	-	0.11	4.61	2.75	1.84	6.12	0

Analysefilen for 1:5,000, opløsningen 15 µm og maskestørrelsen 12.5 m. før iterationsprocessen.



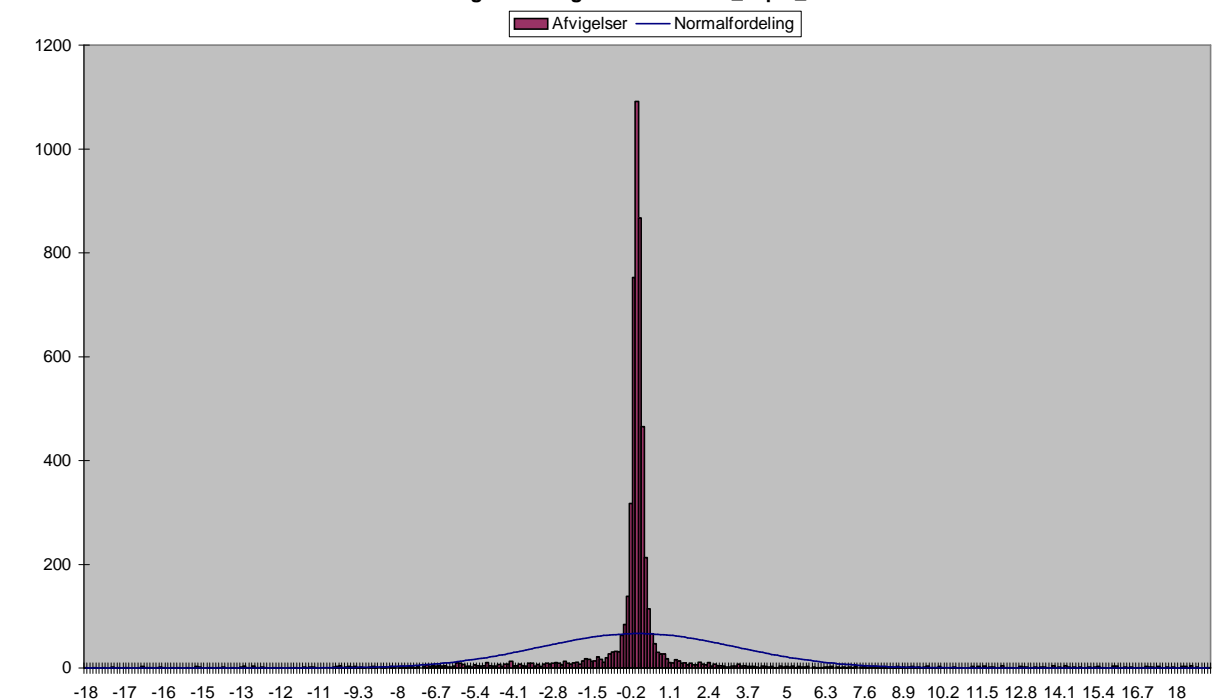
Fordelingen af afvigelser efter eliminering af grove fejl 1:5.000, 15 µm, 12,5 m.



	Total	Fladt A 12	Grusgrav 34	Landsby 56	Bakket A 78	Skov 90	Ukendt 00
Min	-25.60	-0.49	-2.87	-20.25	-23.28	-25.60	0
Max	16.23	0.88	16.23	3.45	11.68	1.88	0
Gns	-0.05	0.05	2.67	-0.75	-0.07	-6.64	0
Stnd	3.23	0.11	4.61	2.75	1.84	6.12	0
Sprd	3.23	0.12	5.33	2.85	1.84	9.03	0
Antal	5265	1265	764	1059	1957	220	0
Niv'0.1'	2592	965	171	327	1119	10	0
Niv'0.2'	1180	228	95	339	517	1	0
Niv'0.4'	387	59	45	131	149	3	0
Udklip.pkt	1106	13	453	262	172	206	0
Areal	22293.4	0.0	19316.5	1800.3	0.0	1176.5	0.0
Niv'0.1'	5137.8	0.0	4331.3	691.7	0.0	114.9	0.0
Niv'0.2'	2719.6	0.0	2425.0	294.6	0.0	0.0	0.0
Niv'0.4'	1187.5	0.0	1162.5	25.0	0.0	0.0	0.0
Udklip.pkt	13248.6	0.0	11397.8	789.1	0.0	1061.7	0.0
Udkl. i %	21.01	1.03	59.29	24.74	8.79	93.64	-0-
Offset gns.	-0.05	0.05	2.67	-0.75	-0.07	-6.64	-0-
Min	-23.21	-0.54	-5.54	-19.50	-23.21	-18.96	0
Max	13.56	0.83	13.56	4.20	11.75	8.51	0
Gns	-0.00	-0.00	-0.00	-0.00	0.00	0.00	0
Stnd	2.72	0.11	4.61	2.75	1.84	6.12	0
Sprd	2.72	0.11	4.61	2.75	1.84	6.12	0
Udklippet							
Min	-6.98	-0.32	0	-1.06	-0.39	-6.98	0
Max	0.41	0.41	0	-0.38	0.30	-6.35	0
Gns	0.04	0.05	0	-0.66	0.06	-6.72	0
Stnd	0.33	0.10	0	0.19	0.11	0.23	0
Sprd	0.31	0.11	0	0.68	0.13	6.72	0
Udklippet + Offset							
Min	-	-0.37	0	-0.40	-0.46	-0.26	0
Max	-	0.36	0	0.28	0.24	0.37	0
Gns	-	0.00	0	-0.00	-0.00	0.00	0
Stnd	-	0.10	0	0.19	0.11	0.23	0
Sprd	-	0.10	0	0.19	0.11	0.23	0

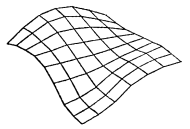
Analysefilen for 1:5,000, opløsningen 15 µm og maskestørrelsen 12.5 m. efter iterationsprocessen.

Fordelingen af afvigelser for 1:5000_15µm_25m.

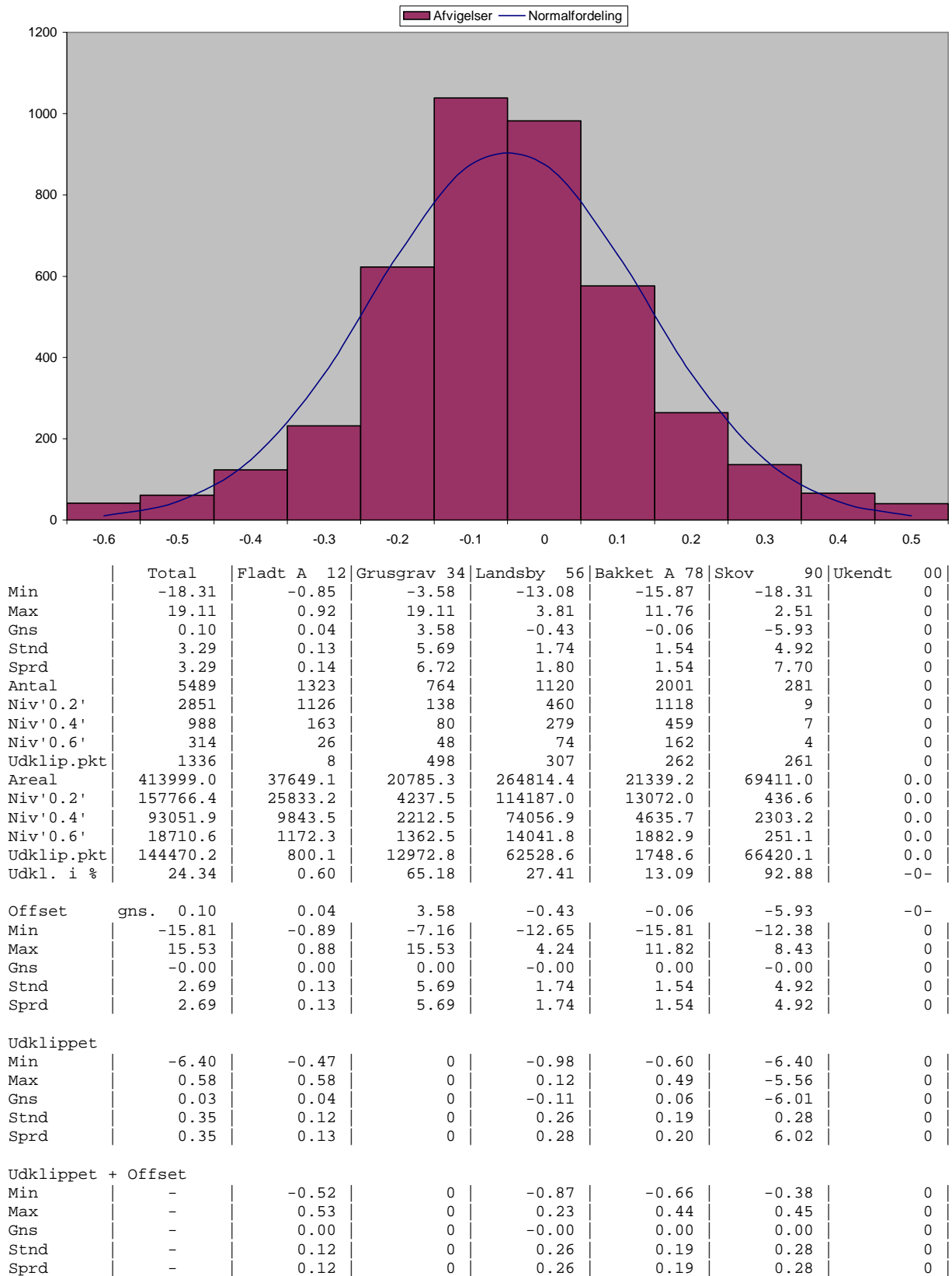


	Total	Fladt A 12	Grusgrav 34	Landsby 56	Bakket A 78	Skov 90	Ukendt 00
Min	-18.31	-0.85	-3.58	-13.08	-15.87	-18.31	0
Max	19.11	0.92	19.11	3.81	11.76	2.51	0
Gns	0.10	0.04	3.58	-0.43	-0.06	-5.93	0
Stnd	3.29	0.13	5.69	1.74	1.54	4.92	0
Sprd	3.29	0.14	6.72	1.80	1.54	7.70	0
Antal	5489	1323	764	1120	2001	281	0
Niv'200.0'	5489	1323	764	1120	2001	281	0
Niv'400.0'	0	0	0	0	0	0	0
Niv'600.0'	0	0	0	0	0	0	0
Udklip.pkt	0	0	0	0	0	0	0
Areal	413999.0	37649.1	20785.3	264814.4	21339.2	69411.0	0.0
Niv'200.0'	413999.0	37649.1	20785.3	264814.4	21339.2	69411.0	0.0
Niv'400.0'	0.0	0.0	0.0	0.0	0.0	0.0	0.0
Niv'600.0'	0.0	0.0	0.0	0.0	0.0	0.0	0.0
Udklip.pkt	0.0	0.0	0.0	0.0	0.0	0.0	0.0
Udkl. i %	0.00	0.00	0.00	0.00	0.00	0.00	-0-
Offset gns.	0.10	0.04	3.58	-0.43	-0.06	-5.93	-0-
Min	-15.81	-0.89	-7.16	-12.65	-15.81	-12.38	0
Max	15.53	0.88	15.53	4.24	11.82	8.43	0
Gns	-0.00	0.00	0.00	-0.00	0.00	-0.00	0
Stnd	2.69	0.13	5.69	1.74	1.54	4.92	0
Sprd	2.69	0.13	5.69	1.74	1.54	4.92	0
Udklippet							
Min	-18.31	-0.85	-3.58	-13.08	-15.87	-18.31	0
Max	19.11	0.92	19.11	3.81	11.76	2.51	0
Gns	0.10	0.04	3.58	-0.43	-0.06	-5.93	0
Stnd	3.32	0.13	5.69	1.74	1.54	4.92	0
Sprd	3.29	0.14	6.72	1.80	1.54	7.70	0
Udklippet + Offset							
Min	-	-0.89	-7.16	-12.65	-15.81	-12.38	0
Max	-	0.88	15.53	4.24	11.82	8.43	0
Gns	-	0.00	0.00	-0.00	0.00	-0.00	0
Stnd	-	0.13	5.69	1.74	1.54	4.92	0
Sprd	-	0.13	5.69	1.74	1.54	4.92	0

Analysefilen for 1:5,000, opløsningen 15 µm og maskestørrelsen 25 m. før iterationsprocessen.

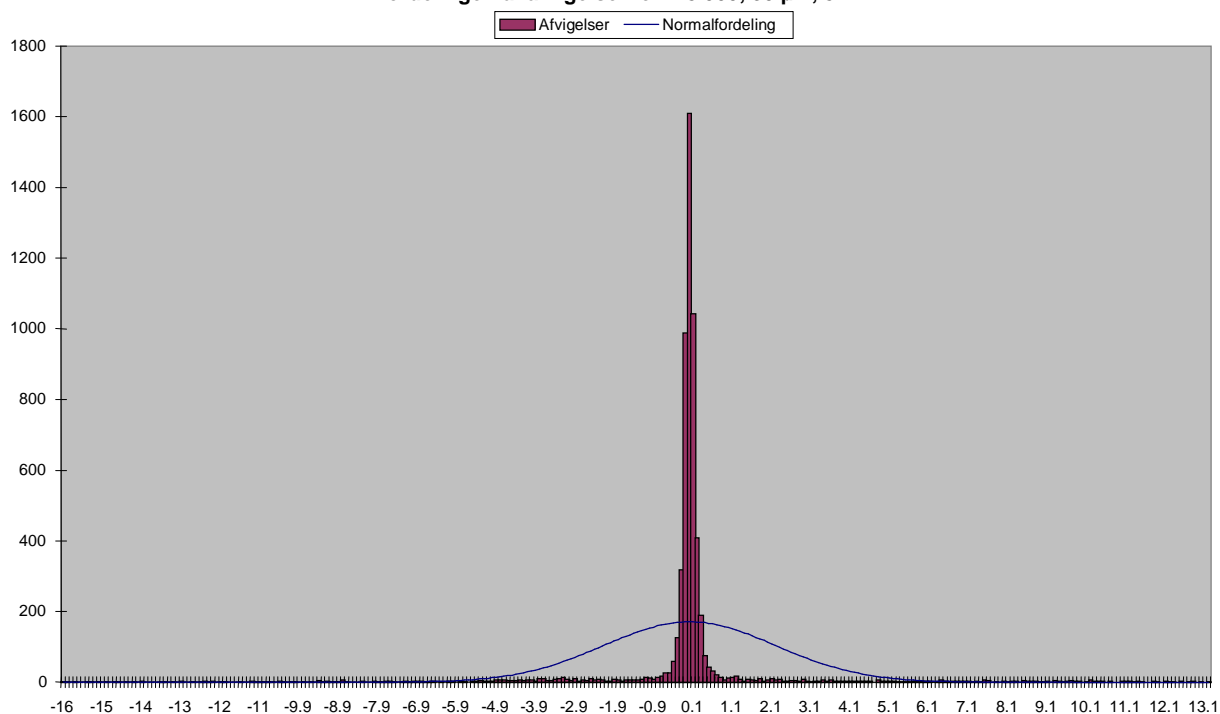


Fordelingen af afvigelser efter eliminering af grove fejl 1:5.000, 15 µm, 25 m.



Analysefilen for 1:5.000, opløsningen 15 µm og maskestørrelsen 25 m. efter iterationsprocessen.

Fordelingen af afvigelser for 1:5.000, 30 µm, 5 m.



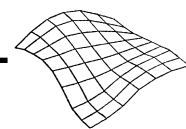
	Total	Fladt A 12	Grusgrav 34	Landsby 56	Bakket A 78	Skov 90	Ukendt 00
Min	-15.81	-0.52	-2.49	-9.34	-11.81	-15.81	0
Max	13.29	1.03	13.29	3.43	3.52	4.01	0
Gns	0.07	0.04	1.54	-0.31	-0.02	-3.59	0
Stnd	2.19	0.12	3.15	1.41	0.80	4.76	0
Sprd	2.19	0.13	3.50	1.44	0.80	5.96	0
Antal	5795	1319	1143	1105	1942	286	0
Niv'200.0'	5795	1319	1143	1105	1942	286	0
Niv'400.0'	0	0	0	0	0	0	0
Niv'600.0'	0	0	0	0	0	0	0
Udklip.pkt	0	0	0	0	0	0	0
Areal	37.4	0.0	0.0	0.0	0.0	37.4	0.0
Niv'200.0'	37.4	0.0	0.0	0.0	0.0	37.4	0.0
Niv'400.0'	0.0	0.0	0.0	0.0	0.0	0.0	0.0
Niv'600.0'	0.0	0.0	0.0	0.0	0.0	0.0	0.0
Udklip.pkt	0.0	0.0	0.0	0.0	0.0	0.0	0.0
Udkl. i %	0.00	0.00	0.00	0.00	0.00	0.00	-0-

Offset	gns.	0.07	0.04	1.54	-0.31	-0.02	-3.59	-0-
Min	-12.21	-0.56	-4.04	-9.03	-11.79	-12.21	0	
Max	11.74	0.99	11.74	3.74	3.54	7.60	0	
Gns	0.00	0.00	0.00	0.00	-0.00	-0.00	0	
Stnd	1.91	0.12	3.15	1.41	0.80	4.76	0	
Sprd	1.91	0.12	3.15	1.41	0.80	4.76	0	

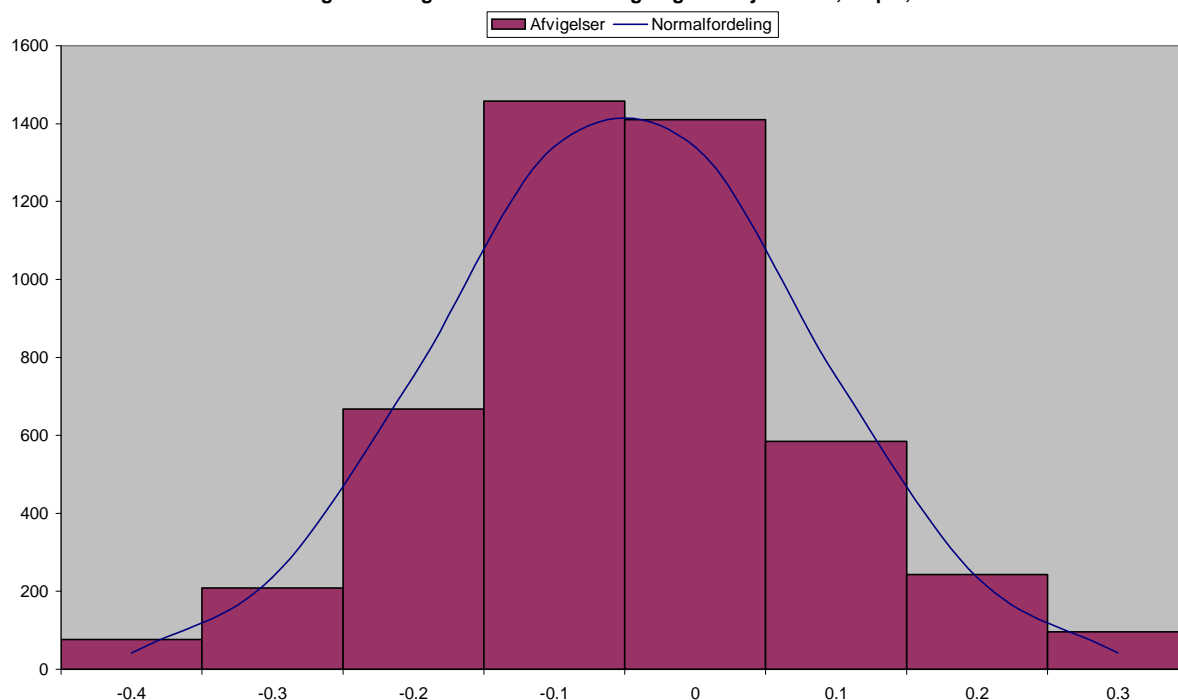
Udklippet							
Min	-15.81	-0.52	-2.49	-9.34	-11.81	-15.81	0
Max	13.29	1.03	13.29	3.43	3.52	4.01	0
Gns	0.07	0.04	1.54	-0.31	-0.02	-3.59	0
Stnd	2.21	0.12	3.15	1.41	0.80	4.76	0
Sprd	2.19	0.13	3.50	1.44	0.80	5.96	0

Udklippet + Offset							
Min	-	-0.56	-4.04	-9.03	-11.79	-12.21	0
Max	-	0.99	11.74	3.74	3.54	7.60	0
Gns	-	0.00	0.00	0.00	-0.00	-0.00	0
Stnd	-	0.12	3.15	1.41	0.80	4.76	0
Sprd	-	0.12	3.15	1.41	0.80	4.76	0

Analysefilen for 1:5,000, opløsningen 30 µm og maskestørrelsen 5 m. før iterationsprocessen.



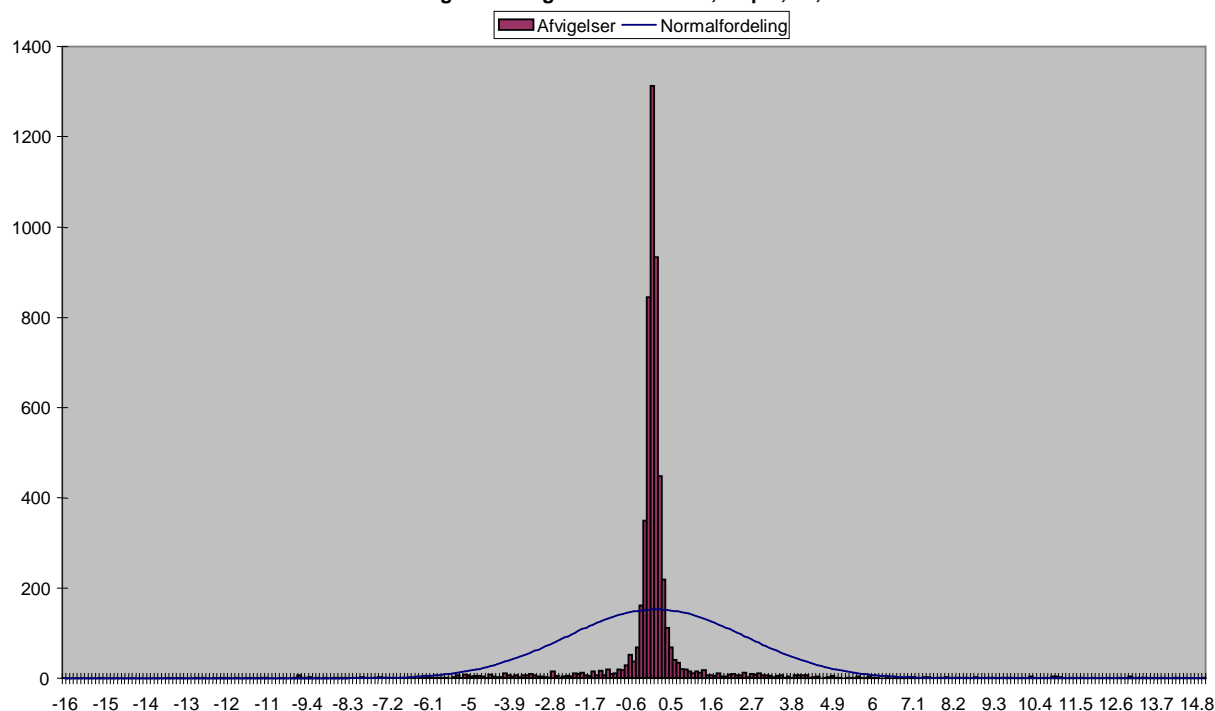
Fordelingen af afvigelser efter eliminering af grove fejl 1:5.000, 30 µm, 5 m.



	Total	Fladt A 12	Grusgrav 34	Landsby 56	Bakket A 78	Skov 90	Ukendt 00
Min	-15.81	-0.52	-2.49	-9.34	-11.81	-15.81	0
Max	13.29	1.03	13.29	3.43	3.52	4.01	0
Gns	0.07	0.04	1.54	-0.31	-0.02	-3.59	0
Stnd	2.19	0.12	3.15	1.41	0.80	4.76	0
Sprd	2.19	0.13	3.50	1.44	0.80	5.96	0
Antal	5795	1319	1143	1105	1942	286	0
Niv'0.1'	3146	1019	452	370	1289	16	0
Niv'0.3'	1200	245	190	299	457	9	0
Niv'0.4'	368	41	88	134	102	3	0
Udklip.pkt	1081	14	413	302	94	258	0
Areal	37.4	0.0	0.0	0.0	0.0	37.4	0.0
Niv'0.1'	0.0	0.0	0.0	0.0	0.0	0.0	0.0
Niv'0.3'	0.0	0.0	0.0	0.0	0.0	0.0	0.0
Niv'0.4'	18.7	0.0	0.0	0.0	0.0	18.7	0.0
Udklip.pkt	18.7	0.0	0.0	0.0	0.0	18.7	0.0
Udkl. i %	18.65	1.06	36.13	27.33	4.84	90.21	-0-
Offset gns.	0.07	0.04	1.54	-0.31	-0.02	-3.59	-0-
Min	-12.21	-0.56	-4.04	-9.03	-11.79	-12.21	0
Max	11.74	0.99	11.74	3.74	3.54	7.60	0
Gns	0.00	0.00	0.00	0.00	-0.00	-0.00	0
Stnd	1.91	0.12	3.15	1.41	0.80	4.76	0
Sprd	1.91	0.12	3.15	1.41	0.80	4.76	0
Udklippet							
Min	-3.95	-0.34	1.15	-0.65	-0.40	-3.95	0
Max	1.89	0.42	1.89	0.08	0.37	-3.34	0
Gns	0.04	0.04	1.47	-0.05	0.06	-3.64	0
Stnd	0.30	0.11	0.25	0.13	0.11	0.19	0
Sprd	0.30	0.11	1.49	0.14	0.13	3.64	0
Udklippet + Offset							
Min	-	-0.38	-0.31	-0.60	-0.46	-0.31	0
Max	-	0.38	0.42	0.13	0.31	0.29	0
Gns	-	0.00	0.00	0.00	-0.00	0.00	0
Stnd	-	0.11	0.25	0.13	0.11	0.19	0
Sprd	-	0.11	0.25	0.13	0.11	0.19	0

Analysefilen for 1:5,000, opløsningen 30 µm og maskestørrelsen 5 m. efter iterationsprocessen.

Fordelingen af afvigelser for 1:5.000, 30 µm, 12,5 m.



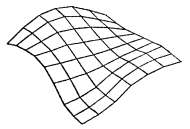
	Total	Fladt A 12	Grusgrav 34	Landsby 56	Bakket A 78	Skov 90	Ukendt 00
Min	-15.91	-0.45	-2.85	-13.13	-15.91	-15.44	0
Max	15.04	0.59	15.04	2.84	8.59	10.00	0
Gns	0.15	0.04	2.38	-0.40	0.00	-1.14	0
Stnd	2.43	0.11	4.24	1.64	1.25	4.32	0
Sprd	2.44	0.12	4.86	1.69	1.25	4.47	0
Antal	5741	1320	764	1180	2001	476	0
Niv'200.0'	5741	1320	764	1180	2001	476	0
Niv'400.0'	0	0	0	0	0	0	0
Niv'600.0'	0	0	0	0	0	0	0
Udklip.pkt	0	0	0	0	0	0	0
Areal	23792.7	0.0	19316.5	1800.3	0.0	2675.8	0.0
Niv'200.0'	23792.7	0.0	19316.5	1800.3	0.0	2675.8	0.0
Niv'400.0'	0.0	0.0	0.0	0.0	0.0	0.0	0.0
Niv'600.0'	0.0	0.0	0.0	0.0	0.0	0.0	0.0
Udklip.pkt	0.0	0.0	0.0	0.0	0.0	0.0	0.0
Udkl. i %	0.00	0.00	0.00	0.00	0.00	0.00	-0-

Offset	gns.	0.15	0.04	2.38	-0.40	0.00	-1.14	-0-
Min		-15.91	-0.50	-5.23	-12.73	-15.91	-14.30	0
Max		12.66	0.55	12.66	3.24	8.59	11.14	0
Gns		0.00	-0.00	0.00	-0.00	-0.00	-0.00	0
Stnd		2.25	0.11	4.24	1.64	1.25	4.32	0
Sprd		2.25	0.11	4.24	1.64	1.25	4.32	0

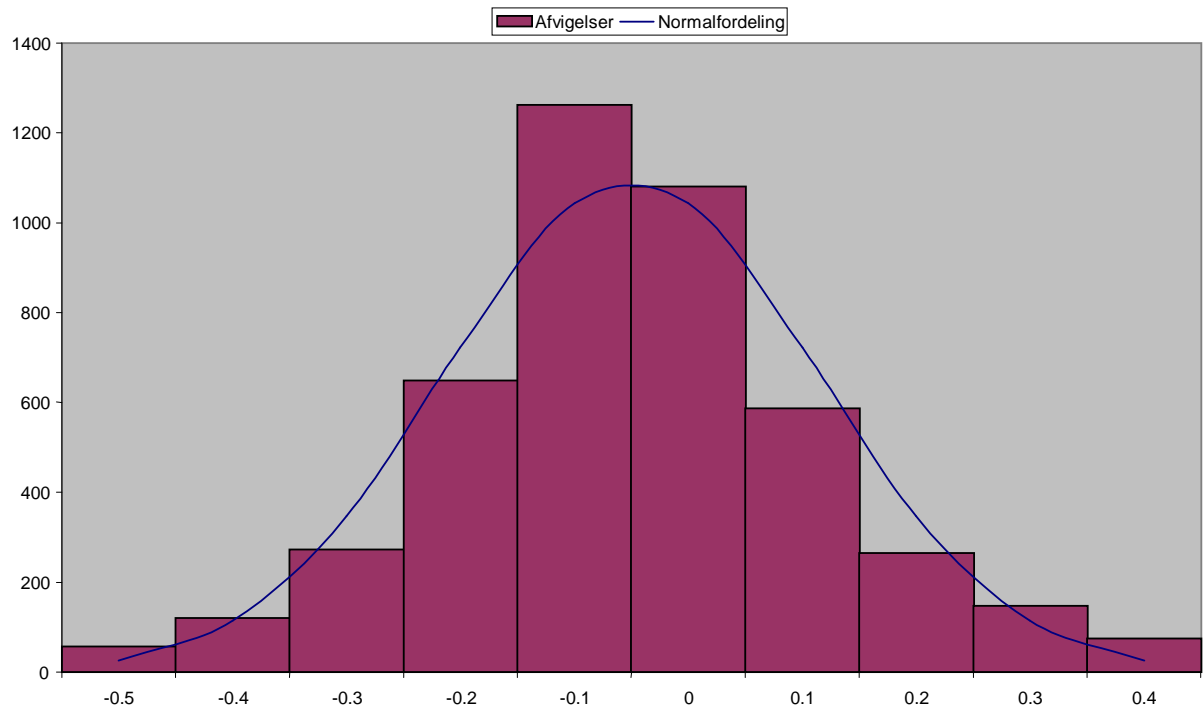
Udklippet								
Min	-15.91	-0.45	-2.85	-13.13	-15.91	-15.44	0	
Max	15.04	0.59	15.04	2.84	8.59	10.00	0	
Gns	0.15	0.04	2.38	-0.40	0.00	-1.14	0	
Stnd	2.47	0.11	4.24	1.64	1.25	4.32	0	
Sprd	2.44	0.12	4.86	1.69	1.25	4.47	0	

Udklippet + Offset							
Min	-	-0.50	-5.23	-12.73	-15.91	-14.30	0
Max	-	0.55	12.66	3.24	8.59	11.14	0
Gns	-	-0.00	0.00	-0.00	-0.00	-0.00	0
Stnd	-	0.11	4.24	1.64	1.25	4.32	0
Sprd	-	0.11	4.24	1.64	1.25	4.32	0

Analysefilen for 1:5,000, opløsningen 30 µm og maskestørrelsen 12.5 m. før iterationsprocessen.



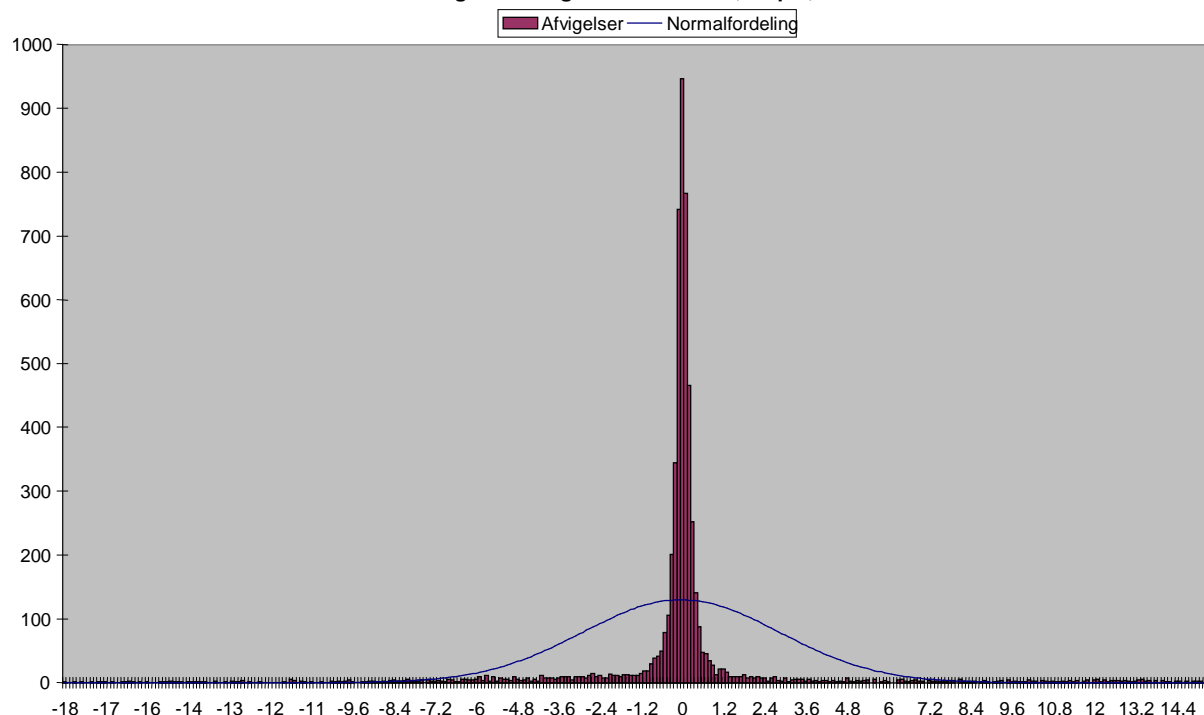
Fordelingen af afvigelser efter eliminering af grove fejl 1:5.000, 30 µm, 12,5 m.



	Total	Fladt A	12 Grusgrav	34 Landsby	56 Bakket A	78 Skov	90 Ukendt	00
Min	-15.91	-0.45	-2.85	-13.13	-15.91	-15.44		0
Max	15.04	0.59	15.04	2.84	11.46	10.00		0
Gns	0.14	0.04	2.38	-0.39	0.01	-1.18		0
Stnd	2.44	0.11	4.24	1.64	1.26	4.32		0
Sprd	2.45	0.12	4.86	1.69	1.26	4.48		0
Antal	5816	1320	764	1190	2041	501		0
Niv'0.2'	3139	1132	195	480	1301	31		0
Niv'0.3'	1069	166	115	330	433	25		0
Niv'0.5'	335	19	47	110	127	32		0
Udklip.pkt	1273	3	407	270	180	413		0
Areal	23880.6	0.0	19316.5	1800.3	0.0	2763.7		0.0
Niv'0.2'	6223.5	0.0	4968.8	1133.7	0.0	121.1		0.0
Niv'0.3'	3109.9	0.0	2937.5	172.4	0.0	0.0		0.0
Niv'0.5'	1187.5	0.0	1187.5	0.0	0.0	0.0		0.0
Udklip.pkt	13359.6	0.0	10222.8	494.3	0.0	2642.6		0.0
Udkl. i %	21.89	0.23	53.27	22.69	8.82	82.44		-0-
Offset	gns.	0.14	0.04	2.38	-0.39	0.01	-1.18	-0-
Min	-15.92	-0.50	-5.23	-12.74	-15.92	-14.26		0
Max	12.66	0.55	12.66	3.23	11.45	11.18		0
Gns	0.00	0.00	0.00	-0.00	0.00	0.00		0
Stnd	2.25	0.11	4.24	1.64	1.26	4.32		0
Sprd	2.25	0.11	4.24	1.64	1.26	4.32		0
Udklippet								
Min	-1.60	-0.45	1.92	-0.89	-0.47	-1.60		0
Max	2.85	0.54	2.85	0.11	0.51	-0.72		0
Gns	0.04	0.04	2.38	-0.07	0.06	-1.17		0
Stnd	0.31	0.11	0.30	0.19	0.16	0.28		0
Sprd	0.30	0.12	2.39	0.21	0.17	1.20		0
Udklippet + Offset								
Min	-	-0.50	-0.45	-0.82	-0.53	-0.43		0
Max	-	0.50	0.47	0.18	0.45	0.45		0
Gns	-	0.00	0.00	0.00	0.00	-0.00		0
Stnd	-	0.11	0.30	0.19	0.16	0.28		0
Sprd	-	0.11	0.30	0.19	0.16	0.28		0

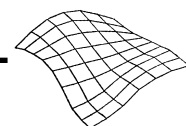
Analysefilen for 1:5.000, opløsningen 30 µm og maskestørrelsen 12.5 m. efter iterationsprocessen.

Fordelingen af afvigelser for 1:5.000, 30 µm, 25 m.

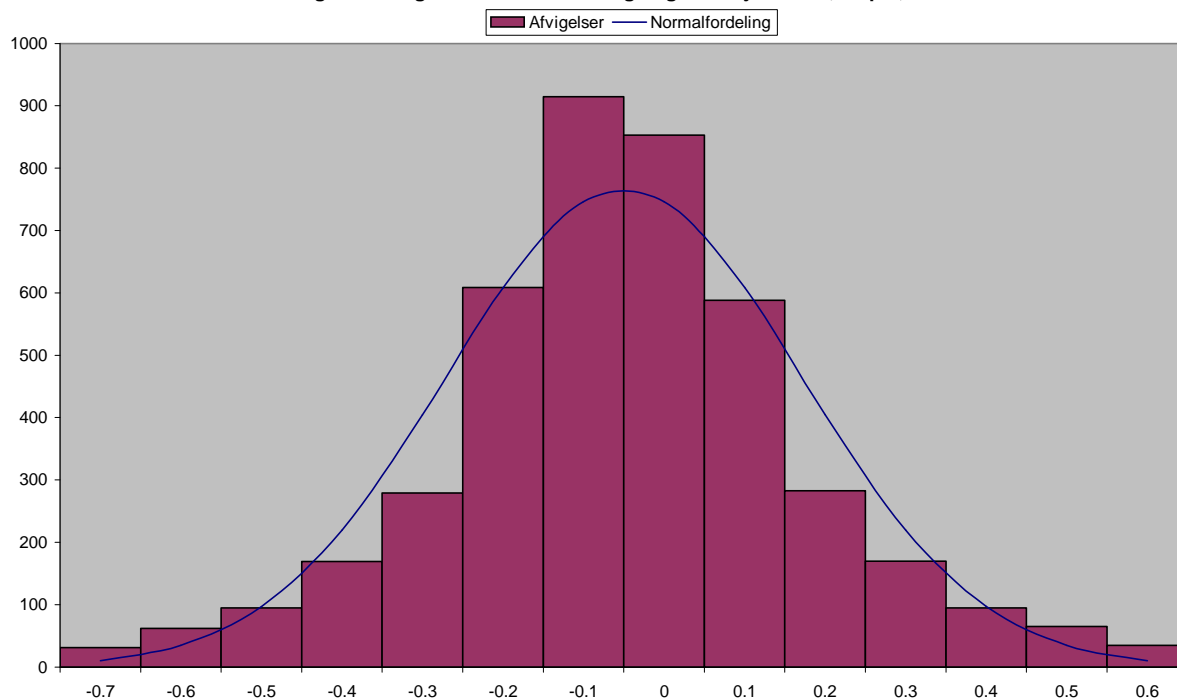


	Total	Fladt A 12	Grusgrav 34	Landsby 56	Bakket A 78	Skov 90	Ukendt 00
Min	-17.93	-0.62	-3.44	-15.08	-17.93	-17.61	0
Max	15.55	0.70	15.55	3.28	11.73	3.44	0
Gns	0.01	0.04	2.70	-0.51	-0.09	-4.63	0
Stnd	2.87	0.14	4.63	1.96	1.67	5.01	0
Sprd	2.87	0.14	5.37	2.03	1.68	6.82	0
Antal	5489	1323	764	1120	2001	281	0
Niv'200.0'	5489	1323	764	1120	2001	281	0
Niv'400.0'	0	0	0	0	0	0	0
Niv'600.0'	0	0	0	0	0	0	0
Udklip.pkt	0	0	0	0	0	0	0
Areal	413999.0	37649.1	20785.3	264814.4	21339.2	69411.0	0.0
Niv'200.0'	413999.0	37649.1	20785.3	264814.4	21339.2	69411.0	0.0
Niv'400.0'	0.0	0.0	0.0	0.0	0.0	0.0	0.0
Niv'600.0'	0.0	0.0	0.0	0.0	0.0	0.0	0.0
Udklip.pkt	0.0	0.0	0.0	0.0	0.0	0.0	0.0
Udkl. i %	0.00	0.00	0.00	0.00	0.00	0.00	-0-
Offset	gns. 0.01	0.04	2.70	-0.51	-0.09	-4.63	-0-
Min	-17.85	-0.66	-6.14	-14.58	-17.85	-12.98	0
Max	12.84	0.66	12.84	3.78	11.82	8.08	0
Gns	0.00	0.00	-0.00	0.00	0.00	0.00	0
Stnd	2.47	0.14	4.63	1.96	1.67	5.01	0
Sprd	2.47	0.14	4.63	1.96	1.67	5.01	0
Udklippet							
Min	-17.93	-0.62	-3.44	-15.08	-17.93	-17.61	0
Max	15.55	0.70	15.55	3.28	11.73	3.44	0
Gns	0.01	0.04	2.70	-0.51	-0.09	-4.63	0
Stnd	2.90	0.14	4.63	1.96	1.67	5.01	0
Sprd	2.87	0.14	5.37	2.03	1.68	6.82	0
Udklippet + Offset							
Min	-	-0.66	-6.14	-14.58	-17.85	-12.98	0
Max	-	0.66	12.84	3.78	11.82	8.08	0
Gns	-	0.00	-0.00	0.00	0.00	0.00	0
Stnd	-	0.14	4.63	1.96	1.67	5.01	0
Sprd	-	0.14	4.63	1.96	1.67	5.01	0

Analysefilen for 1:5,000, opløsningen 30 µm og maskestørrelsen 25 m. før iterationsprocessen.



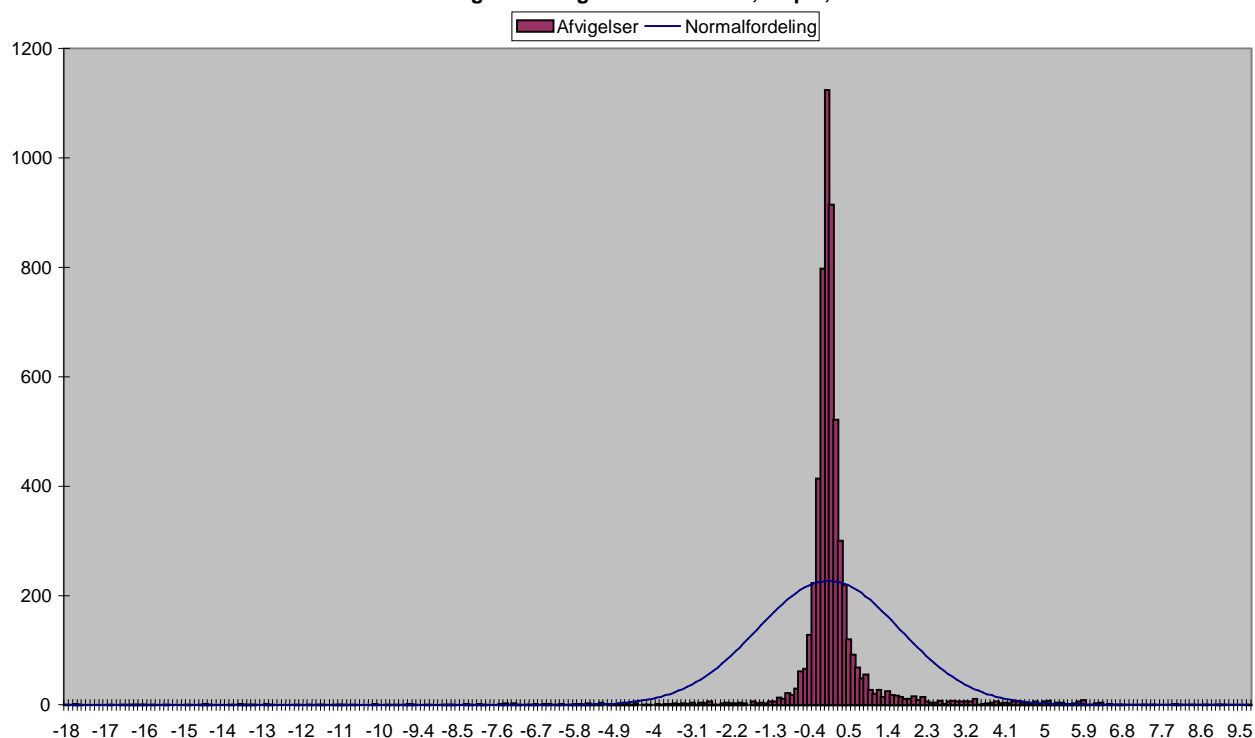
Fordelingen af afvigelser efter eliminering af grove fejl 1:5.000, 30 µm, 25 m.



	Total	Fladt A 12	Grusgrav 34	Landsby 56	Bakket A 78	Skov 90	Ukendt 00
Min	-17.93	-0.62	-3.44	-15.08	-17.93	-17.61	0
Max	15.55	0.70	15.55	3.28	11.73	3.44	0
Gns	0.01	0.04	2.70	-0.51	-0.09	-4.63	0
Stnd	2.87	0.14	4.63	1.96	1.67	5.01	0
Sprd	2.87	0.14	5.37	2.03	1.68	6.82	0
Antal	5489	1323	764	1120	2001	281	0
Niv'0.2'	2965	1172	155	509	1111	18	0
Niv'0.4'	968	134	104	297	418	15	0
Niv'0.7'	297	16	58	76	139	8	0
Udklip.pkt	1259	1	447	238	333	240	0
Areal	413999.0	37649.1	20785.3	264814.4	21339.2	69411.0	0.0
Niv'0.2'	173501.5	27824.9	4562.5	123359.7	14693.6	3060.8	0.0
Niv'0.4'	93479.1	8240.4	3025.0	75680.6	3563.1	2970.0	0.0
Niv'0.7'	23950.1	1583.8	1675.0	18245.2	1340.9	1105.2	0.0
Udklip.pkt	123068.3	0.0	11522.8	47528.9	1741.6	62275.0	0.0
Udkl. i %	22.94	0.08	58.51	21.25	16.64	85.41	-0-
Offset gns.	0.01	0.04	2.70	-0.51	-0.09	-4.63	-0-
Min	-17.85	-0.66	-6.14	-14.58	-17.85	-12.98	0
Max	12.84	0.66	12.84	3.78	11.82	8.08	0
Gns	0.00	0.00	-0.00	0.00	0.00	0.00	0
Stnd	2.47	0.14	4.63	1.96	1.67	5.01	0
Sprd	2.47	0.14	4.63	1.96	1.67	5.01	0
Udklippet							
Min	-5.09	-0.49	0	-1.09	-0.73	-5.09	0
Max	0.58	0.58	0	0.14	0.56	-4.04	0
Gns	0.02	0.04	0	-0.12	0.03	-4.64	0
Stnd	0.31	0.13	0	0.26	0.24	0.35	0
Sprd	0.30	0.14	0	0.29	0.24	4.66	0
Udklippet + Offset							
Min	-	-0.53	0	-0.97	-0.77	-0.45	0
Max	-	0.54	0	0.26	0.53	0.60	0
Gns	-	0.00	0	-0.00	-0.00	0.00	0
Stnd	-	0.13	0	0.26	0.24	0.35	0
Sprd	-	0.13	0	0.26	0.24	0.35	0

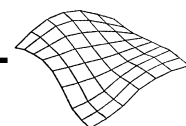
Analysefilen for 1:5,000, opløsningen 30 µm og maskestørrelsen 25 m. efter iterationsprocessen.

Fordelingen af afvigelser for 1:5.000, 60 µm, 5 m.

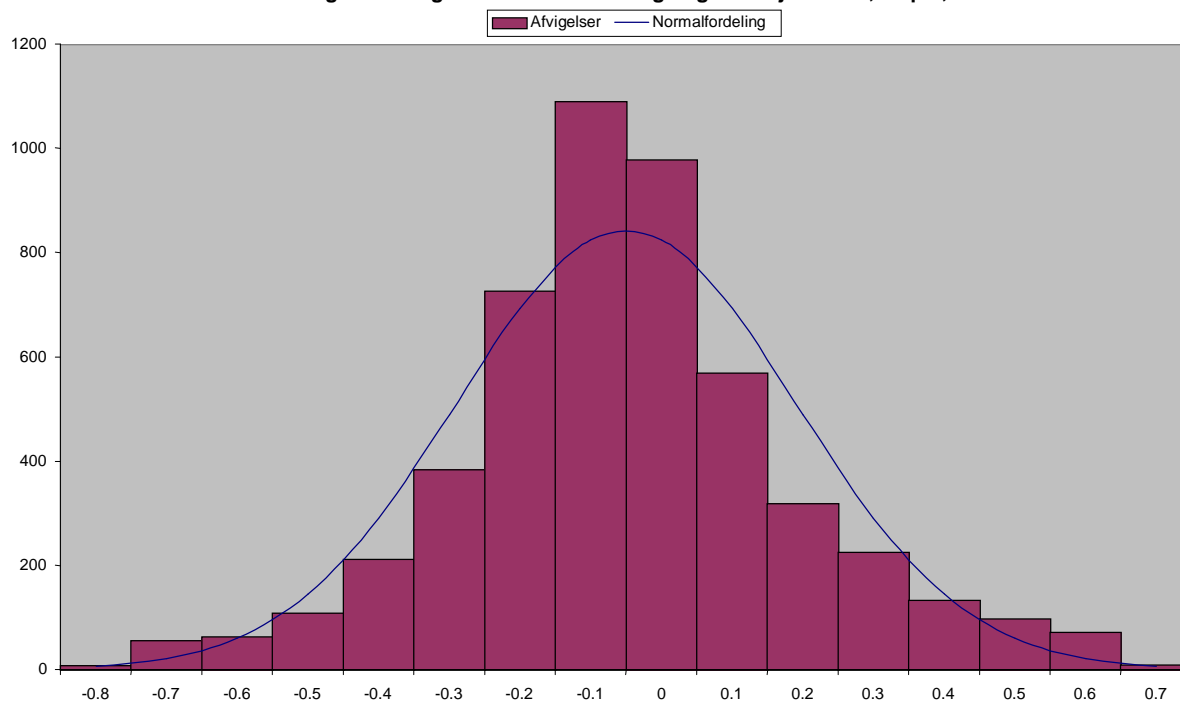


	Total	Fladt A 12	Grusgrav 34	Landsby 56	Bakket A 78	Skov 90	Ukendt 00
Min	-17.42	-0.63	-3.54	-2.06	-3.38	-17.42	0
Max	9.75	1.61	5.15	6.56	9.75	5.36	0
Gns	0.10	0.08	0.08	0.80	0.20	-3.14	0
Stnd	1.65	0.18	0.79	1.31	0.93	5.27	0
Sprd	1.65	0.20	0.80	1.53	0.96	6.14	0
Antal	5874	1323	1143	1121	2001	286	0
Niv'200.0'	5874	1323	1143	1121	2001	286	0
Niv'400.0'	0	0	0	0	0	0	0
Niv'600.0'	0	0	0	0	0	0	0
Udklip.pkt	0	0	0	0	0	0	0
Areal	37.4	0.0	0.0	0.0	0.0	37.4	0.0
Niv'200.0'	37.4	0.0	0.0	0.0	0.0	37.4	0.0
Niv'400.0'	0.0	0.0	0.0	0.0	0.0	0.0	0.0
Niv'600.0'	0.0	0.0	0.0	0.0	0.0	0.0	0.0
Udklip.pkt	0.0	0.0	0.0	0.0	0.0	0.0	0.0
Udkl. i %	0.00	0.00	0.00	0.00	0.00	0.00	-0-
Offset gns.	0.10	0.08	0.08	0.80	0.20	-3.14	-0-
Min	-14.28	-0.71	-3.61	-2.86	-3.58	-14.28	0
Max	9.56	1.53	5.07	5.76	9.56	8.50	0
Gns	-0.00	0.00	0.00	-0.00	0.00	-0.00	0
Stnd	1.45	0.18	0.79	1.31	0.93	5.27	0
Sprd	1.45	0.18	0.79	1.31	0.93	5.27	0
Udklippet							
Min	-17.42	-0.63	-3.54	-2.06	-3.38	-17.42	0
Max	9.75	1.61	5.15	6.56	9.75	5.36	0
Gns	0.10	0.08	0.08	0.80	0.20	-3.14	0
Stnd	1.73	0.18	0.79	1.31	0.93	5.27	0
Sprd	1.65	0.20	0.80	1.53	0.96	6.14	0
Udklippet + Offset							
Min	-	-0.71	-3.61	-2.86	-3.58	-14.28	0
Max	-	1.53	5.07	5.76	9.56	8.50	0
Gns	-	0.00	0.00	-0.00	0.00	-0.00	0
Stnd	-	0.18	0.79	1.31	0.93	5.27	0
Sprd	-	0.18	0.79	1.31	0.93	5.27	0

Analysefilen for 1:5,000, opløsningen 60 µm og maskestørrelsen 5 m. før iterationsprocessen.



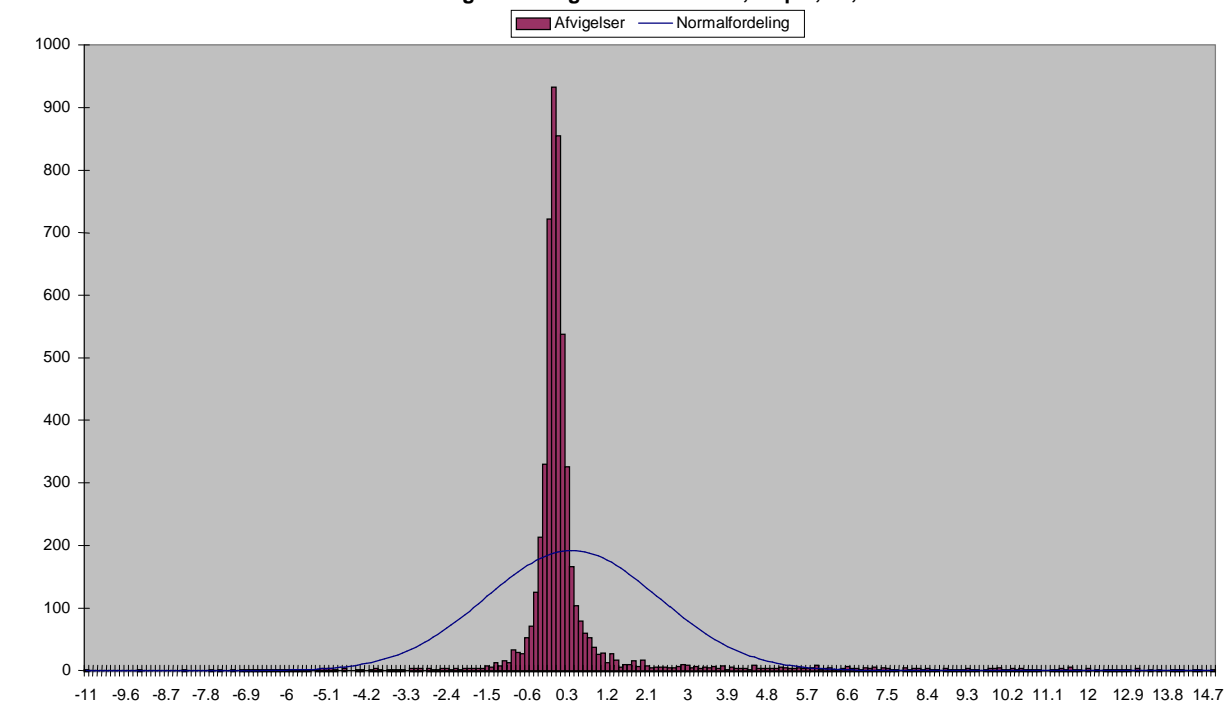
Fordelingen af afvigelser efter eliminering af grove fejl 1:5.000, 60 µm, 5 m.



	Total	Fladt A 12	Grusgrav 34	Landsby 56	Bakket A 78	Skov 90	Ukendt 00
Min	-17.42	-0.63	-3.54	-2.06	-3.38	-17.42	0
Max	9.75	1.61	5.15	6.56	9.75	5.36	0
Gns	0.10	0.08	0.08	0.80	0.20	-3.14	0
Stnd	1.65	0.18	0.79	1.31	0.93	5.27	0
Sprd	1.65	0.20	0.80	1.53	0.96	6.14	0
Antal	5874	1323	1143	1121	2001	286	0
Niv'0.2'	3598	1104	601	415	1454	24	0
Niv'0.5'	1052	187	276	247	322	20	0
Niv'0.7'	382	22	103	129	108	20	0
Udklip.pkt	842	10	163	330	117	222	0
Areal	37.4	0.0	0.0	0.0	0.0	37.4	0.0
Niv'0.2'	0.0	0.0	0.0	0.0	0.0	0.0	0.0
Niv'0.5'	0.0	0.0	0.0	0.0	0.0	0.0	0.0
Niv'0.7'	0.0	0.0	0.0	0.0	0.0	0.0	0.0
Udklip.pkt	37.4	0.0	0.0	0.0	0.0	37.4	0.0
Udkl. i %	14.33	0.76	14.26	29.44	5.85	77.62	-0-
Offset gns.	0.10	0.08	0.08	0.80	0.20	-3.14	-0-
Min	-14.28	-0.71	-3.61	-2.86	-3.58	-14.28	0
Max	9.56	1.53	5.07	5.76	9.56	8.50	0
Gns	-0.00	0.00	0.00	-0.00	0.00	-0.00	0
Stnd	1.45	0.18	0.79	1.31	0.93	5.27	0
Sprd	1.45	0.18	0.79	1.31	0.93	5.27	0
Udklippet							
Min	-3.81	-0.63	-0.64	0.08	-0.52	-3.81	0
Max	1.52	0.76	0.78	1.52	0.90	-2.49	0
Gns	0.11	0.08	-0.00	0.49	0.08	-3.11	0
Stnd	0.44	0.17	0.28	0.35	0.22	0.40	0
Sprd	0.38	0.18	0.28	0.60	0.23	3.14	0
Udklippet + Offset							
Min	-	-0.70	-0.64	-0.41	-0.60	-0.70	0
Max	-	0.68	0.78	1.03	0.82	0.62	0
Gns	-	0.00	0.00	-0.00	0.00	-0.00	0
Stnd	-	0.17	0.28	0.35	0.22	0.40	0
Sprd	-	0.17	0.28	0.35	0.22	0.40	0

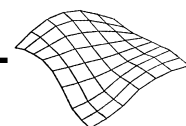
Analysefilen for 1:5,000, opløsningen 60 µm og maskestørrelsen 5 m. efter iterationsprocessen.

Fordelingen af afvigelser for 1:5.000, 60 µm, 12,5 m.

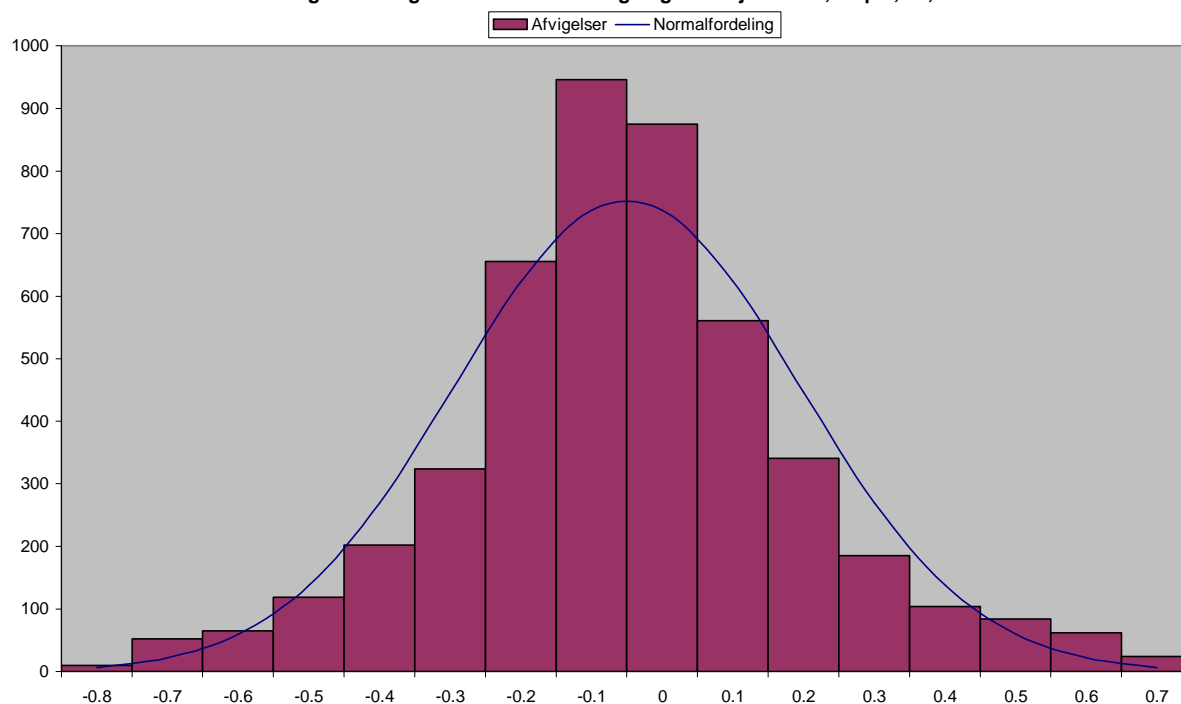


	Total	Fladt A 12	Grusgrav 34	Landsby 56	Bakket A 78	Skov 90	Ukendt 00
Min	-10.46	-0.77	-2.10	-5.51	-7.67	-10.46	0
Max	14.84	1.11	14.84	3.78	8.83	9.01	0
Gns	0.46	0.08	2.13	0.22	0.06	1.45	0
Stnd	1.95	0.17	3.91	0.69	0.61	4.12	0
Sprd	2.00	0.19	4.46	0.72	0.61	4.37	0
Antal	5466	1320	764	1104	2001	277	0
Niv'200.0'	5466	1320	764	1104	2001	277	0
Niv'400.0'	0	0	0	0	0	0	0
Niv'600.0'	0	0	0	0	0	0	0
Udklip.pkt	0	0	0	0	0	0	0
Areal	22563.3	0.0	19316.5	1800.3	0.0	1446.4	0.0
Niv'200.0'	22563.3	0.0	19316.5	1800.3	0.0	1446.4	0.0
Niv'400.0'	0.0	0.0	0.0	0.0	0.0	0.0	0.0
Niv'600.0'	0.0	0.0	0.0	0.0	0.0	0.0	0.0
Udklip.pkt	0.0	0.0	0.0	0.0	0.0	0.0	0.0
Udkl. i %	0.00	0.00	0.00	0.00	0.00	0.00	-0-
Offset gns.	0.46	0.08	2.13	0.22	0.06	1.45	-0-
Min	-11.90	-0.85	-4.23	-5.73	-7.73	-11.90	0
Max	12.70	1.02	12.70	3.56	8.77	7.57	0
Gns	-0.00	0.00	-0.00	0.00	0.00	-0.00	0
Stnd	1.80	0.17	3.91	0.69	0.61	4.12	0
Sprd	1.80	0.17	3.91	0.69	0.61	4.12	0
Udklippet							
Min	-10.46	-0.77	-2.10	-5.51	-7.67	-10.46	0
Max	14.84	1.11	14.84	3.78	8.83	9.01	0
Gns	0.46	0.08	2.13	0.22	0.06	1.45	0
Stnd	1.95	0.17	3.91	0.69	0.61	4.12	0
Sprd	2.00	0.19	4.46	0.72	0.61	4.37	0
Udklippet + Offset							
Min	-	-0.85	-4.23	-5.73	-7.73	-11.90	0
Max	-	1.02	12.70	3.56	8.77	7.57	0
Gns	-	0.00	-0.00	0.00	0.00	-0.00	0
Stnd	-	0.17	3.91	0.69	0.61	4.12	0
Sprd	-	0.17	3.91	0.69	0.61	4.12	0

Analysefilen for 1:5,000, opløsningen 60 µm og maskestørrelsen 12.5 m. før iterationsprocessen.



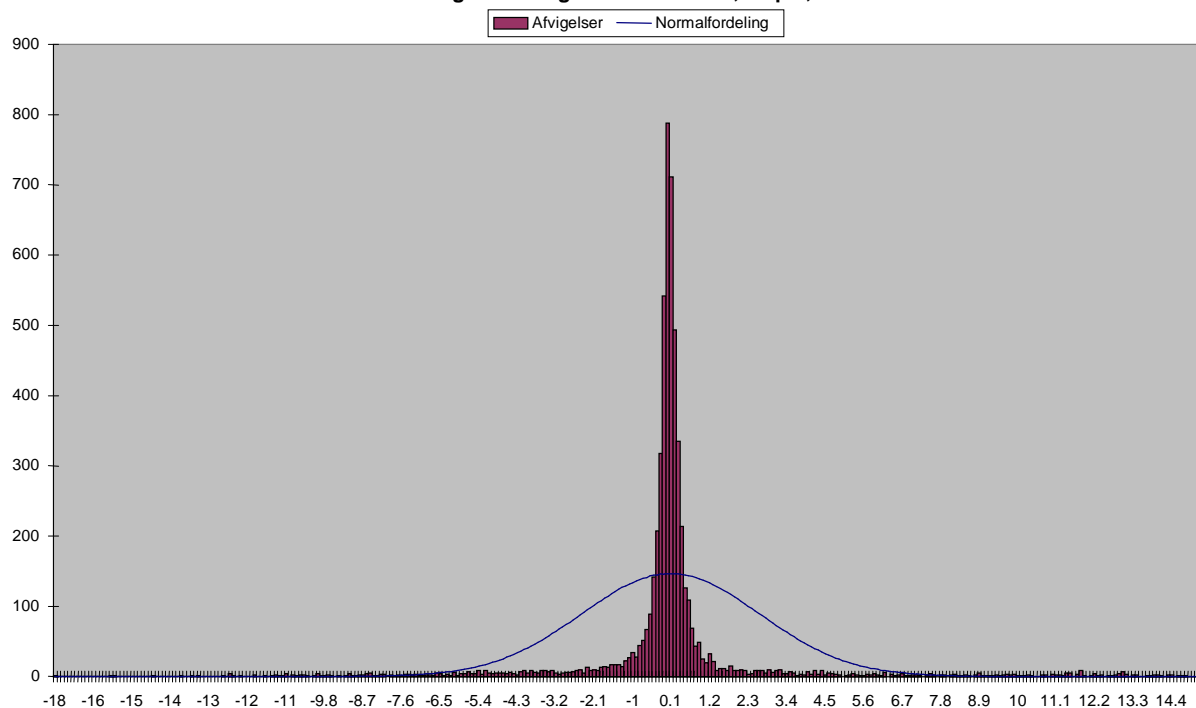
Fordelingen af afvigelser efter eliminering af grove fejl 1:5.000, 60 µm, 12,5 m.



	Total	Fladt A 12	Grusgrav 34	Landsby 56	Bakket A 78	Skov 90	Ukendt 00
Min	-10.46	-0.77	-2.10	-5.51	-7.67	-10.46	0
Max	14.84	1.11	14.84	3.78	8.83	9.01	0
Gns	0.46	0.08	2.13	0.22	0.06	1.45	0
Stnd	1.95	0.17	3.91	0.69	0.61	4.12	0
Sprd	2.00	0.19	4.46	0.72	0.61	4.37	0
Antal	5466	1320	764	1104	2001	277	0
Niv'0.2'	3186	1108	206	452	1409	11	0
Niv'0.5'	1050	185	155	320	381	9	0
Niv'0.7'	338	20	60	149	100	9	0
Udklip.pkt	892	7	343	183	111	248	0
Areal	22563.3	0.0	19316.5	1800.3	0.0	1446.4	0.0
Niv'0.2'	6162.7	0.0	5268.8	764.1	0.0	129.8	0.0
Niv'0.5'	4194.6	0.0	3925.0	269.6	0.0	0.0	0.0
Niv'0.7'	2141.1	0.0	1512.5	498.8	0.0	129.8	0.0
Udklip.pkt	10065.0	0.0	8610.3	267.9	0.0	1186.8	0.0
Udkl. i %	16.32	0.53	44.90	16.58	5.55	89.53	-0-
Offset gns.	0.46	0.08	2.13	0.22	0.06	1.45	-0-
Min	-11.90	-0.85	-4.23	-5.73	-7.73	-11.90	0
Max	12.70	1.02	12.70	3.56	8.77	7.57	0
Gns	-0.00	0.00	-0.00	0.00	0.00	-0.00	0
Stnd	1.80	0.17	3.91	0.69	0.61	4.12	0
Sprd	1.80	0.17	3.91	0.69	0.61	4.12	0
Udklippet							
Min	-0.66	-0.51	0	-0.50	-0.66	0.91	0
Max	2.16	0.81	0	0.95	0.78	2.16	0
Gns	0.12	0.08	0	0.23	0.06	1.57	0
Stnd	0.28	0.16	0	0.29	0.22	0.38	0
Sprd	0.29	0.18	0	0.36	0.23	1.61	0
Udklippet + Offset							
Min	-	-0.59	0	-0.73	-0.72	-0.66	0
Max	-	0.72	0	0.73	0.72	0.60	0
Gns	-	0.00	0	-0.00	-0.00	0.00	0
Stnd	-	0.16	0	0.29	0.22	0.38	0
Sprd	-	0.16	0	0.29	0.22	0.38	0

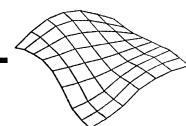
Analysefilen for 1:5,000, opløsningen 60 µm og maskestørrelsen 12.5 m. efter iterationsprocessen.

Fordelingen af afvigelser for 1:5.000, 60 µm, 25 m

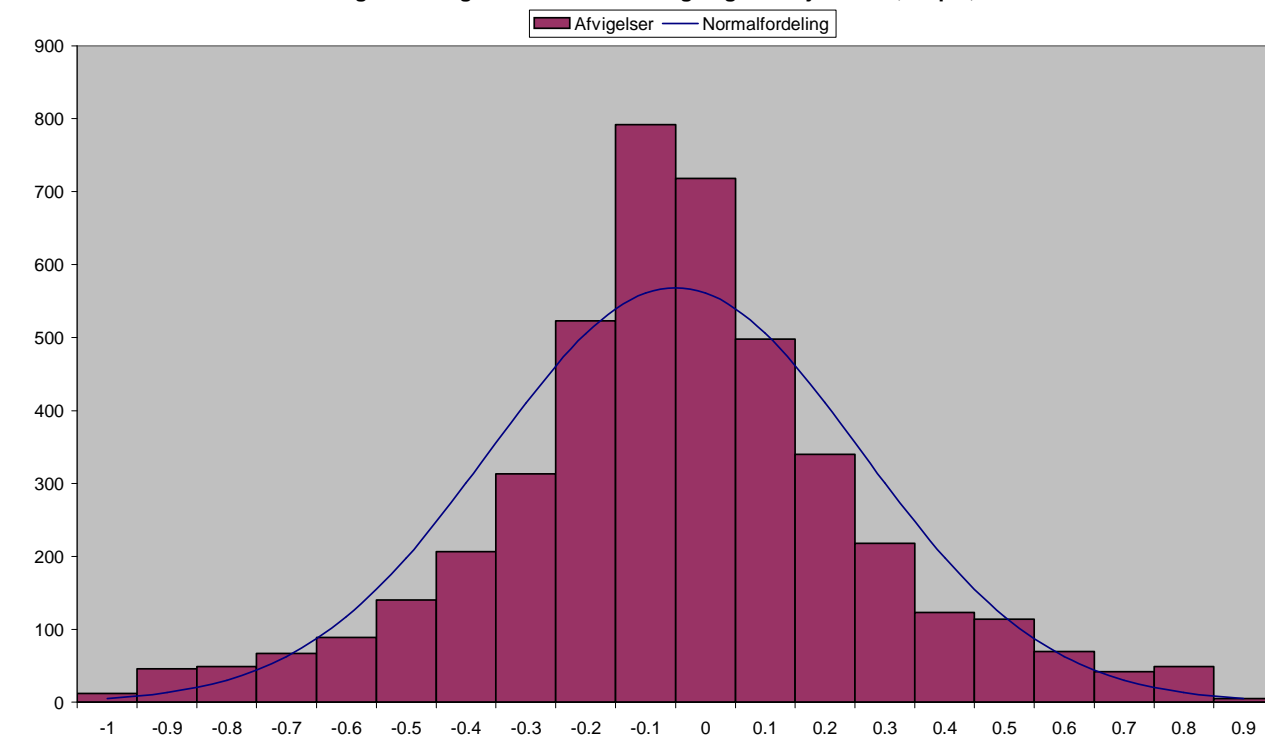


	Total	Fladt A 12	Grusgrav 34	Landsby 56	Bakket A 78	Skov 90	Ukendt 00
Min	-17.47	-0.64	-3.35	-14.63	-17.47	-15.74	0
Max	15.35	0.95	15.35	3.24	9.59	7.26	0
Gns	0.13	0.09	2.40	-0.47	-0.05	-2.17	0
Stnd	2.55	0.17	4.43	1.95	1.47	4.68	0
Sprd	2.55	0.19	5.03	2.01	1.47	5.16	0
Antal	5489	1323	764	1120	2001	281	0
Niv'200.0'	5489	1323	764	1120	2001	281	0
Niv'400.0'	0	0	0	0	0	0	0
Niv'600.0'	0	0	0	0	0	0	0
Udklip.pkt	0	0	0	0	0	0	0
Areal	413999.0	37649.1	20785.3	264814.4	21339.2	69411.0	0.0
Niv'200.0'	413999.0	37649.1	20785.3	264814.4	21339.2	69411.0	0.0
Niv'400.0'	0.0	0.0	0.0	0.0	0.0	0.0	0.0
Niv'600.0'	0.0	0.0	0.0	0.0	0.0	0.0	0.0
Udklip.pkt	0.0	0.0	0.0	0.0	0.0	0.0	0.0
Udkl. i %	0.00	0.00	0.00	0.00	0.00	0.00	-0-
Offset gns.	0.13	0.09	2.40	-0.47	-0.05	-2.17	-0-
Min	-17.42	-0.73	-5.75	-14.16	-17.42	-13.57	0
Max	12.95	0.87	12.95	3.71	9.64	9.43	0
Gns	-0.00	-0.00	0.00	-0.00	-0.00	0.00	0
Stnd	2.33	0.17	4.43	1.95	1.47	4.68	0
Sprd	2.33	0.17	4.43	1.95	1.47	4.68	0
Udklippet							
Min	-17.47	-0.64	-3.35	-14.63	-17.47	-15.74	0
Max	15.35	0.95	15.35	3.24	9.59	7.26	0
Gns	0.13	0.09	2.40	-0.47	-0.05	-2.17	0
Stnd	2.59	0.17	4.43	1.95	1.47	4.68	0
Sprd	2.55	0.19	5.03	2.01	1.47	5.16	0
Udklippet + Offset							
Min	-	-0.73	-5.75	-14.16	-17.42	-13.57	0
Max	-	0.87	12.95	3.71	9.64	9.43	0
Gns	-	-0.00	0.00	-0.00	-0.00	0.00	0
Stnd	-	0.17	4.43	1.95	1.47	4.68	0
Sprd	-	0.17	4.43	1.95	1.47	4.68	0

Analysefilen for 1:5,000, opløsningen 60 µm og maskestørrelsen 25 m. før iterationsprocessen.

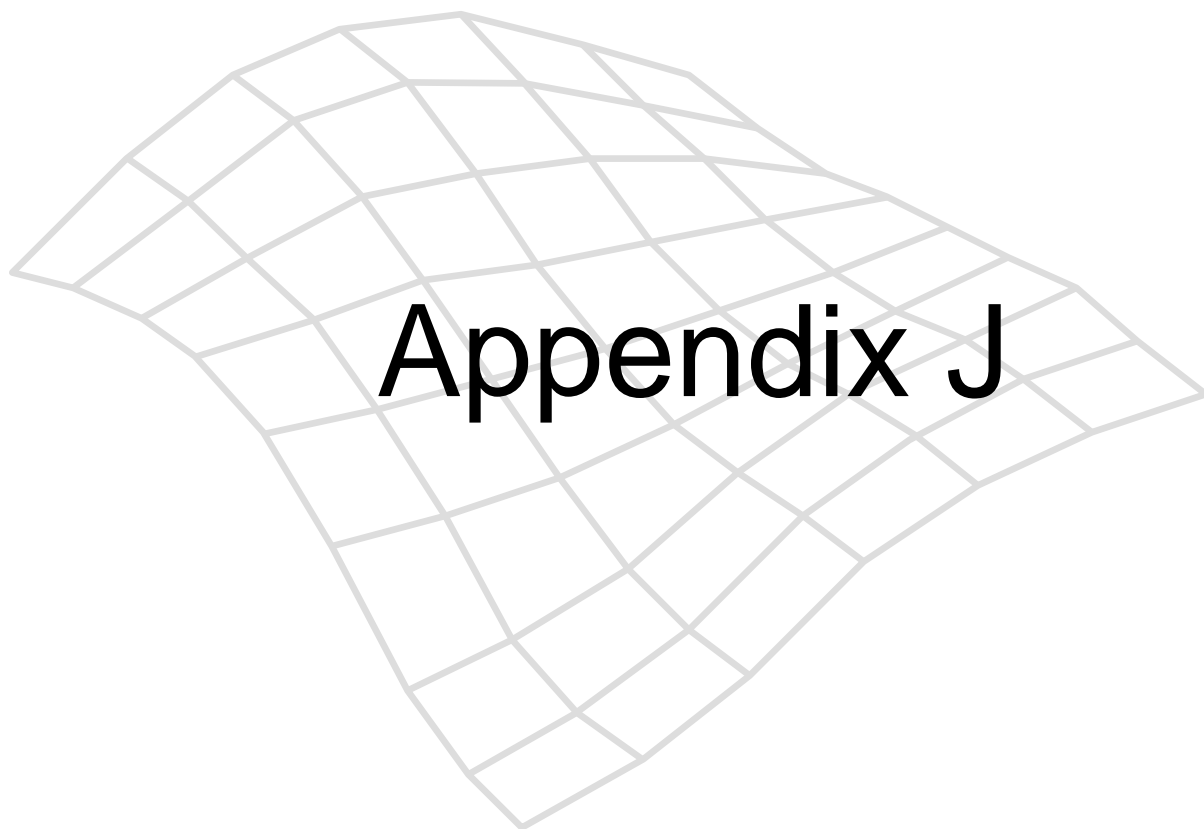


Fordelingen af afvigelser efter eliminering af grove fejl 1:5.000, 60 µm, 25 m.

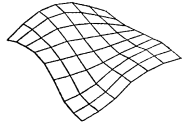


	Total	Fladt A 12	Grusgrav 34	Landsby 56	Bakket A 78	Skov 90	Ukendt 00
Min	-17.47	-0.64	-3.35	-14.63	-17.47	-15.74	0
Max	15.35	0.95	15.35	3.24	9.59	7.26	0
Gns	0.13	0.09	2.40	-0.47	-0.05	-2.17	0
Stnd	2.55	0.17	4.43	1.95	1.47	4.68	0
Sprd	2.55	0.19	5.03	2.01	1.47	5.16	0
Antal	5489	1323	764	1120	2001	281	0
Niv'0.3'	3105	1186	159	490	1243	27	0
Niv'0.6'	965	126	134	292	401	12	0
Niv'0.9'	330	10	81	100	128	11	0
Udklip.pkt	1089	1	390	238	229	231	0
Areal	413999.0	37649.1	20785.3	264814.4	21339.2	69411.0	0.0
Niv'0.3'	169599.6	32020.1	4687.5	114951.2	14508.7	3432.2	0.0
Niv'0.6'	89891.8	5264.0	3850.0	75064.1	4623.2	1090.6	0.0
Niv'0.9'	33516.9	365.0	2162.5	27908.6	799.2	2281.5	0.0
Udklip.pkt	120990.8	0.0	10085.3	46890.6	1408.1	62606.7	0.0
Udkl. i %	19.84	0.08	51.05	21.25	11.44	82.21	-0-
Offset gns.	0.13	0.09	2.40	-0.47	-0.05	-2.17	-0-
Min	-17.42	-0.73	-5.75	-14.16	-17.42	-13.57	0
Max	12.95	0.87	12.95	3.71	9.64	9.43	0
Gns	-0.00	-0.00	0.00	-0.00	-0.00	0.00	0
Stnd	2.33	0.17	4.43	1.95	1.47	4.68	0
Sprd	2.33	0.17	4.43	1.95	1.47	4.68	0
Udklippet							
Min	-2.90	-0.64	0	-1.18	-0.97	-2.90	0
Max	0.95	0.95	0	0.46	0.88	-1.41	0
Gns	0.06	0.09	0	0.06	0.05	-2.08	0
Stnd	0.31	0.17	0	0.31	0.32	0.44	0
Sprd	0.31	0.19	0	0.32	0.32	2.12	0
Udklippet + Offset							
Min	-	-0.73	0	-1.25	-1.02	-0.83	0
Max	-	0.87	0	0.40	0.83	0.67	0
Gns	-	-0.00	0	0.00	0.00	0.00	0
Stnd	-	0.17	0	0.31	0.32	0.44	0
Sprd	-	0.17	0	0.31	0.32	0.44	0

Analysefilen for 1:5,000, opløsningen 60 µm og maskestørrelsen 25 m. efter iterationsprocessen.



Appendix J

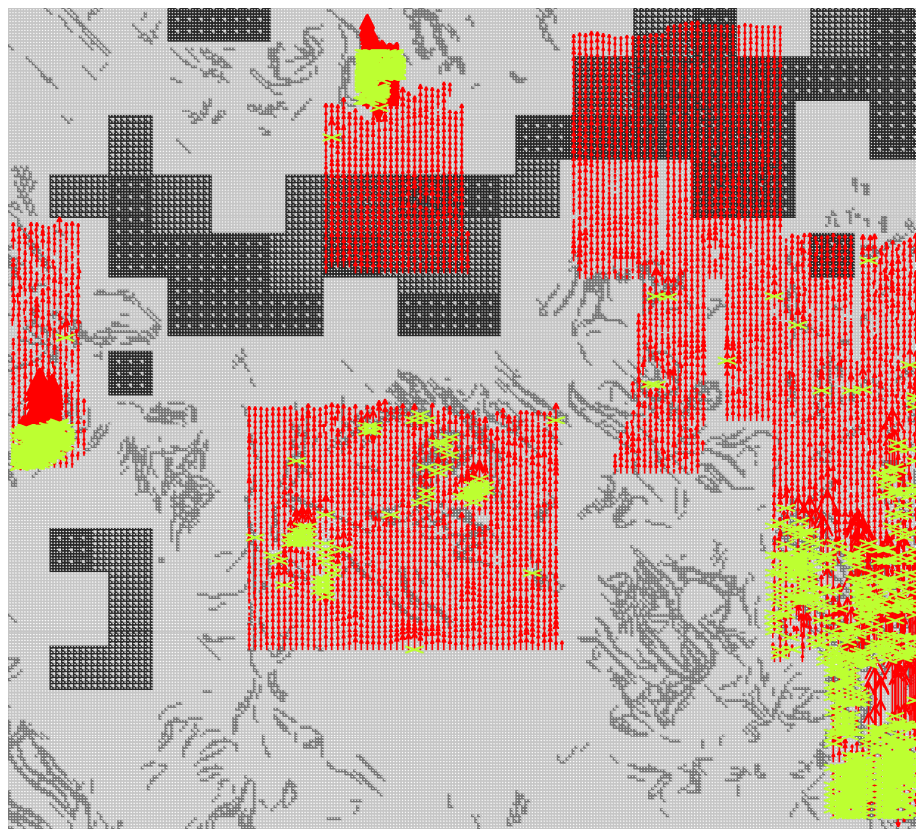


Appendix J: Code specification and error arrows

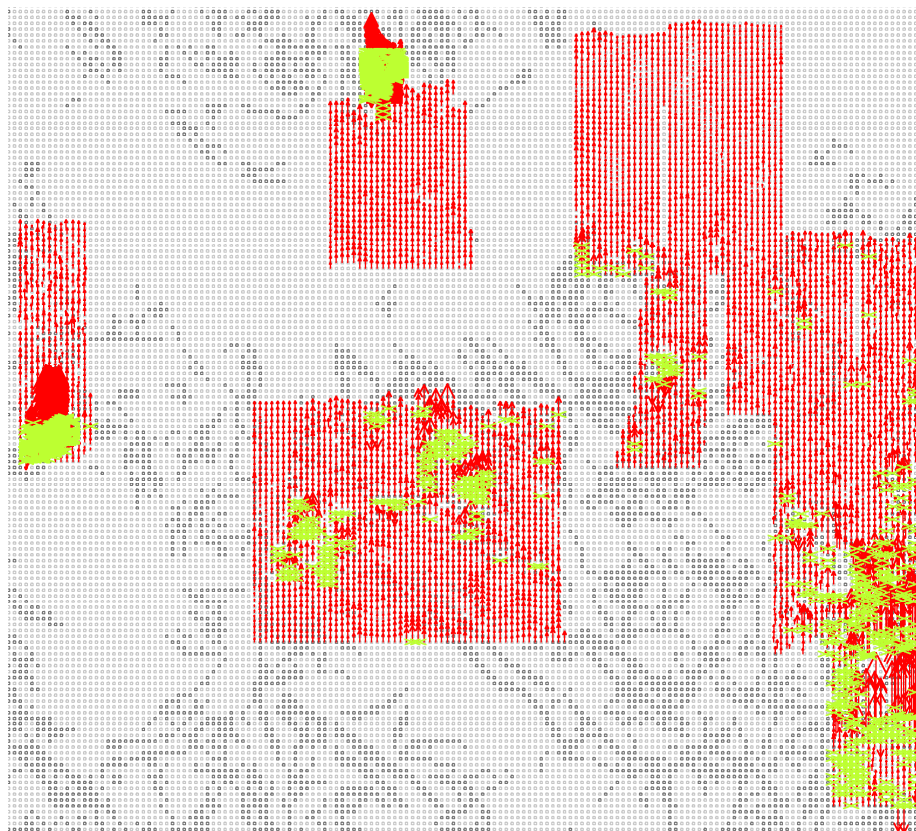
J.1 Code specification and error arrows

Appendix J contains the automatically generated grids shown with their code specifications without boundaries. The code specifications are defined as:- light grey = grid points OK, medium grey = grid points with double code and dark grey = grid points defective. The (red) error arrows are superimposed on the grid. The length of the arrow is related to the deviation between the frame of reference and the automatically generated grids. Arrows which should have been deleted are marked with a green cross.

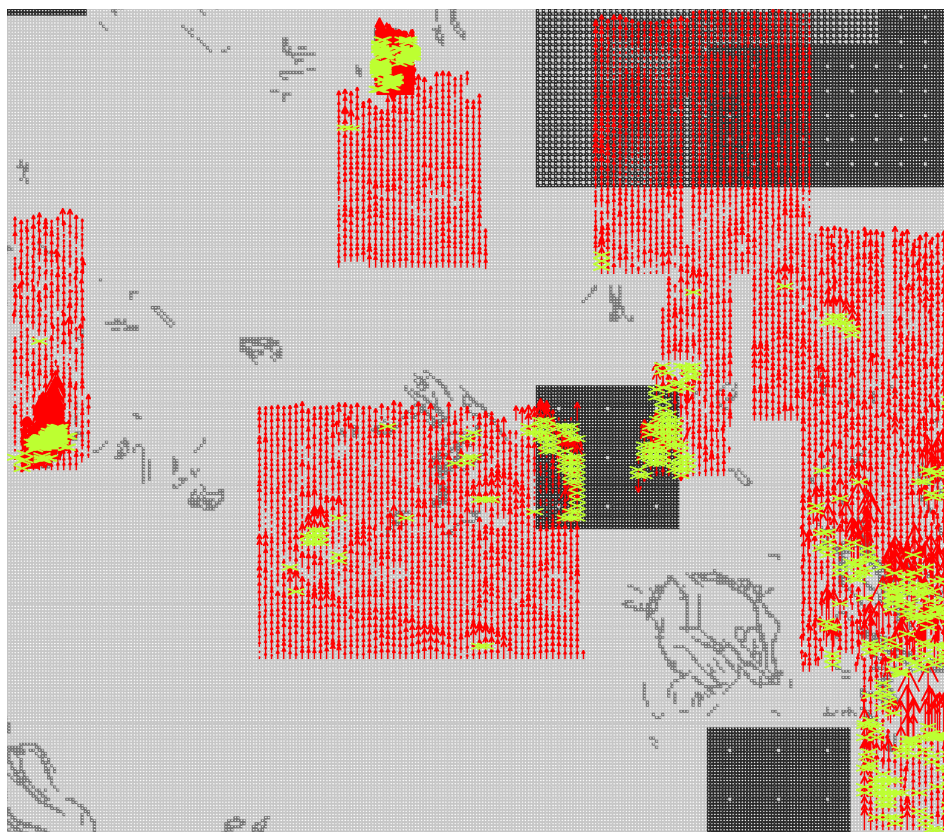
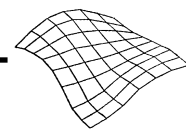
Positive deviations are depicted as upward facing arrows, and negative deviations as downward facing arrows. The size of the deviation is multiplied with a scale 20.



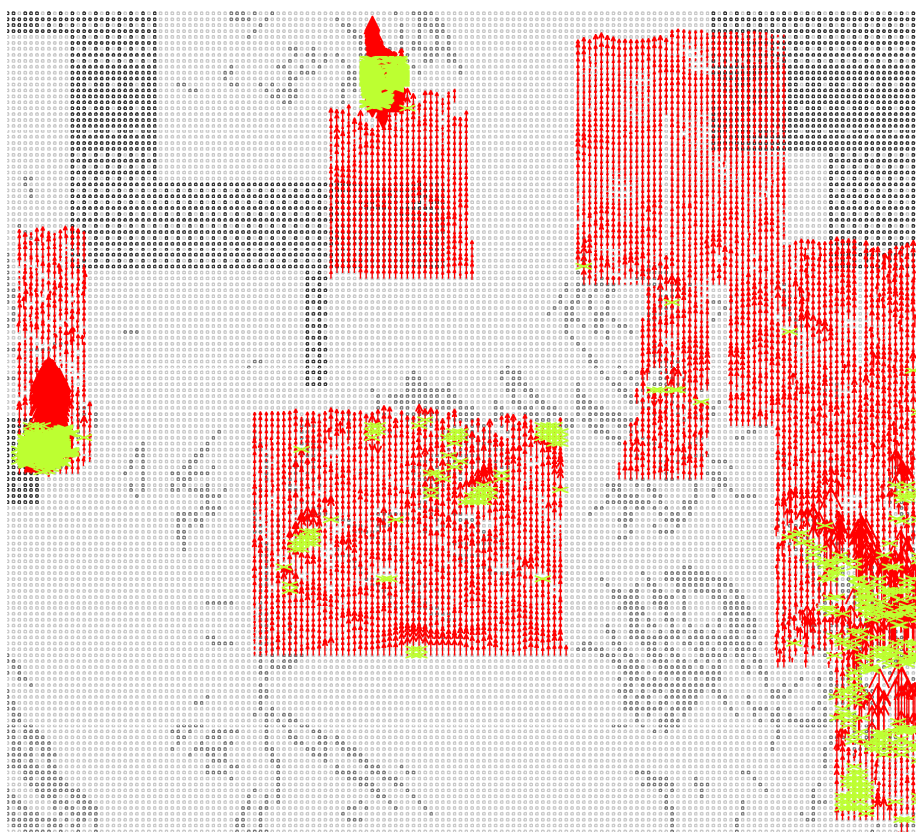
Code specification and errors arrows (red) for images in scale 1:25.000, resolution 15 μm and mesh size 12.5 x 12.5 m. Points which should have been deleted are shown as green crosses.



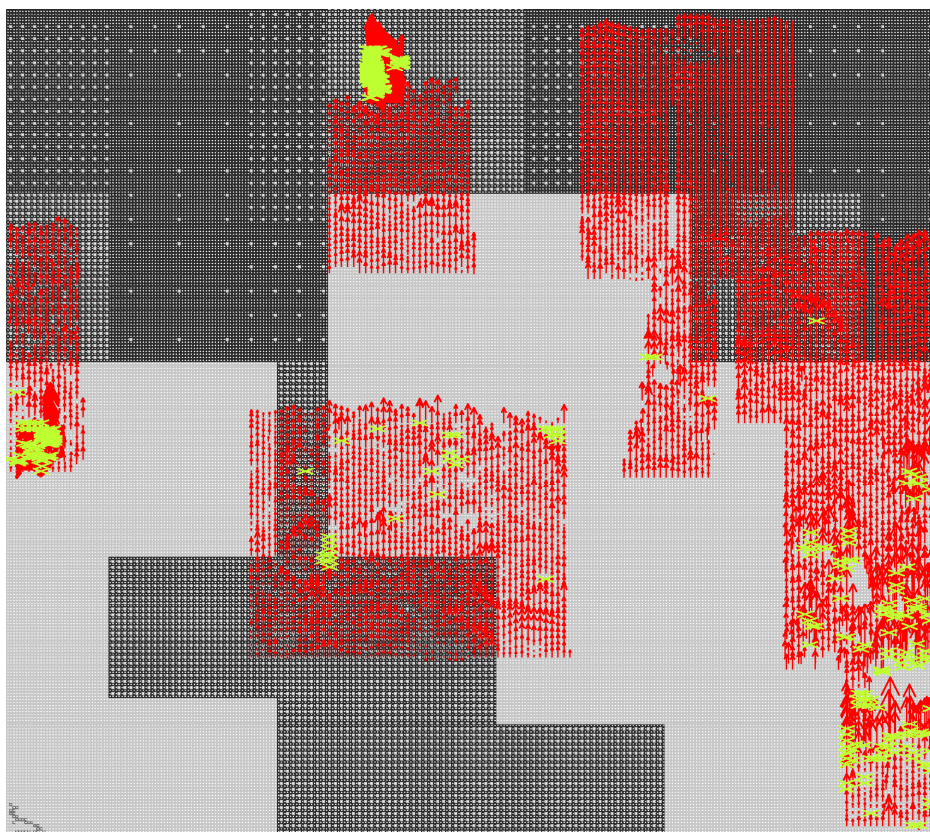
Code specification and errors arrows (red) for images in scale 1:25.000, resolution 15 μm and mesh size 25 x 25 m. Points which should have been deleted are shown as green crosses.



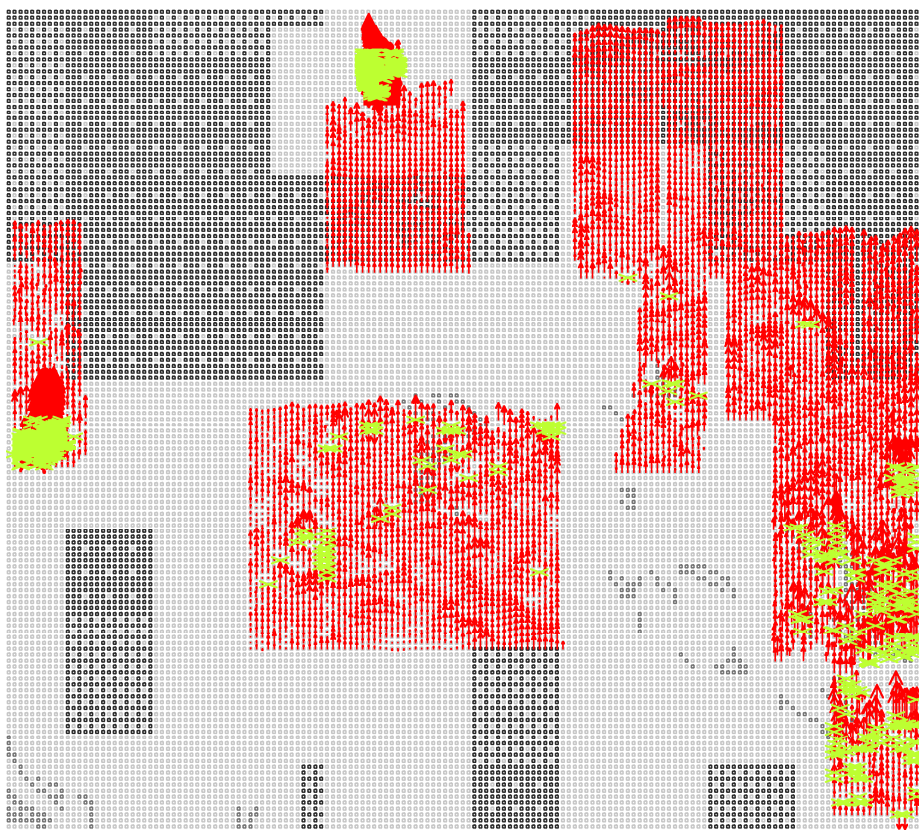
Code specification and errors arrows (red) for images in scale 1:25.000, resolution 30 μm and mesh size 12.5 x 12.5 m. Points which should have been deleted are shown as green crosses.



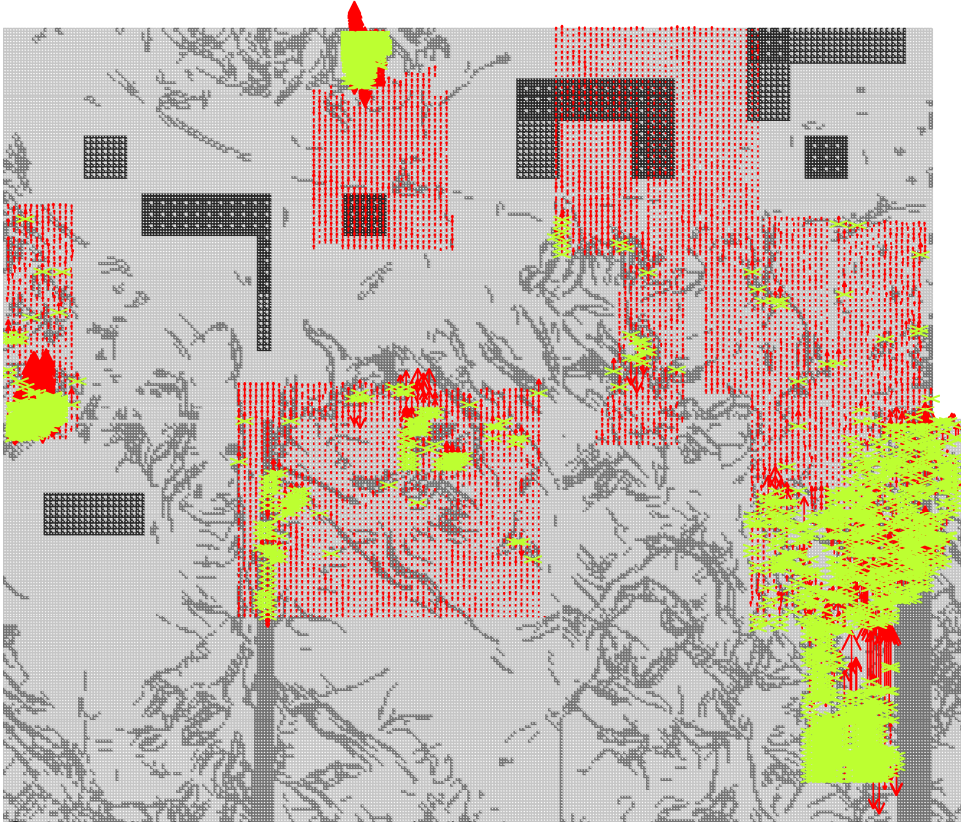
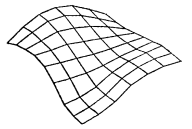
Code specification and errors arrows (red) for images in scale 1:25.000, resolution 15 μm and mesh size 12.5 x 12.5 m. Points which should have been deleted are shown as green crosses.



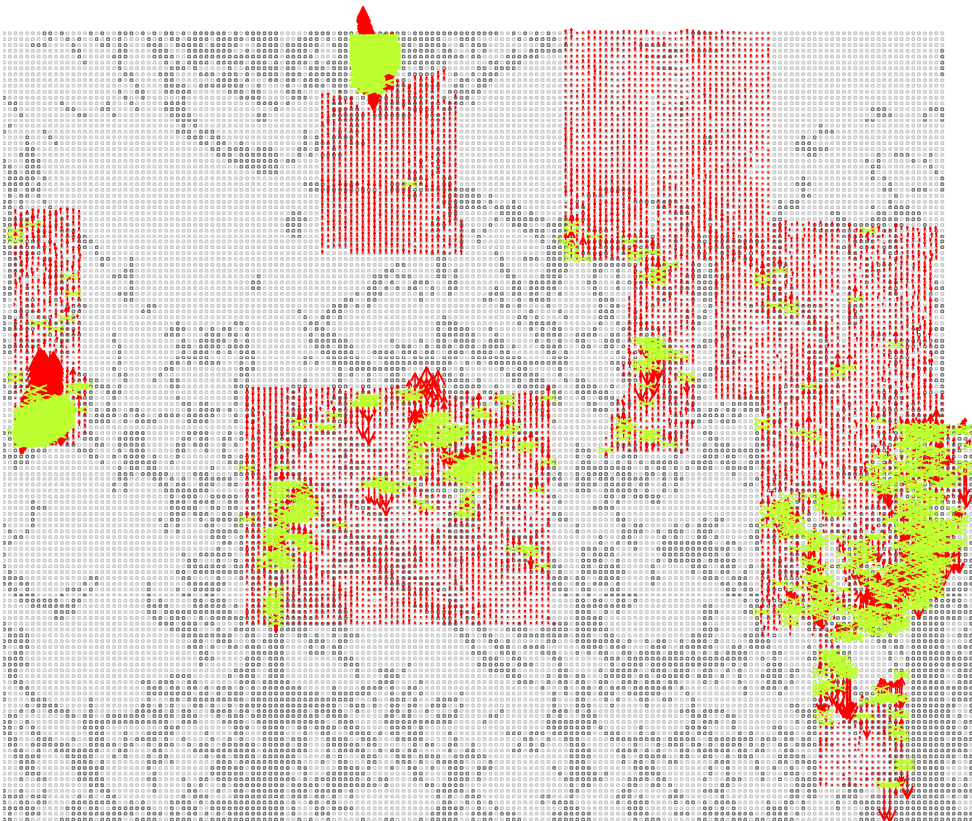
Code specification and errors arrows (red) for images in scale 1:25.000, resolution 60 μm and mesh size 12.5 x 12.5 m. Points which should have been deleted are shown as green crosses.



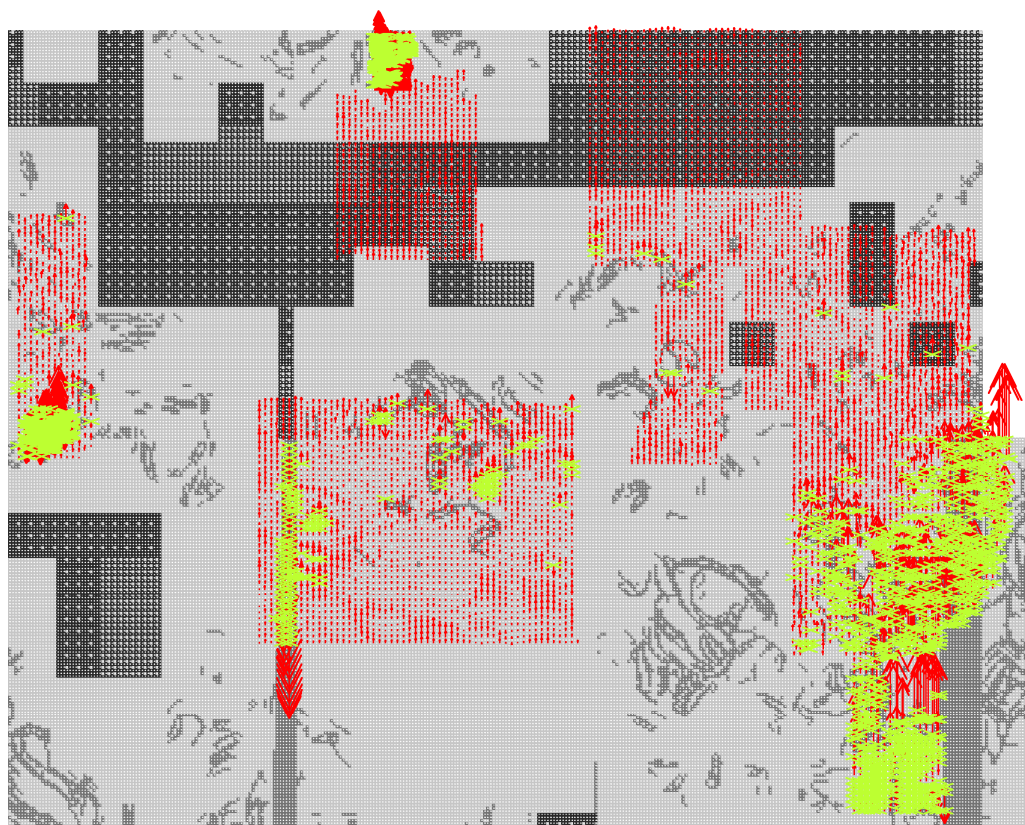
Code specification and errors arrows (red) for images in scale 1:25.000, resolution 60 μm and mesh size 25 x 25 m. Points which should have been deleted are shown as green crosses.



Code specification and errors arrows (red) for images in scale 1:15.000, resolution 15 μm and mesh size 12.5 x 12.5 m. Points which should have been deleted are shown as green crosses.



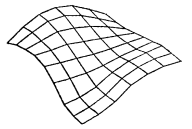
Code specification and errors arrows (red) for images in scale 1:15.000, resolution 15 μm and mesh size 25 x 25 m. Points which should have been deleted are shown as green crosses.



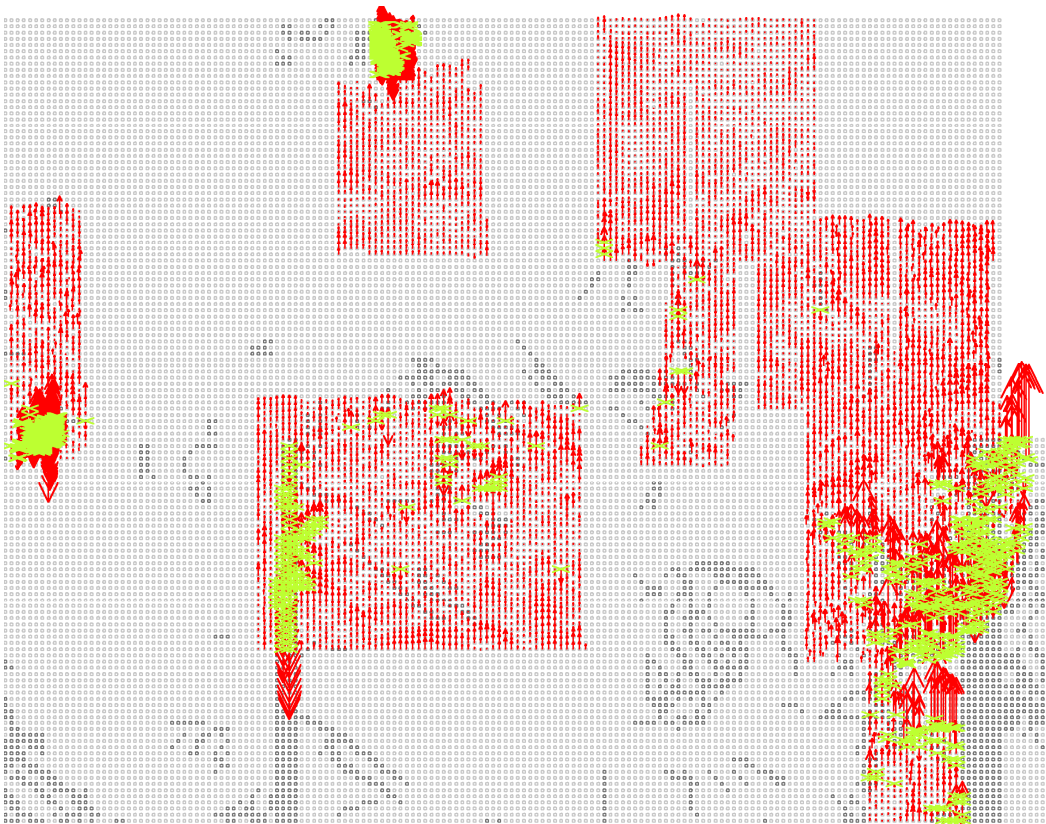
Code specification and errors arrows (red) for images in scale 1:15,000, resolution 30 μm and mesh size 12.5 x 12.5 m. Points which should have been deleted are shown as green crosses.



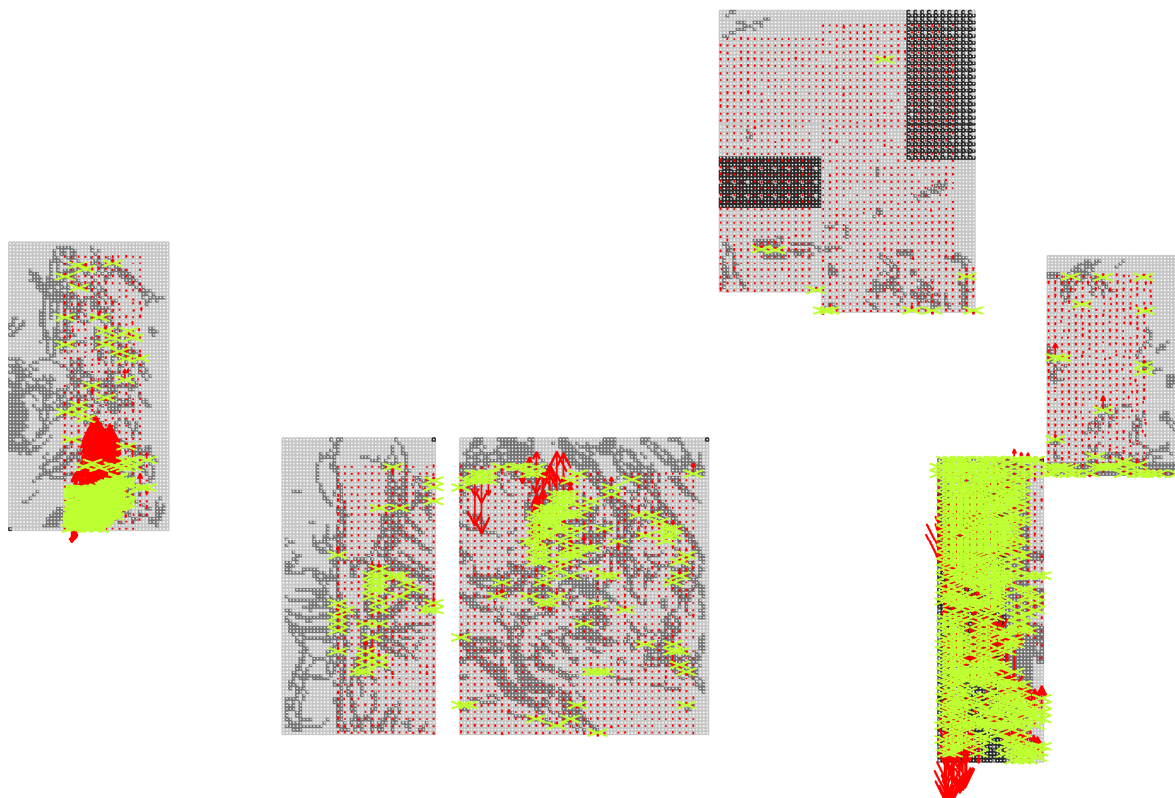
Code specification and errors arrows (red) for images in scale 1:25,000, resolution 30 μm and mesh size 25 x 25 m. Points which should have been deleted are shown as green crosses.



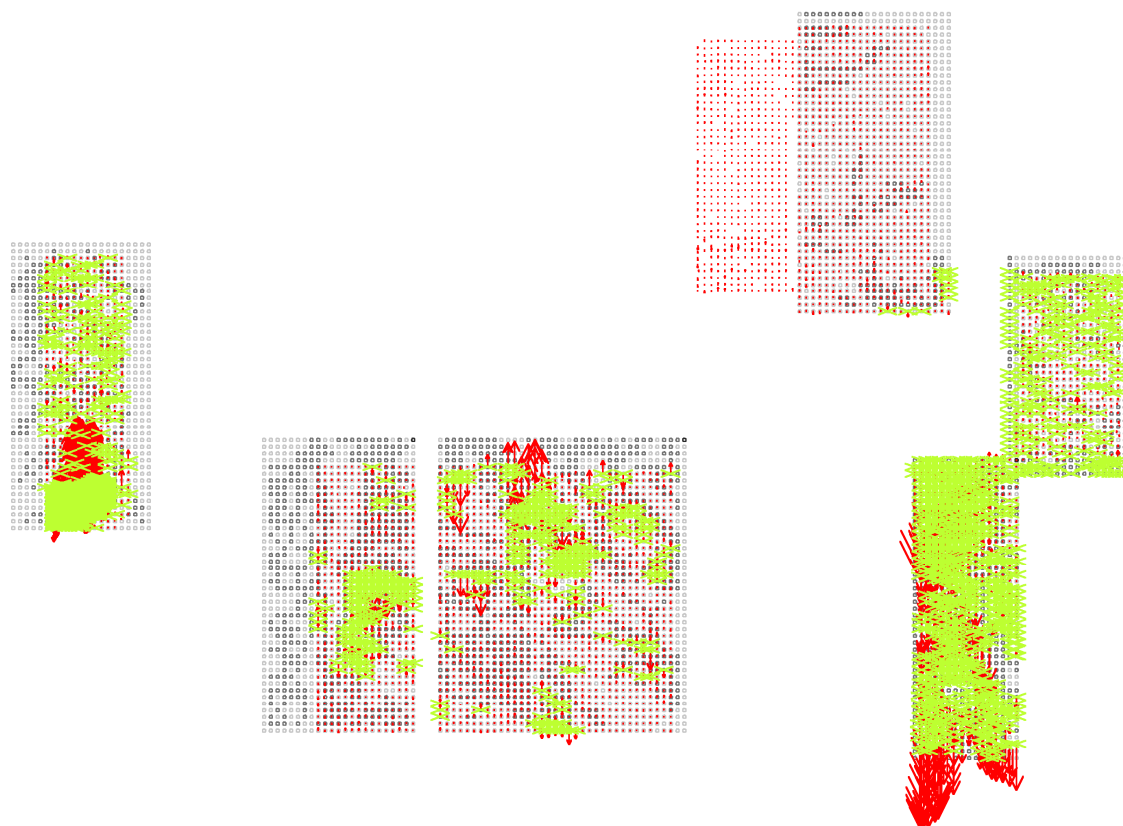
Code specification and errors arrows (red) for images in scale 1:15,000, resolution 60 μm and mesh size 12.5 x 12.5 m. Points which should have been deleted are shown as green crosses.



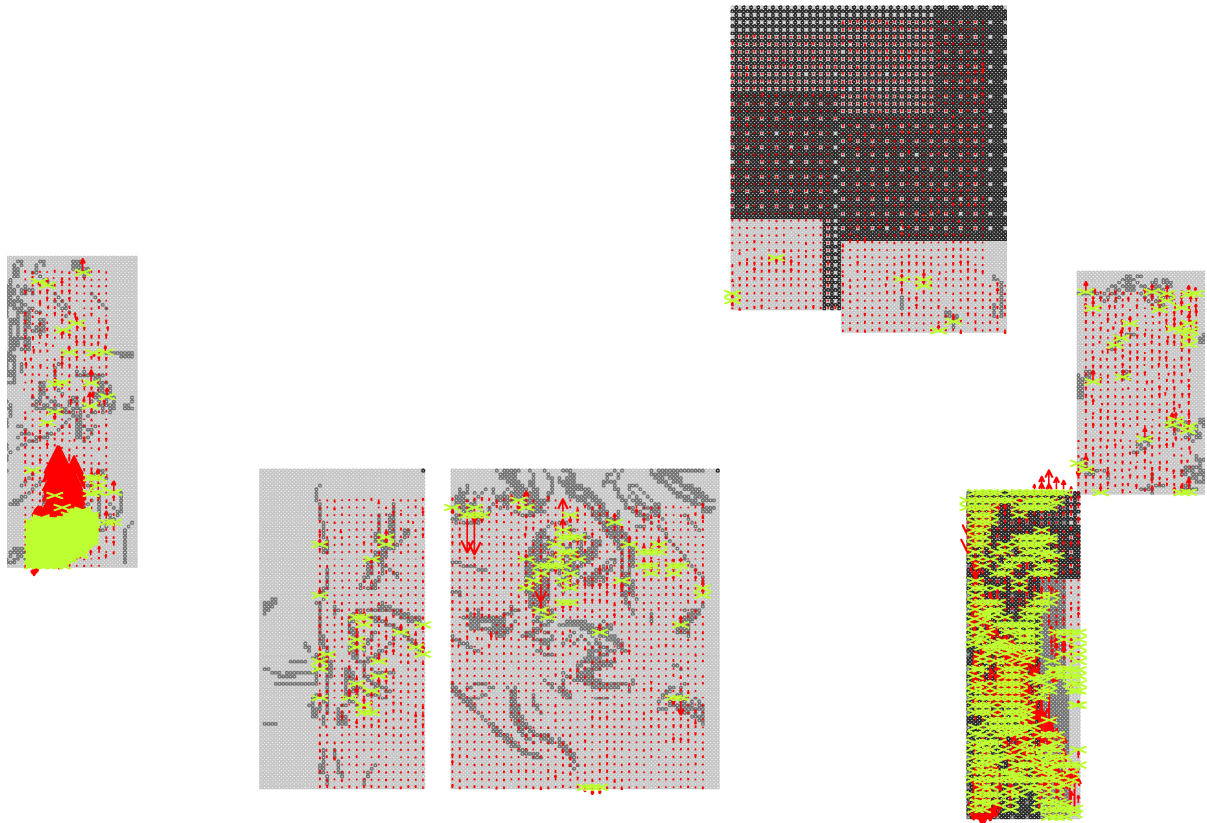
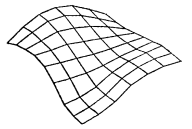
Code specification and errors arrows (red) for images in scale 1:15,000, resolution 60 μm and mesh size 25 x 25 m. Points which should have been deleted are shown as green crosses.



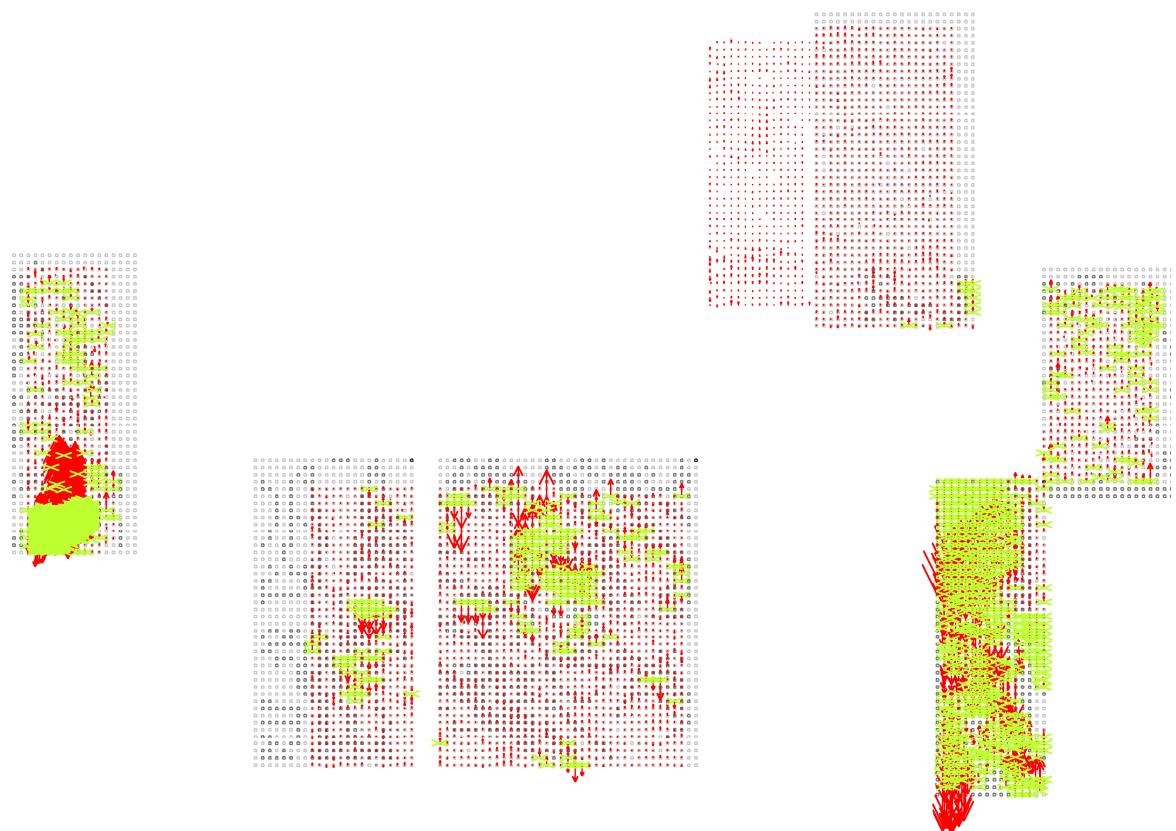
Code specification and errors arrows (red) for images in scale 1:5,000, resolution $30\ \mu\text{m}$ and mesh size $12.5 \times 12.5\ \text{m}$. Points which should have been deleted are shown as green crosses.



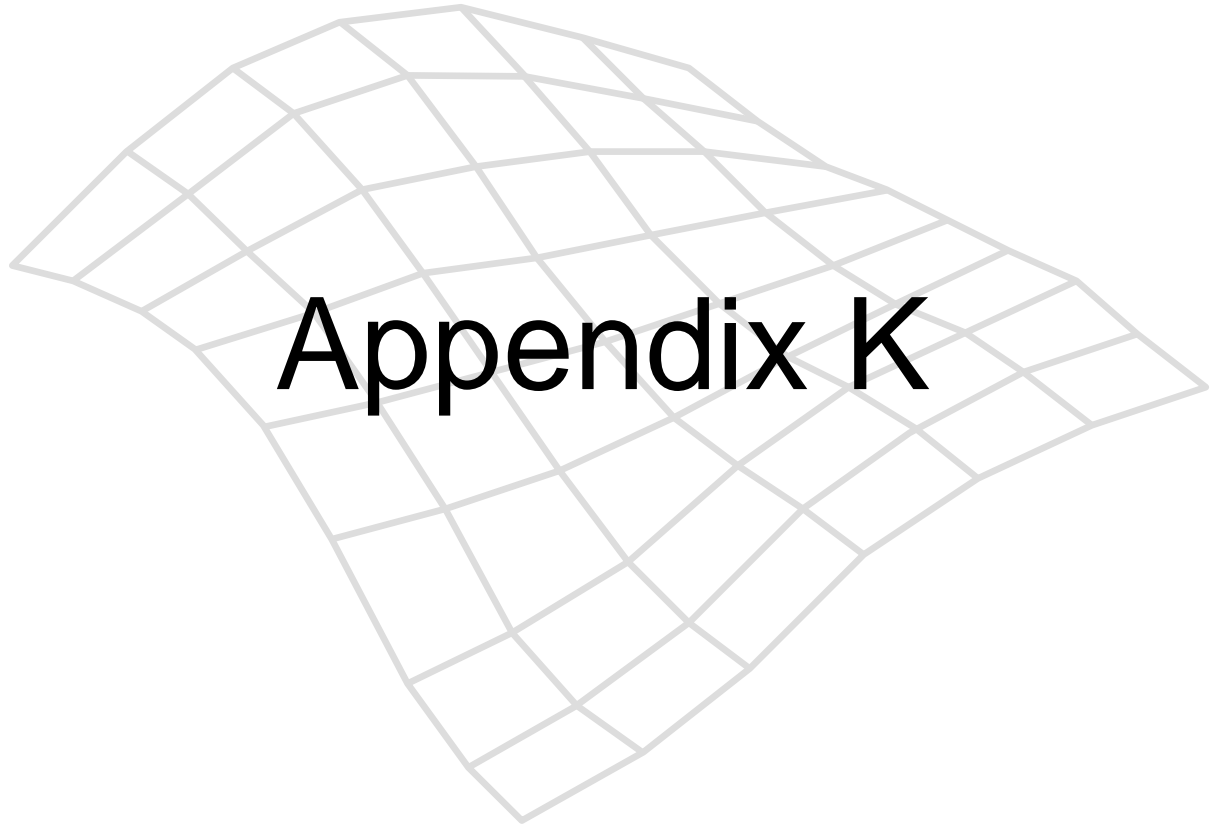
Code specification and errors arrows (red) for images in scale 1:5,000, resolution $30\ \mu\text{m}$ and mesh size $25 \times 25\ \text{m}$. Points which should have been deleted are shown as green crosses.

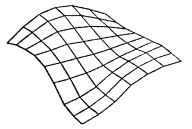


Code specification and errors arrows (red) for images in scale 1:5,000, resolution 60 μm and mesh size 12.5 x 12.5 m. Points which should have been deleted are shown as green crosses.



Code specification and errors arrows (red) for images in scale 1:5,000, resolution 60 μm and mesh size 25 x 25 m. Points which should have been deleted are shown as green crosses.





Appendix K: Orthophoto and error arrows

K.1 Orthophoto and error arrows

In this Appendix, the deviations (scale 20) are superimposed on an orthophoto of the test area. The Appendix contains all 24 calculations.

Error arrows are shown with different colours. The colour indicates the landscape type:-

- *Green = flat terrain*
- *Yellow/orange = gravel pit*
- *Red = village*
- *Violet = hilly terrain*
- *Blue = woods*

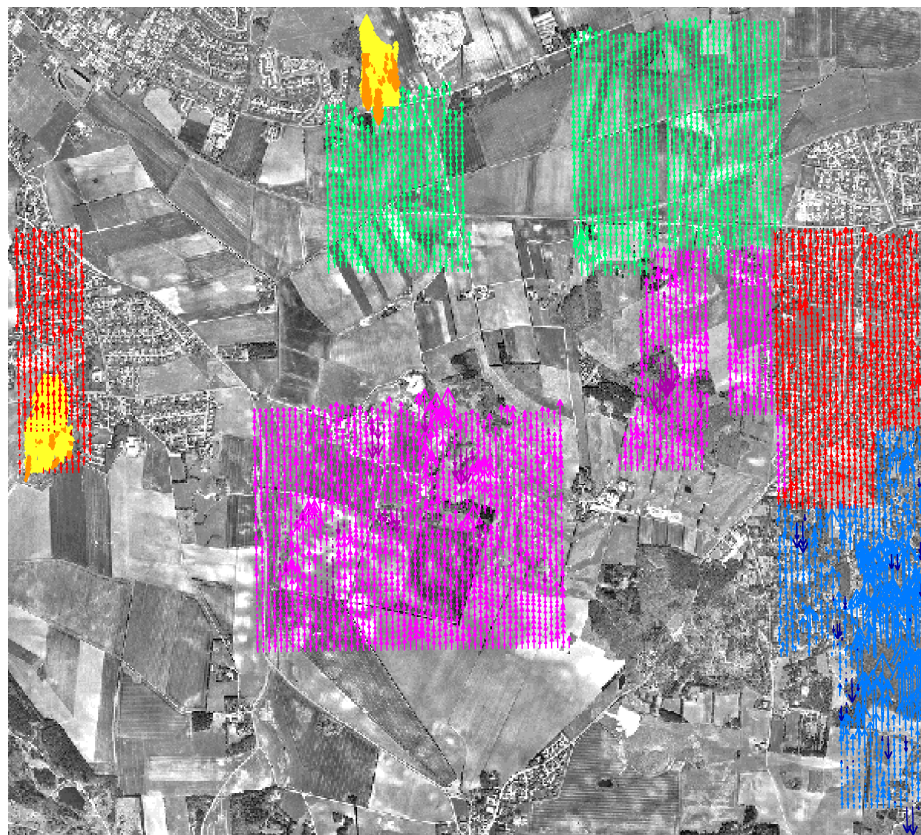
Positive deviations are depicted with upward facing light coloured error arrows and negative with downward facing dark coloured error arrows.



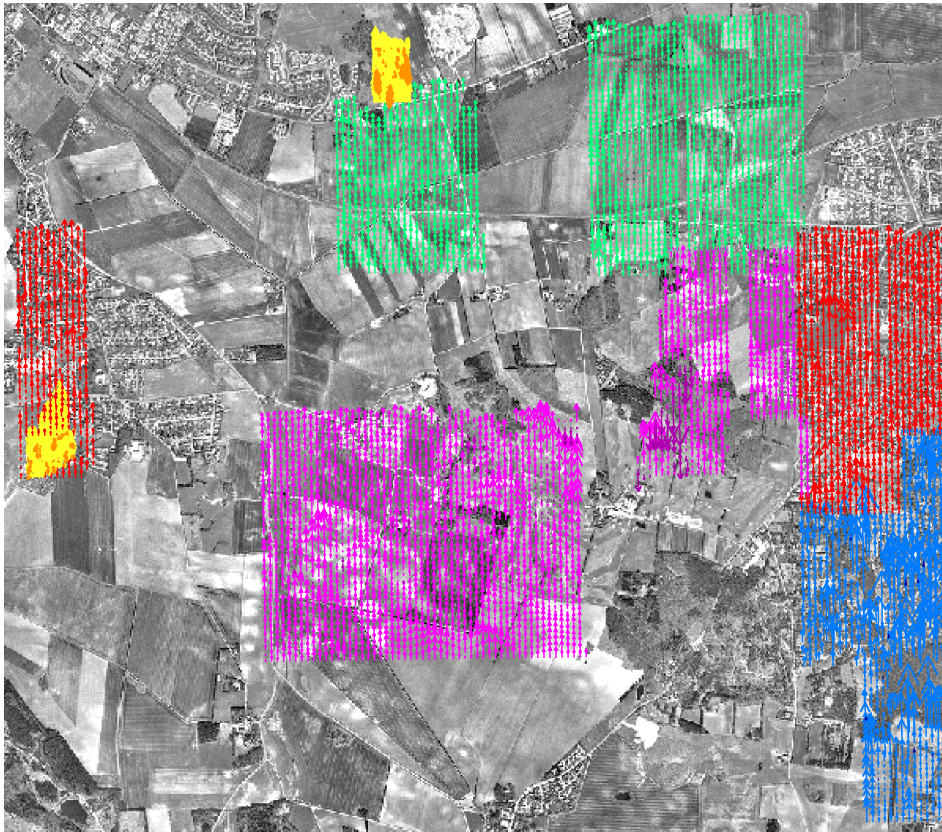
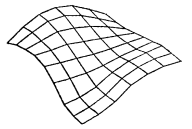
Error arrows coloured as the landscape type superimposed on an orthophoto for images in scale 1:25,000, resolution 15 μ m and mesh size 5 x 5 m.



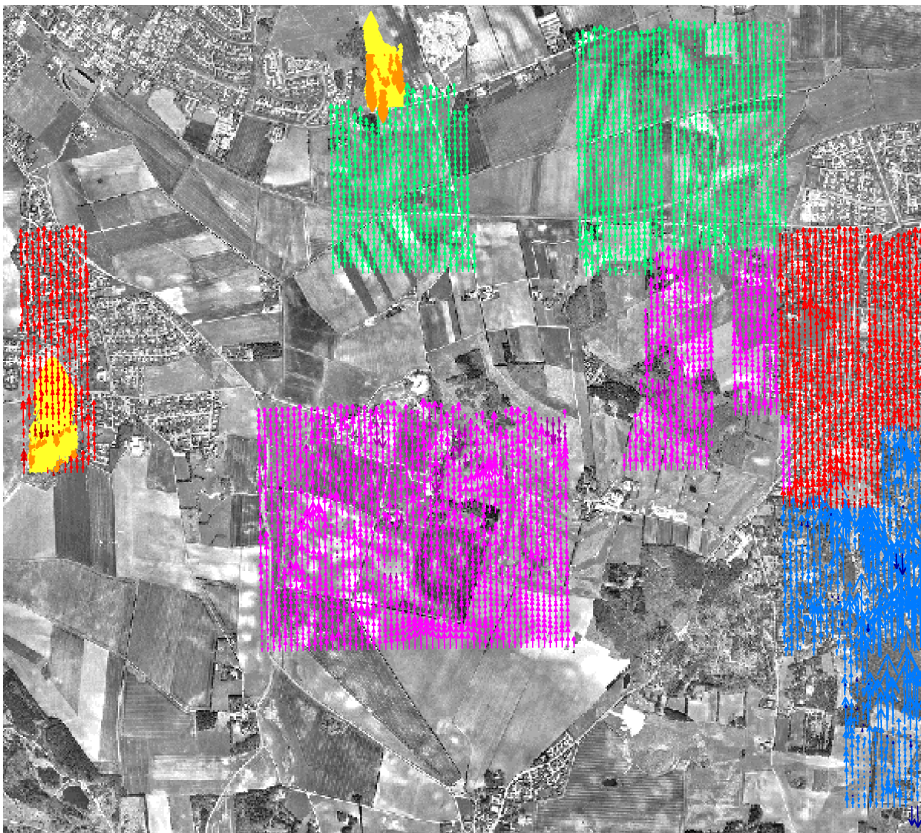
Error arrows coloured as the landscape type superimposed on an orthophoto for images in scale 1:25,000, resolution 15 μ m and mesh size 12.5 x 12.5 m.



Error arrows coloured as the landscape type superimposed on an orthophoto for images in scale 1:25,000, resolution 15 μ m and mesh size 25 x 25 m.



Error arrows coloured as the landscape type superimposed on an orthophoto for images in scale 1:25,000, resolution 30 μm and mesh size 12.5 x 12.5 m.



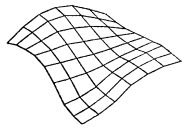
Error arrows coloured as the landscape type superimposed on an orthophoto for images in scale 1:25,000, resolution 30 μm and mesh size 25 x 25 m.



Error arrows coloured as the landscape type superimposed on an orthophoto for images in scale 1:25,000, resolution 60 μm and mesh size 12.5 x 12.5 m.



Error arrows coloured as the landscape type superimposed on an orthophoto for images in scale 1:25,000, resolution 60 μm and mesh size 25 x 25 m.



Error arrows coloured as the landscape type superimposed on an orthophoto for images in scale 1:15,000, resolution 15 μm and mesh size 5 x 5 m.



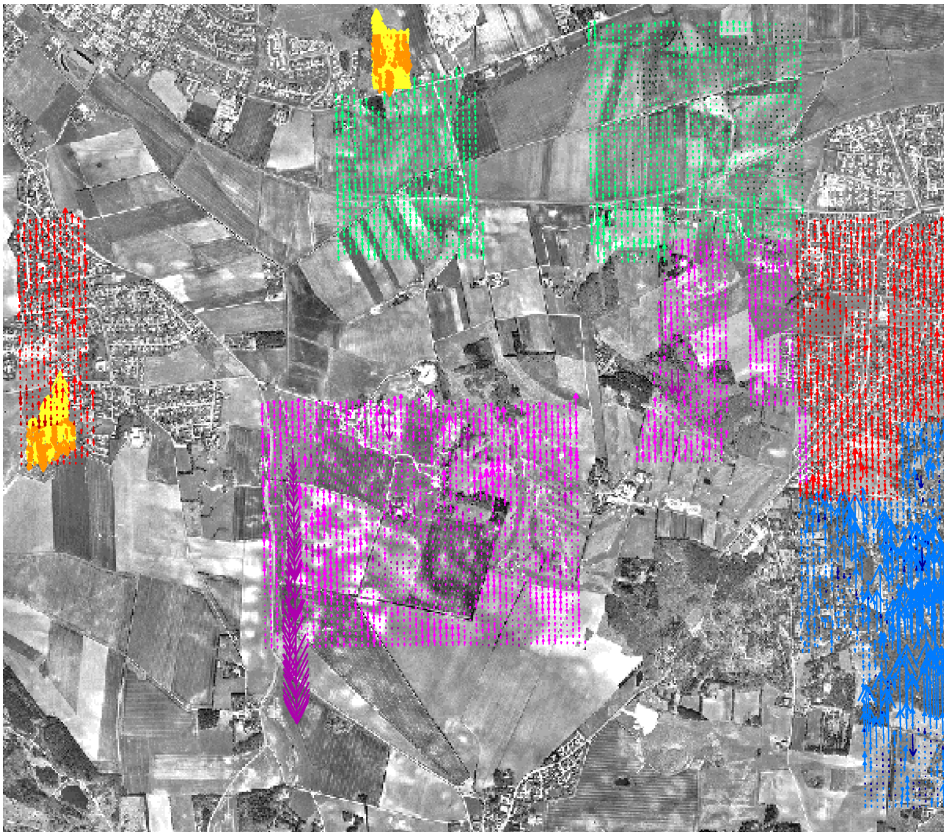
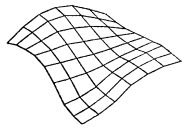
Error arrows coloured as the landscape type superimposed on an orthophoto for images in scale 1:15,000, resolution 15 μm and mesh size 12.5 x 12.5 m.



Error arrows coloured as the landscape type superimposed on an orthophoto for images in scale 1:15.000, resolution 15 μ m and mesh size 25 x 25 m.



Error arrows coloured as the landscape type superimposed on an orthophoto for images in scale 1:15,000, resolution 30 μ m and mesh size 5 x 5 m.



Error arrows coloured as the landscape type superimposed on an orthophoto for images in scale 1:15,000, resolution 30 μm and mesh size 12.5 x 12.5 m.



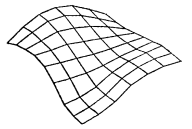
Error arrows coloured as the landscape type superimposed on an orthophoto for images in scale 1:15,000, resolution 30 μm and mesh size 25 x 25 m.



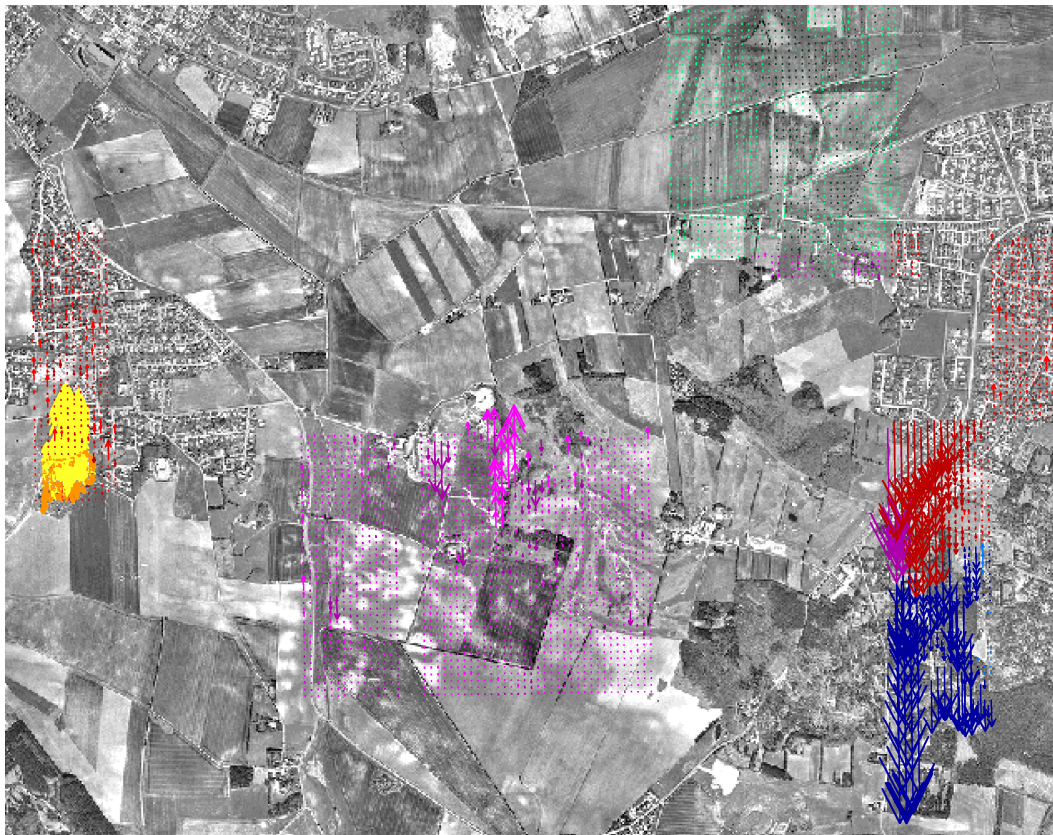
Error arrows coloured as the landscape type superimposed on an orthophoto for images in scale 1:15,000, resolution 60 μ m and mesh size 12.5 x 12.5 m.



Error arrows coloured as the landscape type superimposed on an orthophoto for images in scale 1:15,000, resolution 60 μ m and mesh size 25 x 25 m.



Error arrows coloured as the landscape type superimposed on an orthophoto for images in scale 1:5,000, resolution 15 μ m and mesh size 5 x 5 m.



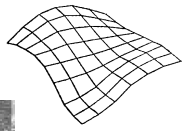
Error arrows coloured as the landscape type superimposed on an orthophoto for images in scale 1:5,000, resolution 15 μ m and mesh size 12.5 x 12.5 m.



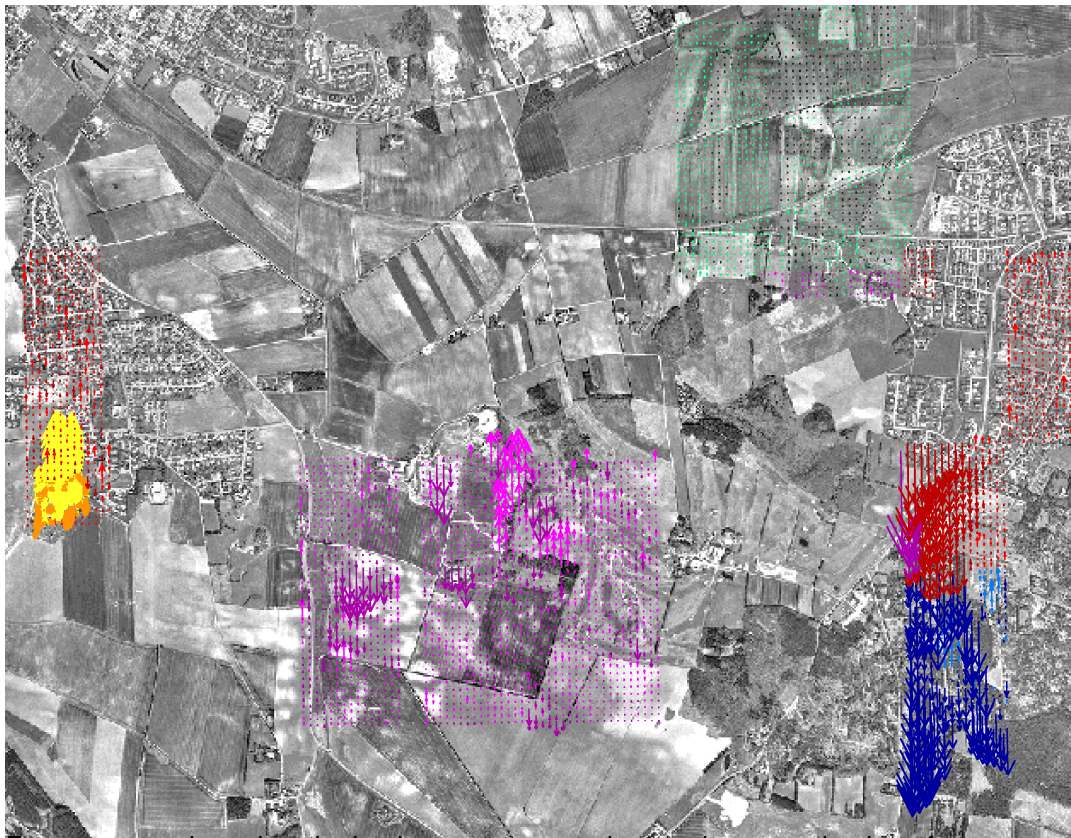
Error arrows coloured as the landscape type superimposed on an orthophoto for images in scale 1:5,000, resolution 15 μ m and mesh size 25 x 25 m.



Error arrows coloured as the landscape type superimposed on an orthophoto for images in scale 1:51,000, resolution 30 μ m and mesh size 5 x 5 m.



Error arrows coloured as the landscape type superimposed on an orthophoto for images in scale 1:5,000, resolution 30 μ m and mesh size 12.5 x 12.5 m.



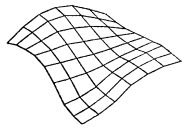
Error arrows coloured as the landscape type superimposed on an orthophoto for images in scale 1:5,000, resolution 30 μ m and mesh size 25 x 25 m.



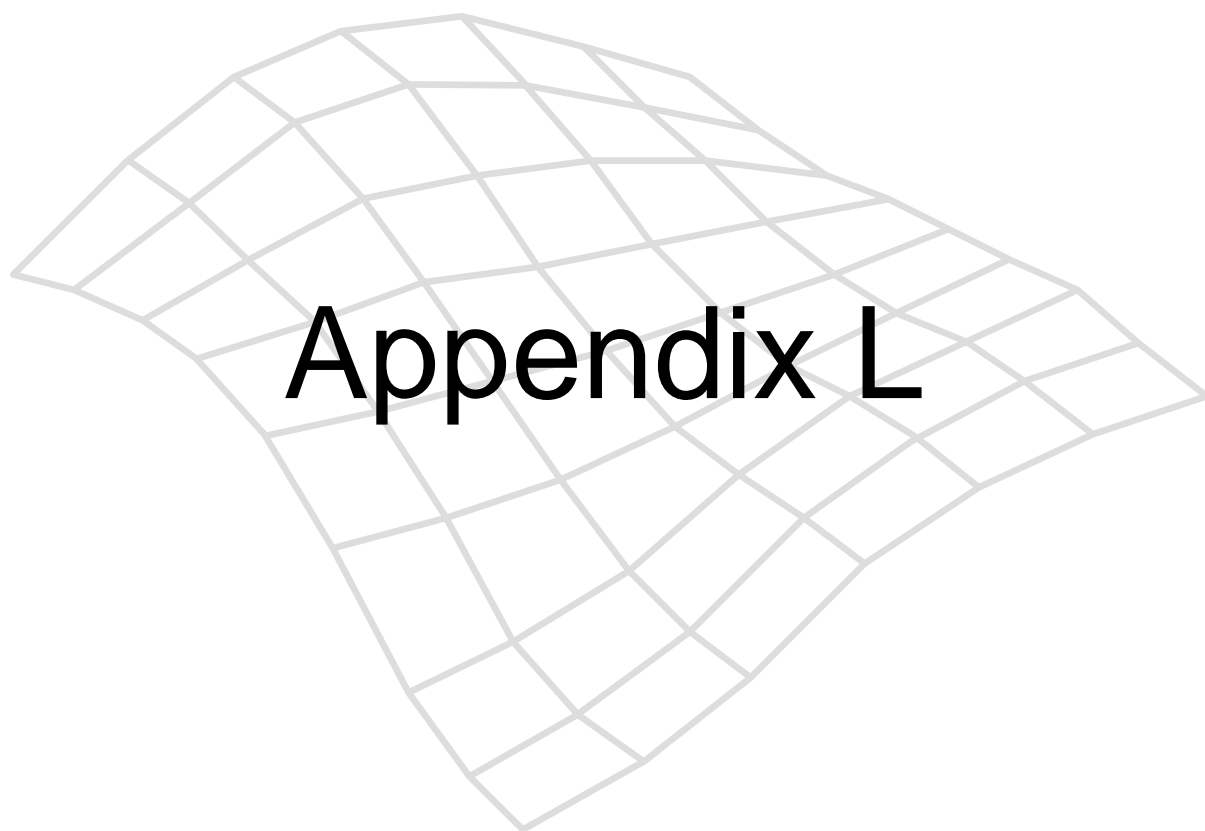
Error arrows coloured as the landscape type superimposed on an orthophoto for images in scale 1:5,000, resolution 60 μ m and mesh size 5 x 5 m.

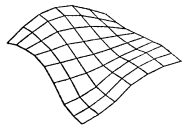


Error arrows coloured as the landscape type superimposed on an orthophoto for images in scale 1:5,000, resolution 60 μ m and mesh size 12.5 x 12.5 m.



Error arrows coloured as the landscape type superimposed on an orthophoto for images in scale 1:5,000, resolution 60 μm and mesh size 25 x 25 m.





Appendix L: STND used as threshold

L.1 STND used as threshold

This Appendix contains a cut out of the results from the excel sheet with the calculations in which the standard deviation has been used as the cut out threshold between the results from images in 15 μ m, 30 μ m and 60 μ m for a given scale and mesh size.

Image scale 1:25,000 and mesh size 25 x 25 m.

Nos. of points	Nos. of points	Good (nos.)	Bad (nos.)		Good (m)	Bad (m)
70	3263	14	56		11,4643	285,899
1,10 %	51,48 %	0,22 %	0,88 %			
Klip after STND	Klip after z	Difference				

Image scale 1:15,000 and mesh size 25 x 25 m.

Nos. of points	Nos. of points	Good (nos.)	Bad (nos.)		Good (m)	Bad (m)
199	850	81	118		37,6113	47
3,09 %	13,21 %	1,26 %	1,83 %			
Cut after STND	Cut after z	Difference				

Image scale 1:15,000 and mesh size 12.5 x 12.5 m.

Nos. of points	Nos. of points	Good (nos.)	Bad (nos.)		Good (m)	Bad (m)
177	676	83	94		38,7559	327,257
2,76 %	10,55 %	1,30 %	1,47 %			
Cut after STDAFV	Cut after Z (ref.)	Difference				

Image scale 1:5,000 and mesh size 5 x 5 m.

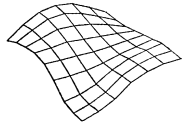
Nos. of points	Nos. of points	Good (nos.)	Bad (nos.)		Good (m)	Bad (m)
158	125	95	63		9,9755	341,525
4,78 %	3,79 %	2,88 %	1,91 %			
Cut after STDAFV	Cut after z	Difference				

Image scale 1:5,000 and mesh size 12.5 x 12.5 m.

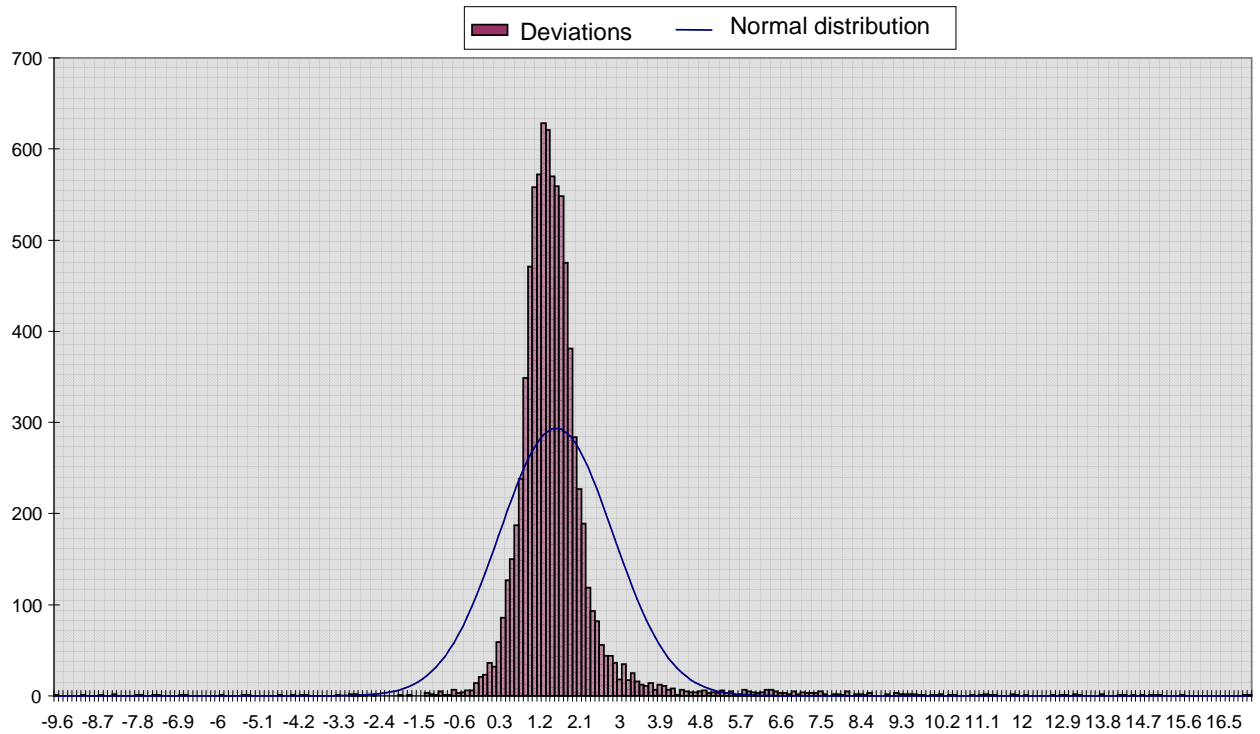
Nos. of points	Nos. of points	Good (nos.)	Bad (nos.)		Good (m)	Bad (m)
170	261	54	116		7,3931	632,185
5,21 %	7,99 %	1,65 %	3,55 %			
Cut after STDAFV	Cut after z	Difference				

Image scale 1:5,000 and mesh size 25 x 25 m.

Nos. of points	Nos. of points	Good (nos.)	Bad (nos.)		Good (m)	Bad (m)
340	583	140	200		19,5477	597,353
10,11 %	17,33 %	4,16 %	5,95 %			
Cut after STDAFV	Cut after z	Difference				



Distribution of the deviations for images in scale 1:xx,000, resolution xx µm and mesh size xx m



	Total	Flat A 12	Gravel pit 34	Village 56	Hilly A 78	Woods 90	Unknown 00
Min	-9.51	-0.07	-0.98	0.06	-2.73	-9.51	0
Max	17.13	4.65	2.89	6.98	8.40	17.13	0
Mean	1.64	1.55	1.05	1.65	1.70	2.39	0
Stnd	1.27	0.45	0.54	0.68	0.89	3.22	0
RMSE	2.07	1.61	1.18	1.79	1.92	4.02	0
Nos. of pts	8342	2092	1168	1410	2811	861	0
Level '200'	8342	2092	1168	1410	2811	861	0
Level '400'	0	0	0	0	0	0	0
Level '600'	0	0	0	0	0	0	0
Nos. of cut out pts	0	0	0	0	0	0	0
Area	202.0	0.0	107.3	0.0	0.0	94.6	0.0
Level '200'	202.0	0.0	107.3	0.0	0.0	94.6	0.0
Level '400'	0.0	0.0	0.0	0.0	0.0	0.0	0.0
Level '600'	0.0	0.0	0.0	0.0	0.0	0.0	0.0
Area cut out	0.0	0.0	0.0	0.0	0.0	0.0	0.0
Area cut out in %	0.0	0.00	0.00	0.00	0.00	0.00	-0-

Offset (mean)	1.64	1.55	1.05	1.65	1.70	2.39	-0-
Min	-11.90	-1.62	-2.03	-1.59	-4.43	-11.90	0
Max	14.73	3.10	1.83	5.33	6.70	14.73	0
Mean	-0.00	0.00	0.00	0.00	-0.00	0.00	0
Stnd	1.23	0.45	0.54	0.68	0.89	3.22	0
RMSE	1.23	0.45	0.54	0.68	0.89	3.22	0

							Cut out
Min	-9.51	-0.07	-0.98	0.06	-2.73	-9.51	0
Max	17.13	4.65	2.89	6.98	8.40	17.13	0
Mean	1.64	1.55	1.05	1.65	1.70	2.39	0
Stnd	1.27	0.45	0.54	0.68	0.89	3.22	0
RMSE	2.07	1.61	1.18	1.79	1.92	4.02	0

							Cut out + Offset
Min	-	-1.62	-2.03	-1.59	-4.43	-11.90	0
Max	-	3.10	1.83	5.33	6.70	14.73	0
Mean	-	0.00	0.00	0.00	-0.00	0.00	0
Stnd	-	0.45	0.54	0.68	0.89	3.22	0
RMSE	-	0.45	0.54	0.68	0.89	3.22	0

